R-10-60

Hydrogeochemical Evolution of the Laxemar Site

María J. Gimeno, Luís F. Auqué, Javier B. Gómez
University of Zaragoza, Spain

Joaquín Salas, Jorge Molinero
Amphos 21, Spain

November 2010

Svensk Kärnbränslehantering AB
Swedish Nuclear Fuel
and Waste Management Co

Box 250, SE-101 24 Stockholm
Phone +46 8 459 84 00

SKB

ISSN 1402-3091
SKB R-10-60

Hydrogeochemical Evolution of the Laxemar Site

María J. Gimeno, Luís F. Auqué, Javier B. Gómez
University of Zaragoza, Spain

Joaquín Salas, Jorge Molinero
Amphos 21, Spain

November 2010

Keywords: Performance assessment, Laxemar, Geochemical modelling, groundwater evolution, SKBdoc 1271303.

Abstract

The chemical composition of groundwater in the rock volume surrounding a spent nuclear fuel repository is of importance to many variables that affect repository performance. One of the questions to be addressed is whether the chemical environment will remain favourable over time under the expected environmental evolution. Different groundwater compositions will prevail around the repository as a result of the different types of climate domains and their corresponding hydraulic conditions. The successions of temperate, periglacial and glacial climate domains will affect both the groundwaters' flow and composition around the repository. For a specific location, the evolution between climate domains will be gradual. For example, during a temperate domain, temperatures may slowly decrease such that periglacial conditions slowly develop within parts of the repository region.

In SR-Site, the evaluation of geochemical effects is restricted to using separate specifications for the different climatic domains. During the initial temperate period after closure, the infiltration of meteoric waters, the displacement of the Baltic shoreline, and the changes in annual precipitation are the key processes controlling the evolution of the hydrogeology of the site. On the other hand, the groundwater chemistry for periods in which the repository is under permafrost or under an ice sheet (during periglacial and glacial conditions, respectively) is expected to change by the infiltration of glacial melt waters, and by the upconing of deep saline groundwaters. Immediately after the retreat of an ice sheet, isostatic depression will set the ground surface at the repository site below the Baltic Sea surface level for a period of time. In the reference evolution, the Laxemar site is expected to be flooded under a lake of glacial melt water and, then, under marine or brackish waters during a period of time from a few thousand years up to, perhaps, ten thousand years.These phenomena will induce changes in the geochemical composition of groundwater around the repository. In this way, the present report summarizes the results obtained by the geochemical simulations performed to simulate the hydrogeochemical evolution of groundwaters in the Laxemar area.

In the safety assessment of the candidate repository site, a series of functions and parameters must be evaluated. From a geochemical point of view, the most important are redox properties, pH and concentration of solutes. Other factors to be considered are the groundwater content of potassium, sulphide and iron, as they might affect the chemical stability of the buffer and the canister. Additionally, the effects of grouting in the geosphere and cement materials in the engineered barriers could affect groundwater's pH. Discussions of the results will be focused on these aspects.

The starting point of the geochemical calculations is a series of hydrological models (using ConnectFlow and DarcyTools), which, based on the understanding of the palaeohydrogeological history of the sites (which assumes the presence of different water mixing events due to the input of different reference waters over the time), have provided information on (1) the transport of fractions of selected reference waters (deep saline, old meteoric, glacial, marine and present meteoric waters), in the case of the temperate period, or (2) the transport of salts, in the case of the glacial cycle. In the latter case, the rock volume initially contains a mixture of two reference waters: a deep saline groundwater and a dilute water from meteoric origin. The proportion of these two waters can be obtained from the salinity at any point in the rock volume. With the advancement and retreat of the glacier, the proportion of a third mixing end-member is calculated from the decrease of salinity at any point in the rock volume (a newly incoming glacial melt-water), changing the proportions of the other two reference waters correspondingly. Finally, groundwater compositions are modelled through mixing and chemical reactions with the reactive minerals present in the bedrock and fracture fillings (calcite, quartz, hydroxyapatite and a redox mineral, either haematite or amorphous Fe(II) monosulphide,(FeS(am)), using PHREEQC.

It should be noted that the hydrogeological and geochemical modelling are not fully coupled: the results of the regional-scale groundwater flow modelling (in the form of mass fractions of the reference waters) are used as input to a geochemical mixing and reaction model (in the form of mixing proprotions of these waters, end members). The aim has been to obtain equivalent groundwater models for hydrology and geochemistry. The coupling of the two models also allows a description of the geochemical heterogeneity, which otherwise would be hard to attain.

In the framework of the assessment of the hydrogeological evolution of the Laxemar site, three hydrological and climatic cases have been discussed: the open repository stage, the temperate period and the remaining glacial cycle (including periglacial and glacial conditions). The geochemical evolution of groundwaters during the stage of the open repository has been conceptually analysed. Aspects such as salinity, redox conditions, oxygen consumption in the backfill, precipitation and/or dissolution of minerals and the effects of grout, shotcrete and concrete on pH have been extensively discussed.

During the temperate period, the main hydrogeochemical process is the infiltration of modern meteoric waters, mainly focused along the hydraulically more conductive deformation zones. As a consequence, salinities decrease within the candidate repository volume, whereas pH is maintained in equilibrium with calcite, in a range of 6.5–8.0, depending on the concentrations obtained by the mixing processes. Despite the salinity decrease, cationic contents keep high enough to ensure the unstability of montmorillonite colloids guaranteing the buffer stability during the simulated temperate period. On the other hand, the redox potentials and the concentrations of iron and sulphide are other parameter that may affect the performance of the repository. In general, the computed concentrations of iron and sulphide are limited by values of 10^{-4} and 10^{-5} mol/L, respectively, and the calculated Eh values remains below –125 mV during most of the temperate period.

During the glacial cycle, infiltration of new glacial melt waters, upconing and the hypothetical existence of a permafrost, are the key mechanisms which control the geochemistry of the groundwaters within the candidate repository volume. In contrast with the temperate period simulations, potential perturbations to the repository performance have been elucidated. Glacial melt waters are very dilute and the results show that montmorillonite colloids may be stable during especific stages of the glacial period in most of the deposition locations during glacial conditions. The computed pH values remain below 9.75 during the simulated glacial cycle, and Eh shows a wide variability, in a range between –25 and –375 mV.

The expected evolution of other geochemical parameters not included in the calculations (such as colloids, nitrite, ammonia, molecular hydrogen, acetate, methane and DOC concentrations), has been extensively analysed. This discussion is based on the analytical data avalaible for the Forsmark, Laxemar and other Swedish sites.

Contents

1 Introduction

1.1 Background

With the objective of siting a final repository for spent nuclear fuel according to the KBS-3 concept (see Section 1.4), the Swedish Nuclear Fuel and Waste Management Company (SKB) has conducted site investigations at the Laxemar and the Fosrmark areas. Despite the fact that Forsmark has been selected for the licence application, a full assessment was initially carried out for both sites and this report details the information available for the Laxemar site.

Hydrogeochemical conditions are a crucial factor in the safety assessment of an underground repository for spent fuel. The Swedish concept for a deep geological repository for spent fuel foresees a geological environment that must fulfill a number of hydrogeochemical constraints and safety functions related to pH, Eh, and the concentrations of dissolved oxygen, sulphide, calcium, sodium, potassium and phosphate, among the most relevant (see Section 1–4). In addition, the safety assessment for spent fuel disposal in Sweden must consider the hypothetical hydrological evolution of the site from the contruction and the operation periods. The hydrogeochemical evolution at repository depth will be strongly conditioned by the hydrogeology of the site,which is in turn, dependent upon the different climatic domains. Hydrogeological models have been used to simulate the hydrogeological behaviour of the sites during these climatic periods. In this way, several climate domains such as temperate (and an enhanced greenhouse effect period[1]), periglacial, glacial and submerged (under a lake of glacial melt waters and under sea waters) have been considered of importance to SKB. The computed evolution of the geochemical parameters involved in the safety function indicators must be especially analysed.

1.2 Objectives and scope

The main objectives of the present work are (1) to estimate the hydrogeochemical conditions of the Laxemar site for the different periods of interest in the SR-Site assessment, and (2) to identify the hypothetical conditions under which the safety functions defined in the KBS-3 concept are not fulfilled at the repository depths. With this aim (and based on the input of hydrogeological data estimated in previous calculations), a numerical methodology has been developed in order to combine and integrate the results obtained from the hydrogeological models with the hydrogeochemical calculations. The methodology should be able to evaluate the most likely hydrogeochemical evolution of the sites taking into account the computed hydrogeological framework. Such a methodology was already developed and used in the previous SR-Can exercise /Auqué et al. 2006/, and was successfully applied and checked with the present-day groundwaters for both sites, Forsmark and Laxemar.

The groundwater evolution in the Laxemar site has been studied during (1) a temperate period of 13,000 years from the present day (including the excavation and the operational stages /Joyce et al. 2010, Svensson and Follin 2010/, despite no calculations have been performed to simulate the operational phase of the repository), (2) a periglacial period and a complete glacial cycle (ice advance and retreat; /Vidstrand et al. 2010/) compromising approximately 13,000 years between two successive temperate interglacial periods. The final stage of the glacial cycle occurs when the site is submerged under a sheet of glacial melt waters and, finally (3) under seawaters. The simulations carried out are shown in Figure 1-1.

[1] These climatic conditions have not been analysed for the Laxemar site.

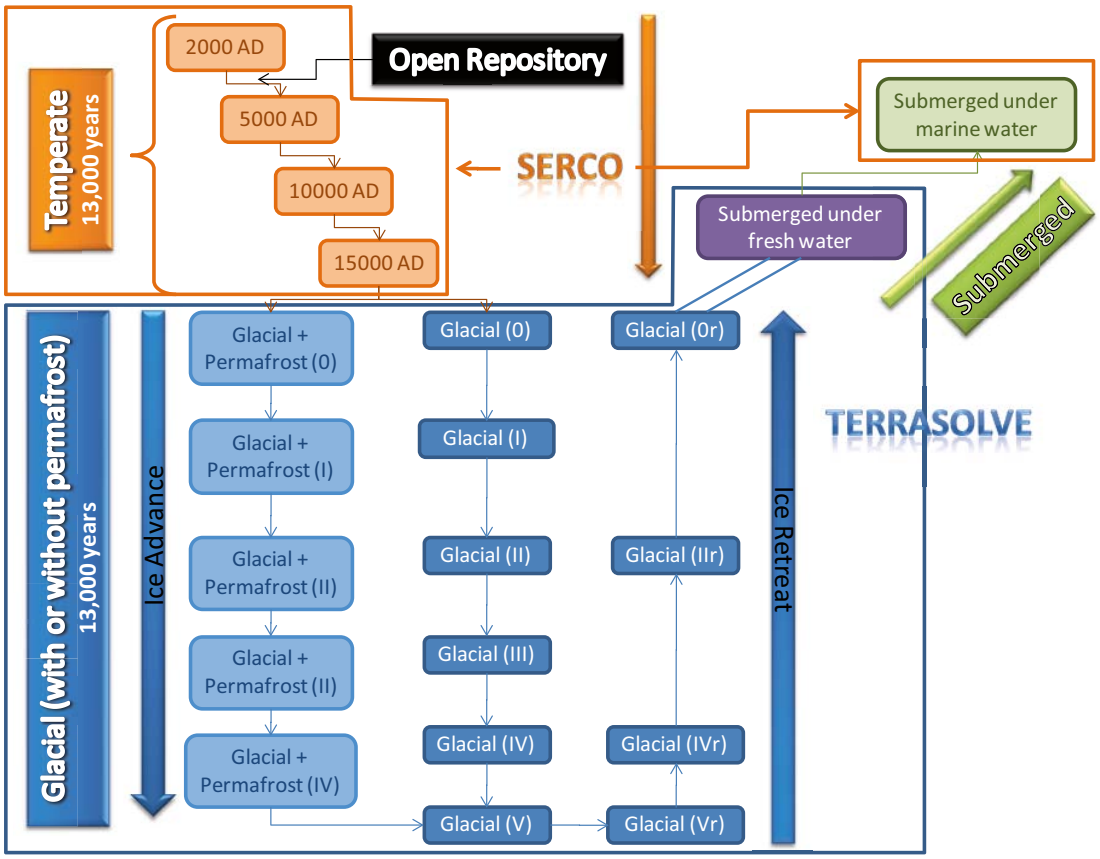

Figure 1-1. *Scheme of the different temporal periods studied here and the hydrogeological teams that have provided the data. The temperate period is simulated (Serco) to last 13,000 years from the present day (2000 AD to 15,000 AD) including the excavation and the operational stage (orange colours). The glacial cycle simulated for Laxemar (Terrasolve; blue colours) compromise approximately 13,000 years between the first ice front passage until the site once again becomes ice free, however sub-merged beneath a fresh water lake. Finally a period where the site is submerged under marine waters is considered (green colours).*

1.3 Approach

The methodology of the calculations is explained in Chapter 3, and summarized in Figure 1-2. In short, the general strategy to evaluate groundwater compositions in SR-Site consists of combining the results from the hydrological flow models (provided by SKB and performed by TerraSolve and Serco) with mixing and reaction models. Based on the understanding of the palaeohydrogeological history of the sites (which assumes the presence of different water mixing events due to the input of different reference waters over the time), the hydrogeological models provide the mass fractions of these reference waters for each point in the discretised volume of the whole area. Using these data as mixing proportions of the end member waters and knowing the chemical composition of these reference waters, the final groundwater compositions have been modelled through mixing of groundwaters and chemical reactions with fracture-filling and rock-forming minerals (Figure 1-2).

The input data used in the hydrogeochemical calculations are:

- hydrogeological data provided by Serco, TerraSolve and Computed Aided Fluid Engineering AB and SF GeoLogic AB,
- chemical composition of the reference waters,
- definition of reactions between aqueous species and mineral equilibria.

Consequently, the most relevant data needed for this investigation are the geological structure of the site, the hydrogeological data and associated conceptual assumptions, the hydrogeochemical and mineralogical data from the Laxemar site descriptive model (SDM) work /Laaksoharju et al. 2009/, and the thermodynamic data used in the geochemical calculations.

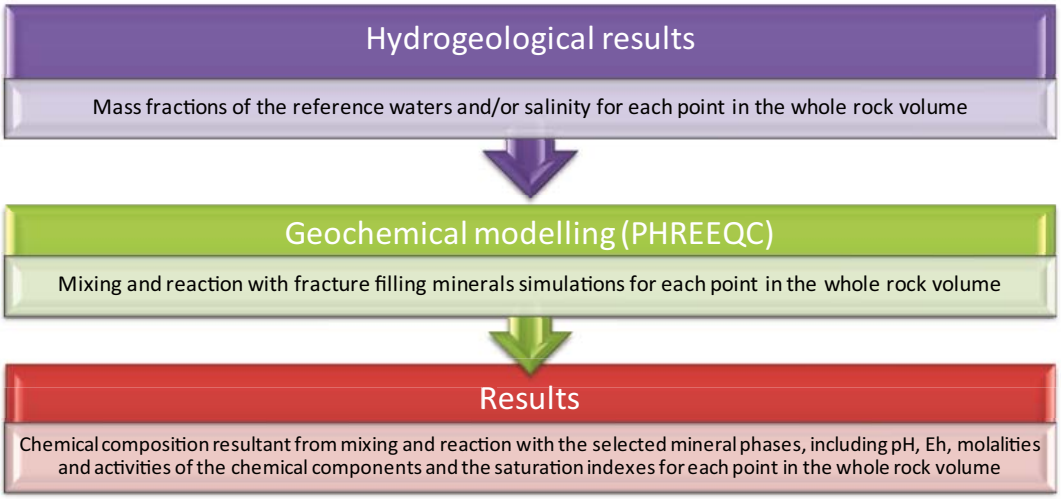

Figure 1-2. *Steps followed for the geochemical simulations.*

Hydrogeological models are constructed to simulate complex three-dimensional geological conditions, including main hydraulic conductor domains and heterogeneous hydraulic properties based on the upscaling of discrete fracture network models. Such hydrogeological models solve the groundwater flow equation (accounting for variable density driven flow) and the classical advection-dispersion transport equation. Also, matrix diffusion is accounted for. This not only allows accounting for density driven flow. The most important impact is on the exchange of solutes between the porewater in the matrix and the mobile water in the fractures.

The hydrogeochemical study of the Laxemar groundwaters has confirmed the existence of at least five reference waters: an old brine (Deep Saline), an old dilute meteoric water (Old Meteoric), a glacial melt-water (Glacial), a marine water (ancient Littorina Sea), and a modern meteoric water (Altered Meteoric) /Laaksoharju et al. 2009/. Hydrogeological model results have provided groundwater composition as mass fractions of these reference waters (in the case of the temperate and submerged under marine waters periods), or salinities (in the case of the operation period and the glacial and periglacial periods). When salinities have been provided (TerraSolve and Computer-Aided Fluid Engineering), they have been transformed to end-members proportions. These spatial and time distributions of the mixing proportions of the end-member groundwaters have been used as inputs for hydrogeochemical calculations. The chemical composition of end-member waters is known from the SDM reports /Laaksoharju et al. 2008a, 2009, Gimeno et al. 2008, 2009/, although they needed adjustments for this task.

Groundwater compositions have been simulated using PHREEQC /Parkhurst and Appelo 1999/ by mixing of the reference groundwaters. Finally, hydrogeochemical speciation and geochemical water-rock interaction calculations have been done in all the selected nodes and selected times, in order to evaluate the hydrogeochemical conditions of the sites.The simulated groundwater compositions have been assumed to be in thermodynamic equilibrium with respect to calcite, quartz, hydroxyapatite and Fe(III) oxyhydroxides (haematite). However, other geochemical assumptions have been evaluated, such as equilibrium with respect to amorphous Fe(II) monosulphides instead of haematite, and uncoupling the redox reactions between S(VI) and S(–II) species.

1.4 Key geochemical parameters in the analysis of the safety assessment of the candidate repository

In order to assess the suitability of the future repository, a series of geochemical “safety functions” have been defined as requirements of the groundwater composition (Figure 1-3). The primary safety function of the KBS-3 concept is to completely isolate the spent nuclear fuel within copper canisters over the entire assessment period /SKB 2011/. Should a canister be damaged, the secondary safety function is to retard any contaminant released from the canisters. For the part of the geosphere surrounding the repository, most of the function indicators concern the composition of groundwaters in the fracture network; several of the groundwater characteristics are essential for providing a chemically favourable environment for the repository.

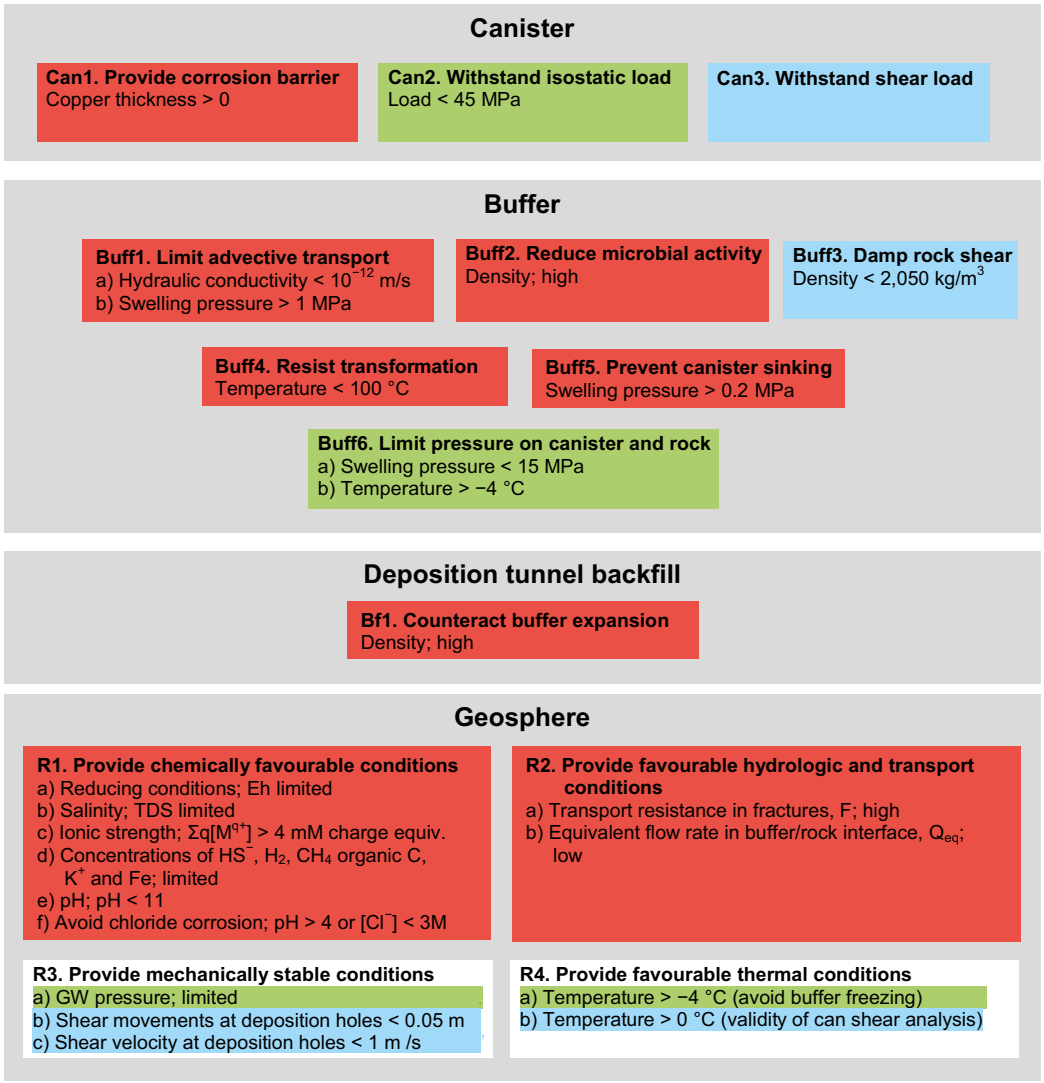

Figure 1-3. *Safety functions (bold), safety function indicators and safety function indicator criteria. When quantitative criteria cannot be given, terms like "high", "low" and "limited" are used to indicate favourable values of the safety function indicators. The colour coding shows how the functions contribute to the canister safety functions Can1 (red; provide corrosion barrier), Can2 (green; withstand isostatic load) or Can3 (blue; withstand shear load), see /SKB 2011/.*

1.4.1 Salinity and concentration of solutes

The salinity of the groundwater should be neither too high nor too low. Groundwaters of high ionic strengths would have a negative impact on the buffer and backfill properties, in particular on the backfill swelling pressure and hydraulic conductivity. In general, ionic strengths corresponding to NaCl concentrations of approximately 1.2 mol/L are a safe limit for maintaining backfill properties, whereas the corresponding limit for the buffer is around 1.7 mol/L /SKB 2006a/. The limit of tolerable ionic strength is, however, strongly dependent on material properties, in particular for the backfill.

Groundwater salinities in the Laxemar area are mainly controlled by the concentration of chloride, sodium and calcium. Chloride is not listed among the safety function indicator criteria, but it is used when selecting radionuclide transport properties (sorption coefficients). It behaves almost conservatively as it rarely participates in chemical reactions between solutes and the solid phases. The distribution of salinity may initially be affected, during repository operation, by perturbations in the hydraulic conditions, although it is thought to be negligible /Auque et al. 2006, Svensson and Follin 2010/. Salinities during the first temperate period following repository closure will remain limited, ensuring that the swelling properties of the buffer and backfill are not negatively affected. Afterwards, groundwaters will be affected by increasing amounts of waters of meteoric origin, which will produce a gradual decrease of salinity, especially in the upper part of the modelled domain.

The concentration of cations is important because their presence decreases the stability of colloids. In groundwaters that are too dilute, colloids might enhance the transport of radionuclides. In addition, as the buffer swells into fractures, montmorillonite colloids may be transported away by dilute groundwaters. The criterion for the safety function indicator is $2\cdot\Sigma[M^{2+}] + \Sigma[M^{+}] = \Sigma qM^{q+} \geq 0.002–0.004$ mol/L, where $\Sigma[M^{2+}]$ and $\Sigma[M^{+}]$ are the summation of the concentrations of the divalent and monovalent cationic species, respectively. In this way, available experimental data suggest that montmorillonite colloids are not stable at concentrations above this limit.

Calcium participates in water-rock interactions such as calcite dissolution and precipitation, feldspars weathering and cation exchange. However, deep saline groundwaters at the Laxemar site are quite rich in calcium and they are in equilibrium with gypsum /Gimeno et al. 2009/. Moreover examination of the groundwaters at depths below 100 m shows that calcium concentrations are also significantly controlled by mixing processes. The other major divalent cation is magnesium, which is a tracer of marine inputs in the studied systems and, therefore, is basically controlled by mixing when marine intrusions occur /Laaksoharju et al. 2008a, 2009/ despite it is also modulated by cation exchange /Gimeno et al. 2009/. Magnesium is also regulated in granitic groundwaters by the precipitation and dissolution of chlorite, a mineral that may have a wide range of compositions. In general, magnessium concentrations in groundwaters are much lower than those of calcium. As a consequence of the low solubility of chlorites and the uncertainty in the composition of this mineral, the modelling of magnessium concentrations is much more uncertain than that of calcium. Potassium is other of the main cations but it will be discussed as a detrimental agent in the following section.

1.4.2 Concentration of detrimental agents: sulphide, iron and potassium

Regarding canister corrosion, it is desirable to have low groundwater concentrations of agents detrimental to the long-term stability of the buffer and backfill, in particular sulphide. On the other hand, it is desirable to have low iron and potassium concentrations to the long-term stability of the buffer /SKB 2006b/.

Potassium concentrations are generally low in the groundwaters sampled at Laxemar. Solubility control by sericite or illitic clays has been proposed as a mechanism controlling the maximum concentrations of potassium /Nordstrom et al. 1989/, but ion-exchange cannot be ruled out. Even if the exact mechanism is not known, all available groundwater data indicate that the increased infiltration of waters of meteoric origin will not increase present potassium concentrations due to their low contents in this element /Gimeno et al. 2009/. In the mixing models presented later in this study, potassium has been treated as a conservative aqueous species.

Sulphide concentrations are variable in Laxemar groundwaters, from below the detection limit ($\approx 10^{-7}$ mol/L) to about $8\cdot10^{-5}$ mol/L. Under oxidizing conditions, sulphide is quickly oxidized to sulphate whereas under reducing conditions the common presence of dissolved Fe(II) facilitates the precipitation of Fe(II)-monosulphides, thus keeping low maximum sulphide concentrations[2]. In most Laxemar groundwaters, Fe(II) concentrations are lower than 10^{-6} mol/L, which sets the maximum S(–II) concentrations in the range 10^{-4}–10^{-5} mol/L /Gimeno et al. 2009/.

The concentration of Fe(II) is basically regulated by the slow dissolution of Fe(II)-silicates, such as chlorite and biotite, the precipitation of Fe(II)-sulphides and also by redox reactions. Concentrations of Fe(III) aqueous species are, in general, negligible in granitic groundwaters, as Fe(III)-oxyhydroxides are quite insoluble and precipitate quickly. Moreover, under the reducing conditions identified in the groundwaters of Laxemar, haematite has been found in fracture fillings at all examined depths /Drake and Tullborg 2009, Gimeno et al. 2009/. Thus, apart from assuming the equilibrium with FeS(am), equilibrium with respect to haematite and redox equilibrium between Fe(II) and Fe(III)-oxyhydroxides are assumed (which is also controlled by pH) as an important variant case in the geochemical calculations.

[2] The inorganic reductive dissolution of iron oxyhydroxides by dissolved sulphide could also diminish the amount of dissolved sulphide. It is a kinetically fast process that proceeds via the oxidation of dissolved sulphide at the mineral surface, followed by the release of the produced Fe(II) to solution (see /Gimeno et al. 2009/ and references therein).

1.4.3 pH values

Regarding pH, near-neutral values are preferred for buffer and backfill stability /SKB 2006b/. This is fulfilled by all natural groundwaters in the Laxemar area. However, two events can give rise to higher pH values: contamination of groundwater by concrete and other materials during the construction period, and the input of glacial melt-waters during the glacial and periglacial periods. The criterion for the safety function indicator R1e is that pH should always remain lower than 11.

A further requirement is that the combination of low pH values (< 4) and high chloride concentrations (> 3 mol/L) should be avoided in order to exclude chloride corrosion of the canister.

1.4.4 Sulphate and phosphate concentrations

Sulphate /Geipel et al. 1996/ and phosphate /Sanding and Bruno 1992/ aqueous species may complex significant fractions of uranyl cations. Soluble complexes not only limit sorption, but often result in enhanced transport of uranium /Choppin and Wong 1998, Gabriel et al. 1998, McCarthy et al. 1998/. Sulphate is also important when determining solubility limits for radium. In the present study, dissolved sulphate is computed considering (1) the proposed mixing fractions of the reference waters, and (2) the redox stability of the S(VI) aqueous species (e.g. presence or absence of sulphate reducing agents). In the case of phosphate, the computed concentrations have been asumed to be in equilibrium with hydroxyapatite.

1.4.5 Redox conditions

A fundamental safety requirement is that of reducing conditions. One of the necessary conditions is the absence of dissolved oxygen, because any evidence of its presence would indicate that no reducing conditions have been reached. The presence of reducing agents that react quickly with oxygen, such as Fe(II) and sulphide is sufficient to indicate anoxic conditions. Other proxies of redox conditions, such as negative Eh, are not always well defined or easily measured and thus less practical as indicators. Nevertheless, the redox potential is useful as a measure of the availability of all kinetically active oxidizing species in a groundwater.

Anoxic conditions minimise the canister corrosion. Furthermore, should a canister be penetrated by groundwaters, reducing conditions are essential to ensure a low dissolution rate of the fuel matrix, low solubilities of several radioelements and, for some elements, also high sorption affinities for buffer, backfill and host rock materials.

The hydrological model of the site predicts an increase with time of the proportion of waters of meteoric origin at repository depth during the temperate period. This evolution is not expected to change the reducing character of the groundwater, as infiltrating meteoric waters become depleted of oxygen by microbial activity in the soil layers or after some tens of metres along fractures in the bedrock, as observed in the natural system during the SDM studies /Laaksoharju et al. 2009/. Evidence from the Äspö laboratory and other Swedish sites indicate that anoxic conditions prevail in the host rock even at a short distance from tunnel walls or the ground surface.

However, the potential penetration of oxygen-rich meltwaters to repository depth during the reference glacial cycle could drastically alter the safe reducing conditions. This possibility is not examined in the present work.

1.4.6 Colloids and other geochemical parameters

The evolution of colloids and the concentration of other geochemical components such as $H_2(g)$, $CH_4(g)$, NH_4^+, NO_2^-, CH_3COO^-, TOC and DOC, have not been included in our calculations. This apparently heterogeneous group of parameters include components for which either the available information is insufficient for a precise quantitative evaluation of their future evolution or cannot be modelled using the same methodology as the rest of the geochemical parameters in this work. Most of these components are intimately related to microbial activity or being conditioned by different redox processes. This fact makes their evaluation a difficult task due both to the their intrinsic complexity and to the limited present knowledge of microbial processes in the groundwaters of crystalline systems.

Pernicious effects of these components are mainly related to canister corrosion as most are corroding agents or can enhance contents of such agents through different metabolic processes. This is the case of dissolved sulphide, whose content in low temperature environments depends on the activity of sulphate reducing bacteria (SRB). This activity is in turn conditioned by the amount and availability of suitable substrates which, in the case of SRBs, include dissolved organic carbon, acetate, methane and molecular hydrogen. Therefore, an assessment of the potential amounts of these components over the future evolution of the groundwater system at Laxemar has been performed and is presented below.

Other parameters such as nitrite, ammonia and acetate are also metabolic by-products of different microbial processes and they may enhance some specific types of corrosion, like stress corrosion cracking (SCC). This type of corrosion may affect copper and copper alloys and is considered to be a potential canister corrosion failure mechanism. The activation of SCC requires that a susceptible metal be exposed to a large enough tensile stress in the presence of an SCC agent like the aforementioned nitrite, ammonia or acetate (e.g. /King 2007/ and references therein). A substantial experimental work has been done to assess copper SCC in nitrite-, ammonia- and acetate-containing environments, both at room temperature /Arilahti et al. 2000, Ikeda and Litke 2000, Ikeda et al. 2004, Betova et al. 2005, Litke and Ikeda 2006/ and at elevated temperature (100–130°C; /Kinnunen 2006, Ikeda and Litke 2007/). Overall, results indicate that copper SCC susceptibility decreases with decreasing concentrationsof SCC agents. Furthermore, SCC susceptibility appears to decrease with increasing chloride concentration and temperature (the inhibiting effect of chloride on SCC susceptibility also appears to be enhanced at elevated temperatures; /King 2007/).

In the Swedish and Finnish concepts, SCC is considered highly unlikely in repository conditions because of the low probability of the simultaneous occurrence of SCC-promoting factors in the repository /King et al. 2001, Posiva 2006, SKB 2006c/. However, an evaluation of the likely amounts of SCC agents (nitrite, ammonia and acetate) during the evolution of the groundwater system at Laxemar has also been performed.

Finally, another important component, difficult to include in the predictive modelling, is the concentration of colloids (particles with diameters between 1 and 1,000 nm). Colloids are thermodynamically metastable and consequently their occurrence and stability cannot be approached from an equilibrium point of view /SKB 2010/. In groundwaters, natural colloids form by the erosion of rock-forming minerals and alteration products, the precipitation of mineral oxides and the degradation of organic material[3]. In addition, the bentonite barrier may represent an additional source of colloids (bentonite is in itself colloidal) under certain conditions, mainly through interaction with dilute glacial meltwaters.

There is a fairly large body of literature on the colloidal contents in the investigated sites and in other groundwater systems. Also, bentonite colloid generation, stability and transport in dilute waters mimicking glacial water have been investigated in a number of projects (such as SKB's Colloid Dipole Project and SKB's Colloid Transport Project) and research articles (see review by /Wold 2010/). As the concentration of natural and bentonite-derived colloids should remain low to avoid transport of radionuclides by them, the available information has been reviewed in order to estimate colloidal contents during the possible evolution of the Laxemar site.

All the above parameters will be analysed separately from the rest of the calculations and the results presented in Chapter 5.

1.5 Report Layout

Considering the main objectives of this work, the report has been structured starting with the presentation of the site with a summary of the main hydrogeochemical features and the processes controlling their evolution (Chapter 2) with special emphasis on the behaviour of the geochemical parameters related to the main geochemical safety functions considered for the integrity of the repository (summarised in Section 1.4). This will help to understand the different simulations performed later on.

[3] Viruses (2 to 80 nm) and bacteria (200 nm to several microns) can be considered a special group of colloids although, presently, there are little data to assess the importance of these types of biogenic colloids for performance assessment purposes.

Chapter 3 presents the methodology followed to perform the geochemical calculations, including the initial step of coupling the hydrogeological results as input data to the geochemical module. After defining what kind of calculations have been done and why, Chapter 4 shows the main results obtained for each of the studied parameters over the different time periods analysed. Chapter 5 deals with a set of parameters of geochemical interest that have not been included in the calculations because they can not be treated in the same way. Chapter 6 summarises the main conclusions of this work. Finally a series of appendices has been added to complement the information shown in this report.

2 Hydrogeochemical conceptual model for the Laxemar site

2.1 Introduction

From the site descriptive model (SDM) a hydrogeochemical conceptual understanding of the Laxemar-Simpevarp area was described in /Gimeno et al. 2009, Laaksoharju et al. 2009/. Explorative analyses and modelling of groundwater chemistry data measured in samples from cored boreholes, percussion boreholes, porewater from bedrock and shallow soil boreholes, have been used to evaluate the hydrogeochemical conditions at the site in terms of origin of the groundwater and the processes that control their chemical composition. The effects from changing climate (and shoreline movement) on the groundwater and matrix porewater compositions and on the fracture filling minerals have also been determined /Laaksoharju et al. 2009/.

Although the data set is rather limited, the results provide an overall understanding of the site.

2.2 Present status of hydrogeochemical understanding at the Laxemar site

The predominant rock-types in this area are granite and quartz-monzodiorite. Most of them were formed between 1,900 and 1,800 Ma ago and then suffering both ductile and brittle deformation. The majority of the fracture systems that are water conducting today were activated or reactivated during the Palaeozoic and have probably been water conducting pathways ever since /Tullborg et al. 2008/.

The complex groundwater evolutionary patterns at Laxemar-Simpevarp are a result of many factors such as: a) past changes in hydrogeology related to glaciation/deglaciation, land uplift and cyclic marine/lake water regressions/transgressions (Figure 2-1; Section 2.2.1), b) the present day topography and proximity to the Baltic Sea coastline, and c) organic or inorganic changes of the groundwater composition caused by microbial or water-rock interaction processes /Laaksoharju et al. 2009/. Thus, the hydrogeochemical evolution of groundwaters flowing through fracture zones results from hydrodynamic mechanisms, transport processes and water-rock interactions driven by past and present changes in the climate that have induced the input of different recharge waters at least since the last glaciation (e.g. /Laaksoharju and Wallin 1997, Laaksoharju et al. 1999, 2008b, Pitkänen et al. 1999, 2004, Waber and Smellie 2008, Waber et al. 2009, Gimeno et al. 2009/).

A summary of the palaeohydrogeological conceptual model is presented next (Section 2.2.1), and then a thourough description of the main geochemical processes driven by these changes and affected by different chemical reactions due to water rock interaction and/or microbial activity processes is shown.

2.2.1 Present palaeohydrological conceptual model

Mixing has been mainly induced by the alternating or simultaneous input, into the upper part of the crystalline basement, of glacial melt-waters and meteoric waters during the succession of glacial and interglacial periods over the Quaternary period. Moreover, these waters (or their mixtures) have mixed with the saline groundwaters that occupy most parts of the deeper basement and which have been geochemically modified in the crystalline bedrock (covered by several kilometres of sediments) over hundreds of millions of years mainly by water-rock interaction /Smellie et al. 2008/.

The conceptual model for the palaeohydrogeological evolution at Laxemar has changed with respect to the one used for the SR-Can. The SDM-Site Laxemar hydrogeochemical investigations /Laaksoharju et al. 2009/ have showed that changes in the groundwater chemistry during the Quaternary were not restricted to post glacial time. There are groundwater and porewater evidences that indicate the existence of an old, warm-climate derived meteoric water component, at depths higher than 600 m. This water would have infiltrated during climatic periods with temperature maxima prior to the last glaciation and during the Holocene. Without recognising this older component, the hydrogeochemistry (and hydrogeology) cannot be adequately explained /Laaksoharju et al. 2009/. Therefore, in this

new version of the hydrogeological model, they include a fifth reference water (not used in SR-Can calculations) which represents this old dilute water (see Section 3.2.2.3). However, the conceptual model for the period since the last deglaciation, represented in Figure 2-1, remains unaltered. The Holocene evolution from the last glacial period has influenced most of the groundwater chemistry in the Laxemar-Simpevarp area, above 600 m depth.

During the most recent post-glacial period, when the continental ice melted and retreated from the Laxemar-Simpevarp area around 12,000 BC, glacial meltwater was hydraulically injected under considerable head pressure into the bedrock (Figure 2-1a). The penetration depth is not accurately known but, according to hydraulic simulations, depths exceeding several hundred metres are possible. Although the last deglaciation of the Laxemar-Simpevarp region coincided with the end of the Yoldia period (Figure 2-1b), there are no signs of Yoldia Sea water in the bedrock.

The Ancylus Lake (years 8800 to 7500 BC) was developed after the deglaciation (Figure 2-1c). This period was followed by the brackish Littorina Sea (since the year 7500 BC to present, Baltic Sea). During the Littorina Sea stage (Figure 2-1d), the salinity was considerably higher than at present, reaching a maximum of about 15‰ in the period 4500 to 3000 BC (see the review by /Gimeno et al. 2008/). Dense brackish sea water from the Littorina Sea initially penetrated most of the rock in the Simpevarp subarea and, probably, a more diluted variety penetrated the eastern and southeastern zones of the bedrock at Laxemar[4].

This resulted in a density-driven intrusion that affected the groundwater in the more conductive parts of the bedrock. In the areas not covered by the Littorina Sea water (most of the Laxemar subarea), infiltration of meteoric water began around the year 12,000 BC forming a freshwater layer on top of the older saline water.

Finally, as a result of post-glacial rebound and uplift less than 1,000 years ago, the submerged area emerged from the sea, allowing modern meteoric waters penetrating into the upper part of the groundwater system (Figure 2-1e). However, this has been limited, and consequently post glacial water dominates at depths of about 20–300 m and remnants of glacial water still dominate within the approximate 300–600 m depth interval /Laaksoharju et al. 2009/. Additionally the Littorina signature was diluted in the bedrock as a result of meteoric water infiltration driven by land uplift.

Present regional groundwater flow in the Laxemar subarea is driven by topography with a general gradient from the high elevated areas (in the west) to the Baltic Sea (in the east). The flow regimes are considered local and believed to extend down to depths of approximately 600 to 1,000 m depending on local topography. The flow pattern is largely governed by the connections between deformation zones in the region. The topography also results in localised areas of recharge/discharge which represent groundwater circulation cells of varying depth and extent, and therefore of varying groundwater ages.

Close to the Baltic Sea coastline in the Simpevarp subarea, where topographical gradient is negligible, groundwater penetration to depth will be less marked. In contrast, the Laxemar subarea is characterised by higher topographic gradients, resulting in a much more dynamic groundwater circulation. The effects of this advective fluid flow appears to extend to at least 500 to 600 m depth in most boreholes. At these depths and below there is a change in the bedrock hydrogeological properties and low flow conditions and weak hydraulic gradients begin to dominate /Laaksoharju et al. 2009/. There is a diminishing effect of groundwater circulation down to a depth of about 1,000 m, and below about 1,200 m the groundwater is effectively stagnant /Rhén and Hartley 2009/.

Overall, the Holocene evolution has influenced most of the groundwater chemistry in the Laxemar-Simpevarp area, but above 600 m this is not restricted to post glacial time. At these depths the hydrochemistry of the Laxemar-Simpevarp has been also affected by an older groundwater component /Laaksoharju et al. 2009/. Present groundwaters, therefore, are a result of mixing and reactions over a long period of geological time. Furthermore, the interfaces between different groundwater types are not sharp and reflect the anisotropy in the hydrostructural properties of the bedrock.

[4] The Littorina period affected in a different way the Laxemar and Forsmark areas. Whereas the Forsmark area was under marine waters for around 7,000 years and, as a consequence, these waters percolated deep down into the basement, the Laxemar-Simpevarp area was only partly covered (with maximum depths of around only 15 m, Figure 2-1d) and only for a short period of time /Laaksoharju et al. 2008a, 2009/.

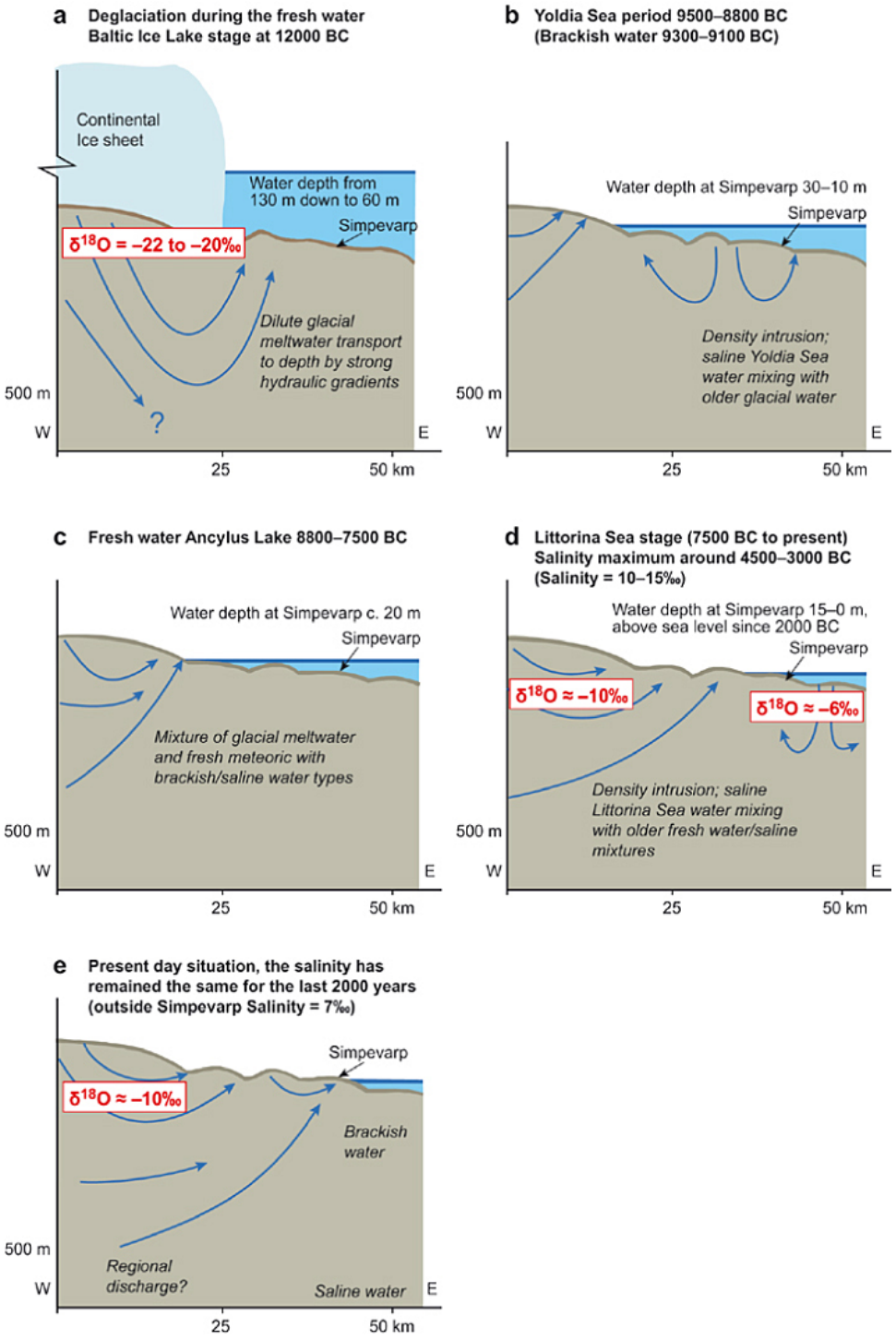

Figure 2-1. *Conceptual model of the period since the last deglaciationl for the Laxemar-Simpevarp area. The different stages are: a) deglaciation and the development of the Baltic Ice Lake (> 12,000 BC), b) the Yoldia Sea stage (9500 to 8800 BC), c) freshwater Ancylus Lake between 8800 to 6500 BC, d) minor portions of Littorina Sea water introduced by density intrusion between 7500 BC to 0 AD, and e) the present day situation. Blue arrows indicate possible groundwater flow pattern /Laaksoharju et al. 2009/.*

2.2.2 Groundwater evolution: geochemical processes

The main processes determining the overall geochemical evolution of Laxemar-Simpevarp groundwater systems are mixing and reaction processes. As stated in the previous section, mixing has taken place between different types of waters (reference waters or end members) over time, making discrimination of the main influences complex. In addition to mixing processes, different chemical reactions have taken place in the system due to the water rock interaction processes and/or microbial activity (e.g. aluminosilicate and carbonate dissolution/precipitation, cation exchange, gypsum dissolution, main redox reactions, etc). Some elements (Cl or $\delta^{18}O$) behave conservatively in groundwater while others are affected by chemical reactions to differing degrees, especially the redox sensitive elements.

Major groundwater characteristics and residence times allow the identification of different hydrochemical intervals in the Laxemar zone:

- The 0–20 m depth interval (overburden) is hydrogeologically active (residence times in the order of years to decades) and dominated by modern recharge meteoric water or Fresh groundwater (< 200 mg/L Cl; $5.6 \cdot 10^{-3}$ mol/L) of Na-Ca-HCO_3 (SO_4) type showing large variations in pH and redox conditions.
- The 20–250 m depth interval is dominated by Fresh–Mixed Brackish–Brackish Glacial groundwaters of Na-Ca-HCO_3 (SO_4) to Na-Ca-Cl-HCO_3 type, showing a transition to stable reducing conditions with increasing depth. The residence times of the groundwaters are in the order of decades to several thousands of years.
- The 250–600 m depth interval is dominated by Brackish Glacial–Brackish Non-marine– Transition groundwaters of Na-Ca-Cl-(HCO_3) type. Redox conditions are reducing with low Eh values (–245 to –303 mV). The significant fractions of glacial waters in this depth interval, and the equally significant increase of non-marine groundwaters with depth, indicates that groundwaters older than the last deglaciation at around 14,000 years ago are becoming increasingly important.
- The 600–1,200 m depth interval is dominated by Brackish Non-marine–Saline (±Brackish Glacial and Transition) groundwater of Na-Ca Cl-(SO_4) to Ca-Na Cl-(SO_4) type. These groundwaters show very low magnesium contents and are clearly reducing (–220 to –265 mV). Interpretation of chlorine-36 measurements suggests long residence times of hundreds of thousands of years. This is hydrogeologically supported by very low flows to stagnant conditions.

Overall, two main domains can be differentiated in the hydrochemical evolution of the groundwater system: the overburden (near surface groundwaters) and the bedrock (deeper groundwater system). Geochemical processes in both domains are decribed below.

2.2.2.1 Near surface groundwaters (overburden)

The overburden (down to 20 m depth) is hydrogeochemically dominated by water-rock interactions between the recharging meteoric water and the soil, till sediments and bedrock (Figure 2-2). Thus, the compositional evolution of the near surface and shallow groundwaters is mainly controlled by the existence of weathering reactions.

Typical weathering reactions in the subsurface systems are mainly triggered by biogenic CO_2 input derived from organic matter decay (e.g. plant debris) and root respiration. This input of CO_2 promotes a pH decrease and a CO_2 partial pressure increase in the waters, which may favour the dissolution of carbonate or aluminosilicate mineral phases if present in the system (Figure 2-2).

In carbonate or aluminosilicate dissolution reactions, cations (Na, Ca, Mg, K, etc), silica and bicarbonate are released (Figure 2-2). The intensity of these weathering reactions during infiltration of the surface waters in the overburden is mainly conditioned by the input of atmospheric or biogenic CO_2.

Due to the variable influence of this CO_2 input on the reactions in the overburden, alkalinity, fluoride, major cations, silica and pH values in this part of the system show the greatest variability among the Laxemar-Simpevarp groundwaters. Na, K and Mg concentrations display a clear increase with the weathering intensity, which also causes an increase in the alkalinity production. The incongruent dissolution of aluminosilicates (mainly plagioclase and mafic minerals such as biotite and hornblende) seems to be generally the most important process in their control. However, the partial incorporation of

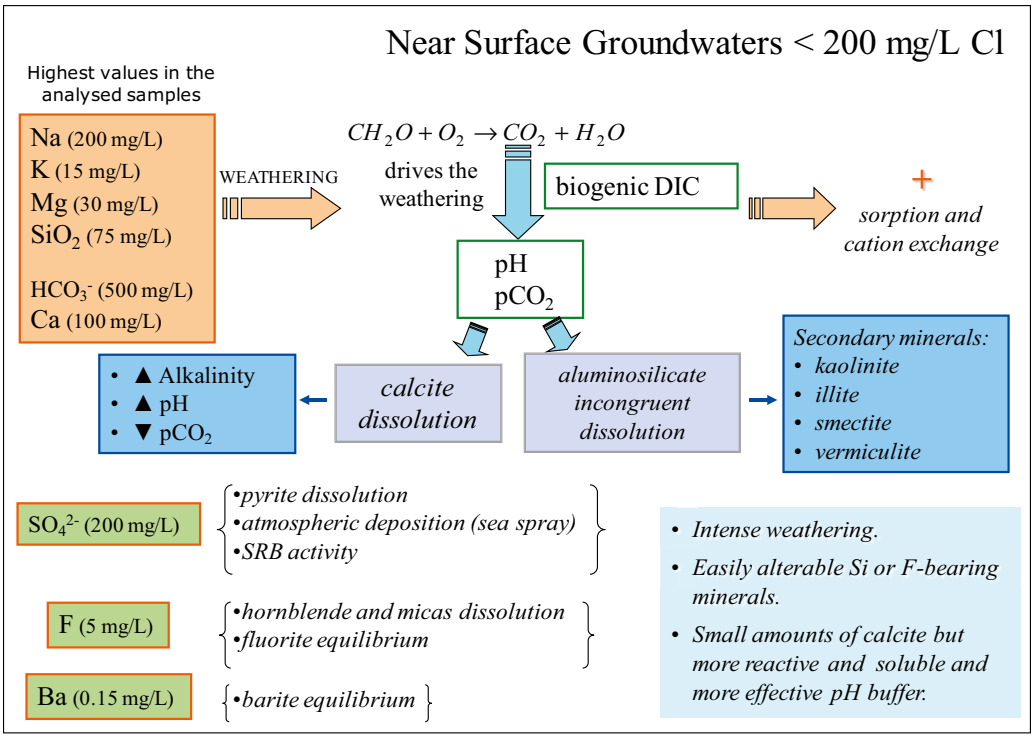

Figure 2-2. *The evolution of the near surface groundwater in the Laxemar-Simpevarp area where typical weathering reactions control the hydrochemistry; SRB = Sulphate-Reducing Bacteria. Concentration data on the left correspond to the maximum contents found in the near surface groundwaters from Laxemar. Processes involved in their control are also indicated (taken from /Gimeno et al. 2009/).*

these cations into secondary clays (e.g. kaolinite, illite), their use as nutrients for plants (e.g. Mg, K) or their participation in cation exchange processes also play a role in modulating their concentrations in the near surface groundwaters.

Dissolved calcium in the fresh near-surface groundwaters shows maximum concentrations of about 100 mg/L ($2.5 \cdot 10^{-3}$ mol/L). Calcite and aluminosilicate weathering reactions (hornblende and plagioclase dissolution), cation exchange reactions or calcite and fluorite equilibrium may participate in the control of this element in the near surface and shallow groundwaters from Laxemar-Simpevarp (Figure 2-2). Bicarbonate reaches maximum concentrations around 500 mg/L ($8.2 \cdot 10^{-3}$ mol/L) and calcite equilibrium is only attained for the waters with the largest bicarbonate contents. Overall, calcite appears to contribute to the chemical and isotopic (C and Sr) characters of the near-surface groundwaters much more than expected from the small amounts of this mineral detected in the Laxemar-Simpevarp overburden (Figure 2-2). Thus, calcite dissolution is the main pH-buffer in the near surface groundwaters /Gimeno et al. 2009/.

Dissolved sulphate contents in the fresh, near-surface groundwaters are always below 200 mg/L ($2.1 \cdot 10^{-3}$ mol/L). Isotopic constraints ($\delta^{34}S$ values of dissolved sulphate) support an important contribution from pyrite dissolution to the dissolved sulphate pool in these waters. The effect of atmospheric deposition or the direct influence from seawater deposition (sea spray) or even the existence of sulphate reducing activity, are also supported by the range of $\delta^{34}S$ values found in some waters. Neither calcium nor strontium solubility is limited by precipitation of sulphate phases but barium appears to reach a solubility limitation (barite) in these near-surface groundwaters, also contributing to modulate the dissolved sulphate concentrations.

As indicated above, higher values and variability of silica and fluoride concentrations have been found in the near-surface groundwaters of Laxemar-Simpevarp compared with other systems (e.g. Forsmark). This would indicate a more important presence of easily alterable silica and fluoride-bearing minerals, and/or a more intense weathering in the Laxemar-Simpevarp overburden. Dissolved fluoride is mainly controlled by hornblende and micas dissolution and fluorite participates as solubility-limiting phase (Figure 2-2).

Dissolved silica concentrations are mainly controlled by the incongruent dissolution of aluminosilicates (although dissolution of amorphous silica -diatoms- in marine sediments outcrops may also play an important role). Silica is released from primary minerals (mainly plagioclase and mafic minerals such as hornblende) and partially incorporated into secondary clays. The net effect of these reactions on the increase of dissolved silica concentrations depends on the type of the secondary mineral phase formed (kaolinite, illite, smectites and vermiculite). Sorption-desorption processes involving fine-grained materials in the overburden can also participate in the control of dissolved silica. Surface reactions with clays and aluminium or ferric oxyhydroxides are common processes in soils /Gimeno et al. 2009/. Chalcedony and quartz saturation indices in the near-surface groundwaters indicate that most of the waters are oversaturated with respect to both phases and they are not solubility-limiting phases for this element at these depths.

Near-surface groundwaters show large variations in redox conditions. Variable and high dissolved Fe(II), S(–II) and Mn(II) concentrations are found, indicating the presence of anoxic environments with effective reductive dissolution of Fe-silicates (e.g. Fe(II)-bearing clay minerals) or ferric and manganese oxyhydroxides (post-oxic environment) and bacterial S(–II) production (sulphidic environment) already in the very shallow parts of the system. These reducing conditions are conditioned by the biological and microbial activity developed in the overburden and mainly in the soils, where organic matter decay may lead to complete redox sequences (from oxic to post-oxic, sulphidic and methanic environments) at the centimetre to metre scale.

Different bacterial metabolic activities (IRB, SRB and MRB) may contribute to the dissolved Fe(II), S(–II) and Mn(II) concentrations. But inorganic processes are also involved in the control of these elements: reduction of ferric and manganese oxyhydroxides by dissolved sulphides as well as siderite and rhodochrosite equilibrium or iron monosulphide precipitation have been identified as the main effective processes /Gimeno et al. 2009/. In the exposed bedrock outcrops of the overburden, the reducing capacity is lower than in the soils and therefore, oxygenated waters may reach greater depths. However, the present redox front in the Laxemar subarea is located at about 15–20 m depth, in a zone affected by seasonal and annual variations in the recharge waters /Drake et al. 2009, Drake and Tullborg 2008/. Thus, the oxic conditions in the surface waters appear to change to anoxic and reducing when passing through the soil cover and/or the near surface bedrock fractures. Both degradation of organic matter and the interaction with Fe(II)-minerals would consume the dissolved oxygen in the fresh, near-surface groundwaters, promoting clear reducing conditions in the overburden and the shallowest bedrock. The possible maximum penetration depth of oxygenated groundwaters in the past (within the last 300,000 years) has been estimated to be around 80 m /Drake and Tullborg 2008/. These oxidising episodes have not been intense enough to exhaust the reducing capacity of fracture filling minerals, not even in the shallowest part of the system where chlorite and pyrite are still present.

2.2.2.2 Groundwater system

In the bedrock system (20–1,200 m depth), mixing processes progressively dominate and the effects of water-rock interactions and microbes are superimposed on mixing signatures. The temporal sequence of the deep groundwater evolution and the composition is illustrated in Figure 2-3 assuming that there is a continuous recharge and downward advective flow of groundwater to maximum depth of around 1,000 m. Below this depth, very low flow and stagnant conditions prevail and solute transport is increasingly diffusion controlled. Groundwater water-rock interaction (e.g.mineral equilibrium features) and microbiological processes, supported by mineralogical, microbial and modelling studies are shown in Figure 2-4.

$\delta^{18}O$ is a conservative component that can be used to trace mixing processes but also to distinguish between recharge waters corresponding to different (cold or warm) climates. There is a wide range of variation in $\delta^{18}O$ contents for waters down to 600 m (Figure 2-3 from –16‰ to –7‰. As also described for Forsmark, the heaviest values appear in the brackish-marine type waters (especially in Äspö). The lightest values are associated with brackish waters with a significant Glacial component, whereas fresh, mixed, transition and brackish-non marine types display intermediate values. From 900 m down, $\delta^{18}O$ values tend to increase towards the values of the Deep Saline end member (–8‰; Figure 2-3). Such enrichment has also been observed in Olkiluoto from 500 m down and in deep brines of the Canadian Shield /Gimeno et al. 2009/.

Chloride, sodium, calcium and sulphate distrubution with depth show similar trends. The concentrations of these components increase with depth (from 800–900 m depth down in the Laxemar subarea; Figure 2-3) reflecting the influence of a mixing with the Deep Saline end-member. The thermodynamic simulations performed by /Gimeno et al. 2009/ indicate that Ca and Na contents show a quasi-conservative behavior in mixed groundwaters with Cl > 0.2 mol/L. Groundwaters with Cl < 0.2 mol/L are affected by other mixing processes (mainly with Littorina, although its effects on the sodium contents are less evident than in Forsmark) and by the effects of water-rock interaction, especially in dilute groundwaters down to 500 m depth.

Potassium contents in the Laxemar subarea increase very slowly with depth showing the influence of mixing with a saline (non marine) water enriched in this component, as it happens at Forsmark and Olkiluoto. In the Simpevarp-Aspö subareas this trend is obscured as the highest potassium contents are restricted to the shallow groundwaters from Äspö with a significant Littorina contribution (Figure 2-3). Magnesium also shows the influence of old marine contributions in the Simpevarp subarea where the highest contents occur in groundwaters with a Littorina contribution down to 500 m depth. This marine contribution is lower in the Laxemar subarea (see Section 2.2.1).

Low dissolved sulphate concentrations characterise the shallow 0–400 m groundwaters in Laxemar and Simpevarp subareas.With regard to Äspö (and some waters from the Laxemar subarea), most groundwaters display higher sulphate contents down to 400 m depth) as an inherited character from the Littorina contribution.

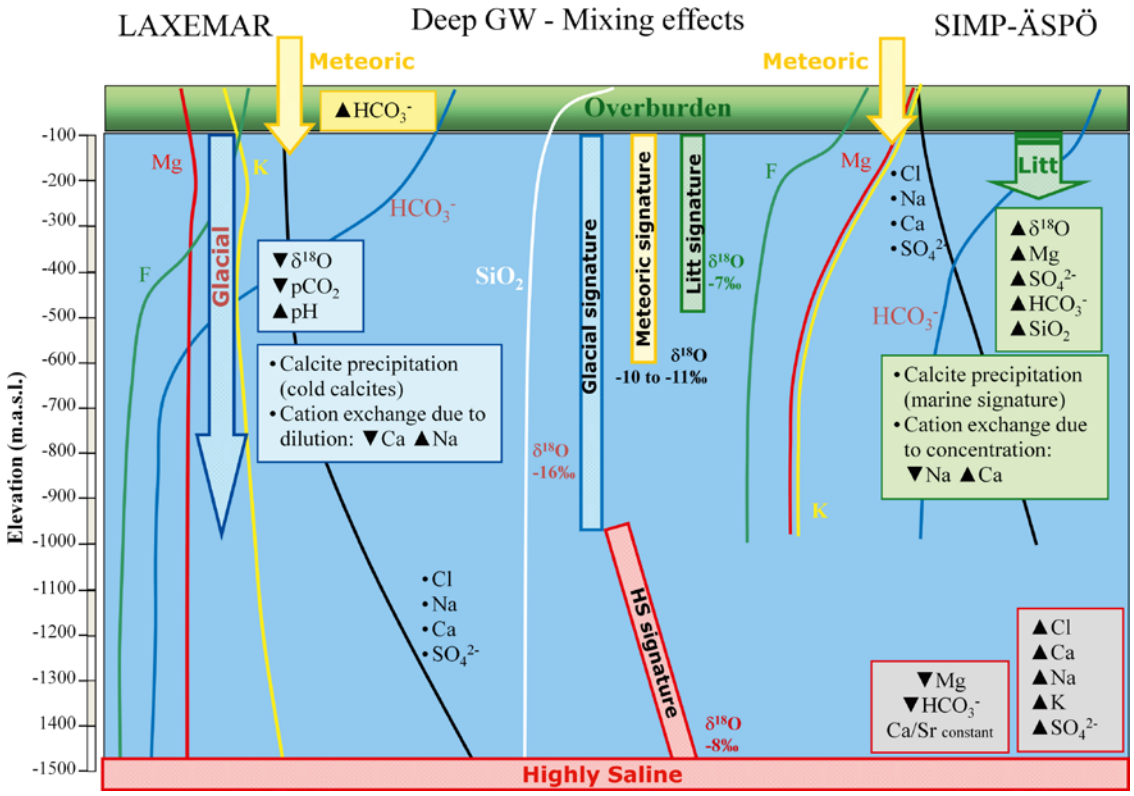

Figure 2-3. *The evolution of the groundwaters in the Laxemar (left zone) and Simpevarp-Äspö (right zone) subareas. Coloured trend lines indicate relative measured variations of different elements with depth. Also indicated are element or isotope increases/decreases associated with reactions and end-member influences. The end members are: Meteoric (yellow), Littorina (green), Glacial (blue) and Deep or Highly saline (red). The central part of the profile shows the common evolution of silica (in white) and the relative $\delta^{18}O$ variations with depth for both subareas (taken from /Gimeno et al. 2009/).*

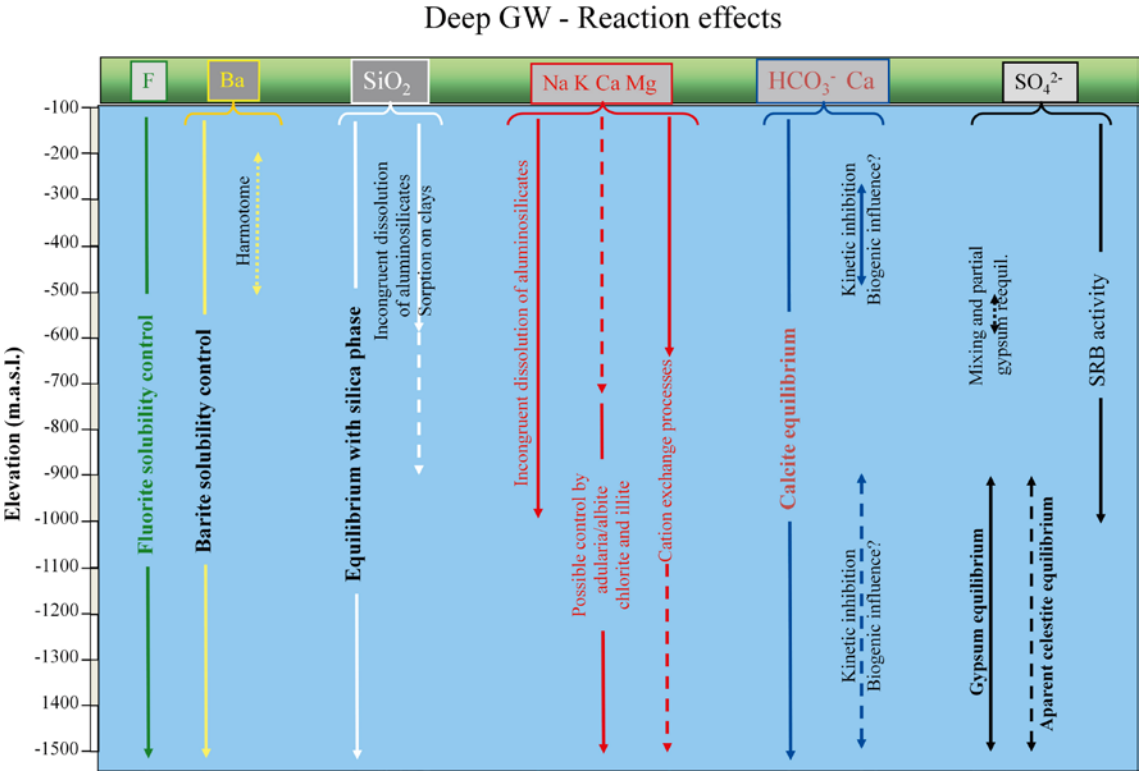

Figure 2-4. *Simplified sketch of the effects of reactions on the dissolved contents of the major components which are supported by mineralogical and microbial observations (taken from /Gimeno et al. 2009/).*

Groundwater saturation indices with respect to gypsum define a clear trend towards equilibrium with increasing depth (and chloride content; see /Gimeno et al. 2009/). The existence of this equilibrium in saline groundwaters below 900 m depth is also supported by the presence of that mineral in the fracture fillings. Apart from the influence of gypsum equilibrium, dissolved sulphate in some waters seems to be affected by other reaction processes superimposed on mixing, such as microbial sulphate reduction by SRB (Figure 2-4).

Alkalinity contents show a sharp decrease with increasing depth (Figure 2-3) and chloride concentration. High and variable values can be found down to 400 m depth at the Äspö and Laxemar subareas. In the Laxemar subarea they seem to be related to fresh and "recent" recharging groundwaters, although open-hole mixing effects are also possible in some samples. Below 500 m depth, alkalinity in the saline groundwaters drastically decreases to a narrow range of values, as also observed in the Forsmark and Olkiluoto groundwaters. This indicates the existence of a clear mineral solubility control on bicarbonate contents superimposed to the effects of mixing.

The pH-buffering capacity in Laxemar appears to be controlled by the carbonate system as calcite is the most abundant mineral (together with chlorite) in the fracture fillings /Drake and Tullborg 2009/. Most groundwaters, even at shallower levels, are in equilibrium with respect to calcite though some oversaturation situations have been detected whose origin (kinetic inhibition, biogenic influence; Figure 2-4) should be further studied (see /Gimeno et al. 2009/).

Silica contents show greater variability in the shallowest groundwaters waters (from 10 to 18 mg/L SiO_2; $1.7 \cdot 10^{-4}$ to $3.0 \cdot 10^{-4}$ mol/L) and in the brackish waters with clear Littorina contributions (from 5 to 13 mg/L SiO_2; $8.3 \cdot 10^{-5}$ to $2.2 \cdot 10^{-4}$ mol/L). Similar silica behaviour is observed in Forsmark where the brackish groundwaters have the highest silica concentrations as inherited from the significant Littorina contribution. However, deeper groundwaters show silica concentrations within a narrow range around 10 mg/L ($1.7 \cdot 10^{-4}$ mol/L; white trend in the common area of Figure 2-3). Different water-rock interaction processes related to clays (incongruent dissolution of feldspars, clay mineral transformations, silica adsorption-desorption reactions in clays, etc; Figure 2-4) can participate in

the control of dissolved silica, at least in the dilute groundwaters of recent meteoric origin. In any case, the net effect of these heterogeneous processes leads to a progressive restriction of the dissolved silica range with depth and residence time. As a consequence, most of the old groundwaters in the Laxemar-Simpevarp area are in equilibrium or near equilibrium with respect to quartz or another silica variety with similar solubility (Figure 2-4).

Fluoride contents in the shallow dilute groundwaters (< 200 m depth) of the Laxemar-Simpevarp area are very high and variable, up to 7 mg/L ($3.7 \cdot 10^{-4}$ mol/L; green trend in Figure 2-3). This is due to weathering and dissolution of F-bearing minerals such as hornblende, micas or fluorite present in the overburden or in fracture fillings at very shallow levels. As a result, waters reach fluorite saturation and fluoride derived from weathering reactions can be re-precipitating at present as fluorite in some points. Fluoride variability decreases below 200 m depth at the Simpevarp subarea and below 400 m depth at the Laxemar subarea, as salinity increases, as resulting from the fluorite solubility control. For chloride contents greater than 5,000 mg/L (0.14 mol/L), fluoride concentrations are always between 1 and 2 mg/L ($5.3 \cdot 10^{-5}$ and $1.05 \cdot 10^{-4}$ mol/L;, as in the Forsmark and Finnsjön groundwaters. Mineralogical control of fluorite is also effective during all the mixing processes affecting this system (Figure 2-4). Therefore, there is a generalised fluorite control on the dissolved fluoride in the Laxemar-Simpevarp area groundwaters (Figure 2-4). It will be superimposed on the calcite control of dissolved calcium, giving rise to a clear relationship between pH, alkalinity and calcium and fluoride contents, which will be controlled by both phases /Gimeno et al. 2009/, calcite and fluorite.

Overall, the successive mixing events have left a more or less clear imprint in the groundwater's chemistry even in the non conservative elements. Furthermore, those mixing events have promoted calcite disequilibrium situations and have catalysed the development of cation exchange processes through dilution-concentration effects, as modeled by /Gimeno et al. 2009/.

In this way, with the onset of the last glaciation/deglaciation, the input of dilute waters (meteoric or glacial meltwaters) over time, modified the pre-existing concentration profile from the surface to depth. These different mixtures promoted calcite precipitation and cation exchange due to dilution, i.e. led to a decrease of calcium and an increase of sodium in the groundwaters (Figure 2-3). The input of a marine water (Littorina Sea) into the bedrock (following several diagenetic processes during its passage through marine sediments) also promoted this type of processes. The higher density of these Littorina waters mixed with the previous dilute waters resulted in calcite precipitation and cation exchange to produce a decrease of sodium and an increase in calcium in the waters (Figure 2-3). Eventually, the mixed groundwaters become more enriched in magnesium, sulphate, bicarbonate and silica as traces of the marine influence.

According to the measured data and the modelling of the redox system /Gimeno et al. 2009/, reducing conditions currently prevail at depths greater than about 20 m where the redox front is presently located in the Laxemar subarea. The Eh values in groundwaters at depths between 100 and 700 m are clearly reducing between –200 to –310 mV.

Iron and sulphur systems are very important for the control of the redox processes in the groundwaters at Laxemar-Simpevarp. Iron (II) and (III) minerals are widely distributed in the studied systems and the presence of IRB has been documented /Hallbeck and Pedersen 2008b/. However, the bioenergetic calculations and the redox modelling approach performed from a partial equilibrium assumption for iron reduction and sulphate reduction processes /Gimeno et al. 2009/ indicate that sulphate reduction is the thermodynamically favoured process. Sulphur isotope ratios in dissolved sulphate show large variations indicating that sulphide has been produced in the system and also that microbial sulphate reduction is ongoing. Furthermore, sulphate-reducing bacteria are present at all sampled depths (although showing wide variations in population levels; /Haveman and Pedersen 2002, Hallbeck and Pedersen 2008b/).

The key role played by SRB in the stabilisation of these reducing conditions is supported by several lines of evidence including the microbially influenced $\delta^{34}S$ values found in pyrites from the Laxemar-Simpevarp area at shallow to intermediate depths, and the low $\delta^{13}C$ values found in calcites from fracture fillings from the same area /Laaksoharju et al. 2009/.

Measurements of sulphide at different sampling occasions have given very ambiguous results and a continuous sampling in conjunction with a monitoring programme has been initiated to determine the reason for these observations. One of the main conclusion is that the relatively high concentrations of Fe(II) in the groundwater system, together with the S(-II) values, might be controlled by Fe-monosulphide solubility during undisturbed conditions. However, more information is needed prior to any future detailed interpretation and, therefore, the magnitude and variability of sulphide at repository depth remain an open question.

As a summary, it could be said that all the hydrogeochemical and microbiological data indicate the presence of clear reducing conditions in the groundwaters. Furthermore, mineralogical studies indicate that the system has retained a significant reducing capacity to the present day /Drake et al. 2009, Drake and Tullborg 2009/.

2.2.3 Gases and colloids

The main gas in samples from the Laxemar-Simpevarp area groundwaters is nitrogen followed by carbon dioxide in the more shallow groundwaters, and helium in the deeper parts of the system. Other gases present are methane, argon and hydrogen. The available data indicate that the total gas content is less than would be expected in the Fennoscandian Shield groundwaters. Although their concentrations generally increase with depth, the gases are not oversaturated at the depths at which they were sampled /Laaksoharju et al. 2009/.

Maximum amounts of methane and hydrogen (important gases related to metabolic activities and to redox processes) in the groundwaters in the Laxemar subarea are generally lower than those found in Forsmark or Olkiluoto /Gimeno et al. 2009/. The highest methane concentration in Laxemear is found in the KLX03 at –380 m elevation, the only section at Laxemar showing a significant number of anaerobic and heterotrophic methanogenic bacteria. All other sections show numbers of methanogens below the detection limit. There are few samples taken for gas analyses and the isotopic composition of these important gases is missing. The description of the origin of gases should therefore be considered as preliminary /Gimeno et al. 2009, Laaksoharju et al. 2009/.

Hydrogen and methane are included as other parameters of interest in the evolution of the Laxemar site (Chapter 5) and a further a discussion can be seen in Sections 5.2.3 and 5.2.4.

The concentration of colloids in Laxemar-Simpevarp groundwaters is lower than 90 μg/L /Hallbeck and Pedersen 2008b/. Both inorganic and organic colloids exist at Laxemar and some colloids are probably microbes and potentially viruses (phages). The measured colloid concentration is in agreement with measurements from other crystalline groundwater environments (see Section 5.2.6).

2.2.4 Confidence and important issues in site understanding

The site investigations in the Laxemar-Simpevarp area have produced a good hydrogeochemical understanding of the site, both of present and past conditions, and have emphasised the different groundwater behaviour. Looking at the conditions in the candidate repository volume, these do not represent a site characterised by a continuous and systematic hydrogeochemical evolution from surface recharge to the maximum sampled depth. Instead, the large variation in climate and hydrogeological properties have resulted in a complicated addition (of e.g. brackish marine waters) and mixing of water types of different origin.

There is generally a high confidence in the description and understanding of the current spatial distribution of groundwater composition, mainly due to the consistency between different analyses and modelling of the chemical data, but also due to the general agreement with the hydrogeological understanding of the area. Some important points for the performance assessment can be highlighted:

Redox and pH buffer capacity in the bedrock. Mineralogical studies indicate that calcite is one of the most abundant fracture filling phases (together with chlorite) at all examined depths in the fracture fillings from Laxemar. Calcite is also present in the overburden and in the shallower bedrock and calcite dissolution is the main pH-buffer in the near-surface groundwaters. Calcite leaching is observed in the upper 20–30 m although without complete dissolution /Drake and Tullborg 2008/.

Though feasible at these shallow levels in the Laxemar and Simpevarp subareas, calcite dissolution would probably be very limited due to the fact that shallow dilute groundwaters are already in equilibrium or oversaturated with respect to this mineral. In fact, the isotopic compositions of shallow calcite fracture fillings in this area indicate that calcite was effectively precipitating from the present-day groundwaters at those levels (around 200 m depth; /Wallin and Peterman 1999/). In any case, the detected amounts of calcite in the shallowest levels of the Laxemar and Simpevarp subareas suggest an important buffering capacity for future recharge waters.

Redox front. Based on the shallow groundwater chemistry a near-surface redox reaction zone appears to be also well established. Mineralogical and geochemical studies performed on the fracture fillings in Laxemar indicate that the transition from oxidising to reducing conditions mainly takes place in the upper 20 m. Importantly, the presence of Fe(II)-bearing minerals (mainly chlorite and pyrite) in the fracture fillings at all depths (even in the uppermost 100 m of the bedrock) indicates that past oxidising episodes have not exhausted the reducing capacity of the fracture minerals, even in the shallowest part of the system. These findings, together with the significant Fe(II) content of the host rock (also in the red-stained altered wall rock), suggest that the buffering capacity against infiltrating dilute groundwater remains efficient in maintaining pH values in the range 7.5 to 8.5 and Eh values lower than –200 mV.

Glacial meltwaters. Glacial signatures are most prominent at depths between 300–600 m. Assuming similar conditions for a future glaciation as experienced during the last glaciation, it is likely that large volumes of glacial meltwaters will penetrate to repository depth within the candidate repository volume. Accepting this, the probability of the glacial meltwaters retaining their oxidising character for a long period of time is unlikely considering the buffer capacity of the bedrock and the fracture system mentioned above. This assumed outcome is supported by detailed mineralogical studies from the Laxemar-Simpevarp area and Äspö, all of which indicate that even though glacial meltwater signatures are found in the bedrock, there are no signs of this water having been oxidising at depths below 100 m /Laaksoharju et al. 2009/.

Calcium contents. A groundwater calcium content of more than 0.001 mol/L was the limit set for repository safety analysis in SR-Can /SKB 2006a/ and it could also be valid for the new criterion used in SR-Site ($\Sigma qM^{q+} \geq 0.002$–$0.004$ mol/L; see Section 1.4.1 /SKB 2011) and based on a preliminary assessment on the stability of bentonite colloids. Shallow groundwaters in Laxemar are characterised by relatively low calcium contents and a few groundwaters sampled from intermediate depth also show low calcium contents, although still exceeding 0.001 mol/L. Calcium content in groundwater is governed by mixing and reactions (calcite equilibrium and cation exchange). With regard to potential effects of dilute groundwater on the buffer material, there are two critical events that may entail potential lowering of the calcium content and will have to be analysed: the incursion of dilute glacial meltwaters (described above) and, less probably, the subsequent meteoric recharge following land uplift.

Dissolved sulphide contents. Sulphur isotope ratios in dissolved sulphate show large variations indicating that sulphide has been produced in the system and, also, geochemical calculations indicate that microbial sulphate reduction is ongoing /Gimeno et al. 2009/. Furthermore, sulphate-reducing bacteria are present at all sampled depths, but show wide variations in population levels. Measurements of sulphide at different sampling occasions have yielded very ambiguous results and continuous sampling in conjunction with the monitoring programme has been initiated to determine the reason for these observations. The relatively high concentrations of Fe(II) in the groundwater system, together with the S(-II) values, might be controlled by Fe-monosulphide solubility during undisturbed conditions. However, more information is needed prior to any future detailed interpretation. In conclusion, the magnitude and variability of sulphide at repository depth remain an open question.

3 Geochemical calculations methodology

As mentioned in the Introduction, the general strategy to evaluate groundwater compositions in SR-Site consists in combining results of hydrological flow models with mixing and reaction models. Hydrogeological models have been calibrated to reproduce, in the best possible way, present-day groundwater data for non-reactive chemical components in boreholes, as described in /Selroos and Follin 2010, Svensson and Follin 2010, Joyce et al. 2010, Vidstrand et al. 2010/. The results from these calibrated hydrological models are used as input for geochemical reaction and mixing calculations.

The main aim of the geochemical calculations is to produce a detailed chemical evolution of the groundwaters for Laxemar. Calculations performed with PHREEQC /Parkhurst and Appelo 1999/ achieve the coupling of the results of the hydrogeological model (discretised for specific time intervals over a regional site model) via a set of chemical processes (mixing, aqueous equilibrium and mineral reactions) to obtain groundwater compositions which are compatible with the hydrology and with the geochemistry of the site. The coupling of the two modules (the flow model and the chemical model) also allows a description of the geochemical heterogeneity of the repository volume, which otherwise would be hard to attain.

In order to understand the complete calculation methodology, this chapter presents a short description of the type of data given by the hydrogeological model and the procedure followed to couple them to the geochemical calculation model (Section 3.1). Then, a thorough explanation of the geochemical simulations performed in this work is presented (Section 3.2) including a description of the thermodynamic data base used for the calculations, the reference water's composition and the calculation procedure.

3.1 Hydrogeological results

Hydrogeological model results have been provided by the hydrogeological team of SKB through the standard QA procedures specified for SR-Site. Hydrogeological descriptions needed for the calculations have been selected from published SKB reports from the site characterisation activities, in particular /Rhén and Hartley 2009/ has been used. This hydrogeological conceptual model has been updated accordingly with the results obtained by the hydrogeological team along the process of the SR-Site hydrogeological modelling. Updates have been provided by SKB and through the Trac system /Selroos and Follin 2010, Svensson and Follin 2010, Joyce et al. 2010, Vidstrand et al. 2010/.

Several technical modelling teams have provided the hydrological results from which the hydrogeochemical calculations have been started:

1. Serco /Joyce et al. 2010/ has simulated the hydrodynamic evolution of the site during (1) the temperate period, and (2) the case when the repository area is submerged under seawater (Figure 1-1). The modelling consists of the transport of the selected reference waters (a.k.a. end members: Deep Saline, DS, Old Meteoric, OM, Glacial, G, Littorina, Lit, and present Altered Meteoric, AM). By this approach, the mass fractions of these waters are obtained at any time for all the discretised points in the studied rock volume. Although the chemical composition of the end-members has been updated during this project, the starting point was the estimated compositions used in SR-Can and reported in /Auque et al. 2006/ (additional explanation about the end members is reported below; Section 3.2.2.3).
2. Terrasolve AB has studied the hydrodynamic evolution of the site during (1) a periglacial period, (2) a hypothetical glacial cycle, and (3) when the candidate site is submerged under a glacial melt-water lake (Figure 1-1). One of the processes modelled is the transport of salts and, contrary to the modelling of the initial temperate period, these models do not included the fractions of selected reference waters. Therefore results in this case consist of the estimated salinity in all the discretised points in the studied rock volume. This will affect the way in which Terrasolve results will be coupled to the geochemical model.

3. The stage of the open repository has not been numerically treated in the present work, and it has been conceptually discussed from the data provided by /Svensson and Follin 2010/. The fluid flow simulations were carried out with DarcyTools and they provide inflow rates, drawdown of the groundwater table and upconing of deep saline water. Besides informing about possible effects of the excavation and operational periods, they also present tentative modelling results for the saturation phase, which starts once the completed parts of the repository are being backfilled.

3.1.1 Hydrogeological results for the temperate period and submerged under marine water periods

The hydrogeological data files include 1,484,756 points in the rock volume of Laxemar, representing the whole regional area of the site down to 2.3 km depth. These files contain the X-Y-Z coordinates together with the mass fractions of the five reference waters (Deep Saline, Old Meteoric, Glacial, Littorina and Altered Meteoric) and a column with the salinity. There is a file for each simulated year: 2000 AD, 5000 AD, 10,000 AD and 15,000 AD corresponding to the temperate period (Figure 1.1) and another file for the year 3000 BC (Littorina stage) representing the equivalent to the submerged period under marine waters at the end of the glacial cycle.

3.1.2 Hydrogeological results for the glacial period, permafrost and submerged under fresh water periods

The hydrogeological data files for the glacial and permafrost periods contain 2,816,619 and 2,021,866, respectively, in the rock volume of Laxemar, representing the whole regional area of the sites down to 1 km depth. These files contain the X-Y-Z coordinates together with calculated pressure (Pa) and salinity (%) for the groundwater in the fractures and in the matrix. The X and Y coordinates are given in metres in the DarcyTools local coordinate system with the origin at x = 1,539,000 and y = 6,360,000 for Laxemar. The Z coordinate is in metres above sea level. The three coordinates are referred to the DarcyTools cell centre.

The glacial cycle simulated for Laxemar compromise approximately 13,000 years between the first ice front passage until the site once again becomes ice free, however submerged beneath a fresh water lake. As indicated in Figure 1-1 and Table 3-1, the simulations carried out include (1) a pre-LGM stage (Last Glacial Maximum; the ice sheet was as extensive as it ever was believed to be), which means the advancing period of a short duration, (2) the LGM stage, which represents the long period with static gradient for Laxemar (11,000 years) and, finally, (3) the post-LM stage, which represents the ice front retreat.

There is a file for each period including the advance and retreat of the ice front and different cases depending on the direction of the ice front movement (NW-SE: the base case, and N-S: the variant case) and on the ice front angle (45º: the base case, and 0º: the variant case). In all the cases the initial state (at time t = 0) and the model network are the same and correspond to the end of the temperate period and, therefore, free of ice and assuming that the present day Baltic Sea is occupied by a fresh water lake.

Geochemical calculations have been carried out with the hydrological base case[5] where the ice front has a frontal angle of 45 degrees, and moves over an unfrozen surface in a NW-SE direction (Table 3-1). The periods include the advance of the ice front to different [X,Y] locations (in m, in the local Darcy tools): from [–31,000, 0] (Ice 0) to [1,100, 0] (Ice I), [3,200, 0] (Ice II), [4,400, 0] (Ice III), [27,800, 0] (Ice IV) and ice covering the entire model domain (Ice V); and then its retreat to some of the previously considered positions: Ice Vr, IVr, IIr and 0r, ice-free again after a full glacial cycle (with the entire domain covered by 100 metres of fresh water).

In the variant case where permafrost develops during the glacial period, the initial stage represents frozen conditions (periglacial period) with "taliks" before the ice advance ("xyzpss_lax_frozen-ground_IFL0.txt", see Table 3-1). The other files correspond to the progressive advance of the ice (Ice I, Ice II, Ice III and Ice IV) with permafrost development to 2 km under the ice margin and with the presence of taliks ("xyzpss_lax_perm_IFLI.txt", "xyzpss_IP2_perm_IFLII.txt", "xyzpss_IP2_perm_IFLIII.txt" and "xyzpss_IP4_perm_IFLIV.txt", Table 3-1).

[5] There are several variant hydrogeological cases but they have not been included in the geochemical calculations (see /Selroos and Follin 2010, Svensson and Follin 2010, Joyce et al. 2010, Vidstrand et al. 2010/).

Table 3-1. Cases and stages obtained from Terrasolve for which geochemical simulations over the glacial cycle have been performed /Vidstrand et al. 2010/, giving the name of the hydrogeological file, the position of the sea level and the ice front location, movement, angle and coordinates. The initial state (at time = 0) and the model network are the same in all cases.

File name	Special Case	Sea Level	Ice movement	Ice Front Angle	Ice Front location	Ice Front Location Coordinates				Local Darcy Tools	
						Local Darcy Tools		RT90		Origo (RT90)	
						X(km)	Y(km)	X(km)	Y(km)	X0(km)	Y0(km)
Chem_delivery_Laxemar_0.txt		0	–		Temperate	–31.3	0	1,507.7	6,360.0	1,539	6,360
Chem_delivery_Laxemar_I.txt		0	advance	–45	Ice I	1.1	0	1,540.1	6,360.0	1,539	6,360
Chem_delivery_Laxemar_II.txt		0	advance	–45	Ice II	3.2	0	1,542.2	6,360.0	1,539	6,360
Chem_delivery_Laxemar_III.txt		0	advance	–45	Ice III	4.4	0	1,543.4	6,360.0	1,539	6,360
Chem_delivery_Laxemar_IV.txt		0	advance	–45	Ice IV	27.8	0	1,566.8	6,360.0	1,539	6,360
xyzpss_lax_BC_IFLVa.txt		100	advance	–45	Ice Va						
xyzpss_IPV2.txt		100	retreat	–45	Ice Vr						
Chem_delivery_Laxemar_IVr.txt		100	retreat	–45	Ice IVr	27.8	0	1,566.8	6,360.0	1,539	6,360
Chem_delivery_Laxemar_IIr.txt		100	retreat	–45	Ice IIr	4.4	0	1,543.4	6,360.0	1,539	6,360
Chem_delivery_Laxemar_0r.txt		100	–		Temperate						
DEVELOPMENT OF PERMAFROST											
xyzpss_lax_frozenground_IFL0.txt	Perm_2km	–28?	–	–	frozen						
xyzpss_lax_perm_IFLI.txt	Perm_2km	–28?	advance	–45	Ice I	1.1	0	1,540.1	6,360.0	1,539	6,360
xyzpss_lax_perm_IFLII.txt	Perm_2km	–28?	advance	–45	Ice II	3.2	0	1,542.2	6,360.0	1,539	6,360
xyzpss_lax_perm_IFLIII.txt	Perm_2km	–28?	advance	–45	Ice III	4.4	0	1,543.4	6,360.0	1,539	6,360
xyzpss_lax_perm_IFLIV.txt	Perm_2km	–28?	advance	–45	Ice IV	27.8	0	1,566.8	6,360.0	1,539	6,360

As indicated above, the main difference between these results and those obtained for the temperate and submerged under marine water periods is that in the case of the glacial and permafrost models, the hydrological results are given as salinities. Due to the fact that the interface programs that couple these results to the geochemical codes are based on mixing proportions not on salinity /Auqué et al. 2006/ the hydrological results for the glacial and permafrost periods, given in the form of salinity values, require a pre-treatment to transform salinities into mixing proportions for each time slice. This new interface program has been developed (Appendix 1) and will be explained below.

Calculations over the glacial and permafrost periods follow the steps summarised below and in Figure 3-1:

- The initial state (at time t = 0) and the model network are the same in all cases. As the only data contained in the hydrogeology files are salinities, these are converted into chloride using the following relations:

$$\text{TDS (g/L)} = \rho \frac{S}{100} \qquad \text{(Equation 3-1)}$$

$$\text{Cl (g/L)} = \frac{\text{TDS (g/L)}}{1.646}, \qquad \text{(Equation 3-2)}$$

where S is percent salinity and $\rho = \rho_0 (1 + \alpha S)$, with $\rho_0 = 1{,}000$ g/L and $\alpha = 0.00741$. Factor 1.646 is the slope of the correlation line ($R^2 = 0.99$) between TDS and chloride for Laxemar and Forsmark groundwaters (Figure 4-2 in /Salas et al. 2010/).

- With salinity (converted into chloride) as the sole starting point, (t = 0) the initial assumption of the existence of just two end member waters must be made which, upon mixing in different proportions, give the known chloride content. The end members used represent a saline water and a dilute water. This is the weakest point in the approach as the "saline water" should be represented by the two more saline end members considered during the temperate period (including Littorina) and the "dilute water" should be represented by the three most diluted end members (Old Meteoric, Glacial and Altered Meteoric). The saline water has been assigned to the Deep Saline end-member and the dilute water to the Altered Meteoric end-member. Only with more information on other parameters (isotopes or magnesium, for example) could additional end members be included in the transformation of chloride to mixing proportions (like, e.g., Old Meteoric, Glacial, and Littorina). This will be discussed in more detail below.
- Therefore, from the salinity values, a new file with the mixing proportions of Deep Saline and Altered Meteoric is generated. The rest of the end members have at t = 0 a mixing proportions of zero.
- The hydrogeological data files for the next period (Glacial I) contain new salinity values calculated at the same grid points as before; so, they can be compared with the previous ones. Then, as the two main processes able to affect the groundwaters between the two time periods are the input of new glacial melt waters and the upconing of saline waters, depending on the result of the comparison, the program calculates the new mixing proportion at each point in the following way: if the new salinity at a given grid point is lower than the t = 0 one, an amount of Glacial end member water is added to the mixture (and the other two already existing proportions, Deep Saline and Altered Meteoric end members are recalculated, keeping their ratio constant)[6]; if the new salinity at a given grid point is higher that the t = 0 one, an extra amount of Deep Saline water is added to the mixture (the Altered Meteoric proportion is recalculated and the proportion of Glacial remains zero).
- The next steps will follow the same procedure as in step 4, that is, comparison of the salinities and addition of Glacial or Deep Saline proportions according to the differences found between the salinity in the previous period and the salinity in the period under consideration.

[6] This could be another weakness of the model. Irrespective to the origin of the dilute input, the program considers that it is a Glacial-melt water even in the first stages of the ice front advance. Then, in some cases where meteoric water could have been the entering end member, the program will calculate it as an extra amount of the Glacial end-member.

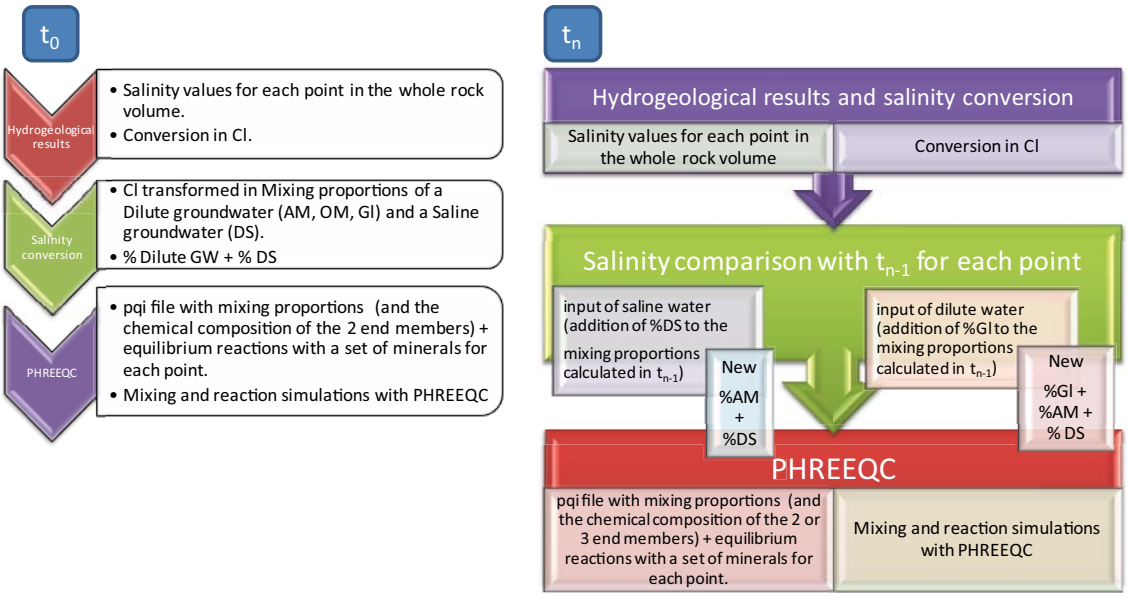

Figure 3-1. *Conversion of salinity in mixing proportions for the glacial and periglacial periods.*

As indicated above, this procedure has many uncertainties in the calculated mixing proportions, but with the available data and the restrictions imposed by the hydrogeological model, this is the most appropriate strategy. In any case, the conversion of salinity to mixing proportions affects only to the glacial and periglacial periods which are mainly characterised by a very important dilution which involves two waters with very different compositional characters: a pre-existing saline water (at the end of the temperate period) and a very dilute glacial melt water. Under these conditions, the simulated evolution is expected to reproduce, at least qualitatively, the main effects of the dilution process.

On the other hand, as will be shown in Chapter 4, the groundwater composition at the end of the temperate period (calculated from the mass fractions provided by the SERCO model) does not deviate drastically from the initial water of the glacial period (estimated from the salinities given by the TERRASOLVE model) in the bedrock. That is, there is a certain degree of coherence in the link between the two different hydrogeological models used.

Finally, and this is specific to the Laxemar case, the fact that very low Littorina proportion is present in the bedrock (less than 1.5% in all the the cases), the post-temperate evolution is better matched in those simulation cases where this end member is not used. For example, in the glacial and/or glacial + periglacial periods using the Terrasolve input files, the initial step (end of the temperate period) should be comparable with the last step obtained for the temperate period using the Serco input files. Therefore, the calculated mixing proportions for the saline waters in the first glacial stage should be comparable with the proportion of Deep Saline end-member in the temperate period (year 15,000 AD) and the mixing proportions for the dilute waters should be comparable to the sum of all the dilute waters present in the same final temperate stage (Old Meteoric, Glacial and Altered Meteoric). This comparison is plotted in Figure 3-2. These plots not only show that the calculated mixing proportions coincide, but also the distribution in the repository volume are fairly similar. Therefore, the approach used here to obtain mixing proportions from salinity could be considered acceptable. However, for future performance assessment, it would be advisable that the hydrological models used for the complete Glacial Cycle would provide homogeneous results (fractions of the reference groundwaters as a result of their models).

Accepting the limitations of this approach, from this point in the report onwards all the hydrogeological data for all periods are expressed as mixing proportions. However, instead of working with the whole rock volume, the first step is to extract several data subsets in order to reduce the number of grid points and to facilitate visualizations.

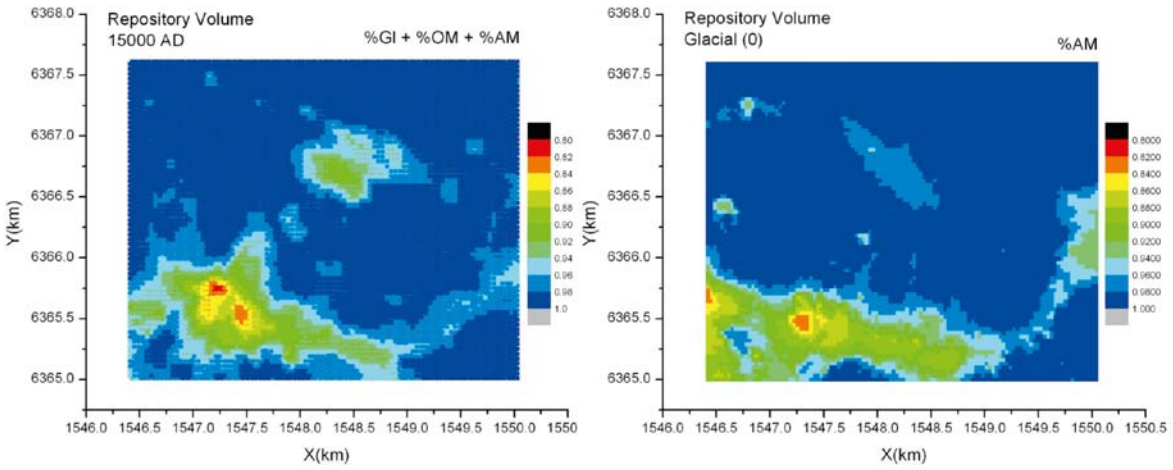

Figure 3-2. *Mixing proportion distribution of the dilute waters at the end of the temperate period (sum of Old meteoric, Glacial and Altered meteoric mixing proportions) and at the beginning of the glacial period.*

3.1.3 Extraction of the data for the geochemical simulations

From each of the original hydrogeological data files, different subsets are extracted (Figure 3-3):

- all data points at repository depth, that is, a complete horizontal slice at 500 m depth, with different thickness depending on the simulated period: 500 ± 60 m for the temperate (with 106,776 points), between –528 and –464 m depth for the glacial (around 50,000 points), between –544 and –448 m for the permafrost (around 50,000 points) and between –556 and –442 m for the open periods (806,578 points).
- a subset of the above, including the data points within the candidate repository volume (included in the domain inside the following coordinates: [1,546.40, 6,367.62, –0.5]; [1,550.05, 6,367.62, –0.5]; [1,550.05, 6,365.00, –0.5]; and [1,546.40, 6,365.00, –0.5]) with 35,762 for the temperate, 28,044 points for the glacial and permafrost and 790,110 points for the open periods.
- A vertical slice approximately parallel to the shoreline (Figure 3-3) (NW: 1,544,500 m / 6,370,000; SE: 1,551,500 m / 6,363,025), through boreholes KLX13A, KLX18A, the entrance to the repository, and boreholes KLX12A and KLX05[7], with 33,115, 20,372 and 101,761 points for the temperate, the glacial and permafrost and the open periods simulations, respectively.

A complete explanation of the procedure for the extraction of the different slices can be found in Appendix 1.

Once these data subsets are extracted, they are used to create input files for PHREEQC. The still large number of points (i.e., water samples) on which PHREEQC calculations had to be performed, led to the development of simple interface programs for the automatic import and export of data. This software (developed in-house by the GMG, University of Zaragoza, for SR-Can and updated for SR-Site; Appendix 1) accepts as input a hydro file with the mixing proportions and a file with the composition of the end-members to calculate the final chemical composition of the waters at each point. This interface program allows also the selection of the chemical processes that will be imposed to the waters. All this procedure is presented next and explained in Appendix 1.

[7] An additional slice has also been selected to include the Simpevarp peninsula. It is W-E and goes through boreholes KLX20A, KLX11A, KLX18A, KLX10, KLX21B, KSH01 and KSG03. The coordinates are W: 1,544,500 m / 6,366,500; E: 1,554,000 m / 6,366,000 (Figure 3-3).

3.2 Geochemical numerical model setup

3.2.1 Conceptual model

The conceptual model on which the geochemical calculation strategies are based, assumes that the chemical characteristics of these groundwaters are the result of complex mixing events driven by the input of different recharge waters during the palaeogeographic history of the site (see Chapter 2 and /Laaksoharju et al. 2009/). The successive penetration at different depths of dilute cold and warm waters, including the last glacial melt-waters and Littorina Sea marine waters, has triggered complex, density and hydraulically driven flows that have mixed them with highly saline and long residence time waters (brines) present in the fractures and the rock matrix. The recent infiltration of present meteoric and Baltic Sea marine waters has only affected the shallowest (≤ 200 m) part of the aquifer system.

The hydrogeochemical study of the Laxemar groundwaters has confirmed the existence of at least five component waters: an old brine (Deep Saline), an old dilute meteoric water (Old meteoric), a glacial melt-water (Glacial), a marine water (ancient Littorina Sea), and a modern meteoric water (Altered Meteoric) /Laaksoharju et al. 2009/. As a result, from a purely geochemical viewpoint, mixing can be considered the prime irreversible process responsible for the chemical evolution of the groundwater system in the Laxemar area. The successive disequilibrium states resulting from mixing conditioned the subsequent water-rock interaction processes and hence the re-equilibration pathways of the mixed groundwaters.

Mixing provides a satisfactory interpretation for several of the groundwater components partly because the rates of reaction between the rock and the circulating groundwater are relatively slow, as mentioned above. Besides, an important aspect is that there are large differences in concentrations between the mixing waters (e.g. between the meteoric infiltrating waters and the Deep Saline end member found at the deepest parts of the site). Under such circumstances, the relative effects of water-rock interactions on the concentrations of the main groundwater components are small when compared with the large effects caused by mixing. There are, however, important parameters mainly controlled by equilibrium reactions (homogeneous and heterogeneous) and these must be taken into account. But even in that case, the intensity of water-rock interactions depends on salinity/TDS (for example, mineral solubility depends on the salinity or ionic strength of the waters) and, therefore, on mixing proportions. Moreover, mixing produces non-linear effects on the thermodynamic activities of the species controlling the water-mineral reactions (e.g. through the ionic activity product) and controls the direction (precipitation or dissolution) and extent of most subsequent heterogeneous reactions in the system (see /Gimeno et al. 2009, pp 133–137/ and references therein). Therefore, the coupling of the hydrogeological results with the geochemical calculation is necessary.

3.2.2 PHREEQC calculations

Hydrogeochemical calculations have been performed with PHREEQC /Parkhurst and Appelo 1999/. Data subsets as defined above, including the mixing proportions for each point, were used to create input files for the PHREEQC code in order to “translate” these mixing proportions into chemical compositions for each point. The procedure involved combining the file with the hydrogeological mixing proportions with the file containing the chemical composition of each end member water. With a simple option of mixing, the final chemical composition, speciation and saturation states of the groundwaters at each point is obtained.

However, knowing that some chemical equilibrium reactions are important controls on the non-conservative parameters of the system, apart from the mixing simulation, PHREEQC is forced to equilibrate each water with a set of minerals. The selected phases are present in the system as rock-forming minerals and fracture fillings and have fast kinetics for the simulated time intervals. The results obtained include the detailed chemical compositions of the groundwaters at each point and the amount of mass transfer for the equilibrated minerals.

This simulation methodology corresponds to classical reaction-path calculations: mixing of waters constitutes the irreversible process in the evolution of the hydrochemical system, while the equilibrium reactions represent reversible processes modifying its effects /Zhu and Anderson 2002, Bethke 2008/.

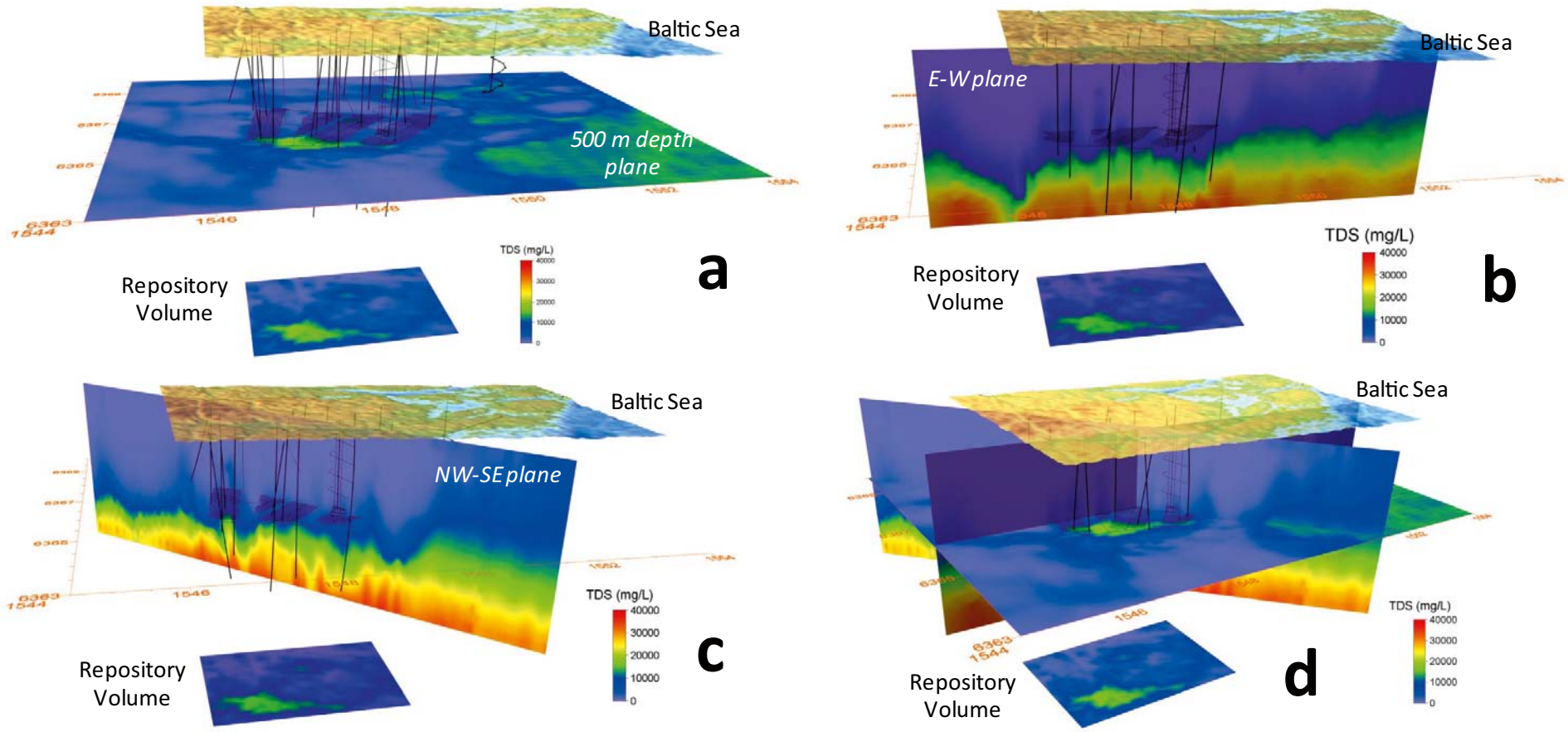

Figure 3-3. *3D plots showing the distribution of the computed salinity (TDS in mg/L)at the year 2000 AD for Laxemar in the different planes in which the geochemical calculations have been performed. In all the cases, the topographical surface, the boreholes and the repository layout are drawn. The x and y axes represent the X and Y coordinates. (a) horizontal plane at the repository depth. (b) vertical slice perpendicular to the coast (E-W plane) cross-cutting the repository volume; (c) vertical slice parallel to the coast (NWSE) cross-cutting the repository volume; (d) salinity distribution in the three previous planes together. Additionally, in the four plots, a small picture of the distribution in the repository volume is also shown.*

To create these PHREEQC input files, apart from the hydro file with the mixing proportions calculated at each point, two additional files are needed: a file containing the end members to be mixed and the mineral phases to be equilibrated (Appendix 1), and another file with the complete chemical composition of the end members. With these two files, the dedicated interface programs create the input files that PHREEQC uses to calculate the chemical composition in all the grid points and times selected from the hydrogeological models.

Finally, when running PHREEQC two very important aspects need to be considered: the thermodynamic data base and the composition of the end member. A comprehensive explanation of these key aspects of the geochemical calculations is presented next.

3.2.2.1 Thermodynamic database

Consistency between this model exercise and other SR-Site geochemical models using thermodynamic data is an important issue. This is the reason why, instead of using the same WATEQ4F database as in previous geochemical calculations for SR-Can /Auqué et al. 2006/, a thermodynamic database from SKB's Trac system has been used, known as TDB_SKB-2009_Amphos21.dat (a.k.a. SKB-SR-Site). This database is the one developed by /Hummel et al. 2002/ with specific modifications carried out by Amphos21 /Duro et al. 2006/ and used for the solubility limits calculations by /Grivé et al. 2010/.

The use of this database has limited the capacity of simulating processes such as cation exchange because this database cannot deal with them without including the necessary data (which would have needed a complete verification exercise as an indispensable QA requirement). The same problem has been encountered with some specific solubility data (already included and verified in the WATEQ4F database /Ball and Nordstrom 2001/ by /Auqué et al. 2006[8]/) for some important phases in the groundwater systems under study /Gimeno et al. 2009/. These new data have been included in each simulation using the "Phases" option in each PHREEQC input file. The affected phases are:

- Iron(III) oxy-hydroxides and amorphous or crypto-crystalline iron mono-sulphides. Both groups of solids are involved in the redox processes that control the Eh of the groundwaters, and their solubility is highly dependent on the degree of crystallinity, specific surface area, and re-crystallization or ripening.

$Fe(OH)_3$(hematite_grenthe): $Fe(OH)_3 + 3H^+ = Fe^{3+} + 3H_2O$ (log_k = –1.10)

FeS(ppt): $FeS + H^+ = Fe^{2+} + HS^-$ (log_k = –3.00)

- Aluminosilicate phases. They are present as rock forming minerals and as fracture filling minerals in most granitic systems. Due to extensive solid-solution between end-member phases, their thermodynamic properties are not well known. The following data have been used:

Albite: $NaAlSi_3O_8 + 8H_2O = Al(OH)_4^- + 3Si(OH)_4 + Na^+$ (log_k = –19.98).

K-Feldspar: $KAlSi_3O_8 + 8H_2O = Al(OH)_4^- + 3Si(OH)_4 + K^+$ (log_k = –22.62).

Kaolinite_G: $Al_2Si_2O_5(OH)_4 + 7H_2O = 2Al(OH)_4^- + 2H^+ + 2Si(OH)_4$ (log_k = –37.3).

Additionally, two mineral phases not included in the database were also added:

- Hydroxyapatite: $Ca_5(PO_4)_3OH + 4H^+ = 5Ca^{2+} + 3HPO_4^{2-} + H_2O$ (log_k = –3.421).
- Rhodochrosite: $MnCO_3 = Mn^{2+} + CO_3^{2-}$ (log_k = –11.13).

The reasons behind the selection of these phases and their equilibrium constants are detailed in /Auque et al. 2006/ and /Gimeno et al. 2009/.

Besides these additions and corrections, and based on the study performed and reported in SR-Can (see /Auqué et al. 2006/ for more details), the possibility of redox disequilibria has been taken into account, trying to cover all possible redox situations in the natural system.

[8] Appendix A in /Auqué et al. 2006/ contains a detailed discussion of the main difficulties encountered when working with these type of phases, the range of solubility values found in the literature, and the values selected for the SR-Can modelling.

Due to the redox approach implemented in most geochemical codes (including PHREEQC), based on redox equilibrium assumption (see /Auqué et al. 2006/ for more details), the only way to prevent equilibration between redox couples in PHREEQC is to define the individual redox states in each couple as separated "chemical elements". This can only be done by modifying the thermodynamic database /Parkhurst and Appelo 1999/. Therefore, a modified version of the thermodynamic database was implemented by /Salas et al. 2010/ in order to obtain redox disequilibrium between the HCO_3^-/CH_4, SO_4^{2-}/HS^- and $Fe(OH)_3(s)/Fe^{2+}$ redox pairs. This modified database will be named here the "un-coupled" database. The modification essentially prevents the redox pairs SO_4^{2-}/HS^- and HCO_3^-/CH_4 participating in the homogeneous redox equilibrium during the mixing and reaction simulations. The procedure followed to implement this modification is explained in /Auqué et al. 2006/.

In summary, the "un-coupled" database has allowed to obtaining groundwater Eh values controlled by the $Fe(OH)_3/Fe^{2+}$ redox pair. The resulting Eh values are similar to the ones measured in some of the Swedish groundwaters believed to be controlled by the electro-active $Fe(OH)_3/Fe^{2+}$ redox pair /Grenthe et al. 1992/. With the original "coupled" database, the resulting Eh values correspond to homogeneous redox equilibrium, consistent with the agreement between Eh values for the $Fe(OH)_3/Fe^{2+}$, SO_4^{2-}/HS^- and HCO_3^-/CH_4 couples which has been observed in some groundwater samples at Laxemar /Gimeno et al. 2009/.

Therefore, the use of these two databases covers the measured and calculated Eh values in SKB's site characterisation studies and, although some problems in the treatment and interpretation of redox potential still persists, this methodology gives a reasonable range of Eh values in SR-Site simulations. They will be treated as geochemical variant cases.

3.2.2.2 Sensitivity of the results to the thermodynamic data base

A sensitivity analysis of the geochemical results to the thermodynamic data base was performed in order to test the differences between the results obtained when using the WATEQ4F data base (previously used for SR-Can; /Auqué et al. 2006/) and those obtained with the data base suggested by SKB to be applied for the SR-Site calculations[9]. Different geochemical variant cases have been done assuming two different redox minerals and the possibility of coupling or uncoupling the sulphide and carbon system in the data base (see also Figure 3-5) and therefore, the effects of these different cases have also been analysed with the two different thermodynamic data bases.

In general, the results for the total contents of the major ions (even for those affected by the equilibrium imposed with with calcite, quartz and hydroxyapatite) and salinity are the same irrespective of using WATEQ4F or SKB-SrSite thermodynamic data base. Even the pH values are the same.

The results obtained for the redox parameters (Eh, S(-II) and Fe(II)), are very sensible to the redox mineral considered to be in equilibrium for each variant case. There are no differences between the results obtained for Eh with the two data bases when the equilibrium mineral is the Fe(III)-oxyhydroxide (with the coupled or the uncoupled data base). When the equilibrium mineral is FeS(am), the Eh values obtained with SKB-SrSite TDB are only slightly lower (but negligible) than the ones obtained with the WATEQ4F data base.

For Fe(II) and S(-II) contents, some differences between the results obtained when using the two different data bases are seen for the geochemical variant case that equilibrates Fe(III)-oxyhydroxide and uses the so-called coupled data base. However the differences found for Fe(II) are negligible while for S(-II) can be one order of magnitude (lower when using the SKB-SrSite TDB).

This analysis, therefore, indicates that the results obtained with WATEQ4F and with SKB-SrSite are very similar. And, in general, they are lower than the differences produced when applying the different geochemical variant cases or the different hydrogeological results.

[9] Other sensitivity analysis was also done in order to check the effects of considering different cases, including: (a) the hydrogeological model (SR-Can vs. SR-Site) and (b) the different geochemical model: Only mixing vs. mixing + equilibrium reactions, Mixing + equilibrium reactions vs. Mixing-Equilibrium-Exchange.

3.2.2.3 Estimation of the end-member waters compositions

All the geochemical calculations start with mixing proportions of the end-member waters instead of with the chemical compositions themselves, which therefore have to be calculated. The results will be strongly affected by the assumed original composition of the end-member waters.

Table 3-2 shows the original compositions of the end-member waters that have been used for the site characterisation studies /Gimeno et al. 2008, 2009/ and that have been considered as reference waters in the hydrogeological models. Some of these waters are represented by real samples from natural systems and some others are estimated from diverse geological sources (for more detailed information on the approach, see /Gimeno et al. 2008, 2009/). In both cases there are some unknown fundamental parameters for some of these waters (pH, Eh, concentration of Al, Fe, or S^{2-}), and they have been obtained assuming a series of mineral equilibrium reactions thought to be controlling these variables (e.g. with calcite, quartz, haematite and/or Fe(II)-monosulphides). The final chemical composition of the end members as they have been used in the geochemical modelling performed for SR-Site is shown in Tables 3-3 and 3-4.

The main assumptions for the derivation of the composition of the end member are summarised next.

The **Deep Saline end member** corresponds to the deepest and most saline water sampled in Laxemar (from borehole KLX02 at 1,631–1,681 m depth with a salinity of 75 g/L TDS). It is 1.5 million years old (estimated from ^{36}Cl data /Louvat et al. 1997, 1999/), has a Ca-Na-Cl composition and a significant deviation from the MWL (Meteoric Water Line in $\delta^{18}O$ vs $\delta^{2}H$ plots) due to its long interaction with the bedrock in a near-stagnant environment /Laaksoharju and Wallin 1997, Laaksoharju et al. 1999/.

This water must have been in the rock for hundreds of thousands of years and therefore it must be in equilibrium with the rock-forming minerals and the fracture fillings. Thus, the original composition of this water has been equilibrated with albite, K-feldspar, calcite, haematite (Grenthe's equilibrium constant; /Grenthe et al. 1992/), and quartz at a constant pH = 8.0. The redox potential of these waters is assumed to be controlled by an iron mineral phase (haematite) with the equilibrium constant proposed by /Grenthe et al. 1992/.

The Old Meteoric end member. As reported in Chapter 2, the SDM-Site Laxemar hydrogeochemical investigations showed that changes in the groundwater chemistry during the Quaternary were not restricted to post glacial time as there is groundwater and porewater evidence that indicates an old, warm-climate derived meteoric water component. Without recognising this older component, the hydrogeochemistry (and hydrogeology) cannot be adequately explained /Laaksoharju et al. 2009/. Therefore, in this new version of the hydrogeological model, the hydrogeologic models have included a fifth end member (not used in SR-Can calculations) which represents an old dilute water ("**Old meteoric end member**") whose composition is similar to the Altered Meteoric end member but with a longer residence time and therefore, longer interaction time with the rock. This water has been equilibrated with calcite, haematite, kaolinite, quartz and a $\log P_{CO2} = -4.1$.

Table 3-2. Original end members (used by the hydrogeologists; Table F-1 in /Joyce et al. 2010/). Units in mg/L except for isotopes and pH.

	DeepSaline	Old Meteoric	Glacial	Littorina	Altered Meteoric
pH	8	8	5.8	7.6	8.17
Alkalinity	14.1	10	0.12	92.5	265.0
Cl	47,200	5,000	0.5	6,500	23.0
SO_4^{2-}	906.0	375	0.5	890	35.8
Br	323.66	34		22.2	b.d.l.
Ca	19,300	1,585	0.18	151	11.2
Mg	2.12	2	0.1	448	3.6
Na	8,500	1,440	0.17	3,674	110.0
K	45.5	4	0.4	134	3
Si	2.9	—	—	3.94	7
Fe(II)	—	—	—	0.002 (Fe tot)	0.08
$\delta^{2}H$ (‰)	–44.9	—	–158.0	–37.8	–76.5
$\delta^{18}O$ (‰)	–8.9	–5	–21.0	–4.7	–10.9

Glacial end member. The composition adopted for the Glacial end-member (used in the SDM-Site Laxemar) in the site investigation program corresponds to present melt-waters from one of the largest glaciers in Europe, the Josterdalsbreen in Norway, located on a crystalline granitic bedrock /Laaksoharju and Wallin 1997/. These waters represent the chemical composition of surface melt-waters prior to the water-rock interaction processes undergone during their infiltration into the bedrock. They have a very low content of dissolved solids, even lower than present-day meteoric waters, a pH value of 5.8, and an isotopically light signature /Gimeno et al. 2009, Salas et al. 2010/.

To obtain the possible compositional characteristics of these waters after water-rock interaction in the upper parts of the rock (even in the first 100 m) prior to mixing with other groundwater components, equilibrium with respect to quartz and kaolinite has been assumed. Calcite saturation index has been fixed to −1.0 (originally glacial meltwaters are strongly under-saturated with respect to calcite) and the redox potential has been assumed to be controlled by an iron mineral phase (microcrystalline $Fe(OH)_3$) common in environments that buffer the input of oxygenated waters.

Compared with the original composition of glacial melt-waters (compare values in Tables 3-2 and 3-3), these already reacted waters have a more alkaline pH (around 9) and higher TDS values as a consequence of water-rock interaction (see Appendix 2; /Gimeno et al. 2009, Salas et al. 2010/). The differences are of orders of magnitude, especially for chloride, sodium and alkalinity. However, the final salt content is still very low in absolute terms. The presence of geochemically-reactive minerals like calcite, even at the trace amounts found in many crystalline systems, exert an important control in the compositional evolution of glacial melt-waters /Brown 2002, Mitchell and Brown 2007/. This control is very fast and dominant in environments out of contact with the atmospheric CO_2 and where other sources of acidity (e.g. pyrite dissolution) are limited (calcite is one of the most abundant minerals at all depths in the fracture fillings of Laxemar whereas pyrite is much more scarce and evenly distributed; /Drake and Tullborg 2009/), as it occurs during the infiltration of melt-waters in the bedrock. See Appendix 2 for further discussion.

Littorina end member. The chemical composition of seawater during the Littorina stage has been selected as one of the reference waters used in the hydrogeological and hydrogeochemical modelling of the Laxemar site. The Littorina stage in the postglacial evolution of the Baltic Sea commenced at ≈ 6500 BC. The salinity increased more or less continuously until ≈ 4500–4000 BC, reaching estimated maximum values twice as high as modern Baltic Sea water and this maximum prevailed at least from 4000 to 3000 BC. This period was followed by a stage where substantial dilution took place. During the last 2,000 years, the salinity has remained almost constant and equal to present Baltic Sea values.

The chemical composition of the Littorina Sea used here (as well as in SR-Can and in the site characterisation studies /Gimeno et al. 2008, 2009/) is based on the maximum salinity estimation of 12‰ or 6,500 mg/L Cl^- /Kankainen 1986/, while the concentration of other main elements were obtained by diluting the global mean ocean water /Pitkänen et al. 1999, 2004/. Apart from the uncertainty in the salinity estimated for this end member (vertical and lateral, /Gimeno et al. 2008/), the main uncertainty is in the fact that seawater intruding in the sub-surface may be modified by reactions in the sediments. The main processes are: sulphate reduction, carbonate precipitation and cation exchange.

Because of these reactions, it must be understood that the composition of the Littorina Sea component in mixing calculations is quite uncertain. Thus, mineral equilibrium with calcite, quartz, FeS(am) and kaolinite[10] have been considered.

The **Altered Meteoric end member** corresponds to a real sample (sample #10231; Table 3-2; the selection of this sample is thoroughly described in /Gimeno et al. 2008, 2009/). This sample represents a typical shallow dilute groundwater (less than 100 m depth) of recent meteoric origin and, therefore, it should reflect the chemical characteristics of meteoric waters after a short interaction with soils, overburden and granite. Their tritium content and low chloride concentrations are representative of their recent meteoric origin and the absence of mixing processes with more saline waters.

[10] Equilibrium with respect to FeS(am) reflects the expected microbial sulphate reduction and the common presence of this sulphide phase in anoxic marine sediments. Equilibrium with quartz and kaolinite is an attempt to approximate the interaction with aluminosilicates in the sea sediments or in the first metres of the bedrock.

In this case, as the selected end member water is a real sample, the chemical composition is well known though it does not include aluminium concentrations or measured Eh data. These values have been obtained by equilibrating the sample with kaolinite, quartz and micro-crystalline $Fe(OH)_3$ and imposing a calcite saturation index of −0.5.

Once the main reactions have been established, the composition of each end member was calculated using PHREEQC with the SKB-SrSite thermodynamic data base with the sulphur coupled (Table 3-3) and uncoupled (Table 3-4).

3.2.3 Methodology of the geochemical calculations

Groundwater compositions are modelled through mixing (using the mixing proportions from the hydrogeologic models) and chemical reactions with fracture-filling and rock-forming minerals. Geochemical calculations have been performed for the following periods: the temperate, the glacial (with and without permafrost) and the submerged periods (under marine and fresh waters). Figure 1-1 shows the succesive stages considered in these calculations.

For each case, the geochemical simulations follow the steps shown in Figure 3-4. Once the files with the extracted slices containing the mixing proportions for each node have been obtained, each file is used, together with the file with the chemical composition of the end members, and the file with the list of end members and the mineral phases imposed to be in equilibrium, to create the input file for the geochemical code (PHREEQC[11]). For each point, apart from the mixing, a set of mineral equilibria is also imposed.

The minerals selected for the equilibria are those present at the site as fracture fillings, with fast kinetics compared with the simulated time intervals (calcite and Fe-III oxide -haematite; this last one with the equilibrium constant derived for deep Swedish groundwaters by /Grenthe et al. 1992/) or those with apparent equilibrium situations in present groundwaters (quartz, hydroxyapatite and amorphous Fe-II monosulphide, FeS(am)). The use of haematite or FeS(am) represents two alternative groundwater evolutions: equilibrium with haematite implies a situation where the redox state is not affected by sulphate-reducing bacteria, while equilibrium with FeS(am) characterises a situation with significant activity of sulphate-reducing bacteria.

Table 3-3. Equilibrated end members, calculated with the coupled data base used for the geochemical simulations. Units in molal units (mol/kg) except for pH, T and pe.

mol/kg	DeepSaline	Old Meteoric	Glacial	Littorina	Altered Meteoric
pH	8.00	8.64	9.30	7.95	7.84
T (ºC)	15	15	15	15	15
pe	–4.45	–5.12	–5.26	–4.42	–1.05
Al	$7.37\cdot10^{-9}$	$1.21\cdot10^{-6}$	$5.21\cdot10^{-6}$	$3.25\cdot10^{-7}$	$2.03\cdot10^{-7}$
Br	$4.16\cdot10^{-3}$			$2.81\cdot10^{-4}$	
C	$3.68\cdot10^{-5}$	$6.91\cdot10^{-4}$	$8.52\cdot10^{-5}$	$1.63\cdot10^{-3}$	$4.26\cdot10^{-3}$
Ca	0.49	$5.26\cdot10^{-4}$	$7.18\cdot10^{-5}$	$3.87\cdot10^{-3}$	$1.79\cdot10^{-4}$
Cl	1.37	$6.49\cdot10^{-4}$	$1.41\cdot10^{-5}$	0.19	$6.49\cdot10^{-4}$
F	$8.64\cdot10^{-5}$	$2.03\cdot10^{-4}$		$2.61\cdot10^{-5}$	$2.03\cdot10^{-4}$
Fe_{Tot}	$2.53\cdot10^{-7}$	$5.72\cdot10^{-9}$	$8.00\cdot10^{-7}$	$8.26\cdot10^{-6}$	$1.79\cdot10^{-6}$
K	$8.22\cdot10^{-4}$	$7.60\cdot10^{-5}$	$1.02\cdot10^{-5}$	$3.47\cdot10^{-3}$	$7.60\cdot10^{-5}$
Li	$6.86\cdot10^{-4}$	$1.59\cdot10^{-6}$		$1.02\cdot10^{-5}$	$1.59\cdot10^{-6}$
Mg	$8.95\cdot10^{-5}$	$1.48\cdot10^{-4}$	$4.11\cdot10^{-6}$	$1.87\cdot10^{-2}$	$1.48\cdot10^{-4}$
Mn	$2.62\cdot10^{-6}$	$1.06\cdot10^{-6}$			$1.06\cdot10^{-6}$
Na	0.38	$4.79\cdot10^{-3}$	$7.40\cdot10^{-6}$	0.16	$4.79\cdot10^{-3}$
SO_4^{2-}	$9.68\cdot10^{-3}$	$3.73\cdot10^{-4}$	$5.31\cdot10^{-6}$	$9.39\cdot10^{-3}$	$3.73\cdot10^{-4}$
Si	$8.81\cdot10^{-5}$	$1.42\cdot10^{-4}$	$1.67\cdot10^{-4}$	$1.28\cdot10^{-4}$	$1.35\cdot10^{-4}$
Sr	$3.95\cdot10^{-3}$			$3.10\cdot10^{-5}$	

[11] As pointed out before, the large number of points (or waters) obtained in the hydrogeological spatial discretisation for which PHREEQC calculations had to be performed led to the development of simple interface software in order to make the input and output of data automatically (Appendix 1).

Table 3-4. Equilibrated end members calculated with the "un-coupled" thermodynamic data base, used for the geochemical simulations. Units in molal units (mol/kg) except for pH (standard units), T (degrees centigrades) and pe.

mol/kg	DeepSaline	Old Meteoric	Glacial	Littorina	Altered Meteoric
pH	8.00	8.64	9.29	7.95	7.84
T (ºC)	15	15	15	15	15
pe	–5.91	–7.08	–2.62	–3.91	–1.05
Al	$7.37 \cdot 10^{-9}$	$1.21 \cdot 10^{-6}$	$5.21 \cdot 10^{-6}$	$3.25 \cdot 10^{-7}$	$2.03 \cdot 10^{-7}$
Br	$4.16 \cdot 10^{-3}$			$2.81 \cdot 10^{-4}$	
C	$3.68 \cdot 10^{-5}$	$6.91 \cdot 10^{-4}$	$8.61 \cdot 10^{-5}$	$1.63 \cdot 10^{-3}$	$4.26 \cdot 10^{-3}$
Ca	0.49	$5.26 \cdot 10^{-4}$	$7.18 \cdot 10^{-5}$	$3.87 \cdot 10^{-3}$	$1.79 \cdot 10^{-4}$
Cl	1.37	$6.49 \cdot 10^{-4}$	$1.41 \cdot 10^{-5}$	0.19	$6.49 \cdot 10^{-4}$
F	$8.64 \cdot 10^{-5}$	$2.03 \cdot 10^{-4}$		$2.61 \cdot 10^{-5}$	$2.03 \cdot 10^{-4}$
Fe_{Tot}	$7.28 \cdot 10^{-6}$	$5.23 \cdot 10^{-7}$	$2.11 \cdot 10^{-9}$	$8.28 \cdot 10^{-6}$	$1.79 \cdot 10^{-6}$
K	$8.22 \cdot 10^{-4}$	$7.60 \cdot 10^{-5}$	$1.02 \cdot 10^{-5}$	$3.47 \cdot 10^{-3}$	$7.60 \cdot 10^{-5}$
Li	$6.861 \cdot 10^{-4}$	$1.59 \cdot 10^{-6}$		$1.02 \cdot 10^{-5}$	$1.59 \cdot 10^{-6}$
Mg	$8.95 \cdot 10^{-5}$	$1.48 \cdot 10^{-4}$	$4.11 \cdot 10^{-6}$	0.019	$1.48 \cdot 10^{-4}$
Mn	$2.62 \cdot 10^{-6}$	$1.06 \cdot 10^{-6}$			$1.06 \cdot 10^{-6}$
Na	0.38	$4.79 \cdot 10^{-3}$	$7.40 \cdot 10^{-6}$	0.16	$4.79 \cdot 10^{-3}$
SO_4^{2-}	$9.68 \cdot 10^{-3}$	$3.73 \cdot 10^{-4}$	$5.21 \cdot 10^{-6}$	$9.38 \cdot 10^{-3}$	$3.73 \cdot 10^{-4}$
S(-II)	$1.03 \cdot 10^{-15}$	$1 \cdot 10^{-15}$	$1.00 \cdot 10^{-7}$	$8.25 \cdot 10^{-6}$	$1.00 \cdot 10^{-15}$
Si	$8.81 \cdot 10^{-5}$	$1.42 \cdot 10^{-4}$	$1.66 \cdot 10^{-4}$	$1.28 \cdot 10^{-4}$	$1.35 \cdot 10^{-4}$
Sr	$3.95 \cdot 10^{-3}$			$3.10 \cdot 10^{-5}$	

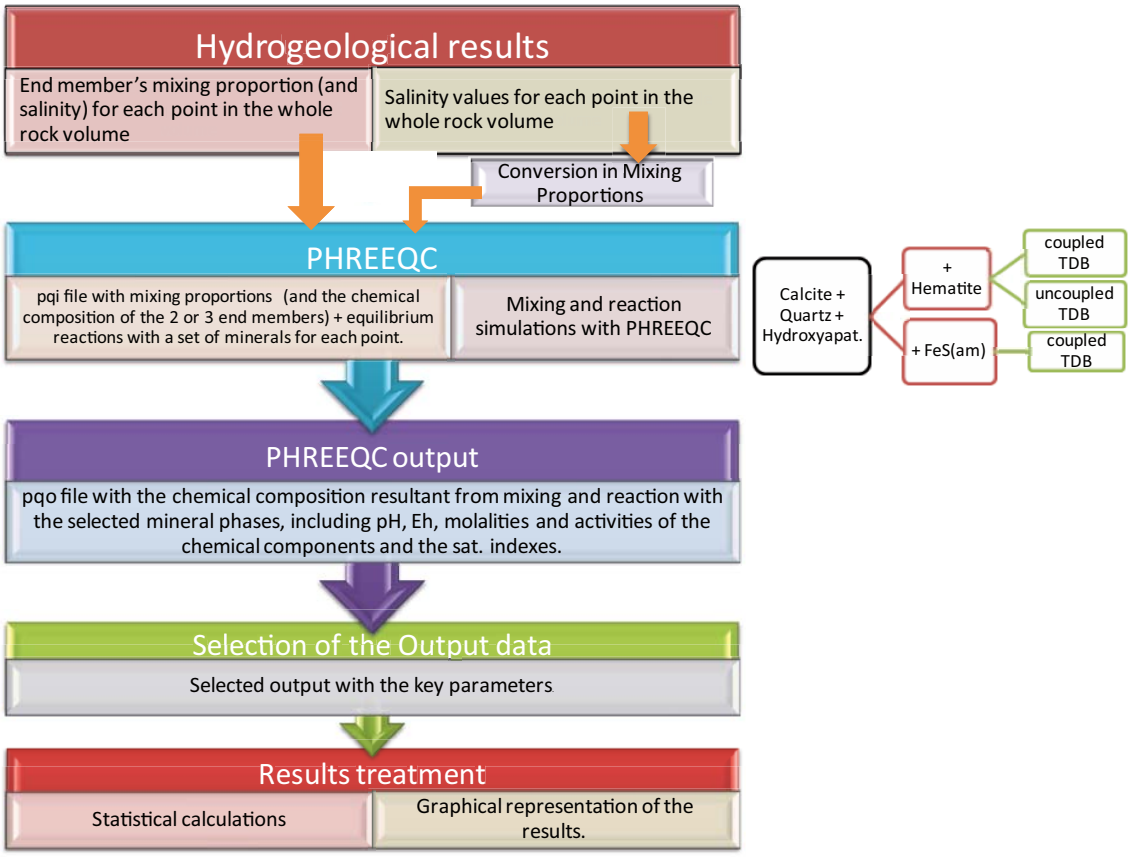

Figure 3-4. *Steps followed for the geochemical simulations.*

The existence of haematite has been described at all depths in the fracture fillings /Drake and Tullborg 2009/ and FeS(am) equilibrium situations have been identified in the groundwaters from Laxemar /Gimeno et al. 2009/. Thus, both geochemical cases have been evaluated through two geochemical variant cases. Apart from these two cases, an additional one has also been tested considering the possible control of Eh by the iron system and the $Fe(OH)_3/Fe^{2+}$ redox pair (mantaining homogeneous redox disequilibrium; Section 3.2.2.1) and, therefore, using the un-coupled thermodynamic database. This analysis has been only performed under the assumption of equilibrium with respect to haematite.

What cannot be forgotten is the fact that this is an oversimplication of the problem as these simulations are applied to the whole rock volume even knowing that the processes imposed are not homogeneously distributed at all depths.

As a summary, the geochemical simulations performed are shown in Figure 3-5: mixing and equilibrium reactions with calcite, quartz and hydroxyapatite are imposed in all the cases, and then a different redox mineral is alternatively equilibrated (haematite or FeS(am)) with the additional possibility of using the coupled or the uncoupled TDB. This gives three different cases (variant geochemical cases in Figure 3-5; in red): (a) Case 1, equilibrium with haematite and the coupled TDB; (b) Case 2, equilibrium with FeS(am) and the coupled TDB; and (c) Case 3, equilibrium with haematite and the un-coupled TDB.

As will be shown in the next chapter, the different cases provide very similar values for most of the chemical components (including pH). However, this is not valid for the redox sensitive parameters considered here, Eh, Fe(II) and (S-II) concentration. Therefore, in order to take into account all the possible values within the repository volume, the numerical results obtained by the two models which consider the equilibrium of solutions with haematite (Case 1) or FeS(am) (Case 2) have been integrated in the so-called "Base Case". For the non-redox parameters, this Base Case includes the results obtained only with the simulations in equilibrium with haematite (which are the same as those obtained with the rest of the geochemical variant cases). Unless otherwise stated, the figures and tables in Chapter 4 show results obtained with this Base Case. Alternative simulation strategies will be discussed only when appropriate.

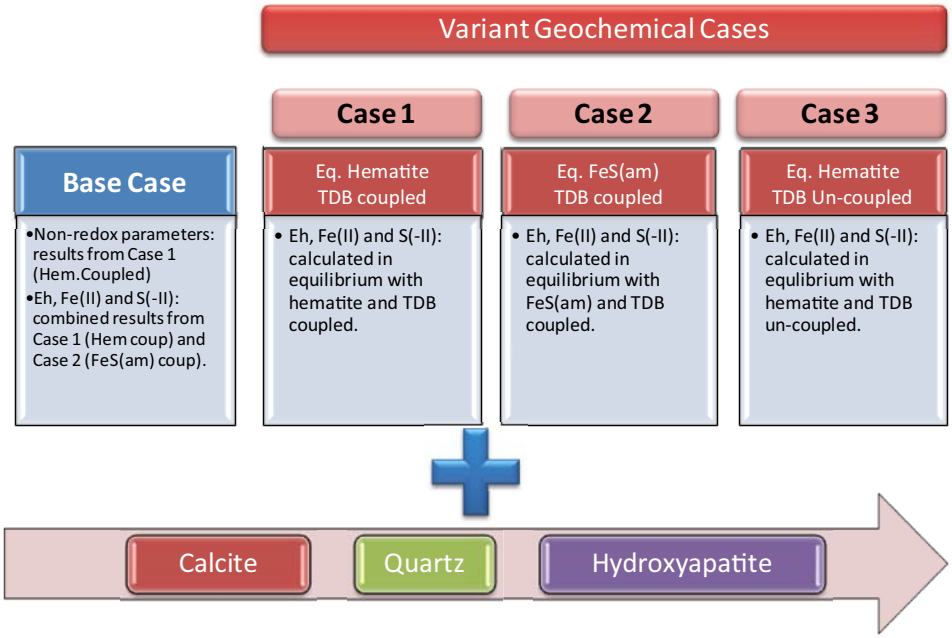

Figure 3-5. *Different geochemical simulations performed for all the periods analysed. The so-called Base Case includes the results obtained with the variant case 1 (equilibration with haematite) for all parameters except the redox ones (Eh, Fe(II) and S(-II)) for which, it includes also the results obtained with the variant case 2 (equilibration with FeS(am)).*

As stated in Section 3.2.2.1, some important processes in the hydrochemical evolution of the Laxemar groundwaters (e.g. /Gimeno et al. 2008, 2009/), like cation exchange, have not been modelled in the present work. Available CEC values for fracture filling minerals (a basic parameter for this type of simulations) are very scarce and uncertain /Selnert et al. 2008/ and the thermodynamic data base used for the calculations (SKB-SrSite) does not include the possibility to deal with cation exchange processes. However, knowing the importance of cation exchange, the UZ group has developed the methodology and software needed to deal with cation exchange from the results provided by the hydrogeologists (mixing proportions).

Cation exchange reactions were already implemented for SR-Can simulations as a variant case. The conceptual model assumed the presence of an unique type of exchanger (i.e., the same composition for all the points in the whole volume and for all the time slices), whose composition was in equilibrium with the waters with the longest residence time, the Deep Saline end member. The model proposed for SR-Site has been improved, assuming the composition of the exchanger to be in equilibrium with the water at each point for the first time slice. Then, each exchanger is transferred to the next time slice, and the new mixed water is equilibrated at each grid point with the previous exchanger, modifying its final composition.

Scoping calculations with some "deduced" CEC values /Gimeno et al. 2008, 2009/ have been performed with the WATEQ4F.dat database (widely used to deal with exchange processes and previously used in the SR-Can exercise). Results suggest that no important differences with respect to the simulations without cation exchange are expected. However, some interesting indications on the qualitative effect of these processes over the main master variables have been found and deserve a more thorough study in future (see Appendix 3 for some examples).

In any case, when more data on CEC become available and the SKB-SrSite data base is upgraded (and verified) for the simulation of this type of processes, their inclusion in the PA calculation will be straightforward as the methodology is ready.

Once the PHREEQC output files have been obtained, another interface program is used to extract in a tabulated form the desired information contained in them (a Selected Output interface, Figure 3-4). Files generated with the Selected Output interface program are in the form of tables with the extracted information in columns and the grid points in rows. These files contain information on the composition of the waters at each grid point. The information included is indicated by the user in a specific format file (Appendix 1). The data extracted for this work as columns in these files are:

- X, Y, Z coordinates[12].
- Mixing proportions of the end-member waters for each point: Deep Saline, Old Meteoric, Glacial, Littorina and Altered Meteoric.
- Mass transfers for the equilibrated minerals.
- TDS.
- Molality of the elements included in the selected output's format file: result of mixing and reaction.
- pH, pe, ionic strength, total alkalinity, charge balance.
- Activity and molality of the selected species.
- Saturation indexes of the waters with respect to the selected mineral phases.

These selected results have been post-processed with different graphical tools (Origin and VOXLER; from OriginLab Corp. 2007, and Golden Software, Inc. 2006, respectively). In the case of the repository domain calculations (data points within the candidate repository volume), a specific statistic analysis has been performed for all the geochemical cases and all the studied periods. They have been compiled in tables and plotted as "Box-and-whisker plots", using ORIGIN, showing the statistical distribution of the chosen parameters. The statistical measures included are the median, the 1st, 5th, 25th, 75th, 95th and 99th percentiles, the mean, the maximum and the minimum values.

[12] The distance along the line calculated for the vertical plane is not stored here as it is not included in the PHREEQC output; therefore if the user wants to plot spatial distributions, this value must be calculated again using the following equation: $\text{Distance} = \sqrt{X^2 + Y^2}$.

4 Geochemical evolution of groundwaters over the time

As indicated at the beginning of this report, the main aim of the work presented here is to calculate and describe the chemical composition of the groundwaters in the rock volume around the repository in the Laxemar site. Because the barrier functions of a spent nuclear fuel repository will be required for periods of time of at least 100,000 years, changes in groundwater chemistry over at least one glacial cycle are evaluated.

Therefore, the future stages considered here cover the time span of a Quaternary glacial cycle, which is about 120,000 years. Hence, they include (Figure 1-1) the initial temperate period (including the operational period) and the evolution during the remaining glacial cycle[13] following that initial period. Immediately after the retreat of an ice sheet, isostatic depression will place the ground surface at the repository site under either glacial melt water lakes or brackish marine waters during a period of time between a few thousand years up to perhaps ten thousand years.

In this scheme, as it was done for Forsmark /Salas et al. 2010/ the excavation-operation period (that includes the re-saturation phase of the repository[14]; /SKB 2011/) has been conceptually treated in this chapter from the works performed by /Svensson and Follin 2010/. Moreover, no geochemical calculations were made for a series of key geochemical parameters over the whole glacial cycle due to the fact that they cannot be modelled with the available information and tools. They will be treated separately in Chapter 5.

In general terms, during the initial temperate period after closure, the infiltration of meteoric waters, the displacement of the Baltic shore line, and the changes in annual precipitation will influence the hydrology of the site. These phenomena will induce changes in the geochemical composition of groundwater around the repository. For the glacial cycle of the reference evolution (about 120,000 years) the Laxemar site will be covered by inland ice during a few periods with a total duration of less than 30,000 years (/SKB 2006d/, see Figure 1-1). The permafrost will not occur over a continuous period of time, but rather thawing will occur between more or less short periods of permafrost. Some of these permafrost periods will furthermore coincide with the time when the site is covered by an ice sheet, with “basal frozen” conditions.

It is expected that different groundwater compositions will prevail around the repository as a result of the different types of climate domains and their corresponding hydraulic conditions. The evolution between climate domains will be gradual, without a clear boundary between them.

This chapter has been organised around the different parameters of geochemical interest for the safety case (see Section 1.4). They will be treated in separate sections indicating their values and changes over the complete glacial cycle. When different geochemical variant cases have been analysed, the main results for all of them will be shown. Moreover, in order to test the reliability of the results, calculated data for the year 2000 AD in a vertical plane parallel to the coast and cross-cutting the repository volume (Figure 3-3) will be compared with the values measured in the natural system at present.

However, as all these geochemical parameters have been obtained from the salinity for each period (as given by the hydrogeological models), the first section of this chapter will show the raw data (salinity) to visualise the general expected evolution of the hydraulic and salinity conditions of the site over the time.

Then, the rest of the sections will go through each geochemical parameter or set of parameters using a common structure, indicating the results for the calculated values over time, with the evaluation of their contents and uncertainties, and a general description of their expected behaviour in each of the considered future stages (open repository, temperate period, glacial and periglacial periods and submerged period).

[13] In this section, the term “glacial period” includes the permafrost and glacial stages.

[14] It will take several hundreds of years for the repository to reach full saturation /SKB 2011/.

The chemical characteristics of Laxemar groundwaters prior to the construction of the repository are set out in detail in their corresponding Site Descriptive Model, version 2.3 /Laaksoharju et al. 2009/ and have been summarised in Chapter 2.

The statistical results within the candidate repository volume are graphically presented as box and whisker plots. When variant geochemical cases have been constructed, their corresponding plots are also shown. All these statistical results, including the corresponding values obtained for the vertical slice parallel to the coast cross-cutting the repository, are included in the form of tables in Appendix 4.

4.1 Salinity evolution from the hydrogeological models

This section shows the evolution of salinity, as given by the hydrogeological models, over the whole cycle. The results obtained for the natural conditions previous to the repository construction (panels a in Figures 4-1 and 4-2; distribution of values at repository depth and in a vertical plane, respectively) show a narrow range of salinity values for almost all grid points between 5.6 and 24 g/L. When the effects of the repository construction are simulated (panels b in Figures 4-1 and 4-2) a clear decrease in the salinity in almost all the volume (green, from 0.3 to 1.3 g/L) is predicted.

During the temperate period previous to the development of the glacial cycle (panels c, d, e and f in Figures 4-1 and 4-2), salinities in the repository volume are predicted to be in a range between 0.3 and 24 g/L slightly higher than during the open repository conditions. However from the year 2000 to the year 15000, a clear decrease in the number of grid points with high values (orange colour) is seen.

The salinity distribution simulated for the Stage Ice 0 of the glacial period (panels g in Figures 4-1 and 4-2) is quite similar to the one obtained for the last time slice in the temperate period (despite the different methodology used in the construction of the two hydrogeological models; see Section 3-1). When the glacier advances over an unfrozen soil (stages Ice I, Ice II and Ice III; panels h, i and j in Figures 4-1 and 4-2), higher salinities (between 12 and 30 g/L) have been computed in the repository volume just ahead of the ice front as a consequence of upconing processes.

However, behind the ice front (covered by the ice sheet), salinities decrease from 0.3 down to 0.001 g/L due to the infiltration of glacial melt waters in all the domain. The same dilution is seen once the ice sheet totally covers the area of the Laxemar site (stages Ice IV and Ice V; panels k and l in Figures 4-1 and 4-2).

After 11,000 years, during which the unfrozen soil of the Laxemar area remains under the ice sheet, the glacier begins to retreat (stages Ice Vr, IVr and IIr; panels m, n and o in Figures 4-1 and 4-2). In these stages, upconing (in front of the ice front, as shown in the picture corresponding to Ice IIr stage; panels o in Figures 4-1 and 4-2) is again responsible of transporting saline groundwaters to repository depths, reaching values locally between 0.3 and 1.3 g/L. At the end of the glacial cycle, a lake of glacial melt waters is supposed to cover the Laxemar region (stage Ice 0r; panels p in Figure 4-1 and 4-2). In this period, the same range of salinities (0.3 to 0.7 g/L) will affect the candidate repository volume. It is expected that salinity will decrease with time.

A periglacial condition is simulated as well for the first stages of the glacial period, assuming that the ground is frozen to some extent under the ice sheet. Permafrost and freezing of groundwater reach greater depths at Forsmark than at Laxemar. This is mainly due to differences in climate and bedrock thermal properties. Results are compared with the ones just presented above for the glacial period in Figures 4-1 and 4-2. Stage Permafrost 0 (panels c in Figures 4-3 and 4-4), at the beginning of this period, predicts salinities in the repository volume slightly lower than when permafrost is not considered (panels b in Figures 4-3 and 4-4) in general between 0.3 to 1.3 g/L and only in the SE area they can reach 5.6 g/L. As soon as the glacier begins its advance over the frozen ground and before its front arrives to the superficial domain over the candidate repository volume, salinities, in general, decrease behind the ice front (to a maximum of 0.32 g/L) maintaining values up to 5.6 g/L ahead of the ice front (mainly in the SE zone), even at slightly shallower depth, by upconing, although not as marked as when the ice advances over an unfrozen ground. It seems that the presence of a permafrost system is one of the key factors controlling the change of salinities in groundwaters during the glacial and the periglacial conditions.

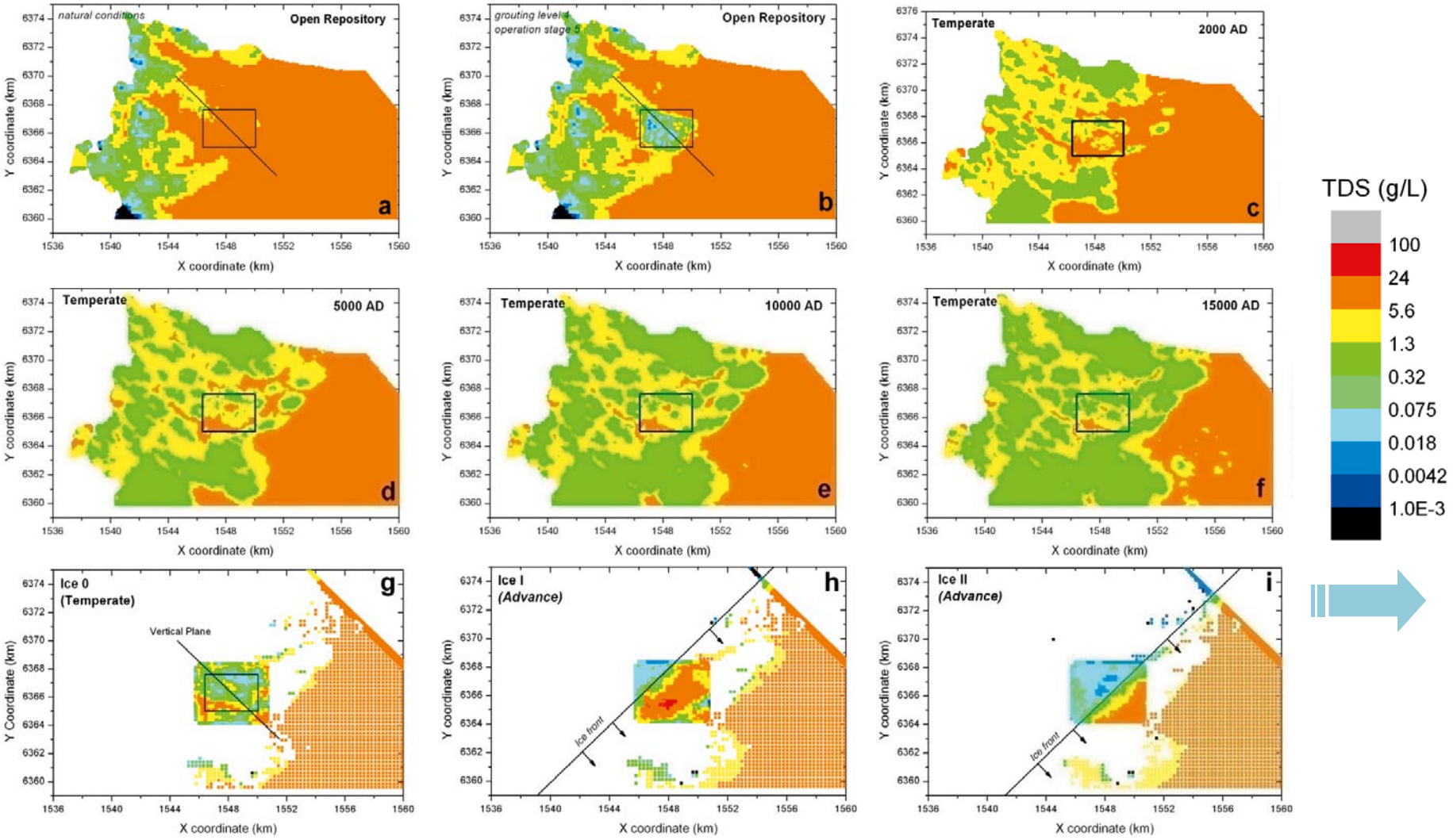

Figure 4-1. *Sequence of salinity time frame as estimated by the hydrological calculations (expressed as TDS: total dissolved solids, g/L) in a 500 m depth plane over the open repository (a, b), temperate (c, d, e, f), and the beginning of the glacial (Ice 0 to Ice II; g, h, i) periods. The area enclosed by the black rectangle corresponds to the repository volume.*

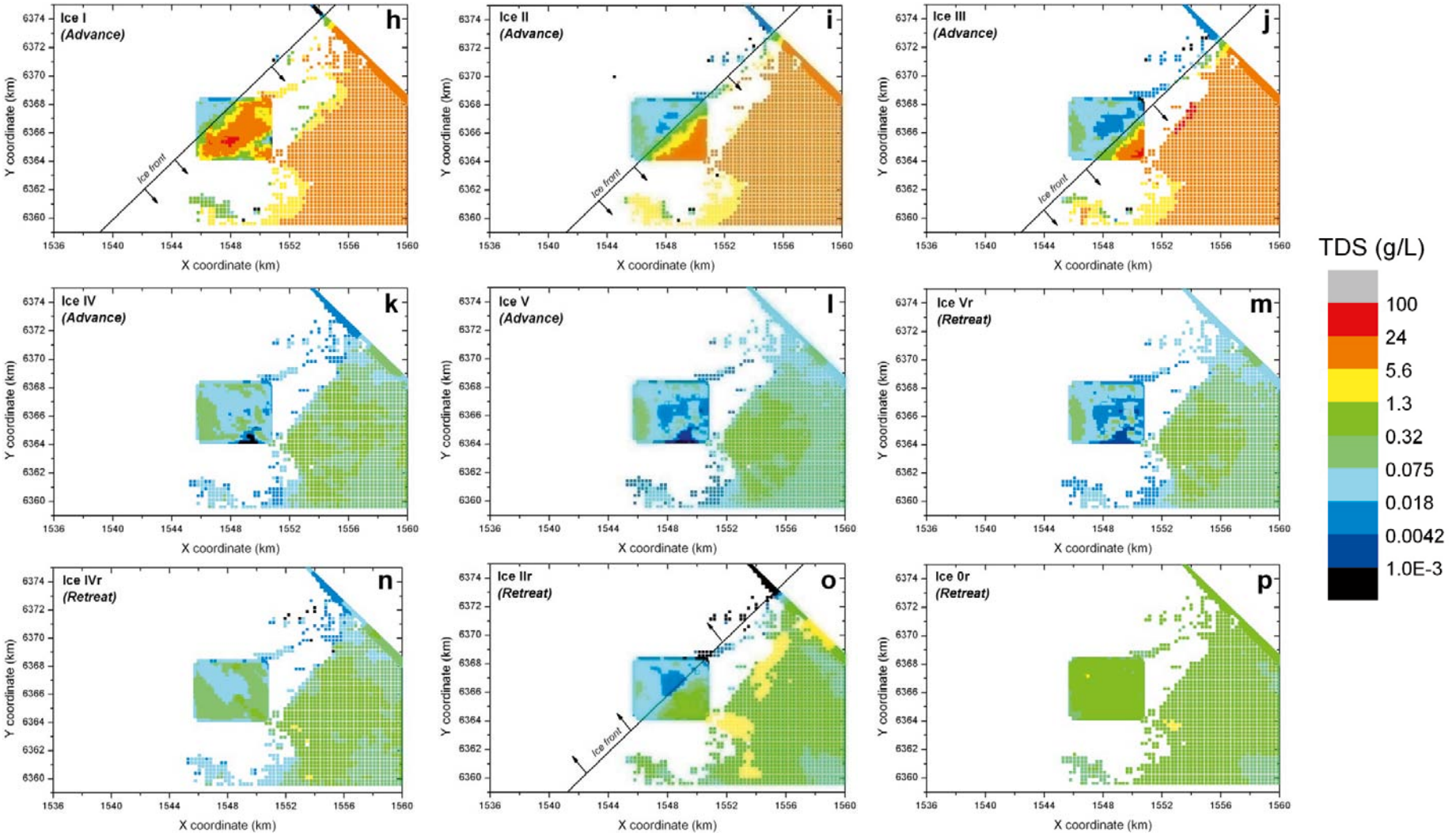

Figure 4-1 cont. *Sequence of salinity time frame as estimated by the hydrological calculations (expressed as TDS: total dissolved solids, g/L) in a 500 m depth plane over the remaining glacial cycle (advance: Ice I to Ice V, h to l; retreat: Ice Vr to Ice 0r, m to p).*

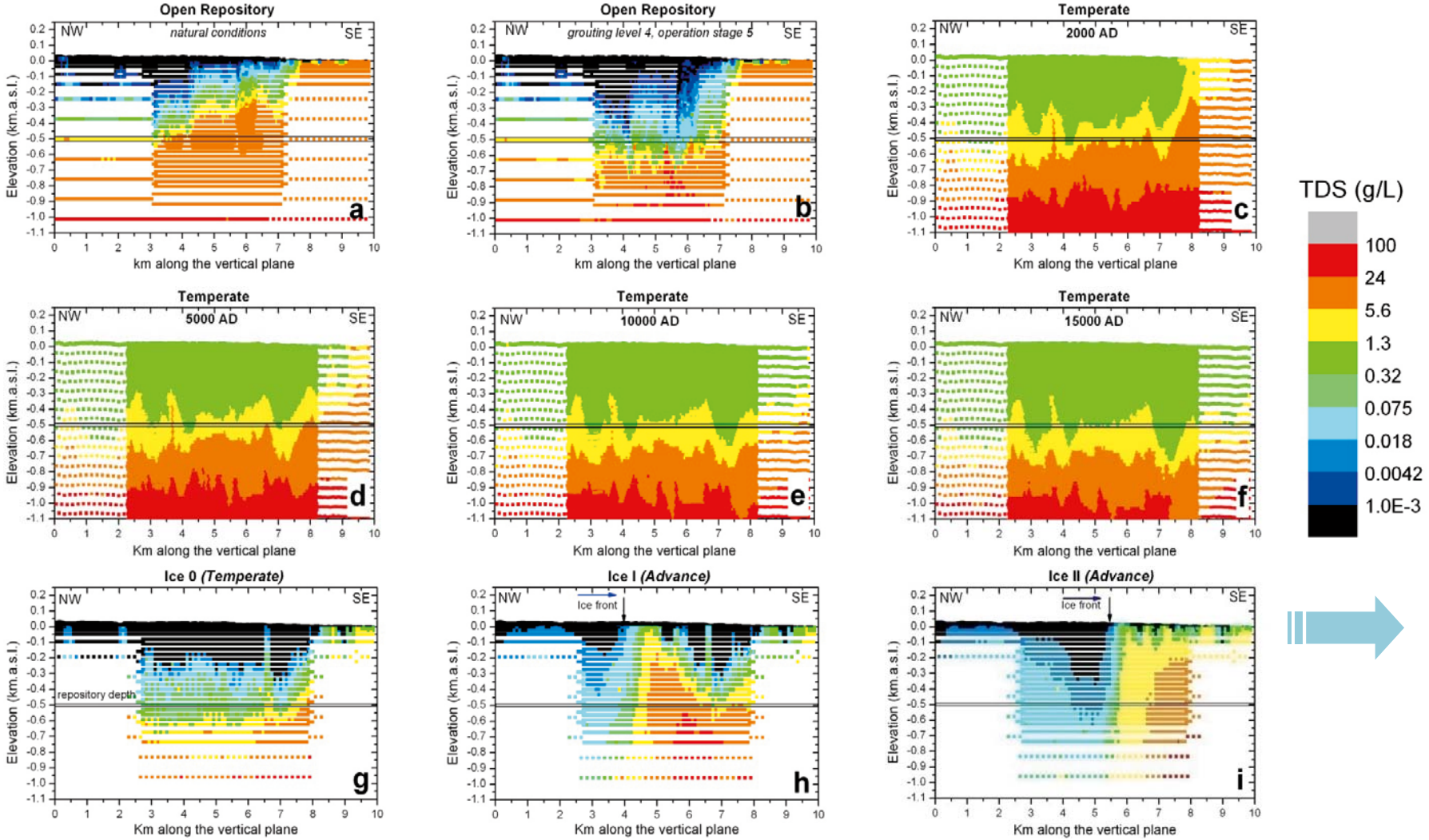

Figure 4-2. *Sequence of salinity time frames as estimated by the hydrological calculations (expressed as TDS, total dissolved solids, g/L) in a vertical section (parallel to the coast cutting across the repository volume) over the open repository (a, b), temperate (c, d, e, f) and the beginning of the glacial periods (Ice 0 to Ice II; g, h, i). The vertical scale is enlarged 20 times with respect to the horizontal scale.*

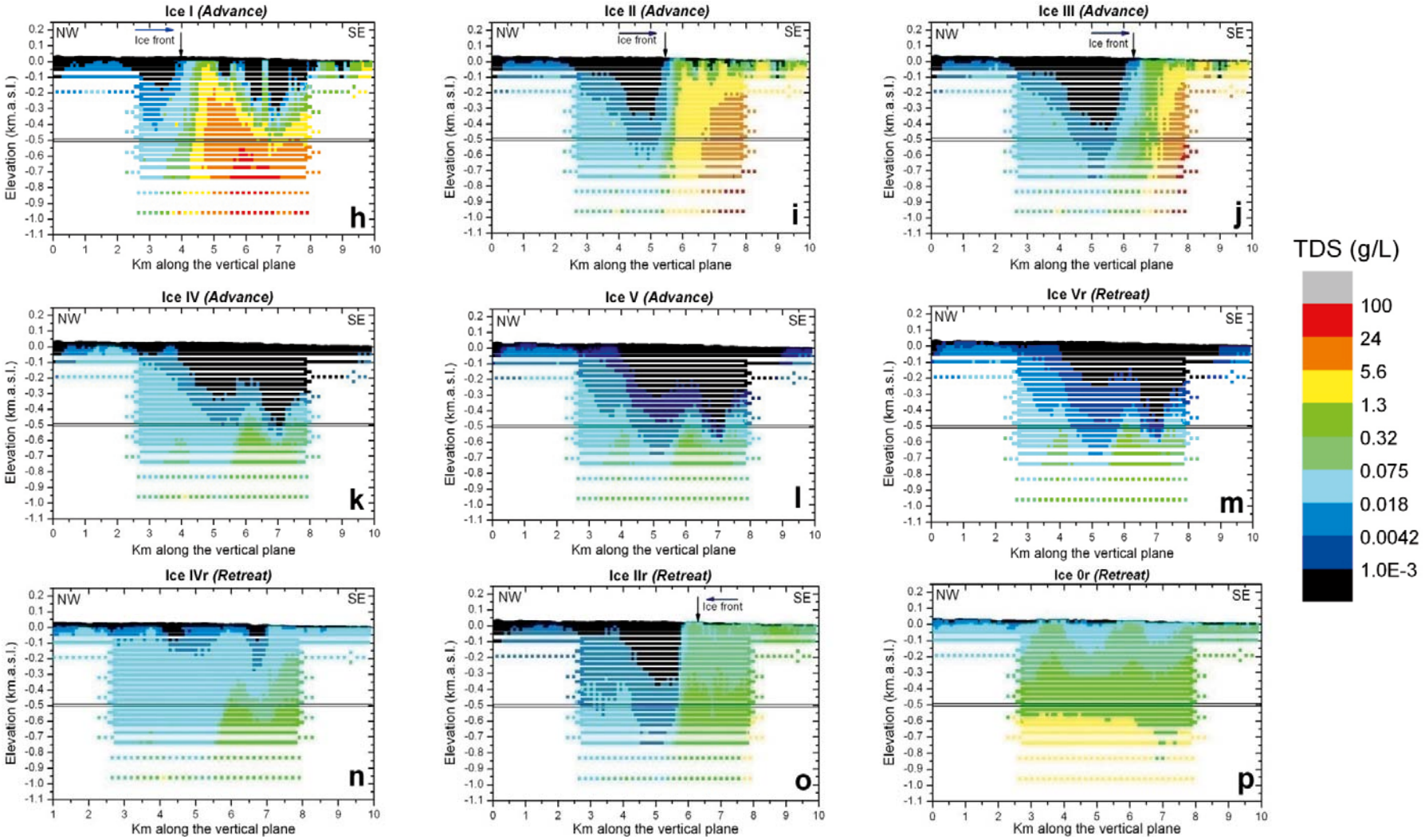

Figure 4-2 cont. *Sequence of salinity time frames as estimated by the hydrological calculations (expressed as TDS, total dissolved solids, g/L) in a vertical section (parallel to the coast cutting across the repository volume) over the remaining glacial cycle (advance: Ice I to Ice V, h to l; retreat: Ice Vr to Ice 0r, m to p). The vertical scale is enlarged 20 times with respect to the horizontal scale.*

When the whole area is covered by the ice sheet (stage Permafrost IV; panels k in Figures 4-3 and 4-4) the distribution of salinity is very similar to the one obtained for the glacial period (panels j in Figures 4-3 and 4-4) and the rest of the evolution is expected to be the same.

Then, immediately after the retreat of the ice sheet, isostatic depression will place the ground surface at the repository site below the Baltic Sea surface level for a period of time. In the reference evolution, the Laxemar site is expected to be below glacial melt water lakes and then below marine or brackish waters for a period of time between a few thousand years up to perhaps ten thousand years. The first period corresponds to the last stage of the glacial evolution (stage Ice 0r) and it is denoted as the "submerged under fresh waters period" in Figure 4-5 (panels a and c). The second period is thought to be the same as during the maximum of salinity of the Littorina stage at the year 3000 BC and it is denoted as "submerged under marine waters period" in Figure 4-5 (panels b and d). A relatively fast turnover of groundwaters, where glacial melt is replaced by a succession of waters penetrating from the surface, is expected during this period: the equivalent to the Littorina sea gradually evolving into the equivalent to the present-day Baltic Sea.

The distribution of salinity during the submerged periods is shown in Figure 4-5. Panels a and c in this figure are the same as panels i in Figures 4-1 and 4-2 corresponding to the glacial stage Ice 0r. Then, panels b and c in Figure 4-5, showing the TDS distribution over the period in which the site is submerged under marine waters resemble those for the present time (open repository period under natural conditions, panels a in Figures 4-1 and 4-2, or year 2000 AD, panels c in Figures 4-1 and 4-2) though salinities are slightly higher, with almost all the repository volume having salinity values from 0.6 to 19 g/L.

The salinity distribution has been translated into mass fractions (or mixing proportions) of the reference waters, either by the hydrogeologists themselves (temperate and submerged under marine water periods) or by the authors of this report (glacial and permafrost periods; see Section 3.1.2). Plots showing the distribution of the different reference waters over time are included in Appendix 5, but a summary of the main findings is included below.

During the temperate period, the main hydrological process controlling the hydrogeochemical evolution in the Laxemar area is the infiltration of meteoric origin groundwaters from the surface. Meteoric waters displace and dilute the groundwaters already present in the Laxemar fractures. Groundwater convection and the evolution of the compositional fronts are strongly controlled and modified by the existence of high conductive areas associated with the fracture zones.

In general, the fraction of meteoric waters (represented by the Altered Meteoric end member, AM in the plots) increases over the temperate period in such a way that starting from a wide range of proportions (from 0 to 1) in the year 2000 AD, it is almost 1 in all the repository volume by the end of the temperate period. At the same time, the rest of the reference waters already present in the fractures (before the input of meteoric recharge), decrease their importance. The most saline end member (Deep Saline, DS in the plots) tends to disappear (from fraction values between 0 and 0.2 in the repository volume at year 2000 AD, to less than 0.1 at 15,000 AD in most of the points). The same happens with the Old Meteoric and the Glacial waters (OM and Gl in the plots, respectively): their fractions decrease from maxima values of 0.2 from OM and 0.4 for Glacial in most of the repository volume at 2000 AD, to less than 0.1 at 15,000 AD in most of the points. Littorina was barely present at repository depth in the Laxemar area during the temperate period, only in the Eastern part of the regional area, closer to the sea, some zones show Littorina fractions up to 0.5 but the number of grid points with such values tends to decrease with time.

During the remaining glacial cycle, salinities are basically controlled by (1) the infiltration of glacial melt waters and (2) the transport of saline waters from the deepest areas by upconing. Another key factor for the solute distribution is the existence of a frozen soil (permafrost conditions). The development of permafrost increases groundwater salinities within the candidate repository volume during the first stage of the glacier advance. This is clearly seen in the distribution of mixing proportions. Meteoric waters occupy almost the whole repository volume at the beginning of the glacial cycle (even more if the ground is frozen). But then, its fraction decreases as the ice front advances until the final stage of the submerged under fresh waters period is reached. Only when the submerged under marine waters case is included, some influence of meteoric waters is seen in the Western part of the system, though the repository volume does not show any evidence of that. Deep Saline fractions only increase during the upconing events (and only up to a maximum of 0.2) ahead of the ice front. Otherwise they are always lower than 0.1 except when the site is finally submerged under marine waters when slightly higher fractions (up to 0.2) can be found in the repository volume (reaching 0.3 in some grid points).

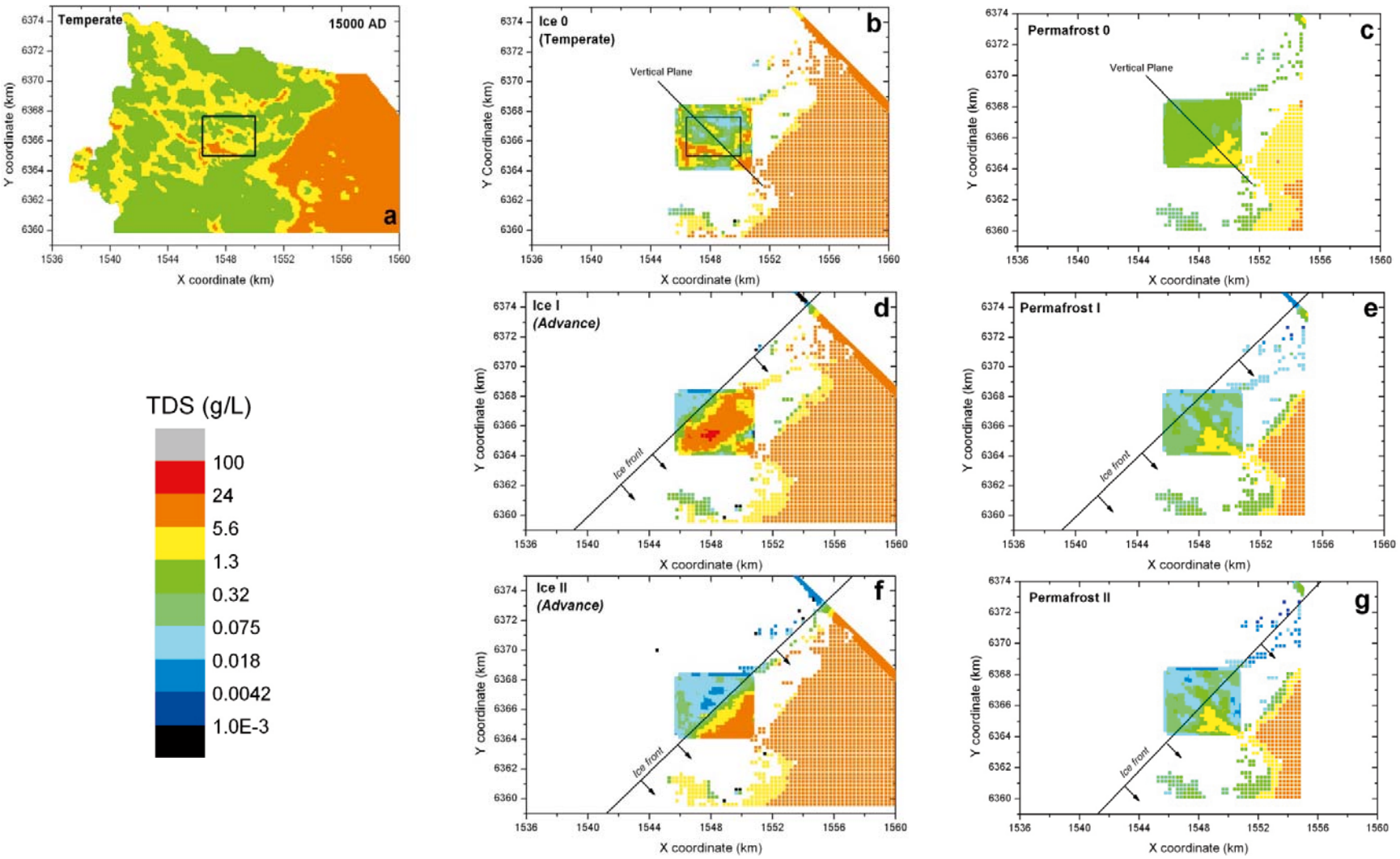

Figure 4-3. *Sequence of salinity time frames as estimated by the hydrological calculations (expressed as TDS, total dissolved solids, g/L) in a 500 m depth plane for the final stage of the temperate period (a), and the stages Ice 0 (b, c), Ice I (d, e) and Ice 2 (f, g) of the glacial period without (left plots; b, d, f) and with permafrost (right plots;c, e, g) development.*

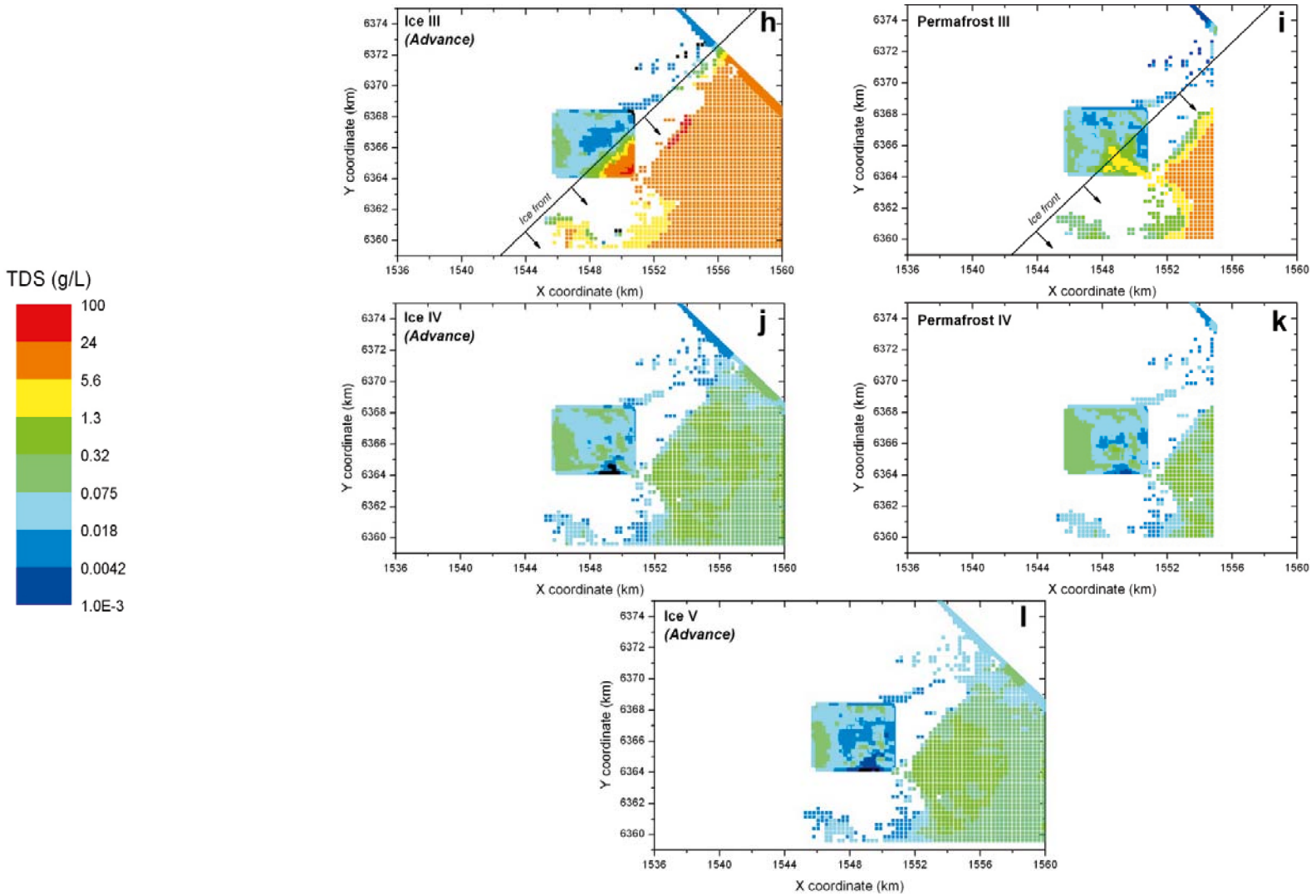

Figure 4-3 cont. *Sequence of salinity time frames as estimated by the hydrological calculations (expressed as TDS, total dissolved solids, g/L) in a 500 m depth plane for the stages Ice III (a, b), Ice IV (c, d) and Ice V (e) of the glacial period without (left plots; a, c, e) and with permafrost (right plots, b, d) development.*

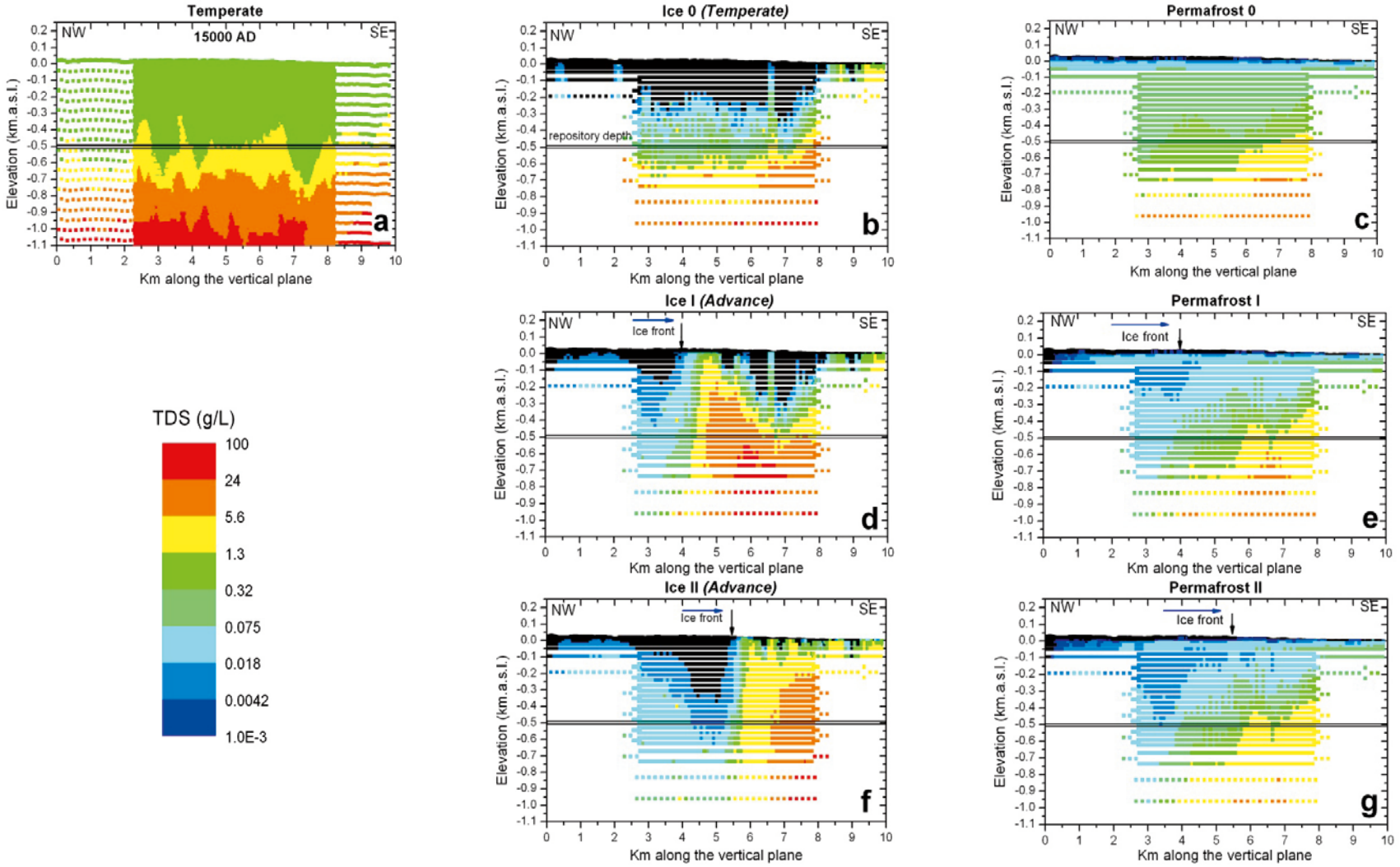

Figure 4-4. *Sequence of salinity time frames as estimated by the hydrological calculations (expressed as TDS, g/L) in a vertical section parallel to the coast cross-cutting the repository volume, for the final stage of the temperate period (a), and the stages Ice 0 to Ice II (b to g) of the glacial period without (left plots; b, d, f) and with permafrost (right plots;c, e, g) development. The vertical scale is enlarged 20 times with respect to the horizontal scale.*

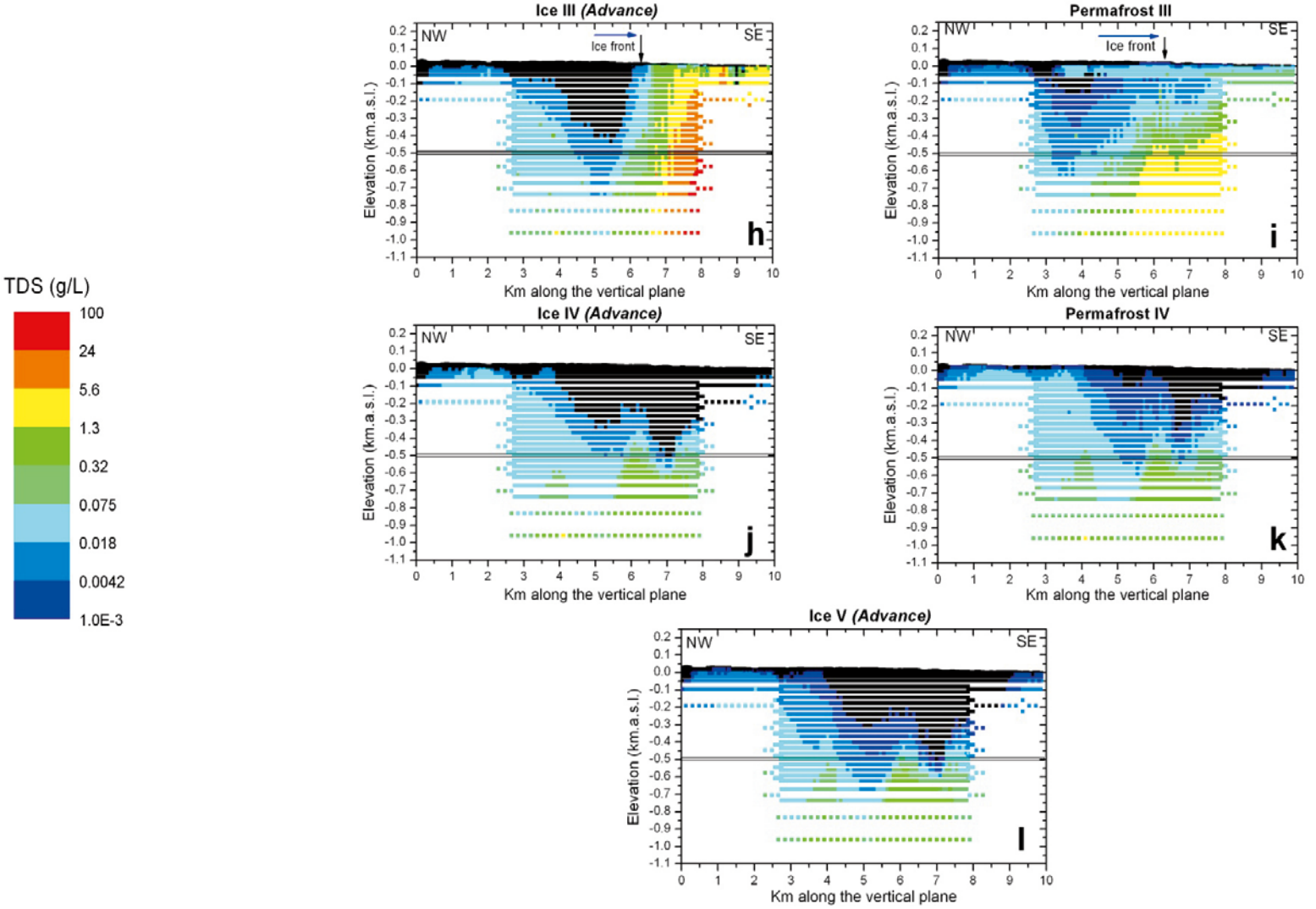

Figure 4-4 cont. *Sequence of salinity time frames as estimated by the hydrological calculations (expressed as TDS, g/L) in a vertical section parallel to the coast cross-cutting the repository volume, for the stages Ice III to Ice V of the glacial period without (left plots; h, j, l) and with permafrost (right plots, i, k) development. The vertical scale is enlarged 20 times with respect to the horizontal scale.*

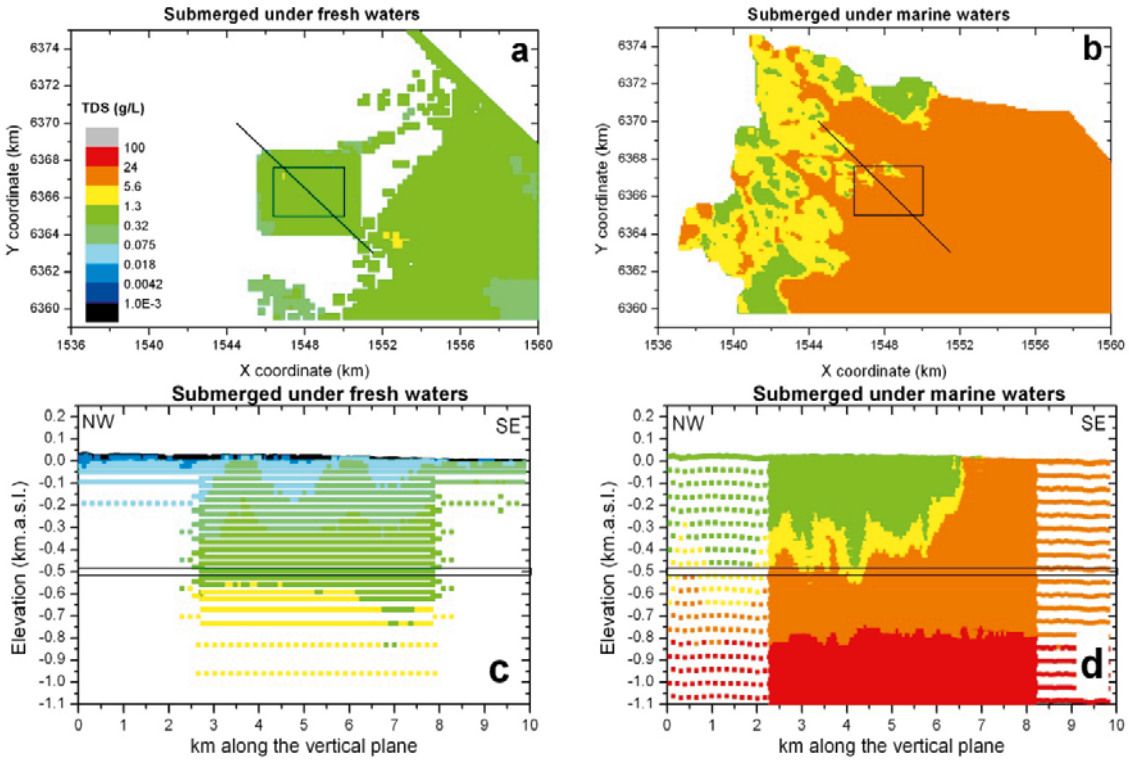

Figure 4-5. *Sequence of salinity time frames as estimated by the hydrological calculations (expressed as TDS, total dissolved solids, g/L) in a 500 m depth plane (a and b) and in a vertical section parallel to the coast cross-cutting the repository volume (c and d; with the vertical scale enlarged 20 times with respect to the horizontal scale) for the final stages of the glacial cycle where the site is submerged under fresh (a and c) or marine (b and d) waters.*

As already indicated in Section 3.1.2, the results obtained for the Glacial end member must be taken with care due to the simplification of the approach to obtain the mixing proportions from the salinity results. It must be kept in mind that the procedure to obtain the mixing proportions (Figure 3-1) evaluates the difference of salinity in a point between two consecutive stages; if the new salinity is higher than the previous one, it is assumed that some saline water fraction has been added. This is not a big problem as the only saline end member present in the system is the Deep Saline. But if the new salinity is lower than the previous one, it is also assumed (simplified assumption) that the only water able to dilute the mixture is the glacial water, which is true underneath the glacial sheet but not ahead of it in the uncovered area. The problem is that with only the information of salinity (TDS) values there is no way to discriminate between the different dilute end-members. Thus, some odd results can locally occur although these do not modify the general picture (see Section 3.1.2 and Figure 3-2). In any case, these results should be read as follows: at the beginning of the glacial cycle, the glacial fraction at repository depth is lower the 0.1, however, as the ice moves towards the site, the amount of glacial melt-water in the system increases up to fractions of 1 just below the ice front. However, the vertical section shows some important glacial fractions ahead of the ice front and towards the south-east which cannot be interpreted as glacial melt water. They would correspond to non-glacial dilute waters, probably meteoric water.

During the final stage of the glacial cycle, when the repository is covered by fresh waters, all the repository volume is dominated by Glacial melt waters (fractions from 0.8 to 1). However, when seawater covers the area, the infiltration of marine water could affect the transient amount of solutes in groundwaters within the candidate repository domain as the marine water fractions are predicted to reach values up to 0.5.

The following sections describe the evolution of the main geochemical parameters over the different periods, either through the description of the calculated results (temperate, glacial, with or without permafrost, and submerged under fresh or marine water periods), or through some considerations based on what it is expected (open repository).

4.2 Evolution of the main geochemical groundwater components

This section describes the evolution of the main chemical components of the groundwaters over the simulated periods. These salinity-related components are: TDS, ionic strenght, chloride (as one of the main component of salinity) and the sum of the four main cations (Ca, Mg, Na and K) expressed as the safety function $\sum q[M^{q+}]$ indicated in Chapter 1 (Figure 1-3; /SKB 2011/). Finaly some comments on sulphate and bicarbonate are also included. The main common character of all these parameters is that their concentrations do not depend on the geochemical variant case used for the calculations (different redox model, and coupled or uncoupled thermodynamic data base).

4.2.1 Open repository period

As no geochemical calculations have been done for this period, no additional information on salinity, to the one indicated in the previous section for salinity, can be added.

The groundwater salinity and composition in the vicinity of the repository will change during this period because of the inflow into open tunnel sections. This will cause an unnatural infiltration of meteoric and Baltic seawater and, as a consequence, upconing may occur. This phenomenon has been observed, for example, in some boreholes at Äspö. In extreme cases, if groundwaters at greater depth have high salinities, upconing might decrease the swelling pressure of the backfill (safety function indicator R1b; Section 1.4.1, Figure 1-3; /SKB 2011/). However, no such highly saline groundwaters have been found in the simulations performed for this period (see Section 4.1).

Inflow to the tunnels will be reduced by injecting grout into the surrounding fractures. This will reduce the depression of groundwater levels near the ground surface and the corresponding inflow of meteoric and seawaters as well as the upconing of saline waters.

Once the repository has been backfilled and closed it is expected that groundwater salinities (and therefore its main chemical components) will return to normal conditions after some time.

4.2.2 Temperate period

Geochemical calculations were performed for this period and a more detailed description on the different parameters evolution is included here.

However, before describing the main results of the geochemical modelling, it is worth seeing how reliable these results are by comparing the values obtained for the present time (year 2000 AD) with the actual values measured in the system. These values have been taken from the SDM work /Laaksoharju et al. 2009, Gimeno et al. 2009/. Considering that the groundwater samples have been taken in the system in punctual locations in the boreholes, at different depths, this comparison has been made with respect to the results obtained for the vertical section parallel to the coast and crossing the repository volume (see Figure 3-3). Therefore, these results cover a wider range of groundwater compositions[15].

As the main components of salinity, Figure 4-6 shows the distribution with depth of the concentration of chloride (Figure 4-6a), the sum of the main cations (Figure 4-6b; safety function indicator, $\sum q[M^{q+}]$; Section 1.4.1, Figure 1-3; /SKB 2011/) and the contents of the main cations separately (Ca, Na, Mg and K, Figure 4-6 c, d, e and f[16]). The figure compares the measured values with those predicted by geochemical modelling. The graphs only show the system below 100 m depth as the upper part of the bedrock cannot be appropriately simulated with this approach[17].

[15] Basic statistics of this section (for this and all other periods) are not included in the plots but can be found in Appendix 4 (Tables A4-17 to A4-20).

[16] Ions concentration is expressed as molality (mol/kg H_2O) in all the cases (plots and text) and the units are indicated as mol/kg. Except for the Deep Saline reference water, with a density of 1.05 kg/L, molality is equivalent to Molarity (mol/L) in all the cases.

[17] Shallow waters are mainly controlled by reaction processes and mixing proportions obtained at these depths are meaningless.

The trends and the range of variation found in the real samples and in the calculated results agree qualitatively between them, not only for elements mainly controlled by mixing (Cl and Na) but also for other elements more affected by water-rock reactions (Ca, Mg and K). Apart from the fact that these results give confidence in the rest of the calculations for future stages, it suggests that most significant processes involved in the groundwater evolution have been taken into account in the conceptual model.

As known from the Site Descriptive Model /Laaksoharju et al. 2009, Gimeno et al. 2009/ calcium mainly participates in the equilibrium with calcite and in cation-exchange reactions. However, the high Ca content of the present mixed waters (derived from the calcium-rich Deep Saline end member) obliterates the effects of mass transfers associated with those reactions (see /Gimeno et al. 2009/. Thus, calcium in groundwaters deeper than ≈100 m (the ones shown in the plots) may be simulated by mixing of the different end members (reference waters) with minor influence of chemical reactions.

Magnesium contents are considerably lower than those of calcium and mainly controlled by water-rock reactions (chlorite and/or cation exchange, see Appendix 3) although these reactions have not been included in the simulations. In spite of this, the fit between calculated and measured values is very good. Potassium concentrations are also low in groundwaters (as is the case in other Fennoscandian sites in granitic rocks) and they could be solubility controlled by sericite /Nordstrom et al. 1989/, as well as by cation-exchange (Appendix 3). However, as indicated for Mg, these reactions have not been included in the simulations.

Although sulphate is not listed in the safety function indicator criteria, it is important when determining the solubility limits for radium or as electron acceptor for sulphate reducing bacteria activity. Alkalinity (bicarbonate) is another important parameter to take into account according to its role in chemical reactions. The comparison of measured *versus* predicted sulphate and bicarbonate values is shown in Figure 4-7. Considering all the uncertainties, simplifications and limitations of this approach, it is noticeable that the results in general cover the ranges and follow the trends found in the natural system, giving more confidence to the whole calculations procedure. For sulphate some of the lowest and highest values in the system (at shallow and deep depths, respectively) have not been reproduced by the simulations[18]. Calculated alkalinity reproduce quite satisfactorily the range of variability and the distribution with depth observed in the natural system.

As shown in Chapter 2, deep Laxemar groundwaters tend to reach equilibrium with gypsum (something that has not been found in Forsmark; /Gimeno et al. 2008/). When the saturation indices of the simulated waters with respect to this mineral (Figure 4-7c) are compared with the values obtained for the real groundwaters, a fairly good agreement in the values and trend can be seen, except for a small group of groundwaters in equilibrium with gypsum. This group of groundwaters mainly correspond to the deep groundwaters in Figure 4-7a which are outside the simulated range. To go into this problem in more detail, equilibrium with gypsum should have been imposed in the simulations. However, as these equilibrium situations are only locally found in the deeper levels of the real system, they have not been included in the calculations.

Having shown the reliability of the approach, the description of the future evolution of groundwater chemistry, specifically groundwaters enclosed into the repository volume, as obtained by applying the methodolgy presented in Chapter 3 is now described.

Starting with the TDS (or the ionic strength obtained with PHREEQC) its depth gradient in the Laxemar domain is large due to the presence of saline groundwaters at depths below 600-700 m (see Appendix 5), and to the existence of some dilute groundwaters down to those depths resulting from the infiltration of meteoric waters in the shallowest parts of the fractured aquifer. During the temperate period, groundwaters are affected by increasing amounts of meteoric waters (see also Appendix 5). On a regional scale this corresponds to a gradual decrease of salinity, especially in the upper part of the modelled rock volume (see previous section). TDS mean values decrease progresively with time in the repository volume from about 5,000 mg/L for the year 2000 AD, to around 2,000 mg/L for the year 15,000 AD (Figure 4-8a). The minimum salinity calculated at repository depth is around 500 mg/L since the beginning of the temperate period and remains fairly constant until its end.

[18] The lowest values are associated with dilute waters found at quite deep locations (down to 300 m). These dilute groundwaters are being investigated at present as they may be related to leakages during sampling.

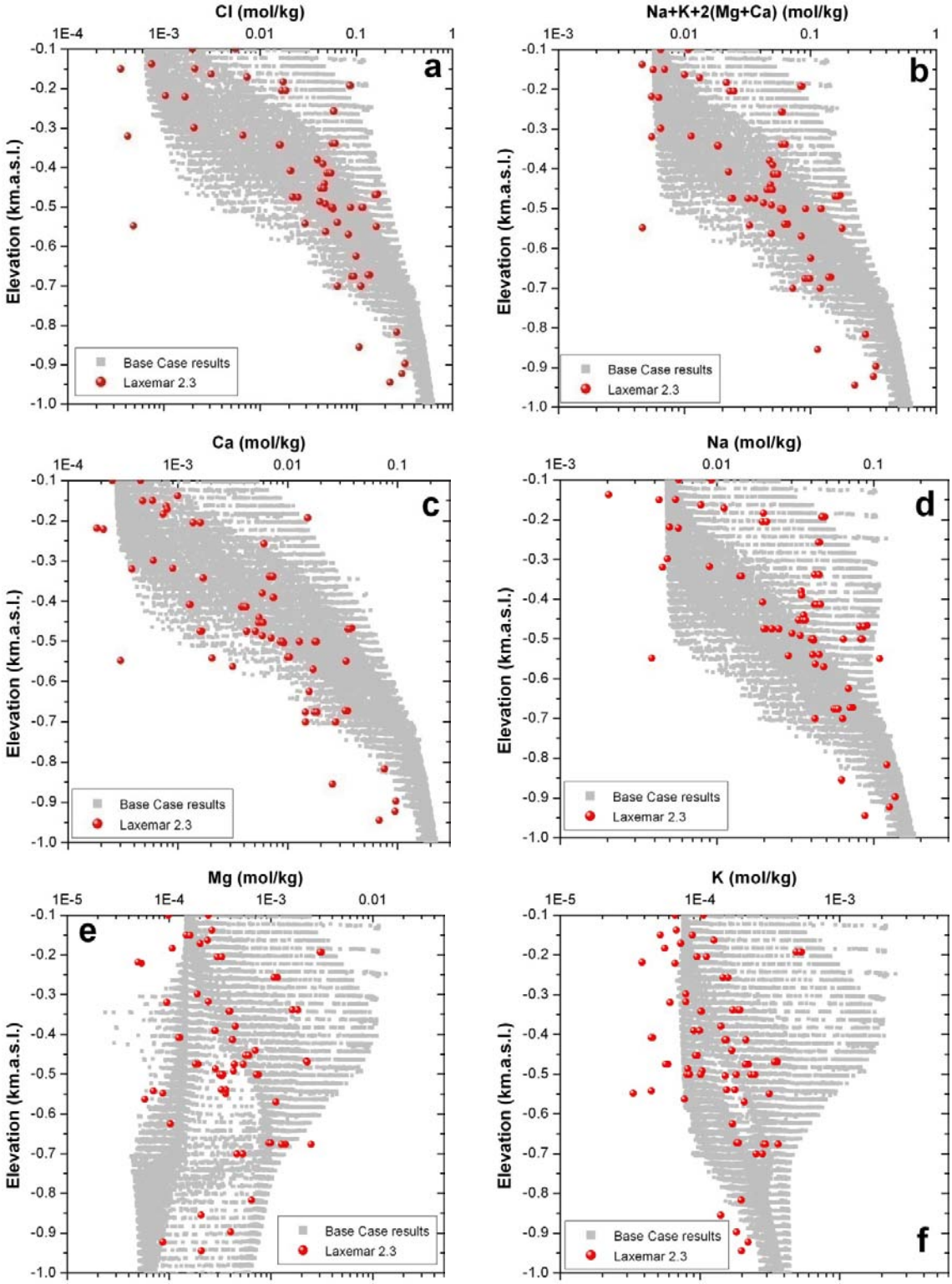

Figure 4-6. *Concentration-depth graphs for chloride and the main cations measured in groundwater samples (red spheres) and obtained by geochemical modelling for the year 2000 AD (grey squares) in a vertical section parallel to the coast (NW-SE) cross-cutting the repository volume. Concentrations are expressed as molality (mol/kg). (a) chloride, (b) sum of cations, (c) calcium, (d) sodium, (e) magnesium and (f) potassium. Groundwater data taken from /Laaksoharju et al. 2009/.*

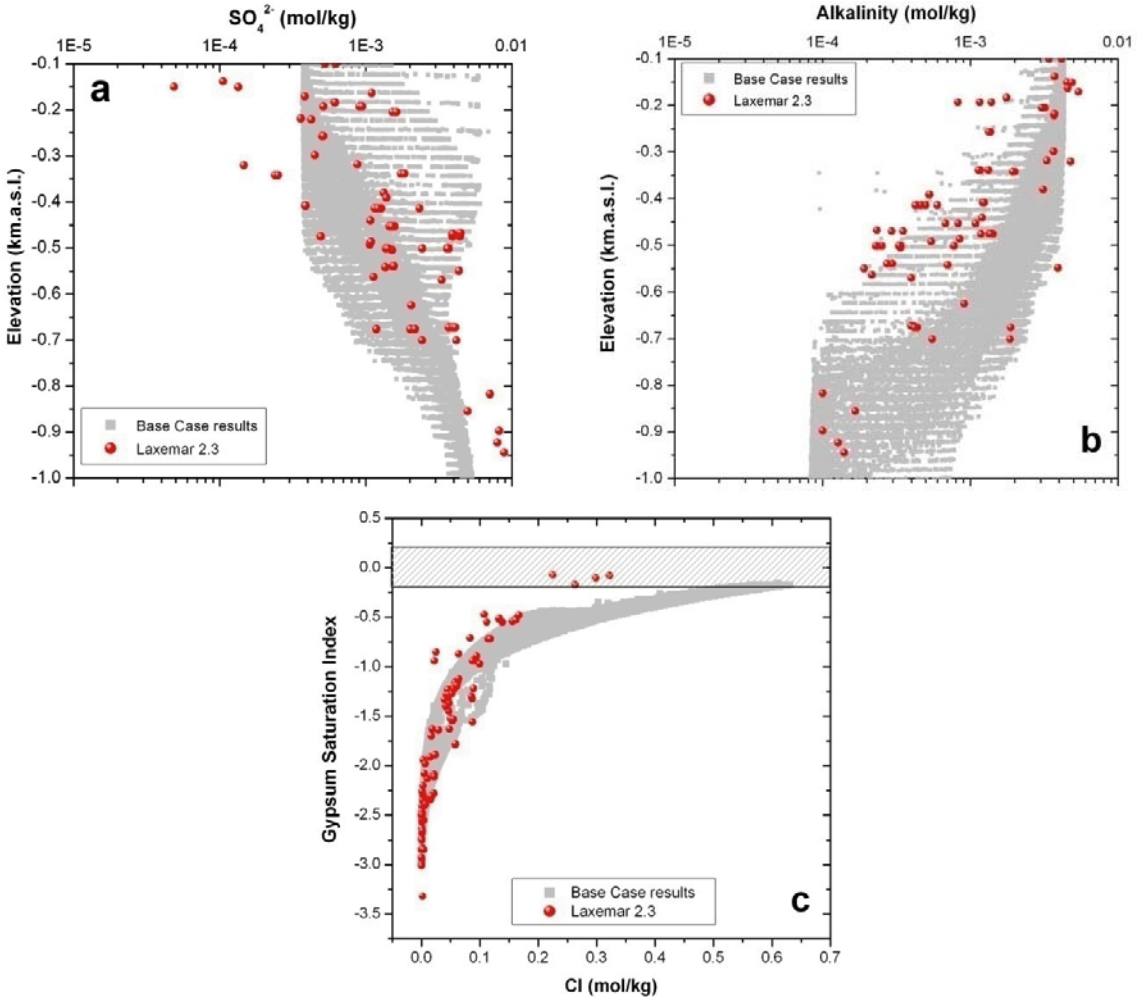

Figure 4-7. *Concentration-depth graphs for sulphate (a) and alkalinity (b) measured in the groundwater samples (red spheres) and predited by geochemical modelling for the year 2000 AD (grey squares) in a vertical section parallel to the coast (NW-SE) cross-cutting the repository volume. Concentrations are expressed as molality (mol/kg). Panel (c) shows the saturation index of the real waters with respect to gypsum compared with the values obtained for the simulated waters.*

As a summary, it could be said that at the beginning of this period, all waters have a TDS value above 1,000 mg/L while towards the end of the modelled period (15,000 AD; Figure 4-8a), approximately 25% of the groundwaters within the repository volume have less than 800 mg/L of dissolved salts. The ionic strength and chloride values[19] mimic the ones shown for TDS (Figure 4-8b and c). Therefore, salinities during the first temperate period following repository closure will probably remain limited at Laxemar, ensuring that the swelling properties of the buffer and backfill are not negatively affected.

As indicated above, the presence of specific cations is important as their concentration decreases the stability of colloids. The criterion for the safety function indicator is expressed in charge equivalents as $\sum q[M^{q+}]$ (Figure 4-8d). This value has to be higher than 0.004 mol/kg /SKB 2011/. Figure 4-8d shows the evolution of this safety function along the simulated temperate period. It is clear that for the period following repository closure, cation charged concentrations in the repository volume in Laxemar will probably remain higher than 0.004 mol/kg, guaranteing that montmorillonite colloids are unstable in solution. Even when waters of meteoric origin are the major groundwater contributor in the mixing (15,000 AD), the safety function indicator $\sum q[M^{q+}]$ remains higher than 0.004 mol/kg.

[19] Despite not being listed in the safety function indicator criteria, chloride is used when selecting radionuclide transport properties (sorption coefficients). It behaves conservatively and has been modelled by mixing calculations in SR-Site.

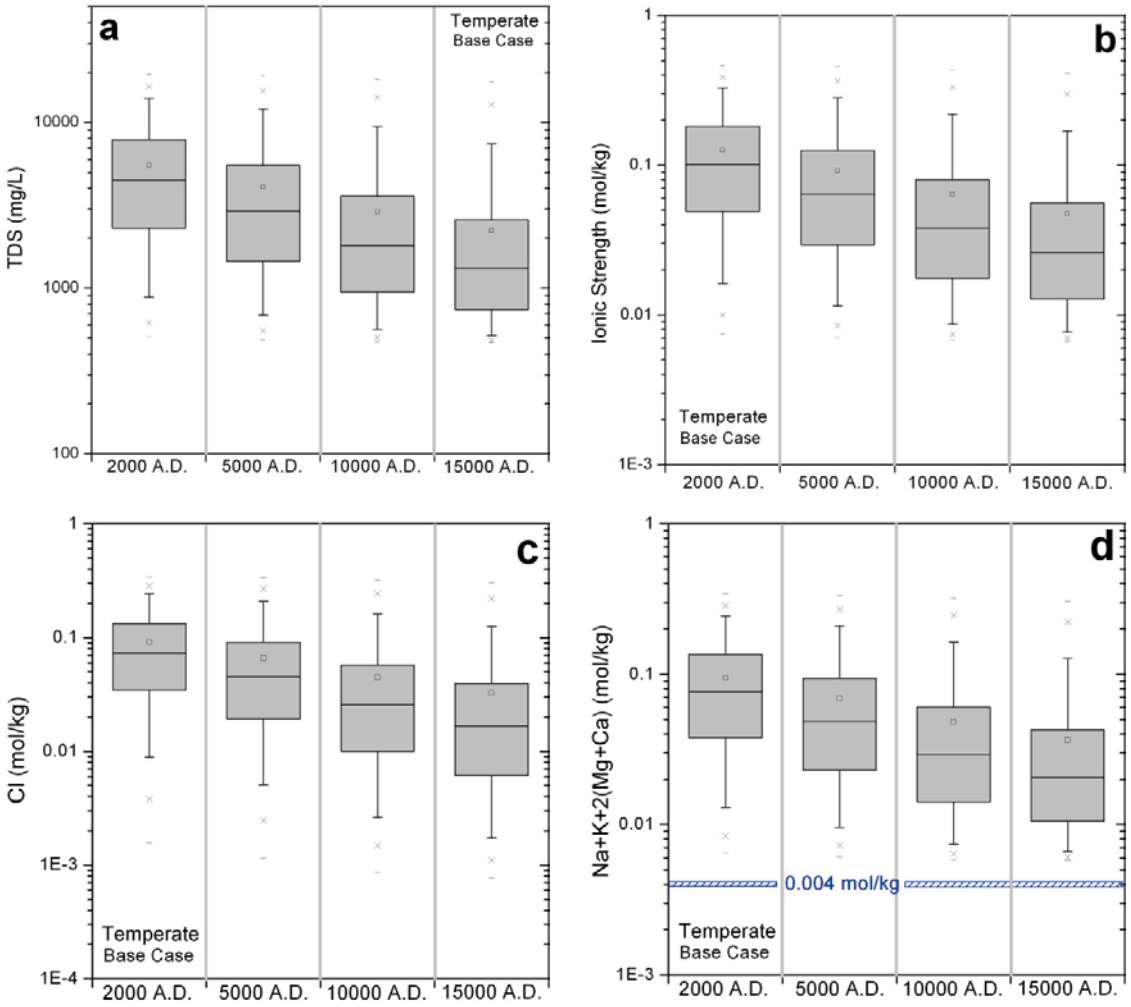

Figure 4-8. *Box-and-whisker plots showing the statistical distribution in the repository volume of TDS values (a, in milligrams per liter), ionic strength, chloride, and the sum of the main cations expressed in charge equivalents as $\sum q[M^{q+}]$ (see Section 1.4 and /SKB 2011/; b, c and d, in mols per kilogram of water, mol/kg) for the "Base Case" defined in the text. The statistical measures plotted here and in all the following box and whiskers plots, are the median (horizontal line inside the grey box), the 25th and 75th percentiles (bottom and top of the box), the mean (square), the 5th and 95th percentiles ("whiskers"), the 1st and 99th percentile (crosses) and the maximum and the minimum values (horizontal bars).*

Figure 4-9 shows the evolution of the main cations over the temperate period within the repository volume. Two aspects are worth remarking: (1) mean values for Ca and Na decrease with time, although their maximum and minimum values remain quite constant; and (2) the variation of Mg and K during the whole period are negligible (mean values around 10^{-4} mol/kg), showing only a progressive narrowing of their range with time (as expressed by the 25th and 75th percentiles).

The predicted evolution of sulphate concentrations follows the same trend as the one already described for the Deep Saline end member (Section 4.1; Appendix 5); this is because the Deep Saline end-member has the highest concentration of sulphate ($9.38 \cdot 10^{-3}$ mol/kg), one order of magnitude higher than in the other end members[20]. Bicarbonate follows the same trend of the Altered Meteoric end member for the same reason (this end member contains the highest concentration of bicarbonate). Figure 4-10 shows that the concentration of sulphate at repository level tends to decrease with time, although only slightly, as waters of meteoric origin become increasingly dominant; on the other hand, bicarbonate contents increase slightly. Silica and phosphate, both controlled by the imposed equilibrium with a mineral phase (quartz and hydroxyapatite respectively), maintain very constant values over time.

[20] Difference with Forsmark where the only possible source of sulphate is Littorina, the saline waters have low sulphate concentrations.

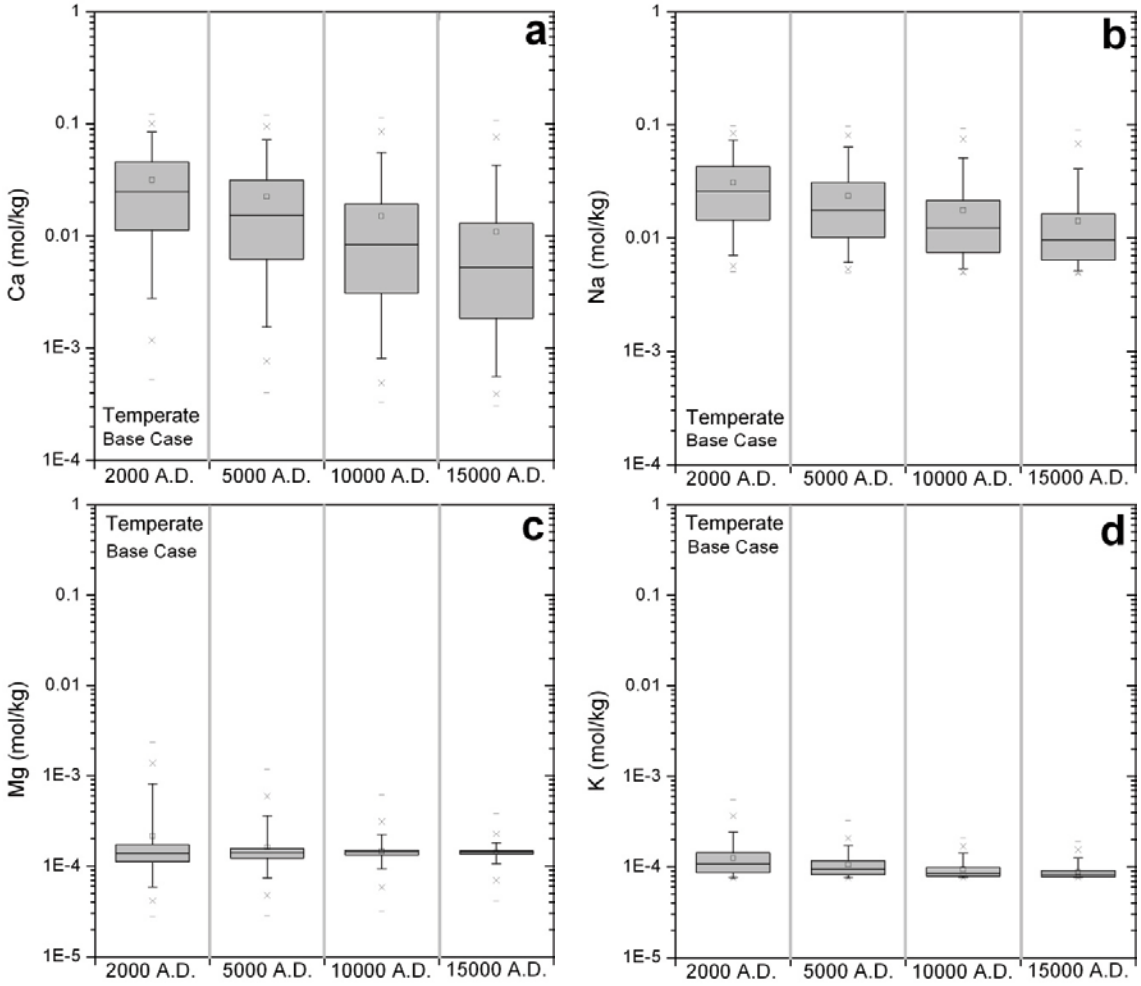

Figure 4-9. *Box-and-whisker plots showing the statistical distribution of the calculated Ca (a), Na (b), Mg (c) and K (d) concentrations (in mol/kg) for the groundwaters located within the candidate repository volume at Laxemar. See the caption of Figure 4-8 for the statistical meaning of the different symbols.*

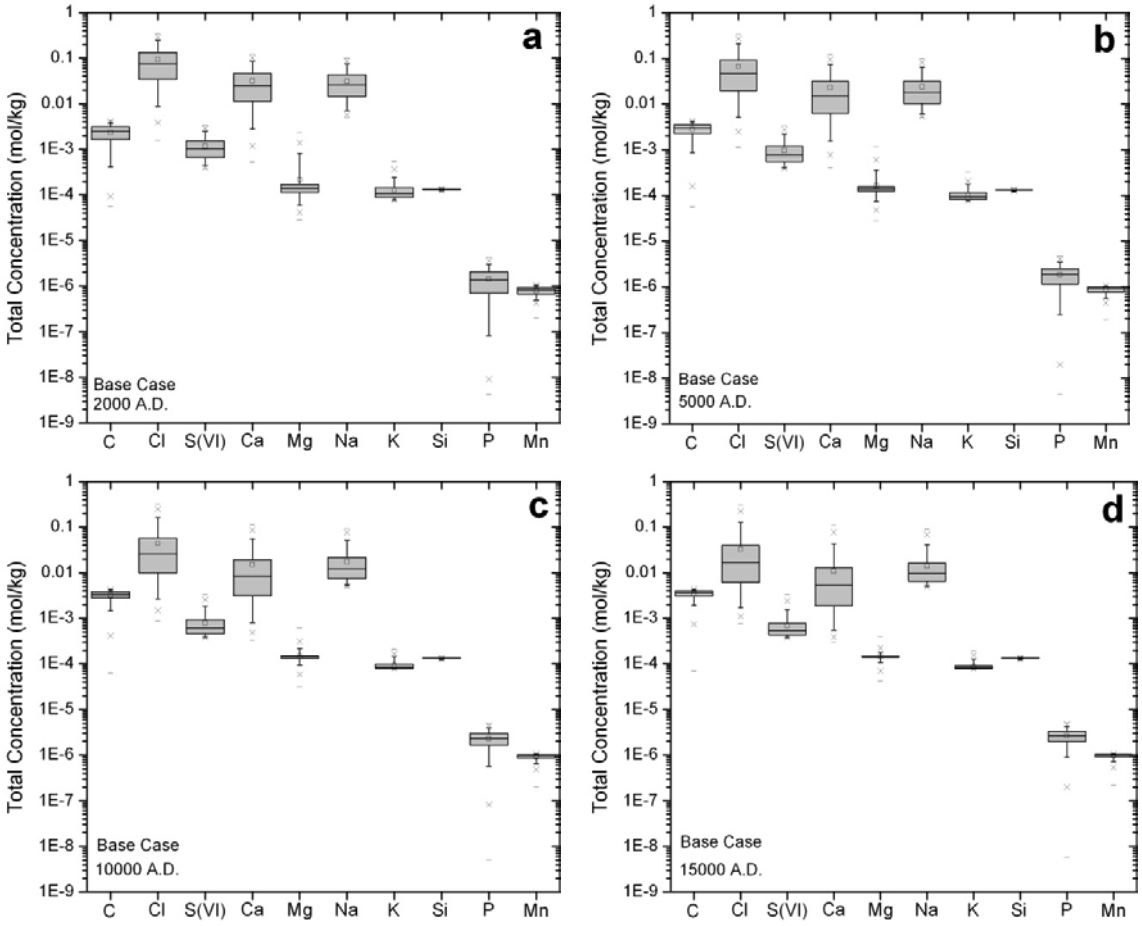

Figure 4-10. *Box-and-whisker plots showing the statistical distribution of the predicted total concentration for the different major water components (in mol/kg) calculated for the different stages of the temperate period (2000 AD to 15,000 AD, a to d) within the candidate repository volume at Laxemar. See the caption of Figure 4-8 for the statistical meaning of the different symbols.*

4.2.3 Glacial period

As shown in the previous section, the hydrogeological results indicate a decrease in the range of salinity at the beginning of the glacial period (Ice 0, equivalent to the end of the temperate; panels g in Figures 4-1 and 4-2). The same decrease has been obtained for TDS through geochemical modelling considering mixing and reaction (Figure 4-11a). Chemical components not participating extensively in chemical reactions, such as Cl and Na (but also to some extent more reactive elements like Ca, Mg and K), follow a similar decreasing trend. This can be seen in Figure 4-11c where the values for the safety function $\sum q[M^{q+}]$ (see Section 1.4 and /SKB 2011/) within the candidate repository volume are shown. The decrease in salinity is shown here by the decrease in the values to below 0.004 mol/kg for some periods of time during the advance and retreat of an ice sheet (Figure 4-11c; stages Ice III, IV, V, Vr, IVr and IIr, with the mean values below the accepted 0.004 mol/kg threshold).

Only the expected effect of upconing in front of the glacier would produce a fairly important increase in salinity (and, therefore, in the concentration of the main ions) at repository depth (see stages Ice I and II in Figure 4-11c). However, as the advancement of the ice sheet is a relatively fast process and the retreat even more so, the high-salinity conditions are predicted to last at most a few centuries.

In the periglacial case (ground frozen down to some extent) salinities in the repository volume are slightly different to the ones obtained when the ground is not frozen. Comparing the evolution of both cases during the first 5 stages, the presence of the permafrost seems to buffer to some extent the sharp changes in salinity due to upconing or dilution as both TDS and $\sum q[M^{q+}]$ show (Figure 4-11 b and d). However, results indicate that since the moment the ice starts its advance, an important fraction of the waters in the repository volume will have values lower than the 0.004 mol/kg threshold accepted for the safety function $\sum q[M^{q+}]$ /SKB 2011/.

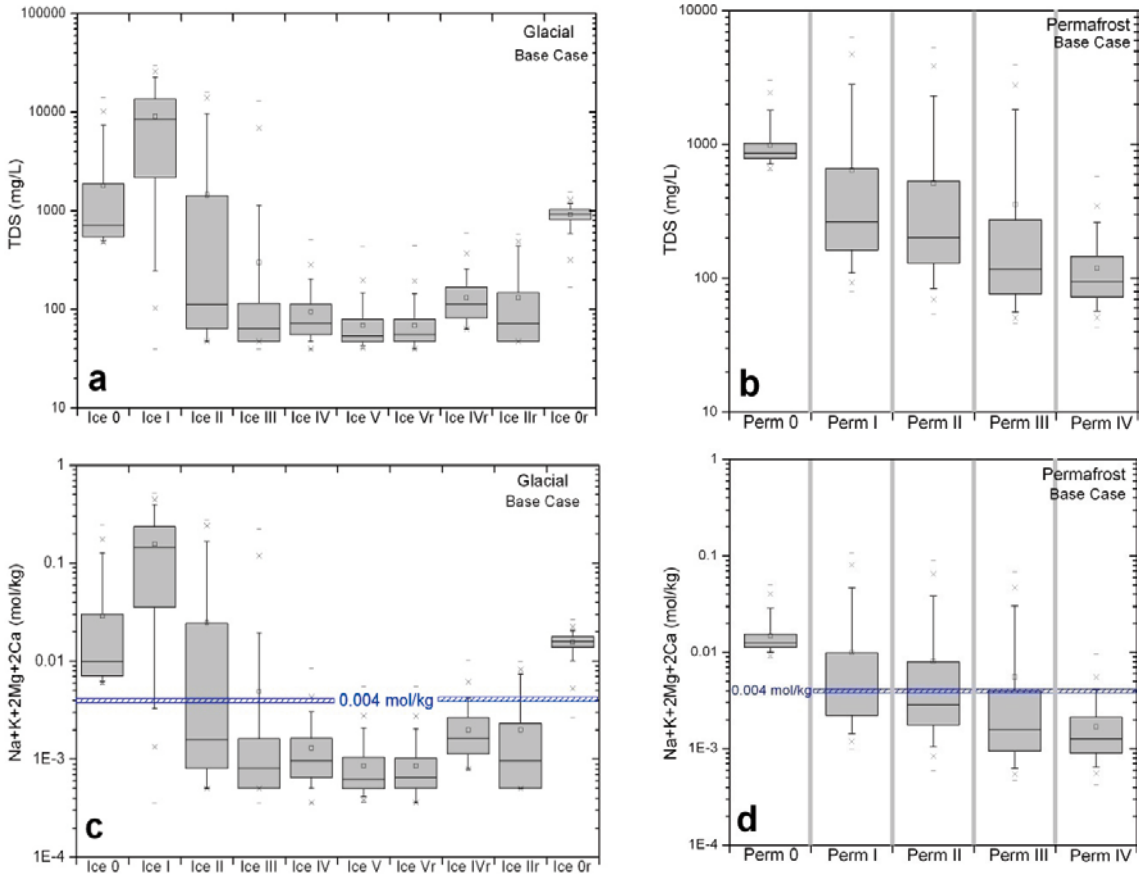

Figure 4-11. *Box-and-whisker plots showing the predicted statistical distribution of TDS (in mg/L) and ∑q[M^{q+}] (in mol/kg; /SKB 2011/) for the different stages of the glacial period without (a and c) and with permafrost (b and d) for groundwaters within the candidate repository volume at Laxemar. See the caption of Figure 4-8 for the statistical meaning of the different symbols.*

After the complete retreat of the ice sheet salinities and concentration of cations (Figure 4-11c and 4-12b, stage 0r) seem to be back, approximately, to the levels estimated before the onset of the glacial period (though with a narrower range of variability).

The evolution of the other main water components is shown in Appendix 6. Silica and phosphate, both controlled by the imposed equilibrium with a mineral phase (quartz and hydroxyapatite), maintain very constant values over time. This is specially true for silica, with contents around 10^{-4} mol/kg for all the simulated periods. In the case of phosphate, most values are between 10^{-7} and 10^{-8} mol/kg during the whole glacial period. In the permafrost case, a narrow range of phosphate concentrations is also obtained, although an order of magnitude higher (from 10^{-6} to 10^{-7} mol/kg).

4.2.4 Submerged period

The initial stage of this period is supposed to be under a glacial melt water lake (fresh water) similar to the final stage of the glacial period (stage 0r, Figures 4-9a and 4-10a). The salinities obtained by the hydrogeological models, as shown in the previous section, are slightly higher than the ones existing during the glacial period. This is reflected in the TDS and in the ∑q[M^{q+}] (Figures 4-12a, b).

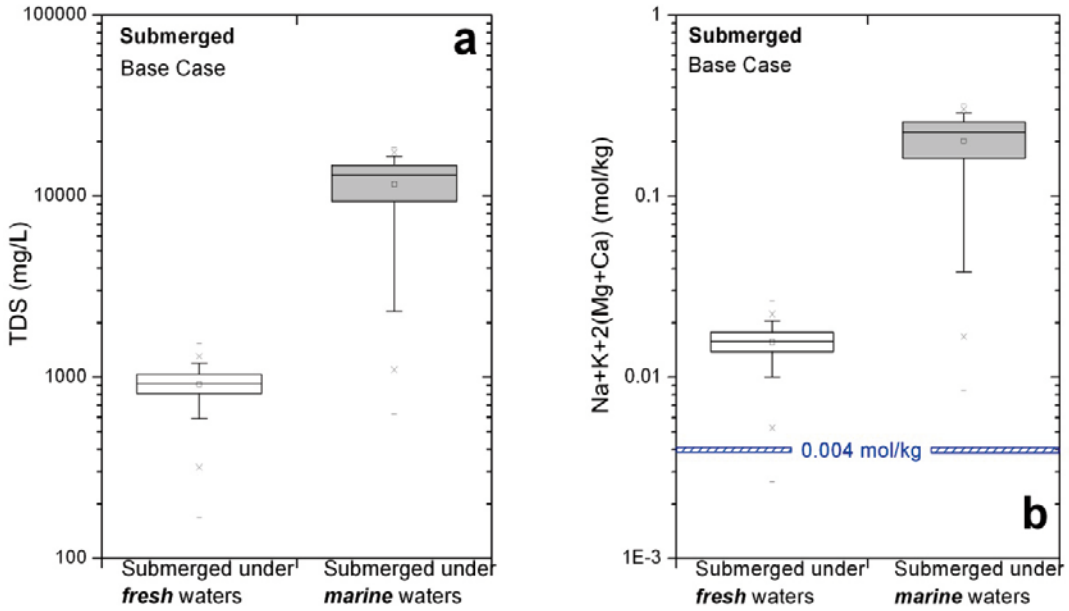

Figure 4-12. *Box-and-whisker plots showing the predicted statistical distribution of the TDS (mg/L; panel a) and the $\sum q[M^{q+}]$ (in mol/kg; panel b) during the two different submerged situations (under fresh waters and under marine waters, respectively) for the groundwaters located within the candidate repository volume at Laxemar. See the caption of Figure 4-8 for the statistical meaning of the different symbols.*

During the last simulated stage the area will be submerged under marine waters, in a situation equivalent to the Littorina Sea episode that had its salinity maximum at 3000 BC. The salinity of groundwaters at repository depth could increase due to density-driven groundwater flow, reaching values slightly higher than at the beginning of the temperate period. This effect is clearly seen in most geochemical parameters (Appendix 6), with values remarkably similar to those calculated for the initial stage of the temperate period. Most predicted TDS values (Figure 4-12a) are between 2,500 and 16,600 mg/L, with maximum values of about 18,500 mg/L and minimun values higher than 600 mg/L. The safety function $\sum q[M^{q+}]$ (Figure 4-12b) is higher than $8.4 \cdot 10^{-3}$ mol/kg. As salinities are not expected to increase above those of sea water during any period of time, the swelling capacity of the backfill would not be affected.

4.3 pH values and total inorganic carbon concentrations

4.3.1 Open repository period

The excavation period will be accompanied by grouting, and , in general, cementitious grouts will increase the pH of the water, involving the safety function indicator R1e (pH < 11; /SKB 2011/). The potential impact on the site hydrogeology is generally ignored. In this way, a programme of experimental studies is currently ongoing internationally to further assess this point. The current status is laid out in /Alexander 2010/.

Injection of grout into fractures surrounding the repository tunnels might be necessary to avoid inflow of groundwater. Traditionally, cement-based grout is used when excavating tunnels. After significant leaching of cement, Standard Portland cement paste has porewater which is highly alkaline (pH ≈12.5). However, the early-phase pH will be 13.3–13.4, sometimes even higher, depending on formulation. In order to avoid detrimental effects from porewater diffusing out of the cement matrix, cement recipes with porewaters having pH ≤ 11 will probably be used in the vicinity of deposition tunnels. It is to be expected that the development of recipes for such materials will be an ongoing process at SKB and elsewhere during the whole period of repository operation. Although the effects of these porewaters are limited, they must be considered, because it is possible that relatively large quantities of cement will be used.

Large volumes of shotcrete are needed for worker safety. However, the distribution of shotcrete and concrete in the repository will be spatially restricted and so will be their potential impact during the excavation and operational phases. Most porewaters leaking from these materials will mix with groundwater infiltrating into the tunnel and be pumped away. A small part of the cement materials will be in contact with the backfill, and cement porewaters could migrate and diffuse into the bentonite. As discussed in /Alexander and Neall 2007/, as long as low-alkalinity cement materials are used, the consequences on the properties of the buffer and backfill may be probably neglected.

Grout could have a large impact on geosphere conditions, as it is widely and diffusely distributed in the fracture system. Grouting is, however, necessary to avoid a large groundwater drawdown (increased meteoric water influx) and the corresponding upconing of saline waters. Grouting is also needed for construction purposes; the ingress of water needs to be limited for the engineering installation and for worker safety. Two types of grout are envisaged in the vicinity of the deposition tunnels in the final repository: low-alkalinity cement-based grouts and suspensions of nano-sized silica particles (Silica Sol). The solidified Silica Sol grout is similar in its properties to the silica present in large quantities in the rock and fracture fillings and, therefore, it is likely to present no problems. Cement-based grouts on the other hand have chemical properties quite different from the surrounding rock, and their effects have to be considered.

Boreholes crossing cement grouted fractures at the Olkiluoto site in Finland have yielded waters with elevated pH values since sampling started. The more limited experience from Äspö shows that a pulse of alkaline solutions may be generated in the immediate vicinity of the grouted fractures. This pulse of alkaline waters is believed to be due to two factors: (1) pore water released while the liquid grout solidifies; and (2) erosion and dilution of grout by flowing groundwater in the outer edge of the grouted volume. These effects in the non-grouted fractures at Äspö were transitory and, after a few days, the chemical composition of the groundwater returned to its original state. The pH values were sufficiently low as to indicate that substantial dilution had occurred. The data from Olkiluoto indicate that the intensity of this short alkaline pulse will be decreased by the use of "low-alkalinity" cement. Because of its short duration and its low intensity, its effect is negligible.

After this short initial transient period grout will start to react with circulating groundwater, and a slightly alkaline plume will develop downstream in the grouted fractures /Luna et al. 2006/. According to these authors, this process could modify the geochemistry of groundwaters around the affected points during thousands of years. However, the development of the alkaline plume depends on many factors, such as the geochemistry and the fluid flow of the recharge groundwaters arriving to the affected points, the neutralization capacity of the system (precipitation of mineral phases), and the fluid flow regime, among others.

4.3.2 Temperate period

As in the previous section, before describing the expected evolution of pH as calculated by geochemical modelling, a comparison between measured and calculated pH values for the year 2000 AD (in a vertical plane) is shown. The pH values mesured *in situ* with the Chemmac proble at Laxemar are, in general, between 7.6 and 8.5 pH units showing a large variability (Figure 4-13).

The pH values calculated with the Base Case (equilibrium with calcite, quartz, hydroxyapatite and haematite, shown in Figure 4-13 a) do not reproduce the extreme values found in some real groundwater samples. Using the other geochemical variant cases, in which the Fe-bearing mineral changes to FeS(am), or the redox processes are not coupled, results do not change. That is, pH is not very sensitive to these effects.

This apparent disagreement between the measured and the calculated values may simply be related to the well known problems in downhole pH measurements, even with the sophisticated methodology used in the Finnish and Swedish sites (see /Pitkänen et al. 2004/ and /Gimeno et al. 2009/ for further discussion).

Some of the measured pH data shown in Figure 4-13 a that are out of the predicted range correspond to *in situ* measurements giving positive saturation indices for calcite (Figure 4-13 b). Considering that this outcome is an "error" in the pH measurement, the usual procedure is to re-calculate pH assuming equilibrium with respect to calcite (see /Gimeno et al. 2009/ for further details). After re-calculation, most pH values for the real groundwaters are inside the range predicted by geochemical simulations. However, some of these pH values and their corresponding oversaturation states with

respect to calcite can be real (see /Gimeno et al. 2009/ for a thourough explanation of the possible meanings of this oversaturation). Therefore, an additional variant case was simulated considering the possibility of a slight oversaturation with respect to calcite (SI = 0.5). The results of this simulation are shown in Figure 4-13 c as green triangles.

The agreement in this case is better as the calculated pH values cover almost all the measured pH. Obviously, the effect of this oversaturation on other chemical parameters was also checked, with the following results: negligible changes for calcium or bicarbonate (which were already well reproduced), an improved fit for Eh (which will be shown in Section 4.4.2.2), and a slight change for Fe(II) and S(-II) without any improvement with respect to what is obtained in the Base Case (see Section 4.4.1.2).

For the Base Case average pH values within the repository volume show an increasing trend (from 7 to 7.35 pH units) over the simulated period of time (Figure 4-13 d). Maximum and minimum values are almost constant during the whole time span (around 8.2 and 6.85, respectively). Only the range of variability (expressed as the 25th and 75th percentiles) changes over time, widening from 0.15 pH units at 2000 AD, to almost 0.5 units at 15,000 AD.

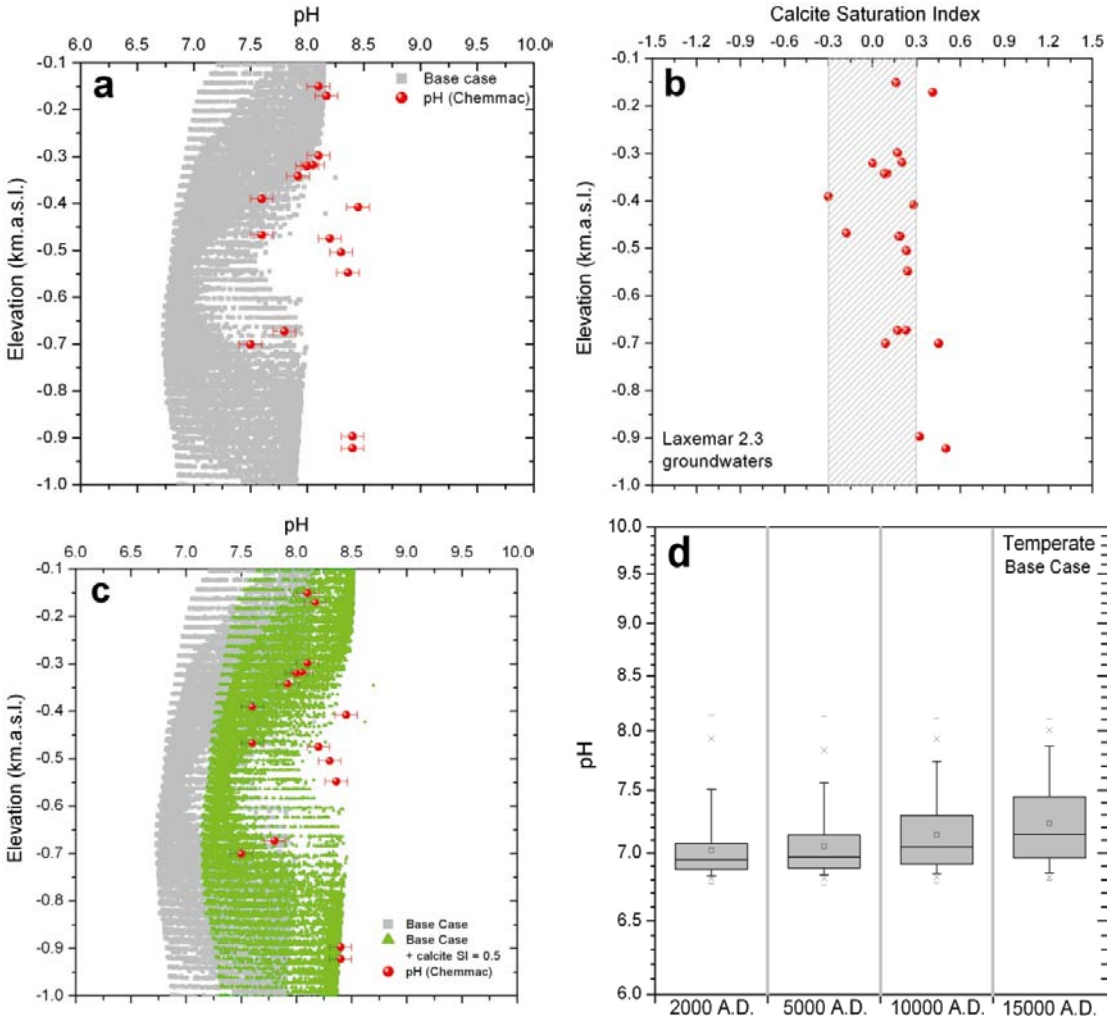

Figure 4-13. *(a) pH values measured in the groundwater samples (red spheres) and obtained by geochemical modelling for the year 2000 AD (grey squares) in a vertical section parallel to the coast (NW-SE) cross-cutting the repository volume, with respect to depth assuming equilibrium with calcite at SI = 0; error bars of 0.1 pH units are also shown; (b) calcite saturation indexes calculated for the real groundwaters from Laxemar; (c) same comparison as in (a) but equilibrating the waters with calcite at SI = 0.5; (d) box-and-whisker plot showing the statistical distribution of the pH (in standard units) calculated over the temperate period for the groundwaters located within the candidate repository volume at Laxemar. The criterion for the safety function indicator R1e (pH < 11; /SKB 2011/) is clearly fulfilled during this period. See the caption of Figure 4-8 for the statistical meaning of the different symbols.*

The concentration of total inorganic carbon and the partial pressure of dissolved carbon dioxide increase with time (Figure 4-14). This is so because it is assumed in the modelling that infiltrating meteoric waters have a higher bicarbonate and CO_2 content than the other waters in the system.

As time progresses, dissolved carbon concentrations increase as a consequence of the infiltration of meteoric waters. These waters will dissolved calcite up to equilibrium producing the slight increase in pH.

In conclusion, mixing and reaction calculations for pH and total inorganic carbon are dominated by equilibrium (or slight oversaturation in some cases) with respect to calcite. The numerical results show that pH values remain approximately in the range 6.8 to 8 (or 8.5 when assuming oversaturation with respect to calcite), and that dissolved inorganic carbon increases gradually with time, from a mean value of $2.3 \cdot 10^{-3}$ mol/kg at 2000 AD to $3.4 \cdot 10^{-3}$ mol/kg at 15,000 AD. Thus, the criterion for the safety function indicator R1e (pH < 11; /SKB 2011/) is fulfilled during the whole temperate period following repository closure.

4.3.3 Glacial period

Calculations indicate that the onset of glacial conditions may result in a general increase of pH values (Figure 4-15), an effect which is commonly observed in this type of glacial groundwaters (see Appendix 2). Except for a decrease in pH during the Ice I stage (beginning of the ice front advance), which is not observed when the presence of permafrost is considered (compare figures 4-15 a and b), the pH obtained for almost all the glacial period (Ice III to Ice IIr) is fairly high and most of the time quite constant with 50% of the samples in the repository volume having pH values between 9.25 and 9.7. The widest pH range is predicted for the Ice II stage, just before the ice front is above the repository, that is, when upconing affects the repository volume. During this stage 90% of pH values are in the range 6.5–9.7 and 50% of the samples are in the range 8–9.5. The final stage (Ice 0r) shows a decrease in the mean pH value (from 9.5 to 8.75) and a narrowing of its range. In any case, the safety function criterion R1e (pH < 11; /SKB 2011/) will be fulfilled as pH will remain lower than 11.

The effect of permafrost over the repository on the calculated pH values is clearly seen in Figure 4-15 b. There is a constant increase of pH, with quite a wide range of variability, reaching values (up to 9.5) not as high as the ones found when the ground is not frozen.

As shown in Figure 4-15 c and d, log pCO_2 behaves exactly opposite to pH. Total inorganic carbon (TIC) during the glacial period shows a progressive decrease from mean values around $3 \cdot 10^{-3}$ mol/kg before the arrival of the ice front over the repository (stage Ia; Figure A6-2 in Appendix 6), to mean values around $2.2 \cdot 10^{-4}$ mol/kg when the ice sheet is retreating.

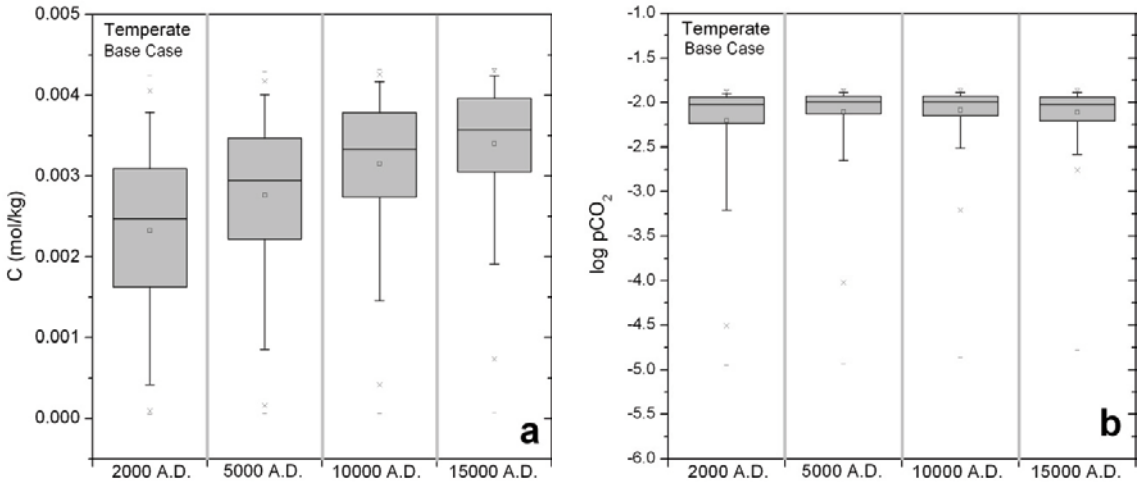

Figure 4-14. *Box-and-whisker plot showing the statistical distribution of total carbon (mol/kg) and log pCO_2 (logaritmic units) calculated over the temperate period for the groundwaters located within the candidate repository volume at Laxemar. See the caption of Figure 4-8 for the statistical meaning of the different symbols.*

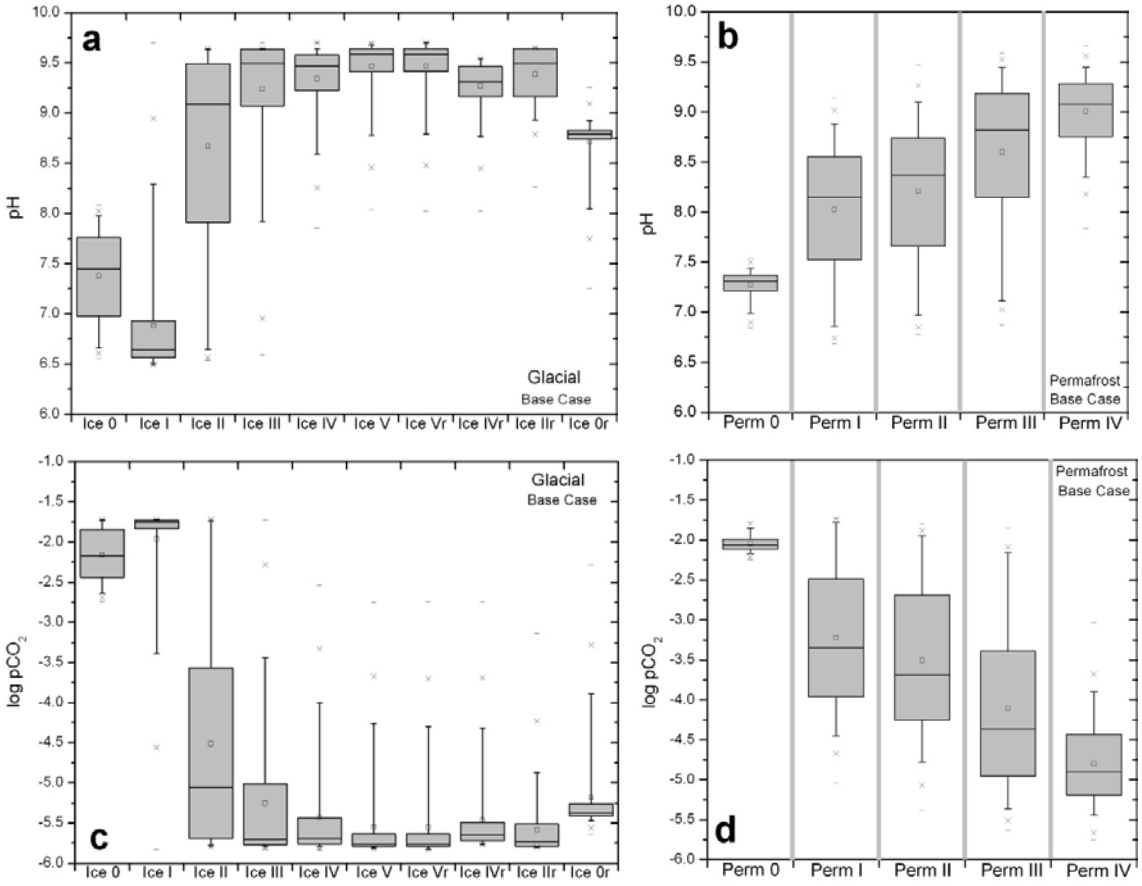

Figure 4-15. *Box-and-whisker plot showing the statistical distribution of the pH (in standard units, a and b) and the log pCO_2 (c and d), calculated over the glacial period considering the absence of permafrost (left) or its presence (righ) for the groundwaters located within the candidate repository volume at Laxemar. See the caption of Figure 4-8 for the statistical meaning of the different symbols.*

4.3.4 Submerged period

Figure 4-16 shows pH and log pCO_2 values for the two submerged cases. When the area is covered by fresh waters, pH remains high and the pCO_2 low (as inherited from the previous glacial period). However, when the waters covering the area are of marine origin, a clear decrease in pH (mean: 7,6; range: 7-8) in the repository volume is produced. However, pH is still higher than during the temperate period, and pCO_2 considerably lower than before.

4.4 Redox parameters

As previously indicated in Chapter 3, a "Base Case" has been defined. The Base Case assumes that, apart from equilibrium with calcite, quartz and hydroxyapatite, groundwaters are also in thermodynamic equilibrium with haematite (Figure 3-5). The parameters described so far have not shown great sensitivity to the different geochemical variant cases and for their calculation the Base Case could have been any of these variant cases, in fact, the results shown in the plots correspond to case 1 (equilibrium with haematite as redox controlling mineral). However, as described below, the redox parameters are very sensitive to the specific redox mineral considered to be in equilibrium, and to the coupling or uncoupling of the thermodynamic data base. Therefore, for the redox parameters, the Base Case includes not only the results obtained with the variant case 1, but also the results obtained with the variant case 2. Apart from considering these two sets of results together (named as Base Case for these parameters), the specific results found with each variant case (Case 1: equilibrium with haematite only; and Case 2: equilibrium with FeS(am) only) will also be shown and interpreted.

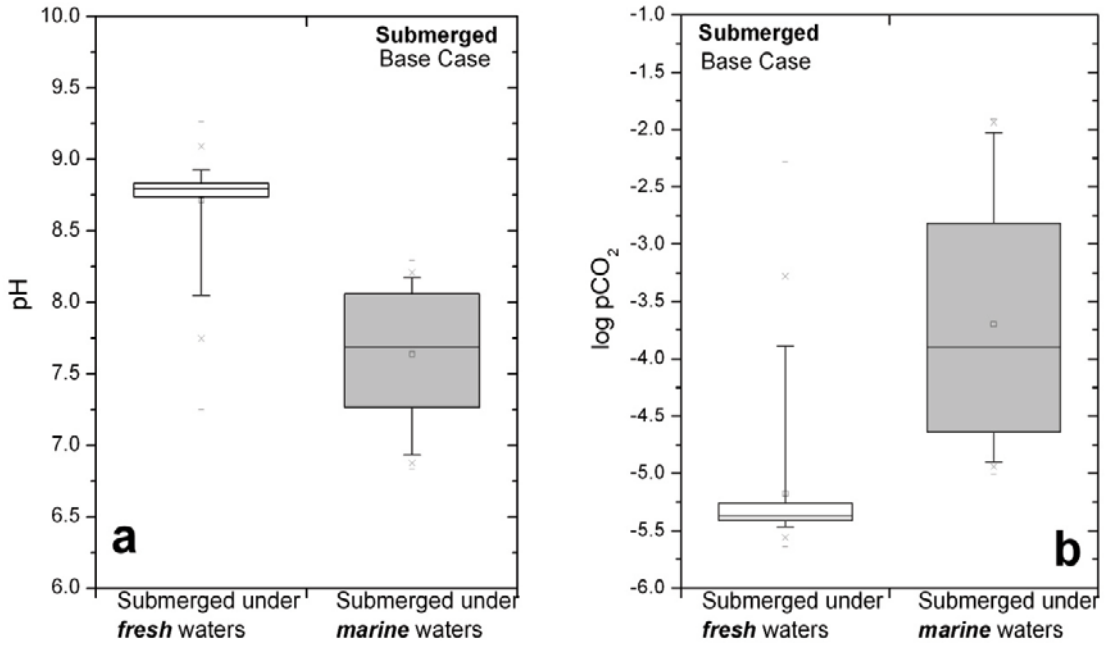

Figure 4-16. *Box-and-whisker plot showing the statistical distribution of the pH (in standard units; a) and the log pCO_2 (b), calculated for the two submerged cases for the groundwaters located within the candidate repository volume at Laxemar.The statistical values are the same as indicated in Figure 4-8 caption.*

An additonal variant case (Case 3) has been devised considering the control of Eh by the $Fe(OH)_3$/Fe^{2+} redox pair, assuming redox homogeneous disequilibrium between the redox pairs S(-II) /S(VI) and C(-IV)/C(IV) and, therefore, using the un-coupled thermodynamic database. Figure 3-5 sumarises the conditions of the Base Case and the three Variant Cases.

What follows next is the discussion of the statistical distribution of S(-II), Fe(II) and Eh for the Base Case and for the 3 geochemical variants.

4.4.1 Sulphide and iron concentrations

The content of sulphide in groundwaters is controlled by the interplay between microbial sulphate reduction and inorganic processes that remove sulphide: oxidation and precipitation with metals. Under oxidising conditions sulphide is quickly oxidised to sulphate. Under reducing conditions, dissolved Fe(II) is normally present and maximum sulphide concentrations are controlled by the precipitation of Fe(II)-sulphide.

Sulphide concentrations have been analysed during the Site Characterisation Program and in the following groundwater monitoring program /Tullborg et al. 2010a, b/. Values are often below the detection limit of the analytical method ($\approx 10^{-7}$ mol/kg), but in some borehole sections sulphate reduction has taken place and relatively high sulphide concentrations have been observed (to about $8 \cdot 10^{-5}$ mol/L).

The concentration of Fe(II) is regulated by a complicated set of reactions including homogeneous redox reactions, the slow dissolution of Fe(II)-silicates (e.g. chlorite) and the precipitation of Fe(II)-monosulphides. The concentrations of Fe(III) are, in general, negligible in granitic groundwaters as Fe(III)-oxyhydroxides are quite insoluble and precipitate quickly. In the simulations, the concentration levels of dissolved sulphide and Fe(II) have been regulated by the interplay between groundwater flow (mixing of reference waters) and the redox equilibrium assumptions (geochemical variant cases 1, 2 and 3), which are also controlled by pH /Auqué et al. 2006/.

4.4.1.1 Open repository period

During the operational phase, inflow of groundwater into the tunnel and mixing of groundwaters of different origin within the rock fractures will probably result in precipitation or dissolution of minerals. Performed numerical simulations /Domènech et al. 2006, Acero et al. 2010/ indicate that Fe(III) oxy-hydroxides are expected to precipitate (as it has been observed at Äspö) while oxic conditions prevail. Thus, dissolved iron contents would be very low, and the same could be said for sulphide, as it is totally unstable under oxic conditions.

After closure, decomposition of organic materials (including biofilms, tobacco, plastics, cellulose, hydraulic oil, surfactants and cement additives) could enhance the reducing capacity of the repository near-field and contribute to a quick consumption of any oxygen left in the repository. It may also favour an increase in DOC and acetate contents that, in turns, would increase SRB activity and, thus, dissolved sulphide contents after closure. In addition, corrosion processes may also represent an additional source of hydrogen that may also increase SRB activity (see Chapter 5).

An inventory of organic materials and an assessment of their impact on microbial processes have been prepared by /Hallbeck 2010/ for SR-Site. Three main pools of organic material in the repository have been identified. The largest pool is the organic material in bentonite although it may be questionable whether this material is available for degradation /Hallbeck 2010/; the second largest pool are the biofilms formed on rock surfaces, while the third main pool is the organic material that can be produced by microorganisms with hydrogen from anaerobic corrosion of iron in steel as the energy source /Hallbeck 2010, SKB 2011/.

Several calculations were performed on the theoretical concentration of sulphide that can be produced with H_2 from anaerobic iron corrosion (via acetogenesis and sulphate-reduction) and from biodegradation of biofilms with sulphate-reduction. The results indicate that the cumulated dissolved sulphide concentration from total corrosion and biodegradation is still below $2 \cdot 10^{-4}$ mol/kg (6.5 mg/L). However important uncertainties remain and further discussion can be found in Chapter 5.

4.4.1.2 Temperate period

Before describing the expected evolution of the redox parameters, Figure 4-17 compares the measured S(-II) and Fe(II) values with the ones obtained in the simulations performed for SR-Site following the Base Case defined for the redox parameters, that is, the results obtained in equilibrium with haematite (light grey squares; Case 1) together with those obtained when imposing the equilibrium with FeS(am) (dark grey squares, Case 2).

These plots must be read with care as the low values calculated for Fe(II) and specially for S(-II) are frequently below the detection limit of the analytical techniques available at present (and used for the groundwater samples) and, therefore, they cannot be compared. One of the main conclusions obtained from these plots is the observation that to reproduce the whole range of measured S(-II) and Fe(II) values in the real system, the combined results of both geochemical variant cases must be considered (and that is why the Base Case used for these parameters include all these results). This was not needed for Forsmark as measured values (mainly for S(-II)) are lower. However, for Laxemar, the FeS(am) equilibrium assumption is necessary to explain some of the high-sulphide and high-Fe(II) values measured in the groundwaters. This is very important as to know these possible maximum sulphide values is the main interest for PA to determine the possible canister corrosion rates.

Although not shown in Figure 4-17, the results obtained with the geochemical variant case 3, where equilibrium with haematite is also imposed but using the un-coupled thermodynamic data base, reproduce quite well the lower S(-II) and Fe(II) values and their range of variation is narrower than when using the coupled data base. However, these results do not improve much on what has already been considered and they have been left only as a variant case.

The results presented next correspond to the Base Case which, as mentioned, is the combination of all the results obtained with Case 1 and Case 2, for the points enclosed into the repository volume. However, some comments will also be included refering to specific results obtained with each variant case separately (data tables with the statistical results can be found in Appendix 4).

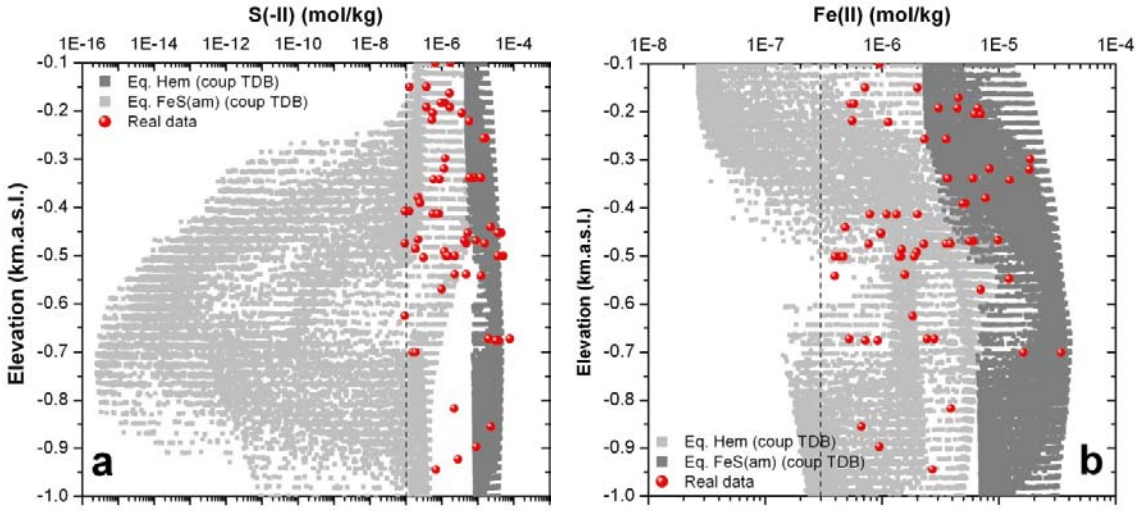

Figure 4-17. *Concentration-depth graphs for S(-II) and Fe(II) measured in the groundwater samples (red spheres; mol/kg) and obtained by geochemical modelling using Case 1 and Case 2 (grey squares: light grey for the equilibrium with haematite, case 1, and dark grey for the equilibrium with FeS(am), case 2) for the year 2000 AD in a vertical section parallel to the coast (NW-SE) cross-cutting the repository volume. Together, these results constitue the Base Case. See Figure 3-5 for more explanations on the variant cases. The dashed lines indicate the detection limit of the analytical technique used for the analysis of the groundwater samples.*

Figure 4-18 shows the box and whisker plots for S(-II) and Fe(II) in the repository volume during the temperate period for the Base Case. The calculations predict few changes in these two parameters over this period although in the case of sulphide the range of variability decreases substantialy (from seven orders of magnitude at 2000 AD to four orders of magnitude at 15,000 AD). However, the mean (around 10^{-5} mol/kg), the median and even the 75th percentile are almost the same over the time. The calculated iron(II) concentration are in the range $3\cdot10^{-5}$ to $1.5\cdot10^{-6}$ mol/kg.

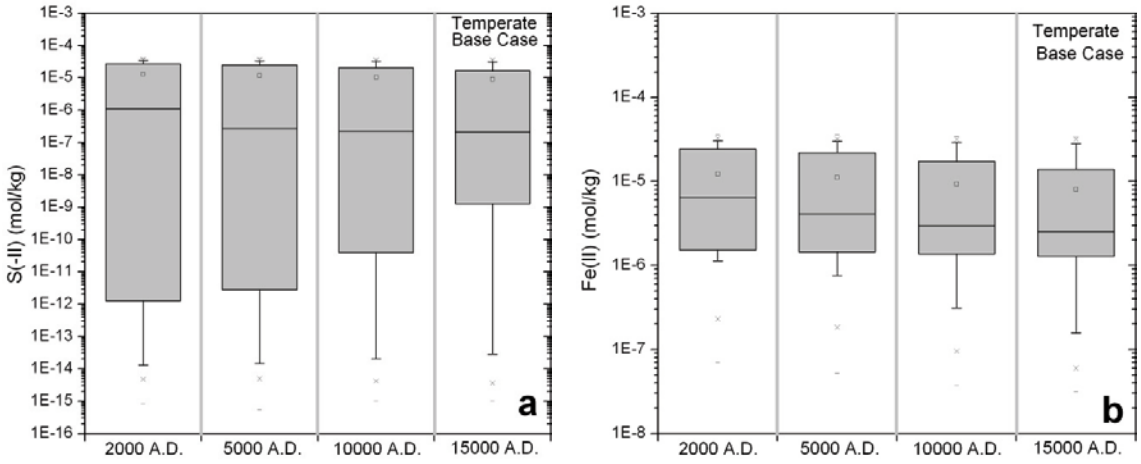

Figure 4-18. *Box-and-whisker plot showing the statistical distribution of S(II) and Fe(II) (in mol/kg) obtained with the Base Case simulations over the temperate period for the groundwaters located within the candidate repository volume at Laxemar. See the caption of Figure 4-8 for the statistical meaning of the different symbols.*

Looking now separately at the results obtained with the two geochemical variant cases which compose the Base Case (Figures 4-19 for S(-II) and 4-20 for Fe(II)), it becomes clear that the wide variability for sulphide comes from the equilibrium with haematite which gives the lowest concentrations, while the values obtained in equilibrium with FeS(am) are considerably higher, with a narrow range of variability and quite constant over the time. Results obtained with Case 3 are quite interesting as they are also fairly constant (with a narrow range of variability) and give values similar to those near the 75th percentile in Case 1 (note that Case 3 uses the same equilibrium minerals as Case 1 but the thermodynamic data base is un-coupled). In other words, un-coupling the pair sulphate-sulphide gives higher concentrations of dissolved sulphide.

For iron (Figure 4-20) both the variability range and the mean values are quite constant over time. The range is quite narrow for all the cases, and expands slightly with time. When the waters are equilibrated with haematite (irrespective of the coupling of the database, Cases 1 and 3) values are the lowest (about 10^{-6} mol/kg), while equilibrium with FeS(am) gives values around $2{\cdot}10^{-5}$ mol/kg.

Results obtained with these two simulations point to the important role that the two redox minerals considered in them can play in controlling the dissolved contents of ferrous iron and sulphide. As described in Chapter 3, the methodology used for these simulations simplify the behaviour of the system by assuming that the imposed equilibria are taking place in the whole volume of rock, which obviously is not true. It is clear (from the SDM /Laaksoharju et al. 2009, Gimeno et al. 2009/ and from results obtained here) that in some parts of the system the equilibrium with haematite is the main control, while in other parts sulphate reduction is important enough to allow monosulphides to impose control. In any case, the use of the Base Case, combining the results from variant cases 1 and 2, gives a practical range of values to be used for future predictions.

In summary, sulphide concentrations averaged over the temperate period are similar to those found at present (up to 10^{-4} mol/L). In any given deposition hole, oscillations in sulphide levels will take place, but time-averaged concentrations are expected to be always lower than 10^{-4} mol/kg.

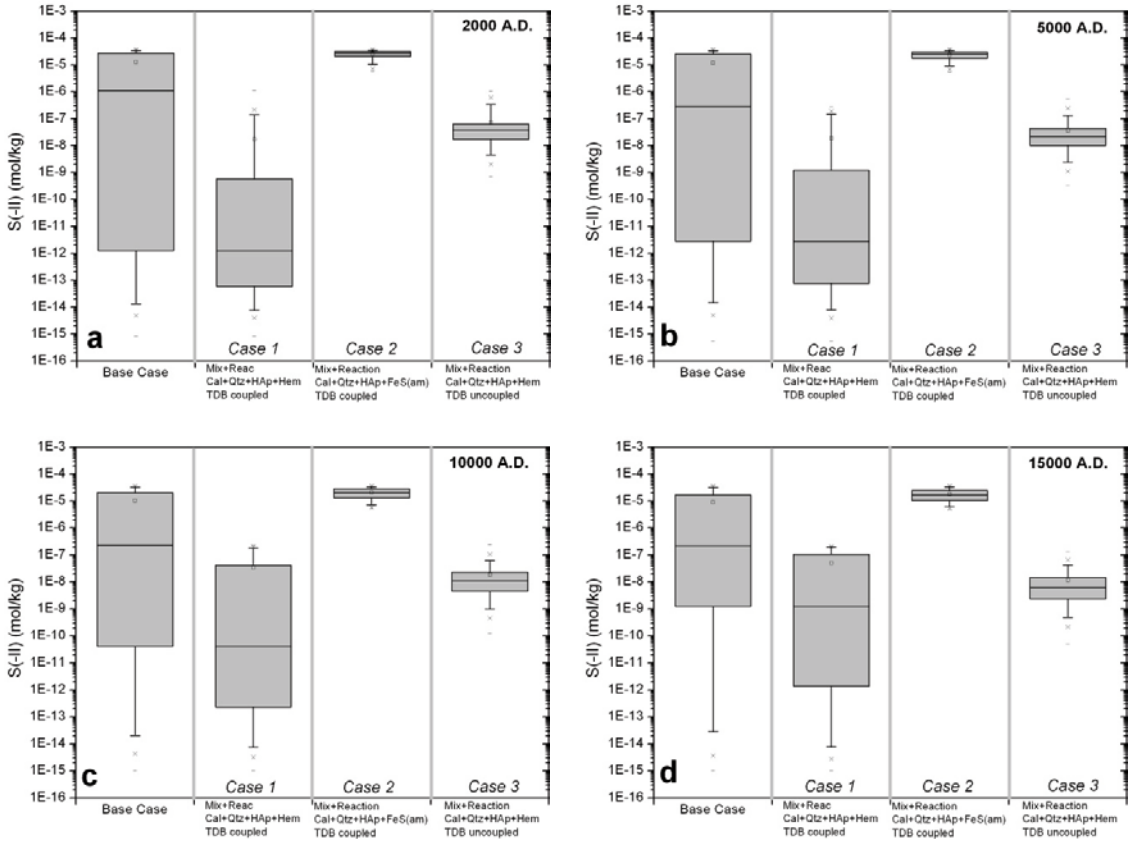

Figure 4-19. *Box-and-whisker plot showing the statistical distribution of S(-II) (mol/kg) obtained for the different geochemical variant cases over the temperate period for the groundwaters located within the candidate repository volume at Laxemar.* See *the caption of Figure 4-8 for the statistical meaning of the different symbols.*

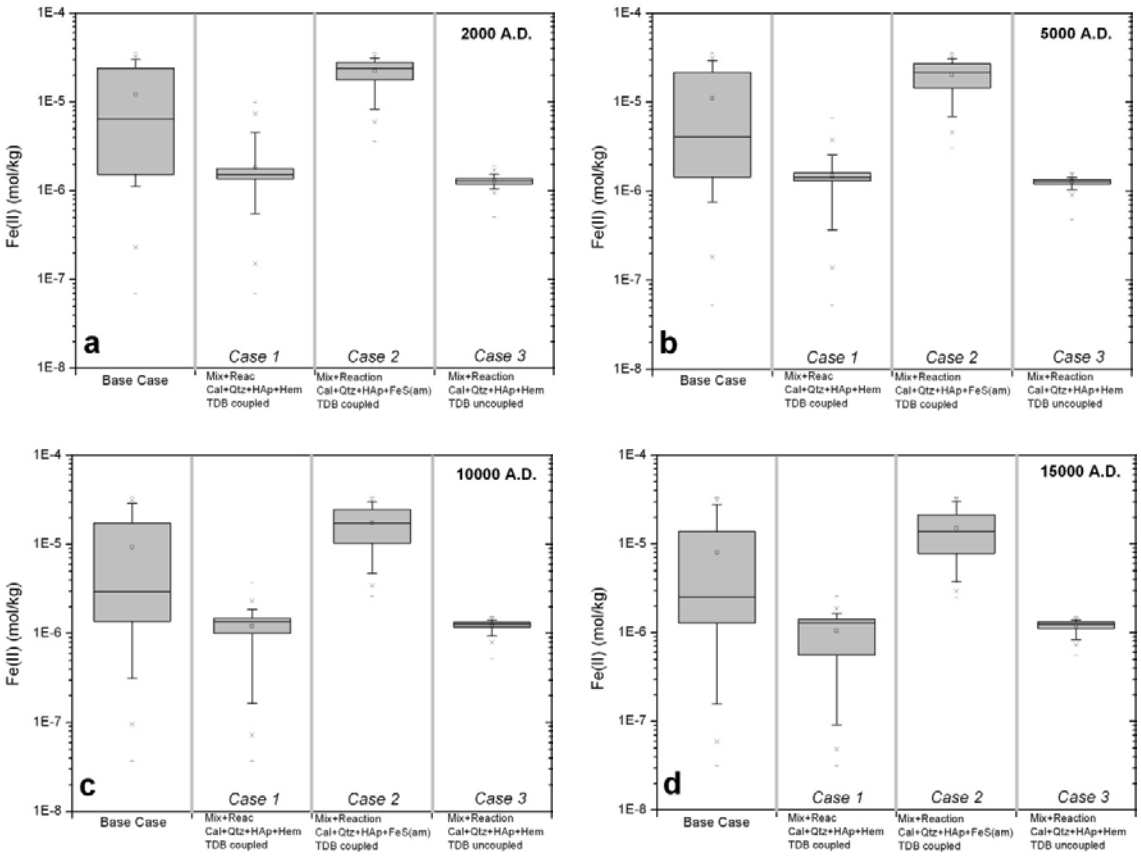

Figure 4-20. *Box-and-whisker plot showing the statistical distribution of Fe(II) (mol/kg) obtained for the different geochemical variant cases over the temperate period for the groundwaters located within the candidate repository volume at Laxemar.* See *the caption of Figure 4-8 for the statistical meaning of the different symbols.*

4.4.1.3 Glacial period

Under glacial conditions the intensity of microbially-mediated sulphate reduction to produce sulphide will probably decrease under an ice sheet, as inflow of organic matter from the surface will become negligible. Compared with the previous temperate and periglacial periods, sulphate concentrations might increase during the short episodes of upconing (in front of the ice front advance or retreat) but they will decrease substantially during the longer periods of intrusion of glacial melt waters. In the absence of superficial organic carbon, deep-sourced H_2 and CH_4 might be the key players in the control of the sulphate reduction considered to exist. Sulphate reduction activity in groundwaters may be supported by autotrophic methane oxidation (see reaction 5.3 at Section 5.2.3.2, Chapter 5) or, indirectly, by suitable organic matter liberated by other H_2-utilising microorganisms (e.g. autotrophic acetogens),

Under these conditions, if microbial sulphide production occurs during upconing periods, it will be limited by the availability of sulphate, hydrogen and methane. The amounts of hydrogen and methane will be controlled by its production and flow from the deeper parts of the bedrock. There is not enough information at present to quantify this process, but some estimations of fluxes and maximum production rates of methane and hydrogen have been performed by /Delos et al. 2010/ for the Forsmak and Laxemar sites. Based on these estimations, sulphate reduction rates of 10^{-6} to 10^{-8} mM/year are obtained, in the lowest range of sulphate reduction rates in groundwater systems and in agreement with the values obtained by /Onstott et al. 2009/ in deep groundwaters from the Lupin Mine (see Appendix 3 in /Tullborg et al. 2010a/ for further details). Thus there is currently no evidence to support increased sulphide production under ice sheets.

During the glacial period, iron concentrations would be mainly controlled by inorganic reactions. Under these stringent conditions for electron donors and the lack of suitable electron acceptors (poorly crystalline iron-oxyhidroxides; see /Gimeno et al. 2009/ for further discussion) microbially mediated iron (Fe(III)-oxides) reduction could be extremely limited.

S(-II) values obtained at the beginning of the glacial period with the Base Case (Figure 4-21 a, b) are very similar to the ones obtained at the end of the temperate (minimum around 10^{-8} and maximum up to $5{\cdot}10^{-5}$ mol/kg), even considering the different calculation approaches (see Chapter 3, hydrogeological simulations over the glacial and permafrost periods). The first stage of the ice advance (Ice I) has a very wide range of variability, up to 13 orders of magnitude with maximum values of 10^{-4} mol/kg and minimum values down to very low, and meaningless, concentrations (10^{-17} mol/kg). For the rest of the stages most of the samples in the repository volume have sulphide contents between 10^{-7} to 10^{-5} mol/kg. The last stage (equivalent to the submerged under fresh water period) is characterised by a slightly broader range of sulphide values, displaced towards higher values (minimum around 10^{-8} and maximum up to $5{\times}10^{-5}$ mol/kg). Half of the samples in the respository volume at the end of the glacial period have values between 10^{-7} and 10^{-6} mol/kg, which is a narrower range (and a mean value slightly lower) than at the end of the temperate.

The presence of permafrost does not change the results in terms of mean values and ranges except for the fact that the minumum values are higher than for the non-permafrost case.

As shown in Figures 4-21 c and d, Fe(II) values for the Base Case at the beginning of the glacial period are also similar to those found at the end of the temperate period but with a broader range of variation (maximum: $6{\cdot}10^{-5}$ mol/kg; minimum: $5{\cdot}10^{-8}$ mol/kg). The advance of the ice sheet produces first a slight increase in Fe(II) contents in the respository volume followed by a general decrease in mean and maximum values and an increase in the range of variation. The end of the glacial period (Ice 0r stage) shows a slight increase in Fe(II) values with 50% of the grid points between $3{\cdot}10^{-10}$ and 10^{-5} mol/kg, still lower than the values found at the end of the temperate period. When permafrost is included, a more constant and regular decrease of Fe(II) contents is predicted (Figure 4-21 d); the range of variation (as expressed by the 25th and 75th percentiles) increases with time from one order of magnitude (between 10^{-5} and 10^{-6} mol/kg) to more than three orders of magnitude (between 10^{-6} and 10^{-10} mol/kg).

Looking now at S(-II) and Fe(II) concentrations as predicted by each of the different geochemical variant cases (Figures 4-22 and 4-23, with the upper graphs on both figures showing again the Base Case for comparison), one can see the effect that the different mineral equilibria (haematite or FeS(am)) have on the final content of these elements.

The highest S(-II) and Fe(II) concentrations and the narrower ranges are obtained when equilibrium with FeS(am) is imposed (variant case 2). Except for the first stages in the advance of the ice sheet (Ice 0, 1 and 2), the concentrations are relatively constant.When the permafrost is included, a decreasing concentration trend is seen (not perceived in the Base Case).

Variant cases 1 and 3 (equilibrium with haematite, with the coupled and the un-coupled data base, respectively) show similar results between them, but different from the ones obtained with Case 2 (equilibrium with FeS(am)). Fe(II) contents are very variable in both cases and, in general, lower than 10^{-6} mol/kg, with a clear decreasing trend during the permafrost stages. On the other hand, dissolved S(-II) contents are roughly constant at 10^{-7} mol/kg over the whole glacial period, irrespective of the coupling or uncoupling of the data base.

When the un-coupled data base is used, total S(-II) contents are only conditioned by the mixing of different water types and, therefore, by the sulphide content of the end members. The Deep Saline and Altered Meteoric end-members have an initial S(-II) content of 10^{-15} mol/kg, while the Glacial end-member has a content of 10^{-7} mol/kg (Table 3-4, Chapter 3). Thus, the fraction of glacial water in the mixture determines the concentration of sulphide in the groundwater.

When using the coupled data base and the equilibrium with haematite (Case 1) the redox potential imposed by such equilibrium propagates to dissolved sulphide contents through the redox pair S(-II)/S(VI). Because in this variant case the pair is coupled, it is conditioned by the Eh. However, this effect is only visible in the first stages of the glacial period (e.g. Ice 0, I and II) when glacial waters are still insignificant and S(-II) contents are low. When glacial waters start to dominate the system, S(-II) content increases rapidly to around 10^{-7} mol/kg. Although the redox equilibrium effect is still visible, predicted sulphide contents are those imposed by mixing and, therefore, strongly dependent on the initial assumptions made for the composition of the end-member.

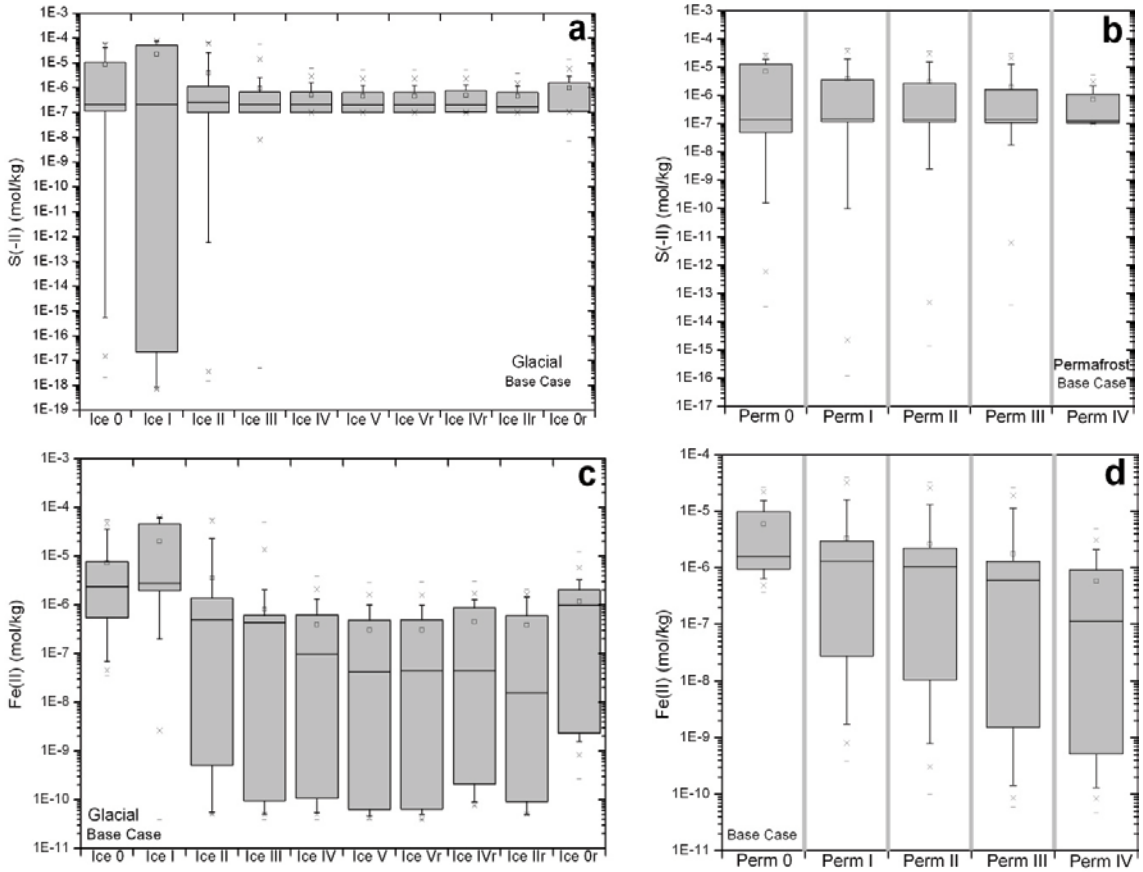

Figure 4-21. *Box-and-whisker plot showing the statistical distribution of S(-II) and Fe(II) (mol/kg) obtained for the Base Case over the glacial period without (a, b) and with permafrost (c, d) for the groundwaters located within the candidate repository volume at Laxemar. See the caption of Figure 4-8 for the statistical meaning of the different symbols.*

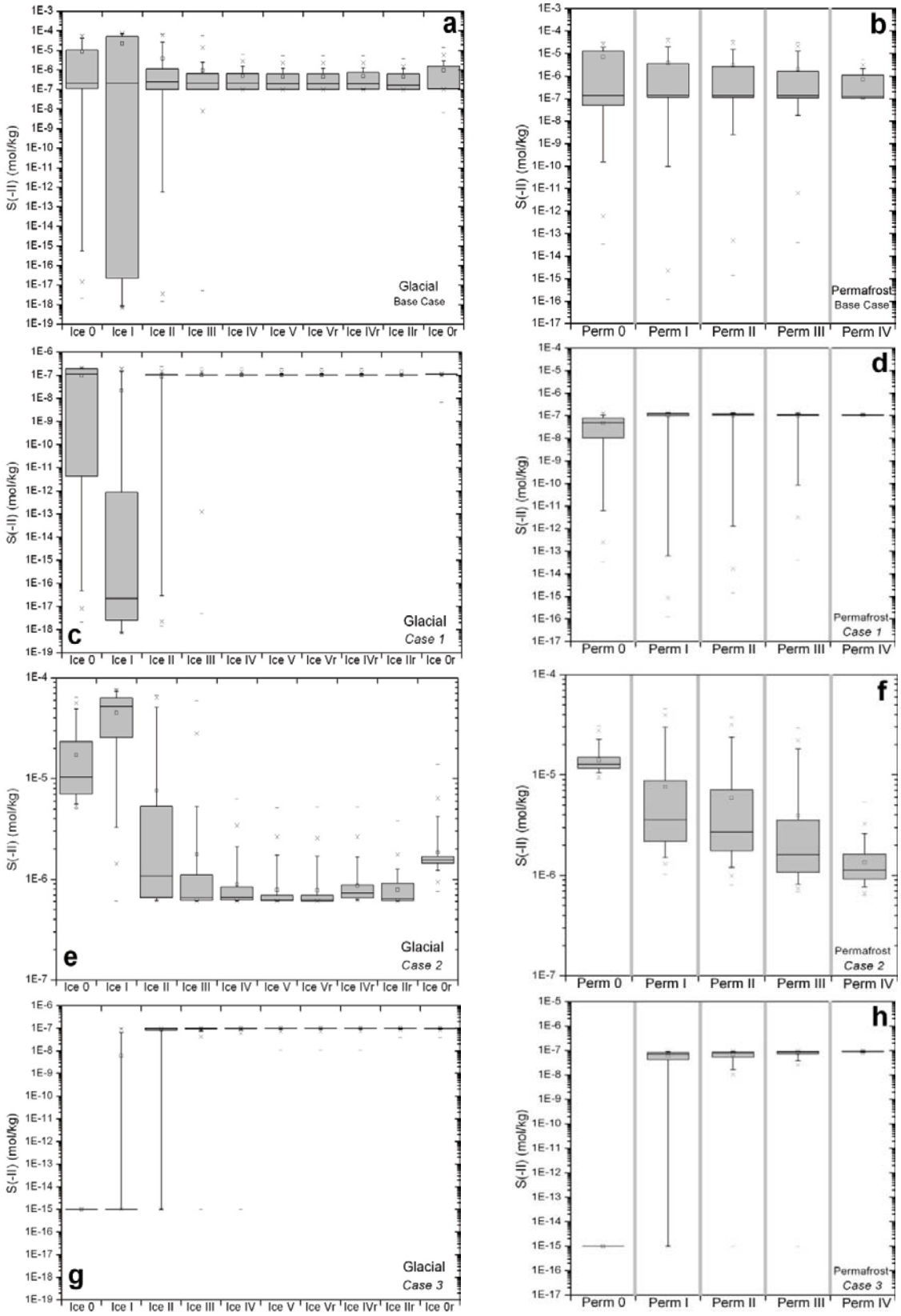

Figure 4-22. *Box-and-whisker plot showing the statistical distribution of S(-II) (mol/kg) obtained for the different geochemical variant cases (Base Case, a and b, Case 1, c and d, Case 2, e and f, and Case 3, g and h) over the glacial (a, c, e, g) and the permafrost periods (b, d, f, h) for the groundwaters located within the candidate repository volume at Laxemar. See the caption of Figure 4-8 for the statistical meaning of the different symbols.*

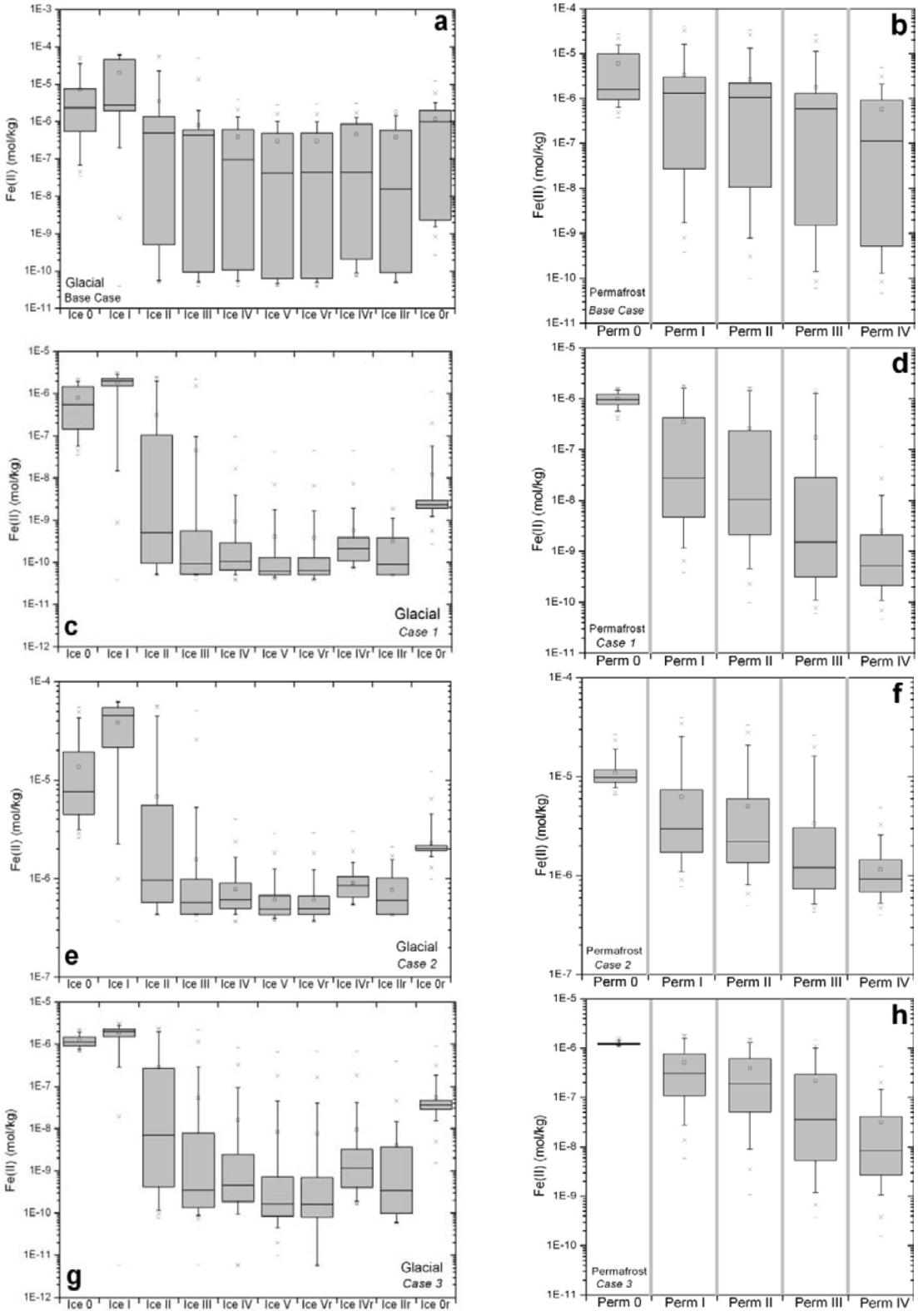

Figure 4-23. *Box-and-whisker plot showing the statistical distribution of Fe(II) (mol/kg) obtained for the different geochemical variant cases (base case, a and b, case 1, c and d, case 2, e and f, and case 3, g and h) over the glacial (a, c, e, g) and the permafrost periods (b, d, f, h) for the groundwaters located within the candidate repository volume at Laxemar. See the caption of Figure 4-8 for the statistical meaning of the different symbols.*

4.4.1.4 Submerged Period

Dissolved S(-II) and Fe(II) concentrations calculated for the submerged period are shown in Figure 4-24. S(-II) values for the case where the area is covered by fresh waters are the same as the ones calculated for the end of the glacial period and range from 10^{-7} to $3{\cdot}10^{-6}$ mol/kg. Fe(II) has values between $3{\cdot}10^{-10}$ and 10^{-5} mol/kg, still lower than at the end of the temperate period. As for the submerged case under marine waters, both elements have higher concentrations and narrower ranges. Computed mean S(-II) concentrations are between $5{\cdot}10^{-6}$ and $3{\cdot}10^{-5}$ mol/kg and mean Fe(II) concentrations between 10^{-7} and $3{\cdot}10^{-5}$ mol/kg in both cases, similar to the ones obtained during the temperate period.

The results obtained for the different geochemical variant cases are shown Figure 4-25. There is a large variability of S(-II) and Fe(II) in the Base Case for the simulation of the repository submerged under fresh waters. However, one can see how this variability is actually the combination of two extreme values given by the variant Cases 1 and 2, with the lowest values obtained for Case 1 and the highest for Case 2. Case 3 gives similar values to Case 1 for S(-II), as this component is not affect by the equilibrium with haematite, and intermediate values for Fe(II), between the two extreme values obtained for Cases 1 and 2.

In the submerged under marine waters stage, S(-II) values are almost identical for Cases 1 and 2 (and, therefore, for the Base Case). Fe(II), however, has lower values when equilibrated with haematite and the coupled data base (Case 1), and higher values when the equilibrium is imposed with FeS(am) (Case 2). Case 3 gives the lowest values of sulphide and intermediate values of Fe(II).

4.4.1.5 Remarks

The methodology used for redox simulations simplify the behaviour of the system by assuming that the imposed equilibria are taking place in the whole volume of rock, which obviously is not true. But the use of the Base Case, combining the results from variant cases 1 and 2, gives a practical range of values to be used for future predictions as they cover the whole range of measured of Fe(II) and, especially, of S(-II) values in the present groundwater system.

The equilibrium with FeS(am) is necessary to explain some of the high-sulphide and high-Fe(II) samples at Laxemar and this is very important as to know these possible maximum sulphide values is the main interest for PA to determine the possible canister corrosion rate. However, these high dissolved sulphide values in the Laxemar groundwaters are punctual situations and they cannot be generalized to the whole rock volume. Thus, the S(-II) concentrations obtained using the geochemical variant case 2 (equilibrium with FeS(am)) can be considered as maxima contents locally expected as long as the Fe(II) source is not exhausted.

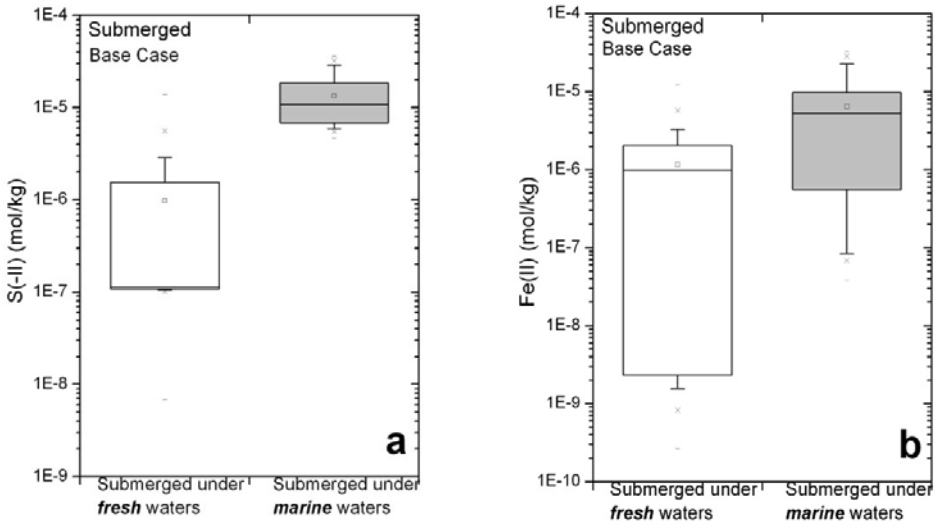

Figure 4-24. *Box-and-whisker plot showing the statistical distribution of (a) S(-II) and (b) Fe(II) (mol/kg), obtained for the Base Case over the two different stages simulated for the submerged period (under fresh and under marine waters), for the groundwaters located within the candidate repository volume at Laxemar. See the caption of Figure 4-8 for the statistical meaning of the different symbols.*

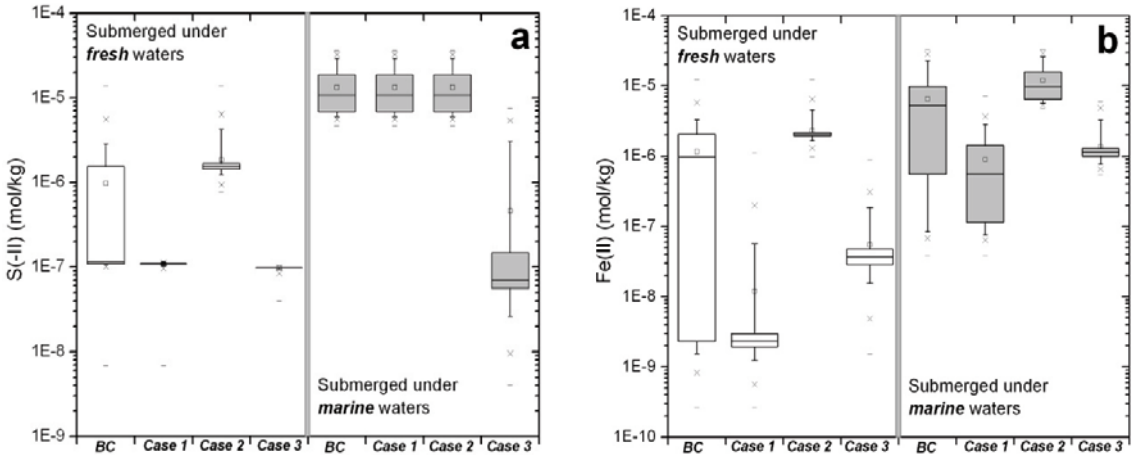

Figure 4-25. *Box-and-whisker plot showing the statistical distribution of (a) S(-II) and (b) Fe(II) (mol/kg) obtained for the different geochemical variant cases over the two different submerged simulations, for the groundwaters located within the candidate repository volume at Laxemar. See the caption of Figure 4-8 for the statistical meaning of the different symbols.*

This is specially valid for the maxima S(-II) values obtained for the glacial period when imposing the equilibrium with FeS(am). During this period electron donors (the input of organic carbon with the recharging groundwater) and acceptors (dissolved sulphate) for SRB activity are expected to be lower than at present and, thus, also the sulphate reduction rates (see Chapter 5).

4.4.2 Redox potential

4.4.2.1 Open repository period

During the excavation period and during the relatively long operational period, the hydraulic and geochemical conditions of the Laxemar site will be subjected to an important number of disturbancies /Laaksoharju et al. 2009, Mårtensson et al. 2009, Acero et al. 2010/. The bedrock and the groundwater at repository depth will be exposed to open atmospheric conditions and this exposure will shift their redox state towards more oxidising conditions. Carbon content will also change due to reequilibration with atmospheric partial pressures of CO_2(g).

After closure, during the return to "natural conditions", microbial degradation of organic materials accumulated in the repository (e.g. biofilms, plastics, cellulose, hydraulic oil, surfactants, etc) and/or corrosion affecting metallic parts used as repository components, may affect the chemical evolution of most of the parameters of interest (Chapter 5), including Eh. The expected effects may occur during the re-saturation phase but also during the temperate period.

The role of stray materials must be assessed, as well as that of any other process that could possibly change the chemical conditions in the repository, such as the corrosion of metal in rock-bolts due to air trapped in the porous buffer and backfill. These processes might, for example, affect the safety function indicators Can1 (copper canister thickness), R1a (reducing conditions), R2d and R2e (generation of colloids and the sorption properties of minerals /SKB 2011/).

Even with moderate inflows to the open tunnels, large amounts of superficial waters are predicted to percolate in when considering the whole period of repository operation. Infiltrating waters will initially be equilibrated with oxygen in the atmosphere, irrespective of their origin (marine, lacustrine, fluvial or meteoric). Therefore, it could be expected that the redox stability of the rock volume on top of the repository area might be challenged at the time of repository closure by the large amounts of infiltrating O_2-rich waters.

However, microbial oxygen consumption takes place already in the overburden and in the first metres of rock, as well as in lacustrine, fluvial and marine sediments and, as described in Chapter 2, the redox buffering capacity of the rock assures that waters reaching the repository volume are free of dissolved O_2. Oxygen consumption in saturated soils is well documented, see for example /Drew 1983, Silver et al. 1999, Pedersen 2006, Alexander and Neall 2007/. The Äspö Redox Zone experiment /Banwart 1999, Molinero et al. 2004/ also showed that microbial respiration in the upper metres of a fracture zone effectively consumes the oxygen in infiltrating waters. In addition groundwater samples from Äspö and Stripa are always found to contain dissolved Fe(II) /Nordstrom et al. 1989/ indicating that groundwaters remain reducing even after prolonged periods of inflow into the tunnels.

In conclusion, the reducing capacity of transmissive fracture zones is not affected during the excavation and operational periods, because consumption of oxygen in infiltrating waters takes place already in soils, sediments as well as in the upper metres of fractures by microbial processes. Evidence from the Äspö laboratory and other Swedish sites, shows that anoxic conditions prevail in the host rock even at a short distance from tunnel walls or from the ground surface.

Air will be trapped in the porous buffer and backfill when deposition tunnels are plugged. Most of the oxygen in this air will be in the backfill because of its larger volume. This oxygen can diffuse to the canister surface and cause some initial corrosion until anoxic conditions are achieved, and, therefore, it is valuable to estimate the reducing capacity of the backfill. Both chemical processes and microbial activities are expected to consume oxygen.

Numerical calculations /Grandia et al. 2006, Yang et al. 2007/ coupling chemical processes consuming oxygen with the hydrodynamic saturation of the backfill have been used to estimate the time scale for reaching anoxic conditions in the tunnels of the repository. These studies show that several inorganic O_2 consumption processes may take place with the accessory minerals present in the bentonite in the buffer and in the backfill. These reactions are, in order of decreasing rate, the dissolution of Fe(II)-containing carbonates, the oxidation of pyrite, and the oxidation of Fe(II)-bearing silicates such as mica and montmorillonite. The calculated oxygen consumption times are highly dependent on the postulated value for the surface area of the reacting minerals. Nevertheless, it may be concluded that anoxic conditions are likely to be reached after a period of the order of one month after the backfill becomes completely water saturated. The density of the backfill is low enough to allow microbial activity and the effect of this will be to shorten the time to reach anoxic conditions in the backfill. Diffusion of oxygen to the surrounding granite would be also an effective mechanism for oxygen consumption by aerobic bacteria populations that could develop in the backfill/granite interface. The REX experiment in the Äspö HRL showed that oxygenated water in contact with a granite surface will be reduced in a few weeks.

In the Prototype Repository Project at the Äspö Hard Rock Laboratory, a programme is in progress for sampling and analysing gases at different locations in the buffer and backfill. One of the specific aims is to monitor the consumption of oxygen /Pedersen et al. 2004/. The two sections of the Prototype Repository were sealed in September 2001 and September 2003, respectively. The resulting oxygen content in the gas phase ranged from almost zero to practically full air atmosphere, although there is a general decreasing trend with time. However, for technical reasons the backfill is not fully water saturated in all parts. These data, therefore, provide further indications that the oxygen consumption will be rapid.

Thus, air will be entrapped in the buffer and backfill, but anoxic conditions are expected to be established soon after the tunnels become re-saturated. Even if the buffer or backfill do not become fully saturated during this period, oxygen consumption processes will take place in the partially saturated materials, as shown from the data obtained at the FEBEX and Prototype experiments /Jockwer and Wieczorek 2003/.

In conclusion, both inorganic reactions and microbial processes will quickly consume O_2 in the air trapped in the backfill, which has the largest pore volume in the deposition tunnels. The majority of the oxygen in the backfill will react before it can diffuse into the buffer and reach the surface of a canister.

4.4.2.2 Temperate period

Figure 4-26 shows the Eh-pH diagrams plotting the values measured in the system (red spheres) and the predicted values obtained for the different geochemical variant cases in a vertical section NW-SE cross-cutting the repository volume. Panel a shows the results obtained with the 3 variant cases (cases 1, 2 and 3) and panel 2, apart from these, shows also (as green triangles) the results obtained with Case 1 and Case 2 but assuming the "equilibrium" with calcite at SI = 0.5. Even taking into account the uncertainty of ± 50 mV and ± 0.1 pH units in the measurements, it is clear from Figure 4-26a that the modelled values are a poor representation for the lowest redox potentials and the highest pH values. However most of these values are better reproduced in Figure 4-26b, when the oversaturation with respect to calcite is assumed in some groundwaters (green symbols; see /Gimeno et al. 2009/).

These results do not allow selecting a unique model that fits the measured Eh values. But in any case, considering all the uncertainties always related to the redox modelling and also the important simplifications made when applying this methodology (the difference between the heterogeneous behaviour of the real system and the homogeneous geochemical model considered for the simulation of the whole volume), the agreement is reasonable and the results do not contradict what has been found in the system. Moreover, as it was indicated for sulphide, the most important point considered in the PA is to find the more oxidant values that could be found in the system and these results show that even in the worst case, the system will be kept under reducing conditions.

Figure 4-27 shows the statistical results for the Eh predicted for the Base Case (results from Case 1 plus results from Case 2) over the complete temperate period in the repository volume. The hydrogeological modelling suggests that the proportion of meteoric waters will increase with time (Appendix 5). This evolution is not expected to change the reducing characteristics of the groundwater, because infiltrating meteoric waters become depleted in oxygen by microbial processes in the soil layers of the site, or after some tens of metres along fractures in the bedrock, as has been shown in the REX experiment /Puigdomenech 2001/ and in groundwaters sampled at 40 to 70 m depth during the "Redox Zone" experiment at Äspö /Banwart 1999, Banwart et al. 1999/.

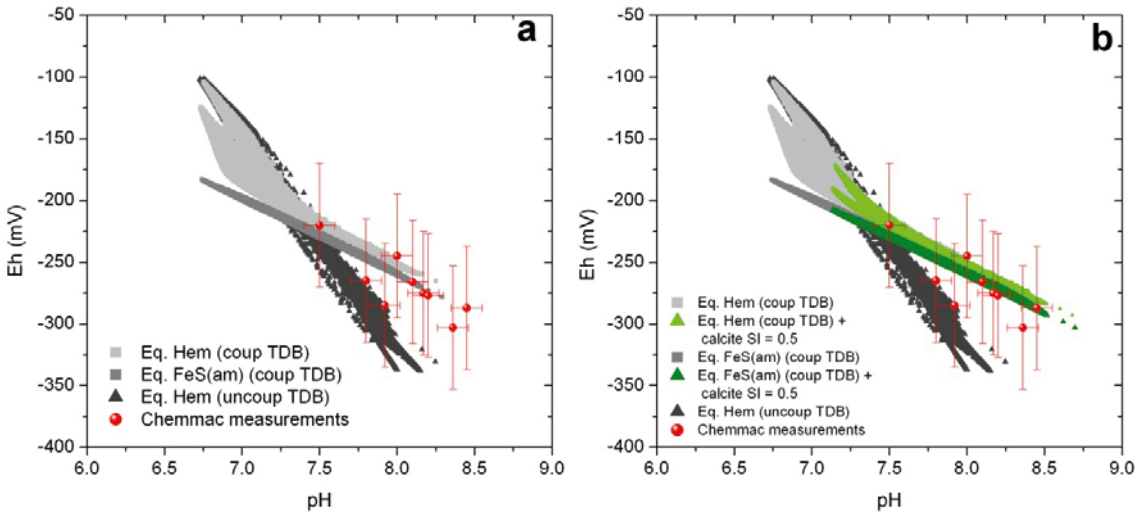

Figure 4-26. *(a) Eh-pH plots (in mV and standard pH units, respectively) measured in the groundwater samples with the Chemmac probe (red spheres) and obtained from the geochemical calculations performed with Case 1 (Eq. Hem. coup. TDB; light grey squares), Case 2 (Eq. FeS(am) coup. TDB; dark grey squares) and Case 3 (Eq. Hem. uncoup. TDB; black triangles) for year 2000 AD in a vertical section parallel to the coast (NW-SE) cross-cutting the repository volume. (b) Same results as in (a) plus two other variant cases in which calcite has been equilibrated at SI = 0.5 (green triangles): light green corresponds to the equilibrium with haematite and dark green represents the equilibrium with FeS(am). The error bars for the measured values are shown in both plots as red bars, the horizontal one represents an error of ±0.1 for pH and the vertical one, an error of ±50 mV for Eh.*

At 2000 AD, most waters in the repository volume are predicted to have Eh values between –225 and –125 mV[21]. Figure 4-27 shows how this range progressively evolves to slightly more reducing values down to minimum values around –270 mV for the year 15,000 AD.

The results for each different geochemical variant case are shown in Figure 4-28. The Eh values obtained considering equilibrium with respect to haematite and FeS(am) (Cases 1 and 2) are similar and mainly in the range from –250 to –125 mV for the repository volume. However, equilibrium with haematite using the uncoupled database (Case 3) enlarges the range of Eh values and moves them towards more reducing levels. This is the only parameter for which the simulations performed with variant case 3 give values in ranges different from what has been considered in the Base Case. It is mentioned here as these results support what was found during the SDM studies /Laaksoharju et al. 2009, Gimeno et al. 2009/. There are parts of the bedrock where the redox conditions are controlled by the iron system with slight or no influence of sulphate reduction (which is the meaning of uncoupling the sulphur redox system in the data base). In any case, these results are favourable from the safety point of view as the predicted conditions are more reducing (numerical results are included in Appendix 4). Thus, they are conservatively excluded from the Base Case, but they are nevertheless discussed also in the next sections.

It may, therefore, be concluded that the reducing groundwater conditions now prevailing at repository depth will continue to dominate for the whole temperate period following the closure of the repository, despite the increasing proportion of meteoric waters with time.

4.4.2.3 Glacial period

The evolution of Eh during the glacial period (with or without permafrost), calculated with the Base Case and the three separate geochemical variant cases is shown in Figure 4-29. The results over the whole glacial period not considering the perfamorst development are quite similar for all the variant cases (more so considering the uncertainty range of ± 50 mV; see Figure 4-29 a, c, e, g).

Compared with the end of the temperate period where Eh values range from –125 mV to –275 mV (as maximum and minimum values), the beginning of the glacial period shows some slightly higher values (up to –75 mV). However, 50% of the samples in the repository volume have more reducing values (between –200 and –250 mV) than at the end of the temperate (between –175 and –225 mV).

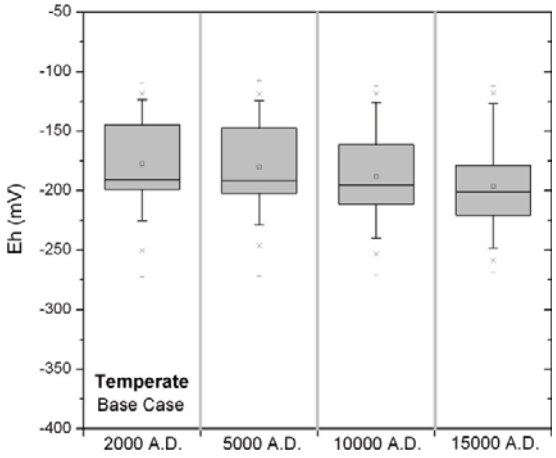

Figure 4.27. *Box-and-whisker plot showing the statistical distribution of Eh (mV) obtained for the Base Case over the temperate period for the groundwaters located within the candidate repository volume at Laxemar. See the caption of Figure 4-8 for the statistical meaning of the different symbols.*

[21] As in all the rest of the parameters discussed in this Chapter, these results correspond to the repository volume and therefore the range of the values is narrower than the one shown in Figure 4-26 where the results plotted correspond to a complete vertical plane.

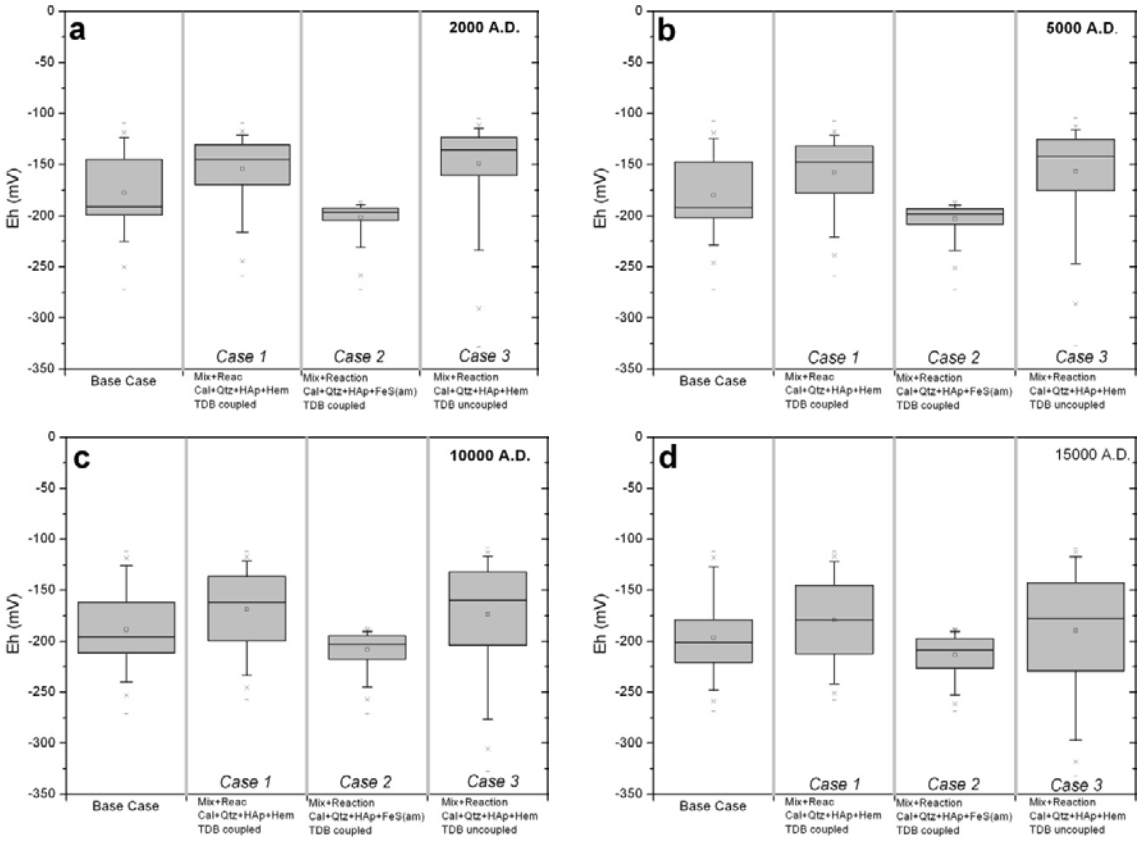

Figure 4-28. *Box-and-whisker plot showing the statistical distribution of Eh (mV) obtained for the different geochemical variant cases over the temperate period for the groundwaters located within the candidate repository volume at Laxemar. See the caption of Figure 4-8 for the statistical meaning of the different symbols.*

During the first stages of the ice advance, more reducing waters reach de repository volume due to the upconing ahead of the ice front, and therefore the mean Eh values decrease. This effect is seen in all the simulations but is more evident when equilibrium with haematite is considered (Case 1) and less marked when the equilibrium is impossed with FeS(am) (Case 2). Then, for the rest of the evolution stages, all the simulations predict very low Eh values (mean around –375 mV) until the final stage is reached, when a slight increase can be seen in Cases 1 and 2. Equilibrium with haematite and the uncoupled data base (Case 3) gives the lowest values for all stages and are mantained very low (around –400 mV) at the end of the glacial period.

When permafrost is considered, Eh evolves progressively towards more reducing situations (Figure 4-29 b, d, f and h). This is common for all three variant cases simulated here and, as seen above, the most reducing values correspond to Case 3 (equilibrium with haematite and un-coupled data base).

In conclusion, for most of the glacial periods, the redox potential of the groundwaters within the candidate repository domain is expected to be clearly reducing.

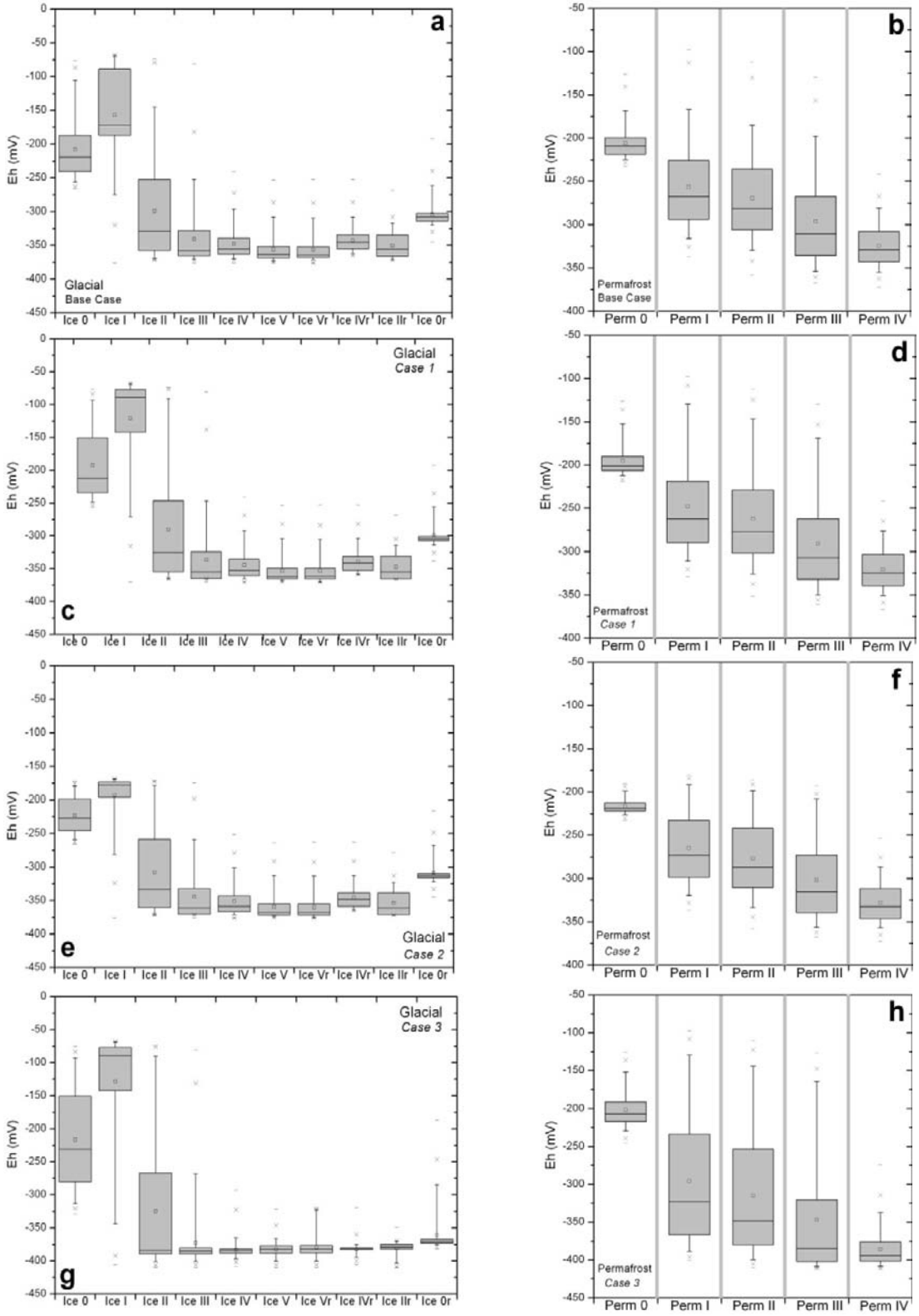

Figure 4-29. *Box-and-whisker plot showing the statistical distribution of Eh (mV) obtained for the different geochemical variant cases (Base Case, a and b, Case 1, c and d, Case 2, e and f, and Case 3, g and h) over the glacial (a, c, e, g)) and the permafrost periods (b, d, f, h) for the groundwaters located within the candidate repository volume at Laxemar. See the caption of Figure 4-8 for the statistical meaning of the different symbols.*

4.4.2.4 Submerged period

Figure 4-30 shows the predicted Eh values for the submerged period considering the two stages (under fresh and marine waters) for the Base Case (panel a) and its comparison with the three variant cases (panel b). The results show that by the end of the glacial period, redox conditions in the repository volume will be very reducing in the submerged under fresh water stage (between –260 and –320 mV for 90% of the grid points) and more if the iron system controls the redox processes (Case 3, with mean values around –400 mV). When the presence of marine waters is considered, all the models predict an increase of Eh towards less reducing conditions, although always below –100 mV, irrespective of the case simulated. These values are quite similar to those predicted (and measured) at present.

4.4.2.5 Remarks

The results obtained for Eh are affected by different uncertainties and limitations and they do not perfectly reproduce the conditions observed in the groundwater system at present. However the only non-reproduced Eh values are the lowest ones, which would mean that the case considered here as de Base Case is the most conservative one from the PA point of view.

The methodology used for redox simulations simplify the behaviour of the system by assuming that the imposed equilibria are taking place in the whole volume of rock, which obviously is not true: there are parts of the bedrock where the redox conditions are controlled by the iron system with slight or no influence of sulphate reduction. However, as indicated for S(-II) and Fe(II), the use of the Base Case, combining the results from variant cases 1 and 2, gives a practical range of values to be used for future predictions as they cover almost the whole range of measured Eh values in the present groundwater system, mainly the less reducing ones and, therefore, those of major concern for PA purposes.

Thus, these results indicate that the anoxic and reducing groundwater conditions now prevailing at repository depth will continue to dominate for the whole temperate period following the closure of the repository, despite the increasing proportion of meteoric waters with time. This is in agreement with the expected reducing capacity of the system, able to exhaust the oxygen present in the recharge waters in the soil layers or after some tens of metres along fractures in the bedrock.

For most of the glacial stages with or without permafrost, the redox potential of the groundwaters within the candidate repository domain is expected to be also clearly reducing. And the same can be said for the submerged final stages, although with less reducing values for the stage in which the area will be submerged under marine waters.

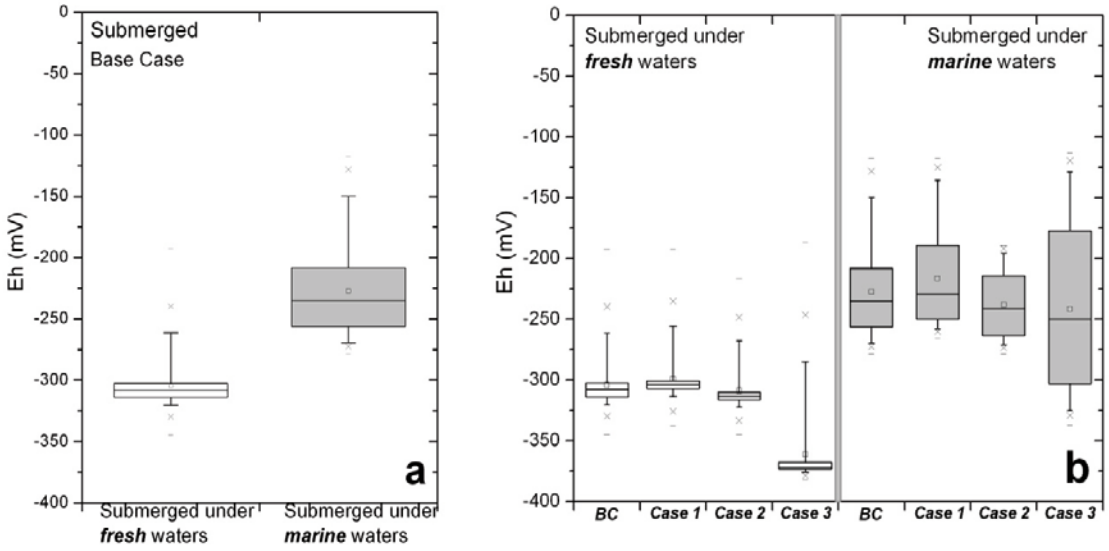

Figure 4-30. *Box-and-whisker plot showing the statistical distribution of Eh (mV) obtained for the different geochemical variant cases over the submerged period (under either fresh or marine waters), for the groundwaters located within the candidate repository volume at Laxemar. See the caption of Figure 4-8 for the statistical meaning of the different symbols.*

5 Evolution over time of other geochemical parameters

5.1 Introduction

The main aim of this section is the assessment of the possible contents of certain components (colloids, dissolved and total organic carbon, nitrite, ammonia, acetate, methane and molecular hydrogen) expected over the future evolution of the Laxemar groundwaters. As stated in Section 1.4.6, this apparently heterogeneous group of parameters include components for which either the available information is insufficient for a precise quantitative evaluation of their future evolution or cannot be modelled in the same way and with the same tools as the rest of the geochemical parameters in this work. Most of them are intimately related to the microbial activity conditioning or being conditioned by different redox processes. This fact makes their evaluation a difficult task due to the complexity and the present limited knowledge of microbial processes in the groundwaters of crystalline systems.

Pernicious effects of these components are mainly related to canister corrosion as many of them are corroding agents or can enhance contents of such agents through different metabolic processes. Therefore, an assessment of the potential amounts of these components over the future evolution of the groundwater system at Laxemar has been performed and is presented next.

All these parameters will be analysed in the following sections using a common structure: a) Overview/general description, including the significance in the performance assessment, factors controlling their contents, available data from the studied sites (or other natural systems); and b) Estimated values over time, with the evaluation of their contents and uncertainties in each of the considered future stages (open repository, temperate period, glacial period and submerged period).

5.2 Evaluation of the parameters

As just stated above, the components that will be analysed here are dissolved organic carbon (DOC)[22], acetate, methane, molecular hydrogen, nitrite, ammonia, and colloids.

Data and discussions included in this section are based on those presented in the report on the hydrogeochemical evolution of the Forsmark site /Salas et al. 2010/. In that report, important limitations on the availability or reliability of data related to some of these parameters were identified, both in the present hydrogeochemical conditions and/or in some of the considered future stages; thus, an important effort has been made in order to delimit these uncertainties. The analysis of potential contents of these parameters over time is based on a larger literature survey:

- The available data and interpretations for the two sites, Laxemar and Forsmark, from the Site Descriptive Modelling. The data used here can be found in the SICADA tables and a general overview is documented in the corresponding background reports /Laaksoharju et al. 2008a, 2009/. A more detailed presentation of the data together with interpretations of most of these parameters are available in /Gimeno et al. 2008, 2009, Hallbeck and Pedersen 2008 a, b/. Furthermore, available data on the SFR site (final repository for short-lived radioactive waste, constructed near Forsmark) in /Nilsson et al. 2010/ have also been included as they give some useful information on the effects of marine intrusion and of the repository construction over the hydrogeochemistry of groundwaters.
- Information on some "non-natural" boundary conditions such as those imposed by the accumulation of organic materials during the construction and operation of the repository /Hallbeck et al. 2006, Hallbeck 2010/ or by the presence of the bentonite barrier as source of colloids /Wold 2010/.

[22] The contents of TOC (analysed in unfiltered samples) and DOC (analysed in filtered samples) in the Laxemar and Forsmark groundwaters are usually very similar. Only locally TOC was found to be significantly greater than DOC. Thus, only the values of dissolved organic carbon will be discussed in this section.

- The available data in other crystalline systems such as Olkiluoto (Finland; /Pitkänen et al. 1999, 2004, Pitkänen and Partamies 2007, Pedersen 2008/), Stripa (Sweden; /Nordstrom et al. 1989/), Grimsel (Switzerland; /Degueldre 1994, Degueldre et al. 1996/), Tono Mine (Japan; /Iwatsuki et al. 2004, 2005/), the Canadian Shield /Vilks et al. 1991, Gascoyne and Thomas 1997, Stroes-Gascoyne and Gascoyne 1998, Gascoyne 2004, Stotler et al. 2009/ and the Witwatersrand basin (South Africa; /Lin et al. 2006/).
- The available data on the chemical characteristics of groundwaters under permafrost conditions in crystalline rock environments. There is very little information about this subject to be used in the evaluation of the future permafrost/glacial stages. The main source comes from the studies in the Lupin Mine or High Lake sites (Canada), but important problems affect some of the performed hydrochemical characterization of these groundwaters (contamination with drilling fluids or mine work; /Stotler et al. 2009/). However, some useful data can be found, specially in the last published works and the available information on these sites has been reviewed /Ruskeeniemi et al. 2002, 2004, Onstott et al. 2009, Stotler et al. 2009, 2010a, b/.
- Finally, data on acetate contents in groundwaters from crystalline systems (as acetate concentrations were not determined during the site characterization programs in Sweden or Finland). Analytical data are available from the sulphide monitoring program under progress at Laxemar and Äspö. Some additional information can be obtained from the replica experiment in REX project /Trotignon et al. 2002/ and from the MICROBE experiment at Äspö /Hallbeck and Pedersen 2008c/. Additional data have been obtained from the Lupin Mine and the Witwatersrand basin /Onstott et al. 2009, Kieft et al. 2005, Moser et al. 2005, Lin et al. 2006/ and they have been used to verify the deductions made in /Salas et al. 2010/ on the contents and possible evolution of acetate in this type of systems.

The future stages considered here cover the time span of a Quaternary glacial cycle, which is 120,000 years. Hence, they include the excavation/operation period, the initial temperate period, and the evolution during the glacial period[23] following the initial temperate period. In addition, immediately after the retreat of an ice sheet, isostatic depression will set the ground surface at the repository site below the Baltic Sea surface level.

In the reference evolution, which is a repetition of the last glacial cycle, the Weichselian, the Laxemar site is expected to be below glacial melt water lakes (such in the Ancylus period in the past), and sea or brackish waters (such as the Littorina sea water periods in the past) during a period of time between a few thousand years up to perhaps ten thousand years. The model results presented above indicate that the conditions when the site is submerged under a glacial melt water lake are similar to those found before the onset of the glaciation. Thus, only a "marine" submerged period is discussed in this section.

In this scheme, the excavation/operational period (that includes the re-saturation phase of the repository[24];/ SKB 2011/) is treated in a "special way". During the excavation and operation phases, the chemical situation close to the repository may undergo several changes. Increased infiltration of meteoric waters, upconing of deep saline waters, oxygen intrusion, changes in microbial communities etc, will promote the existence of variable chemical conditions that, in turn, will affect most of the considered parameters in a very short time perspective.

After closure, during the return to "natural conditions", degradation of organic materials (e.g. microbial biofilms, plastics, cellulose, hydraulic oil, surfactants, etc) accumulated in the repository and/or corrosion affecting the metallic parts used as repository components, may affect the chemical evolution of most of the parameters of interest. The expected effects may occur during the re-saturation phase but also during the temperate period. However, in order to make the description easier, these effects will only be discussed in the section of the excavation/operational period.

Finally, most of the parameters analysed here have fairly similar sources, sinks and conditioning factors (e.g. those related to microbial activities). Hence, in the following text the reader will find a certain degree of redundancy when reviewing the different parameters. This redundancy has been kept in order to make each description self-consistent and easier.

[23] In this section, the term "glacial period" includes the permafrost and glacial stages.

[24] It will take several hundreds of years for the repository to reach full saturation /SKB 2011/.

5.2.1 Dissolved organic carbon (DOC)

5.2.1.1 Overview/general description

The concentration of dissolved organic carbon (DOC) is of special interest for microbiological interpretations as DOC is expected to be related to microbiology: DOC can be used as a source of energy, electrons and carbon by heterotrophic microorganisms, while autotrophic microorganisms will produce DOC (e.g. acetate; see Section 5.2.2). DOC contents may favour reducing environments through microbial activities but also may have detrimental effects if sulphate reduction (and sulphide generation) is the favoured microbial activity. Moreover, the formation of organic complexing compounds and organic colloids might enhance the potential for radionuclide transport during later periods.

As already presented in /Salas et al. 2010/ DOC contents show significant variations in the Forsmark area (Figure 5-1a) at the shallower and more hydraulically active levels (down to 200 m depth) and the highest value, up to around 35 mg/L (2.92 mM), is observed in a brackish marine groundwater. Deeper down (below 200 m depth), DOC values are between 1 and 5 mg/L (0.08–0.42 mM) except for a few exceptions with higher values (around 12 mg/L ≈ 1.0 mM) in some brackish non-marine to saline groundwaters (Figure 5-1a). A similar behaviour is observed at the Laxemar and Äspo areas with the highest values, up to around 20 mg/L (1.67 mM) and 27 mg/L (2.25 mM), respectively in mixed brackish type groundwaters (Figure 5-1b).

DOC (or TOC) values at depth in crystalline systems are expected to be low. Extremely low concentrations have been found in Grimsel Test Site (glacial derived groundwaters) or in the grondwaters at deep granitic fractures (1,000 m depth) from the Henderson mine (below $5{\cdot}10^{-2}$ mM or 0.6 mg/L; Table 5-1). However, in the rest of the examined crystalline systems, concentrations from $8{\cdot}10^{-2}$ to $5{\cdot}10^{-1}$ mM (1–6 mg/L) are more frequently found. This is true even at depths as great as 2.8–3.3 km in the mines from South Africa (Table 5-1) or in deep groundwaters where only autotrophic metabolisms are active like in the Mponeng Mine (/Lin et al. 2006, Chivian et al. 2008/; Table 5-1). Thus, this range ($8{\cdot}10^{-2}$ to $5{\cdot}10^{-1}$ mM) could be considered as the "usual" in groundwaters from crystalline systems.

In this context, the reason for the slightly increased values found in Laxemar and Forsmark below 200 m depth or for the high values found in the brackish-marine groundwaters is not clearly known. Contamination during drilling/sampling, new routines for cleaning the equipment, natural sources such as asphaltite or autotrophic metabolisms, Littorina Sea influences, etc have been discussed. It is hoped that additional data from the monitoring program will clarify the long term behaviour of DOC /Laaksoharju et al. 2009/.

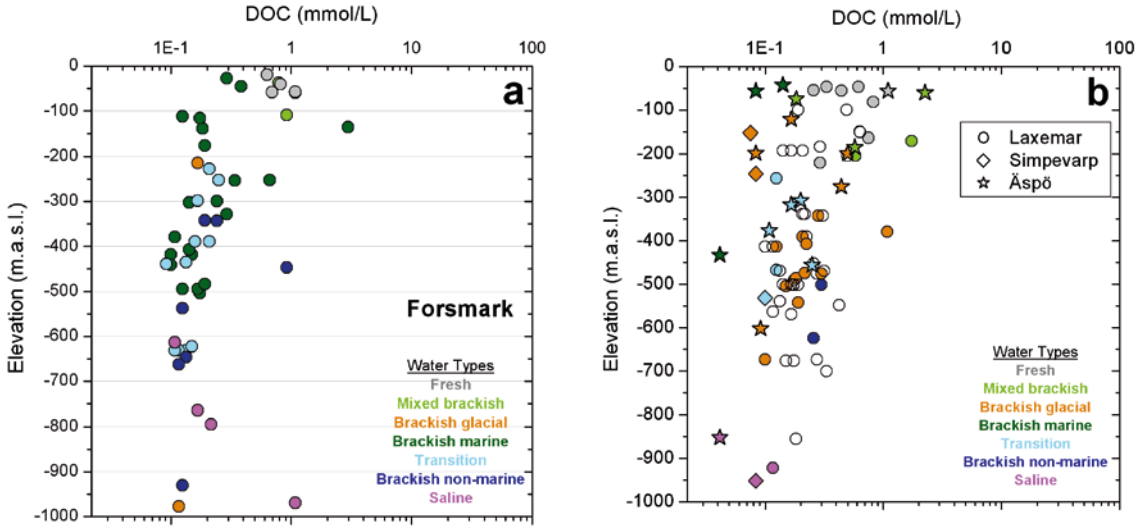

Figure 5-1. *Depth distribution of dissolved organic carbon (DOC) in the Forsmark (a) and Laxemar-Simpevarp-Äspö (b) areas. Samples are coloured by water type as indicated in the legends (see also /Laaksoharju et al. 2008a, 2009/). Open symbols in the Laxemar-Simpevarp plot corresponds to samples for which a water type has not been defined.*

5.2.1.2 Estimated values over time

The excavation and operational phases

Decomposition of organic materials (including microbial biofilms, tobacco, plastics, cellulose, hydraulic oil, surfactants and cement additives) may increase DOC contents promoting an increase in microbial activity. This effect could in turn enhance the reducing capacity of the repository near-field and contribute to a quick consumption of any oxygen left in the repository. However, it may also favour an increase in the activity of SRB and thus in dissolved sulphide contents after closure.

An inventory of organic materials and an assessment of their impact on microbial processes were prepared by /Hallbeck et al. 2006, Hallbeck 2010/ for SR-Can and SR-Site, respectively. In the latest work, three main pools of organic material in the repository have been identified. The largest pool is the organic material in bentonite although it may be questionable whether this material is available for degradation /Hallbeck 2010/; the second largest pool are the biofilms formed on rock surfaces, while the third main pool is the organic material that can be produced by microorganisms with hydrogen from anaerobic corrosion of iron in steal as energy source /Hallbeck 2010, SKB 2010/.

If all the estimated organic carbon in the deposition tunnels would dissolve in their pore space it would result in a DOC concentration as high as 0.45 M /SKB 2011/. However, if the amount of organic carbon with the bentonite is excluded (assuming that it is insoluble) the DOC concentration would be around 1.2 mM. From the calculations performed by /Hallbeck 2010/, maximum concentrations around 0.36 mM of DOC (only from hydrogen produced during the anaerobic corrosion of steel and from biofilms) can be deduced for the deposition tunnels and other areas at the repository in Laxemar and Forsmark. Thus, these are highly uncertain values that strongly depend on the assumptions and simplifications considered in the calculations.

Moreover, the degradation rate of organic materials, especially man-made materials, is still poorly known /SKB 2011/. Some of the problems related to degradation of man-made materials can be exemplified by the results obtained in the REX project. In the supporting laboratory experiment of that project (the replica experiment; /Trotignon et al. 2002/), waters with dissolved oxygen were injected periodically (pulses) during 1 year in a core section extracted from the REX borehole. The return from oxic to reducing conditions was monitored between each series of pulses, including chemical (e.g. DOC, TOC, dissolved sulphide and acetate) and microbiological analysis of waters. Also, biofilm investigations were performed on solid surface samples collected at the end of the experiment, both from the core and from the experimental setup (resins, PETP – polyethylenetereph-thalate- cap, O-ring, etc).

An artefact, associated with an unexpected carbon source supplied by the experimental setup, was discovered. DOC and TOC concentrations in solution reached more than 40 mM during the anoxic periods. Some of the main organic contributors to the bulk DOC and TOC were identified as coming from the PETP cap and the epoxy resin used to seal the cylindrical part of the core. Biofilm investigations confirmed this finding: fermentative anaerobes were present mostly on the sealing epoxy resin; aerobes and IRB were present at significant levels both on plastic surfaces and on the core.

Organic carbon concentration increased in solution from the first to the last pulses (from 0.1 to 46 mM) and because of this extra carbon source, “explosive” iron reducing and fermentative bacteria development was favoured in this experiment. However, the concentration of preferred bacterial substrates such as acetate remained low (below 70 μM; see Section 5.2.2.1) suggesting that organics released by the resin or PETP cap are slow to transform into easily assimilated molecules at the temporal scale of the experiment (one year; /Trotignon et al. 2002/).

The conditions and scale of the replica experiment are not equivalents to those of the repository after closure. However, it would indicate that high DOC contents may develop locally from degradation of some artificial materials, clearly enhancing microbiological activities although the bulk amounts of DOC were not totally bioavailable.

Thus, all the estimations on the DOC contents in this stage must be taken cautiously as important uncertainties remain in the degradation rate of organic materials but also in the biodegradability of the organic matter in the bentonite /SKB 2011/.

Table 5-1. Contents for certain parameters of interest (DOC, acetate, NO_3^-, NO_2^- and NH_4^+) in Laxemar groundwaters compared with those in fracture groundwaters from different crystalline systems. All concentrations in molar units.

	Cl	DOC	Acetate	NO_3^-	NO_2^-	NH_4^+
Laxemar (Sweden) (1)	$1.6\cdot10^{-4}$ to 1.28	$4.0\cdot10^{-5}$ to $2.2\cdot10^{-3}$		$2.1\cdot10^{-8}$ to $3.2\cdot10^{-7}$	$7\cdot10^{-9}$ to $2.0\cdot10^{-7}$	$2.0\cdot10^{-7}$ to $2.8\cdot10^{-5}$
Forsmark (Sweden) (2)	$2.5\cdot10^{-4}$ to $4.2\cdot10^{-1}$	$1.0\cdot10^{-4}$ to $2.9\cdot10^{-3}$		$2.1\cdot10^{-8}$ to $4.3\cdot10^{-7}$	$1.05\cdot10^{-8}$ to $1.0\cdot10^{-7}$	$1.1\cdot10^{-6}$ to $1.9\cdot10^{-4}$
SFR (Sweden) (3)	$5.3\cdot10^{-2}$ to $1.4\cdot10^{-1}$	$5.9\cdot10^{-5}$ to $4.2\cdot10^{-4}$		$1.4\cdot10^{-8}$ to $2.2\cdot10^{-4}$	$1.4\cdot10^{-8}$ to $6.4\cdot10^{-7}$	$3.6\cdot10^{-7}$ to $3.9\cdot10^{-5}$
Olkiluoto (Finland) (4)	$1\cdot10^{-4}$ to 1.27			$3.2\cdot10^{-7}$ to $5.6\cdot10^{-6}$	$4.3\cdot10^{-7}$ to $5.4\cdot10^{-6}$	$1.1\cdot10^{-6}$ to $5.0\cdot10^{-5}$
Stripa (Sweden) (5)	$1\cdot10^{-4}$ to $2\cdot10^{-2}$	$5.9\cdot10^{-5}$ to $3.3\cdot10^{-4}$		$1.6\cdot10^{-6}$ to $1.25\cdot10^{-4}$	1.0 to $8.0\cdot10^{-7}$	1.0 to $3.3\cdot10^{-6}$
Tono Mine (Japan) (6)	$3.1\cdot10^{-5}$ to $3.7\cdot10^{-2}$	$9.2\cdot10^{-5}$ to $3.3\cdot10^{-4}$		1.6 to $8.1\cdot10^{-7}$	$< 4.3\cdot10^{-6}$	$5.5\cdot10^{-7}$ to $2.5\cdot10^{-4}$
Grimsel (Switz.) (7)	1.5. to $4\cdot10^{-4}$	$4.2\cdot10^{-5}$ to $7.5\cdot10^{-5}$		10^{-6}	bdl	$5\cdot10^{-10}$
Lupin Mine (Canada) (8)	$4.6\cdot10^{-2}$ to $6.6\cdot10^{-1}$	1.5 to $3.6\cdot10^{-4}$	2.2 to $8.1\cdot10^{-8}$	$3.1\cdot10^{-6}$ to $6.3\cdot10^{-5}$		1.3 to $3.5\cdot10^{-6}$
Henderson Mine (USA) (9)	1.0 to $1.4\cdot10^{-4}$	3.0 to $5.0\cdot10^{-5}$		1.7 to $7.2\cdot10^{-5}$	2.7 to $4.8\cdot10^{-5}$	$5.0\cdot10^{-6}$ to $1.13\cdot10^{-4}$
Columbia River Fm. (USA) (10)	0.1 to $4.6\cdot10^{-3}$	1.6 to $1.9\cdot10^{-4}$		$1.1\cdot10^{-7}$	$< 2\cdot10^{-7}$	
Kloof 7 Mine (South Africa) (11)	0.23	$4.9\cdot10^{-4}$	$6.2\cdot10^{-5}$	$9.7\cdot10^{-6}$		$< 6.7\cdot10^{-5}$
Driefontein Mine (South Africa) (12)	2.6 to $3.1\cdot10^{-2}$	1.7 to $4.0\cdot10^{-4}$	1.3 to $4\cdot10^{-5}$			$5.8\cdot10^{-6}$ to $6.9\cdot10^{-5}$
Mponeng Mine (South Africa) (13)	5.4 to $8.5\cdot10^{-2}$	$3.58\cdot10^{-4}$	2.25 to $3.57\cdot10^{-5}$	1.5 to $5.6\cdot10^{-7}$		$7.4\cdot10^{-5}$ to 1.10^{-4}

(1) Data from /Gimeno et al. 2009/ and /Laaksoharju et al. 2009/ between 20 and 1,500 m depth.

(2) Data from /Gimeno et al. 2008/ and /Laaksoharju et al. 2008a/ between 20 and 1,000 m depth.

(3) Data from /Nilsson et al. 2010/ between 30 and 390 m depth.

(4) Data from /Pitkänen et al. 2004/ in gneissic bedrocks between 60 and 950 m depth.

(5) Data from granitic rocks between 50 and 1,200 m depth. Available DOC data are between 60 and 350 m depth. NO_3^-, NO_2^- and NH_4^+ are usually below the detection limit. See /Nordstrom et al. 1989/.

(6) Data from /Iwatsuki et al. 2004, 2005/ in the Toki Granite Formation between 180 and 1,000 m depth. As DOC values are not available, TOC concentrations are indicated. NO_3^-, NO_2^- and NH_4^+ are usually below the detection limit.

(7) Data from /Deguledre et al. 1996/ and /Smith et al. 2001/ in the granitic bedrock from the Grimsel Test Site (Switzerland). As DOC values are not available, TOC concentrations are indicated.

(8) Data from /Onstott et al. 2009/ in metamorphic bedrocks (archaean metaturbidites) at 890–1,130 m depth.

(9) Data from /Salh et al. 2008/ in grantic bedrocks at 1,000 m depth.

(10) Data from /Stevens and McKinley 1995/ and /Fry et al. 1997/ in basaltic bedrocks at 300–1,200 m depth.

(11) Data from /Kieft et al. 2005/ in the metavolcanic rocks from Ventersdorp Supergroup at 3.1 km depth. As DOC values are not available, TOC concentrations are indicated.

(12) Data from /Moser et al. 2005/ in the metasedimentary (quartzite) rocks from Witwatersrand Supergourp at 3.3 km depth. As DOC values are not available, TOC concentrations are indicated.

(13) Data from /Lin et al. 2006/ in the metavolcanic rocks from Ventersdorp Supergroup at 2.8 km depth.

Temperate period

The performed simulations indicate that dilute waters will reach greater depths, mainly at the end of the temperate period and, thus, an increment in the DOC contents would also be expected. In Forsmark present fresh and shallow (< 100 m) groundwaters have DOC concentrations around 10–15 mg/L (0.83–1.25 mM; Figure 5-1a). In Laxemar, which is more active hydraulically and where fresh groundwaters reach presently greater depths, DOC contents are lower (0.25–0.83 mM; Figure 5-1b).

DOC contents are expected to decrease during infiltration due to microbial activity. Moreover, DOC at deeper levels is a less suitable substrate for microbial use because it has been exposed to microbial degradation at shallower depths /Kotelnikova 2002/ reducing the metabolic suitable part of DOC (e.g. short-chain organic molecules like acetate; see Section 5.2.2). Thus, neither the amounts of "superficial" DOC reaching the repository level during the temperate period nor the effect of a potential increase in DOC at this depth on microbial activity are clear. In any case, an estimation could be a DOC concentration of about 3–10 mg/L (0.25–0.83 mM) from the present fresh and shallow groundwaters at Laxemar, near the usual range found in crystalline systems (Section 5.2.1.1 and Table 5-1).

Glacial period

During this period the input of organic carbon with the recharging groundwater is expected to be low, because photosynthetic production of organic carbon will cease. Measured values of DOC in several glacier ice samples range from 0.06 to 46.6 ppb ($5 \cdot 10^{-6}$ to $3.9 \cdot 10^{-3}$ mM; /Barker et al. 2006/). Thus, it is not expected in this period an increase in the microbial degradation of organic matter promoted by this "external" input (microbial activity will be sustained mainly by autotrophic metabolisms). A conservative estimation may be a DOC content of 6 mg/L (0.5 mM) for this period, in the usual range observed in the crystalline systems reviewed in Table 5-1. However, this value may be extremely conservative if it is compared with the concentrations found in some groundwaters from glacial origin like those from Grimsel (Table 5-1).

Submerged period under marine waters

In periods where sea water covers the repository site, greater amounts of organic matter (and sulphate) would be expected in the marine recharge groundwaters, enhancing microbial activity (e.g. Fe (III) reduction, sulphate reduction) at shallower levels (sediments). However, the efficiency of DOC at deeper levels would diminish because, as stated above, DOC is a less suitable substrate for microbial utilisation the further from the surface.

Presently, some of the groundwaters at the sites with a high old-marine Littorina contribution have the highest DOC concentrations (up to 2.92 mM; Figure 5-1). However, other groundwaters with similar characteristics have very low DOC contents. As stated above, the origin of these high values is not known and more data are needed to clarify the long term behaviour of DOC /Laaksoharju et al. 2009/.

At the SFR, significant drawdown of modern Baltic Sea water has been observed since the excavation and construction of the facility some twenty years ago and, as in Forsmark, important old marine (Littorina) contributions remain in some of the groundwaters. In this case, high values of DOC/TOC would be expected due to past and present input of brackish sea water. However, the DOC contents in these groundwaters range from 0.7 to 5.1 mg/L ($5.9 \cdot 10^{-2}$ to $4.2 \cdot 10^{-1}$ mM) whereas in the groundwaters with a clear present Baltic signature concentrations the DOC concentrations are even lower (below 3 mg/L or $2.5 \cdot 10^{-4}$ M).

Moreover, some estimate on the amount of suitable DOC for metabolic activities (e.g. acetate) can be made (see Section 5.2.2.2). This estimate also suggests that the input of marine waters does not provide an important source of carbon additional to that already present at repository depth.

Thus, it could be argued that the amount of bulk DOC, eventually reaching the repository depth should not be significant or represent drastic modifications in the intensity of the metabolic processes. However, important uncertainties remain and therefore, the minimum DOC value found in the waters from the sites with more clear marine signature (2.92 mM), could be used as a recommended value for this period.

5.2.2 Acetate

5.2.2.1 Overview/general description

Acetate, as well as molecular H_2 and other simple organic molecules, are continuously produced by fermentative bacteria from complex organic compounds during the degradation sequence of organic matter. It is also produced by autotrophic acetogens using hydrogen as electron donor (reduction of CO_2 via the acetyl-CoA pathway; e.g. /Drake et al. 2006, Konhauser 2007/). The produced acetate

serves as an important substrate for a variety of microorganisms, including sulphate reducing bacteria and, thereby, it may contribute to the amount of produced sulphide. Moreover, acetate contents may contribute, as one of the involved factors (oxidising agent), to stress corrosion cracking (SSC) of the copper canister (see Section 5.1).

Acetate is one of the components included in the bulk DOC concentration. But, unfortunately, acetate contents in the groundwaters were not determined during the site characterization programs in Sweden (or Finland) and, as far as the authors know, there are few available data on acetate contents in other crystalline systems. However, some analytical data are available from the sulphide monitoring program under progress at Laxemar and Äspö; also, some additional information can be obtained from the replica experiment in the REX project /Trotignon et al. 2002/ and from the MICROBE experiment at Äspö /Hallbeck and Pedersen 2008c/.

As there are few published works on the behaviour of acetate in crystalline systems, the scarce available information will be analysed below in the context defined by the state of the art in other low temperature natural systems.

In natural low-temperature and reducing water systems, both biogenic H_2 (Section 5.2.4.1) and acetate are key intermediate metabolites for different dissimilatory metabolic pathways. Thus, they have rather short turnover times (minutes to hours; /Konhauser 2007/) which translates in to the existence of low concentrations in waters from sediments and superficial aquifers. H_2 concentrations are measured in nanomols (Section 5.2.4.1) while acetate concentrations are in the micromolar range (usually tenths of micromoles, reaching occasionally several hundreds of micromoles; /Wellsbury and Parkes 1995, King 1991, Hansen et al. 2001, Koizumi et al. 2004, Konhauser 2007, Jakobsen and Cold 2007, Heuer et al. 2009/)[25].

Higher acetate concentrations may locally appear in low temperature systems where changes (e.g. seasonal) in the microbial population occur (e.g. /Hoehler et al. 1999/). They are promoted by the transient decoupling of acetate production (by fermentative bacteria) and consumption (by heterotrophic metabolisms) but these effects are of short duration (months).

As indicated above, the only available information of acetate in the groundwaters of the sites comes from the sulphide monitoring program at Laxemar (borehole KLX06) and Äspö (boreholes KAS03 and KAS09), and from previous studies like the replica experiment in the REX project /Trotignon et al. 2002/ or the MICROBE experiment at Äspö /Hallbeck and Pedersen 2008c/.

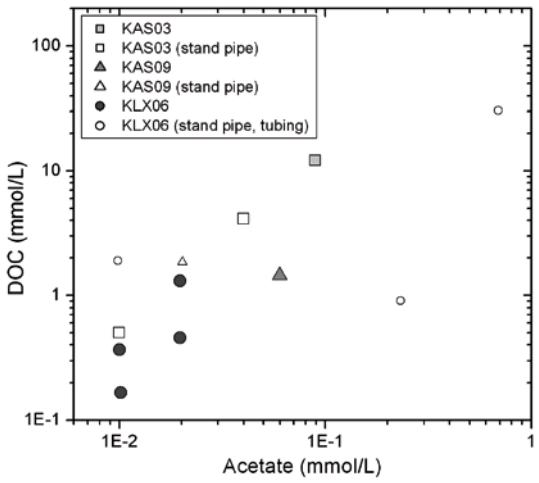

Figure 5-2. *DOC versus acetate contents measured during the on going monitoring program in groundwaters from KLX06 (Laxemar) and KAS03, and 09 (Äspö) boreholes in the Laxemar and Äspö zones. Samples with open symbols correspond to standpipe and tubing samples and, therefore, they are not representative of natural groundwaters.*

[25] Only at high temperatures (60–100°C), in deeply-buried sediments, acetate concentrations can reach levels of 10 mM and higher /Wellsbury et al. 1997, Parkes et al. 2007/.

In the ***sulphide monitoring program*** the highest values of acetate were measured in KLX06 borehole: samples KLX06-1 and KLX06-2-1 with 13.7 mg/L (232.2 μM) and 40.6 mg/L (688 μM), respectively (Figure 5-2), but they correspond to standpipe and tubing samples. The representative groundwater samples have acetate concentrations below 13.7 mg/L (≈ 232.2 μM). Acetate appears to be a minor constituent of bulk DOC in the studied groundwaters, usually contributing less than 10%.

Under *in situ* laboratory conditions in the MICROBE experiment quantitative information on acetate contents and production rate have also been obtained. A circulation system connected to a conductive fracture was installed at a depth of 447 m. Groundwater is pumped from the fracture through flow cells and then back to the fracture again while being maintained under *in situ* conditions. Acetate determinations were performed in a closed mode, where the connection to the aquifer was blocked but pressure was maintained and groundwater was re-circulated through the flow cells in the system.

The concentration of acetate (and also the dissolved sulphide) increased from 2.3 to 14.9 mg/L (39 to 252 μM) in approximately 60 days, when it ceased at the same time as the most probable numbers of both sulphate reducing bacteria and autotrophic acetogens started to decrease. The increments of acetate would correspond to production rates of 0.14 mg acetate L^{-1} day^{-1} (2.37 μmol L^{-1} day^{-1}).

The acetate production rates found in the experiment were large relative to the concentrations of acetate found in the monitored sections from Laxemar and Äspö or to the DOC found in the analysed groundwaters from the potential repository sites (Figure 5-1). Assuming these production rates it would only take 40 days and three months to reach, respectively, the highest acetate and DOC concentrations found in the studied systems. However, the available data indicate that a very large increase of acetate in the analysed groundwaters, promoted by such production rate, is not observed. This fact would suggest that acetate is consumed by heterotrophic microorganisms at approximately the same rate as it is produced in these crystalline environments /Hallbeck and Pedersen 2008c/, in agreement with what has been observed in other natural systems.

In the supporting laboratory experiment of the REX project (the replica experiment; /Trotignon et al. 2002/), waters with dissolved oxygen were injected periodically (pulses) in a core section extracted from the REX borehole. The return from oxic to reducing conditions was monitored between each series of pulses, including chemical (e.g. dissolved sulphide and acetate) and microbiological analysis.

During the anoxic periods between oxygen pulses fermentative anaerobes increased, strongly favoured by an extra carbon source supplied by the experimental setup (resins, polyethylenterephthalate, etc). This increment in the amount of fermentative bacteria could represent a source of additional acetate. However, acetate concentrations remained at low levels, always below 70 μM, during the experiment. The increase in the fermentative activity agreed with the explosive development of iron reducing bacteria (IRB) which would consume the additional acetate, lowering the concentration at the observed low levels.

The rare acetate data in groundwaters of other crystalline systems seems to agree with the picture above. The acetate concentrations in the deep and old groundwaters (2.8 to 3.3 km depth and average subsurface residence time of 4 to 160 Ma; /Kieft et al. 2005, Moser et al. 2005, Lin et al. 2006/) from the crystalline materials in the Witwatersrand Basin (South Africa) are between $1.3 \cdot 10^{-5}$ to $6.2 \cdot 10^{-5}$ M (Table 5-1), in the usual micromolar range observed in the rest of low temperature water systems. Moreover, acetate appears to be a minor constituent of bulk DOC in those groundwaters, usually contributing less than 10% (as in the monitoring program; see above). In the Lupin Mine, at 890–1130 m depth, the acetate contents are even lower, in the nannomolar range (Table 5-1). In these groundwaters, other organic acids like butanoate, pentanoate, hexanoate and, specially, formate ($1.3 \cdot 10^{-7}$ to $8.8 \cdot 10^{-6}$ M) occur in higher concentrations than acetate. However, the combined concentration of the organic acids comprised, again, less than 10% of the measured DOC in these groundwaters /Onsttot et al. 2009/.

All these observations suggest that maximum acetate contents and limiting factors are common to all low temperature natural systems. The acetate pool would be controlled by a balance of acetate producing and consuming processes: acetate production by fermentation of organic matter or by autotrophic acetogens and acetate consumption by heterotrophic metabolisms (e.g. sulphate reducing bacteria or acetoclastic methanogens).

Microbiological analysis performed at Forsmark and Laxemar suggest the existence of the same sources and sinks. Acetogens, both autotrophic and fermentative-heterotrophic, were the dominant microorganisms in the studied sections (there are often one or two orders of magnitude more acetogens than the second most common organism type; /Hallbeck and Pedersen 2008 a, b/). A wide variety of heterotrophic, acetate consuming metabolisms has also been detected and, therefore, acetate concentration in groundwaters is expected to remain low, in the micromolar range.

In summary, as acetate is one of the organic molecules utilised by most microbes, increments in acetate production should be compensated by a parallel increase in its consumption by heterotrophic metabolims, especially in the low-nutrient conditions of groundwaters in crystalline systems. Acetate accumulation could arise from decreasing rates of acetate consumption but, as stated above, this situation appears to be very transient (months) in low temperature environments. Finally, the possible increments in the acetate production rate (by fermentative processes) and its reflection in an enhanced sulphate-reducing activity must be assessed in a generic way considering the present state of knowledge. The easiest way is considering the supply of complex organic components as basic constituents of the organic matter degradation chain, able to induce an increase in the fermentative activity and, subsequently, in the sulphate-reducing activity. Therefore, the analysis presented below has a clear parallelism with that performed for DOC in Section 5.2.1.2.

5.2.2.2 Estimated values over time

The excavation and operational phases

Important changes in the microbial communities are expected during this stage, with extensive microbial activity promoted by the large amounts of organic materials found at or near the repository and the variable environmental conditions associated with oxygen intrusion, mixing of oxidising and reducing waters, etc.

After closure, degradation of organic materials could contribute to quick consumption of oxygen left in the repository but also to higher rates of acetate production that may induce higher rates of sulphide production in the vicinity of the deposition holes. Moreover, the anaerobic corrosion of steel could contribute indirectly to the pool of organic material in the repository. The hydrogen produced in the corrosion process may act as an energy source for various microbial processes, including acetogens. These microorganisms would increase the amounts of acetate that, in turns, would increase SRB activity.

In the inventory of organic materials prepared by /Hallbeck et al. 2006/ for SR-Can, net acetate concentrations of 32–36 μM from fermentation of carbohydrates and biofilms were obtained for deposition tunnels and other cavities in the repository. From the mass balance calculations presented by /Hallbeck 2010/ for SR-Site, concentrations of around 200 μM of acetate (contributed by biofilms and in a lesser extend by hydrogen produced in the anaerobic corrosion of steel) can be deduced for Laxemar and Forsmark areas.

Acetate may be used by SRB, increasing the amounts of dissolved sulphides. The reaction involving acetate and dissolved sulphide is equimolar with respect to both components (see reaction 5–6); thus, from the above estimations of 0.2 mM for acetate, similar amounts of sulphide should be produced (around 6.5 mg/L of dissolved sulphide; /Hallbeck 2010/).

Some of the sulphide could diffuse to the canister where corrosion would take place. But, it must be taken into account that these values are “cumulative” and non time-average values expressed in a per liter basis that must be relaxed during the evolution of the excavation/operational period and, probably, during the temperate period as well. Moreover, not all the acetate will be used by SRB as other, more energetically favoured metabolisms will have used part of this organic carbon previously. Furthermore, most of the sulphide produced will either react with Fe(II) in the groundwater or with the corrosion products, or will diffuse away from the canister and, therefore, this sulphide would have a negligible impact on the copper casing of the canisters.

However, the acetate and sulphide values are largely uncertain /Hallbeck 2010/ and, also, they are based only in a part of the bulk organic pool in the repository (i.e. excluding the organic matter in bentonite; see Section 5.2.1.2).

In any case, the maximum concentrations of acetate allowed by the balance between microbial producing and consuming processes at any time would be in the micromolar range. Immediately after repository closure, microbial activity will continue at a high rate due to the high temperature and, therefore, some transient increments in the acetate concentrations would be expected (e.g. in the millimolar range). However, once the repository has cooled down, microbial processes rates will go down and a decrease of the acetate concentrations at "normal" levels in low temperature systems (micromolar range) is expected.

Temperate period

The performed simulations (Chapter 4) indicate that dilute waters will reach greater depths than today (mainly at the end of the temperate period) and thus an increment in bulk DOC contents would be expected. Present fresh and shallow (< 100 m) groundwaters in Forsmark have concentrations of about 10–15 mg/L (0.83–1.25 mM; Figure 5-1a). In Laxemar, more hydraulically active and with fresh groundwaters reaching greater depths, DOC contents are lower (0.25–0.83 mM; Figure 5-1b).

DOC contents are expected to decrease during infiltration due to microbiological activity. Moreover, this activity will decrease the proportions of the adequate substrates like acetate, included in the bulk DOC and, therefore, the DOC reaching deeper levels will be a less suitable substrate for microbial use.

Thus, the amount of acetate reaching the repository level during the temperate period is expected to be in the micromolar range (as most of the low temperature aquatic systems) which will not represent an important additional source for heterotrophic metabolisms such as sulphate reduction.

Glacial period

During this period, due to the suspension of photosynthetic production of organic carbon, the input of organic carbon and acetate with recharging groundwater is expected to be low. Therefore, an increment in the microbial degradation of organic matter promoted by this "external" input over the glacial period is not anticipated and microbial activity will be mainly sustained by autotrophic metabolisms. Thus, micromolar concentrations of acetate would be also expected from the relationship between acetate production (by fermentative or autotrophic metabolisms) and consumption (by heterotrophic metabolisms).

Submerged period under marine waters

It is expected that the infiltrating recharge waters through marine sediments will follow the known degradation sequence of organic matter controlled by microbiological processes and, thus, with acetate concentrations in the micromolar range.

5.2.3 Methane

5.2.3.1 Overview/general description

Methane may be generated both by organic processes (methanogenic microorganisms) and inorganic processes at depth in crystalline systems (/Pitkänen and Partamies 2007, Hallbeck and Pedersen 2008a, b/ and references therein). Inorganic methane may come from this deep source and move slowly by diffusion towards the surface, mixing with methane from biogenic origin if present. This possible dual origin makes the prediction of methane contents in a specific period very difficult.

Methane is a chemically active gas that may participate or control the redox state of the groundwater system at different depths, under different conditions and with variable rates or intensities depending on its origin. Also, the oxidation of methane may contribute to oxygen reduction in the case of oxygen intrusion /Puigdomenech 2001/ and it is a substrate for different metabolic activities. It may be used, for example, by methanotrophs under oxic conditions but it can participate as well in a special type of microbial sulphate reduction coupled to CH_4 oxidation in anaerobic conditions /Kotelnikova 2002, Pitkänen et al. 1999, 2004/, increasing dissolved sulphide contents.

Methane contents are very low in the Forsmark area. They are always below $5.5 \cdot 10^{-3}$ mM, except in the case of KFM01D borehole at 445 m depth where a value as high as 4.2 ml/L (0.2 mM) was measured (Figure 5-3a), without any evident correlation with depth or with the presence of methanogens

(barely present in this area, usually below 10 cell/mL; /Hallbeck and Pedersen 2008a/). A similar situation can be observed for methane in the Laxemar-Simpevarp area (Figure 5-3b; /Hallbeck and Pedersen 2008b/) with the highest value of methane below $3.9 \cdot 10^{-2}$ mM.

Furthermore, the still scarce data on methane contents in the SFR site indicate also the presence of low concentrations, between $1.23 \cdot 10^{-3}$ and $5.3 \cdot 10^{-3}$ mM, at depths between 94 and 134 m.

These observations contrast with those from other systems like Olkiluoto where methane contents (and also the total amount of dissolved gases) are much higher. This is especially clear for the most saline and deepest Olkiluoto groundwaters, where methane is the most abundant gas /Pitkänen and Partamies 2007/ and its concentrations clearly increase with depth from around 0.1 ml/L ($4.5 \cdot 10^{-3}$ mM) in the near-surface groundwaters to around 1,000 ml/L ($44.6 \cdot 10^{-3}$ mM) at 750 m depth (Figure 5-3c). However, the amounts of methanogens in the Olkiluoto groundwaters were usually at or below the detection limits due to unclear causes (see the discussion by /Pedersen 2008/, pp. 102–103).

The available data for the Laxemar area indicate that methane originates mostly from an inorganic source. The samples with the highest proportion of biogenic methane correspond to KLX03 borehole at 171 and 380 m depth in the sections with the highest volume of methane measured in that area (Figure 5-3b; /Hallbeck and Pedersen 2008b/). Also, a dominant inorganic source has been proposed for Forsmark and, again, the sample with the highest proportion of biogenic methane (KFM01D borehole at 445 m depth) corresponds to the section with the highest volume of methane measured

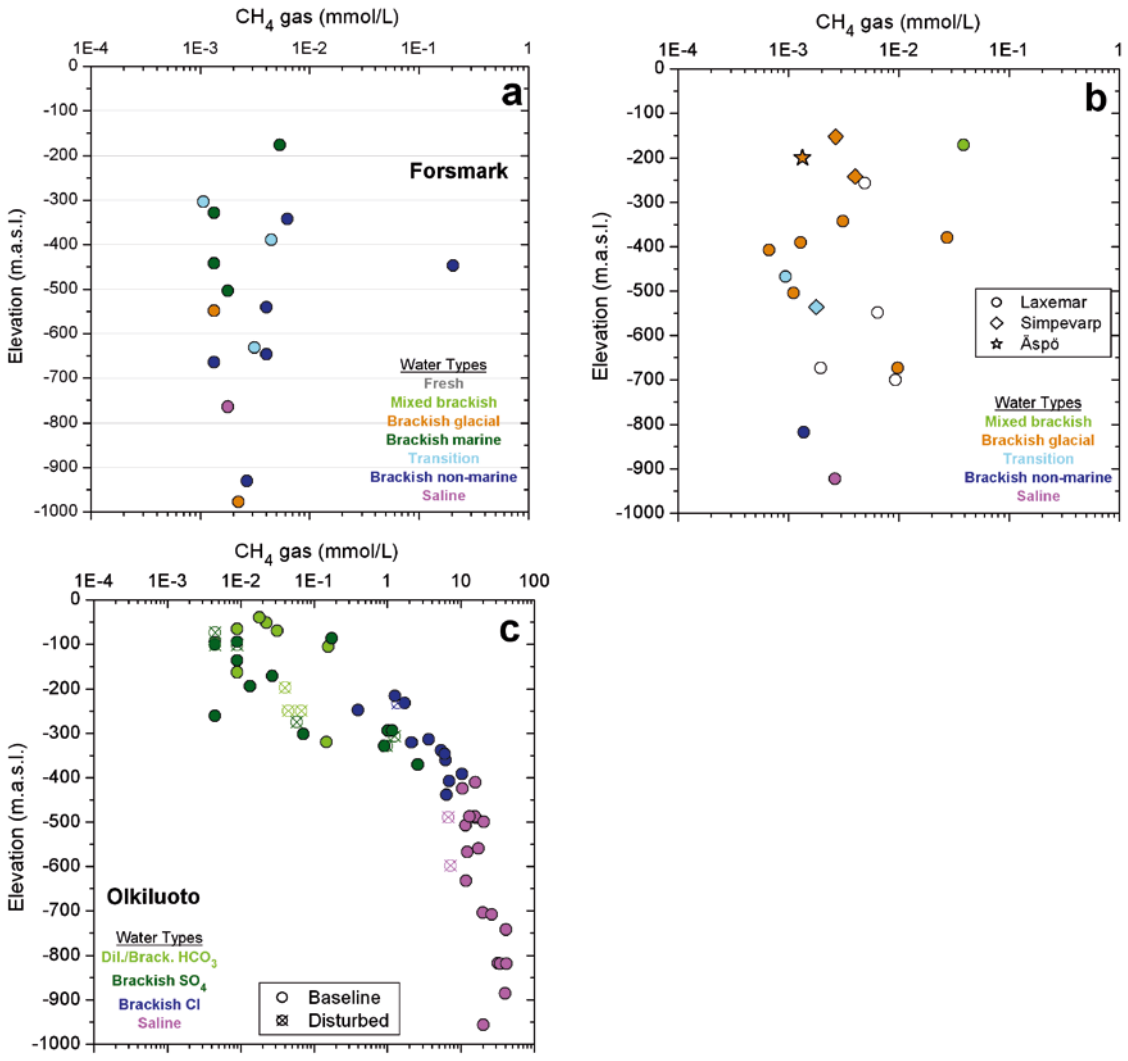

Figure 5-3. *Depth distributions of methane in Forsmark (a), Laxemar (b) and Olkiluoto(c) groundwaters. Data for the Forsmark and Laxemar groundwaters from /Gimeno et al. 2009/ and for the Olkiluoto groundwaters from /Pitkänen and Partamies 2007/.*

in that area (Figure 5-3a; /Hallbeck and Pedersen 2008a/). In Olkiluoto, isotopic data have allowed a more precise determination on the origin and distribution of methane. This gas seems to have two primary sources: a thermal origin from inorganic hydrocarbons, predominant in the deepest groundwaters, and a bacterial origin, steadily increasing in importance towards the shallowest and CH_4-poor parts of the system /Pitkänen and Partamies 2007/.

Therefore, methane from biogenic and abiogenic sources is present and "mixed" in the Laxemar, Forsmark, and Olkiluoto groundwaters. However, the sparseness of data for the examined rock volume in Laxemar and Forsmark prevent identification of any clear trends. All these circumstances highlight the need for more data in order to clarify its origin and distribution in the studied systems and to fill these important gaps in the overall understanding of the redox processes. On top of that, methodological improvements in the sampling procedures are also badly needed (see /Hallbeck and Pedersen 2008a, b/).

5.2.3.2 Estimated values over time

The excavation and operational phases

Decomposition of organic materials accumulated in the repository will increase microbial activity. Methanogenesis is usually the last metabolic step in the degradation sequence of organic matter and could probably be an effective process during this period. Acetoclastic methanogens disproportionate acetate to form methane and CO_2:

$$CH_3COOH \rightarrow CH_4 + CO_2 \quad (5\text{-}1)$$

Also, autotrophic (hydrogenotrophic) methanogens may use H_2 and CO_2:

$$CO_2 + 4H_2 \rightarrow CH_4 + 2H_2O \quad (5\text{-}2)$$

The intensity of these processes and the amounts of methane generated are unclear. Some rough estimations can be made from the net amount of acetate (see Section 5.2.2.2) or hydrogen (from corrosion; see Section 5.2.4.2) produced in the repository. Thus, through reaction (5-1) a concentration of methane of around 200 μM can be obtained; and through reaction (5-2) the calculated concentration of methane is 27 μM.

The concentration of methane is of importance as a nutrient source for microbially mediated sulphate reduction to sulphide:

$$SO_4^{2-} + CH_4 \rightarrow HS^- + HCO_3^- + H_2O \quad (5\text{-}3)$$

and, from the above estimations, a net value of around 7.0 mg/L of dissolved sulphide can be obtained. This estimation may be extremely conservative because not all the acetate or hydrogen will be used by the SRB as other more energetically favoured metabolisms will have used part of these components previously. Moreover, most of the sulphide produced will either react with Fe(II) in the groundwater or in the corrosion products, or diffuse away from the canister, drastically diminishing its impact on the copper casing of the canisters. However, these values are derived from mass balance results largely uncertain /Hallbeck 2010/ based on the inventory of organic materials in the repository (see Sections 5.2.1.2. and 5.2.2.2).

Temperate period

The performed simulations (Chapter 4) indicate that dilute waters will reach deeper depths than today, mainly at the end of the temperate period. Unfortunately, there are no data on CH_4 contents of fresh groundwaters in the Swedish sites that could serve as reference for this dilution case. At Olkiluoto, the maximum CH_4 content in dilute, shallow groundwaters is around 0.2 mM (Figure 5-3c).

Assuming that the concentration of dissolved natural gases remains substantially the same as those before repository construction /SKB 2010/, a mean value of $6.7 \cdot 10^{-3}$ mM can be obtained from the present groundwaters (Table 5-3) with a maximum value (in one the samples with high biogenic contribution in KLX03 borehole; see above) of $3.9 \cdot 10^{-2}$ mM. This maximum value can be used tentatively as a reference value for this period.

If the maximum contents of methane in the Laxemar groundwaters were quantitatively used by microbes in sulphate reduction (assuming that CH_4 contents are not replenished), the sulphide concentration would increase at up to of $3.9 \cdot 10^{-2}$ mM (1.25 mg/L) according to reaction (5-3).

Glacial period

During permafrost, the perennial freezing of rock volumes will effectively shut down the hydraulic circulation in the bedrock, at least locally. In this way, microbial populations could be isolated from the surface, with negligible inflow of organic matter; also, methane gas can be trapped as clathrate hydrates. Under these conditions, the intensity of sulphide production due to microbially mediated $SO4^{2-}$ reduction will probably decrease. However, sulphide production could be sustained by methane and hydrogen (e.g. through reactions 5-3 and 5-4) depending on the balance between 1) the production and flow of CH_4 and H_2 from the deep bedrock and from biogenic origin, 2) the impervious frozen layers at the top of the site, and 3) the incorporation of CH_4 in the ice as clathrates. If clathrate formation occurs, the dissociation of these compounds to release methane during permafrost decay would add to the nutrient sources for microbial populations in the bedrock at the end of the glacial period (see, for example, the discussion in /SKB 2006b, 2010/). Taking into account all these processes and feedbacks, any estimation of the concentration of methane is difficult, if not impossible.

Under glacial conditions, the presence of significant amounts of CH_4 and H_2 may have a positive effect on the chemical stability of the groundwaters by contributing to the consumption of the oxygen potentially capable of reaching the repository. It may be envisaged that methane and hydrogen dissolved in deep groundwaters (or the up-welling of methane and hydrogen from deep crustal layers) can be used by microbes to consume the oxygen infiltrated from the surface. During the Matrix experiments at Äspö, it was observed that the rock matrix contained methane and other dissolved gases in concentrations similar to those found in groundwater. Consequently, if methane is consumed or flushed out from the fractures of an aquifer, it will diffuse from the rock matrix into the fractures and the process will continue. As the volume of water in the rock matrix porosity is larger than the volume of groundwater in the fractures, this process could continue throughout a glaciation cycle /SKB 2011/. This aspect merits further studies as CH_4 and H_2 can also have a negative effect, enhancing sulphate reduction.

In conclusion, there are not enough data at present to quantify the concentration of CH_4 and H_2 during this period. Having no better options, the maximum concentrations of hydrogen and methane detected presently in the Laxemar groundwaters could be used tentatively as recommended values for this glacial period.

Submerged period under marine waters

During the submerged period marine waters will recharge the aquifer system infiltrating through the sediments and at the same time advancing in the redox sequence, including methanogenesis. In other words, the infiltration of marine water would incorporate exclusively biogenic methane into the system.

In the Forsmark groundwaters with clear Littorina signature this conclusion cannot be confirmed (as performed for ammonium in Section 5.2.5.2) as they do not have higher methane contents (always below $6 \cdot 10^{-3}$ mM; Figure 5-2a). Similarly, groundwaters with the most clear Littorina signature in the SFR site show methane contents between $2.54 \cdot 10^{-3}$ and $4.28 \cdot 10^{-3}$ mM. This can be due to the fact that not all the methane produced in the marine sediments diffuses downwards: some of it can go upwards decreasing the level in the infiltrating groundwaters. Additionally, methane can also disappear (e.g. consumed) during infiltration in the bedrock.

In any case, the maximum value of methane in the Laxemar groundwaters at present ($3.9 \cdot 10^{-2}$ mM) can be used as a reference value for this period.

5.2.4 Molecular Hydrogen

5.2.4.1 Overview/general description

Molecular hydrogen, like methane, can be generated by biological and inorganic processes at depth in crystalline systems. In the degradation sequence of organic matter, biogenic molecular H_2 and simple organic molecules (e.g. acetate, Section 5.2.2) are continuously produced by fermentative bacteria and heterotrophic acetogens from complex organic compounds. In turn, the produced H_2 (or acetate) is quickly metabolised by other microorganisms (e.g. turnover times from minutes to hours; /Konhauser 2007/) using different terminal electron acceptors (TEAs) and lowering hydrogen concentrations to values below 50 nM /Lovley and Goodwin 1988, Hoehler et al. 1998, Christensen et al. 2000, Lin et al. 2005/ or to values below 150 nM if acetogenesis is involved /Hoehler et al. 1998, Heimann et al. 2010/.

This behaviour is the consequence of the strong coupling of hydrogen to a very broad spectrum of inter-related microbial activities. Hydrogen is an excellent electron donor for a large number of microbial metabolisms, including methanogenesis, acetogenesis, sulphate reduction, iron reduction, and manganese reduction, among others /Postma and Jakobsen 1996, Hoehler et al. 1998, Christensen et al. 2000, Appelo and Postma 2005/. However, the existence of an additional, inorganic source for H_2 (at least, six different inorganic processes may produce abiogenic H_2; e.g. /Hallbeck and Pedersen 2008a, b/) makes this analysis considerably more difficult. It may increase the intensity and diversity of the aforementioned heterotrophic metabolisms and it may be metabolised by autotrophic methanogens and, especially, acetogens, to create a background level of suitable organic carbon, such as acetate, in crystalline groundwater systems /Pedersen 2001, Lin et al. 2005/. Since the produced acetate can be used by different heterotrophic organisms, it could increase the overall metabolic intensity, including sulphate reduction.

High hydrogen concentrations may favour high metabolic intensities and, even, diversities (indirectly, through acetate production by acetogens or, directly, as electron donor for a wide number of metabolic activities). The net effects of all these linked processes will depend, in the last term, on the inflow and consumption rate of hydrogen (for example, radiolysis can produce millimolar concentrations of H_2 for every million years of subsurface isolation if there is no H_2 consumption; /Lin et al. 2005/).

Thus, abiogenic and biogenic sources of hydrogen in the studied systems are of major concern because hydrogen concentrations may be determined by (and may determine) most of the proposed microbiological metabolic activities in the groundwaters. Hydrogen may not only couple oxidative and reductive processes, but also regulate the flow of carbon and electrons in virtually every step in the breakdown of organic matter /Hoehler et al. 1998/ and of the overall food chain emanated from the "Deep Biosphere" concept /Pedersen 1993, 1997a, b/. For further discussion, see /Gimeno et al. 2009/.

The available data on hydrogen contents in the Forsmark area are very scarce. From the sixteen analysed samples only six have values above the detection limit, in the range 0.24–19.2 μM, with maximum values between 300 and 500 m depth (Figure 5-4a). These maximum values are higher than those found in the Laxemar area (8.5 μM; Figure 5-4b). At Olkiluoto, the latest data presented by /Pedersen 2008/ show a rough increase of hydrogen with depth, reaching maximum values of around 3.5 μM at the maximum sampled depth (742 m). Much higher contents were found at higher depths by /Pitkänen and Partamies 2007/, with concentrations from 300 to 1,000 μM in 800–1,000 m depth interval (Figure 5-4c).

Overall, the maximum detected amounts of hydrogen in the Laxemar area (and also in Forsmark) are lower than at Olkiluoto (in the milimolar range, similar to other groundwaters in crystalline systems; /Lin et al. 2005, Sherwood Lollar et al. 2007/). However they are several orders of magnitude higher than the maximum values (from biogenic origin) found in marine sediments, soils or shallow aquifers (with maximum values around 50–150 nM; /Lovley and Goodwin 1988, Hoehler et al. 1998, Christensen et al. 2000, Lin et al. 2005/). The heterogeneity and variability in the distribution of hydrogen contents in the compared systems is still not well understood.

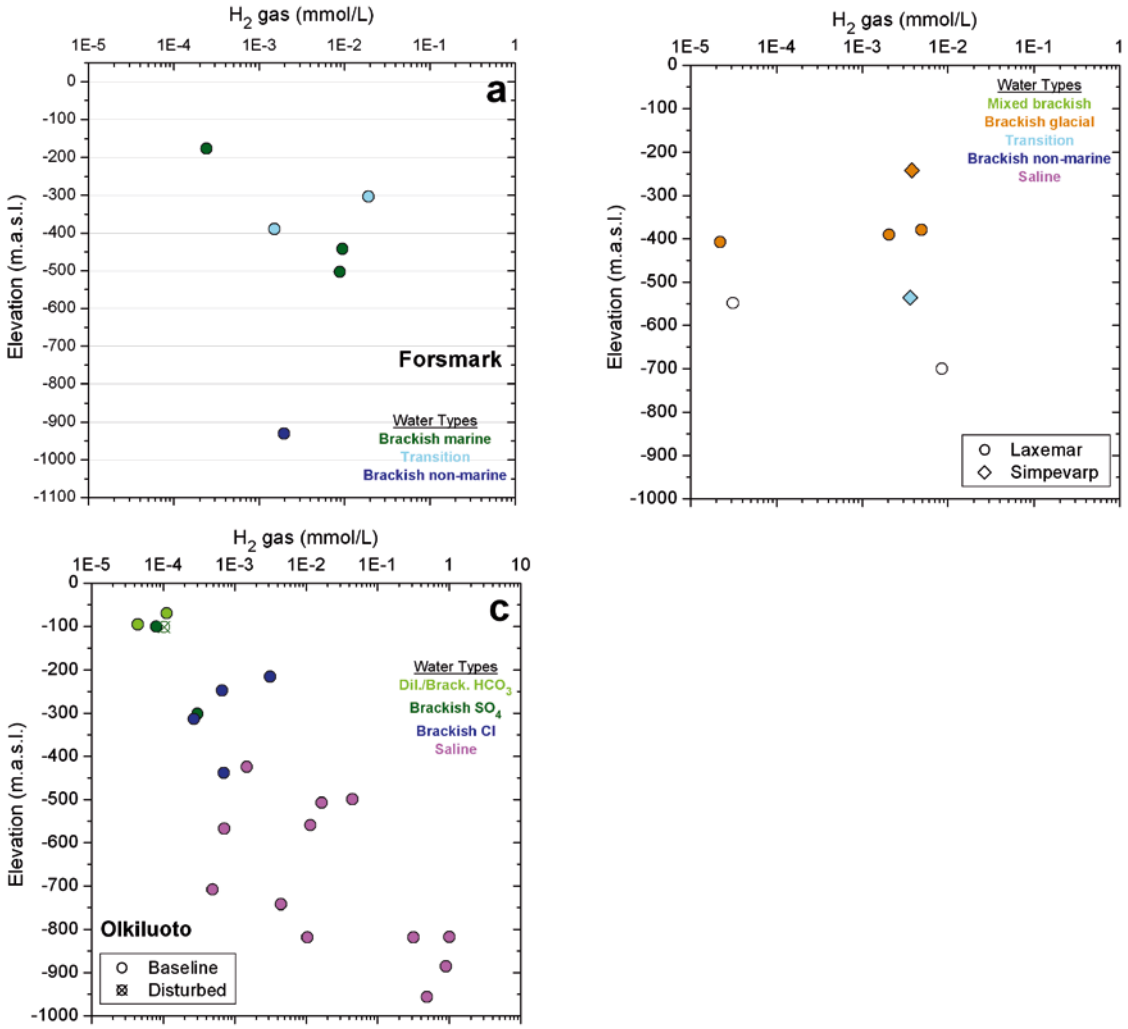

Figure 5-4. *Depth distributions of hydrogen in Forsmark (a), Laxemar(b) and Olkiluoto(c) groundwaters. Data for the Forsmark and Laxemar groundwaters from /Gimeno et al. 2009/ and for the Olkiluoto groundwaters from /Pitkänen and Partamies 2007/.*

5.2.4.2 Estimated values over time

The excavation and operational phases

During excavation and operation, a large pool of organic material will be introduced as structural and stray material promoting an overall increase in the microbial activity. Fermentative metabolisms would increase the amounts of hydrogen and other simple organic molecules that, in turn, would enhance other types of metabolisms, including sulphate reduction. The interplay between sources and sinks would probably maintain low hydrogen contents (below 150 nM) though an increment in sulphate reduction activity and thus in the amount of dissolved sulphide is also possible. However, it is considered that fermentative processes cannot produce high concentrations of hydrogen /SKB 2010/.

In addition, corrosion processes may also represent an additional source of hydrogen that may increase SRB activity, either directly through the reaction:

$$SO_4^{2-} + 4H_2 + H^+ \rightarrow HS^- + 4H_2O, \quad (5\text{-}4)$$

or indirectly through the acetate produced by autotrophic acetogens using hydrogen as electron donor:

$$4H_2 + 2CO_2 \rightarrow CH_3COO^- + H^+ + 2H_2O \quad (5\text{-}5)$$

followed by

$$CH_3COO^- + SO_4^{2-} \rightarrow HS^- + 2HCO_3^- \quad (5\text{-}6)$$

From the calculations performed by /Hallbeck 2010/, this source of hydrogen could rise to net values of $1.6 \cdot 10^{-2}$ and $2.7 \cdot 10^{-2}$ mM in the deposition tunnels from Forsmark and Laxemar, respectively, assuming 100% iron corrosion.

The estimated amounts of hydrogen-mediated dissolved sulphide in the repository (via reaction 5-4 or reactions 5-5 and 5-6) are very low, between 0.13 and 0.22 mg/L ($4.06 \cdot 10^{-3}$ and $6.9 \cdot 10^{-3}$ mM), compared to those previously estimated from other organic sources like organic material in biofilms (around 6.4 mg/L ≈ 0.2 mM of dissolve sulphide; see Section 5.2.1.2).

As it happens for acetate, these values are "cumulative" and non time-average values expressed in a per liter basis that must be relaxed during the evolution of the excavation/operational period. The maximum concentrations of hydrogen allowed by the balance between microbial producing and consuming processes at any time would be in the nanomolar range.

Temperate period

For this period, concentrations of dissolved natural gases (including hydrogen) are expected to remain the same as before repository construction /SKB 2010/. Thus, from present Laxemar groundwater data, mean and maximum values of $3.8 \cdot 10^{-3}$ mM and $8.5 \cdot 10^{-3}$ mM can be given for hydrogen (Table 5-3).

As reactions 5-4 to 5-6 suggest, hydrogen is an important source of nutrients for the microbially-mediated reduction of sulphate to sulphide. If the maximum values of hydrogen were quantitatively used by microbes in sulphate reduction, the amount of sulphide would increase at most by $10^{-5.7}$ M (0.07 mg/L of dissolved sulphide assuming that H_2 is not replenished). If the maximum hydrogen concentrations found in Olkiluoto are considered in the predictive calculations, the amount of dissolved sulphide would be higher, $10^{-3.6}$ M (8 mg/L). However, such a high hydrogen content has not been found at repository levels in any of the studied systems.

Glacial period

Methane and hydrogen have been treated together in Section 5.2.3.2 (glacial period of methane) and their behaviour can be considered parallel, except for clathrates.

Submerged period under marine waters

It is expected that infiltrating recharge waters through marine sediments follows the known degradation sequence of organic matter controlled by microbiological processes and, thus, with hydrogen concentrations below 150 nM (see above). In that case, the concentration of hydrogen at repository depth during this period would depend on abiotic sources, still poorly known. Having no better option, the maximum concentration of hydrogen detected presently in the Laxemar groundwaters ($8.5 \cdot 10^{-3}$ mM) could be used tentatively as recommended values.

5.2.5 Nitrite and Ammonia

5.2.5.1 Overview/general description

As stated above, nitrite and ammonia may contribute, as oxidising agents, to stress corrosion cracking (SSC) of the copper canister. Whereas nitrite is often found in natural aquatic systems at trace levels, ammonia (NH_3) is only stable in alkaline (pH > 9) and very reducing conditions (close to the stability boundary for water; /Kehew 2001, Appelo and Postma 2005/. Thus, it is not expected to find significant amounts of ammonia during the evolution of the sites. In this section the possible evolution of nitrate, nitrite and ammonium is evaluated.

In natural waters nitrogen occurs in various oxidation states from N(+V) to N(-III) and the transformation between them is almost exclusively facilitated by microorganisms /Kehew 2001/. Organic nitrogen is converted to ammonium (ammonification) and, under oxidizing conditions, ammonium is oxidised to nitrite (NO_2^-) or further oxidised to nitrate (NO_3^-) by specialised nitrifying bacteria (two-step nitrification).

Under anaerobic conditions, nitrate is the most thermodynamically favoured electron acceptor for the oxidation of organic substrates and it is used by nitrate reducing bacteria (NRB) for respirative energy production. This nitrate reduction process (denitrification) occurs in different steps, each of which is catalyzed by specific NRB, producing nitrite, nitrous oxide, ammonium or nitrogen gas /Hallberg and Keeney 1993, Chapelle 2001/. The nitrification-denitrification cycle can be broken into aerobic and anaerobic conditions. Under aerobic conditions nitrification may lead to nitrate accumulation and under anaerobic conditions nitrate is depleted by denitrification processes. This usually results in an overall depletion of nitrogen species in anaerobic groundwater systems /Chapelle 2001/.

Therefore, it could be said that the behaviour of nitrogen species in groundwater systems is strongly affected by the existence of aerobic or anaerobic conditions. The observed evolution in the Laxemar groundwaters shows the general depletion of nitrogen usually observed in anaerobic groundwater systems as residence time and/or depth increase.

In general, near-surface groundwaters in Laxemar and Forsmark /Gimeno et al. 2009/ have the widest variability and highest concentrations of nitrogen species. In Laxemar the highest contents reach 0.18 mM for nitrate (though most of them are below ≈ 0.02mM), 0.02 mM for nitrite (the rest are clearly below ≈ $5.5 \cdot 10^{-4}$ mM) and 16.6 to 33.2 mM for NH_4^+ (although most of the available data are below ≈0.22 mM). In Forsmark maximum measured values are 0.032 mM for NO_3^-, 0.003mM for NO_2^- and 0.55 mM for NH_4^+.

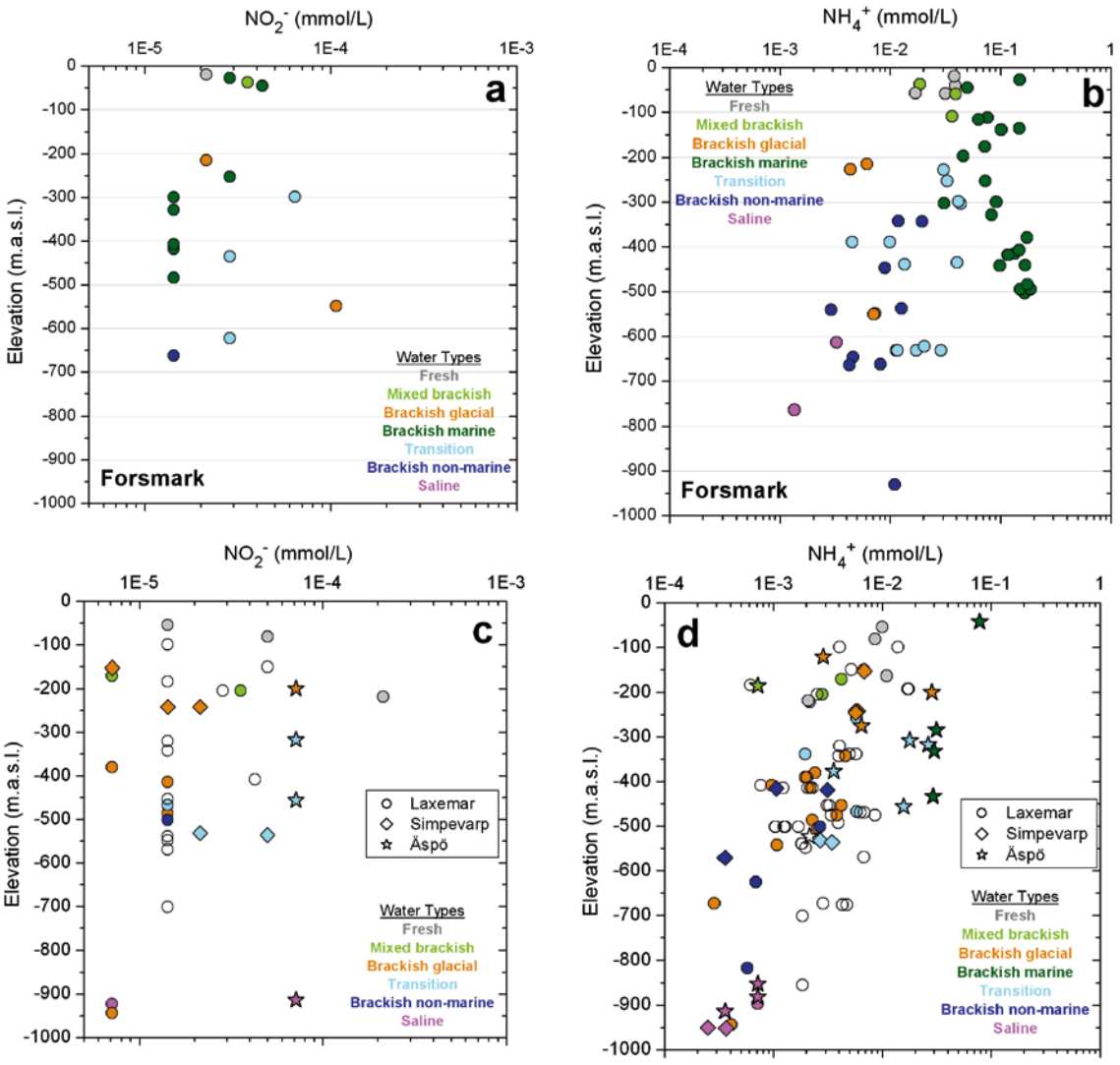

Figure 5-5. *Depth distribution of nitrite (a) and ammonium (b) in the Forsmark and Laxemar (c and d) groundwaters. Data from /Smellie et al. 2008/ and /Gimeno et al. 2009/.*

The range of variation and maximum contents of nitrogen species drastically decrease with depth in crystalline systems /Gascoyne 2004, Pitkänen et al. 2004, Gimeno et al. 2009/. In Laxemar the maximum contents of dissolved NO_3^- and NO_2^- are around $3 \cdot 10^{-4}$ and $2 \cdot 10^{-4}$ mM, respectively (Figure 5-5c for nitrite). In Forsmark dissolved NO_3^- and NO_2^- are very low and in many cases below detection limit; the highest analysed contents are $4 \cdot 10^{-4}$ mM and 10^{-4} mM, respectively (Figure 5-5a nitrite). This situation is in agreement with nitrate instability in the reducing conditions generally found in these groundwaters and with the aforementioned depletion of nitrogen species in anaerobic groundwater systems.

With respect to NH_4^+, its content in deep groundwaters from Forsmark is also restricted in range compared with the shallow groundwaters. High NH_4^+ values (from 0.055 to 0.19 mM) down to 500 m depth (Figure 5-5b) are systematically associated with brackish marine groundwaters with the highest Littorina contributions /Gimeno et al. 2009/. In Laxemar-Simpevarp groundwaters, the largest variability is found also in the first 500 m with contents up to 1.4 mg/L (0.078 mM; Figure 5-5d) in the brackish marine groundwaters located at Äspö. This association also occurs in the Olkiluoto area where groundwaters with a high Littorina contribution have variable and high NH_4^+ concentrations (with maximum values near 0.9 mg/L ≈0.05 mM; /Pitkänen et al. 2004/). These observations indicate that high NH_4^+ concentrations could represent an inherited character from an old marine origin /Gimeno et al. 2009/.

Overall, nitrate and nitrite concentrations in the groundwaters from Laxemar (and Forsmark) are similar or, more frequently, lower than those found in the crystalline and anoxic groundwater systems reviewed in Table 5-1. Ammonium contents in the Laxemar groundwaters are lower than those found in Forsmark but also, they are lower than those determined in the rest of the reviewed crystalline systems (except in the case of the Stripa and Lupin Mine groundwaters; Table 5-1). Thus, the nitrogen system in the Laxemar groundwaters shows the same characters and contents observed in crystalline systems with clearly anoxic/reducing conditions.

In summary, the main sustainable source of nitrate to groundwater should be from surface ecosystems (currently also from soil fertilisers). Oxygen is rapidly removed by microbial respiration in shallow, infiltrating groundwater. When oxygen is exhausted, nitrate will be reduced. Most deep groundwater systems are, consequently, depleted not only in oxygen and nitrate but also in nitrite (as seen in Forsmark, Laxemar and other crystalline systems when residence time and/or depth increase; Table 5-1), a metastable intermediate product in the denitrification process, with very low concentration in most natural waters /Appelo and Postma 2005/.

5.2.5.2 Estimated values over time

The excavation and operational phases

If large amounts of organic structural stray material occur in the repository, decomposition of organic materials may increase the microbial activity during this stage. After the consumption of oxygen, bacterial nitrate reduction[26] is by far the most favoured heterotrophic respirative pathway, even independent of fermentative bacteria /Appelo and Postma 2005, Konhauser 2007/. If dissolved nitrate is present in the repository at this stage, activity of nitrate reduction bacteria will quickly consume it /Hallbeck et al. 2006, Hallbeck 2010/. This effect would enhance the reducing capacity of the repository near-field but it may also increase the amounts of dissolved nitrite and ammonium.

Nitrate derived from agricultural uses or blasting residues are the main potential sources of this component at this stage. From the present concentrations in the near surface groundwaters in the Laxemar or Forsmark areas, it is expected that intruding superficial waters do not represent a meaningful source of nitrates. Remnants of blasting, however, may be an important source of nitrate for groundwaters at the repository level. Also, some of the 'alternative' grouts currently under consideration contain nitrate. These sources has been evaluated for Olkiluoto /Alexander and Neall 2007/. However, as far as the authors know, there are not available estimations on this source for the excavation and operational phases as it would depend on the method used for construction, blasting or rock-drilling machines /Hallbeck et al. 2006, Hallbeck 2010/.

[26] The existence of meaningful amounts of nitrate-reducing microorganisms has been identified in the present groundwaters at the repository level both in Laxemar and Forsmark sites /Hallbeck and Pedersen 2008a, b/.

The effects of blasting relative to nitrate have been studied in some works at the Whiteshell Underground Research Laboratory site (Canada). Increases in NO_3^- concentrations were observed in fractures adjacent to blast sites /Gascoyne and Thomas 1997/ and it was estimated that this nitrate "pollution" could increase groundwater bacterial populations by several orders of magnitude /Stroes-Gascoyne and Gascoyne 1998/. These observations were confirmed in the Blast Damage Assessment Project developed at that URL where it was concluded that blasting residues (nitrates) can enhance microbial growth one to four orders of magnitude with respect to nutrient-poor groundwaters /Martino et al. 2004/.

The main source of nitrate pollution in mine waters and mine water effluents is the explosives used in the mining process /Stroes-Gascoyne and Gascoyne 1998/. Thus, some information can be extracted from this source. The effect of blasting in mine-related groundwaters appears to be variable. From the nearly fifty Canadian and Fennoscandian Shield sites reviewed by /Stotler et al. 2009/ samples from only three mines have recorded nitrate concentrations higher than 100 mg/L (1.61 mM). But in the Lupin Mine (Canada), exceptionally high nitrate concentrations (423–2,630 mg/L ≈ 6.8 to 42.4 mM), attributed to remnants of blasting, have been recorded in the permafrost groundwaters between 200 and 600 m depth /Stotler et al. 2009/. The persistence of such amounts of nitrate was due to oxic to suboxic conditions identified at these depths and to the absence of a significant denitrification process (by nitrate reducing bacteria).

Finally, around the SFR facility (final repository for short-lived radioactive waste, excavated and constructed some twenty years ago), nitrate levels at present are only locally higher (but not especially high; Table 5-1) than those observed in pristine conditions at Forsmark or Laxemar. This would suggest that nitrate from blasting residues are not accumulated in high proportion or that it has been removed quickly under the mildly reducing conditions observed in the groundwaters of that site /Nilsson et al. 2010/.

In any case, if blasting is used in the repository construction, the residual amounts of nitrate and the processes that may mitigate its accumulation[27] should be evaluated. The presence of nitrate is relevant if, as expected, meaningful amounts of organic structural stray material occur in the repository. Under these conditions, the production of nitrites, ammonium or even nitrogen (the stable endpoint of the denitrification chain) can be large, at least locally /SKB 2010/.

A dramatical time-substained increase[28] in nitrite concentrations would be not expected as it is a metastable intermediate product in the overall denitrification processes and it is often found at trace levels in most aqueous systems /Appelo and Postma 2005, Rivett et al. 2008/. However, ammonium may be stable in reducing conditions and, with the available data, it is not possible to estimate the amount of this component.

Temperate period

The performed simulations (Chapter 4) indicate that dilute waters will reach deeper depths than today, mainly at the end of the temperate period. Present fresh and shallow (< 200 m) groundwaters in Laxemar have very low concentrations of NO_3^- (below $2 \cdot 10^{-3}$ mM; /Gimeno et al. 2009/) and also of NO_2^- and NH_4^+ (below $2 \cdot 10^{-4}$ mM and 10^{-2} mM, respectively; Figure 5-5c,d) as is the case in Forsmark (Figure 5-5a,b) with slightly higher NH_4^+ contents ($3.5 \cdot 10^{-2}$ mM) and Olkiluoto /Gimeno et al. 2008, Pitkänen et al. 2004/.

Assuming that concentrations of dissolved NO_2^- and NH_4^+ will remain substantially the same as before repository construction, mean values of $4.4 \cdot 10^{-5}$ mM for NO_2^- and $6.79 \cdot 10^{-3}$ mM for NH_4^+as measured in present groundwaters (Table 5-3) can be expected. Maximum values of $2.1 \cdot 10^{-4}$ mM and $7.8 \cdot 10^{-2}$ mM for NO_2^- and NH_4^+, respectively, would represent a conservative estimate, specially for NH_4^+as maximum values of this component are associated with groundwaters with marked Littorina characters and therefore, with important marine contribution. Thus, a value of $1.5 \cdot 10^{-2}$ mM for NH_4^+ (the maximum value excluding the groundwaters with Littorina contribution) could be proposed.

[27] For instance, the continuous process of input and evacuation of groundwaters to and from the repository (during its construction and operation) is able to "wash" part of the nitrate blasting residues.

[28] A build-up of nitrite may temporally occur due to the time lag between the onset of nitrate reduction and the subsequent onset of nitrite reduction /Rivett et al. 2008/.

Glacial period

During the infiltration of glacial meltwaters, nitrate is expected to decrease due to the decrease of superficial biological activity under such conditions. Nitrate content in present glacier ice and snow is very low (e.g. $4.5 \cdot 10^{-3}$ to $6.8 \cdot 10^{-3}$ mM; /Hallbeck 2009/) and even lower in the Grimsel groundwaters of prbably glacial origin (Table 5-1). Considering that nitrite and ammonium can only be produced by bacterial activity on nitrate, the expected concentrations of these two nitrogen species are also low, below the expected contents for the temperate period.

Submerged period under marine waters

In marine sediments with organic matter, bacterial activity promotes the transformation of organic nitrogen compounds and the formation of NH_4^+. Therefore, during the submerged period, the high biological activity in the marine sediments will lead to a noticeable increase, at least in the ammonium contents in the recharging marine waters infiltrating through them. This is observed at present: seawater has very low NH_4^+ concentrations (usually well below 0.05 mg/L or $2.8 \cdot 10^{-3}$ mM in the available samples from the present Baltic Sea) but increasing ammonium concentrations with depth in the interstitial waters from marine sediments is a common observation. It also occurs in the present sediments of the Baltic Sea, where NH_4^+ concentrations from 0.22 to 0.89 mM are frequent /Carman and Rahm 1997/. However, ammonium is not a conservative component and reactions (e.g. exchange reactions) can reduce NH_4^+ concentrations during circulation of these marine waters through the fractured bedrock.

This situation would be comparable to the Littorina period and, as indicated above, NH_4^+ contents in groundwaters with a clear Littorina signature range from 0.055 to almost 0.19 mM in the Forsmark groundwaters (in the present Laxemar groundwaters, the Littorina imprint is weaker; /Gimeno et al. 2009/). These values, considerably higher than the contents found in the rest of the Forsmark groundwaters, are slightly lower than the ones found in Baltic Sea sediments, probably due to the decreasing effect of cation exchange. However, cation exchange has not been able to completely mask the marine signature in Forsmark, Laxemar-Simpevarp and Olkiluoto groundwaters, probably favoured by the stability of dissolved ammonium in reducing environments. A value for NH_4^+ of 0.19 mM could be proposed for this period.

5.2.6 Colloids

5.2.6.1 Overview/general description

The concentration of natural and bentonite derived colloids should be low to avoid colloid-mediated transport of radionuclides. The stability of the colloidal fraction in groundwaters is mainly linked to the neutralising electric repulsions between charges in their surfaces. In turn, these charges depend on pH, ionic strength and counterions. Overall, colloid stability is largely decreased at high ionic strengths and/or if the concentration of divalent cations exceeds 1 mM.

Most of the measured colloid concentrations in Forsmark groundwaters are below 60 μg/L.Three samples exceeded that amount with maximum contents of 164 μg/L (Figure 5-6a; /Hallbeck and Pedersen 2008a/). In Laxemar the concentrations are below 40 μg/L except in two samples with values around 90 μg/L (Figure 5-6b; /Hallbeck and Pedersen 2008b/). These values are in agreement with those found in other crystalline rock groundwaters such as in Switzerland (30 ± 10 and 10 ± 5 μg/L; /Degueldre 1994/) or in Canada (300 ± 300 μg/L; /Vilks et al. 1991/).

Plotting colloid concentration versus elevation (Figure 6-6) shows that the greatest colloid concentration in the Laxemar groundwaters is found in fresh and dilute waters at 320–340 m depth in boreholes KLX08 (Cl = 15 mg/L, 0.42 mM) and KLX17A (Cl = 565 mg/L, 16 mM) with concentrations of 45 and 90 μg/L respectively. The lowest content was found at 380 m depth in borehole KLX08 (Cl ≈ 1,600 mg/L, 45.1 mM) and, in general, in the most saline groundwaters as it also occurs in the Forsmark area (high ionic strength increases colloidal aggregation and sedimentation; e.g. /Degueldre et al. 1996, 2000/). However, the greatest colloid concentration in the Forsmark area (in the range between 120 and 164 μg/L) is found in waters with a clear brackish marine signature (mainly at the shallowest depth, < 100 m, but also at 442 and 328 m depth in boreholes KFM03A and KFM10A, respectively). The reason for these values is not clear yet and drilling or sampling artefacts can not be discarded. However, they are in the range of other groundwaters in crystalline systems.

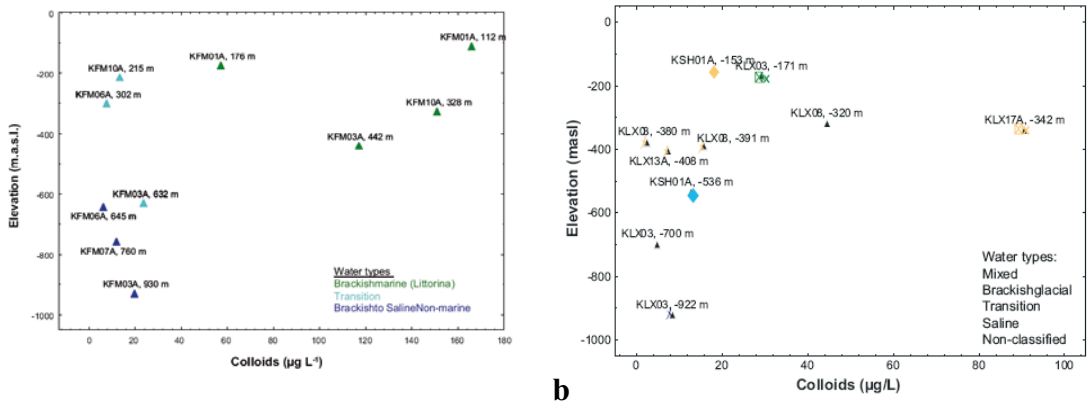

Figure 5-6. *Colloid concentration (µg/L) plotted against elevation and in relation to the groundwater types in the Forsmark (a) and Laxemar (b) areas. In the Forsmark area silica data for KFM01A: 112 m and KFM08D are omitted due to sampling artefacts. In the Laxemar area data from KLX15A: 467 are also excluded due to sampling artefacts. Data taken from /Hallbeck and Pedersen 2008 a, b/.*

Inorganic and organic colloids exist at Laxemar and Forsmark and some colloids have been identified as bacteria and even viruses. Clay colloids seem to be the dominant fraction, whereas organic colloids (humic and fulvic acids), bacteria and viruses appear to represent only a minor part /Nilsson and Degueldre 2007, Hedqvist and Degueldre 2008, Wold 2010/. However, contribution of microorganisms to the colloidal fraction may be higher than thought /Hallbeck and Pedersen 2008 a, b/ and additional investigations are needed to assess the importance of these type of biogenic colloids.

5.2.6.2 Estimated values over time

The excavation and operational phases

During the excavation and operational phases, substantial amounts of colloids may be formed by microbial activity, bentonite erosion by diluted meteoric waters, precipitation of amorphous Fe (III) hydroxides, etc. These colloids are expected to be short-lived, mainly because colloids will aggregate and sediment in moderately saline waters /Degueldre et al. 1996/. Other processes contributing to the elimination of colloids are microbial decomposition of organics, and the re-crystallization and deposition of amorphous materials. In conclusion, an increased formation of colloids during the excavation and operational phases is not expected to affect the performance of the repository in the long-term, because colloid concentrations will quickly decrease and return to natural values.

In any case, a maximum pessimistic value of 0.5 mg/L for the concentration of colloids has been proposed for this period in /SKB 2010/ from /Laaksoharju et al. 1995/.

Temperate period

As stated above, colloid stability is controlled by pH, salinity and cation concentrations. In groundwaters containing more than either 1 mM of Ca^{2+} or 100 mM Na^{+}, colloids are not stable and colloid concentration must be low (e.g. below 100 µg/L; /Degueldre et al. 1996/). Results coming from modelling indicate that pH, salinity and calcium concentration in the groundwaters at that period will be high enough to destabilise colloids, for which their concentrations are expected to remain at the levels measured at present during the site investigation program, i.e. less than 180 µg/L.

Glacial period

Under glacial conditions the inflow of organic matter from the surface will be negligible and the input of organic colloids (e.g. fulvic or humic acids) to the groundwaters must drastically decline. However, the generation of inorganic colloids is favoured at low ionic strengths and low concentrations of cations. As during the glacial stage the expected groundwater composition will be predominantly dilute, the possible generation and transport of colloids by these groundwaters cannot be excluded.

Hence, there is a potential for higher colloid concentrations in groundwaters during a glacial period, especially during the advance and retreat of the ice sheet, when groundwater velocities are higher. A reasonable upper limit would be in the mg/L range from the highest measured colloid concentrations in groundwaters from crystalline environments at repository depths (from the reviews by /Degueldre et al. 2000/ or /Wold 2010/).

In addition, as the buffer swells into fractures, the bentonite barrier can release montmorillonite colloids in contact with dilute groundwaters, increasing the concentration of colloids in the vicinity of the bentonite barrier. Under this situation, experimental results reviewed by /Wold 2010/ suggest that a maximum of about 10–20 mg/L of montmorillonite colloids can be expected in a Grimsel-type groundwater (with Na and Ca concentrations of 0.001 and 0.0001 M respectively) in contact with the bentonite barrier. However, this value may be much higher during brief periods when highly dilute glacial melt water enters the geosphere. The maximum concentration of clay colloids in very dilute waters has been determined to be ~40 g/l in the buffer/groundwater boundary /Birgersson et al. 2009/.These values can be considered a conservative estimation as colloid contents drastically decrease with distance from the barrier /Wold 2010/.

Submerged period under marine waters

Promoted by the density-driven intrusion of marine water, an increase in the salinity (and cation concentration) of the groundwaters is expected to occur in this period and therefore, geochemical conditions would not be favourable for colloid stability. The available data for present groundwaters with an important Littorina contribution at Forsmark indicate that some of them have the highest colloid concentration (around 120–170 μg/L; Figure 5-6a) in the site. The reason for these values is not clear although, in any case, they are in the normal range of other groundwaters in crystalline systems. The conclusion is that colloid concentrations are expected to decrease or, in the worst case, remain at the levels that have been measured at present during the site investigations, i.e. less than 180 μg/L.

5.3 Compilation of values

The proposed concentration values for the parameters analysed in this section (DOC, acetate, CH_4, H_2, NO_2^-, NH_4^+ and colloids) in the different stages are summarised in Table 5-2. One of the main information sources for the compilation has been measured data in the present groundwaters at the two Swedish sites (Laxemar-Simpevarp and Forsmark). Therefore, the main statistics for the values of the parameters measured in the groundwaters from Laxemar and Forsmark are shown in Tables 5-3 and 5-4 respectively, while acetate and DOC values measured during the on-going monitoring program in the Laxemar area are presented in Table 5-5.

Values and ranges included in Table 5-2 come from different sources and these are summarized next. For the ***Excavation/Operational period*** two types of values have been proposed for acetate, CH_4 and H_2 (Table 5-2). Values shaded in blue are deduced from the inventory of organic materials in the repository and mass balance calculations performed by /Hallbeck 2010/. They represent "cumulative" and non time-averaged values expressed in a per liter basis that must be relaxed during the evolution of the Excavation/Operation period and, probably, during the temperate period as well. Values in white cells represent the maximum amounts of acetate and hydrogen allowed by the balance between microbial producing and consuming processes in low temperature systems. They represent the expected time-averaged concentrations during this period (H_2 concentrations in the nanomolar range and acetate in the micromolar range) and, in the case of acetate, also during the other examined periods (for hydrogen, this microbiological balance may be broken by the existence of different inorganic sources for this component). The cumulated values and their possible consequences must be used with caution. The data used in the mass balance estimations are largely uncertain /Hallbeck 2010/ and different assumptions must be verified.

Most of the values proposed for ***the temperate period*** are extrapolated from contents in present groundwaters and assume that they would remain substantially the same after repository construction. Thus, the maximum measured concentrations in present groundwaters have been selected as recommended values. Except DOC, the recommended values are in the range observed in other crystalline systems (Table 5-1). The proposed DOC value is still subjected to different uncertainties and a value of $4 \cdot 10^{-4}$ mM could be used instead as the maximum concentration observed in the crystalline systems reviewed in Table 5-1.

Table 5-2. Recommended values of DOC, acetate, CH_4, H_2, NO_2^-, NH_4^+ and colloids for the different periods during the evolution of the Laxemar site. Concentrations in mol/L, except when indicated. Blue cells indicate values deduced from the mass balance calculations performed by /Hallbeck 2010/.

Evolutive Periods	DOC	Acetate	CH_4	H_2	NO_2^-	NH_4^+	Colloids (µg/L)
Excavation/Operation	$1.2 \cdot 10^{-3}$	$2 \cdot 10^{-4}$ µM range	$2 \cdot 10^{-4}$	$2.7 \cdot 10^{-5}$ (1) $1.5 \cdot 10^{-7}$	$< 2 \cdot 10^{-5}$	$< 3 \cdot 10^{-2}$	500
Temperate	$8.3 \cdot 10^{-4}$	µM range	$3.9 \cdot 10^{-5}$	$8.5 \cdot 10^{-6}$	$2.1 \cdot 10^{-7}$	$1.5 \cdot 10^{-5}$	< 180
Glacial	$5. \cdot 10^{-4}$		$3.9 \cdot 10^{-5}$	$8.5 \cdot 10^{-6}$	$< 2.1 \cdot 10^{-7}$	$< 1.5 \cdot 10^{-5}$	$2 \cdot 10^4$ to $4 \cdot 10^7$
Submerged (marine)	$2.9 \cdot 10^{-3}$		$3.9 \cdot 10^{-5}$	$8.5 \cdot 10^{-6}$	$2.1 \cdot 10^{-7}$	$1.9 \cdot 10^{-4}$	< 180

(1) Value estimated from iron corrosion.

Except for CH_4 and H_2, the selected values for ***the glacial period*** are based in measurements performed in glacier ice samples and in different crystalline systems (DOC), in comparative deductions from contents in present-day groundwaters (NO_2^- and NH_4^+) and in experimental results on the interaction between bentonite and glacial waters.

As for the temperate period, most of the values selected for the ***submerged (marine) period*** are based on the maximum concentrations measured in present-day groundwaters with a clear Littorina contribution. Effects of this marine intrusion are more intense in Forsmark than in Laxemar-Simpevarp /Laaksoharju et al. 2008a, 2009, Gimeno et al. 2009/ and, thus, the selected values for DOC, NH_4^+ and colloids correspond to those observed in the marine-derived groundwaters from Forsmark.

All proposed values have important uncertainties but, in some cases, they are especially large. This is the case of DOC, NO_2^- and NH_4^+ for the Excavation/Operation period, of CH_4 y H_2 for the glacial period and of DOC for the submerged period:

- The value proposed for DOC for the Excavation/Operation period is derived from the inventory of organic materials in the repository /Hallbeck 2010/, excluding the amounts of organic carbon with the bentonite. However, this value is highly uncertain as the degradation rates of organic materials, especially man-made materials, and biodegradability of the organic matter in the bentonite are still poorly known.
- NO_2^- and NH_4^+ contents for the Excavation/Operation period have been impossible to fix or bracket due to the lack of estimations of nitrate contents, the principal source of NO_2^- and NH_4^+ through denitrification. Moreover, the effects of blasting residues have to be evaluated. Thus, the proposed values are the highest values found during the Site Characterization Program in some soil pipes from Laxemar (SSM000241 and SSM000242) and associated with an especially intense microbial degradation of organic matter /Gimeno et al. 2009/. However, nitrite is often found in natural aquatic systems at trace levels and ammonia (NH_3, the involved component in stress corrosion cracking, SSC, of the copper canister), is only stable in alkaline (pH > 9) and very reducing conditions (close to the water stability boundary; /Kehew 2001, Appelo and Postma 2005/). Thus, the existence of meaningful amounts of ammonia during this stage would not be expected, although more detailed analysis is needed.
- The values proposed for CH_4 and H_2 during the glacial period are extrapolated from the highest contents in present groundwaters. The estimation of CH_4 and H_2 concentrations in this period is complicated by the existence of additional processes and different boundary conditions to those present and/or expected in the other periods. The concentration of these gases will be controlled by their production and flow from the deep bedrock and by the active microbial metabolisms (acting as sources and sinks) but also by the impervious frozen layers at the top of the site and by the formation/dissociation of clathrates during permafrost advance and decay.
- As for DOC values during the submerged period, they have been extrapolated from the highest DOC values in present-day Forsmark groundwaters with an important marine contribution (up to 2.92 mM). However, they are still subjected to different uncertainties (e.g. contamination during drilling/sampling) and, therefore, they remain uncertain.

Table 5-3. Main statistics for the values of the analysed parameters measured in the present groundwaters at Laxemar.

	TOC (mgl)	DOC (mgl)	NO_2^- (mol/L)	NH_4^+ (mol/L)	CH_4 g (mol/L)	H_2 g (mol/L)
Number of samples	66	100	34	88	18	6
Minimum	bdl	bdl	$7.14 \cdot 10^{-9}$	$2.50 \cdot 10^{-7}$	$9.38 \cdot 10^{-7}$	$3.13 \cdot 10^{-8}$
Median	2.35	2.2	$1.78 \cdot 10^{-8}$	$3.24 \cdot 10^{-6}$	$2.66 \cdot 10^{-6}$	$3.71 \cdot 10^{-6}$
Mean	3.34	3.37	$4.41 \cdot 10^{-8}$	$6.79 \cdot 10^{-6}$	$6.69 \cdot 10^{-6}$	$3.81 \cdot 10^{-6}$
Standard Deviation	3.15	4.08	$7.78 \cdot 10^{-8}$	$1.10 \cdot 10^{-5}$	$1.02 \cdot 10^{-5}$	$2.84 \cdot 10^{-6}$
Maximum	20	27.2	$4.28 \cdot 10^{-7}$	$7.85 \cdot 10^{-5}$	$3.88 \cdot 10^{-5}$	$8.48 \cdot 10^{-6}$
P0.1	bdl	bdl	$7.14 \cdot 10^{-9}$	$2.50 \cdot 10^{-7}$	$9.38 \cdot 10^{-7}$	$3.13 \cdot 10^{-8}$
P5	bdl	bdl	$7.14 \cdot 10^{-9}$	$3.64 \cdot 10^{-7}$	$9.38 \cdot 10^{-7}$	$3.13 \cdot 10^{-8}$
P95	7.6	9.95	$2.14 \cdot 10^{-7}$	$2.93 \cdot 10^{-5}$	$3.88 \cdot 10^{-5}$	$8.48 \cdot 10^{-6}$
P99.5	20	27.2	$4.28 \cdot 10^{-7}$	$7.85 \cdot 10^{-5}$	$3.88 \cdot 10^{-5}$	$8.48 \cdot 10^{-6}$

Table 5-4. Main statistics for the values of the analysed parameters measured in the present groundwaters at Forsmark.

	TOC (mgl)	DOC (mgl)	NO_2^- (mol/L)	NH_4^+ (mol/L)	CH_4 g (mol/L)	H_2 g (mol/L)
N total	56	62	16	60	16	12
Minimum	bdl	bdl	$1.43 \cdot 10^{-8}$	0	$1.07 \cdot 10^{-6}$	bdl
Median	2.55	1.95	$2.50 \cdot 10^{-8}$	$3.22 \cdot 10^{-5}$	$2.46 \cdot 10^{-6}$	$6.03 \cdot 10^{-8}$
Mean	4.85	3.5	$3.08 \cdot 10^{-8}$	$5.42 \cdot 10^{-5}$	$1.55 \cdot 10^{-5}$	$3.37 \cdot 10^{-6}$
Standard Deviation	6.21	5.51	$2.44 \cdot 10^{-8}$	$5.62 \cdot 10^{-5}$	$5.07 \cdot 10^{-5}$	$6.09 \cdot 10^{-6}$
Maximum	40.3	35.7	$1.07 \cdot 10^{-7}$	$1.86 \cdot 10^{-4}$	$2.05 \cdot 10^{-4}$	$1.92 \cdot 10^{-5}$
P0.1	bdl	bdl	$1.43 \cdot 10^{-8}$	0	$1.07 \cdot 10^{-6}$	bdl
P5	bdl	bdl	$1.43 \cdot 10^{-8}$	$2.13 \cdot 10^{-6}$	$1.07 \cdot 10^{-6}$	bdl
P95	13	13	$1.07 \cdot 10^{-7}$	$1.70 \cdot 10^{-4}$	$2.05 \cdot 10^{-4}$	$1.92 \cdot 10^{-5}$
P99.5	40.3	35.7	$1.07 \cdot 10^{-7}$	$1.86 \cdot 10^{-4}$	$2.05 \cdot 10^{-4}$	$1.92 \cdot 10^{-5}$

Table 5-5. Main statistics for the values of acetate and DOC measured during the monitoring program on going at Laxemar and Äspö.

	Acetatate (M)	DOC (M)
N total	16	20
Mean	$7.55 \cdot 10^{-5}$	$2.92 \cdot 10^{-3}$
Standard Deviation	$1.73 \cdot 10^{-4}$	$7.04 \cdot 10^{-3}$
Sum	$1.21 \cdot 10^{-3}$	$5.84 \cdot 10^{-2}$
Minimum	0	$1.67 \cdot 10^{-4}$
Median	$1.49 \cdot 10^{-5}$	$4.79 \cdot 10^{-4}$
Maximum	$6.88 \cdot 10^{-4}$	$3.06 \cdot 10^{-2}$
P0.1	0	$1.67 \cdot 10^{-4}$
P5	0	$1.84 \cdot 10^{-4}$
P95	$6.88 \cdot 10^{-4}$	$2.14 \cdot 10^{-2}$
P99.9	$6.88 \cdot 10^{-4}$	$3.06 \cdot 10^{-2}$

6 Conclusions

The hydrochemical evolution of the Laxemar site has been modelled through fluid flow and solute transport, simulating groundwaters mixing and chemical reactions with fracture-filling minerals. Different climatic and hydrodynamic conditions of interest in the SR-Site assessment have been simulated using a methodology which integrates hydrological calculations (provided by Serco and TerraSolve teams) and geochemical simulations, performed with PHREEQC. The coupling of the two models allows a description of the geochemical heterogeneity, which otherwise would be hard to attain. The cases discussed for the hydrogeological evolution of the Laxemar site in the framework of SR-Site are: the open repository stage, the temperate period and the remaining glacial cycle.

The methodology used here to integrate the hydrogeological results and the geochemical simulation is based on using the mass fractions of the different reference waters (considered as mixing proportions of end members in the geochemical calculations) thought to be present in the system to create an input file for the geochemical calculations. Then, different geochemical variant cases have been used for calculating the value of all the parameters over the different periods in order to assess their variability under specific hydrogeochemical conditions.

This methodology has a series of uncertainties, already indicated over the document, that are summarised here in Section 6.1. However, despite the usual constraints associated with predictive numerical models, the main objective of the present work has been achieved (the assessment of the safety functions shown in Figure 1-3 within the candidate repository volume). The main results obtained for the geochemical parameters of interest (related to the safety functions) through the different climatic and hydrological conditions are presented in Sections 6-2 to 6-6 and summarised in Table 6-1 and Figures 6-1 to 6-5. The statistical results are compiled in tables in Appendix 2.

6.1 Uncertainties

Four main sources of uncertainties can be identified in the predictive geochemical simulations performed for SR-Site: 1) the number and composition of the end-members used to transform the hydrological data in water compositions for the whole rock volume through mixing calculations; 2) the heterogeneous reactions considered to participate in the control of the composition of the mixed waters through equilibrium situations; 3) the thermodynamic data used for this equilibrium reactions; and, finally, 4) some additional uncertainties arising from the coupling between hydrological and geochemical data.

There are other types of uncertainties related to the evaluation of some key-parameters (colloids, dissolved and total organic carbon, nitrite, ammonia, acetate, methane and molecular hydrogen) that cannot be modelled in the same way and with the same tools as the rest of the geochemical parameters assessed in the SR-Site. These other uncertainties are also described next in Section 6-6.

6.1.1 Number and composition of the end-members

Estimation of the number of reference waters (end-members) involved in the palaeohydrological evolution of the sites and their chemical compositions are key parameters in the performed simulations. The effects of the associated uncertainties have been widely discussed in the context of the Swedish and Finnish Site Characterisation programs (e.g. /Gómez et al. 2008, Gimeno et al. 2008, 2009/ and references therein).

In particular, for the SR-Site the original compositions of the end-member waters used in the geochemical simulations have been carefully reviewed in the SDM works (detailed evaluation on the end-member compositions and the associated uncertainties can be seen in /Gimeno et al. 2008, 2009/). Some of these waters are represented by real samples from the natural systems and some others (for the old end-members) are estimated from diverse geological sources. Thus, compositional uncertainties in these old end-members are greater. Moreover, in some cases, there are some unknown fundamental geochemical parameters (pH, Eh, and dissolved Fe(II) and S(-II)

concentrations), that have been obtained assuming a series of mineral equilibrium reactions thought to be controlling these variables (e.g. equilibrium with calcite, quartz, hematite and/or Fe(II)-monosulphides). Thus, although the selected compositons for the end-members are able to simulate the overall geochemical characters of the present groundwaters, some degree of uncertainty remains.

The number of end-members used in simulations depends on the knowledge of the natural system under study. Thus, it has changed as more information and knowledge is available from the sites. In the SR-Site exercise a fifth reference water ("Old meteoric end member"), not used in SR-Can calculations, has been included based on the works by /Smellie et al. 2008/ and /Laaksoharju et al. 2009/. It would be valuable to compare the results from the previous SR-Can simulations with the presently available results from SR-Site to analyse the effects of this change in the number of end-members. But, in any case, this type of uncertainty can be included in the usual refinement of the models.

6.1.2 Heterogeneous reactions and equilibrium assumptions

The mineral reactions chosen to be in equilibrium with the groundwater mixtures are reasonable as they include those with a fast kinetics compared to the simulated time intervals (like calcite) or those identified in apparent equilibrium situations in the present groundwaters (like quartz). In fact, they effectively represent the chemical effects observed in the reactive components discussed in this work. However, they represent only a limited subset of those present in the fractures and, thus, other minerals (e.g. chlorite, illite or K-feldspar, frequently found in the fracture fillings) could participate through dissolution-precipitation reactions. Other solid phases, such as aluminosilicates, could be stipulated as equilibrium constraints, but their selection would be difficult to justify because their solubility data show important uncertainties (as they depend on the particular mineral composition, order/disorder degree, etc). Moreover, previous scoping calculations performed for the SR-Can /Auqué et al. 2006/ showed that including chlorite and illite equilibrium in the calculations had a negligible effect on the concentrations of Mg and K.

Other processes diferent from dissolution-precipitation reactions, like cation exchange, could partcipate in the hydrochemical evolution of the groundwaters. Cation exchange reactions are kinetically fast and can exert an important control on the major cationic composition of the groundwaters (/Drever 1997, Appelo and Postma 2005, Andersen et al. 2005/ and references therein). These reactions may be specially activated during the mixing processes as the salinity of the groundwaters exerts a major control on the intensity and selectivity of the exchangers for the different cations (e.g. /Appelo and Postma 2005/).

Despite their potential importance, cation exchange proceses have not been included in the present simulations due to two main reasons: a) the available cation exchange capacties (CEC) values for fracture filling minerals, a basic parameter to include cation-exchange processes in the predictive simulations, are very scarce and uncertain /Selnert et al. 2008/; and b) the thermodynamic database selected by SKB does not have the possibility to deal with cation exchange processes (see below).

Finally, whereas most equilibrium assumptions are generalized in the present groundwaters over the whole studied rock volume, it is not the case of the heterogeneous redox equilibria. The work done for the SDM in Laxemar indicates that in some localised zones of the system, equilibrium with haematite is observed whereas in others, waters seem to be in equilibrium with FeS(am). The approach used for the geochemical calculations simplifies the behaviour of the system imposing, alternatively, the equilibrium conditions in the whole volume of rock. This uncertainty has been dealt combining, in the Base Case for the redox processes, the results obtained from both equilibrium assumptions giving a wider range of variation for these parameters but being able to explain the two possible situations present in the real system.

The uncertainties related to redox disequilibrium situations have also been take into account. A modified version of the thermodynamic database was implemented by /Salas et al. 2010/ in order to account for the groundwater Eh values controlled by the $Fe(OH)_3/Fe^{2+}$ redox pair. The only way to do this is un-coupling the equilibrium between the HCO_3^-/CH_4, SO_4^{2-}/HS^- and $Fe(OH)_3(s)/Fe^{2+}$ redox pairs. This modified database has been named the "un-coupled" database and essentially

prevents the redox pairs SO_4^{2-}/HS^- and HCO_3^-/CH_4 to participate in the homogeneous redox equilibrium during the chemical mixing and reaction simulations. The resulting Eh values are similar to the ones measured in some of the Swedish groundwaters believed to be controlled by the electro-active $Fe(OH)_3/Fe^{2+}$ redox pair /Grenthe et al. 1992/. With the original "coupled" database the resulting Eh values correspond to homogeneous redox equilibrium, consistent with the agreement between Eh values for the $Fe(OH)_3/Fe^{2+}$, SO_4^{2-}/HS^- and HCO_3^-/CH_4 couples which has been observed in some groundwater samples at Laxemar /Gimeno et al. 2009/.

Therefore, the use of these two databases and the combination of the results obtained in equilibrium with haematite and those obtained in equilibrium with FeS(am) cover the measured and calculated Eh values in SKB's site characterisation studies and although some problems in the treatment and interpretation of redox potential still persist, this methodology gives a reasonable range of Eh values in SR-Site simulations.

6.1.3 Thermodynamic data and thermodynamic database

The thermodynamic data for the mineral phases included in the simulations have been reviewed in /Auque et al. 2006/ and /Gimeno et al. 2009/. Moreover, these data have been applied, verified and refined in the WATEQ4F database /Ball and Nordstrom 2001/ during the study of the present groundwaters in the site characterization programs both in Laxemar and Forsmark.

Consistency between this model exercise and other SR-Site geochemical models using thermodynamic data is an important issue. This is the reason why, instead of using the same WATEQ4F database as in previous geochemical calculations for SR-Can /Auqué et al. 2006/ and for Site Descriptive Modeling (/Gimeno et al. 2008, 2009/ and references therein), SKB decided to use a new thermodynamic database (available from SKB's Trac system) known as TDB_SKB-2009_Amphos21.dat (SKB-SR-Site), and already used for the solubility limits calculations /Grivé et al. 2010/. This database was developed by /Hummel et al. 2002/ and was substantially modified by /Duro et al. 2006/.

The use of this database has limited the capacity of simulating processes such as cation exchange because this database cannot deal with them without including the necessary data into it (which would have needed a complete verification exercise as an indispensable QA requirement). The same problem has been encountered with some specific solubility data (already included and verified in the WATEQ4F database /Auqué et al. 2006, Gimeno et al. 2009[29]/) for some important phases in the groundwater systems under study /Gimeno et al. 2009/.

The *first problem* has precluded the inclusion of cation exchange processes (known to be effective in the groundwater evolution from the works in the SDM; e.g. /Gimeno et al. 2008, 2009/) in the geochemical calculations. Knowing the importance of cation exchange, the University of Zaragoza group has developed the methodology and software needed to deal with cation exchange from the results provided by the hydrogeologists (mixing proportions). Some scoping calculations have been performed suggesting that these processes would not introduce drastical changes in the results. However, they also evidence that cation exchange processes must be included, at least, as variant cases in future assessments. When more precise data on CEC become available and the SKB thermodynamic data base is upgraded and verified for the simulation of this type of processes, their inclusion in the PA calculation would be straightforward as the calculation methodology is ready.

The *second problem* has been solved including the necessary solubility data for the mineral phases of interest in the SKB-SR-Site database and comparing the results with those obtained with WATEQ4F database. This comparison indicates that the results obtained with both databases are very similar (see Section 3.2.2.2). However, the consitency of the included mineral phases in the SKB-SrSite has not been extensively verified as it was done with the previous database used in SR-Can.

[29] Appendix A in /Auqué et al. 2006/ and Appendix C in /Gimeno et al. 2009/ contain detailed discussions of the main difficulties encountered when working with these types of phases, the range of solubility values found in the literature, and the values selected for the SR-Can modelling.

6.1.4 Coupling between hydrological and geochemical data

Hydrogeological model results have been provided by the hydrogeological team of SKB through the standard QA procedures specified for SR-Site. However two types of hydrological model results have been provided: the mass fractions of the considered reference waters for the temperate and submerged under marine water periods and the salinities for the glacial, permafrost and submerged under fresh water periods.

Transformation of salinities (without any other data available) in mixing proportions has different uncertainties and, as it has been described in Sections 3.1.2 and 4.1 (Chapters 3 and 4), several simplified assumptions have been made. With the applied approach, the groundwater composition at the end of the temperate period (calculated from the mass fractions provided by the SERCO model) does not deviate drastically from the initial water of the glacial period (estimated from the salinities given by the TERRASOLVE model) in the bedrock. That is, there is a certain degree of coherence in the link between the two different hydrogeological models used.

However, for future performance assessment, it would be advisable that the hydrological models used for the complete Glacial Cycle would provide homogeneous results (fractions of the reference groundwaters as a result of their models).

6.2 Salinity evolution

During the excavation and operational period the hydrogeochemical evolution is mainly conditioned by the disturbance of the natural system caused by the construction of the repository. The results obtained when simulating the effects of the repository construction indicate a clear decrease in the salinity in almost all the volume. Groundwater upconing is assessed to be negligible.

During the temperate period, after closure and previous to the development of the glacial cycle, the infiltration of meteoric waters, the displacement of the Baltic shore line and the changes in annual precipitation will influence the hydrology of the site. In this period salinities in the repository volume are between 0.4 and 20 g/L. But from the year 2000 to the year 15,000 AD an overall evident decrease in salinity is observed (from mean values of 5.5 g/L to 2.2 g/L) as the proportion of meteoric waters increases in the repository volume. At the same time, the rest of the reference waters already present in the rock (before the input of meteoric recharge) decrease in importance. In general, the salinity within the candidate repository volume has been predicted to be below 20 g/L during the temperate period and thus, it will remain limited at Laxemar ensuring that the swelling properties of the buffer and backfill are not negatively affected.

During the glacial cycle, salinities are basically controlled by the infiltration of glacial melt waters, the transport of saline waters from the deepest areas by upconing, and the existence (or absence) of a permafrost. The salinity distribution simulated for the Ice 0 stage of the glacial period is quite similar to the one obtained for the last year simulated in the temperate period (despite the different methodology used by the two different hydrogeologists teams). When the glacier advances over an unfrozen soil (Ice I, II and III stages), higher salinities (between 12 and 30 g/L) have been computed in the repository volume just ahead of the ice front as a consequence of upconing. However, behind the front, the salinities decrease from 0.3 down to 0,001 g/L due to the infiltration of glacial melt waters in the domain. The same is seen once the ice sheet totally covers the area of the Laxemar site (Ice IV and V stages). After 11,000 years the glacier begins to retreat (stages Vr, IVr and IIr) and the upconing ahead of the ice front is again responsible of transporting saline groundwaters to repository depths, reaching locally values between 0.3 and 0.7 g/L. At the end of the glacial cycle all the repository volume is dominated by glacial melt waters.

A periglacial period has been simulated for the first stages of the glacial period as well, assuming that the ground is frozen under the ice sheet. Stage 0 at the beginning of this period predicts salinities in the repository volume slightly lower than when permafrost is not considered (in general between 0.7 to 1.3 g/L). As soon as the glacier begins its advance over the frozen ground, salinities tend to decrease behind the ice front (from 0.04 to 0.32 g/L) while maintaining values up to 6.3 g/L ahead of the ice front by upconing (not as high as during the ice advance over an unfrozen ground).

Immediately after the retreat of the ice sheet, isostatic depression will leave the ground surface at the repository site below the Baltic Sea surface level for a period of time. In the reference evolution, the Laxemar site is expected to be below glacial melt water lakes (denoted as the "submerged under fresh waters period" which is the same as the last stage of the glacial evolution), and sea or brackish waters (denoted as "submerged under marine waters period" with conditions thought to be the same as during the maximum of salinity of the Littorina stage at the year 3000 BC) for a period of time between a few thousand years up to perhaps ten thousand years. The distribution of salinity during the submerged under marine waters period is quite similar to the present day distribution (open repository period under natural conditions, or year 2000 AD), though the values are slightly higher, with almost all the repository volume having salinity values from 0.6 to 19 g/L.

6.3 Major element evolution

The trends of the major chemical components (such as chloride, sulphate, calcium and sodium) follow the salinity patterns described above. Other components, such as bicarbonate, silica or phosphate are controlled by relatively fast chemical reactions involving calcite, quartz and hydroxiapatite and they have been calculated assuming these equilibrium situations. Results of cation concentrations in the form of the safety function indicator R1c ($\sum q[Mq+]$) are summarized next.

The salinity decrease in almost all the repository volume promoted by the repository construction would be compensated after closure, when natural conditions return. Thus, violations of the safety function indicator $\sum q[Mq+]$ are not expected.

During the temperate period, and within the candidate repository volume, the values for the safety function $\Sigma q[Mq+]$ will be always higher than 0.004 mol/kg in all the grid points (Figure 6-1a). In this context, colloids are not expected to be especially stable during the temperate period, because calculated pH values (see below), salinities and cation concentrations will be high enough to destabilise them.

However, during the glacial period the overall decrease in salinity facilitates the presence within the candidate repository volume of groundwaters with $\sum q[Mq+]$ lower than 0.004 mol/kg for some period of time during the advance and retreat of the ice sheet (Figure 6-1b, Ice III, IV, V, Vr, IVr and IIr stages, with the mean values below the accepted 0.004 mol/kg). The expected effect of upconing ahead of the glacial front will produce fairly important increases in salinity (and, therefore, in the concentration of the main ions) reaching the depth of the repository (see Ice I and II stages in Figure 6-1b). However, as the advance of the ice sheet is a relatively fast process and the retreat even more so, the high salinity condition is predicted to last only a few centuries at most.

The salinity results shown in the previous section when assuming the periglacial conditions (ground frozen) indicate slightly lower salinities in the repository volume than when permafrost is not considered. This is also seen in the main chemical components and specifically by the values obtained for $\sum q[Mq+]$ within the candidate repository volume (Figure 6-1b').

Comparing the evolution of both cases (Figures 6-1b and 6-1b') during the first 5 stages, the presence of the frozen ground buffers in some extent the sharp changes produced by upconing and dilution. However, the results indicate that since the moment the ice starts its advance, a large percentage of the waters in the repository volume will have values lower than the 0.004 mol/kg threshold accepted for the safety function $\sum q[Mq+]$. After the complete retreat of the ice sheet the salinity and the concentration of cations are predicted to return to the levels attained before the onset of the glacial period (though with a narrower range of variability; Figure 6-1c).

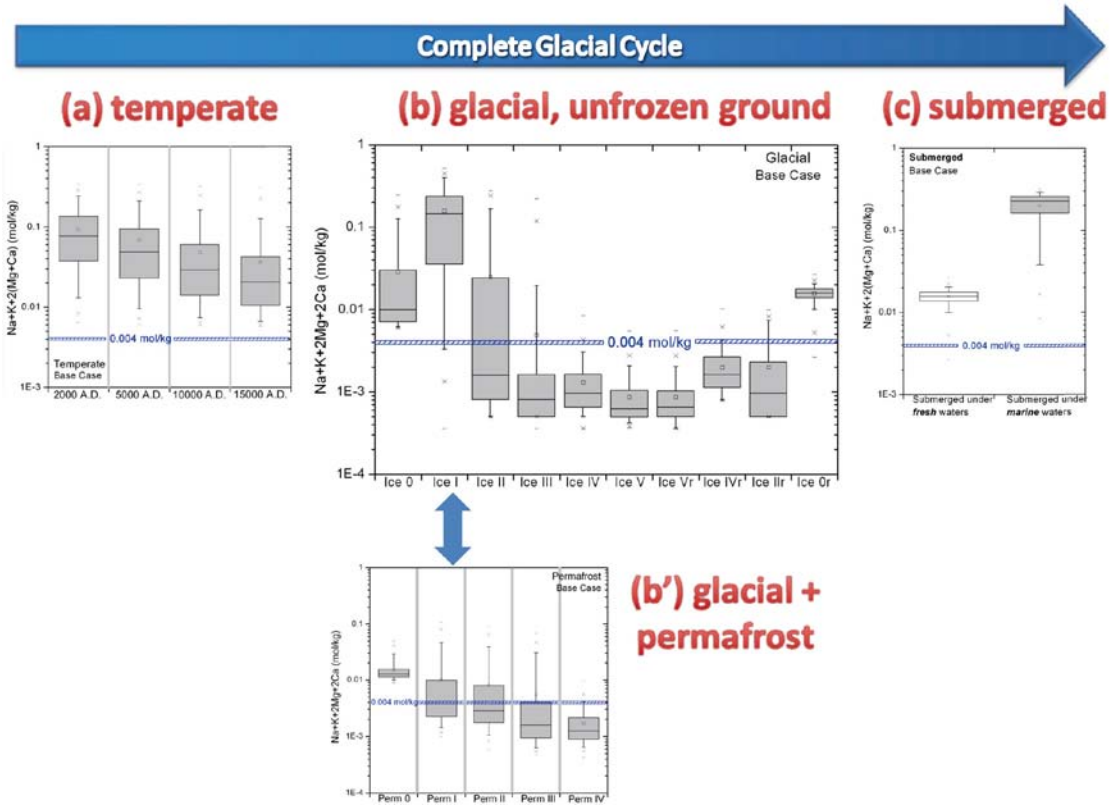

Figure 6-1. *Box-and-whisker plots showing the statistical distribution of the sum of the main cations expressed in charge equivalents as $\sum q[M^{q+}]$ (mol(kg) obtained with the "Base Case" over the complete glacial cycle (temperate,a , glacial,b , glacial + permafrost,b', and submerged, c) for the groundwaters located within the candidate repository volume at Laxemar. The statistical measures plotted here and in all the following box and whiskers plots, are the median (horizontal line inside the grey box), the 25th and 75th percentiles (bottom and top of the box), the mean (square), the 5th and 95th percentiles ("whiskers"), the 1st and 99th percentile (crosses) and the maximum and the minimum values (horizontal bars). The position and size of the different graphs in the Figure is such as the values can be easily compared.*

6.4 pH evolution

During the excavation and operational period a short alkaline pulse in the groundwater from low-alkalinity cement, shotcrete and concrete is likely to form, but its effects are expected to be negligible.

During the temperate period, the average pH values predicted for the groundwaters within the repository volume show an increasing trend with mean values raising from 7 to 7.35 (Figure 6-2a). The maximum and minimum values are almost constant during the whole period and around 8.2 and 6.85, respectively.

Results during the glacial evolution indicate a general increase of pH (Figure 6-2b), an effect which is observed in this type of glacial groundwaters. Except for a decrease in pH during the Ice I stage (beginning of the ice front advance), not observed when the ground is frozen (Figure 6-2b'), the pH obtained for almost all the glacial period is quite high and most of the time quite constant, with 50% of the grid points in the repository volume having pH values between 9.25 and 9.7. In any case, the safety function criteria R1e will be fulfilled as pH will always remain lower than 11.

After the complete retreat of the ice sheet, the entrance of marine waters (submerged under marine waters period; Figure 6-2c) would produce a decrease in pH to values below 8.25.

Table 6-1. Maximum and minimum values of the main geochemical parameters obtained for the base case over the complete glacial cycle in Laxemar. Concentrations are expressed as kmol/m³ and pH as standard pH units.

	Open Repository	Temperate (2000 AD)	Temperate (15,000 AD)	Glacial (stage IIa)	Glacial (stage Vr)	Permafrost 0 (before onset of glaciation)	Permafrost IV (before onset of glaciation)	Sub-merged glacial lake	Sub-merged seawater
Max pH		8.14	8.11	9.64	9.70	7.54	9.66	9.26	8.29
Min pH		6.77	6.80	6.54	8.03	6.84	7.84	7.25	6.83
Max Cl		$3.39\cdot10^{-1}$	$3.04\cdot10^{-1}$	$2.73\cdot10^{-1}$	$4.59\cdot10^{-3}$	$4.69\cdot10^{-2}$	$8.90\cdot10^{-3}$	$2.64\cdot10^{-2}$	$3.21\cdot10^{-1}$
Max Ca/Na		1.25	1.21	3.7	25.00	0.93	4.17	1.39	1.27
Max Ca		$1.21\cdot10^{-1}$	$1.07\cdot10^{-1}$	$9.80\cdot10^{-2}$	$1.71\cdot10^{-3}$	$1.63\cdot10^{-2}$	$3.24\cdot10^{-3}$	$9.59\cdot10^{-3}$	$1.15\cdot10^{-1}$
Max Na		$9.81\cdot10^{-2}$	$8.98\cdot10^{-2}$	$7.96\cdot10^{-2}$	$4.40\cdot10^{-3}$	$1.75\cdot10^{-2}$	$3.03\cdot10^{-3}$	$7.53\cdot10^{-3}$	$1.51\cdot10^{-1}$
Min Ca/Na		0.105	0.063	0.076	0.093	0.230	0.425	0.725	0.051
Min Ca		$5.27\cdot10^{-4}$	$3.04\cdot10^{-4}$	$1.84\cdot10^{-4}$	$1.67\cdot10^{-4}$	$1.33\cdot10^{-3}$	$1.77\cdot10^{-4}$	$9.67\cdot10^{-4}$	$1.26\cdot10^{-3}$
Min Na		$5.03\cdot10^{-3}$	$4.82\cdot10^{-3}$	$5.80\cdot10^{-5}$	$7.40\cdot10^{-6}$	$5.75\cdot10^{-3}$	$4.35\cdot10^{-5}$	$6.95\cdot10^{-4}$	$5.61\cdot10^{-3}$
Max Total Carbon		$4.24\cdot10^{-3}$	$4.33\cdot10^{-3}$	$4.31\cdot10^{-3}$	$3.83\cdot10^{-3}$	$4.12\cdot10^{-3}$	$1.32\cdot10^{-3}$	$1.78\cdot10^{-3}$	$3.96\cdot10^{-3}$
Min Total Carbon		$5.61\cdot10^{-5}$	$6.84\cdot10^{-5}$	$4.84\cdot10^{-5}$	$8.75\cdot10^{-5}$	$3.49\cdot10^{-3}$	$1.44\cdot10^{-4}$	$5.92\cdot10^{-5}$	$5.38\cdot10^{-5}$
Max Ionic strength		$4.63\cdot10^{-1}$	$4.13\cdot10^{-1}$	$3.75\cdot10^{-1}$	$6.53\cdot10^{-3}$	$6.69\cdot10^{-2}$	$1.30\cdot10^{-2}$	$3.65\cdot10^{-2}$	$4.38\cdot10^{-1}$

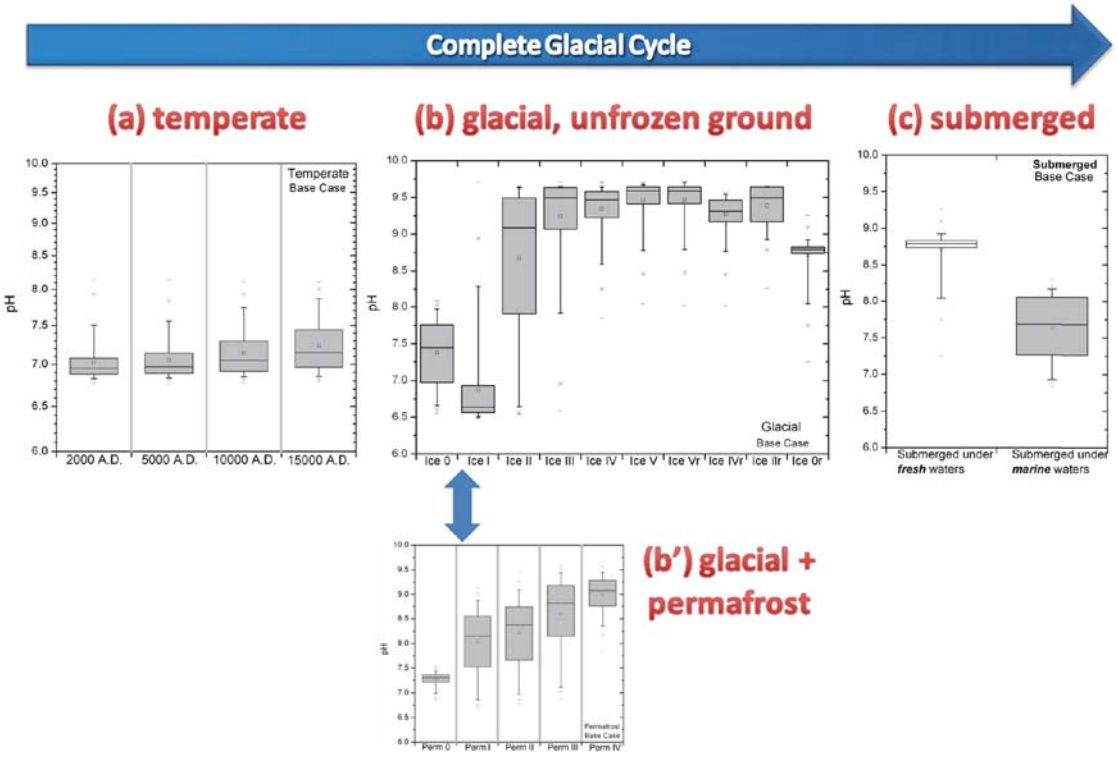

Figure 6-2. *Box-and-whisker plots showing the statistical distribution of pH (standard units) obtained with the "Base Case" over the complete glacial cycle (temperate,a , glacial,b , glacial + permafrost,b', and submerged, c) for the groundwaters located within the candidate repository volume at Laxemar. See the caption of Figure 6-1 for the statistical meaning of the different symbols. The position and size of the different graphs in the Figure is such as the values can be easily compared. The safety function criteria R1e indicates that pH should remain lower than 11.*

6.5 Redox parameters

As indicated above, the results obtained with the different geochemical variant cases for the non-redox parameters are almost the same and therefore, a first important conclusion is that their values and evolution are practically independent of the redox controlling processes. However, the results obtained for the redox parameters are quite different depending on the geochemical model used, basically depending on the redox mineral (haematite or FeS(am)) and on the assumption of redox equilibrium or disequilibrium. This is the reason why the Base Case for the redox parameters is a combinations of the results obtained with variant cases 1 (haematite equilibrium) and 2 (FeS(am) equilibrium).

The use of the un-coupled thermodynamic data base (variant case 3) has little effect on the final picture of the S(-II) and Fe(II) contents and evolution as the results are always inside the range covered by the other two variant cases together (Base Case for redox parameters). However, the Eh values obtained with this case are different from the other two and usually more reducing (thus fulfilling the safety function indicator R1a, reducing conditions, even better).

6.5.1 Iron and sulphide contents

Dissolved S(-II) and Fe(II) contents in the simulations (as seems to be the case for the real system) are regulated by the interplay between groundwater flow (mixing of reference waters) and the different redox equilibrium assumptions (variant cases), which are also controlled by pH.

During the operational phase, inflow of groundwater into the tunnel and mixing of groundwaters of different origin within rock fractures will probably result in precipitation or dissolution of minerals. Some numerical simulations indicate that Fe(III) oxy-hydroxides are expected to precipitate (as it has been observed at Äspö) as far as oxic conditions prevail. Thus, dissolved Fe(II) contents would be very low, and the same could be said for S(-II) (if any), as it is totally unstable under oxic conditions.

After closure, decomposition of organic matter could contribute to a quick consumption of any oxygen left in the repository. It may also favour an increase in the DOC and acetate contents that, in turns, would increase SRB activity and, thus, the dissolved sulphide contents after closure. In addition, corrosion processes may also represent an additional source of hydrogen that may also increase SRB activity. The amounts of dissolved sulphide produced remains uncertain.

The predicted Base Case evolution indicates few changes in these two parameters over the whole temperate period, although in the case of sulphide the variability of contents decreases because low concentrations tend to disappear (the 25th percentile is 10^{-12} mol/kg in the year 2000 AD and $2{\cdot}10^{-9}$ mol/kg in the year 15,000 AD; Figure 6-3a). However, the mean value (around 10^{-5} mol/kg), the median, and even the maximum and the minimum values remain fairly constant over time. Thus, S(-II) concentrations averaged over the temperate period will be very similar to the present ones (up to $\tilde{10}^{-4}$ mol/kg). For any given deposition hole, oscillations in S(-II) levels will take place, but the time-averaged concentrations are expected to be lower than $\tilde{10}^{-4}$ mol/kg. Fe(II) contents are still more constant than sulphide contents, with 50% of the samples in the repository volume inside a range of Fe(II) values between $3{\cdot}10^{-5}$ and $1.5{\cdot}10^{-6}$ mol/kg (Figure 6-4).

The first stages of the ice advance (Ice I, II and III) in the glacial period show maximum and minimum values of S(-II) ranging from high values (up to 10^{-4} mol/kg) down to very low and not meaningful concentrations (10^{-17} mol/kg). However, for the rest of the stages, in most of the repository volume, S(-II) values are between 10^{-7} and 10^{-5} (Figure 6-3b). The last period (equivalent to the submerged under fresh water period) is characterised by a slightly broader range towards higher values (minimum around 10^{-8} and maximum up to $5{\cdot}10^{-5}$ mol/kg). The presence of a frozen ground does not change the results in terms of the values and ranges except for the fact that the minimum values are higher than for the case when permafrost is not considered (compare Figures 6-3b and b').

Fe(II) values in the Base Case at the beginning of the glacial period (Figure 6-4b) range from $6{\cdot}10^{-5}$ to $5{\cdot}10^{-8}$ mol/kg (as maximum and minimum values). The advance of the ice sheet produces first a slight increase in the Fe(II) content followed by a general decrease in mean values and an increase in the variability range (up to a range from $3{\cdot}10^{-11}$ mol/kg to 10^{-6} mol/kg, lower than the maximum values found at the beginning and the end of this period). At the end of the glacial period

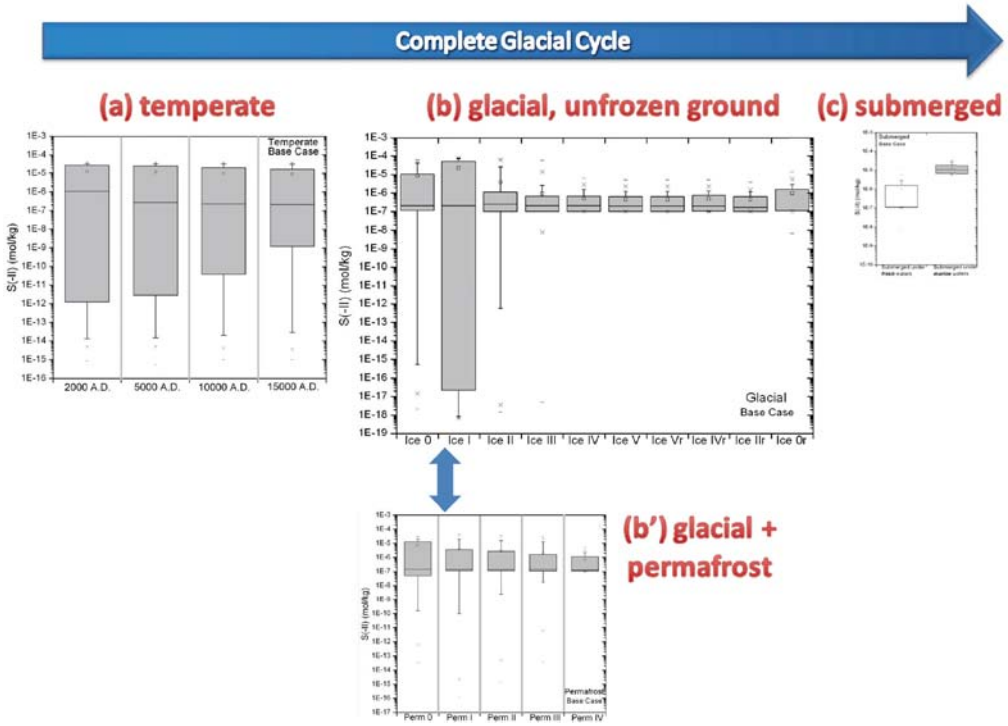

Figure 6-3. *Box-and-whisker plots showing the statistical distribution of S(-II) (mol/kg) obtained with the "Base Case"(including results from variant cases 1 and 2) over the complete glacial cycle (temperate,a , glacial,b , glacial + permafrost,b', and submerged, c) for the groundwaters located within the candidate repository volume at Laxemar. See the caption of Figure 6-1 for the statistical meaning of the different symbols. The position and size of the different graphs in the Figure is such as the values can be easily compared.*

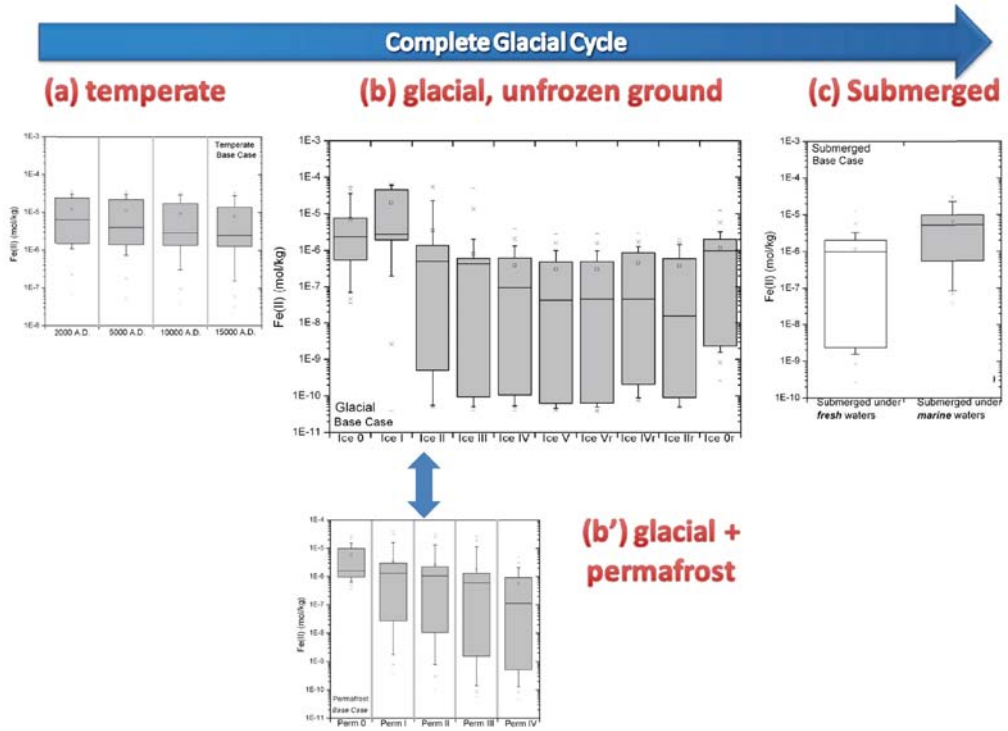

Figure 6-4. *Box-and-whisker plots showing the statistical distribution of Fe(II) (mol/kg) obtained with the "Base Case"(including results from variant cases 1 and 2) over the complete glacial cycle (temperate,a , glacial,b , glacial + permafrost,b', and submerged, c) for the groundwaters located within the candidate repository volume at Laxemar. See the caption of Figure 6-1 for the statistical meaning of the different symbols. The position and size of the different graphs in the Figure is such as the values can be easily compared.*

a slight increase in the Fe(II) values to a range between $3 \cdot 10^{-10}$ and $1 \cdot 10^{-5}$ mol/kg is seen; these values are still lower than those at the end of the temperate period. When permafrost is considered (Figure 6-4b'), a more constant and regular decrease of Fe(II) contents is predicted (from values between 10^{-5} and 10^{-6} mol/kg to values between 10^{-6} and 10^{-10} mol/kg although maximum values are very similar to those found when the ground is not frozen).

For the submerged period, under fresh waters (Figure 6-4c), estimated dissolved S(-II) and Fe(II) concentrations range from 10^{-7} to $3 \cdot 10^{-6}$ mol/kg for S(-II) and from $3 \cdot 10^{-10}$ to 10^{-5} mol/kg for Fe(II). Then in the submerged under marine waters case both elements have higher contents and narrower ranges (S(-II) between $5 \cdot 10^{-6}$ and $3 \cdot 10^{-5}$ mol/kg and Fe(II) between 10^{-7} and $3 \cdot 10^{-5}$ mol/kg; in both cases with similar mean values to the ones predicted for the temperate period).

The different variant cases (equilibrium conditions, haematite or FeS(am) and coupled-uncoupled thermodynamic database) do not significantly change the above conclusions as the Base Case includes the results obtained with the variant cases 1 and 2 (equilibrium with haematite and equilibrium with FeS(am), respectively) and therefore covers the whole range of values. As already mentioned, the main uncertainty of this approach is that it simplifies the behaviour of the system assuming that the equilibrium process imposed is taking place in the whole volume of rock. As a consequence, the statistical results for dissolved sulphide are exaggerated and they correspond to maximum values expected in some points of the repository where sulphate reduction activity is present.

6.5.2 Eh values

Considering the whole period of repository operation, even with moderate inflow to the open tunnels, large amounts of superficial waters are predicted to percolate into the tunnels. Infiltrating waters will initially be equilibrated with oxygen in the atmosphere, whether they are marine, lake, stream or meteoric in origin. However, the reducing capacity of transmissive fracture zones is not affected during the excavation and operation periods, because consumption of oxygen in infiltrating waters takes place already in soils, sediments as well as in the upper metres of fractures by microbial processes. Moreover, after closure, inorganic reactions and decomposition of organic materials could contribute to a quick consumption of any oxygen left in the repository. Thus, the chemical conditions would be reducing shortly after deposition in individual deposition holes, tunnels and, finally, shortly after closure of the repository as a whole.

During the temperate period the increase of the proportion of meteoric waters with time is not expected to change the reducing characteristics of the groundwater. Infiltrating meteoric waters become depleted in oxygen by microbial processes in the soil layers of the site or after some tens of metres along fractures in the bedrock as it occurs presently in the site. The results of Base Case simulation are not against this view. At 2000 AD, the most probable values of calculated Eh (for 90% of the samples in the repository volume) are in the range between –225 and –125 mV. This range progressively evolves to slightly more reducing values, reaching calculated minimum values of around –270 mV in the year 15,000 AD (Figure 6-5a).

The evolution of Eh over the glacial period (with and without permafrost) in the Base Case begins with slightly higher values (up to –75 mV) although 50% of the samples in the repository volume have more reducing values (between –200 and –250 mV) than at the end of the temperate period (between –175 and –225 mV). Then, for the first stages of the ice advance, upconing ahead of the ice front produces quite an important input of more reducing waters and therefore mean Eh values are slightly lower than at stage Ice 0 and I. In the rest of the evolution stages all the simulations indicate very low Eh values (mean around –375mV) until the final stage, when a slight increase is predicted. When a frozen ground is considered (permafrost period), the evolution of the Eh values shows a clear progressive trend towards more reducing situations since the beginning (Figure 6-5b and b').

Finally, after the retreat of the ice sheet, very reducing Eh values (between –260 and –320 mV for 75% of the grid points) are predicted for the submerged situation under fresh waters. When the presence of marine waters is considered, an increase of Eh towards less reducing conditions is predicted, although always below –100 mV and, therefore, fulfilling the safety functions (Figure 6-5c).

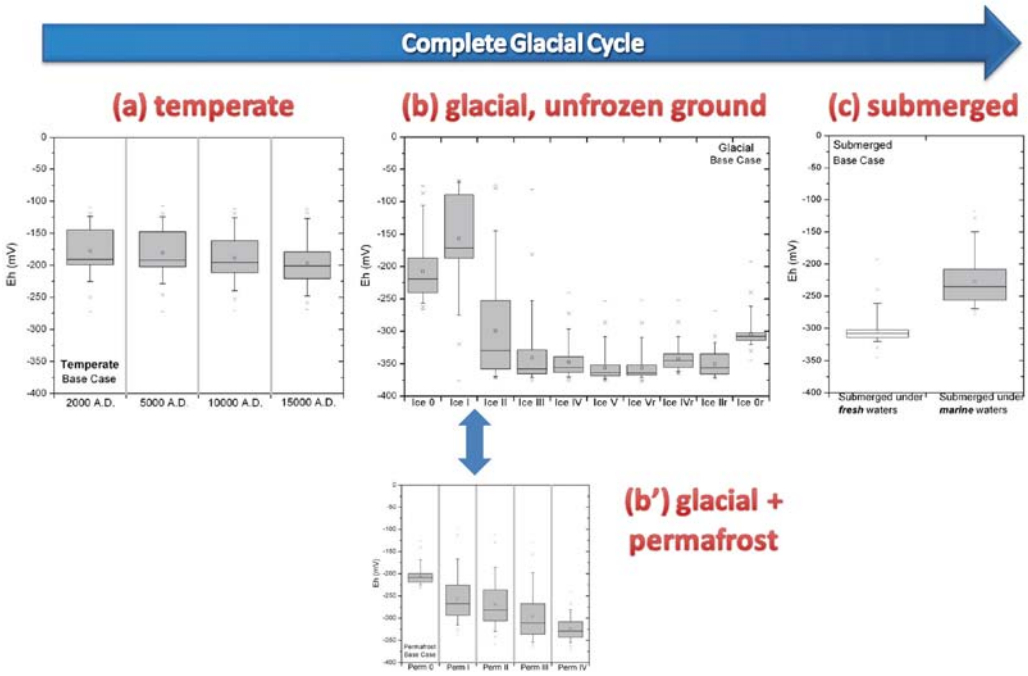

Figure 6-5. *Box-and-whisker plots showing the statistical distribution of Eh (mV) obtained with the "Base Case"(including results from variant cases 1 and 2) over the complete glacial cycle (temperate,a , glacial,b , glacial + permafrost,b', and submerged, c) for the groundwaters located within the candidate repository volume at Laxemar. See the caption of Figure 6-1 for the statistical meaning of the different symbols. The position and size of the different graphs in the Figure is such as the values can be easily compared.*

6.6 Other parameters

The possible contents of certain components (colloids, dissolved and total organic carbon, nitrite, ammonia, acetate, methane and molecular hydrogen) expected over the future evolution of the Laxemar groundwaters have also been assessed in this work. This group of parameters include components for which either the available information is insufficient for a precise quantitative evaluation of their future evolution or cannot be modelled in the same way and with the same tools as the rest of the geochemical parameters in this work.

Pernicious effects of these components are related to enhancement of radionuclide transport (colloids) but, mainly to canister corrosion. Many of them are corroding agents (ammonia, acetate) or can enhance contents of such agents (e.g. dissolved sulphide, nitrite) through different metabolic processes (involving dissolved and total organic carbon, nitrate, acetate, methane and molecular hydrogen).

Most of these parameters are intimately related to the microbial activity conditioning or being conditioned by different redox processes. This fact makes their evaluation a difficult task due to the complexity and the present knowledge of microbial processes in the groundwaters of crystalline systems.

During the operational phase, the accumulation of organic materials and other antropogenic substances (e.g. blasting residues) in the repository introduce "non-natural" disequilibrium conditions that must be relaxed after closure. The increased formation of colloids during the excavation and operational phases is not expected to affect the performance of the repository in the long-term, because colloid concentrations will quickly decrease and resume the natural values.

On the other hand, the expected time-averaged amounts of H_2 (in the nanomolar range) and acetate (in the micromolar range) will be controlled by the usual balance between microbial producing and consuming processes in low temperature systems. However, the total amounts of acetate, methane and, mainly, dissolved carbon contributed by those organic materials are largely uncertain. The value proposed for DOC is derived from the inventory of organic materials in the repository but excluding the amounts of organic carbon associated with the bentonite whose bioavailability is still under study. Moreover degradation rates of organic materials, especially man-made materials, and biodegradability of the organic matter in the bentonite are still poorly known.

NO_2^- and NH_4^+ contents for the Excavation/Operation period have been impossible to fix or bracket due to the lack of estimations of nitrate contents, the principal source of NO_2^- and NH_4^+ through denitrification, and the need to evaluate the effects of blasting residues. However, nitrite is often found in natural aquatic systems at trace levels and ammonia (NH_3, the involved component in stress corrosion cracking, SSC, of the copper canister), is only stable in alkaline (pH > 9) and very reducing conditions. Thus, the existence of meaningful amounts of ammonia during this stage would not be expected, although more detailed analysis is needed.

Most of the values proposed for the temperate period are extrapolated from contents in present groundwaters and has been assumed that they would remain substantially the same after repository construction. Thus, the maximum measured concentrations in present groundwaters have been selected as recommended values for the studied parameters. Except DOC, the recommended values are in the range observed in other crystalline systems. The proposed DOC value is still subjected to different uncertainties and a value of $4 \cdot 10^{-4}$ mM could be used instead as the maximum concentration observed in the crystalline systems reviewed in this work.

As stated above, colloids will not be especially stable during this temperate period because the calculated salinities and cation concentrations will be high enough to destabilise them. Thus, the maximum measured amounts of colloids in present groundwaters have been selected as recommended values.

The selected values for the glacial period (except for CH_4 and H_2) are based on measurements performed in glacier ice samples and in different crystalline systems (DOC), in comparative deductions from contents in present-day groundwaters (NO_2^- and NH_4^+) and in experimental results on the interaction between bentonite and glacial waters.

During this period, due to the suspension of photosynthetic production of organic carbon, the input of organic carbon, acetate or nitrate with recharging groundwater is expected to be low. Moreover, the perennial freezing of rock volumes during permafrost, will effectively shut down the hydraulic circulation in the bedrock, at least locally. Therefore, an increment in the microbial degradation of organic matter promoted by this "external" input over the glacial period is not anticipated. The intensity of sulphide production due to microbially mediated SO_4^{2-} reduction will probably decrease.

However, microbial activity (e.g. sulphate reduction activity) can be sustained by autotrophic metabolisms using CH_4 or H_2 as electron donors. The estimation of CH_4 and H_2 concentrations for this period is complicated by the existence of additional processes and different boundary conditions to those present and/or expected in the other periods. The concentration of these gases will be controlled by their production and flow from the deep bedrock and by the active microbial metabolisms (acting as sources and sinks) but also by the presence of permafrost at the top of the site and by the formation/dissociation of clathrates during permafrost advance and decay. From the preliminary estimations on the fluxes and maximum productions of methane and hydrogen for the Forsmak and Laxemar sites /Delos et al. 2010/, it is not expected an increased sulphide production under ice sheets. However, more data and studies are necessary.

Finally, during this glacial period, the predicted overall decrease in the salinity indicates that groundwaters with $\sum q[Mq^+]$ lower than 4 mM will occur within the candidate repository volume. Thus, as stated above, the possible generation and transport of colloids by these groundwaters cannot be excluded. A reasonable upper limit for this situation would be in the mg/L range from the highest measured colloid concentrations in groundwaters from crystalline environments. In addition, the bentonite barrier can release montmorillonite colloids in contact with dilute groundwaters increasing drastically the concentration of colloids in the vicinity of the bentonite barrier. Under this period, experimental results reviewed suggest that a maximum of about 10–20 mg/l of montmorillonite colloids can be expected.

During the submerged period under marine waters, marine waters will recharge the aquifer system infiltrating through the sediments. Most of the selected values are based on the maximum concentrations measured in present-day groundwaters with a clear Littorina contribution as an expected analogue situation for this period. Effects of this marine intrusion are more intense in Forsmark than in Laxemar-Simpevarp and, thus, the selected values for DOC, NH_4^+ NO_2^-, CH_4 and colloids mainly correspond to those observed in the marine-derived groundwaters from Forsmark.

However, it must be taken into account that the selected DOC contents (corresponding to the highest DOC values in present-day Forsmark groundwaters) are still subjected to different uncertainties (e.g. contamination during drilling/sampling) and, therefore, they must be used with caution.

H_2 and acetate will be controlled by the usual balance between microbial producing and consuming processes in low temperature systems and, thus, contents in the nanomolar and in the micromolar range, respectively, are expected.

7 References

SKB's (Svensk Kärnbränslehantering AB) publications can be found at www.skb.se/publications.

Acero P, Auqué L F, Gimeno M J, Gómez J B, 2010. Evaluation of mineral precipitation potential in a spent nuclear fuel repository. Environmental Earth Sciences, 59, pp 1613–1628.

Alexander W R, 2010. The impact of a hyperalkaline plume on fractured crystalline rock. In: NEA IGSC Workshop on cementitious materials in safety cases for geological repositories for radioactive waste: role, evolution and interaction, Brussels, 17–20 November 2009.

Alexander W R, Neall F B, 2007. Assessment of potential perturbations to Posiva's SF repository at Olkiluoto from the ONKALO facility. Posiva Working Report 2007-35, Posiva Oy, Finland.

Andersen M S, Nyvang V, Jakobsen R, Postma D, 2005. Geochemical processes and solute transport at the seawater/freshwater interface of a sandy aquifer. Geochimica et Cosmochimica Acta, 69, pp 3979–3994.

Appelo C A J, Postma D, 1993. Geochemistry, groundwater and pollution. Rotterdam: Balkema.

Appelo C A J, Postma D, 2005. Geochemistry, groundwater and pollution. 2nd ed. Leiden: Balkema.

Arilahti E, Bojinov M, Mäkelä K, Laitinen T, Saario T, 2000. Stress corrosion cracking investigation of copper in groundwater with ammonium ions. Posiva Working Report 2000-46, Posiva Oy, Finland.

Auqué L F, Gimeno M J, Gómez J B, Puigdomenech I, Smellie J, Tullborg E-L, 2006. Groundwater chemistry around a repository for spent nuclear fuel over a glacial cycle. Evaluation for SR-Can. SKB TR-06-31, Svensk Kärnbränslehantering AB.

Ball J W, Nordstrom D K, 2001. User's manual for WATEQ4F, with revised thermodynamic data base and test cases for calculating speciation of major, trace, and redox elements in natural waters. Open File Report 91-183, U.S. Geological Survey, Denver, Colorado.

Banwart S A, 1999. Reduction of iron(III) minerals by natural organic matter in groundwater. Geochimica et Cosmochimica Acta, 63, pp 2919–2928.

Banwart S A, Gustafsson E, Laaksoharju M, 1999. Hydrological and reactive processes during rapid recharge to fracture zones: the Äspö large scale redox experiment. Applied Geochemistry, 14, pp 873–892.

Barker J D, Sharp M J, Fitzsimons S J, Turner R J, 2006. Abundance and dynamics of dissolved organic carbon in glacier systems. Arctic, Antarctic, and Alpine Research, 38, pp 163–172.

Bath A, 2005. Geochemical investigations of groundwater stability. SKI Report 2006:12, Statens kärnkraftinspekton (Swedish Nuclear Power Inspectorate).

Bethke C M, 2008. Geochemical and biogeochemical reaction modeling. 2nd ed. Cambridge: Cambridge University Press.

Betova I G, Bojinov M S, Heinonen J, Kinnunen P, Lilja C, Saario T, 2005. Development of a rapid screening test for SCC susceptibility of copper in disposal vault conditions. In: Van Iseghem P (ed). Scientific basis for nuclear waste management XXIX: symposium held in Ghent, Belgium, 12–16 September 2005. Warrendale, PA: Materials Research Society. (Materials Research Society Symposium Proceedings 932), pp 821–828.

Birgersson M, Börgesson L, Hedström M, Karnland O, Nilsson U, 2009. Bentonite erosion. Final report. SKB TR-09-34, Svensk Kärnbränslehantering AB.

Brown G H, 2002. Glacier melt water hydrochemistry. Applied Geochemistry, 17, pp 855–883.

Brown G H, Sharp M, Tranter M, 1996. Subglacial chemical erosion: seasonal variations in solute provenance, Haut Glacier d'Arolla, Switzerland. Annals of Glaciology, 22, pp 25–31.

Carman R, Rahm L, 1997. Early diagenesis and chemical characteristics of interstitial waters and sediments in the deep deposition bottoms of the Baltic Proper. Journal of Sea Research, 37, 25–47.

Chapelle F H, 2001. Groundwater microbiology and geochemistry. 2nd ed. New York: John Wiley & Sons.

Chivian D, Brodie E L, Alm E J, Culley D E, Dehal P S, DeSantis T Z, Gihring T M, Lapidus A, Lin L-H, Lowry S R, Moser D P, Richardson P M, Southam G, Wanger G, Pratt L M, Andersen G L, Hazen T C, Brockman F J, Arkin A P, Onstott T C, 2008. Environmental genomics reveals a single-species ecosystem deep within Earth. Science, 322, pp 275–278.

Choppin G R, Wong P J, 1998. The chemistry of actinide behavior in marine systems. Aquatic Geochemistry, 4, pp 77–101.

Christensen T H, Bjerg P L, Banwart S A, Jakobsen R, Heron G, Albrechtsen H-J, 2000. Characterization of redox conditions in groundwater contaminant plumes. Journal of Contaminant Hydrology, 45, pp 165–241.

Degueldre C, 1994. Colloid properties in groundwaters from crystalline formations. Nagra NTB 92-05, National Cooperative for the Disposal of Nuclear Waste, Switzerland.

Degueldre C, Pfeiffer H-R, Alexander W, Wernli B, Bruestch R, 1996. Colloid properties in grantic groundwater systems. I: Sampling and characterization. Applied Geochemistry, 11, pp 677–695.

Degueldre C, Triay I, Kim J, Vilks P, Laaksoharju M, Miekeley R, 2000. Groundwater colloid properties: a global approach. Applied Geochemistry, 15, pp 1043–1051.

Delos A, Trinchero P, Richard L, Molinero J, Dentz M, Pitkänen P, 2010. Quantitative assessment of deep gas migration in Fennoscandian sites. SKB R-10-61, Svensk Kärnbränslehantering AB.

Domènech C, Arcos D, Duro L, Grandia F, 2006. Effect of the mineral precipitation-dissolution at tunnel walls during the operational and post-operational phases. SKB R-06-108, Svensk Kärnbränslehantering AB.

Drake H, Tullborg E-L, 2008. Oskarshamn site investigation. Detecting the near surface redox front in crystalline rock. Results from drill cores KLX09B-G and KLX11B-F. SKB P-08-44, Svensk Kärnbränslehantering AB.

Drake H, Tullborg E-L, 2009. Fracture mineralogy Laxemar. Site descriptive modelling, SDM-Site Laxemar. SKB R-08-99, Svensk Kärnbränslehantering AB.

Drake H L, Küsel K, Matthies C, 2006. Acetogenic prokaryotes. In: Dworkin M, Falkow S, Rosenberg E, Schleifer K-H, Stackebrandt E (eds). The prokaryotes: an evolving electronic resource for the microbiological community. 3rd ed. New York: Springer-Verlag, pp 354–420.

Drake H, Tullborg E-L, MacKenzie A B, 2009. Detecting the near-surface redox front in crystalline bedrock using fracture mineral distribution, geochemistry and U-series disequilibrium. Applied Geochemistry, 24, pp 1023–1039.

Drever J I, 1997. The geochemistry of natural waters: surface and groundwater environments. 3rd ed. Upper Saddle River, NJ: Prentice Hall.

Drew M C, 1983. Plant injury and adaptation to oxygen de ficiency in the root environment: a review. Plant and Soil, 75, pp 179–199.

Duro L, Grivé M, Cera E, Domènech C, Bruno J, 2006. Update of a thermodynamic database for radionuclides to assist solubility limits calculation for performance assessment. SKB TR-06-17, Svensk Kärnbränslehantering AB.

Fry N K, Fredrickson J K, Fishbain S, Wagner M, Stahl D A, 1997. Population structure of microbial communities associated with two deep, anaerobic, alkaline aquifers. Applied and Environmental Microbiology, 63, pp 1498–1504.

Gabriel U, Gaudet J-P, Spadini L, Charlet L, 1998. Reactive transport of uranyl in a goethite column: an experimental and modeling study. Chemical Geology, 151, pp 107–128.

Gaines G L, Thomas H C, 1953. Adsorption studies on clay minerals. II. A formulation of the thermodynamics of exchange adsorption. Journal of Chemical Physics, 21, pp 714–718.

Gascoyne M, 2004. Hydrogeochemistry, groundwater ages and sources of salts in a granitic batholith on the Canadian Shield, southeastern Manitoba. Applied Geochemistry, 19, pp 519–560.

Gascoyne M, Thomas D A, 1997. Impact of blasting on groundwater composition in a fracture in Canada's Underground Research Laboratory. Journal of Geophysical Research, 102, pp 573–584.

Geipel G, Brachmann A, Brendler V, Bernhard G, Nitsche H, 1996. Uranium(VI) sulfate complexation studied by time-resolved laser-induced fluorescence spectroscopy (TRLFS). Radiochimica Acta, 75, pp 199–204.

Gimeno M J, Auqué L F, Gómez J B, Acero P, 2008. Water-rock interaction modelling and uncertainties of mixing modelling. SDM-Site Forsmark. SKB R-08-86, Svensk Kärnbränslehantering AB.

Gimeno M J, Auqué L F, Gómez J B, Acero P, 2009. Water-rock interaction modelling and uncertainties of mixing modelling. Site descriptive modelling, SDM-Site Laxemar. SKB R-08-110, Svensk Kärnbränslehantering AB.

Gómez J B, Auqué L F, Gimeno M J, 2008. Semitivity and uncertainty analysis of mixing and mass balance calculations with standard and PCA-based geochemical codes. Applied Geochemistry, 23, 194-1956.

Grandia F, Domènech C, Arcos D, Duro L, 2006. Assessment of the oxygen consumption in the back fill. Geochemical modelling in a saturated backfill. SKB R-06-106, Svensk Kärnbränslehantering AB.

Grenthe I, Stumm W, Laaksoharju M, Nilsson A C, Wikberg P, 1992. Redox potentials and redox reactions in deep groundwaters systems. Chemical Geology, 98, pp 131–150.

Grivé M, Domènech C, Montoya V, Garcia D, Duro L, 2010. Determination and assessment of the concentration limits to be used in SR-Can. Supplement to TR-06-32. SKB R-10-50, Svensk Kärnbränslehantering AB.

Hallbeck L, 2009. Microbial processes in glaciers and permafrost. A literature study on microbiology affecting groundwater at ice sheet melting. SKB R-09-37, Svensk Kärnbränslehantering AB.

Hallbeck L, 2010. Principal organic materials in a repository for spent nuclear fuel. SKB TR-10-19, Svensk Kärnbränslehantering AB.

Hallbeck L, Pedersen K, 2008a. Explorative analysis of microbes, colloids and gases. SDM-Site Forsmark. SKB R-08-85, Svensk Kärnbränslehantering AB.

Hallbeck L, Pedersen K, 2008b. Explorative analyses of microbes, colloids and gases together with microbial modelling. Site description model. SDM-Site Laxemar. SKB R-08-109, Svensk Kärnbränslehantering AB.

Hallbeck L, Pedersen K, 2008c. Characterization of microbial processes in deep aquifers of the Fennoscandian Shield. Applied Geochemistry, 23, pp 1796–1819.

Hallbeck L, Grivé M, Gaona X, Duro L, Bruno J, 2006. Main organic materials in a repository for high level radioactive waste. SKB R-06-104, Svensk Kärnbränslehantering AB.

Hallberg G R, Keeney D R, 1993. Nitrate. In: Alley W M (ed). Regional ground-water quality. New York: Van Nostrand Reinhold, pp 297–322.

Hansen L K, Jakobsen R, Postma D, 2001. Methanogenesis in a shallow sandy aquifer, Rømø, Denmark. Geochimica et Cosmochimica Acta, 65, pp 2925–2935.

Haveman S A, Pedersen K, 2002. Distribution of culturable microorganisms in Fennoscandian Shield groundwater. FEMS Microbiology Ecology, 39, pp 129–137.

Hedqvist I, Degueldre C, 2008. Oskarshamn site investigation. Granitic groundwater colloids sampling and characterisation. Colloids analysis from KLX17A (416.0 to 437.5 m) and KLX15A (623.0 to 634.5 m). SKB P-08-101, Svensk Kärnbränslehantering AB.

Heimann A, Jakobsen R, Blodau C, 2010. Energetic constraints on H_2-dependent terminal electron accepting processes in anoxic environments: a review of observations and model approaches. Environmental Science & Technology, 44, pp 24–33.

Heuer V B, Pohlman J W, Torres M E, Elvert M, Hinrichs K-W, 2009. The stable carbon isotope biogeochemistry of acetate and other dissolved carbon species in deep subseafloor sediments at the northern Cascadia Margin. Geochimica et Cosmochimica Acta, 73, pp 3323–3336.

Hoehler T M, Alperin M J, Albert D B, Martens C S, 1998. Thermodynamic control on hydrogen concentrations in anoxic sediments. Geochimica et Cosmochimica Acta, 62, pp 1745–1756.

Hoehler T M, Albert D B, Alperin M J, Martens C S, 1999. Acetogenesis from CO_2 in an anoxic marine sediment. Limnology and Oceanography, 44, pp 662–667.

Hummel W, Berner U, Curti E, Pearson F J, Thoenen T, 2002. Nagra/PSI Chemical thermodynamic data base 01/01. Nagra Technical Report 02-16, National Cooperative for the Disposal of Radioactive Waste, Switzerland.

Ikeda B M, Litke C D, 2000. The effect of oxidant flux, nitrite concentration and chloride concentration on the stress corrosion cracking behaviour of non-welded and electronbeam welded copper. Report 06819-REP-01200-10049-R00, Ontario Power Generation, Nuclear Waste Management Division, Canada.

Ikeda B M, Litke C D, 2007. Stress corrosion cracking of copper in nitrite/chloride mixtures at elevated temperatures. NWMO TR-2007-04, Nuclear Waste Management Organization, Canada.

Ikeda B M, Litke C D, Betteridge J S, 2004. Status report for 2003 on stress corrosion cracking of OFP copper in ammonia. Report 06819-REP-01300-10078-R00, Ontario Power Generation, Nuclear Waste Management Division, Canada.

Iwatsuki T, Arthur R, Ota K, Metcalfe R, 2004. Solubility constraints on uranium concentrations in groundwaters of the Tono uranium deposit, Japan. Radiochimica Acta, 92, pp 789–796.

Iwatsuki T, Furue R, Mie H, Ioka S, Mizuno T, 2005. Hydrochemical baseline condition of groundwater at the Mizunami underground research laboratory (MIU). Applied Geochemistry, 20, pp 2283–2302.

Jakobsen R, Cold L, 2007. Geochemistry at the sulfate reduction – methanogenesis transition zone in an anoxic aquifer. A partial equilibrium interpretation using 2D reactive transport modeling. Geochimica et Cosmochimica Acta, 71, pp 1949–1966.

Jockwer N, Wieczorek K, 2003. Gas generation measurements in the FEBETX project. (Abstract). In: Clays in natural and engineered barriers for radioactive waste confinement: proceedings from the international meeting held in Reims, 9–12 December 2002. Châtenay-Malabry: Agence nationale pour la gestion des déchets radioactifs (Andra), pp 108–117.

Joyce S, Simpson T, Hartley L, Applegate D, Hoek J, Jackson P, Roberts D, Swan D, Gylling B, Marsic N, Rhén I, 2010. Groundwater flow modelling of periods with temperate climate conditions – Laxemar. SKB R-09-24, Svensk Kärnbränslehantering AB.

Kankainen T, 1986. Loviisa power station final disposal of reactor waste. On the age and origin of groundwater from the rapakivi granite on the island of Hästholmen. Report YJT-86-29, Nuclear Waste Commission of Finnish Power Companies.

Kehew A E, 2001. Applied chemical hydrogeology. Upper saddle River, NJ: Prentice Hall.

Kieft T L, McCuddy S M, Onstott T C, Davidson M, Lin L-H, Mislowack B, Pratt L, Boice E, Sherwood Lollar B, Lippmann-Pipke J, Pfiffner S M, Phelps T J, Gihring T M, Moser D, van Heerden A, 2005. Geochemically generated, energy-rich substrates and indigenous microorganisms in deep, ancient groundwater. Geomicrobiology Journal, 22, pp 325–355.

King F, 2007. Status of the understanding of used fuel container corrosion processes. Summary of current knowledge and gap analysis. NWMO TR-2007-09, Nuclear Waste Management Organization, Canada.

King F, Ahonen L, Taxén C, Vuorinen U, Werme L, 2001. Copper corrosion under expected conditions in a deep geologic repository. SKB TR 01-23, Svensk Kärnbränslehantering AB.

King G M, 1991. Measurement of acetate concentrations in marine pore waters by using an enzymatic approach. Applied and Environmental Microbiology, 57, pp 3476–3481.

Kinnunen P, 2006. Stress corrosion cracking investigation of copper in groundwater with acetate ions. Posiva Working Report 2006-18, Posiva Oy, Finland.

Koizumi Y, Kojima H, Oguri K, Kitazato H, Fukui M, 2004. Vertical and temporal shifts in microbial communities in the water column and sediment of saline meromictic Lake Kaiike (Japan), as determined by a 16S rDNA-based analysis, and related to physicochemical gradients. Environmental Microbiology, 6, pp 622–637.

Konhauser K, 2007. Introduction to geomicrobiology. Oxford: Blackwell.

Kotelnikova S, 2002. Microbial production and oxidation of methane in deep subsurface. Earth-Science reviews, 58, pp 367–395.

Laaksoharju M, Wallin B (eds), 1997. Evolution of the groundwater chemistry at the Äspö Hard Rock Laboratory. Proceedings of the second Äspö International Geochemistry Workshop, Äspö, Sweden, 6–7 June 1995. SKB HRL International Cooperation Report ICR 97-04, Svensk Kärnbränslehantering AB.

Laaksoharju M, Degueldre C, Skårman C, 1995. Studies of colloids and their importance for repository performance assessment. SKB TR 95-24, Svensk Kärnbränslehantering AB.

Laaksoharju M, Tullborg E-L, Wikberg P, Wallin B, Smellie J, 1999. Hydrogeochemical conditions and evolution at the Äspö HRL, Sweden. Applied Geochemistry, 14, pp 835–859.

Laaksoharju M, Smellie J, Tullborg E-L, Gimeno M, Hallbeck L, Molinero J, Waber N, 2008a. Bedrock hydrogeochemistry Forsmark. Site descriptive modelling, SDM-Site Forsmark. SKB R-08-47, Svensk Kärnbränslehantering AB.

Laaksoharju M, Gascoyne M, Gurban I, 2008b. Understanding groundwater chemistry using mixing models. Applied Geochemistry, 23, pp 1921–1940.

Laaksoharju M, Smellie J, Tullborg E-L, Wallin B, Drake H, Gascoyne M, Gimeno M, Gurban I, Hallbeck L, Molinero J, Nilsson A-C, Waber N, 2009. Bedrock hydrogeochemistry Laxemar. Site descriptive modelling, SDM-Site Laxemar. SKB R-08-93, Svensk Kärnbränslehantering AB.

Lin L-H, Slater G F, Sherwood Lollar B, Lacrampe-Couloume G, Onstott T C, 2005. The yield and isotopic composition of radiolytic H2, a potential source for deep subsurface biosphere. Geochimica et Cosmochimica Acta, 69, pp 893–903.

Lin L-H, Wang P-L, Rumble D, Lippmann-Pipke J, Boice E, Pratt L M, Sherwood Lollar B, Brodie E L, Hazen T C, Anderson G L, DeSantis T Z, Moser D P, Kershaw D, Onstott T C, 2006. Long-term sustainability of a high-energy, low-diversity crustal biome. Science, 314, pp 479–482.

Litke C D, Ikeda B M, 2006. The effect of acetate concentration, chloride concentration, and applied current on stress corrosion cracking of OFP copper. Report 06819-REP-01300-10005-R00, Ontario Power Generation, Nuclear Waste Management Division, Canada.

Louvat D, Michelot J L, Aranyossy J F, 1997. Salinity origin and residence time of the Äspö groundwater system. In: Laaksoharju M, Wallin B (eds). Evolution of the groundwater chemistry at the Äspö Hard Rock Laboratory. Proceedings of the second Äspö International Geochemistry Workshop, Äspö, Sweden, 6–7 June 1995. SKB HRL International Cooperation Report ICR 97-04, Svensk Kärnbränslehantering AB.

Louvat D, Michelot J L, Aranyossy J F, 1999. Origin and residence time of salinity in the Äspö groundwater system. Applied Geochemistry, 14, pp 917–925.

Lovley D R, Goodwin S, 1988. Hydrogen concentrations as an indicator of the predominant terminal electron-accepting reactions in aquatic sediments. Geochimica et Cosmochimica Acta, 52, pp 2993–3003.

Luna M, Arcos D, Duro L, 2006. Effects of grouting, shotcreting and concrete leachates on backfill geochemistry. SKB R-06-107, Svensk Kärnbränslehantering AB.

Martino J B, Kozak E, Woodcock D, Stroes-Gascoyne S, 2004. The Blast Damage Assessment Project at the URL. Report 06819-REP-01200-10123-R00, Ontario Power Generation, Nuclear Waste Management Division, Canada.

McCarthy J F, Czerwinski K R, Sanford W E, Jardine P M, Marsh J D, 1998. Mobilization of transuranic radionuclides from disposal trenches by natural organic matter. Journal of Contaminant Hydrology, 30, pp 49–77.

Mitchell A C, Brown G H, 2007. Diurnal hydrological – physicochemical controls and sampling methods for minor and trace elements in an Alpine glacial hydrological system. Journal of Hydrology, 332, pp 123–143.

Molinero J, 2000. Testing and validation of numerical models of groundwater flow, solute transport and chemical reactions in fractured granites:a quantitative study of the hydrogeological and hydrochemical impact produced by the construction of the Äspö Underground Laboratory (Sweden). Ph.D. thesis. Universidad de A Coruña, Spain.

Molinero J, Samper J, 2006. Large-scale modeling of reactive solute transport in fracture zones of granitic bedrocks. Journal of Contaminant Hydrology, 82, pp 293–318.

Molinero-Huguet J, Samper-Calvete F J, Zhang G, Yang C, 2004. Biogeochemical reactive transport model of the Redox Zone experiment of the Äspö Hard Rock Laboratory in Sweden. Nuclear Technology, 148, pp 151–165.

Moser D P, Gihring T M, Brockman F J, Fredrickson J K, Balkwill D L, Dollhopf M E, Sherwood Lollar B, Pratt L M, Boice E, Southam G, Wanger G, Baker B J, Pfiffner S M, Lin L-H, Onstott T C, 2005. Deep continental fracture system dominated by Desulfotomaculum and Methanobacterium spp. dominate a 4-to 5-kilometer-deep fault. Applied Environmental Microbiology, 71, pp 8773–8783.

Mårtensson E, Gustafsson L-G, Bosson E, 2009. Effects on surface hydrology and near-surface hydrogeology of an open repository in Laxemar. Results of modelling with MIKE SHE. SKB R-09-36, Svensk Kärnbränslehantering AB.

Nilsson A-C, Degueldre C, 2007. Forsmark site investigation. Granitic groundwater colloids sampling and characterisation. SKB P-07-169, Svensk Kärnbränslehantering AB.

Nilsson A-C, Tullborg E-L, Smellie J, 2010. Preliminary Hydrogeochemical Site Description SFR (version 0.2). SKB R-10-38, Svensk Kärnbränslehantering AB.

Nordstrom D K, Ball J W, Donahoe R J, Whittemore D, 1989. Groundwater chemistry and water-rock interactions at Stripa. Geochimica et Cosmochimica Acta, 53, pp 1727–1740.

Onstott T C, McGown D J, Bakermans C, Ruskeeniemi T, Ahonen L, Telling J, Soffientino B, Pfiffner S M, Sherwood Lollar B, Frape S, Stotler R, Johnson E J, Vishnivetskaya T A, Rothmel R, Pratt L M, 2009. Microbial communities in subpermafrost saline fracture water at the Lupin Au Mine, Nunavut, Canada. Microbial Ecology, 58, pp 786–807.

Parkes R J, Wellsbury P, Mather I D, Cobb S J, Cragg B A, Hornibrook E R C, Horsfield B, 2007. Temperature activation of organic matter and minerals during burial has the potential to sustain the deep biosphere over geological timescales. Organic Geochemistry, 38, pp 845–852.

Parkhurst D L, Appelo C A J, 1999. User's guide to PHREEQC (version 2): a computer program for speciation, batch-reaction, one-dimensional transport, and inverse geochemical calculations. Water-Resources Investigations Report 99-4259, U.S. Geological Survey, Denver, Colorado.

Pedersen K, 1993. The deep subterranean biosphere. Earth-Science Reviews, 34, pp 243–260.

Pedersen K, 1997a. Microbial life in deep granitic rock. FEMS Microbiology Reviews, 20, pp 399–414.

Pedersen K, 1997b. Investigations of subterranean microorganisms and their importance for performance assessment of radioactive waste disposal. Results and conclusions achieved during the period 1995 to 1997. SKB TR-07-22, Svensk Kärnbränslehantering AB.

Pedersen K, 2001. Diversity and activity of microorganisms in deep igneous rock aquifers of the Fennoscandian Shield. In: Fredrickson J K, Fletcher M (eds). Subsurface microbiology and biogeochemistry. Chichester: Wiley, pp. 97–139.

Pedersen K, 2006. Microbiology of transitional groundwater of the porous overburden and underlying fractured bedrock aquifers in Olkiluoto, Finland. Posiva Working Report 2006-09, Posiva Oy, Finland.

Pedersen K, 2008. Microbiology of Olkiluoto groundwater, 2004–2006. Posiva 2008-02, Posiva Oy, Finland.

Pedersen K, Kennedy C, Nederfeldt K-G, Bergelin A, 2004. Äspö Hard Rock Laboratory. Prototype repository. Chemical measurements in buffer and backfill; sampling and analyses of gases. SKB IPR-04-26, Svensk Kärnbränslehantering AB.

Pitkänen P, Partamies S, 2007. Origin and implications of dissolved gases in groundwater at Olkiluoto. Posiva 2007-04, Posiva Oy, Finland.

Pitkänen P, Luukkonen A, Ruotsalainen P, Leino-Forsman H, Vuorinen U, 1999. Geochemical modelling of groundwater evolution and residence time at the Olkiluoto site. Posiva 98-10, Posiva Oy, Finland.

Pitkänen P, Partamies S, Luukkonen A, 2004. Hydrogeochemical interpretation of baseline groundwater conditions at the Olkiluoto site. Posiva 2003-07, Posiva Oy, Finland.

Posiva, 2006. Expected evolution of a spent nuclear fuel repository at Olkiluoto. Posiva 2006-05, Posiva Oy, Finland.

Postma D, Jakobsen R, 1996. Redox zonation: Equilibrium constraints on the Fe(III)/SO4-reduction interface. Geochimica et Cosmochimica Acta, 60, pp 3169–3175.

Puigdomenech I (ed), 2001. Hydrochemical stability of groundwaters surrounding a spent nuclear fuel repository in a 100,000 year perspective. SKB TR-01-28, Svensk Kärnbränslehantering AB.

Rhén I, Hartley L 2009. Bedrock hydrogeology Laxemar. Site descriptive modelling, SDM-Site Laxemar. SKB R-08-92, Svensk Kärnbränslehantering AB.

Rivett M O, Buss S R, Morgan P, Smith J W N, Bemmen C D, 2008. Nitrate attenuation in groundwater: a review of biogeochemical controlling processes. Water Research, 42, pp 4215–4232.

Ruskeeniemi T, Paananen M, Ahonen L, Kaija J, Kuivamäki A, Frape S, Moren L, Degnan P, 2002. Permafrost at Lupin: report of Phase I. Report YST-112, Geological Survey of Finland, Nuclear Waste Disposal Research.

Ruskeeniemi T, Ahonen L, Paananen M, Frape S, Stotler R, Hobbs M, Kaija J, Degnan P, Blomqvist R, Jensen M, Lehto K, Moren L, Puigdomenech I, Snellman M, 2004. Permafrost at Lupin: report of Phase II. Report YST-119, Geological Survey of Finland, Nuclear Waste Disposal Research.

Sahl J W, Schmidt R, Swanner E D, Mandernack K W, Templeton A S, Kieft T L, Smith R L, Sanford W E, Callaghan R L, Mitton J B, Spear J R, 2008. Subsurface microbial diversity in deep-granitic-fracture water in Colorado. Applied and Environmental Microbiology, 74, pp 143–152.

Salas J, Gimeno M J, Auqué L, Molinero J, Gómez J, Juárez I, 2010. SR-Site – hydrogeochemical evolution of the Forsmark site. SKB TR-10-58, Svensk Kärnbränslehantering AB.

Sanding A, Bruno J, 1992. The solubility of $(UO_2)_3(PO_4)_2 \cdot 4H_2O$ and the formation of U(VI) phosphate complexes: their influence in uranium speciation in natural waters. Geochimica et Cosmochimica Acta , 56, pp 4135–4145.

Selnert E, Byegård J, Widestrand H, 2008. Forsmark site investigation. Laboratory measurements within the site investigation programme for the transport properties of the rock. Final report. SKB P-07-139, Svensk Kärnbränslehantering AB.

Selroos J-O, Follin S, 2010. Groundwater flow modelling methodology, setup and results – SR-Site Forsmark. SKB R-09-22, Svensk Kärnbränslehantering AB.

Sherwood Lollar B, Voglesonger K, Lin L-H, Lacrampe-Couloume C, Telling J, Abrajano T A, Onstott T C, Pratt L M, 2007. Hydrogeologic controls on episodic H_2 release from precambrian fractured rocks – energy for deep subsurface life on Earth and Mars. Astrobiology, 7, pp 971–986.

Silver W L, Lugo A E, Keller M, 1999. Soil oxygen availability and biogeochemistry along rainfall and topographic gradients in upland wet tropical forest soils. Biogeochemistry, 44, pp 301–328.

SKB, 2006a. Long-term safety for KBS-3 repositories at Forsmark and Laxemar – a first evaluation. Main report of the SR-Can project. SKB TR-06-09, Svensk Kärnbränslehantering AB.

SKB, 2006b. Buffer and backfill process report for the safety assessment SR-Can. SKB TR-06-18, Svensk Kärnbränslehantering AB.

SKB, 2006c. Fuel and canister process report for the safety assessment SR-Can. SKB TR-06-22, Svensk Kärnbränslehantering AB.

SKB, 2006d. Climate and climate-related issues for the safety assessment SR-Can. SKB TR-06-23, Svensk Kärnbränslehantering AB.

SKB, 2010. Geosphere process report for the safety assessment SR-Site. SKB TR-10-48, Svensk Kärnbränslehantering AB.

SKB, 2011. Long-term safety for the final repository for spent nuclear fuel at Forsmark. Main report of the SR-Site project. SKB TR-11-01, Svensk Kärnbränslehantering AB.

Smellie J, Tullborg E-L, Nilsson A-C, Sandström B, Waber N, Gimeno M, Gascoyne M, 2008. Explorative analysis of major components and isotopes. SDM-Site Forsmark. SKB R-08-84, Svensk Kärnbränslehantering AB.

Smith P A, Alexander W R, Heer W, Fierz T, Meier P M, Baeyens B, Bradbury M H, Mazurek M, McKinley I G, 2001. Grimsel Test Site Investigation Phase IV (1994–1996). The Nagra-JNC in situ study of safety relevant radionuclide retardation in fractured crystalline rock. I: Radionuclide migration experiment – overview 1990–1996. Nagra Technical Report Series NTB 00-09, National Cooperative for the Disposal of Radioactive Waste, Switzerland.

Stevens T O, McKinley J P, 1995. Lithoautotrophic microbial ecosystems in deep basalt aquifers. Science, 270, pp 450–454.

Stotler R L, Frape S K, Ruskeeniemi T, Ahonen L, Onstott T, Hobbs M Y, 2009. Hydrogeochemistry of groundwaters in and below the base of thick permafrost at Lupin, Nunavut, Canada. Journal of Hydrology, 373, pp 80–95.

Stotler R L, Frape S K, Ahonen L, Clark I D, Greene S, Hobbs M, Johnson E, Lemieux J-M, Peltier W R, Pratt L, Ruskeeniemi T, Sudicky E A, Tarasov L, 2010a. Origin and stability of a permafrost methane hydrate occurrence in the Canadian Shield. Earth and Planetary Science Letters, 296, pp 384-394.

Stotler R L, Frape S K, Freifeld B M, Holden B, Onstott T C, Ruskeeniemi T, Chan E, 2010b. Hydrogeology, chemical and microbial activity measurement through deep permafrost. Ground Water, doi: 10.1111/j.1745-6584.2010.00724.x.

Stroes-Gascoyne S, Gascoyne M, 1998. The introduction of microbial nutrients into a nuclear waste disposal vault during excavation and operation. Environmental Science & Technology, 32, pp 317–325.

Svensson U, Follin S, 2010. Groundwater flow modelling of the excavation and operation periods – SR-Site Laxemar. SKB R-09-23, Svensk Kärnbränslehantering AB.

Tranter M, Sharp M J, Lamb H R, Brown G H, Hubbard B P, Willis I C, 2002. Geochemical weathering at the bed of Haut Glacier d'Arolla, Switzerland: a new model. Hydrological Processes, 16, pp 959–993.

Trotignon L, Michaud V, Lartigue J-E, Ambrosi J-P, Eisenlohr L, Griffault L, de Combarieu M, Daumas S, 2002. Laboratory simulation of an oxidizing perturbation in a deep granite environment. Geochimica et Cosmochimica Acta, 66, pp 2583–2601.

Tullborg E-L, 1997. How do we recognize remants of glacial water in bedrock?. In: King-Clayton L, Chapman N, Ericsson L O, Kautsky F (eds). Glaciation and hydrogeology. Proceedings of the workshop on the impact of climate change & glaciations on rock stresses, groundwater flow and hydrochemistry: past, present and future, Hässelby, Sweden, 17–19 April 1996. SKI Report 97:13, Statens kärnkraftinspektion (Swedish Nuclear Power Inspectorate).

Tullborg E-L, Drake H, Sandström B, 2008. Palaeohydrogeology: a methodology based on fracture mineral studies. Applied Geochemistry, 23, pp 1881–1897.

Tullborg E-L, Smellie J, Nilsson A-C, Gimeno M J, Auqué L F, Brüchert V, Molinero J, 2010a. SR-Site – sulphide content in the groundwater at Forsmark. SKB TR-10-39, Svensk Kärnbränslehantering AB.

Tullborg E-L, Smellie J, Nilsson A-C, Gimeno M J, Auqué L F, Wallin B, Brüchert B V, Jönsson S, Molinero J, 2010b. SR-Site: Sulphide content in the groundwater at Laxemar. SKB R-10-62, Svensk Kärnbränslehantering AB.

Viani B E, Bruton C J, 1996. Assessing the role of cation exchange in controlling groundwater chemistry during fliud mixing in fractured granite at Äspö, Sweden. Second Äspö International Geochemistry Workshop, Äspö, Sweden, June 6–7, 1995. Report UCRL-JC-121527, Lawrence Livermore National Laboratory.

Vidstrand P, Rhén I, Zugec N, 2010. Groundwater flow modelling of periods with periglacial and glacial climate conditions – Laxemar. SKB R-09-25, Svensk Kärnbränslehantering AB.

Vilks P, Miller H, Doern D C, 1991. Natural colloids and suspended particles in the Whiteshell Research area, Manitoba, Canada, and their potential effect on radiocolloid formation. Applied Geochemistry, 8, pp 565–574.

Waber H N, Smellie J A T, 2008. Characterisation of porewater in crystalline rocks. Applied Geochemistry, 23, pp 1834–1861.

Waber H N, Gimmi T, deHaller A, Smellie J A T, 2009. Porewater in the rock matrix. Site descriptive modelling, SDM-Site Laxemar. SKB R-08-112, Svensk Kärnbränslehantering AB.

Wallin B, 1995. Paleohydrological implications in the Baltic area and its relation to the groundwater at Äspö, south-eastern Sweden. A literature study. SKB TR 95-06, Svensk Kärnbränslehantering AB.

Wallin B, Peterman Z, 1999. Calcite fracture fillings as indicators of paleohydrology at Laxemar at the Äspö Hard Rock Laboratory, southern Sweden. Applied Geochemistry, 14, pp 953–962.

Wellsbury P, Parkes R J, 1995. Acetate bioavailability and turnover in a estuarine sediment. FEMS Microbiology Ecology, 17, pp 85–94.

Wellsbury P, Goodman K, Barth T, Cragg B A, Barnes S P, Parkes R J, 1997. Deep marine biosphere fuelled by increasing organic matter availability during burial and heating. Nature, 388, pp 573–576.

Wold S, 2010. Sorption of prioritized elements on montmorillonite colloids and their potential to transport radionuclides. SKB TR-10-20, Svensk Kärnbränslehantering AB.

Yang C, Samper J, Molinero J, Bonilla M, 2007. Modelling geochemical and microbial consumption of dissolved oxygen after backfilling a high level radioactive waste repository. Journal of Contaminant Hydrology, 93, pp 130–148.

Zhu C, Anderson G M, 2002. Environmental applications of geochemical modeling. Cambridge: Cambridge University Press.

Appendix 1

Example of the calculation procedure

In this section, the methodology used in the process of calculation has been synthesized. This methodology (and the associated programs) has been mainly developed by the University of Zaragoza and consists of:

- slice extraction from the hydrological data, using the program "Select data v4.exe",
- creation of the input files for PHREEQC with the selected data (mixing and mineral equilibrium),
- running PHREEQC,
- creation of the tabulated output, selecting key parameters, and
- statistical analysis and postprocessing.

A1.1 Slice extraction using the program "Select data.exe"

This program selects subsets of data points from the hydrogeological files. These subsets can be planes perpendicular to the X, Y or Z co-ordinate, vertical planes (Z-planes) with any orientation, or sets of points defined by a horizontal polygonal boundary. In each case, different options for their selection are available.

First, one of the input hydro files (corresponding to one site and one year) is selected. Then, the format of the hydro file (x y z + data, Serco-2009, Serco-2006, Serco-2004, Colenco, TerraSolve) is specified. Finally, the subset of data to extract ("Action to take", Figure A1-1) is chosen. Option "run" starts the program and creates a new file with the word "cut" added to the original name, containing the extracted subset of data points in a comma-separated format.

These files are the input files for all the geochemical calculations performed with PHREEQC.

The options for the slices (subsets of data points to be extracted) are described next.

A1.1.1 "Selection based on a X, Y or Z plane"

It creates slices based on coordinates N-S, E-W and depth. This option is used to extract the horizontal plane (Z-plane) at the repository depth. Figure A1-1 shows how to select a set of points in a specific interval (± 60 m for the temperate period case) at the repository depth (–500 in the case of Laxemar).

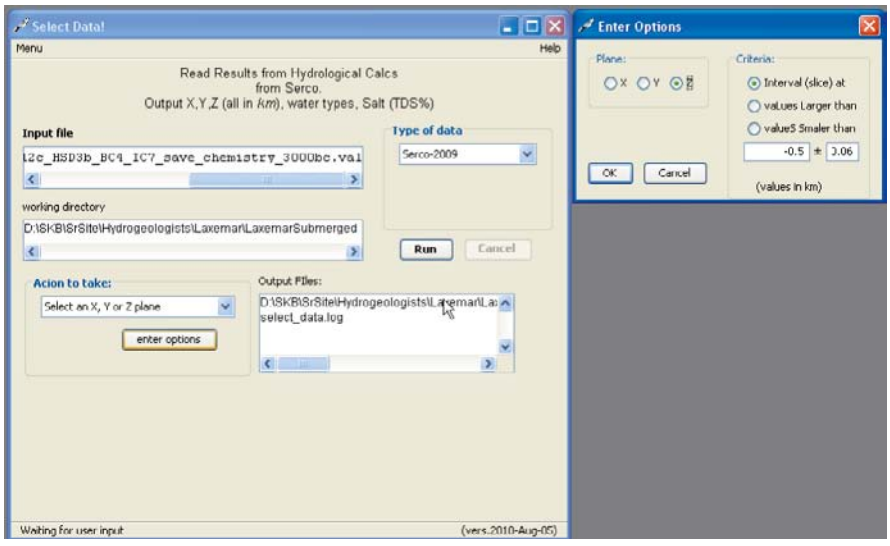

Figure A1-1. Example of the first window when running Select Data.exe for the selection of different types of subsets.

A1.1.2 “Use an X-Y boundary”

This option extracts all data points inside a specified closed horizontal boundary. It is very useful when the user wants to limit the set of points to those inside the repository volume. In this particular case (the one used for most of the calculations in the SR-Site base case) the procedure consists of two steps: (a) extraction of the slice at the desired depth (about 500 m for Laxemar); and (b) the slice just created is selected as the new input file (F_2000.470.val in the example shown in Figure A1-2), using “x y z + data” as Type of data and indicating the number of columns after the coordinates; then the option X-Y boundary is selected and the program asks for a file with the x-y coordinates of the boundary (Figure A1-2).

The boundary coordinates for the repository volume at Laxemar are

- 1,546.40, 6,367.62, –0.5
- 1,550.05, 6,367.62, –0.5
- 1,550.05, 6,365.00, –0.5
- 1,546.40, 6,365.00, –0.5

A1.1.3 “Select a vertical plane based on a line”

This option creates a vertical cross section at any user-defined orientation. It has been used to create vertical sections through the repository volume and parallel or perpendicular to the coast. Apart from asking for the coordinates of the plane, the program also asks for an error range (in meters) and if the user wants to have the data projected onto the extraction plane (to which one must say yes in this case). The vertical planes used in SR-Site for Laxemar are the followings:

- A NW-SE plane (Figures A1-3 and A1-4) roughly parallel to the coast through boreholes KLX13A, KLX18A, entrance to the repository, KLX12A and KLX05 (+-60): NW: 1,544,500 m / 6,370,000, SE: 1,551,500 m / 6,363,025 (see also Figure 3-3).
- An additional slice has also been selected to include the Simpevarp peninsula. It is W-E and goes through boreholes KLX20A, KLX11A, KLX18A, KLX10, KLX21B, KSH01 and KSG03. The coordinates are: W: 1,544,500 m / 6,366,500; E: 1,554,000 m / 6,366,000 (see also Figure 3-3).

When this option is used, apart from the data already contained in the hydrogeological file, the program adds an additional column with the distance along the line. This distance is used to plot the points instead of the X and Y coordinates.

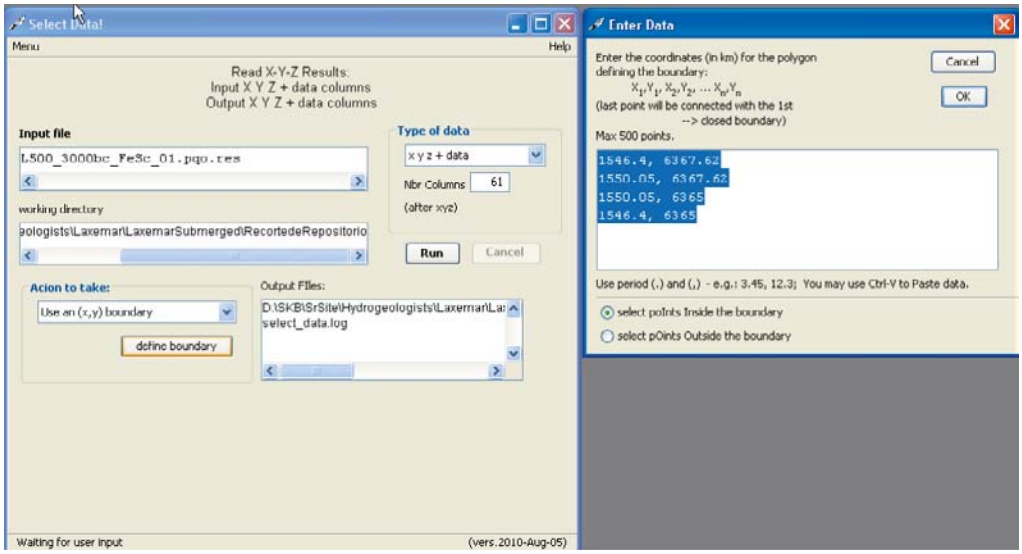

Figure A1-2. *Another example of the Select data program when the choice is an area inside a poligon. When clicking on “define boundary” the program opens the window on the right, and the coordinates of the vertices must be indicated there.*

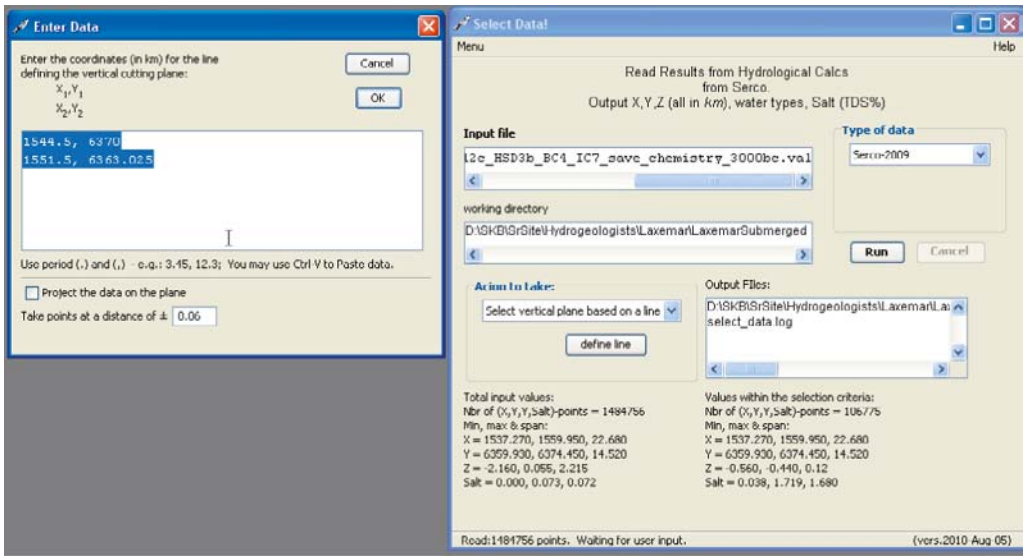

Figure A1-3. *Another example of the Select data program when the choice is a vertical plane. When clicking on "define line" the program opens the window on the left, and the coordinates of the line must be indicated there. In this case, the plane corresponds to the NW-SE vertical slice (see also Figure A1-4).*

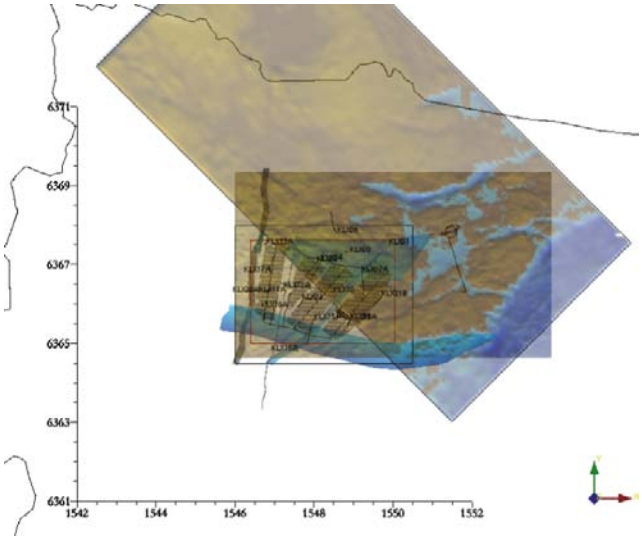

Figure A1-4. *Example of the area selected for Laxemar and the location of the vertical plane NWSE parallel to the coast.*

An additional question that should be taken into account when selecting vertical planes is that the hydrogeological results for the whole volume include points down to 2,500 m depth and the data used here are only those down to around 1,000 m. The rows corresponding to points below those depths can be removed later inside the specific plotting software (e.g. Origin).

A1.2 Salinity transformation into mixing proportions ("Salinity2Mixprop.exe")

In the case of Terrasolve results, they are expressed as salinities and as explained in Chapter 3 these subsets, with the salinity values for each data point, must be transformed in files with mixing proportions for each point. It is the only way to couple these results with the geochemical model PHREEQC using the software generated for the SR-Can. They will be used, as for the temperate period, to create input files for PHREEQC in order to obtain the detailed chemical composition at each point. So, the main difference with respect to the temperate period calculations is the transformation of salinities into mixing proportions.

The specific procedure is explained below. Run the program "Salinity2Mixprop.exe":

1. The program first asks whether the file to be transformed corresponds to the first time slice or not:
   First time slice (y/n)?

If the answer is YES (y) the program will calculate the mixing proportions based only on the salinity values at that time (t = 0).

2. Then it asks for the name of the file with the slice extracted from the hydro files:
   Hydro-data file name (< 40 characters)?
   Eg: .....V0F_sal_0_vert.txt
3. Next it asks for the number of columns with coordinates. This number is 3 for horizontal slices and 4 for vertical slices (with the distance along the projection line added as a new column, see above).
   Number of columns with co-ordinates
   Enter the number 3 or 4 (4 in the example as it is a vertical plane)
4. The program then echoes a message with the number of samples read from the hydro file:
   E.g. 20672 samples read

and produces an output file with the mixing proportions in the points of the selected slice.

Eg: ..... V0F_sal_0_vert.txt.res

If the answer to the first question is NO (n), the program understands that the slice under calculation corresponds to a state (I, II, III, etc) different from the initial state (0), and then it proceeds to compare the salinity in the new state with the salinity in the previous time. Therefore, the program asks for the name of the file under calculation (time t):

Hydro-data file for time t (< 40 characters)?
Eg: ..... V1F_sal_I_vert.txt

And then, it asks for the name of the file with the mixing proportions obtained in the previous time period (time t-1):

Mixprop file for time t-1 (< 40 characters)?
Eg: ..... V0F_sal_0_vert.txt.res

The program then echoes a message with the number of samples read from both files (it must be the same; otherwise the program ends with an error message):

E.g. 20672 samples read

and produces an output file with the mixing proportions in the points of the selected slice.

Eg: ..... V1F_sal_I_vert.txt.res

Now these output files have the same structure as the files provided by the hydrogeologists with the CONNECTFLOW for the temperate period. Therefore, they can be used to create the input files for PHREEQC (pqi_mp.exe)[30]. The procedure to perform the PHREEQC calculations and select the output is the same already explained for the temperate case.

A1.3 Creation of the input file for PHREEQC

Once the different selected slices with the data expressed as mixing proportions have been generated, the following step is to transform these files into input files for PHREEQC. The still large number of points (i.e., water samples) on which PHREEQC calculations had to be performed, led to the development of simple interface programs for the automatic import and export of data. This software (developed in-house by the GMG, University of Zaragoza, for SR-Can and updated for SR-Site) accepts as input a hydro file with the mixing proportions and a file with the composition of the end-members to calculate the final chemical composition of the waters at each point. This interface program allows also the selection of the chemical processes that will be imposed to the waters.

[30] One must be aware of the format files containing the end members, as in these cases only three of them are used.

Two different types of simulations with PHREEQC can be considered: (1) mixing (including aqueous reactions), and (2) mixing and reaction (including equilibrium with minerals). In the case of the SR-Site calculations, only the second option will be applied. This type of simulation is a better approach to what is actually happening in the system as it considers the re-equilibration of groundwaters with specific minerals, as it has been found in the geochemical modelling of the SDM.

The program to create the corresponding PHREEQC input pqi file is "pqi_mp.exe":

1. The program requests the type of simulation (only mixing or mixing and reaction):

   Mixing (M) or mixing+reaction (R)?

   Enter "R" in this case

2. Then it asks for the name of the file containing the extracted slice from the hydro file:

   Hydro-data file name (< 40 characters)?

   e.g. "F_2000_Rep.dat"

3. Next it asks for the number of columns with coordinates. This number is 3 for horizontal slices and 4 for vertical slices (with the distance along the projection line added as a new column, see above)

   Number of columns with co-ordinates

   Enter the number 3 or 4

4. The program then echoes a message with the number of samples read from the hydro file:

   E.g. 35,762 samples read

5. The next question requests the user to define the maximum number of samples to be put onto each output file (preventing this way memory problems with too long PHREEQC output files).

   Maximum number of samples per output file

   The suitable number of samples depends also on the type of simulation to be done, as the more complex a simulation is (mixing + reaction + exchange) the bigger (in size) is the file created by PHREEQC. A rough estimation is around 25,000 samples for complex simulations, and around 50,000 samples for simple mixing-only calculations.

   E.g. 36,000.

6. The program then echoes the number of pqi files that will be created. For example, in the case shown here, the hydro file has 35,762 samples, so we select 36,000 as the maximum number of samples per file to get only one output file.

   Maximum number of samples per output file

   36,000

   Warning: 1 output files will be created

7. The above message is important as it gives the number of files corresponding to each simulation. Let call this number *k*.

8. Then, the program asks for the name of the file containing the chemical composition of the end members.

   End-member file name (< 40 characters)?

   At this point, one must be aware of the type of simulation that is being performed (coupled or uncoupled data base) and the site being analysed (Laxemar or Forsmark) because, as indicated above, there are four different end-member files.

9. Finally, the program asks for the format file in which, apart from the number and name of the end members in the same order as they appear in the hydro file, it contains the number and name of the phases to be considered when performing equilibrium reactions (which will be zero for only mixing) and the number of exchangers (zero in all these simulations). There are different format files depending on the simulation case.

   Format file name (< 40 characters)?

   For mixing and reaction simulations there are two different files, one with haematite "Formatpqi_ mr_ Hem.dat" and the other with the FeS(am) "Formatpqi_ mr_ FeS.dat", and their contents are similar to this one for the haematite set:

```
5 !Number of end members, followed by their names
"Brine" "Littorina" "Meteoric" "Glacial" "PoreWater"
3 !Number of phases for equilibrium calculations
"Calcite" 0 10
"Quartz" 0 10
"Hydroxyapatite" 0 10
"Fe(OH)3(hematite_grenthe)" 0 10
0 !Number of exchangers (for cation exchange)
```

5. After running, the program creates *k* output files with the initial part of the name identical to the hydro file and ending in "_01.pqi", "02_pqi", etc.

   E.g. L_2000_Rep.dat_01.pqi.

These files are then used as input to the batch version of PHREEQC (phreeqc_batch.exe).

As indicated above, if the mineral phases to be used as equilibrium phases are not included in the thermodynamic data base or they have a different thermodynamic value from the one considered suitable for the system under study (e.g., haematite or FeS(am)), these phases must be added by hand to the pqi files already created, For that purpose, the following lines should be added at the beginning of every input file:

```
PHASES
Fe(OH)3(haematite_grenthe)[31]
 Fe(OH)3 + 3 H+ = Fe+3 + 3 H2O
 log_k –1.1
FeS(ppt) 119
 FeS + H+ = Fe+2 + HS–
 log_k –3.00
```

"PHASES" is the keyword used by PHREEQC to do this.

There is an additional problem to be taken into account. When the uncoupled database is used the definition of the sulphide species is different and thus the definition of the thermodynamic data for FeS(ppt) must be different too. It will be as follows:

```
FeS(ppt) 119
 FeS_ + H+ = Fe+2 + HS_–
 log_k –3.00
```

In other words, the expression of the set of minerals added with this option will be different when using the coupled or the uncoupled thermodynamic database.

[31] The user must be aware of the name used here for the mineral phases as they will be used with the same name in the selected output.

As the version used here is a batch version and all the needed information is included in the pqi file, running PHREEQC is exactly the same for all the simulated cases. PHREEQC asks for the names of the input file, the output file, and the thermodynamic database file.

1. First it asks for the input file, which will be the one created with the pqi creator interface program ("pqi_mp.exe").
2. Then it asks for the name of the output file (usually the same name with the extension ".pqo").
3. Finally, it asks for the thermodynamic data base to be used for the calculations (for the mixing case we will use the coupled one).
4. Once the output file has been obtained, it will be passed through the selected output interface program to extract the desired information in a tabular form.

The mixing and chemical reaction simulations (Equilibrium_Phases option in PHREEQC) are used to equilibrate each water with an specific set of mineral phases. In this case the output file includes the detailed chemical composition of the groundwaters at each grid point and the amount of mass transfer for the equilibrated minerals.

The "TDB_SKB-2009_Amphos21.dat" database (and the equivalent uncoupled "TDB_SKB-2009_Amphos21_no_S-redox.dat") has been used to carry out the mixing and reaction simulations. As some of the mineral phases of interest are not included in the database, new phases (solubility for Fe-III oxyhydroxides, iron monosulphides and some aluminosilicates (kaolinite, albite and K-feldspar) were added to the pqi files as PHASES to be considered in the calculations. The detailed description of these phases and the reason for their selection can be found in /Auqué et al. 2006/.

A1.4 Creation of the tabulated output

The procedure is the same for *all* simulations but the interface program to be used and the format files (and obviously the problem files) are different. The dialogue with the interface program in all the cases is the following:

1. The user can chose whether to include or not the sample coordinates in the final table:

   Add coordinates to output file (y/n)?

2. And to include or not the mixing proportions:

   Add mixing proportions to output file (y/n)?

3. Then the program asks for the name of the PHREEQC output file ("F_year_cut_m.pqo").

   PHREEQC .pqo file name (< 20 characters)?

4. Next, it asks for the name of the format file with the information the user wants to extract from the complete pqo file (which will be different for each simulation):

   Input data file name (< 20 characters)?

   For the Mixing and Reaction case. Each of the four simulation cases has a different format file indicating the different minerals in the equilibrium set and the use of the coupled or uncoupled thermodynamic database: "formatsel_mr_Hemunc.dat", "formatsel_mr_FeSunc.dat", "formatsel_mr_Hemcoup.dat" and "formatsel_mr_FeScoup.dat".

   The contents of each format file are shown at the end of this Appendix, Section A1-6.

5. Files generated with the Selected Output interface program are in the form of tables with the extracted information in columns and the grid points in rows. They have the same name as the PHREEQC pqo file but ended in ".res". In the three simulation cases (mixing, mixing+reaction, mixing+reaction+exchange) these file contain information on the composition of the waters at each grid point. The columns in these files are:
   - X, Y, Z coordinates (the distance along the line calculated for the vertical plane is not stored here as it is not included in the PHREEQC output; therefore if the user wants to plot spatial distributions, this value must be calculated again using the following equation: $\text{Distance} = \sqrt{X^2 + Y^2}$
   - Mixing proportions of the end-member waters for each point: Deep Saline, Old Meteoric, Glacial, Littorina and Altered Meteoric.

- Mass transfers for the equilibrated minerals (only if equilibrium reactions are imposed).
- TDS.
- Molality of the elements included in the selected output's format file: result of mixing, or mixing and reaction or mixing, reaction and exchange (depending on the simulation).
- pH, pe, ionic strength total alkalinity, charge balance.
- Activity and molality of the selected species.
- Saturation indexes of the waters with respect to the selected mineral phases.

When a simulation case has been divided into several files (_01, _02, etc), the user must run the selected output interface program on each of them and then combine manually the output into a single file with the whole set of samples (for graphical purposes).

6. All these files have a tabular format and can be easily imported into other software packages for graphical purposes.

A1.5 Postprocessing

In the case of the repository domain calculations (data points within the candidate repository volume), the selected results have been treated with specific statistical analysis. In these cases, the post-processing will be performed by "Box-and-whisker plots", using ORIGIN, showing the statistical distribution of the chosen parameters. The statistical measures included are the median, the 25th and 75th percentile, the mean, the 5th and 95th percentile, the 1st and 99th percentile, and the maximum and the minimum values.

A1.6 Format files. Mixing and equilibrium reaction calculations

Some examples of each type of format file are shown here: the ones to create the input file for PHREEQC, and the ones to select the data from the output file created by PHREEQC The user must keep these files updated for each specific problem to be solved (different end members, different elements or minerals to be obtained, etc).

A1.6.1 Format files for the pqi_mp.exe program

Formatpqi_mr_Hem.dat

```
5     !Number of end members, followed by their names
"Brine" "Littorina" "Meteoric" "Glacial" "PoreWater"
3     !Number of phases for equilibrium calculations
"Calcite" 0 10
"Quartz" 0 10
"Hydroxyapatite" 0 10
"Fe(OH)3(haematite_grenthe)" 0 10
0     !Number of exchangers (for cation exchange)
```

Formatpqi_mr_FeS.dat

```
5     !Number of end members, followed by their names
"Brine" "Littorina" "Meteoric" "Glacial" "PoreWater"
3     !Number of phases for equilibrium calculations
"Calcite" 0 10
"Quartz" 0 10
"Hydroxyapatite" 0 10
«FeS(ppt)» 0 10
0     !Number of exchangers (for cation exchange)
"Hydroxyapatite" 0 10
```

A1.6.2 Format files for the selected output_batchreaction.exe program

formatsel_mr_Hemcoup.dat

```
5 !Number of end-members (ONLY if used in the pqo file)
Brine
Littorina
DGW
Glacial
PoreWater
1 !Compute TDS (Total Dissolved Solids)?
16 !Number of elements, followed by each element (as written in section
"Solution composition", in alphabetical order!)
C
Br
Ca
Al
Cl
F
Fe
K
Li
Mg
Mn
Na
P
S
Si
Sr
4 !Number of phases, followed by each phase (as written in section "Phase
assemblage",in alphabetical order!)
Calcite
Quartz
Fe(OH)3(hematite_grenthe)
Hydroxyapatite
!Write 1 for each paramater to be output (section "Description of solution")
1 !pH
1 !pe
0 !Activity of water
1 !Ionic strength
0 !Mass of water
1 !Total alkalinity
0 !Total CO2
0 !Temperature
0 !Electrical balance
1 !Percent error
0 !Iterations
0 !Total H
0 !Total O
10 !Number of species, followed by each species (as written in section
"Distribution of species")
HCO3-
Ca+2
Na+
K+
H+
Si(OH)4
Mg+2
Fe+2
HS-
```

```
H2S
9 !Number of SI, followed by each phase (as written in section "Saturation
indices")
Albita
CO2(g)
Feldespato_K
Caolinita_Grimaud
FeS(ppt)
Fe(OH)3(am)
Fe(OH)3(mic)
Gypsum
Celestite
```

formatsel_mr_Hemunc.dat

```
5 !Number of end-members (ONLY if used in the pqo file)
Brine
Littorina
DGW
Glacial
PoreWater
1 !Compute TDS (Total Dissolved Solids)?
17 !Number of elements, followed by each element (as written in section
"Solution composition", in alphabetical order!)
C
Br
Ca
Al
Cl
F
Fe
K
Li
Mg
Mn
Na
P
S
S_
Si
Sr
4 !Number of phases, followed by each phase (as written in section "Phase
assemblage",in alphabetical order!)
Calcite
Quartz
Fe(OH)3(hematite_grenthe)
Hydroxyapatite
!Write 1 for each paramater to be output (section "Description of solution")
1 !pH
1 !pe
0 !Activity of water
1 !Ionic strength
0 !Mass of water
1 !Total alkalinity
0 !Total CO2
0 !Temperature
0 !Electrical balance
1 !Percent error
0 !Iterations
```

```
0 !Total H
0 !Total O
8 !Number of species, followed by each species (as written in section
"Distribution of species")
HCO3-
Ca+2
Na+
K+
H+
Si(OH)4
Mg+2
Fe+2
9 !Number of SI, followed by each phase (as written in section "Saturation
indices")
Albita
CO2(g)
Feldespato_K
Caolinita_Grimaud
FeS(ppt)
Fe(OH)3(am)
Fe(OH)3(mic)
Gypsum
Celestite
```

formatsel_mr_FeScoup.dat

```
5 !Number of end-members (ONLY if used in the pqo file)
Brine
Littorina
DGW
Glacial
PoreWater
1 !Compute TDS (Total Dissolved Solids)?
16 !Number of elements, followed by each element (as written in section
"Solution composition", in alphabetical order!)
C
Br
Ca
Al
Cl
F
Fe
K
Li
Mg
Mn
Na
P
S
Si
Sr
4 !Number of phases, followed by each phase (as written in section "Phase
assemblage",in alphabetical order!)
Calcite
Quartz
FeS(ppt)
Hydroxyapatite
!Write 1 for each paramater to be output (section "Description of solution")
1 !pH
```

```
1 !pe
0 !Activity of water
1 !Ionic strength
0 !Mass of water
1 !Total alkalinity
0 !Total CO2
0 !Temperature
0 !Electrical balance
1 !Percent error
0 !Iterations
0 !Total H
0 !Total O
10 !Number of species, followed by each species (as written in section
"Distribution of species")
HCO3-
Ca+2
Na+
K+
H+
Si(OH)4
Mg+2
Fe+2
HS-
H2S
9 !Number of SI, followed by each phase (as written in section "Saturation
indices")
Albita
CO2(g)
Feldespato_K
Caolinita_Grimaud
Fe(OH)3(hematite_grenthe)
Fe(OH)3(am)
Fe(OH)3(mic)
Gypsum
Celestite
```

Appendix 2

Glacial Waters

The composition adopted for the Glacial end-member (used for mass balance and M3 calculations) in the site investigation programmes (Table A2-1) corresponds to present melt waters from one of the largest glaciers in Europe, the Josterdalsbreen in Norway, located on a crystalline granitic bedrock /Laaksoharju and Wallin 1997/. The major element composition of these waters is similar to the one estimated by /Pitkänen et al. 1999, 2004/ in a model study of Olkiluoto (Finland). These glacial melt waters represent the chemical composition of surface melt waters prior to the water-rock interaction processes undergone during their infiltration into the bedrock. They have a very low content of dissolved solids, even lower than present-day meteoric waters, a pH value of 5.8, and an isotopically light signature (Table A2-1).

To obtain the possible compositional characters of these waters after water-rock interaction processes (even in the first 100 m depth), groundwater samples having clear glacial signatures cannot be used because in the Forsmark and Laxemar areas the composition of groundwaters having glacial signatures has been drastically modified by mixing with waters of other origins (e.g. sample 1569 at Äspö, Table A2-1). Therefore, there are no "undisturbed" glacial melt water remnants that could be considered as a pure glacial component modified only by water-rock interaction processes.

Table A2-1. Chemical composition of the glacial end-members used in the Swedish /Laaksoharju and Wallin 1997/ and Finnish /Pitkänen et al. 1999, 2004/ site characterization programs. The composition of a present meteoric water with very low residence time together with one of the real samples with a clear glacial signature (Äspö groundwater, sample 1569), are also shown. Concentrations in mg/L.

	Glacial end-member (Sweden)	Glacial end-member (Finland)	Meteoric water (HBH02, #1931)	Äspö (KAS03, #1569 at 129-134m depth)
(ºC)		1.0	16	10.2
pH	5.8	5.8	6.8	8.0
Eh (mV)	—	—	—	–280
Alkalinity	0.12	0.16	63.0	61
Cl	0.5	0.7	5.0	1,220.0
SO_4^{2-}	0.5	0.05	13.2	31.1
Ca	0.18	0.13	15.4	162
Mg	0.1	0.1	1.9	21.0
Na	0.17	0.15	11.5	613.0
K	0.4	0.15	2.3	2.4
Si	—	0.005	3.4	4.9
δ^2H (‰)	–158.0	–166.0	–77.1	–124.8
$\delta^{18}O$ (‰)	–21.0	–22.0	–10.2	–15.8

Nevertheless, the effect and extent of the expected water-rock interaction processes during the infiltration of glacial melt waters may be inferred from the study of waters in other zones not affected by mixing. The review performed by /Gimeno et al. 2008, 2009/ on the available data from the SKB site characterisation program has identified groundwaters of glacial or meteoric origin (but with high residence times) and corresponding to climates colder than at present (Table A2-2). Despite the fact that many of the sites studied in the Swedish program lack representative hydrochemical data (e.g. because of contamination with drilling water and/or other groundwaters), some indications of ancient glacial melt water are apparent. For example, groundwaters below 500 m depth in Fjällveden seem to be residual melt waters or alternatively meteoric waters from a colder climate /Wallin 1995, Tullborg 1997/. A glacial origin for these groundwaters is suggested in the work of /Bath 2005/ where "apparent" ^{14}C ages of around 12,000 to 14,000 years (i.e. late-glacial) are reported. At Gideå, there seems to be an indication of mixing between meteoric and post-glacial melt waters /Wallin 1995/. Finally, groundwaters in Lansjärv also show the isotopically light signature ($\delta^2H = –109.3‰$ and $\delta^{18}O = –13.8‰$) typical of glacial or old meteoric waters from colder climates.

Table A2-2. Compositional data for different groundwaters from a glacial infiltration or simply cold waters in different zones in Sweden and Switzerland. pH and Eh data in the Swedish sites have been obtained from the continuous logging with Chemmac (only pH data in bold and italics correspond to values determined in laboratory). Chemical contents in mg/L. Taken from /Gimeno et al. 2008/.

	Fjallveden[1]		Gidea[2]	Lansjärv	Svartboberget		Switzerland
	KFJ02 (#267)	KFJ07 (#372)	KGI04 (#194)	KLJ01 (#1410)	KSV04 (#116)	KSV04 (#122)	GTS [3]
Depth (m)	605–607	542–544	404–406	237–500	430–436	630 –633	450
T (ºC)	—	—	—	—	—	—	12
pH	8.9	9.2	9.3	9.2	9.1	9.1	9.6
Eh (mV)	—	–200	–200	—	–75	–150	–171
Alk.	83.0	150.0	18	44.0	130.0	126.0	17.1
Cl	170.0	3.0	178	0.8	8.0	7.0	4.96
SO_4^{2-}	0.2	bdl.	0.1	4.4	1.2	0.8	5.8
Ca	12.0	10.0	21.0	7.7	17.0	17.0	6.61
Mg	0.8	2.0	1.1	1.2	2.0	1.9	0.05
Na	130.0	46	105.0	11.3	35.0	35.0	16.1
K	1.0	3.6	1.9	1.52	0.9	0.7	0.14
Si	4.3	n.a.	4.7	3.7	4.3	6.8	5.6
Fe	0.34	0.51	0.07	0.01	0.25	0.27	0.06
δ^2H (‰)	–102.9	—	–99.4	–109.6	–95.0	–95.4	—
$\delta^{18}O$ (‰)	–14.11	—	–13.63	–13.80	–13.0	–13.1	—

(1) /Wallin 1995, Tullborg 1997, Bath 2005/; (2) /Wallin 1995/; (3) Grimsel Test Site (Switzerland; /Degueldre 1994/).

Compared with the original composition of glacial melt waters (compare values in Table A2-1 and Table A2-2), all the Swedish waters have a more alkaline pH (around 9) and higher TDS values as a consequence of water-rock interaction. The differences are of orders of magnitude, especially for chloride, sodium and alkalinity. However, the final salt contents are still very low in absolute terms, even taking into account potential contamination. This means that, as expected, water-rock interaction modifies the overall compositional characteristics in a quite limited scale but pH values are clearly increased.

Similar conclusions have been obtained when analysing other cold meteoric and glacial waters in crystalline basements. For example, groundwaters from a meteoric origin at 450 m depth in the crystalline rocks of the Grimsel Test Site (Switzerland) are also alkaline, with pH = 9.6, and very dilute /Degueldre et al. 1996/ similar to the ones observed in the Swedish groundwaters (Table A2-2).

The required time to reach these alkaline characters might not be so long as suggested by the residence time of the examined groundwaters. The presence of geochemically-reactive minerals like calcite, even at the trace amounts found in many crystalline systems exert an important control in the compositional evolution of glacial melt waters /Brown 2002, Mitchell and Brown 2007/. This control is dominant in environments out of contact with the atmospheric CO_2 and where other sources of acidity (e.g. pyrite dissolution) are limited (calcite is one of the most abundant minerals at all depths in the fracture fillings of Forsmark and Laxemar, whereas pyrite is much more scarce and evenly distributed; /Drake and Tullborg 2009/), as it occurs during the infiltration of melt waters in the bedrock).

For example, if the Swedish Glacial end-member presented in Table A2-1 dissolves 2.2 mg/L of calcite it would reach a saturation index value of –2.0 (a high undersaturated state) but the pH would be of 9.0. If the amount of calcite dissolved is 4.6 mg/L, the S.I. would be of –1.0 (still a clearly undersaturated situation) but the pH would reach a value of 9.61. The participation of other feasible minerals considered in this evolution (e.g. equilibrium respect to kaolinite and microcrystalline iron oxyhidroxides; see /Auqué et al. 2006/ does not change significantly the obtained results. For instance, the Swedish Glacial end-member equilibrated with kaolinite, microcrystalline iron oxyhidroxide and with calcite at a S.I. value of –2.0 would reach a pH value of 8.81 (dissolving

3 mg/L of calcite); and if the calculation is performed considering a S.I. value for calcite of –1.0, the final pH value would be of 9.3 (dissolving 6.7 mg/L of calcite). This last situation corresponds to the Glacial end-member composition used in the simulations performed in SR-Can (Auqué et al. 2006/ and SR-Site. /Salas et al. 2010/.

Minor amounts of calcite dissolution (even far from equilibrium conditions) could promote clearly alkaline conditions and, thus, this situation can be reached soon during the infiltration of glacial waters in the bedrock. Studies performed at present on the subglacial waters at the ice-bedrock interface in the Haut Glacier d'Arolla in Switzerland (developed on crystalline rocks with disseminated calcite; /Brown et al. 1996, Brown 2002, Tranter et al. 2002/ indicate that despite the existence of an atmospheric CO_2 contribution to the acidity of these waters or the presence of reactive sulphides, the measured pH values range from 7 to 9.1. These values support the ability of the calcite interaction to promote the alkaline conditions in the glacial melt water quite soon during its infiltration.

Thus, a range of pH values between 9.0 and 9.3 can be proposed for the infiltrated glacial melt waters in the bedrock from analytical data of glacial groundwater samples (Table A2-2) and geochemical modelling reasoning.

Appendix 3

Sensitivity analysis to cation exchange processes

Cation exchange reactions are fast and can exert an important control on the major cationic composition of the groundwaters (/Drever 1997, Appelo and Postma 2005, Andersen et al. 2005/ and references therein). These reactions may be especially activate during the periods of mixing (concentration or dilution) as the total dissolved solids or salinity of the solution exerts a major control on the intensity and selectivity of the exchangers for the different cations (e.g. /Appelo and Postma 2005/).

The effects of cation exchange processes on the groundwater evolution have been taken into account since the first steps in the Site Characterization Programs. Their importance in the hydrochemical evolution in Laxemar and Forsmak has been carefully evaluated in /Gimeno et al. 2008, 2009/. But cation exchange processes have not been included quantitatively in the calculations for SR-Site because the methodology is under development and testing. A proposed methodology and the results of some scoping calculations are given in this appendix.

A3.1 Methodological approach

A3.1.1 Conceptual model and procedure

Cation exchange reactions were already implemented in SR-Can simulations as a geochemical variant case /Auqué et al. 2006/. The conceptual model assumed the presence of a unique type of exchanger (i.e., the same composition for all the grid points in the whole volume and for all the time slices), whose composition was in equilibrium with the waters with the longest residence time, the Deep Saline end member.

The model proposed for SR-Site has been improved by assuming the composition of the exchanger to be in equilibrium with the water at each grid point for the first time slice. Then, each exchanger is transferred to the next time slice, and the new mixed water is equilibrated at each grid point with that exchanger, modifying not only the final water composition but also the exchanger composition.

In short, the procedure to create the input and files for PHREEQC, has to take into account the files containing the exchangers composition and the reaction of waters with them at each grid point. Although changes in the exchanger are transferred from one time slice to the next, changes in water composition are not transferred to the following time slice as they are taken from the hydrogeological model (only mixing). However, these results were compared with some calculations made considering the change in water compositions and the differences found between the final values were lower than 1%.

A3.1.2 Cation exchange capacity and composition of the exchange complex

To properly include cation-exchange reactions in the simulations it would be necessary to know the cation exchange capacity (CEC) of the clay minerals in the fracture fillings and the composition of the exchange complex. Available CEC values for fracture filling minerals (a basic parameter for this type of simulations) are very scarce and uncertain /Selnert et al. 2008/. However, several indirect estimates are available, (mainly deduced from cation exchange modelling in Äspö) and the exchange complex compositions can be calculated.

/Viani and Bruton 1996/ estimated an exchange capacity of 0.1 molc/L for Äspö fracture minerals. /Molinero 2000/ and /Molinero and Samper 2006/ deduced a CEC value of 0.6 molc/L as the best fit for the reactive transport simulations performed in the Äspö redox zone. Finally /Gimeno et al. 2009/ deduced values between 0.1 and 0.5 molc/L for the Laxemar groundwaters. Thus, a value of 0.5 molc/L has been selected for these scoping calculations.

The composition of the exchangers has been calculated with PHREEQC assuming equilibrium between a generic exchanger and the selected groundwaters at repository depth. The Gaines-Thomas convention /Gaines and Thomas 1953/ has been used together with the selectivity coefficients proposed by /Appelo and Postma 1993, 2005/, both included in the WATEQ4F database /Ball and Nordstrom 2001/ distributed with PHREEQC.

A3.2 Scoping calculations

The performed calculations have been done over the repository volume for the temperate period and using the three different geochemical variant cases: equilibrium with haematite using the coupled and the uncoupled data base (cases 1 and 3, respectively) and equilibrium with FeS(am) (and the coupled database). Then, these results are compared with the ones shown in this work (Chapter 4) which do not consider the possible cation exchange reactions.

As stated above, these calculations have only been done using the WATEQ4F data base (widely used to deal with exchange processes and previously used in the SR-Can exercise) as the SKB data base is not prepared for this type of simulations.

Calculations start from year 2020 waters and assuming the composition of the exchanger in equilibrium with them at each grid point (with a common value of 0.5 mol/L exchange capacity). Then, the composition of the exchanger at each point is used for the next time slice to equilibrate the waters obtained by the hydrogeologists. So the waters for the new stage will be the result of mixing, equilibrium with the selected minerals and cation exchange reaction. Therefore, the first year with results considering the cation exchange is the year 10,000 AD, which will be the one shown in the plots below as an example.

A3.3 Results

As will be shown next, both for redox and non-redox parameters, the inclusion of cation exhange processes in the simulations affects, in different degree, the obtained results. The main conclusions extracted for the comparison between the values obtained considering exchange or not (Figures A3-1 and A3-2) are the following:

- Ionic strength is not effected.
- Anions such as sulphate and chloride are not effected at all, and alkalinity only slightly.
- Cation exchange directly affects (in more or less extent) Ca, Mg, Na, K, Sr, Mn and Fe(II) contents. In general:
  - Ca, Mg, K, Mn, Fe(II) tend to enter the exchanger, i.e., their content in waters are lower when cation exchange is imposed.
  - Na, K tend to exit the exchanger, and therefore, their content in waters are higher than when only equilibrium reactions are considered.

Calcium tends to enter the exchanger and therefore its content in waters is lower when cation exchange is imposed. However, there is some specific behaviour depending on the total concentration of this cation in the groundwaters. For waters with high concentration of calcium, the effect is negligible (as expected because they are controlled mainly by mixing; see /Gimeno et al. 2009/ for further details); for those with intermediate contents, Ca tends to enter the exchanger, and for dilute waters with very low Ca contents it tends to exit the exchanger, becoming enriched in the waters. Sodium behaviour is just opposite to calcium (see Figures A3-1 and A3-2).

With respect to the redox components, Fe(II) tends to enter the exchanger and, therefore, its content in waters is lower when cation exchange is imposed (except in the case of equilibrium with haematite and the coupled TDB). Indirectly these effects are propagated to pH, Eh and S(-II), and also to the saturation indexes of the redox minerals (haematite and FeS(am)).

Eh mean values when exchange is active are higher when equilibrium with haematite is imposed and slightly lower when equilibrium with FeS(am) is imposed. However, in most cases variations can be considered smaller than the uncertainty range of ± 50 mV. Only when equilibrium with haematite and the un-coupled data base are used (case 3), the values obtained with exchange are clearly less reducing than when only mixing or equilibrium reactions are imposed. For S(-II), apart from the differences obtained when using the different geochemical cases, exchange also produces some indirect effects. For case 1, S(-II) contents are lower in solution while for case 2, there is a clear S(-II) enrichment in waters.

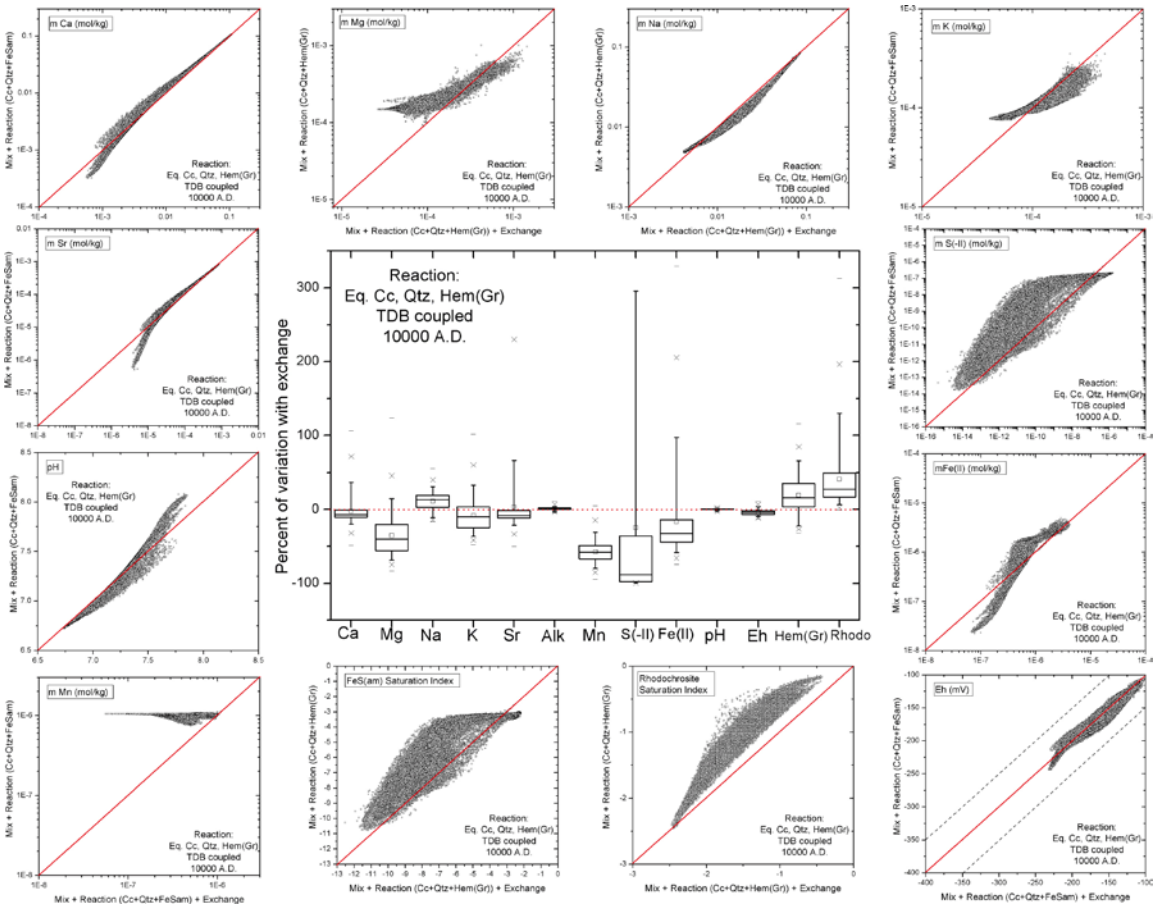

Figure A3-1. *Comparison of the results obtained in mixing and reaction simulations considering equilibrium with calcite, quartz, hydroxyapatite and haematite (Case 1) with and without cation exchange, for the year 10,000 AD (temperate) at Laxemar. X axes indicate the results corresponding to the simulations considering cation exchange processes, and axes Y those obtained not considering these processes. Graph in the middle of the plot show the percent of variation for each parameter when exchange processes are included in the simulations.*

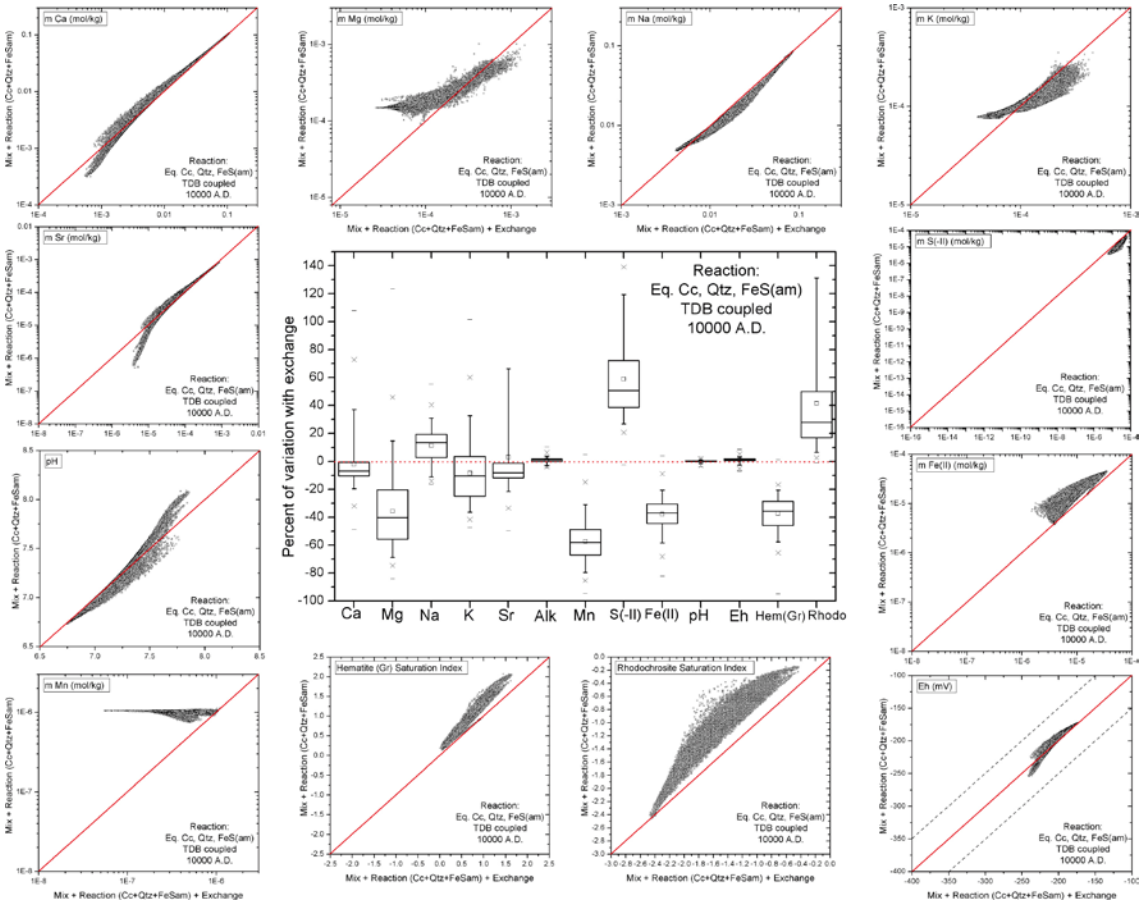

Figure A3-2. *Comparison of the results obtained in mixing and reaction simulations considering equilibrium with calcite, quartz, hydroxyapatite and FeS(am) (Case 2) with and without cation exchange, for the year 10,000 AD (temperate) at Laxemar. X axes indicate the results corresponding to the simulations considering cation exchange processes, and axes Y those obtained not considering these processes. Graph in the middle of the plot show the percent of variation for each parameter when exchange processes are included in the simulations.*

A3.4 Discussion and conclusions

The examples shown here reproduce the known effects of heterovalent exchange reactions[32] during increasing or decreasing salinity periods. During saline intrusion (e.g. marine waters, upconing processes) into more dilute groundwaters, monovalent cations (mainly Na^+) are selectively fixed to the exchangers whereas divalent cations (Ca^{2+} and Mg^{2+}) are released to the solution. The reverse process takes place during freshening (dilution). These trends have been widely observed in natural systems and in laboratory experiments, irrespective of the type of exchangers present in the systems (/Drever 1997, Appelo and Postma 2005/ and references therein).

The hydrochemical evolution during the temperate period represents a generalized dilution of groundwaters due to the increment of meteoric groundwateres with time. The overall results obtained are consistent with this picture and divalent cations (e,g, calcium, magnesium) tend to enter the exchanger and therefore its content in waters is lower when cation exchange is imposed.

These observations allow to advance that cation exchange will favour the same trends in non-redox cations during the periods when more diluted groundwaters dominate represented by the glacial melt-water intrusions during the glacial period (in agreement with the detailed simulations performed by /Gimeno et al. 2008/).

These scoping simulations have been useful to find that even the redox parameters can be, directly or indirectly, affected by cation exchange processes and this merits further studies as these processes have usually been neglected in the quantitative study of redox processes in the sites.

These preliminary results do not change the overall picture presented in this report for the temperate period. It must be remembered that the CEC value used in the simulations is the maximum one deduced in the literature and the net effects of cation exchange processes strongly depends of this value. However, the quantitative effect of these processes over the main master variables may be important (unless the CEC of the fracture fillings are very low) and they should be considered in future assessments, at least, as additional variant cases. The need for precise CEC data is also emphasised. And when more data on CEC become available and the SKB thermodynamic data base is upgraded (and verified) for the simulation of this type of processes, their inclusion in the PA calculation would be straightforward as the methodology is ready.

[32] These effects mainly depend on the stoichiometry of heterovalent exchange reactions (or the exponents used in the corresponding mass action equations) and, therefore, they minimize the uncertainties associated to the absence of site-specific selectivity constants or that associated to the formal convention (e.g. Gapon, Vanselow or Gaines-Thomas conventions; /Appelo and Postma 2005/) used to model exchange reactions.

Appendix 4

Tables with the statistical results

This appendix lists the statistical results obtained for the main geochemical parameters for all the periods simulated over a complete glacial cycle. The results obtained for all the geochemical variant cases are included here. In all the cases, these result correspond to the grid points inside the repository volume. In the case of the temperate period, the results obtained for a vertical section parallel to the coast cross-cutting the repository volume, are also included as these values have been used for comparison with the data measured in the real system.

Table A4-1. Statistical results for the main geochemical parameters obtained with the Base Case geochemical simluation over the temperate period in the repository volume. Chemical components in mol/kg, TDS in mg/L, pH in standard units and Eh in mV. Columns in red indicate the values taken from the geochemical variant Cases 1 and 2 together (Bace Case for the redox parameters).

2000 AD BaseCase: Hem coup (black numbers), Hem coup + FeS coup (red numbers)																		
	pH	Eh(HemC+FeSc)	TDS(mg/l)	IonicStr	mNa	mK	mCa	mMg	Fe(II) (HemC+FeSc)	mC	AlkTot	mCl	mS(VI)	S(-II) (HemC+FeSc)	mSi	mP	Na+K+2Mg+2Ca
N total (samples)	35762	71524	35762	35762	35762	35762	35762	35762	71524	35762	35762	35762	35762	71524	35762	35762	35762
Mean	7.02	-177.47	5547.79	1.27E-01	3.10E-02	1.25E-04	3.15E-02	2.16E-04	1.22E-05	2.33E-03	1.97E-03	9.18E-02	1.17E-03	1.28E-05	1.30E-04	1.41E-06	9.46E-02
Standard Deviation	0.22	33.31	4027.88	9.58E-02	2.04E-02	5.72E-05	2.51E-02	2.54E-04	1.15E-05	1.00E-03	8.73E-04	7.12E-02	6.23E-04	1.38E-05	2.97E-06	8.84E-07	7.04E-02
Minimum	6.77	-272.23	507.62	7.49E-03	5.03E-03	7.41E-05	5.27E-04	2.78E-05	7.02E-08	5.61E-05	8.20E-05	1.57E-03	3.79E-04	8.29E-16	1.22E-04	4.23E-09	6.45E-03
P0.1	6.79	-265.28	539.84	8.21E-03	5.22E-03	7.47E-05	7.11E-04	3.58E-05	1.08E-07	6.69E-05	9.04E-05	2.24E-03	3.85E-04	2.35E-15	1.23E-04	5.57E-09	7.01E-03
P5	6.83	-225.32	884.65	1.62E-02	7.05E-03	7.67E-05	2.78E-03	5.85E-05	1.13E-06	4.18E-04	4.11E-04	8.89E-03	4.39E-04	1.31E-14	1.25E-04	8.37E-08	1.30E-02
Median	6.95	-190.72	4505.44	1.02E-01	2.59E-02	1.07E-04	2.49E-02	1.39E-04	6.47E-06	2.47E-03	2.01E-03	7.34E-02	1.02E-03	3.43E-06	1.31E-04	1.37E-06	7.63E-02
P95	7.50	-123.41	14030.54	3.28E-01	7.37E-02	2.42E-04	8.44E-02	8.20E-04	3.04E-05	3.79E-03	3.43E-03	2.41E-01	2.45E-03	3.40E-05	1.34E-04	2.98E-06	2.43E-01
P99.9	8.06	-114.63	18249.13	4.31E-01	9.20E-02	4.32E-04	1.12E-01	1.80E-03	3.40E-05	4.17E-03	4.04E-03	3.16E-01	3.08E-03	3.81E-05	1.35E-04	4.04E-06	3.17E-01
Maximum	8.14	-109.44	19602.43	4.63E-01	9.81E-02	5.50E-04	1.21E-01	2.36E-03	3.62E-05	4.24E-03	4.15E-03	3.39E-01	3.28E-03	4.06E-05	1.36E-04	4.38E-06	3.40E-01
5000 AD BaseCase: Hem coup (black numbers), Hem coup + FeS coup (red numbers)																		
	pH	Eh(HemC+FeSc)	TDS(mg/l)	IonicStr	mNa	mK	mCa	mMg	Fe(II) (HemC+FeSc)	mC	AlkTot	mCl	mS(VI)	S(-II) (HemC+FeSc)	mSi	mP	Na+K+2Mg+2Ca
N total (samples)	35762	71524	35762	35762	35762	35762	35762	35762	71524	35762	35762	35762	35762	71524	35762	35762	35762
Mean	7.05	-180.12	4092.13	9.20E-02	2.36E-02	1.05E-04	2.25E-02	1.62E-04	1.10E-05	2.76E-03	2.36E-03	6.59E-02	9.58E-04	1.19E-05	1.32E-04	1.83E-06	6.90E-02
Standard Deviation	0.23	33.54	3546.47	8.42E-02	1.79E-02	3.15E-05	2.21E-02	9.65E-05	1.10E-05	9.40E-04	8.72E-04	6.28E-02	5.51E-04	1.31E-05	2.76E-06	9.40E-07	6.20E-02
Minimum	6.76	-272.00	487.57	7.03E-03	4.92E-03	7.53E-05	4.05E-04	2.82E-05	5.28E-08	5.73E-05	8.30E-05	1.14E-03	3.76E-04	5.53E-16	1.21E-04	4.38E-09	6.10E-03
P0.1	6.79	-260.60	509.21	7.51E-03	5.05E-03	7.56E-05	5.29E-04	3.84E-05	9.21E-08	7.45E-05	9.69E-05	1.59E-03	3.81E-04	2.45E-15	1.22E-04	6.63E-09	6.47E-03
P5	6.84	-228.63	686.74	1.15E-02	6.06E-03	7.65E-05	1.54E-03	7.39E-05	7.55E-07	8.54E-04	7.74E-04	5.05E-03	4.12E-04	1.47E-14	1.26E-04	2.47E-07	9.54E-03
Median	6.97	-191.81	2914.75	6.39E-02	1.77E-02	9.42E-05	1.51E-02	1.42E-04	4.11E-06	2.95E-03	2.41E-03	4.53E-02	7.80E-04	2.89E-06	1.32E-04	1.85E-06	4.84E-02
P95	7.56	-124.20	12110.77	2.83E-01	6.38E-02	1.73E-04	7.24E-02	3.62E-04	2.97E-05	4.00E-03	3.75E-03	2.08E-01	2.18E-03	3.32E-05	1.35E-04	3.42E-06	2.09E-01
P99.9	8.02	-115.65	17619.82	4.16E-01	8.94E-02	2.65E-04	1.08E-01	8.21E-04	3.42E-05	4.24E-03	4.15E-03	3.05E-01	3.09E-03	3.84E-05	1.36E-04	4.38E-06	3.06E-01
Maximum	8.13	-107.39	19356.33	4.57E-01	9.71E-02	3.23E-04	1.19E-01	1.18E-03	3.61E-05	4.29E-03	4.23E-03	3.35E-01	3.32E-03	4.05E-05	1.36E-04	4.70E-06	3.36E-01
10000 AD BaseCase: Hem coup (black numbers), Hem coup + FeS coup (red numbers)																		
	pH	Eh(HemC+FeSc)	TDS(mg/l)	IonicStr	mNa	mK	mCa	mMg	Fe(II) (HemC+FeSc)	mC	AlkTot	mCl	mS(VI)	S(-II) (HemC+FeSc)	mSi	mP	Na+K+2Mg+2Ca
N total (samples)	35762	71524	35762	35762	35762	35762	35762	35762	71524	35762	35762	35762	35762	71524	35762	35762	35762
Mean	7.14	-188.41	2895.09	6.35E-02	1.76E-02	9.36E-05	1.50E-02	1.47E-04	9.35E-06	3.16E-03	2.76E-03	4.46E-02	7.90E-04	1.03E-05	1.33E-04	2.29E-06	4.81E-02
Standard Deviation	0.28	34.73	2917.00	6.91E-02	1.49E-02	2.16E-05	1.80E-02	4.07E-05	1.00E-05	8.40E-04	8.48E-04	5.17E-02	4.73E-04	1.20E-05	2.42E-06	9.87E-07	5.09E-02
Minimum	6.78	-270.69	474.83	6.75E-03	4.85E-03	7.57E-05	3.31E-04	3.18E-05	3.70E-08	6.32E-05	8.78E-05	8.64E-04	3.74E-04	1.01E-15	1.21E-04	5.19E-09	5.88E-03
P0.1	6.80	-261.12	486.05	7.00E-03	4.92E-03	7.59E-05	3.87E-04	4.34E-05	5.28E-08	9.06E-05	1.09E-04	1.10E-03	3.77E-04	2.04E-15	1.23E-04	8.97E-09	6.07E-03
P5	6.85	-239.86	561.74	8.68E-03	5.37E-03	7.63E-05	8.08E-04	9.34E-05	3.13E-07	1.46E-03	1.23E-03	2.62E-03	3.92E-04	2.03E-14	1.27E-04	5.76E-07	7.37E-03
Median	7.05	-195.17	1818.40	3.78E-02	1.22E-02	8.53E-05	8.34E-03	1.44E-04	2.96E-06	3.34E-03	2.81E-03	2.57E-02	6.21E-04	2.68E-06	1.33E-04	2.31E-06	2.92E-02
P95	7.74	-125.63	9440.79	2.19E-01	5.07E-02	1.43E-04	5.56E-02	2.22E-04	2.90E-05	4.17E-03	4.02E-03	1.61E-01	1.83E-03	3.25E-05	1.35E-04	3.96E-06	1.63E-01
P99.9	8.02	-115.03	16440.41	3.85E-01	8.50E-02	1.91E-04	1.00E-01	4.28E-04	3.29E-05	4.30E-03	4.24E-03	2.84E-01	3.07E-03	3.67E-05	1.36E-04	4.76E-06	2.85E-01
Maximum	8.12	-111.66	18358.71	4.33E-01	9.30E-02	2.08E-04	1.13E-01	6.22E-04	3.44E-05	4.32E-03	4.28E-03	3.18E-01	3.36E-03	3.87E-05	1.36E-04	4.98E-06	3.19E-01
15000 AD BaseCase: Hem coup (black numbers), Hem coup + FeS coup (red numbers)																		
	pH	Eh(HemC+FeSc)	TDS(mg/l)	IonicStr	mNa	mK	mCa	mMg	Fe(II) (HemC+FeSc)	mC	AlkTot	mCl	mS(VI)	S(-II) (HemC+FeSc)	mSi	mP	Na+K+2Mg+2Ca
N total (samples)	35762	71524	35762	35762	35762	35762	35762	35762	71524	35762	35762	35762	35762	71524	35762	35762	35762
Mean	7.23	-196.52	2227.38	4.76E-02	1.42E-02	8.82E-05	1.09E-02	1.44E-04	8.03E-06	3.40E-03	3.03E-03	3.26E-02	6.94E-04	9.08E-06	1.33E-04	2.63E-06	3.64E-02
Standard Deviation	0.32	35.27	2420.73	5.72E-02	1.25E-02	1.68E-05	1.49E-02	2.35E-05	9.16E-06	7.51E-04	8.11E-04	4.30E-02	4.09E-04	1.09E-05	2.12E-06	1.01E-06	4.22E-02
Minimum	6.80	-268.47	470.19	6.65E-03	4.82E-03	7.59E-05	3.04E-04	4.14E-05	3.19E-08	6.84E-05	9.19E-05	7.63E-04	3.73E-04	9.83E-16	1.22E-04	5.87E-09	5.80E-03
P0.1	6.81	-264.71	475.44	6.76E-03	4.85E-03	7.60E-05	3.31E-04	5.13E-05	3.90E-08	1.07E-04	1.23E-04	8.73E-04	3.75E-04	1.83E-15	1.24E-04	1.21E-08	5.89E-03
P5	6.85	-248.01	516.84	7.67E-03	5.11E-03	7.62E-05	5.56E-04	1.07E-04	1.57E-07	1.91E-03	1.57E-03	1.72E-03	3.84E-04	2.82E-14	1.29E-04	8.96E-07	6.60E-03
Median	7.15	-200.93	1324.01	2.62E-02	9.62E-03	8.16E-05	5.27E-03	1.46E-04	2.52E-06	3.57E-03	3.10E-03	1.67E-02	5.43E-04	2.60E-06	1.34E-04	2.63E-06	2.06E-02
P95	7.87	-126.83	7413.85	1.70E-01	4.09E-02	1.26E-04	4.28E-02	1.81E-04	2.80E-05	4.24E-03	4.15E-03	1.25E-01	1.56E-03	3.15E-05	1.35E-04	4.34E-06	1.27E-01
P99.9	8.07	-114.46	15239.85	3.56E-01	7.99E-02	1.75E-04	9.20E-02	2.96E-04	3.28E-05	4.32E-03	4.28E-03	2.62E-01	3.00E-03	3.67E-05	1.36E-04	4.98E-06	2.64E-01
Maximum	8.11	-111.72	17559.96	4.13E-01	8.98E-02	1.94E-04	1.07E-01	3.88E-04	3.38E-05	4.33E-03	4.30E-03	3.04E-01	3.35E-03	3.78E-05	1.36E-04	5.10E-06	3.04E-01

Table A4-2. Statistical results for the main geochemical parameters obtained with the geochemical variant case 1 (Hem coup) over the temperate period in the repository volume. Chemical components in mol/kg, TDS in mg/L, pH in standard units and Eh in mV.

2000 AD: Eq. Hematite Coupled

	pH	EhmV	TDS(mg/l)	IonicStr	mNa	mK	mCa	mMg	mFe+2	mC	AlkTot	mCl	mS(VI)	mS(-II)	mSi	mP	Na+K+2Mg+2Ca
N total samples	35762	35762	35762	35762	35762	35762	35762	35762	35762	35762	35762	35762	35762	35762	35762	35762	35762
Mean	7.02	-153.77	5547.79	1.27E-01	3.10E-02	1.25E-04	3.15E-02	2.16E-04	1.83E-06	2.33E-03	1.97E-03	9.18E-02	1.17E-03	1.73E-08	1.30E-04	1.41E-06	9.46E -02
Standard Deviation	0.22	30.09	4027.88	9.58E-02	2.04E-02	5.72E-05	2.51E-02	2.54E-04	1.21E-06	1.00E-03	8.73E-04	7.12E-02	6.23E-04	5.21E-08	2.97E-06	8.84E-07	7.04E-0 2
Minimum	6.77	-258.89	507.62	7.49E-03	5.03E-03	7.41E-05	5.27E-04	2.78E-05	7.02E-08	5.61E-05	8.20E-05	1.57E-03	3.79E-04	8.29E-16	1.22E-04	4.23E-09	6.45E- 03
P0.1	6.79	-253.65	539.84	8.21E-03	5.22E-03	7.47E-05	7.11E-04	3.58E-05	9.55E-08	6.69E-05	9.04E-05	2.24E-03	3.85E-04	1.87E-15	1.23E-04	5.57E-09	7.01E- 03
P5	6.83	-216.20	884.65	1.62E-02	7.05E-03	7.67E-05	2.78E-03	5.85E-05	5.58E-07	4.18E-04	4.11E-04	8.89E-03	4.39E-04	7.63E-15	1.25E-04	8.37E-08	1.30E- 02
Median	6.95	-144.72	4505.44	1.02E-01	2.59E-02	1.07E-04	2.49E-02	1.39E-04	1.53E-06	2.47E-03	2.01E-03	7.34E-02	1.02E-03	1.25E-12	1.31E-04	1.37E-06	7.63E -02
P95	7.50	-120.73	14030.54	3.28E-01	7.37E-02	2.42E-04	8.44E-02	8.20E-04	4.58E-06	3.79E-03	3.43E-03	2.41E-01	2.45E-03	1.40E-07	1.34E-04	2.98E-06	2.43 E-01
P99.9	8.06	-112.97	18249.13	4.31E-01	9.20E-02	4.32E-04	1.12E-01	1.80E-03	8.48E-06	4.17E-03	4.04E-03	3.16E-01	3.08E-03	5.09E-07	1.35E-04	4.04E-06	3.17 E-01
Maximum	8.14	-109.44	19602.43	4.63E-01	9.81E-02	5.50E-04	1.21E-01	2.36E-03	9.92E-06	4.24E-03	4.15E-03	3.39E-01	3.28E-03	1.09E-06	1.36E-04	4.38E-06	3.40 E-01

5000 AD: Eq. Hematite Coupled

	pH	Eh(mV)	TDS(mg/l)	IonicStrengt	mNa	mK	mCa	mMg	mFe(II)	mC	AlkalinityTo	mCl	mS(VI)	mS(-II)	mSi	mP	mNa+mK+2mMg+2
N total samples	35762	35762	35762	35762	35762	35762	35762	35762	35762	35762	35762	35762	35762	35762	35762	35762	35762
Mean	7.05	-157.34	4092.13	9.20E-02	2.36E-02	1.05E-04	2.25E-02	1.62E-04	1.47E-06	2.76E-03	2.36E-03	6.59E-02	9.58E-04	1.88E-08	1.32E-04	1.83E-06	6.90E -02
Standard Deviation	0.23	31.83	3546.47	8.42E-02	1.79E-02	3.15E-05	2.21E-02	9.65E-05	6.11E-07	9.40E-04	8.72E-04	6.28E-02	5.51E-04	4.60E-08	2.76E-06	9.40E-07	6.20E-0 2
Minimum	6.76	-258.61	487.57	7.03E-03	4.92E-03	7.53E-05	4.05E-04	2.82E-05	5.28E-08	5.73E-05	8.30E-05	1.14E-03	3.76E-04	5.53E-16	1.21E-04	4.38E-09	6.10E- 03
P0.1	6.79	-250.34	509.21	7.51E-03	5.05E-03	7.56E-05	5.29E-04	3.84E-05	8.17E-08	7.45E-05	9.69E-05	1.59E-03	3.81E-04	2.08E-15	1.22E-04	6.63E-09	6.47E- 03
P5	6.84	-220.65	686.74	1.15E-02	6.06E-03	7.65E-05	1.54E-03	7.39E-05	3.71E-07	8.54E-04	7.74E-04	5.05E-03	4.12E-04	7.99E-15	1.26E-04	2.47E-07	9.54E- 03
Median	6.97	-147.40	2914.75	6.39E-02	1.77E-02	9.42E-05	1.51E-02	1.42E-04	1.45E-06	2.95E-03	2.41E-03	4.53E-02	7.80E-04	2.83E-12	1.32E-04	1.85E-06	4.84E -02
P95	7.56	-121.24	12110.77	2.83E-01	6.38E-02	1.73E-04	7.24E-02	3.62E-04	2.56E-06	4.00E-03	3.75E-03	2.08E-01	2.18E-03	1.47E-07	1.35E-04	3.42E-06	2.09 E-01
P99.9	8.02	-114.80	17619.82	4.16E-01	8.94E-02	2.65E-04	1.08E-01	8.21E-04	4.89E-06	4.24E-03	4.15E-03	3.05E-01	3.09E-03	2.16E-07	1.36E-04	4.38E-06	3.06 E-01
Maximum	8.13	-107.39	19356.33	4.57E-01	9.71E-02	3.23E-04	1.19E-01	1.18E-03	6.59E-06	4.29E-03	4.23E-03	3.35E-01	3.32E-03	2.74E-07	1.36E-04	4.70E-06	3.36 E-01

10000 AD: Eq. Hematite Coupled

	pH	Eh(mV)	TDS(mg/l)	IonicStreng t	mNa	mK	mCa	mMg	mFe(II)	mC	AlkalinityTo	mCl	mS(VI)	mS(-II)	mSi	mP	mNa+mK+2mMg+2
N total samples	35762	35762	35762	35762	35762	35762	35762	35762	35762	35762	35762	35762	35762	35762	35762	35762	35762
Mean	7.14	-168.64	2895.09	6.35E-02	1.76E-02	9.36E-05	1.50E-02	1.47E-04	1.21E-06	3.16E-03	2.76E-03	4.46E-02	7.90E-04	3.44E-08	1.33E-04	2.29E-06	4.81E -02
Standard Deviation	0.28	36.52	2917.00	6.91E-02	1.49E-02	2.16E-05	1.80E-02	4.07E-05	5.11E-07	8.40E-04	8.48E-04	5.17E-02	4.73E-04	6.08E-08	2.42E-06	9.87E-07	5.09E-0 2
Minimum	6.78	-257.24	474.83	6.75E-03	4.85E-03	7.57E-05	3.31E-04	3.18E-05	3.70E-08	6.32E-05	8.78E-05	8.64E-04	3.74E-04	1.01E-15	1.21E-04	5.19E-09	5.88E- 03
P0.1	6.80	-251.66	486.05	7.00E-03	4.92E-03	7.59E-05	3.87E-04	4.34E-05	4.88E-08	9.06E-05	1.09E-04	1.10E-03	3.77E-04	1.72E-15	1.23E-04	8.97E-09	6.07E- 03
P5	6.85	-233.07	561.74	8.68E-03	5.37E-03	7.63E-05	8.08E-04	9.34E-05	1.63E-07	1.46E-03	1.23E-03	2.62E-03	3.92E-04	7.49E-15	1.27E-04	5.76E-07	7.37E- 03
Median	7.05	-161.42	1818.40	3.78E-02	1.22E-02	8.53E-05	8.34E-03	1.44E-04	1.36E-06	3.34E-03	2.81E-03	2.57E-02	6.21E-04	4.00E-11	1.33E-04	2.31E-06	2.92E -02
P95	7.74	-121.30	9440.79	2.19E-01	5.07E-02	1.43E-04	5.56E-02	2.22E-04	1.87E-06	4.17E-03	4.02E-03	1.61E-01	1.83E-03	1.81E-07	1.35E-04	3.96E-06	1.63E -01
P99.9	8.02	-114.40	16440.41	3.85E-01	8.50E-02	1.91E-04	1.00E-01	4.28E-04	2.97E-06	4.30E-03	4.24E-03	2.84E-01	3.07E-03	2.09E-07	1.36E-04	4.76E-06	2.85 E-01
Maximum	8.12	-111.66	18358.71	4.33E-01	9.30E-02	2.08E-04	1.13E-01	6.22E-04	3.77E-06	4.32E-03	4.28E-03	3.18E-01	3.36E-03	2.28E-07	1.36E-04	4.98E-06	3.19 E-01

15000 AD: Eq. Hematite Coupled

	pH	Eh(mV)	TDS(mg/l)	onic Streng	mNa	mK	mCa	mMg	mFe(I)	mC	AlkalinityTo	mCl	mS(VI)	mS(-II)	mSi	mP	mNa+mK+2mMg+2
N total samples	35762	35762	35762	35762	35762	35762	35762	35762	35762	35762	35762	35762	35762	35762	35762	35762	35762
Mean	7.23	-179.46	2227.38	4.76E-02	1.42E-02	8.82E-05	1.09E-02	1.44E-04	1.04E-06	3.40E-03	3.03E-03	3.26E-02	6.94E-04	5.16E-08	1.33E-04	2.63E-06	3.64E -02
Standard Deviation	0.32	38.93	2420.73	5.72E-02	1.25E-02	1.68E-05	1.49E-02	2.35E-05	5.30E-07	7.51E-04	8.11E-04	4.30E-02	4.09E-04	7.17E-08	2.12E-06	1.01E-06	4.22E-0 2
Minimum	6.80	-257.36	470.19	6.65E-03	4.82E-03	7.59E-05	3.04E-04	4.14E-05	3.19E-08	6.84E-05	9.19E-05	7.63E-04	3.73E-04	9.83E-16	1.22E-04	5.87E-09	5.80E-03
P0.1	6.81	-255.19	475.44	6.76E-03	4.85E-03	7.60E-05	3.31E-04	5.13E-05	3.69E-08	1.07E-04	1.23E-04	8.73E-04	3.75E-04	1.59E-15	1.24E-04	1.21E-08	5.89E-03
P5	6.85	-241.74	516.84	7.67E-03	5.11E-03	7.62E-05	5.56E-04	1.07E-04	9.08E-08	1.91E-03	1.57E-03	1.72E-03	3.84E-04	7.80E-15	1.29E-04	8.96E-07	6.60E-03
Median	7.15	-178.81	1324.01	2.62E-02	9.62E-03	8.16E-05	5.27E-03	1.46E-04	1.29E-06	3.57E-03	3.10E-03	1.67E-02	5.43E-04	1.24E-09	1.34E-04	2.63E-06	2.06E -02
P95	7.87	-121.41	7413.85	1.70E-01	4.09E-02	1.26E-04	4.28E-02	1.81E-04	1.66E-06	4.24E-03	4.15E-03	1.25E-01	1.56E-03	1.95E-07	1.35E-04	4.34E-06	1.27E -01
P99.9	8.07	-113.83	15239.85	3.56E-01	7.99E-02	1.75E-04	9.20E-02	2.96E-04	2.27E-06	4.32E-03	4.28E-03	2.62E-01	3.00E-03	2.09E-07	1.36E-04	4.98E-06	2.64 E-01
Maximum	8.11	-111.72	17559.96	4.13E-01	8.98E-02	1.94E-04	1.07E-01	3.88E-04	2.58E-06	4.33E-03	4.30E-03	3.04E-01	3.35E-03	2.12E-07	1.36E-04	5.10E-06	3.04 E-01

Table A4-3. Statistical results for the main geochemical parameters obtained with the geochemical variant case 2 (FeS coup) over the temperate period in the repository volume. Chemical components in mol/kg, TDS in mg/L, pH in standard units and Eh in mV.

2000 AD: Eq. FeS(am) Coupled																	
	pH	EhmV	TDS(mg/l)	IonicStr	mNa	mK	mCa	mMg	mFe+2	mC	AlkTot	mCl	mS(VI)	mS(-II)	mSi	mP	Na+K+2Mg+2Ca
N total samples	35762	35762	35762	35762	35762	35762	35762	35762	35762	35762	35762	35762	35762	35762	35762	35762	35762
Mean	7.03	-201.16	5549.93	1.27E-01	3.10E-02	1.25E-04	3.15E-02	2.16E-04	2.25E-05	2.30E-03	1.98E-03	9.18E-02	1.20E-03	2.55E-05	1.30E-04	1.39E-06	9.45E-02
Standard Deviation	0.23	13.79	4027.87	9.58E-02	2.04E-02	5.72E-05	2.51E-02	2.54E-04	7.04E-06	1.00E-03	8.75E-04	7.12E-02	6.25E-04	7.45E-06	2.96E-06	8.81E-07	7.04E-02
Minimum	6.78	-272.23	509.08	7.49E-03	5.03E-03	7.41E-05	5.21E-04	2.78E-05	3.63E-06	5.01E-05	9.39E-05	1.57E-03	3.91E-04	5.77E-06	1.22E-04	3.55E-09	6.44E-03
P0.1	6.80	-267.33	541.32	8.21E-03	5.22E-03	7.47E-05	7.05E-04	3.58E-05	4.40E-06	6.02E-05	1.02E-04	2.24E-03	3.99E-04	6.42E-06	1.23E-04	4.77E-09	7.00E-03
P5	6.84	-230.74	886.36	1.62E-02	7.05E-03	7.67E-05	2.77E-03	5.85E-05	8.34E-06	4.01E-04	4.21E-04	8.89E-03	4.58E-04	1.06E-05	1.25E-04	7.84E-08	1.30E-02
Median	6.95	-196.54	4507.57	1.02E-01	2.59E-02	1.07E-04	2.49E-02	1.39E-04	2.41E-05	2.44E-03	2.01E-03	7.34E-02	1.06E-03	2.71E-05	1.31E-04	1.34E-06	7.63E-02
P95	7.51	-189.24	14032.17	3.28E-01	7.37E-02	2.42E-04	8.43E-02	8.20E-04	3.16E-05	3.78E-03	3.45E-03	2.41E-01	2.47E-03	3.53E-05	1.34E-04	2.96E-06	2.43E-01
P99.9	8.11	-186.90	18250.63	4.31E-01	9.20E-02	4.32E-04	1.12E-01	1.80E-03	3.45E-05	4.17E-03	4.06E-03	3.16E-01	3.10E-03	3.85E-05	1.35E-04	4.04E-06	3.17E-01
Maximum	8.19	-185.99	19600.00	4.63E-01	9.81E-02	5.50E-04	1.21E-01	2.36E-03	3.62E-05	4.24E-03	4.17E-03	3.39E-01	3.30E-03	4.06E-05	1.36E-04	4.38E-06	3.40E-01

5000 AD: Eq. FeS(am) Coupled																	
	pH	Eh(mV)	TDS(mg/l)	IonicStrength	mNa	mK	mCa	mMg	mFe+2	mC	AlkalityTot	mCl	mS(VI)	mS(-II)	mSi	mP	mNa+mK+2mMg+2mCa
N total samples	35762	35762	35762	35762	35762	35762	35762	35762	35762	35762	35762	35762	35762	35762	35762	35762	35762
Mean	7.06	-202.89	4094.21	9.20E-02	2.36E-02	1.05E-04	2.25E-02	1.62E-04	2.06E-05	2.74E-03	2.37E-03	6.59E-02	9.88E-04	2.37E-05	1.32E-04	1.81E-06	6.90E-02
Standard Deviation	0.23	14.12	3546.55	8.42E-02	1.79E-02	3.15E-05	2.21E-02	9.65E-05	7.65E-06	9.45E-04	8.74E-04	6.28E-02	5.55E-04	7.96E-06	2.75E-06	9.41E-07	6.20E-02
Minimum	6.77	-272.00	488.98	7.03E-03	4.92E-03	7.53E-05	4.01E-04	2.82E-05	3.05E-06	5.12E-05	9.49E-05	1.14E-03	3.88E-04	5.50E-06	1.22E-04	3.70E-09	6.09E-03
P0.1	6.79	-264.20	510.61	7.51E-03	5.05E-03	7.56E-05	5.24E-04	3.84E-05	3.64E-06	6.76E-05	1.08E-04	1.59E-03	3.93E-04	6.06E-06	1.23E-04	5.69E-09	6.46E-03
P5	6.84	-233.81	688.28	1.15E-02	6.06E-03	7.65E-05	1.53E-03	7.39E-05	6.88E-06	8.27E-04	7.80E-04	5.05E-03	4.29E-04	9.21E-06	1.26E-04	2.35E-07	9.52E-03
Median	6.97	-197.79	2916.88	6.39E-02	1.77E-02	9.42E-05	1.51E-02	1.42E-04	2.18E-05	2.92E-03	2.42E-03	4.53E-02	8.13E-04	2.51E-05	1.32E-04	1.82E-06	4.84E-02
P95	7.57	-189.70	12112.84	2.83E-01	6.38E-02	1.73E-04	7.24E-02	3.62E-04	3.08E-05	4.00E-03	3.77E-03	2.08E-01	2.21E-03	3.44E-05	1.35E-04	3.41E-06	2.09E-01
P99.9	8.06	-186.62	17621.88	4.16E-01	8.94E-02	2.65E-04	1.08E-01	8.21E-04	3.46E-05	4.23E-03	4.17E-03	3.05E-01	3.10E-03	3.88E-05	1.36E-04	4.38E-06	3.06E-01
Maximum	8.19	-185.36	19357.96	4.57E-01	9.71E-02	3.23E-04	1.19E-01	1.18E-03	3.61E-05	4.28E-03	4.25E-03	3.35E-01	3.34E-03	4.05E-05	1.36E-04	4.70E-06	3.36E-01

10000 AD: Eq. FeS(am) Coupled																	
	pH	Eh(mV)	TDS(mg/l)	IonicStrength	mNa	mK	mCa	mMg	mFe(II)	mC	AlkalinityTo	mCl	mS(VI)	mS(-II)	mSi	mP	mNa+mK+2mMg+2mCa
N total samples	35762	35762	35762	35762	35762	35762	35762	35762	35762	35762	35762	35762	35762	35762	35762	35762	35762
Mean	7.15	-208.17	2897.07	6.35E-02	1.76E-02	9.36E-05	1.50E-02	1.47E-04	1.75E-05	3.14E-03	2.77E-03	4.46E-02	8.17E-04	2.06E-05	1.33E-04	2.27E-06	4.80E-02
Standard Deviation	0.28	17.26	2917.15	6.91E-02	1.49E-02	2.16E-05	1.80E-02	4.07E-05	8.27E-06	8.47E-04	8.52E-04	5.17E-02	4.78E-04	8.61E-06	2.41E-06	9.92E-07	5.09E-02
Minimum	6.79	-270.69	476.26	6.75E-03	4.85E-03	7.57E-05	3.27E-04	3.18E-05	2.65E-06	5.70E-05	9.96E-05	8.64E-04	3.86E-04	5.13E-06	1.22E-04	4.43E-09	5.87E-03
P0.1	6.81	-263.00	487.46	7.00E-03	4.92E-03	7.59E-05	3.83E-04	4.34E-05	2.96E-06	8.30E-05	1.21E-04	1.10E-03	3.88E-04	5.42E-06	1.23E-04	7.89E-09	6.06E-03
P5	6.85	-244.87	563.19	8.68E-03	5.37E-03	7.63E-05	8.02E-04	9.34E-05	4.77E-06	1.42E-03	1.24E-03	2.62E-03	4.06E-04	7.23E-06	1.27E-04	5.53E-07	7.36E-03
Median	7.05	-202.64	1820.41	3.78E-02	1.22E-02	8.53E-05	8.32E-03	1.44E-04	1.73E-05	3.32E-03	2.83E-03	2.57E-02	6.48E-04	2.06E-05	1.33E-04	2.28E-06	2.92E-02
P95	7.75	-190.21	9442.97	2.19E-01	5.07E-02	1.43E-04	5.56E-02	2.22E-04	3.03E-05	4.17E-03	4.04E-03	1.61E-01	1.87E-03	3.38E-05	1.35E-04	3.95E-06	1.63E-01
P99.9	8.04	-187.47	16442.83	3.85E-01	8.50E-02	1.91E-04	1.00E-01	4.28E-04	3.32E-05	4.29E-03	4.26E-03	2.84E-01	3.08E-03	3.71E-05	1.36E-04	4.76E-06	2.85E-01
Maximum	8.17	-186.05	18360.86	4.33E-01	9.30E-02	2.08E-04	1.13E-01	6.22E-04	3.44E-05	4.32E-03	4.30E-03	3.18E-01	3.37E-03	3.87E-05	1.36E-04	4.98E-06	3.19E-01

15000 AD: Eq. FeS(am) Coupled																	
	pH	Eh(mV)	TDS(mg/l)	IonicStrength	mNa	mK	mCa	mMg	mFe(II)	mC	AlkalinityTo	mCl	mS(VI)	mS(-II)	mSi	mP	mNa+mK+2mMg+2mCa
N total samples	35762	35762	35762	35762	35762	35762	35762	35762	35762	35762	35762	35762	35762	35762	35762	35762	35762
Mean	7.23	-213.58	2229.27	4.76E-02	1.42E-02	8.82E-05	1.09E-02	1.44E-04	1.50E-05	3.38E-03	3.04E-03	3.26E-02	7.18E-04	1.81E-05	1.33E-04	2.61E-06	3.63E-02
Standard Deviation	0.32	19.75	2420.92	5.72E-02	1.25E-02	1.68E-05	1.49E-02	2.35E-05	8.34E-06	7.60E-04	8.15E-04	4.30E-02	4.15E-04	8.73E-06	2.12E-06	1.02E-06	4.22E-02
Minimum	6.81	-268.47	471.62	6.65E-03	4.82E-03	7.59E-05	3.01E-04	4.14E-05	2.50E-06	6.18E-05	1.04E-04	7.63E-04	3.85E-04	4.99E-06	1.22E-04	5.05E-09	5.79E-03
P0.1	6.82	-265.56	476.88	6.76E-03	4.85E-03	7.60E-05	3.27E-04	5.13E-05	2.65E-06	9.98E-05	1.35E-04	8.73E-04	3.86E-04	5.13E-06	1.24E-04	1.07E-08	5.88E-03
P5	6.86	-252.85	518.32	7.67E-03	5.11E-03	7.62E-05	5.51E-04	1.07E-04	3.77E-06	1.87E-03	1.58E-03	1.72E-03	3.97E-04	6.21E-06	1.29E-04	8.67E-07	6.59E-03
Median	7.15	-208.45	1325.95	2.62E-02	9.62E-03	8.16E-05	5.25E-03	1.46E-04	1.38E-05	3.55E-03	3.12E-03	1.67E-02	5.67E-04	1.70E-05	1.34E-04	2.60E-06	2.05E-02
P95	7.88	-190.32	7416.24	1.70E-01	4.09E-02	1.26E-04	4.27E-02	1.81E-04	3.01E-05	4.24E-03	4.16E-03	1.25E-01	1.60E-03	3.36E-05	1.35E-04	4.33E-06	1.27E-01
P99.9	8.08	-187.99	15241.38	3.56E-01	7.99E-02	1.75E-04	9.20E-02	2.96E-04	3.30E-05	4.32E-03	4.30E-03	2.62E-01	3.01E-03	3.69E-05	1.36E-04	4.98E-06	2.64E-01
Maximum	8.13	-187.42	17561.85	4.13E-01	8.98E-02	1.94E-04	1.07E-01	3.88E-04	3.38E-05	4.33E-03	4.32E-03	3.04E-01	3.36E-03	3.78E-05	1.36E-04	5.10E-06	3.04E-01

Table A4-4. Statistical results for the main geochemical parameters obtained with the geochemical variant case 3 (Hem uncoup) over the temperate period in the repository volume. Chemical components in mol/kg, TDS in mg/L, pH in standard units and Eh in mV.

2000 AD: Hematite Uncoupled																	
	pH	EhmV	TDS(mg/l)	IonicStr	mNa	mK	mCa	mMg	mFe+2	mC	AlkTot	mCl	mS(VI)	mS(-II)	mSi	mP	Na+K+2Mg+2Ca
N total	35762	35762	35762	35762	35762	35762	35762	35762	35762	35762	35762	35762	35762	35762	35762	35762	35762
Mean	7.02	-148.77	5547.78	1.27E-01	3.10E-02	1.25E-04	3.15E-02	2.16E-04	1.29E-06	2.33E-03	1.97E-03	9.18E-02	1.17E-03	7.42E-08	1.30E-04	1.41E-06	9.46E-02
Standard Deviation	0.22	37.95	4027.85	9.58E-02	2.04E-02	5.72E-05	2.51E-02	2.54E-04	1.47E-07	1.00E-03	8.72E-04	7.12E-02	6.23E-04	1.16E-07	2.98E-06	8.83E-07	7.04E-02
Minimum	6.77	-328.09	507.51	7.49E-03	5.03E-03	7.41E-05	5.25E-04	2.78E-05	5.17E-07	5.67E-05	8.19E-05	1.57E-03	3.79E-04	7.02E-10	1.22E-04	4.29E-09	6.45E-03
P0.1	6.79	-315.15	539.73	8.21E-03	5.22E-03	7.47E-05	7.10E-04	3.58E-05	8.21E-07	6.75E-05	9.04E-05	2.24E-03	3.85E-04	1.28E-09	1.23E-04	5.64E-09	7.01E-03
P5	6.83	-233.30	884.58	1.62E-02	7.05E-03	7.67E-05	2.78E-03	5.85E-05	1.05E-06	4.22E-04	4.13E-04	8.89E-03	4.39E-04	4.44E-09	1.25E-04	8.47E-08	1.30E-02
Median	6.95	-135.38	4505.37	1.02E-01	2.59E-02	1.07E-04	2.49E-02	1.39E-04	1.28E-06	2.47E-03	2.01E-03	7.34E-02	1.02E-03	3.79E-08	1.31E-04	1.38E-06	7.63E-02
P95	7.50	-114.68	14030.23	3.28E-01	7.37E-02	2.42E-04	8.44E-02	8.20E-04	1.55E-06	3.79E-03	3.43E-03	2.41E-01	2.45E-03	3.40E-07	1.34E-04	2.98E-06	2.43E-01
P99.9	8.06	-108.30	18248.77	4.31E-01	9.20E-02	4.32E-04	1.12E-01	1.80E-03	1.82E-06	4.17E-03	4.04E-03	3.16E-01	3.08E-03	7.89E-07	1.35E-04	4.04E-06	3.17E-01
Maximum	8.13	-105.11	19602.10	4.63E-01	9.81E-02	5.50E-04	1.21E-01	2.36E-03	1.93E-06	4.24E-03	4.15E-03	3.39E-01	3.28E-03	1.07E-06	1.36E-04	4.38E-06	3.40E-01
5000 AD: Hematite Uncoupled																	
	pH	Eh(mV)	TDS(mg/l)	IonicStrength	mNa	mK	mCa	mMg	mFe+2	mC	AlkalinityTot	mCl	mS(VI)	mS(-II)	mSi	mP	mNa+mK+2mMg+2mCa
N total	35762	35762	35762	35762	35762	35762	35762	35762	35762	35762	35762	35762	35762	35762	35762	35762	35762
Mean	7.05	-156.24	4092.11	9.20E-02	2.36E-02	1.05E-04	2.25E-02	1.62E-04	1.27E-06	2.76E-03	2.36E-03	6.59E-02	9.58E-04	3.68E-08	1.32E-04	1.83E-06	6.90E-02
Standard Deviation	0.23	41.21	3546.45	8.42E-02	1.79E-02	3.15E-05	2.21E-02	9.65E-05	1.20E-07	9.39E-04	8.71E-04	6.28E-02	5.51E-04	4.71E-08	2.76E-06	9.39E-07	6.20E-02
Minimum	6.76	-326.84	487.48	7.03E-03	4.92E-03	7.53E-05	4.04E-04	2.82E-05	4.86E-07	5.79E-05	8.29E-05	1.14E-03	3.76E-04	3.42E-10	1.21E-04	4.45E-09	6.10E-03
P0.1	6.79	-308.83	509.10	7.51E-03	5.05E-03	7.56E-05	5.28E-04	3.84E-05	8.00E-07	7.50E-05	9.70E-05	1.59E-03	3.81E-04	6.60E-10	1.22E-04	6.70E-09	6.47E-03
P5	6.84	-246.64	686.63	1.15E-02	6.06E-03	7.65E-05	1.54E-03	7.39E-05	1.05E-06	8.57E-04	7.76E-04	5.05E-03	4.12E-04	2.38E-09	1.26E-04	2.48E-07	9.54E-03
Median	6.97	-141.87	2914.65	6.39E-02	1.77E-02	9.42E-05	1.51E-02	1.42E-04	1.28E-06	2.95E-03	2.41E-03	4.53E-02	7.80E-04	2.20E-08	1.32E-04	1.85E-06	4.84E-02
P95	7.56	-115.94	12110.47	2.83E-01	6.38E-02	1.73E-04	7.24E-02	3.62E-04	1.44E-06	4.00E-03	3.75E-03	2.08E-01	2.18E-03	1.32E-07	1.35E-04	3.42E-06	2.09E-01
P99.9	8.01	-108.41	17619.51	4.16E-01	8.94E-02	2.65E-04	1.08E-01	8.21E-04	1.59E-06	4.24E-03	4.15E-03	3.05E-01	3.09E-03	3.65E-07	1.36E-04	4.38E-06	3.06E-01
Maximum	8.13	-104.48	19356.00	4.57E-01	9.71E-02	3.23E-04	1.19E-01	1.18E-03	1.61E-06	4.29E-03	4.23E-03	3.35E-01	3.32E-03	5.22E-07	1.36E-04	4.70E-06	3.36E-01
10000 AD: Hematite Uncoupled																	
	pH	Eh(mV)	TDS(mg/l)	IonicStrength	mNa	mK	mCa	mMg	mFe(II)	mC	AlkalinityTot	mCl	mS(VI)	mS(-II)	mSi	mP	mNa+mK+2mMg+2mCa
N total	35762	35762	35762	35762	35762	35762	35762	35762	35762	35762	35762	35762	35762	35762	35762	35762	35762
Mean	7.14	-173.26	2895.06	6.35E-02	1.76E-02	9.36E-05	1.50E-02	1.47E-04	1.23E-06	3.16E-03	2.76E-03	4.46E-02	7.90E-04	1.88E-08	1.33E-04	2.29E-06	4.81E-02
Standard Deviation	0.28	50.24	2916.99	6.91E-02	1.49E-02	2.16E-05	1.80E-02	4.07E-05	1.39E-07	8.39E-04	8.48E-04	5.17E-02	4.73E-04	2.27E-08	2.42E-06	9.86E-07	5.09E-02
Minimum	6.78	-327.41	474.73	6.75E-03	4.85E-03	7.57E-05	3.29E-04	3.18E-05	5.26E-07	6.38E-05	8.78E-05	8.64E-04	3.74E-04	1.23E-10	1.21E-04	5.26E-09	5.88E-03
P0.1	6.80	-318.57	485.95	6.99E-03	4.92E-03	7.59E-05	3.86E-04	4.34E-05	7.19E-07	9.11E-05	1.09E-04	1.10E-03	3.77E-04	2.71E-10	1.23E-04	9.05E-09	6.07E-03
P5	6.85	-276.45	561.62	8.68E-03	5.37E-03	7.63E-05	8.07E-04	9.34E-05	9.35E-07	1.46E-03	1.24E-03	2.62E-03	3.92E-04	1.00E-09	1.27E-04	5.77E-07	7.37E-03
Median	7.05	-159.60	1818.46	3.78E-02	1.22E-02	8.53E-05	8.34E-03	1.44E-04	1.27E-06	3.34E-03	2.81E-03	2.57E-02	6.21E-04	1.08E-08	1.33E-04	2.31E-06	2.92E-02
P95	7.74	-116.74	9440.66	2.19E-01	5.07E-02	1.43E-04	5.56E-02	2.22E-04	1.40E-06	4.17E-03	4.02E-03	1.61E-01	1.83E-03	6.37E-08	1.35E-04	3.96E-06	1.63E-01
P99.9	8.02	-110.47	16440.12	3.85E-01	8.50E-02	1.91E-04	1.00E-01	4.28E-04	1.51E-06	4.30E-03	4.24E-03	2.84E-01	3.07E-03	1.73E-07	1.36E-04	4.77E-06	2.85E-01
Maximum	8.11	-108.13	18358.19	4.33E-01	9.29E-02	2.08E-04	1.13E-01	6.22E-04	1.54E-06	4.32E-03	4.28E-03	3.18E-01	3.36E-03	2.46E-07	1.36E-04	4.98E-06	3.19E-01
15000 AD: Hematite Uncoupled																	
	pH	Eh(mV)	TDS(mg/l)	IonicStrength	mNa	mK	mCa	mMg	mFe(II)	mC	AlkalinityTot	mCl	mS(VI)	mS(-II)	mSi	mP	mNa+mK+2mMg+2mCa
N total	35762	35762	35762	35762	35762	35762	35762	35762	35762	35762	35762	35762	35762	35762	35762	35762	35762
Mean	7.23	-189.42	2227.34	4.76E-02	1.42E-02	8.82E-05	1.09E-02	1.44E-04	1.19E-06	3.40E-03	3.03E-03	3.26E-02	6.94E-04	1.16E-08	1.33E-04	2.63E-06	3.64E-02
Standard Deviation	0.32	56.41	2420.73	5.72E-02	1.25E-02	1.68E-05	1.49E-02	2.35E-05	1.65E-07	7.50E-04	8.11E-04	4.30E-02	4.09E-04	1.46E-08	2.12E-06	1.01E-06	4.22E-02
Minimum	6.80	-332.25	470.10	6.65E-03	4.82E-03	7.59E-05	3.03E-04	4.14E-05	5.59E-07	6.90E-05	9.19E-05	7.63E-04	3.73E-04	4.83E-11	1.22E-04	5.94E-09	5.80E-03
P0.1	6.81	-327.47	475.35	6.76E-03	4.85E-03	7.60E-05	3.29E-04	5.13E-05	6.72E-07	1.08E-04	1.23E-04	8.73E-04	3.75E-04	1.23E-10	1.24E-04	1.22E-08	5.89E-03
P5	6.85	-297.08	516.72	7.67E-03	5.11E-03	7.62E-05	5.55E-04	1.07E-04	8.37E-07	1.91E-03	1.57E-03	1.72E-03	3.84E-04	4.83E-10	1.29E-04	8.97E-07	6.60E-03
Median	7.15	-177.84	1324.01	2.62E-02	9.62E-03	8.16E-05	5.27E-03	1.46E-04	1.24E-06	3.57E-03	3.10E-03	1.67E-02	5.43E-04	6.12E-09	1.34E-04	2.63E-06	2.06E-02
P95	7.87	-116.96	7414.07	1.70E-01	4.09E-02	1.26E-04	4.28E-02	1.81E-04	1.38E-06	4.24E-03	4.14E-03	1.25E-01	1.56E-03	4.32E-08	1.35E-04	4.34E-06	1.27E-01
P99.9	8.08	-110.47	15239.43	3.56E-01	7.99E-02	1.75E-04	9.20E-02	2.96E-04	1.47E-06	4.32E-03	4.28E-03	2.62E-01	3.00E-03	1.03E-07	1.36E-04	4.98E-06	2.64E-01
Maximum	8.11	-109.04	17559.63	4.13E-01	8.98E-02	1.94E-04	1.07E-01	3.88E-04	1.51E-06	4.33E-03	4.30E-03	3.04E-01	3.35E-03	1.36E-07	1.36E-04	5.10E-06	3.04E-01

Table A4-5. Statistical results for the main geochemical parameters obtained with the geochemical Base case over the glacial period in the repository volume. Chemical components in mol/kg, TDS in mg/L, pH in standard units and Eh in mV. Columns in red indicate the values taken from the geochemical variant Cases 1 and 2 together (Bace Case for the redox parameters).

Glacial 0: BASE CASE, hem coup (black cells), hem coup + FeS coup (red cells)																		
	pH	Eh(mV) (HemC + FeSc)	TDS(mg/l)	IonicStr	mNa	mK	mCa	mMg	mFe(II) (HemC + FeSc)	mC	AlkTot	mCl	mS(VI)	mS(-II) (HemC + FeSc)	mSi	mP	Na+K+2Mg+2Ca
N total	28044	56088	28044	28044	28044	28044	28044	28044	56088	28044	28044	28044	28044	56088	28044	28044	28044
Mean	7.38	-207.65	1789.15	3.76E-02	1.13E-02	8.90E-05	8.51E-03	1.47E-04	7.27E-06	3.92E-03	3.55E-03	2.44E-02	5.35E-04	8.59E-06	1.34E-04	3.39E-06	2.87E-02
Standard Deviation	0.44	43.95	2246.93	5.32E-02	1.09E-02	2.17E-05	1.41E-02	1.70E-06	1.11E-05	3.72E-04	6.34E-04	3.96E-02	2.70E-04	1.30E-05	2.22E-06	8.80E-07	3.91E-02
Minimum	6.56	-266.08	473.24	6.72E-03	4.83E-03	7.61E-05	3.22E-04	1.38E-04	3.54E-08	2.84E-03	2.09E-03	8.25E-04	3.74E-04	2.10E-18	1.23E-04	1.52E-06	5.85E-03
P0.1	6.57	-266.08	473.24	6.72E-03	4.83E-03	7.61E-05	3.22E-04	1.39E-04	3.54E-08	2.91E-03	2.14E-03	8.25E-04	3.74E-04	4.05E-18	1.24E-04	1.60E-06	5.85E-03
P5	6.66	-256.61	490.38	7.09E-03	4.93E-03	7.63E-05	4.20E-04	1.43E-04	6.88E-08	3.17E-03	2.36E-03	1.18E-03	3.76E-04	5.37E-16	1.29E-04	1.93E-06	6.14E-03
Median	7.45	-219.51	709.72	1.21E-02	6.09E-03	7.86E-05	1.73E-03	1.48E-04	2.48E-06	4.07E-03	3.78E-03	5.39E-03	4.05E-04	2.65E-06	1.35E-04	3.46E-06	9.92E-03
P95	7.98	-105.62	7371.90	1.70E-01	3.83E-02	1.43E-04	4.36E-02	1.48E-04	3.57E-05	4.30E-03	4.24E-03	1.23E-01	1.20E-03	4.09E-05	1.36E-04	4.68E-06	1.26E-01
P99.9	8.08	-79.86	12721.28	2.97E-01	6.40E-02	1.94E-04	7.74E-02	1.48E-04	5.23E-05	4.33E-03	4.30E-03	2.16E-01	1.84E-03	6.01E-05	1.36E-04	5.02E-06	2.19E-01
Maximum	8.08	-76.04	14216.67	3.33E-01	7.12E-02	2.08E-04	8.69E-02	1.48E-04	5.55E-05	4.33E-03	4.30E-03	2.42E-01	2.02E-03	6.41E-05	1.36E-04	5.02E-06	2.45E-01
Glacial I: BASE CASE																	
	pH	Eh(mV) (HemC + FeSc)	TDS(mg/l)	IonicStr	mNa	mK	mCa	mMg	mFe(II) (HemC + FeSc)	mC	AlkTot	mCl	mS(VI)	mS(-II) (HemC + FeSc)	mSi	mP	Na+K+2Mg+2Ca
N total	28044	56088	28044	28044	28044	28044	28044	28044	56088	28044	2.80E+04	28044	28044	56088	28044	28044	28044
Mean	6.88	-156.86	9088.66	2.11E-01	4.63E-02	1.55E-04	5.47E-02	1.33E-04	2.01E-05	2.99E-03	2.36E-03	1.53E-01	1.39E-03	2.24E-05	1.28E-04	1.88E-06	1.56E-01
Standard Deviation	0.56	63.34	7269.82	1.73E-01	3.52E-02	7.49E-05	4.57E-02	2.72E-05	2.31E-05	6.88E-04	6.44E-04	1.27E-01	8.92E-04	2.77E-05	7.44E-06	7.53E-07	1.27E-01
Minimum	6.49	-376.03	39.74	5.50E-04	7.40E-06	1.02E-05	1.67E-04	4.11E-06	3.95E-11	1.80E-04	2.41E-04	1.41E-05	5.31E-06	7.01E-19	1.11E-04	4.18E-08	3.60E-04
P0.1	6.49	-346.62	70.90	1.21E-03	2.91E-04	1.23E-05	2.21E-04	7.73E-06	2.56E-10	2.08E-04	3.08E-04	3.90E-04	1.91E-05	7.01E-19	1.12E-04	5.56E-08	8.93E-04
P5	6.51	-275.25	246.84	3.97E-03	2.02E-03	3.27E-05	4.70E-04	5.21E-05	2.01E-07	1.50E-03	1.52E-03	1.21E-03	1.39E-04	8.17E-19	1.16E-04	8.86E-07	3.30E-03
Median	6.64	-171.86	8482.17	1.96E-01	4.37E-02	1.53E-04	5.06E-02	1.41E-04	2.80E-06	3.03E-03	2.24E-03	1.42E-01	1.34E-03	4.08E-07	1.28E-04	1.76E-06	1.45E-01
P95	8.29	-69.77	22701.05	5.35E-01	1.12E-01	2.89E-04	1.41E-01	1.48E-04	6.10E-05	4.03E-03	3.73E-03	3.90E-01	3.03E-03	7.20E-05	1.39E-04	3.40E-06	3.93E-01
P99.9	9.32	-67.66	28061.57	6.63E-01	1.38E-01	3.40E-04	1.74E-01	1.48E-04	6.29E-05	4.31E-03	4.26E-03	4.84E-01	3.66E-03	7.61E-05	1.69E-04	4.84E-06	4.87E-01
Maximum	9.70	-67.66	29991.63	7.09E-01	1.47E-01	3.58E-04	1.87E-01	1.48E-04	6.29E-05	4.33E-03	4.30E-03	5.17E-01	3.90E-03	7.68E-05	2.14E-04	5.02E-06	5.21E-01
Glacial II: BASE CASE																	
	pH	Eh(mV) (HemC + FeSc)	TDS(mg/l)	IonicStr	mNa	mK	mCa	mMg	mFe(II) (HemC + FeSc)	mC	AlkTot	mCl	mS(VI)	mS(-II) (HemC + FeSc)	mSi	mP	Na+K+2Mg+2Ca
N total	28044	56088	28044	28044	28044	28044	28044	28044	56088	28044	28044	28044	28044	56088	28044	28044	28044
Mean	8.67	-299.05	1449.41	3.34E-02	7.30E-03	3.36E-05	8.64E-03	2.58E-05	3.56E-06	6.22E-04	6.16E-04	2.39E-02	2.25E-04	3.82E-06	1.61E-04	2.90E-07	2.47E-02
Standard Deviation	0.99	74.80	2994.23	7.00E-02	1.51E-02	4.43E-05	1.82E-02	3.71E-05	9.78E-06	8.21E-04	6.13E-04	5.10E-02	4.36E-04	1.11E-05	2.59E-05	5.14E-07	5.17E-02
Minimum	6.54	-371.53	47.12	7.31E-04	5.80E-05	1.04E-05	1.84E-04	4.18E-06	5.07E-11	4.84E-05	7.82E-05	1.90E-04	6.68E-06	1.44E-18	1.22E-04	3.48E-09	4.99E-04
P0.1	6.55	-371.47	47.13	7.31E-04	5.82E-05	1.04E-05	1.84E-04	4.18E-06	5.08E-11	9.96E-05	1.53E-04	1.90E-04	6.69E-06	1.78E-18	1.22E-04	1.51E-08	4.99E-04
P5	6.65	-369.59	47.31	7.33E-04	6.24E-05	1.04E-05	2.08E-04	4.29E-06	5.52E-11	1.17E-04	1.84E-04	1.91E-04	7.02E-06	5.61E-13	1.27E-04	2.06E-08	5.02E-04
Median	9.09	-329.57	112.23	2.06E-03	5.95E-04	1.36E-05	4.54E-04	8.35E-06	4.99E-07	2.08E-04	3.11E-04	1.07E-03	3.11E-05	4.23E-07	1.55E-04	5.08E-08	1.58E-03
P95	9.64	-145.18	9639.00	2.25E-01	4.87E-02	1.55E-04	5.85E-02	1.38E-04	2.28E-05	2.89E-03	2.15E-03	1.63E-01	1.42E-03	2.50E-05	2.03E-04	1.62E-06	1.66E-01
P99.9	9.64	-75.07	15099.86	3.54E-01	7.54E-02	2.16E-04	9.25E-02	1.48E-04	5.63E-05	4.31E-03	4.26E-03	2.58E-01	2.12E-03	6.52E-05	2.04E-04	4.84E-06	2.61E-01
Maximum	9.64	-73.76	15976.48	3.75E-01	7.96E-02	2.25E-04	9.80E-02	1.48E-04	5.75E-05	4.31E-03	4.26E-03	2.73E-01	2.23E-03	6.67E-05	2.04E-04	4.84E-06	2.76E-01
Glacial III: BASE CASE																	
	pH	Eh(mV) (HemC + FeSc)	TDS(mg/l)	IonicStr	mNa	mK	mCa	mMg	mFe(II) (HemC + FeSc)	mC	AlkTot	mCl	mS(VI)	mS(-II) (HemC + FeSc)	mSi	mP	Na+K+2Mg+2Ca
N total	28044	56088	28044	28044	28044	28044	28044	28044	56088	28044	28044	28044	28044	56088	28044	28044	28044
Mean	9.24	-340.42	301.40	6.62E-03	1.44E-03	1.57E-05	1.70E-03	1.07E-05	8.12E-07	3.01E-04	3.94E-04	4.43E-03	5.24E-05	9.39E-07	1.78E-04	1.20E-07	4.87E-03
Standard Deviation	0.58	41.36	1076.16	2.53E-02	5.40E-03	1.57E-05	6.59E-03	1.52E-05	3.11E-06	3.86E-04	3.39E-04	1.84E-02	1.55E-04	3.40E-06	2.44E-05	2.89E-07	1.86E-02
Minimum	6.59	-376.03	39.74	5.50E-04	7.40E-06	1.02E-05	1.67E-04	4.11E-06	3.95E-11	5.02E-05	8.21E-05	1.41E-05	5.31E-06	5.03E-18	1.24E-04	3.88E-09	3.60E-04
P0.1	6.64	-376.03	39.74	5.50E-04	7.40E-06	1.02E-05	1.67E-04	4.11E-06	3.95E-11	1.06E-04	1.68E-04	1.41E-05	5.31E-06	4.65E-17	1.26E-04	1.74E-08	3.60E-04
P5	7.92	-371.30	47.16	7.31E-04	5.90E-05	1.04E-05	2.08E-04	4.21E-06	5.12E-11	1.22E-04	2.00E-04	1.90E-04	6.75E-06	9.99E-08	1.37E-04	2.30E-08	5.00E-04
Median	9.50	-358.02	64.10	1.14E-03	1.92E-04	1.08E-05	2.91E-04	4.60E-06	4.31E-07	1.64E-04	3.06E-04	5.42E-04	1.09E-05	4.06E-07	1.85E-04	4.01E-08	8.08E-04
P95	9.64	-252.74	1139.30	2.65E-02	5.64E-03	3.38E-05	6.85E-03	3.73E-05	2.03E-06	1.02E-03	1.04E-03	1.89E-02	1.93E-04	2.54E-06	2.04E-04	5.27E-07	1.94E-02
P99.9	9.70	-93.94	11012.27	2.58E-01	5.50E-02	1.67E-04	6.71E-02	1.48E-04	4.36E-05	4.30E-03	4.24E-03	1.88E-01	1.58E-03	4.94E-05	2.14E-04	4.68E-06	1.90E-01
Maximum	9.70	-81.11	12814.59	3.00E-01	6.42E-02	1.89E-04	7.83E-02	1.48E-04	5.14E-05	4.31E-03	4.26E-03	2.18E-01	1.82E-03	5.90E-05	2.14E-04	4.84E-06	2.21E-01

Table A4-5. Continuation.

Glacial IV: BASE CASE																	
	pH	Eh(mV) (HemC + FeSc	TDS(mg/l)	IonicStr	mNa	mK	mCa	mMg	mFe(II) (HemC + FeSc)	mC	AlkTot	mCl	mS(VI)	mS(-II) (HemC + FeSc)	mSi	mP	Na+K+2Mg+2Ca
N total	28044	56088	28044	28044	28044	28044	28044	28044	56088	28044	28044	28044	28044	56088	28044	28044	28044
Mean	9.34	-347.50	94.28	1.76E-03	3.94E-04	1.27E-05	4.34E-04	8.32E-06	3.92E-07	2.41E-04	3.39E-04	9.27E-04	2.22E-05	4.96E-07	1.78E-04	9.34E-08	1.29E-03
Standard Deviation	0.33	22.88	55.02	1.15E-03	4.48E-04	5.27E-06	2.71E-04	1.15E-05	4.91E-07	3.26E-04	3.08E-04	8.08E-04	3.00E-05	5.66E-07	1.95E-05	2.62E-07	8.82E-04
Minimum	7.85	-376.03	39.74	5.50E-04	7.40E-06	1.02E-05	1.67E-04	4.11E-06	3.95E-11	8.23E-05	1.32E-04	1.41E-05	5.31E-06	9.96E-08	1.35E-04	1.05E-08	3.60E-04
P0.1	7.98	-376.03	39.74	5.50E-04	7.40E-06	1.02E-05	1.67E-04	4.11E-06	3.95E-11	8.70E-05	1.37E-04	1.41E-05	5.31E-06	9.96E-08	1.36E-04	1.16E-08	3.60E-04
P5	8.59	-370.27	47.20	7.32E-04	5.98E-05	1.04E-05	2.11E-04	4.19E-06	5.34E-11	1.09E-04	1.81E-04	1.90E-04	6.82E-06	9.99E-08	1.42E-04	1.87E-08	5.00E-04
Median	9.47	-355.74	72.71	1.35E-03	2.20E-04	1.09E-05	3.31E-04	4.51E-06	2.33E-07	1.49E-04	2.76E-04	7.18E-04	1.19E-05	4.04E-07	1.82E-04	3.41E-08	9.64E-04
P95	9.64	-296.63	202.80	4.12E-03	1.20E-03	2.20E-05	9.64E-04	2.81E-05	1.32E-06	7.98E-04	8.54E-04	2.49E-03	7.50E-05	1.53E-06	2.03E-04	3.98E-07	3.04E-03
P99.9	9.70	-251.31	490.38	9.43E-03	4.93E-03	7.63E-05	2.47E-03	1.48E-04	3.13E-06	4.30E-03	4.24E-03	6.70E-03	3.76E-04	4.85E-06	2.14E-04	4.68E-06	6.87E-03
Maximum	9.70	-240.71	516.71	1.16E-02	5.08E-03	7.66E-05	3.04E-03	1.48E-04	3.98E-06	4.30E-03	4.24E-03	8.29E-03	3.80E-04	6.30E-06	2.14E-04	4.68E-06	8.45E-03
Glacial V: BASE CASE																	
	pH	Eh(mV) (HemC + FeSc	TDS(mg/l)	IonicStr	mNa	mK	mCa	mMg	mFe(II) (HemC + FeSc)	mC	AlkTot	mCl	mS(VI)	mS(-II) (HemC + FeSc)	mSi	mP	Na+K+2Mg+2Ca
N total	28044	56088	28044	28044	28044	28044	28044	28044	56088	28044	28044	28044	28044	56088	28044	28044	28044
Mean	9.47	-356.18	69.10	1.19E-03	2.36E-04	1.18E-05	2.98E-04	7.08E-06	3.06E-07	2.24E-04	3.42E-04	4.98E-04	1.61E-05	4.42E-07	1.88E-04	7.85E-08	8.59E-04
Standard Deviation	0.28	19.96	35.90	7.05E-04	3.28E-04	3.93E-06	1.47E-04	8.49E-06	3.73E-07	2.36E-04	2.18E-04	4.72E-04	2.24E-05	4.53E-07	2.00E-05	1.78E-07	5.57E-04
Minimum	8.04	-375.86	40.03	5.58E-04	9.54E-06	1.02E-05	1.69E-04	4.12E-06	4.00E-11	8.78E-05	1.44E-04	2.18E-05	5.36E-06	9.96E-08	1.36E-04	1.22E-08	3.66E-04
P0.1	8.14	-375.74	40.14	5.61E-04	1.03E-05	1.02E-05	1.70E-04	4.12E-06	4.02E-11	9.24E-05	1.56E-04	2.45E-05	5.38E-06	9.96E-08	1.37E-04	1.36E-08	3.68E-04
P5	8.78	-373.35	42.71	6.23E-04	2.91E-05	1.03E-05	1.85E-04	4.14E-06	4.57E-11	1.20E-04	2.06E-04	8.65E-05	5.92E-06	9.98E-08	1.45E-04	2.27E-08	4.16E-04
Median	9.59	-363.83	53.84	8.90E-04	1.05E-04	1.05E-05	2.44E-04	4.30E-06	2.07E-07	1.63E-04	2.99E-04	3.29E-04	8.19E-06	4.00E-07	1.96E-04	3.95E-08	6.22E-04
P95	9.68	-308.54	146.58	2.70E-03	8.74E-04	1.93E-05	5.93E-04	2.31E-05	9.89E-07	6.48E-04	7.05E-04	1.44E-03	5.89E-05	1.22E-06	2.09E-04	3.03E-07	2.06E-03
P99.9	9.70	-267.22	371.03	5.61E-03	3.65E-03	5.91E-05	1.25E-03	1.11E-04	2.27E-06	3.23E-03	3.22E-03	3.27E-03	2.80E-04	3.51E-06	2.13E-04	3.14E-06	4.68E-03
Maximum	9.70	-253.31	439.23	6.43E-03	4.38E-03	6.89E-05	1.69E-03	1.32E-04	2.85E-06	3.84E-03	3.80E-03	4.52E-03	3.35E-04	5.09E-06	2.13E-04	3.99E-06	5.50E-03
Glacial Vr: BASE CASE																	
	pH	Eh(mV) (HemC + FeSc	TDS(mg/l)	IonicStr	mNa	mK	mCa	mMg	mFe(II) (HemC + FeSc)	mC	AlkTot	mCl	mS(VI)	mS(-II) (HemC + FeSc)	mSi	mP	Na+K+2Mg+2Ca
N total	28044	56088	28044	28044	28044	28044	28044	28044	56088	28044	28044	28044	28044	56088	28044	28044	28044
Mean	9.47	-356.39	68.80	1.19E-03	2.32E-04	1.18E-05	2.99E-04	6.94E-06	3.04E-07	2.20E-04	3.38E-04	4.99E-04	1.58E-05	4.39E-07	1.89E-04	7.54E-08	8.55E-04
Standard Deviation	0.28	19.65	34.92	6.96E-04	3.14E-04	3.71E-06	1.48E-04	8.00E-06	3.69E-07	2.21E-04	2.04E-04	4.73E-04	2.12E-05	4.44E-07	2.00E-05	1.61E-07	5.47E-04
Minimum	8.03	-376.03	39.74	5.50E-04	7.40E-06	1.02E-05	1.67E-04	4.11E-06	3.95E-11	8.75E-05	1.44E-04	1.41E-05	5.31E-06	9.96E-08	1.36E-04	1.21E-08	3.60E-04
P0.1	8.21	-376.03	39.74	5.50E-04	7.40E-06	1.02E-05	1.67E-04	4.11E-06	3.95E-11	9.23E-05	1.56E-04	1.41E-05	5.31E-06	9.96E-08	1.38E-04	1.37E-08	3.60E-04
P5	8.79	-371.64	39.74	5.50E-04	7.40E-06	1.02E-05	1.67E-04	4.11E-06	5.04E-11	1.20E-04	2.05E-04	1.41E-05	5.31E-06	9.98E-08	1.46E-04	2.25E-08	3.60E-04
Median	9.59	-364.40	55.19	9.27E-04	1.09E-04	1.05E-05	2.58E-04	4.29E-06	2.07E-07	1.62E-04	3.05E-04	3.66E-04	8.15E-06	3.99E-07	1.96E-04	3.94E-08	6.48E-04
P95	9.70	-309.51	143.84	2.72E-03	8.51E-04	1.90E-05	5.97E-04	2.23E-05	9.77E-07	6.24E-04	6.85E-04	1.42E-03	5.67E-05	1.19E-06	2.14E-04	2.85E-07	2.03E-03
P99.9	9.70	-269.10	337.30	4.91E-03	3.29E-03	5.43E-05	1.28E-03	1.00E-04	2.26E-06	2.92E-03	2.93E-03	3.36E-03	2.53E-04	3.41E-06	2.14E-04	2.75E-06	4.21E-03
Maximum	9.70	-252.17	442.13	6.53E-03	4.40E-03	6.89E-05	1.71E-03	1.32E-04	2.94E-06	3.83E-03	3.79E-03	4.59E-03	3.35E-04	5.17E-06	2.14E-04	3.95E-06	5.55E-03
Glacial IVr: BASE CASE																	
	pH	Eh(mV) (HemC + FeSc	TDS(mg/l)	IonicStr	mNa	mK	mCa	mMg	mFe(II) (HemC + FeSc)	mC	AlkTot	mCl	mS(VI)	mS(-II) (HemC + FeSc)	mSi	mP	Na+K+2Mg+2Ca
N total	28044	56088	28044	28044	28044	28044	28044	28044	56088	28044	28044	28044	28044	56088	28044	28044	28044
Mean	9.27	-342.20	132.17	2.72E-03	5.62E-04	1.25E-05	6.97E-04	6.90E-06	4.52E-07	1.81E-04	2.62E-04	1.70E-03	2.40E-05	4.84E-07	1.69E-04	5.82E-08	1.98E-03
Standard Deviation	0.24	17.01	67.64	1.61E-03	3.86E-04	3.47E-06	4.29E-04	7.73E-06	5.00E-07	2.23E-04	2.15E-04	1.22E-03	2.00E-05	4.76E-07	1.37E-05	1.54E-07	1.18E-03
Minimum	8.03	-364.74	63.48	1.05E-03	1.54E-04	1.05E-05	2.34E-04	4.15E-06	7.55E-11	7.22E-05	1.20E-04	3.87E-04	9.04E-06	1.00E-07	1.36E-04	8.46E-09	7.72E-04
P0.1	8.15	-364.74	63.48	1.13E-03	1.54E-04	1.05E-05	2.38E-04	4.15E-06	7.55E-11	7.45E-05	1.23E-04	4.39E-04	9.04E-06	1.00E-07	1.37E-04	8.86E-09	8.00E-04
P5	8.77	-361.95	63.56	1.13E-03	1.56E-04	1.06E-05	3.09E-04	4.17E-06	8.95E-11	8.85E-05	1.50E-04	5.42E-04	9.20E-06	1.00E-07	1.45E-04	1.28E-08	8.01E-04
Median	9.31	-345.08	112.82	2.25E-03	4.97E-04	1.15E-05	5.41E-04	4.40E-06	2.96E-07	1.18E-04	2.12E-04	1.25E-03	1.91E-05	4.04E-07	1.69E-04	2.20E-08	1.62E-03
P95	9.55	-308.20	257.75	5.71E-03	1.24E-03	1.84E-05	1.47E-03	2.10E-05	1.28E-06	5.82E-04	6.35E-04	3.90E-03	5.75E-05	1.27E-06	1.91E-04	2.55E-07	4.22E-03
P99.9	9.55	-265.28	549.43	1.28E-02	3.34E-03	5.44E-05	3.36E-03	1.00E-04	2.48E-06	2.91E-03	2.91E-03	9.16E-03	2.54E-04	3.62E-06	1.91E-04	2.64E-06	9.31E-03
Maximum	9.55	-252.17	600.15	1.40E-02	4.40E-03	6.89E-05	3.68E-03	1.32E-04	3.02E-06	3.83E-03	3.79E-03	1.00E-02	3.35E-04	5.17E-06	1.91E-04	3.95E-06	1.02E-02

Table A4-5. Continuation.

Glacial IIr: BASE CASE																	
	pH	Eh(mV) (HemC + FeSc	TDS(mg/l)	IonicStr	mNa	mK	mCa	mMg	mFe(II) (HemC + FeSc)	mC	AlkTot	mCl	mS(VI)	mS(-II) (HemC + FeSc)	mSi	mP	Na+K+2Mg+2Ca
N total	28044	56088	28044	28044	28044	28044	28044	28044	56088	28044	28044	28044	28044	56088	28044	28044	28044
Mean	9.39	-350.46	132.19	2.75E-03	5.25E-04	1.19E-05	7.20E-04	5.69E-06	3.83E-07	1.65E-04	2.67E-04	1.71E-03	2.10E-05	4.45E-07	1.80E-04	4.63E-08	1.99E-03
Standard Deviation	0.26	18.64	128.72	3.10E-03	6.47E-04	2.37E-06	8.15E-04	4.61E-06	4.70E-07	1.34E-04	1.37E-04	2.33E-03	1.90E-05	3.93E-07	2.02E-05	8.65E-08	2.26E-03
Minimum	8.27	-371.75	47.05	7.30E-04	5.63E-05	1.03E-05	1.84E-04	4.13E-06	5.02E-11	6.69E-05	1.16E-04	1.90E-04	6.55E-06	9.98E-08	1.38E-04	7.37E-09	4.98E-04
P0.1	8.40	-371.75	47.05	7.30E-04	5.63E-05	1.03E-05	1.86E-04	4.13E-06	5.02E-11	6.83E-05	1.18E-04	1.90E-04	6.55E-06	9.98E-08	1.39E-04	7.70E-09	4.98E-04
P5	8.93	-371.70	47.05	7.30E-04	5.65E-05	1.03E-05	2.11E-04	4.13E-06	5.03E-11	7.56E-05	1.28E-04	1.90E-04	6.56E-06	9.98E-08	1.50E-04	9.31E-09	4.98E-04
Median	9.50	-356.28	72.31	1.28E-03	2.04E-04	1.08E-05	3.13E-04	4.28E-06	2.23E-07	1.47E-04	2.74E-04	5.43E-04	1.15E-05	3.86E-07	1.85E-04	3.33E-08	9.59E-04
P95	9.65	-317.03	438.61	1.01E-02	2.03E-03	1.53E-05	2.66E-03	1.34E-05	1.45E-06	3.78E-04	4.59E-04	7.23E-03	5.90E-05	1.14E-06	2.04E-04	1.45E-07	7.38E-03
P99.9	9.65	-286.54	538.69	1.25E-02	2.51E-03	3.97E-05	3.30E-03	6.81E-05	1.79E-06	1.98E-03	2.02E-03	8.98E-03	1.71E-04	2.45E-06	2.04E-04	1.59E-06	9.12E-03
Maximum	9.65	-268.36	579.25	1.35E-02	2.93E-03	4.94E-05	3.55E-03	8.94E-05	2.10E-06	2.61E-03	2.63E-03	9.69E-03	2.25E-04	3.78E-06	2.04E-04	2.34E-06	9.83E-03
Glacial 0r: BASE CASE																	
	pH	Eh(mV) (HemC + FeSc	TDS(mg/l)	IonicStr	mNa	mK	mCa	mMg	mFe(II) (HemC + FeSc)	mC	AlkTot	mCl	mS(VI)	mS(-II) (HemC + FeSc)	mSi	mP	Na+K+2Mg+2Ca
N total	28044	56088.00	28044	28044	28044	28044	28044	28044	56088	28044	28044	28044	28044	56088	28044	28044	28044
Mean	8.71	-304.08	913.19	2.14E-02	4.35E-03	2.01E-05	5.63E-03	6.53E-06	1.16E-06	1.03E-04	1.43E-04	1.54E-02	1.18E-04	9.79E-07	1.46E-04	1.73E-08	1.56E-02
Standard Deviation	0.26	17.42	188.27	4.47E-03	9.31E-04	2.98E-06	1.17E-03	4.60E-06	1.34E-06	1.28E-04	1.18E-04	3.25E-03	2.68E-05	1.15E-06	3.80E-06	4.79E-08	3.27E-03
Minimum	7.25	-344.62	167.93	3.65E-03	6.95E-04	1.17E-05	9.67E-04	4.31E-06	2.65E-10	5.92E-05	1.00E-04	2.48E-03	2.29E-05	6.89E-09	1.34E-04	5.66E-09	2.65E-03
P0.1	7.42	-339.38	207.46	4.60E-03	8.89E-04	1.21E-05	1.21E-03	4.35E-06	3.74E-10	5.96E-05	1.01E-04	3.18E-03	2.78E-05	7.13E-08	1.35E-04	5.72E-09	3.34E-03
P5	8.05	-320.11	589.21	1.38E-02	2.75E-03	1.62E-05	3.62E-03	4.77E-06	1.55E-09	6.06E-05	1.03E-04	9.86E-03	7.57E-05	1.06E-07	1.37E-04	5.94E-09	1.00E-02
Median	8.79	-307.86	922.44	2.16E-02	4.37E-03	1.98E-05	5.64E-03	5.24E-06	9.79E-07	6.49E-05	1.09E-04	1.55E-02	1.18E-04	4.37E-07	1.47E-04	6.78E-09	1.58E-02
P95	8.93	-261.40	1193.58	2.80E-02	5.74E-03	2.54E-05	7.36E-03	1.43E-05	3.29E-06	3.17E-04	3.41E-04	2.02E-02	1.61E-04	2.85E-06	1.50E-04	6.73E-08	2.04E-02
P99.9	9.20	-219.45	1480.89	3.50E-02	7.13E-03	4.65E-05	9.21E-03	6.83E-05	8.41E-06	1.78E-03	1.64E-03	2.54E-02	2.58E-04	8.81E-06	1.62E-04	8.65E-07	2.55E-02
Maximum	9.26	-192.66	1541.98	3.65E-02	7.53E-03	5.75E-05	9.59E-03	8.94E-05	1.23E-05	2.36E-03	2.16E-03	2.64E-02	3.35E-04	1.39E-05	1.65E-04	1.37E-06	2.66E-02

Table A4-6. Statistical results for the main geochemical parameters obtained with the geochemical variant case 1 (Hem coup) over the glacial period in the repository volume. Chemical components in mol/kg, TDS in mg/L, pH in standard units and Eh in mV.

Glacial 0: Hematite coupled																	
	pH	Eh(mV)	TDS(mg/l)	IonicStr	mNa	mK	mCa	mMg	mFe+2	mC	AlkTot	mCl	mS(VI)	mS(-II)	mSi	mP	Na+K+2Mg+2Ca
N total	28044	28044	28044	28044	28044	28044	28044	28044	28044	28044	28044	28044	28044	28044	28044	28044	28044
Mean	7.38	-192.42	1789.15	3.76E-02	1.13E-02	8.90E-05	8.51E-03	1.47E-04	8.10E-07	3.92E-03	3.55E-03	2.44E-02	5.35E-04	9.63E-08	1.34E-04	3.39E-06	2.87E-02
Standard Deviation	0.44	51.81	2246.93	5.32E-02	1.09E-02	2.17E-05	1.41E-02	1.70E-06	6.92E-07	3.72E-04	6.34E-04	3.96E-02	2.70E-04	8.52E-08	2.22E-06	8.80E-07	3.91E-02
Minimum	6.56	-255.82	473.24	6.72E-03	4.83E-03	7.61E-05	3.22E-04	1.38E-04	3.54E-08	2.84E-03	2.09E-03	8.25E-04	3.74E-04	2.10E-18	1.23E-04	1.52E-06	5.85E-03
P0.1	6.57	-255.82	473.24	6.72E-03	4.83E-03	7.61E-05	3.22E-04	1.39E-04	3.54E-08	2.91E-03	2.14E-03	8.25E-04	3.74E-04	3.16E-18	1.24E-04	1.60E-06	5.85E-03
P5	6.66	-248.81	490.38	7.09E-03	4.93E-03	7.63E-05	4.20E-04	1.43E-04	5.65E-08	3.17E-03	2.36E-03	1.18E-03	3.76E-04	4.77E-17	1.29E-04	1.93E-06	6.14E-03
Median	7.45	-212.90	709.72	1.21E-02	6.09E-03	7.86E-05	1.73E-03	1.48E-04	5.46E-07	4.07E-03	3.78E-03	5.39E-03	4.05E-04	1.12E-07	1.35E-04	3.46E-06	9.92E-03
P95	7.98	-93.20	7371.90	1.70E-01	3.83E-02	1.43E-04	4.36E-02	1.48E-04	1.94E-06	4.30E-03	4.24E-03	1.23E-01	1.20E-03	2.03E-07	1.36E-04	4.68E-06	1.26E-01
P99.9	8.08	-78.49	12721.28	2.97E-01	6.40E-02	1.94E-04	7.74E-02	1.48E-04	2.27E-06	4.33E-03	4.30E-03	2.16E-01	1.84E-03	2.08E-07	1.36E-04	5.02E-06	2.19E-01
Maximum	8.08	-76.04	14216.67	3.33E-01	7.12E-02	2.08E-04	8.69E-02	1.48E-04	2.36E-06	4.33E-03	4.30E-03	2.42E-01	2.02E-03	2.08E-07	1.36E-04	5.02E-06	2.45E-01
Glacial I: Hematite coupled																	
	pH	Eh(mV)	TDS(mg/l)	IonicStr	mNa	mK	mCa	mMg	mFe+2	mC	AlkTot	mCl	mS(VI)	mS(-II)	mSi	mP	Na+K+2Mg+2Ca
N total	28044	28044	28044	28044	28044	28044	28044	28044	28044	28044	2.80E+04	28044	28044	28044	28044	28044	28044
Mean	6.88	-120.72	9088.66	2.11E-01	4.63E-02	1.55E-04	5.47E-02	1.33E-04	1.81E-06	2.99E-03	2.36E-03	1.53E-01	1.39E-03	2.11E-08	1.28E-04	1.88E-06	1.56E -01
Standard Deviation	0.56	64.88	7269.82	1.73E-01	3.52E-02	7.49E-05	4.57E-02	2.72E-05	8.07E-07	6.88E-04	6.44E-04	1.27E-01	8.92E-04	5.00E-08	7.44E-06	7.53E-07	1.27E-01
Minimum	6.49	-370.27	39.74	5.50E-04	7.40E-06	1.02E-05	1.67E-04	4.11E-06	3.95E-11	1.80E-04	2.41E-04	1.41E-05	5.31E-06	7.01E-19	1.11E-04	4.18E-08	3.60E-04
P0.1	6.49	-342.06	70.90	1.21E-03	2.91E-04	1.23E-05	2.21E-04	7.73E-06	1.85E-10	2.08E-04	3.08E-04	3.90E-04	1.91E-05	7.01E-19	1.12E-04	5.56E-08	8.93E-04
P5	6.51	-270.98	246.84	3.97E-03	2.02E-03	3.27E-05	4.70E-04	5.21E-05	1.49E-08	1.50E-03	1.52E-03	1.21E-03	1.39E-04	7.34E-19	1.16E-04	8.86E-07	3.30E-03
Median	6.64	-89.09	8482.17	1.96E-01	4.37E-02	1.53E-04	5.06E-02	1.41E-04	2.02E-06	3.03E-03	2.24E-03	1.42E-01	1.34E-03	2.18E-17	1.28E-04	1.76E-06	1.45E-01
P95	8.29	-68.74	22701.05	5.35E-01	1.12E-01	2.89E-04	1.41E-01	1.48E-04	2.82E-06	4.03E-03	3.73E-03	3.90E-01	3.03E-03	1.48E-07	1.39E-04	3.40E-06	3.93E -01
P99.9	9.32	-67.66	28061.57	6.63E-01	1.38E-01	3.40E-04	1.74E-01	1.48E-04	3.08E-06	4.31E-03	4.26E-03	4.84E-01	3.66E-03	2.06E-07	1.69E-04	4.84E-06	4.87E -01
Maximum	9.70	-67.66	29991.63	7.09E-01	1.47E-01	3.58E-04	1.87E-01	1.48E-04	3.17E-06	4.33E-03	4.30E-03	5.17E-01	3.90E-03	2.08E-07	2.14E-04	5.02E-06	5.21E -01
Glacial II: Hematite coupled																	
	pH	Eh(mV)	TDS(mg/l)	IonicStr	mNa	mK	mCa	mMg	mFe+2	mC	AlkTot	mCl	mS(VI)	mS(-II)	mSi	mP	Na+K+2Mg+2Ca
N total	28044	28044	28044	28044	28044	28044	28044	28044	28044	28044	28044	28044	28044	28044	28044	28044	28044
Mean	8.67	-290.38	1449.41	3.34E-02	7.30E-03	3.36E-05	8.64E-03	2.58E-05	3.09E-07	6.22E-04	6.16E-04	2.39E-02	2.25E-04	8.64E-08	1.61E-04	2.90E-07	2.47E -02
Standard Deviation	0.99	83.79	2994.23	7.00E-02	1.51E-02	4.43E-05	1.82E-02	3.71E-05	6.40E-07	8.21E-04	6.13E-04	5.10E-02	4.36E-04	3.99E-08	2.59E-05	5.14E-07	5.17E-02
Minimum	6.54	-365.71	47.12	7.31E-04	5.80E-05	1.04E-05	1.84E-04	4.18E-06	5.07E-11	4.84E-05	7.82E-05	1.90E-04	6.68E-06	1.44E-18	1.22E-04	3.48E-09	4.99E-04
P0.1	6.55	-365.71	47.13	7.31E-04	5.82E-05	1.04E-05	1.84E-04	4.18E-06	5.07E-11	9.96E-05	1.53E-04	1.90E-04	6.69E-06	1.71E-18	1.22E-04	1.51E-08	4.99E-04
P5	6.65	-365.14	47.31	7.33E-04	6.24E-05	1.04E-05	2.08E-04	4.29E-06	5.19E-11	1.17E-04	1.84E-04	1.91E-04	7.02E-06	2.93E-17	1.27E-04	2.06E-08	5.02E-04
Median	9.09	-325.70	112.23	2.06E-03	5.95E-04	1.36E-05	4.54E-04	8.35E-06	5.11E-10	2.08E-04	3.11E-04	1.07E-03	3.11E-05	1.01E-07	1.55E-04	5.08E-08	1.58E-03
P95	9.64	-90.74	9639.00	2.25E-01	4.87E-02	1.55E-04	5.85E-02	1.38E-04	2.01E-06	2.89E-03	2.15E-03	1.63E-01	1.42E-03	1.20E-07	2.03E-04	1.62E-06	1.66E-01
P99.9	9.64	-74.84	15099.86	3.54E-01	7.54E-02	2.16E-04	9.25E-02	1.48E-04	2.41E-06	4.31E-03	4.26E-03	2.58E-01	2.12E-03	2.06E-07	2.04E-04	4.84E-06	2.61E -01
Maximum	9.64	-73.76	15976.48	3.75E-01	7.96E-02	2.25E-04	9.80E-02	1.48E-04	2.46E-06	4.31E-03	4.26E-03	2.73E-01	2.23E-03	2.39E-07	2.04E-04	4.84E-06	2.76E -01
Glacial III: Hematite coupled																	
	pH	Eh(mV)	TDS(mg/l)	IonicStr	mNa	mK	mCa	mMg	mFe+2	mC	AlkTot	mCl	mS(VI)	mS(-II)	mSi	mP	Na+K+2Mg+2Ca
N total	28044	28044	28044	28044	28044	28044	28044	28044	28044	28044	28044	28044	28044	28044	28044	28044	28044
Mean	9.24	-336.40	301.40	6.62E-03	1.44E-03	1.57E-05	1.70E-03	1.07E-05	4.54E-08	3.01E-04	3.94E-04	4.43E-03	5.24E-05	1.01E-07	1.78E-04	1.20E-07	4.87E-03
Standard Deviation	0.58	44.10	1076.16	2.53E-02	5.40E-03	1.57E-05	6.59E-03	1.52E-05	2.37E-07	3.86E-04	3.39E-04	1.84E-02	1.55E-04	1.83E-08	2.44E-05	2.89E-07	1.86E-02
Minimum	6.59	-370.27	39.74	5.50E-04	7.40E-06	1.02E-05	1.67E-04	4.11E-06	3.95E-11	5.02E-05	8.21E-05	1.41E-05	5.31E-06	5.03E-18	1.24E-04	3.88E-09	3.60E-04
P0.1	6.64	-370.27	39.74	5.50E-04	7.40E-06	1.02E-05	1.67E-04	4.11E-06	3.95E-11	1.06E-04	1.68E-04	1.41E-05	5.31E-06	2.17E-17	1.26E-04	1.74E-08	3.60E-04
P5	7.92	-365.60	47.16	7.31E-04	5.90E-05	1.04E-05	2.08E-04	4.21E-06	5.09E-11	1.22E-04	2.00E-04	1.90E-04	6.75E-06	9.98E-08	1.37E-04	2.30E-08	5.00E-04
Median	9.50	-354.94	64.10	1.14E-03	1.92E-04	1.08E-05	2.91E-04	4.60E-06	9.41E-11	1.64E-04	3.06E-04	5.42E-04	1.09E-05	1.00E-07	1.85E-04	4.01E-08	8.08E-04
P95	9.64	-246.98	1139.30	2.65E-02	5.64E-03	3.38E-05	6.85E-03	3.73E-05	9.74E-08	1.02E-03	1.04E-03	1.89E-02	1.93E-04	1.21E-07	2.04E-04	5.27E-07	1.94E -02
P99.9	9.70	-89.43	11012.27	2.58E-01	5.50E-02	1.67E-04	6.71E-02	1.48E-04	2.07E-06	4.30E-03	4.24E-03	1.88E-01	1.58E-03	2.03E-07	2.14E-04	4.68E-06	1.90E-01
Maximum	9.70	-81.11	12814.59	3.00E-01	6.42E-02	1.89E-04	7.83E-02	1.48E-04	2.21E-06	4.31E-03	4.26E-03	2.18E-01	1.82E-03	2.06E-07	2.14E-04	4.84E-06	2.21E-01

Table A4-6. Continuation.

Glacial IV: Hematite coupled																	
	pH	Eh(mV)	TDS(mg/l)	IonicStr	mNa	mK	mCa	mMg	mFe+2	mC	AlkTot	mCl	mS(VI)	mS(-II)	mSi	mP	Na+K+2Mg+2Ca
N total	28044	28044	28044	28044	28044	28044	28044	28044	28044	28044	28044	28044	28044	28044	28044	28044	28044
Mean	9.34	-344.19	94.28	1.76E-03	3.94E-04	1.27E-05	4.34E-04	8.32E-06	9.31E-10	2.41E-04	3.39E-04	9.27E-04	2.22E-05	1.03E-07	1.78E-04	9.34E-08	1.29E-03
Standard Deviation	0.33	23.18	55.02	1.15E-03	4.48E-04	5.27E-06	2.71E-04	1.15E-05	3.96E-09	3.26E-04	3.08E-04	8.08E-04	3.00E-05	8.65E-09	1.95E-05	2.62E-07	8.82E-04
Minimum	7.85	-370.27	39.74	5.50E-04	7.40E-06	1.02E-05	1.67E-04	4.11E-06	3.95E-11	8.23E-05	1.32E-04	1.41E-05	5.31E-06	9.96E-08	1.35E-04	1.05E-08	3.60E-04
P0.1	7.98	-370.27	39.74	5.50E-04	7.40E-06	1.02E-05	1.67E-04	4.11E-06	3.95E-11	8.70E-05	1.37E-04	1.41E-05	5.31E-06	9.96E-08	1.36E-04	1.16E-08	3.60E-04
P5	8.59	-365.48	47.20	7.32E-04	5.98E-05	1.04E-05	2.11E-04	4.19E-06	5.12E-11	1.09E-04	1.81E-04	1.90E-04	6.82E-06	9.99E-08	1.42E-04	1.87E-08	5.00E-04
Median	9.47	-352.77	72.71	1.35E-03	2.20E-04	1.09E-05	3.31E-04	4.51E-06	1.07E-10	1.49E-04	2.76E-04	7.18E-04	1.19E-05	1.01E-07	1.82E-04	3.41E-08	9.64E-04
P95	9.64	-292.07	202.80	4.12E-03	1.20E-03	2.20E-05	9.64E-04	2.81E-05	3.97E-09	7.98E-04	8.54E-04	2.49E-03	7.50E-05	1.20E-07	2.03E-04	3.98E-07	3.04E-03
P99.9	9.70	-248.81	490.38	9.43E-03	4.93E-03	7.63E-05	2.47E-03	1.48E-04	5.65E-08	4.30E-03	4.24E-03	6.70E-03	3.76E-04	2.03E-07	2.14E-04	4.68E-06	6.87E-03
Maximum	9.70	-240.71	516.71	1.16E-02	5.08E-03	7.66E-05	3.04E-03	1.48E-04	9.64E-08	4.30E-03	4.24E-03	8.29E-03	3.80E-04	2.03E-07	2.14E-04	4.68E-06	8.45E-03
Glacial V: Hematite coupled																	
	pH	Eh(mV)	TDS(mg/l)	IonicStr	mNa	mK	mCa	mMg	mFe+2	mC	AlkTot	mCl	mS(VI)	mS(-II)	mSi	mP	Na+K+2Mg+2Ca
N total	28044	28044	28044	28044	28044	28044	28044	28044	28044	28044	28044	28044	28044	28044	28044	28044	28044
Mean	9.47	-353.02	69.10	1.19E-03	2.36E-04	1.18E-05	2.98E-04	7.08E-06	4.08E-10	2.24E-04	3.42E-04	4.98E-04	1.61E-05	1.02E-07	1.88E-04	7.85E-08	8.59E-04
Standard Deviation	0.28	20.15	35.90	7.05E-04	3.28E-04	3.93E-06	1.47E-04	8.49E-06	1.65E-09	2.36E-04	2.18E-04	4.72E-04	2.24E-05	6.73E-09	2.00E-05	1.78E-07	5.57E-04
Minimum	8.04	-370.04	40.03	5.58E-04	9.54E-06	1.02E-05	1.69E-04	4.12E-06	4.00E-11	8.78E-05	1.44E-04	2.18E-05	5.36E-06	9.96E-08	1.36E-04	1.22E-08	3.66E-04
P0.1	8.14	-369.99	40.14	5.61E-04	1.03E-05	1.02E-05	1.70E-04	4.12E-06	4.01E-11	9.24E-05	1.56E-04	2.45E-05	5.38E-06	9.96E-08	1.37E-04	1.36E-08	3.68E-04
P5	8.78	-368.22	42.71	6.23E-04	2.91E-05	1.03E-05	1.85E-04	4.14E-06	4.40E-11	1.20E-04	2.06E-04	8.65E-05	5.92E-06	9.97E-08	1.45E-04	2.27E-08	4.16E-04
Median	9.59	-361.67	53.84	8.90E-04	1.05E-04	1.05E-05	2.44E-04	4.30E-06	6.32E-11	1.63E-04	2.99E-04	3.29E-04	8.19E-06	1.00E-07	1.96E-04	3.95E-08	6.22E-04
P95	9.68	-304.32	146.58	2.70E-03	8.74E-04	1.93E-05	5.93E-04	2.31E-05	1.80E-09	6.48E-04	7.05E-04	1.44E-03	5.89E-05	1.16E-07	2.09E-04	3.03E-07	2.06E-03
P99.9	9.70	-259.81	371.03	5.61E-03	3.65E-03	5.91E-05	1.25E-03	1.11E-04	2.74E-08	3.23E-03	3.22E-03	3.27E-03	2.80E-04	1.81E-07	2.13E-04	3.14E-06	4.68E-03
Maximum	9.70	-253.31	439.23	6.43E-03	4.38E-03	6.89E-05	1.69E-03	1.32E-04	4.20E-08	3.84E-03	3.80E-03	4.52E-03	3.35E-04	1.94E-07	2.13E-04	3.99E-06	5.50E-03
Glacial Vr: Hematite coupled																	
	pH	Eh(mV)	TDS(mg/l)	IonicStr	mNa	mK	mCa	mMg	mFe+2	mC	AlkTot	mCl	mS(VI)	mS(-II)	mSi	mP	Na+K+2Mg+2Ca
N total	28044	28044	28044	28044	28044	28044	28044	28044	28044	28044	28044	28044	28044	28044	28044	28044	28044
Mean	9.47	-353.24	68.80	1.19E-03	2.32E-04	1.18E-05	2.99E-04	6.94E-06	3.82E-10	2.20E-04	3.38E-04	4.99E-04	1.58E-05	1.02E-07	1.89E-04	7.54E-08	8.55E-04
Standard Deviation	0.28	19.84	34.92	6.96E-04	3.14E-04	3.71E-06	1.48E-04	8.00E-06	1.47E-09	2.21E-04	2.04E-04	4.73E-04	2.12E-05	6.38E-09	2.00E-05	1.61E-07	5.47E-04
Minimum	8.03	-370.27	39.74	5.50E-04	7.40E-06	1.02E-05	1.67E-04	4.11E-06	3.95E-11	8.75E-05	1.44E-04	1.41E-05	5.31E-06	9.96E-08	1.36E-04	1.21E-08	3.60E-04
P0.1	8.21	-370.27	39.74	5.50E-04	7.40E-06	1.02E-05	1.67E-04	4.11E-06	3.95E-11	9.23E-05	1.56E-04	1.41E-05	5.31E-06	9.96E-08	1.38E-04	1.37E-08	3.60E-04
P5	8.79	-370.27	39.74	5.50E-04	7.40E-06	1.02E-05	1.67E-04	4.11E-06	3.95E-11	1.20E-04	2.05E-04	1.41E-05	5.31E-06	9.96E-08	1.46E-04	2.25E-08	3.60E-04
Median	9.59	-361.55	55.19	9.27E-04	1.09E-04	1.05E-05	2.58E-04	4.29E-06	6.40E-11	1.62E-04	3.05E-04	3.66E-04	8.15E-06	1.00E-07	1.96E-04	3.94E-08	6.48E-04
P95	9.70	-305.24	143.84	2.72E-03	8.51E-04	1.90E-05	5.97E-04	2.23E-05	1.68E-09	6.24E-04	6.85E-04	1.42E-03	5.67E-05	1.15E-07	2.14E-04	2.85E-07	2.03E-03
P99.9	9.70	-264.59	337.30	4.91E-03	3.29E-03	5.43E-05	1.28E-03	1.00E-04	2.00E-08	2.92E-03	2.93E-03	3.36E-03	2.53E-04	1.74E-07	2.14E-04	2.75E-06	4.21E-03
Maximum	9.70	-252.17	442.13	6.53E-03	4.40E-03	6.89E-05	1.71E-03	1.32E-04	4.53E-08	3.83E-03	3.79E-03	4.59E-03	3.35E-04	1.93E-07	2.14E-04	3.95E-06	5.55E-03
Glacial IVr: Hematite coupled																	
	pH	Eh(mV)	TDS(mg/l)	IonicStr	mNa	mK	mCa	mMg	mFe+2	mC	AlkTot	mCl	mS(VI)	mS(-II)	mSi	mP	Na+K+2Mg+2Ca
N total	28044	28044	28044	28044	28044	28044	28044	28044	28044	28044	28044	28044	28044	28044	28044	28044	28044
Mean	9.27	-338.80	132.17	2.72E-03	5.62E-04	1.25E-05	6.97E-04	6.90E-06	5.74E-10	1.81E-04	2.62E-04	1.70E-03	2.40E-05	1.03E-07	1.69E-04	5.82E-08	1.98E-03
Standard Deviation	0.24	17.10	67.64	1.61E-03	3.86E-04	3.47E-06	4.29E-04	7.73E-06	1.77E-09	2.23E-04	2.15E-04	1.22E-03	2.00E-05	5.93E-09	1.37E-05	1.54E-07	1.18E-03
Minimum	8.03	-358.87	63.48	1.05E-03	1.54E-04	1.05E-05	2.34E-04	4.15E-06	7.55E-11	7.22E-05	1.20E-04	3.87E-04	9.04E-06	1.00E-07	1.36E-04	8.46E-09	7.72E-04
P0.1	8.15	-358.87	63.48	1.13E-03	1.54E-04	1.05E-05	2.38E-04	4.15E-06	7.55E-11	7.45E-05	1.23E-04	4.39E-04	9.04E-06	1.00E-07	1.37E-04	8.86E-09	8.00E-04
P5	8.77	-358.53	63.56	1.13E-03	1.56E-04	1.06E-05	3.09E-04	4.17E-06	7.66E-11	8.85E-05	1.50E-04	5.42E-04	9.20E-06	1.00E-07	1.45E-04	1.28E-08	8.01E-04
Median	9.31	-341.54	112.82	2.25E-03	4.97E-04	1.15E-05	5.41E-04	4.40E-06	2.11E-10	1.18E-04	2.12E-04	1.25E-03	1.91E-05	1.01E-07	1.69E-04	2.20E-08	1.62E-03
P95	9.55	-303.92	257.75	5.71E-03	1.24E-03	1.84E-05	1.47E-03	2.10E-05	1.91E-09	5.82E-04	6.35E-04	3.90E-03	5.75E-05	1.14E-07	1.91E-04	2.55E-07	4.22E-03
P99.9	9.55	-260.60	549.43	1.28E-02	3.34E-03	5.44E-05	3.36E-03	1.00E-04	2.62E-08	2.91E-03	2.91E-03	9.16E-03	2.54E-04	1.72E-07	1.91E-04	2.64E-06	9.31E-03
Maximum	9.55	-252.17	600.15	1.40E-02	4.40E-03	6.89E-05	3.68E-03	1.32E-04	4.53E-08	3.83E-03	3.79E-03	1.00E-02	3.35E-04	1.93E-07	1.91E-04	3.95E-06	1.02E-02

Table A4-6. Continuation.

Glacial IIr: Hematite coupled																	
	pH	Eh(mV)	TDS(mg/l)	IonicStr	mNa	mK	mCa	mMg	mFe+2	mC	AlkTot	mCl	mS(VI)	mS(-II)	mSi	mP	Na+K+2Mg+2Ca
N total	28044	28044	28044	28044	28044	28044	28044	28044	28044	28044	28044	28044	28044	28044	28044	28044	28044
Mean	9.39	-347.17	132.19	2.75E-03	5.25E-04	1.19E-05	7.20E-04	5.69E-06	3.15E-10	1.65E-04	2.67E-04	1.71E-03	2.10E-05	1.02E-07	1.80E-04	4.63E-08	1.99E-03
Standard Deviation	0.26	18.79	128.72	3.10E-03	6.47E-04	2.37E-06	8.15E-04	4.61E-06	5.53E-10	1.34E-04	1.37E-04	2.33E-03	1.90E-05	3.83E-09	2.02E-05	8.65E-08	2.26E-03
Minimum	8.27	-365.94	47.05	7.30E-04	5.63E-05	1.03E-05	1.84E-04	4.13E-06	5.02E-11	6.69E-05	1.16E-04	1.90E-04	6.55E-06	9.98E-08	1.38E-04	7.37E-09	4.98E-04
P0.1	8.40	-365.94	47.05	7.30E-04	5.63E-05	1.03E-05	1.86E-04	4.13E-06	5.02E-11	6.83E-05	1.18E-04	1.90E-04	6.55E-06	9.98E-08	1.39E-04	7.70E-09	4.98E-04
P5	8.93	-365.94	47.05	7.30E-04	5.65E-05	1.03E-05	2.11E-04	4.13E-06	5.03E-11	7.56E-05	1.28E-04	1.90E-04	6.56E-06	9.98E-08	1.50E-04	9.31E-09	4.98E-04
Median	9.50	-354.83	72.31	1.28E-03	2.04E-04	1.08E-05	3.13E-04	4.28E-06	9.16E-11	1.47E-04	2.74E-04	5.43E-04	1.15E-05	1.00E-07	1.85E-04	3.33E-08	9.59E-04
P95	9.65	-314.47	438.61	1.01E-02	2.03E-03	1.53E-05	2.66E-03	1.34E-05	1.13E-09	3.78E-04	4.59E-04	7.23E-03	5.90E-05	1.08E-07	2.04E-04	1.45E-07	7.38E-03
P99.9	9.65	-277.59	538.69	1.25E-02	2.51E-03	3.97E-05	3.30E-03	6.81E-05	8.69E-09	1.98E-03	2.02E-03	8.98E-03	1.71E-04	1.51E-07	2.04E-04	1.59E-06	9.12E-03
Maximum	9.65	-268.36	579.25	1.35E-02	2.93E-03	4.94E-05	3.55E-03	8.94E-05	1.57E-08	2.61E-03	2.63E-03	9.69E-03	2.25E-04	1.66E-07	2.04E-04	2.34E-06	9.83E-03
Glacial 0r: Hematite coupled																	
	pH	Eh(mV)	TDS(mg/l)	IonicStr	mNa	mK	mCa	mMg	mFe+2	mC	AlkTot	mCl	mS(VI)	mS(-II)	mSi	mP	Na+K+2Mg+2Ca
N total	28044	28044	28044	28044	28044	28044	28044	28044	28044	28044	28044	28044	28044	28044	28044	28044	28044
Mean	8.71	-299.30	913.19	2.14E-02	4.35E-03	2.01E-05	5.63E-03	6.53E-06	1.20E-08	1.03E-04	1.43E-04	1.54E-02	1.18E-04	1.08E-07	1.46E-04	1.73E-08	1.56E- 02
Standard Deviation	0.26	17.25	188.27	4.47E-03	9.31E-04	2.98E-06	1.17E-03	4.60E-06	4.67E-08	1.28E-04	1.18E-04	3.25E-03	2.68E-05	3.90E-09	3.80E-06	4.79E-08	3.27E-03
Minimum	7.25	-337.90	167.93	3.65E-03	6.95E-04	1.17E-05	9.67E-04	4.31E-06	2.65E-10	5.92E-05	1.00E-04	2.48E-03	2.29E-05	6.89E-09	1.34E-04	5.66E-09	2.65E- 03
P0.1	7.42	-333.79	207.46	4.60E-03	8.89E-04	1.21E-05	1.21E-03	4.35E-06	3.42E-10	5.96E-05	1.01E-04	3.18E-03	2.78E-05	4.97E-08	1.35E-04	5.72E-09	3.34E- 03
P5	8.05	-313.67	589.21	1.38E-02	2.75E-03	1.62E-05	3.62E-03	4.77E-06	1.23E-09	6.06E-05	1.03E-04	9.86E-03	7.57E-05	1.04E-07	1.37E-04	5.94E-09	1.00E- 02
Median	8.79	-304.21	922.44	2.16E-02	4.37E-03	1.98E-05	5.64E-03	5.24E-06	2.33E-09	6.49E-05	1.09E-04	1.55E-02	1.18E-04	1.09E-07	1.47E-04	6.78E-09	1.58E- 02
P95	8.93	-255.65	1193.58	2.80E-02	5.74E-03	2.54E-05	7.36E-03	1.43E-05	5.67E-08	3.17E-04	3.41E-04	2.02E-02	1.61E-04	1.11E-07	1.50E-04	6.73E-08	2.04E -02
P99.9	9.20	-210.33	1480.89	3.50E-02	7.13E-03	4.65E-05	9.21E-03	6.83E-05	6.95E-07	1.78E-03	1.64E-03	2.54E-02	2.58E-04	1.14E-07	1.62E-04	8.65E-07	2.55E -02
Maximum	9.26	-192.66	1541.98	3.65E-02	7.53E-03	5.75E-05	9.59E-03	8.94E-05	1.11E-06	2.36E-03	2.16E-03	2.64E-02	3.35E-04	1.15E-07	1.65E-04	1.37E-06	2.66E -02

Table A4-7. Statistical results for the main geochemical parameters obtained with the geochemical variant case 2 (FeS coup) over the glacial period in the repository volume. Chemical components in mol/kg, TDS in mg/L, pH in standard units and Eh in mV.

Glacial 0: Eq. FeS(am) Coupled																	
	pH	Eh(mV)	TDS(mg/l)	onicStr	mNa	mK	mCa	mMg	mFe+2	mC	AlkTot	mCl	mS(VI)	mS(-II)	mSi	mP	Na+K+2Mg+2Ca
N total	28044	28044	28044	28044	28044	28044	28044	28044	28044	28044	28044	28044	28044	28044	28044	28044	28044
Mean	7.38	-222.89	1791.02	3.76E-02	1.13E-02	8.90E-05	8.49E-03	1.47E-04	1.37E-05	3.90E-03	3.56E-03	2.44E-02	5.58E-04	1.71E-05	1.34E-04	3.37E-06	2.87E -02
Standard Deviation	0.44	26.73	2247.43	5.32E-02	1.09E-02	2.17E-05	1.41E-02	1.70E-06	1.27E-05	3.88E-04	6.38E-04	3.96E-02	2.84E-04	1.39E-05	2.22E-06	8.96E-07	3.91E-02
Minimum	6.57	-266.08	474.68	6.71E-03	4.83E-03	7.61E-05	3.19E-04	1.38E-04	2.60E-06	2.77E-03	2.09E-03	8.25E-04	3.85E-04	5.09E-06	1.23E-04	1.46E-06	5.84E-03
P0.1	6.58	-266.08	474.68	6.71E-03	4.83E-03	7.61E-05	3.19E-04	1.39E-04	2.60E-06	2.84E-03	2.14E-03	8.25E-04	3.85E-04	5.09E-06	1.24E-04	1.54E-06	5.84E-03
P5	6.67	-259.41	491.79	7.09E-03	4.93E-03	7.63E-05	4.15E-04	1.43E-04	3.13E-06	3.12E-03	2.36E-03	1.18E-03	3.88E-04	5.59E-06	1.29E-04	1.88E-06	6.14E-03
Median	7.45	-227.15	711.32	1.21E-02	6.09E-03	7.86E-05	1.71E-03	1.48E-04	7.59E-06	4.06E-03	3.80E-03	5.39E-03	4.22E-04	1.04E-05	1.35E-04	3.44E-06	9.90E-03
P95	7.98	-179.27	7374.59	1.70E-01	3.83E-02	1.43E-04	4.36E-02	1.48E-04	4.28E-05	4.30E-03	4.25E-03	1.23E-01	1.26E-03	4.89E-05	1.36E-04	4.68E-06	1.26E-01
P99.9	8.09	-173.74	12724.60	2.97E-01	6.40E-02	1.94E-04	7.74E-02	1.48E-04	5.35E-05	4.33E-03	4.31E-03	2.16E-01	1.91E-03	6.15E-05	1.36E-04	5.02E-06	2.19E-01
Maximum	8.09	-172.77	14220.29	3.33E-01	7.12E-02	2.08E-04	8.68E-02	1.48E-04	5.55E-05	4.33E-03	4.31E-03	2.42E-01	2.09E-03	6.41E-05	1.36E-04	5.02E-06	2.45E-01
Glacial I: Eq. FeS(am) Coupled																	
	pH	Eh(mV)	TDS(mg/l)	onicStr	mNa	mK	mCa	mMg	mFe+2	mC	AlkTot	mCl	mS(VI)	mS(-II)	mSi	mP	Na+K+2Mg+2Ca
N total	28044	28044	28044	28044	28044	28044	28044	28044	28044	28044	2.80E+04	28044	28044	28044	28044	28044	28044
Mean	6.89	-192.99	9091.47	2.11E-01	4.63E-02	1.55E-04	5.46E-02	1.33E-04	3.84E-05	2.94E-03	2.37E-03	1.53E-01	1.44E-03	4.48E-05	1.28E-04	1.84E-06	1.56E-01
Standard Deviation	0.55	34.71	7270.49	1.73E-01	3.52E-02	7.49E-05	4.57E-02	2.72E-05	1.99E-05	6.93E-04	6.49E-04	1.27E-01	9.14E-04	2.30E-05	7.46E-06	7.61E-07	1.27E-01
Minimum	6.50	-376.03	40.87	5.51E-04	7.40E-06	1.02E-05	1.67E-04	4.11E-06	3.69E-07	1.80E-04	2.54E-04	1.41E-05	1.22E-05	6.07E-07	1.11E-04	4.11E-08	3.60E-04
P0.1	6.50	-348.90	71.98	1.21E-03	2.91E-04	1.23E-05	2.19E-04	7.73E-06	6.72E-07	2.08E-04	3.20E-04	3.90E-04	2.63E-05	8.47E-07	1.12E-04	5.50E-08	8.91E-04
P5	6.52	-281.30	247.96	3.97E-03	2.02E-03	3.27E-05	4.65E-04	5.21E-05	2.26E-06	1.50E-03	1.53E-03	1.21E-03	1.50E-04	3.27E-06	1.16E-04	8.84E-07	3.29E-03
Median	6.64	-177.78	8485.25	1.96E-01	4.37E-02	1.53E-04	5.06E-02	1.41E-04	4.55E-05	2.97E-03	2.24E-03	1.42E-01	1.40E-03	5.20E-05	1.28E-04	1.70E-06	1.45E-01
P95	8.29	-169.40	22704.03	5.35E-01	1.12E-01	2.89E-04	1.40E-01	1.48E-04	6.20E-05	4.02E-03	3.75E-03	3.90E-01	3.11E-03	7.36E-05	1.39E-04	3.38E-06	3.93E-01
P99.9	9.33	-168.49	28064.71	6.62E-01	1.38E-01	3.40E-04	1.74E-01	1.48E-04	6.29E-05	4.31E-03	4.28E-03	4.84E-01	3.75E-03	7.63E-05	1.69E-04	4.84E-06	4.87E-01
Maximum	9.71	-168.32	29994.77	7.09E-01	1.47E-01	3.58E-04	1.87E-01	1.48E-04	6.29E-05	4.33E-03	4.31E-03	5.17E-01	3.98E-03	7.68E-05	2.14E-04	5.02E-06	5.20E-01
Glacial II: Eq. FeS(am) Coupled																	
	pH	Eh(mV)	TDS(mg/l)	onicStr	mNa	mK	mCa	mMg	mFe+2	mC	AlkTot	mCl	mS(VI)	mS(-II)	mSi	mP	Na+K+2Mg+2Ca
N total	28044	28044	28044	28044	28044	28044	28044	28044	28044	28044	28044	28044	28044	28044	28044	28044	28044
Mean	8.68	-307.72	1450.75	3.34E-02	7.30E-03	3.36E-05	8.63E-03	2.58E-05	6.81E-06	6.14E-04	6.28E-04	2.39E-02	2.39E-04	7.56E-06	1.61E-04	2.84E-07	2.46E -02
Standard Deviation	0.99	63.40	2994.79	7.00E-02	1.51E-02	4.43E-05	1.82E-02	3.71E-05	1.30E-05	8.06E-04	6.10E-04	5.10E-02	4.51E-04	1.48E-05	2.62E-05	5.02E-07	5.17E-02
Minimum	6.55	-371.53	48.25	7.32E-04	5.80E-05	1.04E-05	1.83E-04	4.18E-06	4.31E-07	4.33E-05	9.05E-05	1.90E-04	1.36E-05	6.08E-07	1.22E-04	2.93E-09	4.99E-04
P0.1	6.56	-371.53	48.26	7.32E-04	5.82E-05	1.04E-05	1.83E-04	4.18E-06	4.31E-07	9.83E-05	1.66E-04	1.90E-04	1.36E-05	6.08E-07	1.22E-04	1.47E-08	4.99E-04
P5	6.65	-370.96	48.45	7.34E-04	6.24E-05	1.04E-05	2.08E-04	4.29E-06	4.34E-07	1.16E-04	1.97E-04	1.91E-04	1.39E-05	6.14E-07	1.27E-04	2.02E-08	5.02E-04
Median	9.09	-333.22	113.29	2.06E-03	5.95E-04	1.36E-05	4.50E-04	8.35E-06	9.62E-07	2.06E-04	3.25E-04	1.07E-03	3.84E-05	1.08E-06	1.56E-04	4.99E-08	1.58E-03
P95	9.64	-178.41	9642.24	2.25E-01	4.87E-02	1.55E-04	5.84E-02	1.38E-04	4.47E-05	2.83E-03	2.15E-03	1.63E-01	1.48E-03	5.09E-05	2.03E-04	1.57E-06	1.66E-01
P99.9	9.65	-172.25	15103.53	3.54E-01	7.54E-02	2.16E-04	9.24E-02	1.48E-04	5.65E-05	4.31E-03	4.28E-03	2.58E-01	2.20E-03	6.55E-05	2.04E-04	4.84E-06	2.61E-01
Maximum	9.65	-171.80	15980.35	3.75E-01	7.96E-02	2.25E-04	9.79E-02	1.48E-04	5.75E-05	4.31E-03	4.28E-03	2.73E-01	2.30E-03	6.67E-05	2.04E-04	4.84E-06	2.76E-01
Glacial III: Eq. FeS(am) C oupled																	
	pH	Eh(mV)	TDS(mg/l)	onicStr	mNa	mK	mCa	mMg	mFe+2	mC	AlkTot	mCl	mS(VI)	mS(-II)	mSi	mP	Na+K+2Mg+2Ca
N total	28044	28044	28044	28044	28044	28044	28044	28044	28044	28044	28044	28044	28044	28044	28044	28044	28044
Mean	9.25	-344.44	302.53	6.62E-03	1.44E-03	1.57E-05	1.69E-03	1.07E-05	1.58E-06	2.99E-04	4.08E-04	4.43E-03	6.04E-05	1.78E-06	1.78E-04	1.18E-07	4.86E-03
Standard Deviation	0.58	37.99	1076.32	2.53E-02	5.40E-03	1.57E-05	6.59E-03	1.52E-05	4.26E-06	3.83E-04	3.39E-04	1.84E-02	1.59E-04	4.67E-06	2.46E-05	2.88E-07	1.86E-02
Minimum	6.60	-376.03	40.87	5.51E-04	7.40E-06	1.02E-05	1.67E-04	4.11E-06	3.69E-07	4.58E-05	9.45E-05	1.41E-05	1.22E-05	6.07E-07	1.24E-04	3.36E-09	3.60E-04
P0.1	6.65	-376.03	40.87	5.51E-04	7.40E-06	1.02E-05	1.67E-04	4.11E-06	3.69E-07	1.05E-04	1.81E-04	1.41E-05	1.22E-05	6.07E-07	1.26E-04	1.70E-08	3.60E-04
P5	7.93	-371.41	48.29	7.32E-04	5.90E-05	1.04E-05	2.08E-04	4.21E-06	4.32E-07	1.21E-04	2.13E-04	1.90E-04	1.37E-05	6.09E-07	1.37E-04	2.26E-08	4.99E-04
Median	9.50	-360.98	65.20	1.14E-03	1.92E-04	1.08E-05	2.90E-04	4.60E-06	5.68E-07	1.64E-04	3.21E-04	5.42E-04	1.78E-05	6.49E-07	1.86E-04	3.97E-08	8.07E-04
P95	9.65	-259.35	1140.41	2.65E-02	5.64E-03	3.38E-05	6.85E-03	3.73E-05	5.30E-06	1.01E-03	1.05E-03	1.89E-02	2.04E-04	5.21E-06	2.04E-04	5.25E-07	1.94E-02
P99.9	9.71	-178.30	11015.10	2.58E-01	5.50E-02	1.67E-04	6.71E-02	1.48E-04	4.60E-05	4.30E-03	4.25E-03	1.88E-01	1.64E-03	5.22E-05	2.14E-04	4.68E-06	1.90E-01
Maximum	9.71	-174.82	12817.59	3.00E-01	6.42E-02	1.89E-04	7.82E-02	1.48E-04	5.14E-05	4.31E-03	4.28E-03	2.18E-01	1.89E-03	5.90E-05	2.14E-04	4.84E-06	2.21E-01

Table A4-7. Continuation.

Glacial IV : Eq. FeS(am) Coupled																	
	pH	Eh(mV)	TDS(mg/l)	IonicStr	mNa	mK	mCa	mMg	mFe+2	mC	AlkTot	mCl	mS(VI)	mS(-II)	mSi	mP	Na+K+2Mg+2Ca
N total	28044	28044	28044	28044	28044	28044	28044	28044	28044	28044	28044	28044	28044	28044	28044	28044	28044
Mean	9.35	-350.82	95.38	1.76E-03	3.94E-04	1.27E-05	4.33E-04	8.32E-06	7.83E-07	2.40E-04	3.53E-04	9.27E-04	2.94E-05	8.89E-07	1.78E-04	9.28E-08	1.29E-03
Standard Deviation	0.33	22.10	55.01	1.15E-03	4.48E-04	5.27E-06	2.71E-04	1.15E-05	4.19E-07	3.25E-04	3.08E-04	8.08E-04	3.05E-05	5.77E-07	1.96E-05	2.62E-07	8.81E-04
Minimum	7.86	-376.03	40.87	5.51E-04	7.40E-06	1.02E-05	1.67E-04	4.11E-06	3.69E-07	8.07E-05	1.44E-04	1.41E-05	1.22E-05	6.05E-07	1.35E-04	1.02E-08	3.60E-04
P0.1	7.98	-376.03	40.87	5.51E-04	7.40E-06	1.02E-05	1.67E-04	4.11E-06	3.69E-07	8.56E-05	1.50E-04	1.41E-05	1.22E-05	6.05E-07	1.36E-04	1.12E-08	3.60E-04
P5	8.60	-371.30	48.33	7.33E-04	5.98E-05	1.04E-05	2.11E-04	4.19E-06	4.32E-07	1.08E-04	1.94E-04	1.90E-04	1.37E-05	6.10E-07	1.42E-04	1.83E-08	5.00E-04
Median	9.47	-358.87	73.81	1.35E-03	2.20E-04	1.09E-05	3.28E-04	4.51E-06	6.17E-07	1.49E-04	2.91E-04	7.18E-04	1.88E-05	6.57E-07	1.82E-04	3.37E-08	9.63E-04
P95	9.64	-301.30	203.95	4.12E-03	1.20E-03	2.20E-05	9.63E-04	2.81E-05	1.64E-06	7.97E-04	8.68E-04	2.49E-03	8.33E-05	2.10E-06	2.04E-04	3.96E-07	3.03E-03
P99.9	9.71	-259.41	491.79	9.43E-03	4.93E-03	7.63E-05	2.47E-03	1.48E-04	3.18E-06	4.30E-03	4.25E-03	6.70E-03	3.88E-04	5.59E-06	2.14E-04	4.68E-06	6.87E-03
Maximum	9.71	-251.83	518.13	1.16E-02	5.08E-03	7.66E-05	3.04E-03	1.48E-04	3.98E-06	4.30E-03	4.25E-03	8.29E-03	3.93E-04	6.30E-06	2.14E-04	4.68E-06	8.44E-03
Glacial V: Eq. FeS(am) Coupled																	
	pH	Eh(mV)	TDS(mg/l)	IonicStr	mNa	mK	mCa	mMg	mFe+2	mC	AlkTot	mCl	mS(VI)	mS(-II)	mSi	mP	Na+K+2Mg+2Ca
N total	28044	28044	28044	28044	28044	28044	28044	28044	28044	28044	28044	28044	28044	28044	28044	28044	28044
Mean	9.47	-359.34	70.22	1.19E-03	2.36E-04	1.18E-05	2.98E-04	7.08E-06	6.11E-07	2.24E-04	3.56E-04	4.98E-04	2.32E-05	7.82E-07	1.89E-04	7.79E-08	8.57E-04
Standard Deviation	0.28	19.25	35.89	7.05E-04	3.28E-04	3.93E-06	1.47E-04	8.49E-06	3.03E-07	2.35E-04	2.18E-04	4.72E-04	2.28E-05	4.25E-07	2.01E-05	1.78E-07	5.56E-04
Minimum	8.05	-375.86	41.17	5.59E-04	9.54E-06	1.02E-05	1.69E-04	4.12E-06	3.72E-07	8.64E-05	1.57E-04	2.18E-05	1.23E-05	6.05E-07	1.36E-04	1.18E-08	3.65E-04
P0.1	8.15	-375.74	41.28	5.62E-04	1.03E-05	1.02E-05	1.69E-04	4.12E-06	3.73E-07	9.11E-05	1.69E-04	2.45E-05	1.23E-05	6.06E-07	1.37E-04	1.33E-08	3.68E-04
P5	8.78	-374.03	43.85	6.24E-04	2.91E-05	1.03E-05	1.84E-04	4.14E-06	3.95E-07	1.19E-04	2.20E-04	8.65E-05	1.28E-05	6.06E-07	1.46E-04	2.23E-08	4.16E-04
Median	9.59	-367.54	54.96	8.91E-04	1.05E-04	1.05E-05	2.44E-04	4.30E-06	4.85E-07	1.62E-04	3.13E-04	3.29E-04	1.51E-05	6.19E-07	1.97E-04	3.90E-08	6.21E-04
P95	9.68	-312.99	147.65	2.69E-03	8.74E-04	1.93E-05	5.92E-04	2.31E-05	1.26E-06	6.46E-04	7.18E-04	1.44E-03	6.69E-05	1.73E-06	2.10E-04	3.01E-07	2.06E-03
P99.9	9.70	-270.07	372.35	5.61E-03	3.65E-03	5.91E-05	1.24E-03	1.11E-04	2.52E-06	3.22E-03	3.24E-03	3.27E-03	2.91E-04	4.47E-06	2.14E-04	3.14E-06	4.68E-03
Maximum	9.71	-263.80	440.65	6.43E-03	4.38E-03	6.89E-05	1.69E-03	1.32E-04	2.85E-06	3.84E-03	3.82E-03	4.52E-03	3.46E-04	5.09E-06	2.14E-04	3.99E-06	5.49E-03
Glacial Vr: Eq. FeS(am) Coupled																	
	pH	Eh(mV)	TDS(mg/l)	IonicStr	mNa	mK	mCa	mMg	mFe+2	mC	AlkTot	mCl	mS(VI)	mS(-II)	mSi	mP	Na+K+2Mg+2Ca
N total	28044	28044	28044	28044	28044	28044	28044	28044	28044	28044	28044	28044	28044	28044	28044	28044	28044
Mean	9.47	-359.54	69.91	1.19E-03	2.32E-04	1.18E-05	2.98E-04	6.94E-06	6.08E-07	2.20E-04	3.53E-04	4.99E-04	2.29E-05	7.76E-07	1.89E-04	7.48E-08	8.54E-04
Standard Deviation	0.28	18.95	34.91	6.95E-04	3.14E-04	3.71E-06	1.47E-04	8.00E-06	2.97E-07	2.21E-04	2.04E-04	4.73E-04	2.16E-05	4.09E-07	2.01E-05	1.60E-07	5.46E-04
Minimum	8.03	-376.03	40.87	5.51E-04	7.40E-06	1.02E-05	1.67E-04	4.11E-06	3.69E-07	8.61E-05	1.57E-04	1.41E-05	1.22E-05	6.05E-07	1.36E-04	1.18E-08	3.60E-04
P0.1	8.22	-376.03	40.87	5.51E-04	7.40E-06	1.02E-05	1.67E-04	4.11E-06	3.69E-07	9.11E-05	1.69E-04	1.41E-05	1.22E-05	6.06E-07	1.38E-04	1.33E-08	3.60E-04
P5	8.80	-376.03	40.87	5.51E-04	7.40E-06	1.02E-05	1.67E-04	4.11E-06	3.69E-07	1.19E-04	2.19E-04	1.41E-05	1.22E-05	6.07E-07	1.46E-04	2.22E-08	3.60E-04
Median	9.59	-367.42	56.30	9.28E-04	1.09E-04	1.05E-05	2.57E-04	4.29E-06	4.93E-07	1.62E-04	3.20E-04	3.66E-04	1.51E-05	6.19E-07	1.97E-04	3.90E-08	6.47E-04
P95	9.71	-313.84	144.94	2.72E-03	8.51E-04	1.90E-05	5.96E-04	2.23E-05	1.24E-06	6.22E-04	6.99E-04	1.42E-03	6.48E-05	1.69E-06	2.14E-04	2.84E-07	2.03E-03
P99.9	9.71	-274.68	338.64	4.91E-03	3.29E-03	5.43E-05	1.27E-03	1.00E-04	2.29E-06	2.92E-03	2.95E-03	3.36E-03	2.63E-04	4.09E-06	2.14E-04	2.75E-06	4.20E-03
Maximum	9.71	-262.71	443.55	6.53E-03	4.40E-03	6.89E-05	1.71E-03	1.32E-04	2.94E-06	3.83E-03	3.81E-03	4.59E-03	3.47E-04	5.17E-06	2.14E-04	3.95E-06	5.54E-03
Glacial IVr: Eq. FeS(am) Coupled																	
	pH	Eh(mV)	TDS(mg/l)	IonicStr	mNa	mK	mCa	mMg	mFe+2	mC	AlkTot	mCl	mS(VI)	mS(-II)	mSi	mP	Na+K+2Mg+2Ca
N total	28044	28044	28044	28044	28044	28044	28044	28044	28044	28044	28044	28044	28044	28044	28044	28044	28044
Mean	9.28	-345.59	133.25	2.72E-03	5.62E-04	1.25E-05	6.96E-04	6.90E-06	9.03E-07	1.80E-04	2.76E-04	1.70E-03	3.12E-05	8.64E-07	1.70E-04	5.77E-08	1.98E-03
Standard Deviation	0.24	16.23	67.63	1.61E-03	3.86E-04	3.47E-06	4.29E-04	7.73E-06	3.05E-07	2.23E-04	2.15E-04	1.22E-03	2.04E-05	4.05E-07	1.38E-05	1.53E-07	1.18E-03
Minimum	8.03	-364.74	64.59	1.05E-03	1.54E-04	1.05E-05	2.33E-04	4.15E-06	5.46E-07	7.06E-05	1.33E-04	3.87E-04	1.60E-05	6.16E-07	1.36E-04	8.13E-09	7.71E-04
P0.1	8.16	-364.74	64.59	1.13E-03	1.54E-04	1.05E-05	2.37E-04	4.15E-06	5.46E-07	7.28E-05	1.36E-04	4.39E-04	1.60E-05	6.16E-07	1.37E-04	8.50E-09	7.99E-04
P5	8.78	-364.46	64.68	1.13E-03	1.56E-04	1.06E-05	3.08E-04	4.17E-06	5.48E-07	8.73E-05	1.63E-04	5.42E-04	1.61E-05	6.19E-07	1.45E-04	1.24E-08	8.00E-04
Median	9.32	-348.10	113.86	2.25E-03	4.97E-04	1.15E-05	5.40E-04	4.40E-06	8.58E-07	1.17E-04	2.26E-04	1.25E-03	2.61E-05	7.30E-07	1.69E-04	2.17E-08	1.62E-03
P95	9.55	-312.53	258.79	5.70E-03	1.24E-03	1.84E-05	1.46E-03	2.10E-05	1.47E-06	5.80E-04	6.49E-04	3.90E-03	6.55E-05	1.67E-06	1.91E-04	2.53E-07	4.21E-03
P99.9	9.55	-270.92	550.48	1.28E-02	3.34E-03	5.44E-05	3.36E-03	1.00E-04	2.54E-06	2.91E-03	2.92E-03	9.16E-03	2.65E-04	4.30E-06	1.92E-04	2.64E-06	9.31E-03
Maximum	9.55	-262.71	601.19	1.40E-02	4.40E-03	6.89E-05	3.67E-03	1.32E-04	3.02E-06	3.83E-03	3.81E-03	1.00E-02	3.47E-04	5.17E-06	1.92E-04	3.95E-06	1.02E-02

Table A4-7. Continuation.

Glacial IIr: Eq. FeS(am) Coupled																	
	pH	Eh(mV)	TDS(mg/l)	IonicStr	mNa	mK	mCa	mMg	mFe+2	mC	AlkTot	mCl	mS(VI)	mS(-II)	mSi	mP	Na+K+2Mg+2Ca
N total	28044	28044	28044	28044	28044	28044	28044	28044	28044	28044	28044	28044	28044	28044	28044	28044	28044
Mean	9.39	-353.74	133.29	2.75E-03	5.25E-04	1.19E-05	7.19E-04	5.69E-06	7.65E-07	1.64E-04	2.81E-04	1.71E-03	2.81E-05	7.88E-07	1.81E-04	4.59E-08	1.99E-03
Standard Deviation	0.26	17.89	128.69	3.10E-03	6.47E-04	2.37E-06	8.14E-04	4.61E-06	3.86E-07	1.34E-04	1.38E-04	2.33E-03	1.93E-05	2.70E-07	2.03E-05	8.63E-08	2.26E-03
Minimum	8.27	-371.75	48.18	7.31E-04	5.63E-05	1.03E-05	1.83E-04	4.13E-06	4.30E-07	6.51E-05	1.29E-04	1.90E-04	1.35E-05	6.05E-07	1.38E-04	7.06E-09	4.98E-04
P0.1	8.41	-371.75	48.18	7.31E-04	5.63E-05	1.03E-05	1.85E-04	4.13E-06	4.30E-07	6.66E-05	1.31E-04	1.90E-04	1.35E-05	6.05E-07	1.39E-04	7.39E-09	4.98E-04
P5	8.94	-371.70	48.18	7.31E-04	5.65E-05	1.03E-05	2.10E-04	4.13E-06	4.31E-07	7.40E-05	1.41E-04	1.90E-04	1.35E-05	6.06E-07	1.50E-04	8.97E-09	4.98E-04
Median	9.50	-361.04	73.42	1.27E-03	2.04E-04	1.08E-05	3.13E-04	4.28E-06	6.00E-07	1.47E-04	2.88E-04	5.43E-04	1.85E-05	6.42E-07	1.86E-04	3.29E-08	9.58E-04
P95	9.65	-322.79	439.65	1.01E-02	2.03E-03	1.53E-05	2.66E-03	1.34E-05	1.56E-06	3.77E-04	4.73E-04	7.23E-03	6.65E-05	1.26E-06	2.05E-04	1.44E-07	7.37E-03
P99.9	9.65	-287.28	539.78	1.25E-02	2.51E-03	3.97E-05	3.30E-03	6.81E-05	1.82E-06	1.98E-03	2.03E-03	8.98E-03	1.81E-04	3.15E-06	2.05E-04	1.59E-06	9.12E-03
Maximum	9.65	-278.39	580.29	1.35E-02	2.93E-03	4.94E-05	3.55E-03	8.94E-05	2.10E-06	2.61E-03	2.64E-03	9.69E-03	2.35E-04	3.78E-06	2.05E-04	2.33E-06	9.83E-03
Glacial 0r: Eq. FeS(am) Coupled																	
	pH	Eh(mV)	TDS(mg/l)	IonicStr	mNa	mK	mCa	mMg	mFe+2	mC	AlkTot	mCl	mS(VI)	mS(-II)	mSi	mP	Na+K+2Mg+2Ca
N total	28044	28044	28044	28044	28044	28044	28044	28044	28044	28044	28044	28044	28044	28044	28044	28044	28044
Mean	8.73	-308.85	914.25	1.56E-04	4.35E-03	2.01E-05	5.62E-03	6.53E-06	2.31E-06	1.00E-04	2.14E-02	1.54E-02	1.26E-04	1.85E-06	1.46E-04	1.68E-08	1.56E-02
Standard Deviation	0.26	16.23	188.28	1.18E-04	9.31E-04	2.98E-06	1.17E-03	4.60E-06	9.76E-07	1.27E-04	4.47E-03	3.25E-03	2.75E-05	1.06E-06	3.93E-06	4.72E-08	3.27E-03
Minimum	7.26	-344.62	169.01	1.13E-04	6.95E-04	1.17E-05	9.66E-04	4.31E-06	9.78E-07	5.69E-05	3.65E-03	2.48E-03	3.00E-05	7.60E-07	1.34E-04	5.30E-09	2.65E-03
P0.1	7.42	-340.75	208.53	1.13E-04	8.89E-04	1.21E-05	1.21E-03	4.35E-06	1.08E-06	5.72E-05	4.60E-03	3.18E-03	3.49E-05	8.11E-07	1.35E-04	5.37E-09	3.34E-03
P5	8.05	-322.16	590.26	1.15E-04	2.75E-03	1.62E-05	3.61E-03	4.77E-06	1.68E-06	5.84E-05	1.38E-02	9.86E-03	8.34E-05	1.22E-06	1.37E-04	5.60E-09	1.00E-02
Median	8.81	-313.56	923.50	1.22E-04	4.37E-03	1.98E-05	5.64E-03	5.24E-06	2.04E-06	6.29E-05	2.16E-02	1.55E-02	1.25E-04	1.54E-06	1.47E-04	6.44E-09	1.58E-02
P95	8.94	-267.50	1194.62	3.53E-04	5.74E-03	2.54E-05	7.36E-03	1.43E-05	4.55E-06	3.12E-04	2.80E-02	2.02E-02	1.72E-04	4.22E-06	1.51E-04	6.55E-08	2.04E-02
P99.9	9.21	-227.03	1481.96	1.65E-03	7.13E-03	4.65E-05	9.20E-03	6.83E-05	9.54E-06	1.77E-03	3.50E-02	2.54E-02	2.75E-04	1.04E-05	1.63E-04	8.55E-07	2.55E-02
Maximum	9.27	-216.49	1543.04	2.17E-03	7.53E-03	5.75E-05	9.59E-03	8.94E-05	1.23E-05	2.35E-03	3.65E-02	2.64E-02	3.55E-04	1.39E-05	1.66E-04	1.35E-06	2.66E-02

Table A4-8. Statistical results for the main geochemical parameters obtained with the geochemical variant case 3 (Hem uncoup) over the glacial period in the repository volume. Chemical components in mol/kg, TDS in mg/L, pH in standard units and Eh in mV.

Glacial 0: Hematite Uncoupled																	
	pH	Eh(mV)	TDS(mg/l)	IonicStr	mNa	mK	mCa	mMg	mFe+2	mC	AlkTot	mCl	mS(VI)	mS(-II)	mSi	mP	Na+K+2Mg+2Ca
N total	28044	28044	28044	28044	28044	28044	28044	28044	28044	28044	28044	28044	28044	28044	28044	28044	28044
Mean	7.38	-216.46	1789.07	3.76E-02	1.13E-02	8.90E-05	8.51E-03	1.47E-04	1.22E-06	3.92E-03	3.54E-03	2.44E-02	5.35E-04	1.00E-15	1.34E-04	3.38E-06	2.87E-02
Standard Deviation	0.44	73.57	2246.92	5.32E-02	1.09E-02	2.17E-05	1.41E-02	1.70E-06	3.69E-07	3.71E-04	6.33E-04	3.96E-02	2.70E-04	7.98E-19	2.22E-06	8.80E-07	3.91E-02
Minimum	6.56	-328.89	473.21	6.71E-03	4.83E-03	7.61E-05	3.21E-04	1.38E-04	6.65E-07	2.85E-03	2.09E-03	8.25E-04	3.74E-04	1.00E-15	1.23E-04	1.52E-06	5.85E-03
P0.1	6.57	-328.89	473.21	6.71E-03	4.83E-03	7.61E-05	3.21E-04	1.39E-04	6.65E-07	2.91E-03	2.14E-03	8.25E-04	3.74E-04	1.00E-15	1.24E-04	1.60E-06	5.85E-03
P5	6.66	-313.33	490.28	7.09E-03	4.93E-03	7.63E-05	4.18E-04	1.43E-04	7.55E-07	3.17E-03	2.36E-03	1.18E-03	3.76E-04	1.00E-15	1.29E-04	1.93E-06	6.14E-03
Median	7.45	-231.02	709.67	1.21E-02	6.09E-03	7.86E-05	1.72E-03	1.48E-04	1.13E-06	4.07E-03	3.78E-03	5.39E-03	4.05E-04	1.00E-15	1.35E-04	3.45E-06	9.91E-03
P95	7.98	-93.08	7371.67	1.70E-01	3.83E-02	1.43E-04	4.36E-02	1.48E-04	1.94E-06	4.30E-03	4.23E-03	1.23E-01	1.20E-03	1.00E-15	1.36E-04	4.68E-06	1.26E-01
P99.9	8.09	-78.32	12721.11	2.97E-01	6.40E-02	1.94E-04	7.74E-02	1.48E-04	2.26E-06	4.33E-03	4.30E-03	2.16E-01	1.84E-03	1.00E-15	1.36E-04	5.02E-06	2.19E-01
Maximum	8.09	-75.87	14216.33	3.33E-01	7.12E-02	2.08E-04	8.69E-02	1.48E-04	2.35E-06	4.33E-03	4.30E-03	2.42E-01	2.02E-03	1.01E-15	1.36E-04	5.02E-06	2.45E-01
Glacial I: Hematite Uncoupled																	
	pH	Eh(mV)	TDS(mg/l)	IonicStr	mNa	mK	mCa	mMg	mFe+2	mC	AlkTot	mCl	mS(VI)	mS(-II)	mSi	mP	Na+K+2Mg+2Ca
N total	28044	28044	28044	28044	28044	28044	28044	28044	28044	28044	2.80E+04	28044	28044	28044	28044	28044	28044
Mean	6.88	-128.40	9088.50	2.11E-01	4.63E-02	1.55E-04	5.47E-02	1.33E-04	1.86E-06	2.99E-03	2.37E-03	1.53E-01	1.39E-03	6.10E-09	1.28E-04	1.88E-06	1.56E -01
Standard Deviation	0.56	83.36	7269.70	1.73E-01	3.52E-02	7.49E-05	4.57E-02	2.72E-05	6.89E-07	6.88E-04	6.44E-04	1.27E-01	8.92E-04	1.99E-08	7.43E-06	7.53E-07	1.27E-01
Minimum	6.49	-405.56	39.72	5.50E-04	7.40E-06	1.02E-05	1.67E-04	4.11E-06	5.85E-12	1.81E-04	2.41E-04	1.41E-05	5.21E-06	1.00E-15	1.11E-04	4.20E-08	3.60E-04
P0.1	6.49	-401.68	70.92	1.21E-03	2.91E-04	1.23E-05	2.21E-04	7.73E-06	2.08E-09	2.09E-04	3.08E-04	3.90E-04	1.90E-05	1.00E-15	1.12E-04	5.59E-08	8.94E-04
P5	6.50	-344.22	246.85	3.97E-03	2.02E-03	3.27E-05	4.68E-04	5.21E-05	2.88E-07	1.50E-03	1.52E-03	1.21E-03	1.39E-04	1.00E-15	1.16E-04	8.86E-07	3.30E-03
Median	6.64	-88.95	8482.00	1.96E-01	4.37E-02	1.53E-04	5.06E-02	1.41E-04	2.01E-06	3.03E-03	2.24E-03	1.42E-01	1.34E-03	1.00E-15	1.28E-04	1.76E-06	1.45E-01
P95	8.29	-68.51	22698.87	5.35E-01	1.12E-01	2.89E-04	1.41E-01	1.48E-04	2.80E-06	4.03E-03	3.73E-03	3.90E-01	3.03E-03	6.67E-08	1.39E-04	3.40E-06	3.93E -01
P99.9	9.32	-67.37	28059.45	6.63E-01	1.38E-01	3.40E-04	1.74E-01	1.48E-04	3.06E-06	4.31E-03	4.26E-03	4.84E-01	3.66E-03	9.75E-08	1.69E-04	4.84E-06	4.87E -01
Maximum	9.70	-67.32	29991.87	7.09E-01	1.47E-01	3.58E-04	1.87E-01	1.48E-04	3.15E-06	4.33E-03	4.30E-03	5.17E-01	3.90E-03	1.00E-07	2.13E-04	5.02E-06	5.21E -01
Glacial II: Hematite Uncoupled																	
	pH	Eh(mV)	TDS(mg/l)	IonicStr	mNa	mK	mCa	mMg	mFe+2	mC	AlkTot	mCl	mS(VI)	mS(-II)	mSi	mP	Na+K+2Mg+2Ca
N total	28044	28044	28044	28044	28044	28044	28044	28044	28044	28044	28044	28044	28044	28044	28044	28044	28044
Mean	8.67	-324.49	1449.40	3.34E-02	7.29E-03	3.36E-05	8.64E-03	2.58E-05	2.93E-07	6.23E-04	6.16E-04	2.39E-02	2.25E-04	8.42E-08	1.61E-04	2.91E-07	2.47E -02
Standard Deviation	0.99	102.07	2994.19	7.00E-02	1.51E-02	4.43E-05	1.82E-02	3.71E-05	5.80E-07	8.21E-04	6.13E-04	5.10E-02	4.36E-04	2.71E-08	2.58E-05	5.14E-07	5.17E-02
Minimum	6.54	-410.12	47.11	7.31E-04	5.80E-05	1.04E-05	1.84E-04	4.18E-06	7.80E-11	4.90E-05	7.81E-05	1.90E-04	6.58E-06	1.00E-15	1.22E-04	3.55E-09	4.99E-04
P0.1	6.55	-410.00	47.12	7.31E-04	5.81E-05	1.04E-05	1.84E-04	4.18E-06	7.94E-11	1.00E-04	1.53E-04	1.90E-04	6.59E-06	1.00E-15	1.22E-04	1.53E-08	4.99E-04
P5	6.65	-401.45	47.30	7.33E-04	6.24E-05	1.04E-05	2.08E-04	4.29E-06	1.17E-10	1.17E-04	1.84E-04	1.91E-04	6.92E-06	1.01E-15	1.27E-04	2.08E-08	5.02E-04
Median	9.09	-383.84	112.24	2.06E-03	5.95E-04	1.36E-05	4.53E-04	8.35E-06	7.08E-09	2.09E-04	3.10E-04	1.07E-03	3.10E-05	9.69E-08	1.55E-04	5.10E-08	1.58E-03
P95	9.64	-90.35	9638.89	2.25E-01	4.87E-02	1.55E-04	5.85E-02	1.38E-04	1.97E-06	2.90E-03	2.16E-03	1.63E-01	1.42E-03	9.99E-08	2.03E-04	1.62E-06	1.66E-01
P99.9	9.64	-74.67	15099.52	3.54E-01	7.54E-02	2.16E-04	9.25E-02	1.48E-04	2.40E-06	4.31E-03	4.26E-03	2.58E-01	2.12E-03	1.00E-07	2.04E-04	4.84E-06	2.61E -01
Maximum	9.64	-73.59	15976.14	3.75E-01	7.96E-02	2.25E-04	9.80E-02	1.48E-04	2.44E-06	4.31E-03	4.26E-03	2.73E-01	2.23E-03	1.00E-07	2.04E-04	4.84E-06	2.76E -01
Glacial III: Hematite Uncoupled																	
	pH	Eh(mV)	TDS(mg/l)	IonicStr	mNa	mK	mCa	mMg	mFe+2	mC	AlkTot	mCl	mS(VI)	mS(-II)	mSi	mP	Na+K+2Mg+2Ca
N total	28044	28044	28044	28044	28044	28044	28044	28044	28044	28044	28044	28044	28044	28044	28044	28044	28044
Mean	9.24	-372.68	301.40	6.62E-03	1.44E-03	1.57E-05	1.70E-03	1.07E-05	5.41E-08	3.01E-04	3.94E-04	4.43E-03	5.23E-05	9.53E-08	1.78E-04	1.20E-07	4.87E-03
Standard Deviation	0.58	47.16	1076.15	2.53E-02	5.40E-03	1.57E-05	6.59E-03	1.52E-05	1.96E-07	3.86E-04	3.39E-04	1.84E-02	1.55E-04	1.09E-08	2.43E-05	2.89E-07	1.86E-02
Minimum	6.59	-410.12	39.72	5.50E-04	7.40E-06	1.02E-05	1.67E-04	4.11E-06	5.85E-12	5.09E-05	8.21E-05	1.41E-05	5.21E-06	1.00E-15	1.24E-04	3.97E-09	3.60E-04
P0.1	6.64	-409.77	39.72	5.50E-04	7.40E-06	1.02E-05	1.67E-04	4.11E-06	5.85E-12	1.07E-04	1.68E-04	1.41E-05	5.21E-06	1.00E-15	1.26E-04	1.76E-08	3.60E-04
P5	7.92	-400.71	47.15	7.31E-04	5.90E-05	1.04E-05	2.08E-04	4.21E-06	8.75E-11	1.22E-04	2.00E-04	1.90E-04	6.65E-06	7.63E-08	1.36E-04	2.32E-08	5.00E-04
Median	9.49	-384.75	64.09	1.14E-03	1.92E-04	1.08E-05	2.92E-04	4.60E-06	3.62E-10	1.65E-04	3.06E-04	5.42E-04	1.08E-05	9.96E-08	1.85E-04	4.03E-08	8.08E-04
P95	9.64	-268.53	1139.28	2.65E-02	5.64E-03	3.38E-05	6.85E-03	3.73E-05	2.90E-07	1.02E-03	1.04E-03	1.89E-02	1.93E-04	9.99E-08	2.03E-04	5.27E-07	1.94E -02
P99.9	9.70	-88.69	11011.92	2.58E-01	5.50E-02	1.67E-04	6.71E-02	1.48E-04	1.97E-06	4.30E-03	4.23E-03	1.88E-01	1.58E-03	1.00E-07	2.13E-04	4.68E-06	1.90E -01
Maximum	9.70	-80.88	12814.24	3.00E-01	6.41E-02	1.89E-04	7.83E-02	1.48E-04	2.18E-06	4.31E-03	4.26E-03	2.18E-01	1.82E-03	1.00E-07	2.13E-04	4.84E-06	2.21E -01

Table A4-8. Continuation.

Glacial IV: Hematite Uncoupledp																	
	pH	Eh(mV)	TDS(mg/l)	IonicStr	mNa	mK	mCa	mMg	mFe+2	mC	AlkTot	mCl	mS(VI)	mS(-II)	mSi	mP	Na+K+2Mg+2Ca
N total	28044	28044	28044	28044	28044	28044	28044	28044	28044	28044	28044	28044	28044	28044	28044	28044	28044
Mean	9.34	-383.13	94.28	1.76E-03	3.94E-04	1.27E-05	4.34E-04	8.32E-06	1.62E-08	2.42E-04	3.39E-04	9.27E-04	2.21E-05	9.71E-08	1.78E-04	9.36E-08	1.29E-03
Standard Deviation	0.33	11.91	55.02	1.15E-03	4.47E-04	5.27E-06	2.71E-04	1.15E-05	6.07E-08	3.26E-04	3.08E-04	8.08E-04	3.00E-05	7.96E-09	1.94E-05	2.62E-07	8.82E-04
Minimum	7.85	-408.35	39.72	5.50E-04	7.40E-06	1.02E-05	1.67E-04	4.11E-06	5.85E-12	8.29E-05	1.31E-04	1.41E-05	5.21E-06	1.00E-15	1.35E-04	1.07E-08	3.60E-04
P0.1	7.98	-405.21	39.72	5.50E-04	7.40E-06	1.02E-05	1.67E-04	4.11E-06	5.85E-12	8.76E-05	1.37E-04	1.41E-05	5.21E-06	1.00E-15	1.36E-04	1.17E-08	3.60E-04
P5	8.59	-396.89	47.19	7.32E-04	5.98E-05	1.04E-05	2.11E-04	4.19E-06	9.54E-11	1.09E-04	1.81E-04	1.90E-04	6.72E-06	8.33E-08	1.42E-04	1.88E-08	5.00E-04
Median	9.46	-383.95	72.70	1.35E-03	2.20E-04	1.09E-05	3.30E-04	4.51E-06	4.51E-10	1.50E-04	2.76E-04	7.18E-04	1.18E-05	9.97E-08	1.82E-04	3.42E-08	9.64E-04
P95	9.64	-365.26	202.80	4.12E-03	1.20E-03	2.20E-05	9.65E-04	2.81E-05	9.38E-08	7.99E-04	8.54E-04	2.49E-03	7.49E-05	9.99E-08	2.03E-04	3.98E-07	3.04E-03
P99.9	9.70	-313.33	490.28	9.44E-03	4.93E-03	7.63E-05	2.47E-03	1.48E-04	7.55E-07	4.30E-03	4.23E-03	6.70E-03	3.76E-04	1.00E-07	2.13E-04	4.68E-06	6.87E-03
Maximum	9.70	-292.87	516.61	1.16E-02	5.08E-03	7.66E-05	3.04E-03	1.48E-04	8.51E-07	4.30E-03	4.23E-03	8.29E-03	3.80E-04	1.00E-07	2.13E-04	4.68E-06	8.45E-03
Glacial V: Hematite Uncoupled																	
	pH	Eh(mV)	TDS(mg/l)	IonicStr	mNa	mK	mCa	mMg	mFe+2	mC	AlkTot	mCl	mS(VI)	mS(-II)	mSi	mP	Na+K+2Mg+2Ca
N total	28044	28044	28044	28044	28044	28044	28044	28044	28044	28044	28044	28044	28044	28044	28044	28044	28044
Mean	9.47	-382.46	69.10	1.19E-03	2.36E-04	1.18E-05	2.98E-04	7.08E-06	8.32E-09	2.25E-04	3.41E-04	4.98E-04	1.60E-05	9.79E-08	1.88E-04	7.87E-08	8.59E-04
Standard Deviation	0.28	10.56	35.90	7.05E-04	3.28E-04	3.93E-06	1.47E-04	8.49E-06	3.63E-08	2.36E-04	2.18E-04	4.72E-04	2.24E-05	5.90E-09	1.99E-05	1.78E-07	5.57E-04
Minimum	8.04	-409.60	40.02	5.58E-04	9.53E-06	1.02E-05	1.69E-04	4.12E-06	1.00E-11	8.84E-05	1.44E-04	2.18E-05	5.26E-06	1.12E-08	1.36E-04	1.23E-08	3.66E-04
P0.1	8.14	-407.72	40.14	5.61E-04	1.03E-05	1.02E-05	1.70E-04	4.12E-06	1.13E-11	9.30E-05	1.56E-04	2.45E-05	5.28E-06	2.60E-08	1.37E-04	1.37E-08	3.68E-04
P5	8.78	-400.37	42.70	6.23E-04	2.91E-05	1.03E-05	1.84E-04	4.14E-06	4.53E-11	1.21E-04	2.06E-04	8.65E-05	5.82E-06	8.68E-08	1.45E-04	2.29E-08	4.16E-04
Median	9.59	-382.70	53.83	8.90E-04	1.05E-04	1.05E-05	2.44E-04	4.30E-06	1.69E-10	1.63E-04	2.98E-04	3.29E-04	8.09E-06	9.99E-08	1.96E-04	3.97E-08	6.22E-04
P95	9.68	-366.28	146.61	2.70E-03	8.74E-04	1.93E-05	5.94E-04	2.31E-05	4.54E-08	6.49E-04	7.05E-04	1.44E-03	5.88E-05	1.00E-07	2.09E-04	3.03E-07	2.06E-03
P99.9	9.70	-332.94	370.95	5.61E-03	3.65E-03	5.91E-05	1.25E-03	1.11E-04	5.35E-07	3.23E-03	3.22E-03	3.27E-03	2.80E-04	1.00E-07	2.13E-04	3.14E-06	4.68E-03
Maximum	9.70	-321.82	439.13	6.43E-03	4.38E-03	6.89E-05	1.69E-03	1.32E-04	6.61E-07	3.84E-03	3.80E-03	4.52E-03	3.35E-04	1.00E-07	2.13E-04	4.00E-06	5.50E-03
Glacial Vr: Hematite Uncoupled																	
	pH	Eh(mV)	TDS(mg/l)	IonicStr	mNa	mK	mCa	mMg	mFe+2	mC	AlkTot	mCl	mS(VI)	mS(-II)	mSi	mP	Na+K+2Mg+2Ca
N total	28044	28044	28044	28044	28044	28044	28044	28044	28044	28044	28044	28044	28044	28044	28044	28044	28044
Mean	9.47	-379.14	68.80	1.19E-03	2.32E-04	1.18E-05	2.99E-04	6.94E-06	7.74E-09	2.21E-04	3.38E-04	4.99E-04	1.57E-05	9.80E-08	1.88E-04	7.56E-08	8.55E-04
Standard Deviation	0.28	18.54	34.92	6.96E-04	3.14E-04	3.71E-06	1.48E-04	8.00E-06	3.36E-08	2.21E-04	2.04E-04	4.73E-04	2.12E-05	5.56E-09	1.99E-05	1.61E-07	5.47E-04
Minimum	8.03	-410.12	39.72	5.50E-04	7.40E-06	1.02E-05	1.67E-04	4.11E-06	5.85E-12	8.82E-05	1.44E-04	1.41E-05	5.21E-06	1.12E-08	1.36E-04	1.23E-08	3.60E-04
P0.1	8.21	-409.20	39.72	5.50E-04	7.40E-06	1.02E-05	1.67E-04	4.11E-06	5.85E-12	9.29E-05	1.55E-04	1.41E-05	5.21E-06	3.33E-08	1.38E-04	1.38E-08	3.60E-04
P5	8.79	-400.60	39.72	5.50E-04	7.40E-06	1.02E-05	1.67E-04	4.11E-06	5.85E-12	1.20E-04	2.05E-04	1.41E-05	5.21E-06	8.74E-08	1.46E-04	2.27E-08	3.60E-04
Median	9.59	-382.47	55.18	9.27E-04	1.09E-04	1.05E-05	2.58E-04	4.29E-06	1.64E-10	1.63E-04	3.05E-04	3.66E-04	8.05E-06	9.99E-08	1.96E-04	3.96E-08	6.48E-04
P95	9.70	-322.73	143.85	2.72E-03	8.51E-04	1.90E-05	5.97E-04	2.23E-05	4.05E-08	6.25E-04	6.85E-04	1.42E-03	5.66E-05	1.00E-07	2.13E-04	2.85E-07	2.03E-03
P99.9	9.70	-322.73	337.32	4.91E-03	3.29E-03	5.43E-05	1.28E-03	1.00E-04	4.61E-07	2.92E-03	2.93E-03	3.36E-03	2.53E-04	1.00E-07	2.13E-04	2.75E-06	4.20E-03
Maximum	9.70	-319.31	442.09	6.53E-03	4.40E-03	6.89E-05	1.71E-03	1.32E-04	6.74E-07	3.83E-03	3.79E-03	4.59E-03	3.35E-04	1.00E-07	2.13E-04	3.95E-06	5.55E-03
Glacial IVr: Hematite Uncoupled																	
	pH	Eh(mV)	TDS(mg/l)	IonicStr	mNa	mK	mCa	mMg	mFe+2	mC	AlkTot	mCl	mS(VI)	mS(-II)	mSi	mP	Na+K+2Mg+2Ca
N total	28044	28044	28044	28044	28044	28044	28044	28044	28044	28044	28044	28044	28044	28044	28044	28044	28044
Mean	9.27	-382.20	132.17	2.72E-03	5.62E-04	1.25E-05	6.97E-04	6.90E-06	9.42E-09	1.81E-04	2.62E-04	1.70E-03	2.39E-05	9.80E-08	1.69E-04	5.84E-08	1.98E-03
Standard Deviation	0.24	6.54	67.65	1.61E-03	3.86E-04	3.47E-06	4.29E-04	7.73E-06	3.57E-08	2.23E-04	2.15E-04	1.22E-03	2.00E-05	5.36E-09	1.36E-05	1.54E-07	1.18E-03
Minimum	8.03	-405.56	63.47	1.05E-03	1.54E-04	1.05E-05	2.34E-04	4.15E-06	1.66E-10	7.29E-05	1.20E-04	3.87E-04	8.94E-06	1.12E-08	1.36E-04	8.57E-09	7.73E-04
P0.1	8.15	-401.68	63.47	1.13E-03	1.54E-04	1.05E-05	2.38E-04	4.15E-06	1.66E-10	7.51E-05	1.23E-04	4.39E-04	8.94E-06	3.33E-08	1.37E-04	8.97E-09	8.00E-04
P5	8.77	-394.61	63.55	1.13E-03	1.56E-04	1.06E-05	3.09E-04	4.17E-06	1.92E-10	8.91E-05	1.50E-04	5.42E-04	9.10E-06	8.82E-08	1.45E-04	1.29E-08	8.01E-04
Median	9.31	-381.27	112.85	2.25E-03	4.97E-04	1.15E-05	5.41E-04	4.40E-06	1.16E-09	1.18E-04	2.12E-04	1.25E-03	1.90E-05	9.97E-08	1.68E-04	2.22E-08	1.62E-03
P95	9.54	-375.23	257.76	5.71E-03	1.24E-03	1.84E-05	1.47E-03	2.10E-05	4.23E-08	5.83E-04	6.35E-04	3.90E-03	5.74E-05	1.00E-07	1.90E-04	2.55E-07	4.22E-03
P99.9	9.55	-334.08	549.43	1.28E-02	3.34E-03	5.44E-05	3.36E-03	1.00E-04	5.03E-07	2.91E-03	2.91E-03	9.16E-03	2.54E-04	1.00E-07	1.91E-04	2.64E-06	9.31E-03
Maximum	9.55	-319.31	600.15	1.40E-02	4.40E-03	6.89E-05	3.68E-03	1.32E-04	6.74E-07	3.83E-03	3.79E-03	1.00E-02	3.35E-04	1.00E-07	1.91E-04	3.95E-06	1.02E-02

Table A4-8. Continuation.

Glacial IIr: Hematite Uncoupled																	
	pH	Eh(mV)	TDS(mg/l)	IonicStr	mNa	mK	mCa	mMg	mFe+2	mC	AlkTot	mCl	mS(VI)	mS(-II)	mSi	mP	Na+K+2Mg+2Ca
N total	28044	28044	28044	28044	28044	28044	28044	28044	28044	28044	28044	28044	28044	28044	28044	28044	28044
Mean	9.39	-381.14	132.19	2.75E-03	5.25E-04	1.19E-05	7.20E-04	5.69E-06	4.00E-09	1.65E-04	2.67E-04	1.71E-03	2.09E-05	9.89E-08	1.80E-04	4.65E-08	1.99E-03
Standard Deviation	0.26	9.79	128.72	3.10E-03	6.47E-04	2.37E-06	8.15E-04	4.61E-06	1.38E-08	1.34E-04	1.37E-04	2.33E-03	1.90E-05	3.20E-09	2.02E-05	8.65E-08	2.26E-03
Minimum	8.27	-410.12	47.03	7.30E-04	5.63E-05	1.03E-05	1.84E-04	4.13E-06	5.87E-11	6.75E-05	1.15E-04	1.90E-04	6.45E-06	4.08E-08	1.38E-04	7.48E-09	4.98E-04
P0.1	8.40	-410.06	47.03	7.30E-04	5.63E-05	1.03E-05	1.86E-04	4.13E-06	5.87E-11	6.89E-05	1.18E-04	1.90E-04	6.45E-06	5.56E-08	1.39E-04	7.81E-09	4.98E-04
P5	8.93	-403.62	47.04	7.30E-04	5.65E-05	1.03E-05	2.11E-04	4.13E-06	6.10E-11	7.62E-05	1.28E-04	1.90E-04	6.46E-06	9.36E-08	1.50E-04	9.42E-09	4.98E-04
Median	9.50	-378.94	72.30	1.28E-03	2.04E-04	1.08E-05	3.13E-04	4.28E-06	3.49E-10	1.48E-04	2.74E-04	5.43E-04	1.14E-05	9.99E-08	1.85E-04	3.35E-08	9.59E-04
P95	9.64	-370.22	438.63	1.01E-02	2.03E-03	1.53E-05	2.66E-03	1.34E-05	1.47E-08	3.78E-04	4.59E-04	7.23E-03	5.89E-05	1.00E-07	2.04E-04	1.46E-07	7.38E-03
P99.9	9.64	-362.46	538.74	1.25E-02	2.51E-03	3.97E-05	3.30E-03	6.81E-05	2.67E-07	1.98E-03	2.02E-03	8.98E-03	1.71E-04	1.00E-07	2.04E-04	1.59E-06	9.13E-03
Maximum	9.64	-348.73	579.24	1.35E-02	2.93E-03	4.94E-05	3.55E-03	8.94E-05	3.98E-07	2.61E-03	2.62E-03	9.69E-03	2.25E-04	1.00E-07	2.04E-04	2.34E-06	9.83E-03
Glacial 0r: Hematite Uncoupled																	
	pH	Eh(mV)	TDS(mg/l)	IonicStr	mNa	mK	mCa	mMg	mFe+2	mC	AlkTot	mCl	mS(VI)	mS(-II)	mSi	mP	Na+K+2Mg+2Ca
N total	28044	28044	28044	28044	28044	28044	28044	28044	28044	28044	28044	28044	28044	28044	28044	28044	28044
Mean	8.71	-360.99	913.19	2.14E-02	4.35E-03	2.01E-05	5.63E-03	6.53E-06	5.48E-08	1.03E-04	1.43E-04	1.54E-02	1.18E-04	9.79E-08	1.46E-04	1.75E-08	1.56E-02
Standard Deviation	0.26	28.75	188.27	4.47E-03	9.31E-04	2.98E-06	1.17E-03	4.60E-06	6.24E-08	1.28E-04	1.18E-04	3.25E-03	2.68E-05	3.21E-09	3.75E-06	4.79E-08	3.27E-03
Minimum	7.25	-381.67	167.93	3.65E-03	6.94E-04	1.17E-05	9.67E-04	4.31E-06	1.53E-09	5.99E-05	1.00E-04	2.48E-03	2.28E-05	4.04E-08	1.34E-04	5.76E-09	2.65E-03
P0.1	7.42	-380.25	207.45	4.60E-03	8.89E-04	1.21E-05	1.22E-03	4.35E-06	2.27E-09	6.03E-05	1.01E-04	3.18E-03	2.77E-05	5.51E-08	1.35E-04	5.83E-09	3.34E-03
P5	8.05	-375.57	589.20	1.38E-02	2.75E-03	1.62E-05	3.62E-03	4.77E-06	1.55E-08	6.13E-05	1.03E-04	9.86E-03	7.56E-05	9.24E-08	1.37E-04	6.05E-09	1.00E-02
Median	8.79	-371.81	922.43	2.16E-02	4.36E-03	1.98E-05	5.65E-03	5.24E-06	3.69E-08	6.56E-05	1.09E-04	1.55E-02	1.17E-04	9.87E-08	1.46E-04	6.89E-09	1.58E-02
P95	8.92	-284.89	1193.58	2.80E-02	5.73E-03	2.54E-05	7.36E-03	1.43E-05	1.87E-07	3.18E-04	3.41E-04	2.02E-02	1.61E-04	9.92E-08	1.50E-04	6.75E-08	2.04E-02
P99.9	9.20	-208.91	1480.88	3.50E-02	7.13E-03	4.65E-05	9.21E-03	6.83E-05	6.86E-07	1.78E-03	1.64E-03	2.54E-02	2.58E-04	9.97E-08	1.62E-04	8.66E-07	2.55E-02
Maximum	9.26	-186.96	1541.96	3.65E-02	7.53E-03	5.75E-05	9.59E-03	8.94E-05	8.84E-07	2.36E-03	2.16E-03	2.64E-02	3.35E-04	9.98E-08	1.65E-04	1.37E-06	2.66E-02

Table A4-9. Statistical results for the main geochemical parameters obtained with the geochemical Base case over the glacial period with frozen ground (Permafrost) in the repository volume. Chemical components in mol/kg, TDS in mg/L, pH in standard units and Eh in mV. Columns in red indicate the values taken from the geochemical variant Cases 1 and 2 together (Bace Case for the redox parameters).

Permafrost 0: BaseCase (Red numbers correspond to the values from Hem Coup and FeS Coup.)																	
	pH	Eh(mV) (HemC+FeSc	TDS(mg/l)	IonicStr	mNa	mK	mCa	mMg	mFe(II) (HemC+FeSc)	mC	AlkTot	mCl	mS(VI)	mS(-II) (HemC+FeSc)	mSi	mP	Na+K+2Mg+2Ca
N total	28044	56088	28044	28044	28044	28044	28044	28044	56088	28044	28044	28044	28044	56088	28044	28044	28044
Mean	7.28	-205.86 €	988.11	1.85E-02	7.49E-03	8.14E-05	3.44E-03	1.48E-04	5.96E-06	3.93E-03	3.53E-03	1.05E-02	4.40E-04	7.04E-06	1.34E-04	3.16E-06	1.47E-02
Standard Deviation	0.13	17.52 €	355.44	8.33E-03	1.75E-03	3.48E-06	2.21E-03	2.76E-07	5.53E-06	1.18E-04	2.16E-04	6.37E-03	4.34E-05	7.47E-06	3.87E-07	2.26E-07	6.18E-03
--	--	--	--	--	--	--	--	--	--	--	--	--	--	--	--	--	--
Minimum	6.84	-232.56 €	644.58	1.06E-02	5.75E-03	7.79E-05	1.33E-03	1.46E-04	3.76E-07	3.49E-03	2.75E-03	4.17E-03	3.97E-04	3.32E-14	1.32E-04	2.39E-06	8.79E-03
P0.1	6.86	-232.05 €	646.95	1.06E-02	5.77E-03	7.80E-05	1.35E-03	1.46E-04	3.89E-07	3.51E-03	2.78E-03	4.22E-03	3.97E-04	7.71E-14	1.32E-04	2.42E-06	8.83E-03
P5	6.99	-224.87 €	717.36	1.22E-02	6.13E-03	7.87E-05	1.77E-03	1.47E-04	6.36E-07	3.66E-03	3.04E-03	5.54E-03	4.06E-04	1.56E-10	1.33E-04	2.67E-06	1.01E-02
Median	7.31	-208.68 €	863.70	1.56E-02	6.88E-03	8.02E-05	2.66E-03	1.48E-04	4.06E-06	3.97E-03	3.59E-03	8.24E-03	4.25E-04	4.65E-06	1.34E-04	3.21E-06	1.26E-02
P95	7.44	-168.21 €	1808.14	3.77E-02	1.15E-02	8.94E-05	8.54E-03	1.48E-04	1.55E-05	4.06E-03	3.77E-03	2.52E-02	5.40E-04	1.91E-05	1.35E-04	3.44E-06	2.90E-02
P99.9	7.54	-130.47 €	2858.78	6.26E-02	1.66E-02	9.95E-05	1.51E-02	1.48E-04	2.53E-05	4.12E-03	3.88E-03	4.37E-02	6.66E-04	2.96E-05	1.35E-04	3.62E-06	4.73E-02
Maximum	7.54	-126.26 €	3041.98	6.69E-02	1.75E-02	1.01E-04	1.63E-02	1.48E-04	2.67E-05	4.12E-03	3.89E-03	4.69E-02	6.88E-04	3.12E-05	1.35E-04	3.62E-06	5.05E-02
Permafrost I: BaseCase																	
	pH	Eh(mV) (HemC+FeSc	TDS(mg/l)	IonicStr	mNa	mK	mCa	mMg	mFe(II) (HemC+FeSc)	mC	AlkTot	mCl	mS(VI)	mS(-II) (HemC+FeSc)	mSi	mP	Na+K+2Mg+2Ca
N total	28044	56088	28044	28044	28044	28044	28044	28044	56088	28044	2.80E+04	28044	28044	56088	28044	28044	28044
Mean	8.03	-256.49	642.81	1.31E-02	4.14E-03	4.15E-05	2.87E-03	6.29E-05	3.32E-06	1.67E-03	1.56E-03	8.18E-03	2.10E-04	3.83E-06	1.39E-04	1.03E-06	1.01E-02
Standard Deviation	0.63	48.12	937.84	2.11E-02	5.28E-03	2.72E-05	5.25E-03	4.53E-05	6.17E-06	1.12E-03	9.11E-04	1.51E-02	2.01E-04	7.31E-06	4.77E-06	9.14E-07	1.58E-02
Minimum	6.69	-336.70	80.45	1.32E-03	4.31E-04	1.31E-05	2.50E-04	9.13E-06	3.84E-10	2.33E-04	2.99E-04	4.65E-04	2.57E-05	1.22E-16	1.29E-04	6.35E-08	1.00E-03
P0.1	6.70	-334.02	82.54	1.35E-03	4.64E-04	1.45E-05	2.54E-04	1.18E-05	4.51E-10	3.00E-04	3.52E-04	4.84E-04	3.29E-05	2.93E-16	1.30E-04	8.69E-08	1.03E-03
P5	6.86	-315.95	109.80	1.86E-03	6.95E-04	1.73E-05	3.32E-04	1.86E-05	1.74E-09	5.12E-04	5.70E-04	7.38E-04	4.76E-05	9.81E-11	1.32E-04	2.10E-07	1.44E-03
Median	8.15	-267.44	265.96	4.80E-03	1.93E-03	2.98E-05	8.62E-04	4.41E-05	1.32E-06	1.24E-03	1.25E-03	2.30E-03	1.23E-04	5.83E-07	1.38E-04	6.29E-07	3.79E-03
P95	8.88	-166.90	2835.03	6.20E-02	1.65E-02	9.93E-05	1.50E-02	1.48E-04	1.60E-05	3.85E-03	3.39E-03	4.33E-02	6.63E-04	1.93E-05	1.48E-04	2.98E-06	4.69E-02
P99.9	9.12	-102.54	5945.78	1.36E-01	3.15E-02	1.29E-04	3.46E-02	1.48E-04	3.73E-05	4.02E-03	3.70E-03	9.78E-02	1.03E-03	4.27E-05	1.56E-04	3.33E-06	1.01E-01
Maximum	9.14	-98.10	6335.20	1.45E-01	3.34E-02	1.33E-04	3.71E-02	1.48E-04	3.98E-05	4.05E-03	3.75E-03	1.05E-01	1.08E-03	4.55E-05	1.58E-04	3.41E-06	1.08E-01
Permafrost II: BaseCase																	
	pH	Eh(mV) (HemC+FeSc	TDS(mg/l)	IonicStr	mNa	mK	mCa	mMg	mFe(II) (HemC+FeSc)	mC	AlkTot	mCl	mS(VI)	mS(-II) (HemC+FeSc)	mSi	mP	Na+K+2Mg+2Ca
N total	28044	56088	28044	28044	28044	28044	28044	28044	56088	28044	28044	28044	28044	56088	28044	28044	28044
Mean	8.21	-269.49	515.84	1.05E-02	3.26E-03	3.46E-05	2.32E-03	4.98E-05	2.63E-06	1.33E-03	1.28E-03	6.52E-03	1.65E-04	3.02E-06	1.41E-04	7.55E-07	8.05E-03
Standard Deviation	0.66	48.19	765.56	1.72E-02	4.30E-03	2.22E-05	4.29E-03	3.68E-05	4.99E-06	9.37E-04	7.85E-04	1.23E-02	1.64E-04	5.79E-06	7.16E-06	6.79E-07	1.29E-02
Minimum	6.78	-358.13	54.10	8.21E-04	1.88E-04	1.22E-05	1.88E-04	7.88E-06	9.85E-11	2.09E-04	2.87E-04	1.93E-04	1.69E-05	1.42E-15	1.30E-04	5.56E-08	5.93E-04
P0.1	6.80	-353.34	56.59	8.67E-04	2.13E-04	1.24E-05	1.94E-04	8.59E-06	1.32E-10	2.60E-04	3.22E-04	2.26E-04	1.83E-05	4.87E-15	1.31E-04	7.38E-08	6.32E-04
P5	6.97	-329.86	84.49	1.38E-03	4.88E-04	1.52E-05	2.60E-04	1.43E-05	7.83E-10	3.97E-04	4.68E-04	4.99E-04	3.55E-05	2.48E-09	1.33E-04	1.51E-07	1.05E-03
Median	8.37	-281.81	202.45	3.64E-03	1.42E-03	2.45E-05	6.61E-04	3.34E-05	1.06E-06	9.32E-04	9.63E-04	1.71E-03	9.13E-05	4.73E-07	1.40E-04	4.38E-07	2.85E-03
P95	9.10	-185.48	2318.14	5.09E-02	1.35E-02	8.32E-05	1.23E-02	1.23E-04	1.31E-05	3.11E-03	2.74E-03	3.53E-02	5.43E-04	1.53E-05	1.56E-04	2.10E-06	3.84E-02
P99.9	9.43	-118.45	4839.36	1.11E-01	2.56E-02	1.07E-04	2.82E-02	1.42E-04	3.05E-05	3.82E-03	3.50E-03	7.94E-02	8.42E-04	3.44E-05	1.78E-04	3.04E-06	8.23E-02
Maximum	9.47	-112.01	5295.58	1.21E-01	2.79E-02	1.13E-04	3.10E-02	1.48E-04	3.33E-05	4.01E-03	3.68E-03	8.73E-02	9.05E-04	3.76E-05	1.81E-04	3.32E-06	9.02E-02
Permafrost III: BaseCase																	
	pH	Eh(mV) (HemC+FeSc	TDS(mg/l)	IonicStr	mNa	mK	mCa	mMg	mFe(II) (HemC+FeSc)	mC	AlkTot	mCl	mS(VI)	mS(-II) (HemC+FeSc)	mSi	mP	Na+K+2Mg+2Ca
N total	28044	56088	28044	28044	28044	28044	28044	28044	56088	28044	28044	28044	28044	56088	28044	28044	28044
Mean	8.60	-296.19	357.25	7.32E-03	2.14E-03	2.54E-05	1.66E-03	3.18E-05	1.76E-06	8.59E-04	8.72E-04	4.53E-03	1.06E-04	2.03E-06	1.50E-04	4.24E-07	5.55E-03
Standard Deviation	0.73	51.00	587.31	1.32E-02	3.32E-03	1.71E-05	3.27E-03	2.80E-05	3.76E-06	7.18E-04	6.07E-04	9.31E-03	1.27E-04	4.24E-06	1.46E-05	4.44E-07	9.88E-03
Minimum	6.87	-367.19	46.37	6.79E-04	9.22E-05	1.10E-05	1.74E-04	5.73E-06	5.96E-11	1.98E-04	2.80E-04	1.04E-04	1.02E-05	3.96E-14	1.31E-04	5.22E-08	4.72E-04
P0.1	6.95	-365.88	46.95	6.88E-04	1.01E-04	1.12E-05	1.76E-04	6.18E-06	6.40E-11	2.12E-04	3.08E-04	1.11E-04	1.12E-05	4.69E-13	1.32E-04	6.12E-08	4.79E-04
P5	7.11	-353.91	56.14	8.66E-04	2.04E-04	1.23E-05	1.96E-04	8.33E-06	1.43E-10	2.53E-04	3.59E-04	2.28E-04	1.75E-05	1.73E-08	1.34E-04	8.06E-08	6.28E-04
Median	8.82	-310.82	118.09	2.03E-03	7.58E-04	1.80E-05	3.80E-04	2.00E-05	5.94E-07	5.53E-04	6.08E-04	8.81E-04	5.16E-05	4.11E-07	1.46E-04	2.32E-07	1.57E-03
P95	9.44	-197.68	1831.34	4.02E-02	1.05E-02	6.71E-05	9.73E-03	9.33E-05	1.13E-05	2.41E-03	2.17E-03	2.77E-02	4.25E-04	1.29E-05	1.79E-04	1.41E-06	3.03E-02
P99.9	9.58	-143.18	3508.82	8.03E-02	1.85E-02	8.37E-05	2.04E-02	1.21E-04	2.24E-05	3.14E-03	2.86E-03	5.72E-02	6.15E-04	2.50E-05	1.95E-04	2.20E-06	5.96E-02
Maximum	9.59	-129.90	3988.70	9.15E-02	2.09E-02	9.40E-05	2.34E-02	1.48E-04	2.64E-05	3.79E-03	3.26E-03	6.55E-02	6.99E-04	2.96E-05	1.96E-04	2.86E-06	6.79E-02
Permafrost IV: BaseCase																	
	pH	Eh(mV) (HemC+FeSc	TDS(mg/l)	IonicStr	mNa	mK	mCa	mMg	mFe(II) (HemC+FeSc)	mC	AlkTot	mCl	mS(VI)	mS(-II) (HemC+FeSc)	mSi	mP	Na+K+2Mg+2Ca
N total	28044.00	56088	28044.00	28044	28044	28044	28044	28044	56088	28044	28044	28044	28044	56088	28044	28044	28044
Mean	9.01	-324.49	119.51	2.26E-03	6.23E-04	1.49E-05	5.13E-04	1.30E-05	5.79E-07	3.52E-04	4.21E-04	1.22E-03	3.59E-05	7.24E-07	1.57E-04	1.20E-07	1.69E-03
Standard Deviation	0.35	23.17	67.68	1.52E-03	4.13E-04	2.71E-06	3.65E-04	5.07E-06	7.40E-07	1.33E-04	1.17E-04	1.07E-03	1.82E-05	7.47E-07	1.31E-05	5.98E-08	1.14E-03
Minimum	7.84	-372.27	43.19	6.27E-04	4.35E-05	1.05E-05	1.77E-04	4.66E-06	4.70E-11	1.44E-04	2.16E-04	8.18E-05	7.15E-06	1.00E-07	1.37E-04	3.04E-08	4.22E-04
P0.1	8.02	-368.79	46.20	6.90E-04	7.51E-05	1.07E-05	1.79E-04	4.83E-06	5.62E-11	1.51E-04	2.22E-04	1.32E-04	8.39E-06	1.00E-07	1.37E-04	3.25E-08	4.75E-04
P5	8.35	-355.11	56.99	8.87E-04	2.01E-04	1.18E-05	1.99E-04	6.73E-06	1.30E-10	1.88E-04	2.74E-04	2.43E-04	1.57E-05	1.03E-07	1.40E-04	4.74E-08	6.44E-04
Median	9.08	-329.00	94.78	1.68E-03	4.94E-04	1.41E-05	3.68E-04	1.14E-05	2.56E-07	3.12E-04	3.92E-04	8.14E-04	3.03E-05	3.78E-07	1.55E-04	1.03E-07	1.26E-03
P95	9.45	-280.84	263.10	5.47E-03	1.48E-03	2.01E-05	1.28E-03	2.21E-05	2.10E-06	5.91E-04	6.28E-04	3.43E-03	7.21E-05	2.17E-06	1.79E-04	2.25E-07	4.10E-03
P99.9	9.62	-256.33	486.65	1.08E-02	2.61E-03	2.79E-05	2.68E-03	3.80E-05	3.77E-06	1.05E-03	1.05E-03	7.34E-03	1.19E-04	3.89E-06	2.00E-04	4.46E-07	7.99E-03
Maximum	9.66	-241.22	578.58	1.30E-02	3.03E-03	3.31E-05	3.24E-03	4.80E-05	4.86E-06	1.32E-03	1.31E-03	8.90E-03	1.52E-04	5.37E-06	2.06E-04	6.11E-07	9.58E-03

Table A4-10. Statistical results for the main geochemical parameters obtained with the geochemical variant case 1 (Hem coup) over the glacial period with frozen ground (permafrost) in the repository volume. Chemical components in mol/kg, TDS in mg/L, pH in standard units and Eh in mV.

Permafrost 0: Hematite Coupled																		
	pH	Eh(mV)	TDS(mg/l)	IonicStr	mNa	mK	mCa	mMg	mFe+2	mC	AlkTot	mCl	mS(VI)	mS(-II)	mSi	mP	Na+K+2Mg+2Ca
N total	28044	28044	28044	28044	28044	28044	28044	28044	28044	28044	28044	28044	28044	28044	28044	28044	28044
Mean	7.28	-195.05	988.11	1.85E-02	7.49E-03	8.14E-05	3.44E-03	1.48E-04	9.84E-07	3.93E-03	3.53E-03	1.05E-02	4.40E-04	4.83E-08	1.34E-04	3.16E-06	1.47E-02
Standard Deviation	0.13	17.79	355.44	8.33E-03	1.75E-03	3.48E-06	2.21E-03	2.76E-07	2.82E-07	1.18E-04	2.16E-04	6.37E-03	4.34E-05	3.68E-08	3.87E-07	2.26E-07	6.18E-03
Minimum	6.84	-219.39	644.58	1.06E-02	5.75E-03	7.79E-05	1.33E-03	1.46E-04	3.76E-07	3.49E-03	2.75E-03	4.17E-03	3.97E-04	3.32E-14	1.32E-04	2.39E-06	8.79E-03
P0.1	6.86	-219.11	646.95	1.06E-02	5.77E-03	7.80E-05	1.35E-03	1.46E-04	3.82E-07	3.51E-03	2.78E-03	4.22E-03	3.97E-04	5.83E-14	1.32E-04	2.42E-06	8.83E-03
P5	6.99	-212.21	717.36	1.22E-02	6.13E-03	7.87E-05	1.77E-03	1.47E-04	5.67E-07	3.66E-03	3.04E-03	5.54E-03	4.06E-04	6.33E-12	1.33E-04	2.67E-06	1.01E-02
Median	7.31	-201.21	863.70	1.56E-02	6.88E-03	8.02E-05	2.66E-03	1.48E-04	9.44E-07	3.97E-03	3.59E-03	8.24E-03	4.25E-04	4.95E-08	1.34E-04	3.21E-06	1.26E-02
P95	7.44	-152.30	1808.14	3.77E-02	1.15E-02	8.94E-05	8.54E-03	1.48E-04	1.46E-06	4.06E-03	3.77E-03	2.52E-02	5.40E-04	1.08E-07	1.35E-04	3.44E-06	2.90E-02
P99.9	7.54	-129.05	2858.78	6.26E-02	1.66E-02	9.95E-05	1.51E-02	1.48E-04	1.59E-06	4.12E-03	3.88E-03	4.37E-02	6.66E-04	1.39E-07	1.35E-04	3.62E-06	4.73E-02
Maximum	7.54	-126.26	3041.98	6.69E-02	1.75E-02	1.01E-04	1.63E-02	1.48E-04	1.61E-06	4.12E-03	3.89E-03	4.69E-02	6.88E-04	1.41E-07	1.35E-04	3.62E-06	5.05E-02
Permafrost I: Hematite Coupled																	
	pH	Eh(mV)	TDS(mg/l)	IonicStr	mNa	mK	mCa	mMg	mFe+2	mC	AlkTot	mCl	mS(VI)	mS(-II)	mSi	mP	Na+K+2Mg+2Ca
N total	28044	28044	28044	28044	28044	28044	28044	28044	28044	28044	2.80E+04	28044	28044	28044	28044	28044	28044
Mean	8.03	-247.97	642.81	1.31E-02	4.14E-03	4.15E-05	2.87E-03	6.29E-05	3.45E-07	1.67E-03	1.56E-03	8.18E-03	2.10E-04	9.60E-08	1.39E-04	1.03E-06	1.01E-02
Standard Deviation	0.63	53.56	937.84	2.11E-02	5.28E-03	2.72E-05	5.25E-03	4.53E-05	5.58E-07	1.12E-03	9.11E-04	1.51E-02	2.01E-04	4.72E-08	4.77E-06	9.14E-07	1.58E-02
Minimum	6.69	-329.35	80.45	1.32E-03	4.31E-04	1.31E-05	2.50E-04	9.13E-06	3.84E-10	2.33E-04	2.99E-04	4.65E-04	2.57E-05	1.22E-16	1.29E-04	6.35E-08	1.00E-03
P0.1	6.70	-327.24	82.54	1.35E-03	4.64E-04	1.45E-05	2.54E-04	1.18E-05	4.24E-10	3.00E-04	3.52E-04	4.84E-04	3.29E-05	1.85E-16	1.30E-04	8.69E-08	1.03E-03
P5	6.86	-311.05	109.80	1.86E-03	6.95E-04	1.73E-05	3.32E-04	1.86E-05	1.17E-09	5.12E-04	5.70E-04	7.38E-04	4.76E-05	6.30E-14	1.32E-04	2.10E-07	1.44E-03
Median	8.15	-262.26	265.96	4.80E-03	1.93E-03	2.98E-05	8.62E-04	4.41E-05	2.72E-08	1.24E-03	1.25E-03	2.30E-03	1.23E-04	1.17E-07	1.38E-04	6.29E-07	3.79E-03
P95	8.88	-129.45	2835.03	6.20E-02	1.65E-02	9.93E-05	1.50E-02	1.48E-04	1.59E-06	3.85E-03	3.39E-03	4.33E-02	6.63E-04	1.33E-07	1.48E-04	2.98E-06	4.69E-02
P99.9	9.12	-100.21	5945.78	1.36E-01	3.15E-02	1.29E-04	3.46E-02	1.48E-04	1.85E-06	4.02E-03	3.70E-03	9.78E-02	1.03E-03	1.41E-07	1.56E-04	3.33E-06	1.01E-01
Maximum	9.14	-98.10	6335.20	1.45E-01	3.34E-02	1.33E-04	3.71E-02	1.48E-04	1.87E-06	4.05E-03	3.75E-03	1.05E-01	1.08E-03	1.45E-07	1.58E-04	3.41E-06	1.08E-01
Permafrost II: Hematite Coupled																	
	pH	Eh(mV)	TDS(mg/l)	IonicStr	mNa	mK	mCa	mMg	mFe+2	mC	AlkTot	mCl	mS(VI)	mS(-II)	mSi	mP	Na+K+2Mg+2Ca
N total	28044	28044	28044	28044	28044	28044	28044	28044	28044	28044	28044	28044	28044	28044	28044	28044	28044
Mean	8.21	-262.16	515.84	1.05E-02	3.26E-03	3.46E-05	2.32E-03	4.98E-05	2.64E-07	1.33E-03	1.28E-03	6.52E-03	1.65E-04	9.85E-08	1.41E-04	7.55E-07	8.05E-03
Standard Deviation	0.66	52.54	765.56	1.72E-02	4.30E-03	2.22E-05	4.29E-03	3.68E-05	4.74E-07	9.37E-04	7.85E-04	1.23E-02	1.64E-04	4.14E-08	7.16E-06	6.79E-07	1.29E-02
Minimum	6.78	-351.52	54.10	8.21E-04	1.88E-04	1.22E-05	1.88E-04	7.88E-06	9.85E-11	2.09E-04	2.87E-04	1.93E-04	1.69E-05	1.42E-15	1.30E-04	5.56E-08	5.93E-04
P0.1	6.80	-349.01	56.59	8.67E-04	2.13E-04	1.24E-05	1.94E-04	8.59E-06	1.14E-10	2.60E-04	3.22E-04	2.26E-04	1.83E-05	3.14E-15	1.31E-04	7.38E-08	6.32E-04
P5	6.97	-325.98	84.49	1.38E-03	4.88E-04	1.52E-05	2.60E-04	1.43E-05	4.55E-10	3.97E-04	4.68E-04	4.99E-04	3.55E-05	1.31E-12	1.33E-04	1.51E-07	1.05E-03
Median	8.37	-277.08	202.45	3.64E-03	1.42E-03	2.45E-05	6.61E-04	3.34E-05	1.05E-08	9.32E-04	9.63E-04	1.71E-03	9.13E-05	1.15E-07	1.40E-04	4.38E-07	2.85E-03
P95	9.10	-146.66	2318.14	5.09E-02	1.35E-02	8.32E-05	1.23E-02	1.23E-04	1.43E-06	3.11E-03	2.74E-03	3.53E-02	5.43E-04	1.31E-07	1.56E-04	2.10E-06	3.84E -02
P99.9	9.43	-116.39	4839.36	1.11E-01	2.56E-02	1.07E-04	2.82E-02	1.42E-04	1.64E-06	3.82E-03	3.50E-03	7.94E-02	8.42E-04	1.40E-07	1.78E-04	3.04E-06	8.23E -02
Maximum	9.47	-112.01	5295.58	1.21E-01	2.79E-02	1.13E-04	3.10E-02	1.48E-04	1.69E-06	4.01E-03	3.68E-03	8.73E-02	9.05E-04	1.42E-07	1.81E-04	3.32E-06	9.02E -02
Permafrost III: Hematite Coupled																	
	pH	Eh(mV)	TDS(mg/l)	IonicStr	mNa	mK	mCa	mMg	mFe+2	mC	AlkTot	mCl	mS(VI)	mS(-II)	mSi	mP	Na+K+2Mg+2Ca
N total	28044	28044	28044	28044	28044	28044	28044	28044	28044	28044	28044	28044	28044	28044	28044	28044	28044
Mean	8.60	-290.31	357.25	7.32E-03	2.14E-03	2.54E-05	1.66E-03	3.18E-05	1.72E-07	8.59E-04	8.72E-04	4.53E-03	1.06E-04	9.84E-08	1.50E-04	4.24E-07	5.55E-03
Standard Deviation	0.73	54.35	587.31	1.32E-02	3.32E-03	1.71E-05	3.27E-03	2.80E-05	3.93E-07	7.18E-04	6.07E-04	9.31E-03	1.27E-04	3.53E-08	1.46E-05	4.44E-07	9.88E-03
Minimum	6.87	-361.04	46.37	6.79E-04	9.22E-05	1.10E-05	1.74E-04	5.73E-06	5.96E-11	1.98E-04	2.80E-04	1.04E-04	1.02E-05	3.96E-14	1.31E-04	5.22E-08	4.72E-04
P0.1	6.95	-360.07	46.95	6.88E-04	1.01E-04	1.12E-05	1.76E-04	6.18E-06	6.22E-11	2.12E-04	3.08E-04	1.11E-04	1.12E-05	2.90E-13	1.32E-04	6.12E-08	4.79E-04
P5	7.11	-349.92	56.14	8.66E-04	2.04E-04	1.23E-05	1.96E-04	8.33E-06	1.09E-10	2.53E-04	3.59E-04	2.28E-04	1.75E-05	8.37E-11	1.34E-04	8.06E-08	6.28E-04
Median	8.82	-307.06	118.09	2.03E-03	7.58E-04	1.80E-05	3.80E-04	2.00E-05	1.52E-09	5.53E-04	6.08E-04	8.81E-04	5.16E-05	1.09E-07	1.46E-04	2.32E-07	1.57E-03
P95	9.44	-169.29	1831.34	4.02E-02	1.05E-02	6.71E-05	9.73E-03	9.33E-05	1.26E-06	2.41E-03	2.17E-03	2.77E-02	4.25E-04	1.27E-07	1.79E-04	1.41E-06	3.03E-02
P99.9	9.58	-140.68	3508.82	8.03E-02	1.85E-02	8.37E-05	2.04E-02	1.21E-04	1.43E-06	3.14E-03	2.86E-03	5.72E-02	6.15E-04	1.39E-07	1.95E-04	2.20E-06	5.96E-02
Maximum	9.59	-129.90	3988.70	9.15E-02	2.09E-02	9.40E-05	2.34E-02	1.48E-04	1.54E-06	3.79E-03	3.26E-03	6.55E-02	6.99E-04	1.41E-07	1.96E-04	2.86E-06	6.79E-02
Permafrost IV: Hematite Coupled																	
	pH	Eh(mV)	TDS(mg/l)	IonicStr	mNa	mK	mCa	mMg	mFe+2	mC	AlkTot	mCl	mS(VI)	mS(-II)	mSi	mP	Na+K+2Mg+2Ca
N total	28044	28044	28044	28044	28044	28044	28044	28044	28044	28044	28044	28044	28044	28044	28044	28044	28044
Mean	9.01	-320.55	119.51	2.26E-03	6.23E-04	1.49E-05	5.13E-04	1.30E-05	2.50E-09	3.52E-04	4.21E-04	1.22E-03	3.59E-05	1.07E-07	1.57E-04	1.20E-07	1.69E-03
Standard Deviation	0.35	23.37	67.68	1.52E-03	4.13E-04	2.71E-06	3.65E-04	5.07E-06	5.54E-09	1.33E-04	1.17E-04	1.07E-03	1.82E-05	3.75E-09	1.31E-05	5.98E-08	1.14E-03
Minimum	7.84	-366.34	43.19	6.27E-04	4.35E-05	1.05E-05	1.77E-04	4.66E-06	4.70E-11	1.44E-04	2.16E-04	8.18E-05	7.15E-06	1.00E-07	1.37E-04	3.04E-08	4.22E-04
P0.1	8.02	-363.26	46.20	6.90E-04	7.51E-05	1.07E-05	1.79E-04	4.83E-06	5.51E-11	1.51E-04	2.22E-04	1.32E-04	8.39E-06	1.00E-07	1.37E-04	3.25E-08	4.75E-04
P5	8.35	-350.44	56.99	8.87E-04	2.01E-04	1.18E-05	1.99E-04	6.73E-06	1.08E-10	1.88E-04	2.74E-04	2.43E-04	1.57E-05	1.02E-07	1.40E-04	4.74E-08	6.44E-04
Median	9.08	-325.13	94.78	1.68E-03	4.94E-04	1.41E-05	3.68E-04	1.14E-05	5.17E-10	3.12E-04	3.92E-04	8.14E-04	3.03E-05	1.06E-07	1.55E-04	1.03E-07	1.26E-03
P95	9.45	-276.39	263.10	5.47E-03	1.48E-03	2.01E-05	1.28E-03	2.21E-05	1.25E-08	5.91E-04	6.28E-04	3.43E-03	7.21E-05	1.14E-07	1.79E-04	2.25E-07	4.10E-03
P99.9	9.62	-254.05	486.65	1.08E-02	2.61E-03	2.79E-05	2.68E-03	3.80E-05	5.23E-08	1.05E-03	1.05E-03	7.34E-03	1.19E-04	1.21E-07	2.00E-04	4.46E-07	7.99E-03
Maximum	9.66	-241.22	578.58	1.30E-02	3.03E-03	3.31E-05	3.24E-03	4.80E-05	1.13E-07	1.32E-03	1.31E-03	8.90E-03	1.52E-04	1.26E-07	2.06E-04	6.11E-07	9.58E-03

Table A4-11. Statistical results for the main geochemical parameters obtained with the geochemical variant case 2 (FeS coup) over the glacial period with frozen ground (permafrost) in the repository volume. Chemical components in mol/kg, TDS in mg/L, pH in standard units and Eh in mV.

Permafrost 0: FeS(am) coupled																		
	pH	Eh(mV)	TDS(mg/l)	IonicStr	mNa	mK	mCa	mMg	mFe+2	mC	AlkTot	mCl	mS(VI)	mS(-II)	mSi	mP	Na+K+2Mg+2Ca
N total	28044	28044	28044	28044	28044	28044	28044	28044	28044	28044	28044	28044	28044	28044	28044	28044	28044
Mean	7.28	-216.67	989.90	1.85E-02	7.49E-03	8.14E-05	3.43E-03	1.48E-04	1.09E-05	3.92E-03	3.55E-03	1.05E-02	4.60E-04	1.40E-05	1.34E-04	3.14E-06	1.47E-02
Standard Deviation	0.13	7.99	355.59	8.33E-03	1.75E-03	3.48E-06	2.21E-03	2.76E-07	3.42E-06	1.22E-04	2.17E-04	6.37E-03	4.72E-05	3.74E-06	3.88E-07	2.31E-07	6.17E-03
Minimum	6.85	-232.56	646.16	1.06E-02	5.75E-03	7.79E-05	1.32E-03	1.46E-04	6.51E-06	3.45E-03	2.76E-03	4.17E-03	4.12E-04	9.15E-06	1.32E-04	2.35E-06	8.77E-03
P0.1	6.86	-232.33	648.54	1.06E-02	5.77E-03	7.80E-05	1.34E-03	1.46E-04	6.55E-06	3.47E-03	2.79E-03	4.22E-03	4.13E-04	9.20E-06	1.32E-04	2.38E-06	8.81E-03
P5	6.99	-226.58	718.97	1.22E-02	6.13E-03	7.87E-05	1.76E-03	1.47E-04	7.72E-06	3.64E-03	3.05E-03	5.54E-03	4.23E-04	1.05E-05	1.33E-04	2.64E-06	1.00E-02
Median	7.31	-218.60	865.44	1.56E-02	6.88E-03	8.02E-05	2.65E-03	1.48E-04	9.80E-06	3.96E-03	3.61E-03	8.24E-03	4.44E-04	1.28E-05	1.34E-04	3.19E-06	1.26E-02
P95	7.44	-199.27	1810.28	3.77E-02	1.15E-02	8.94E-05	8.52E-03	1.48E-04	1.90E-05	4.05E-03	3.79E-03	2.52E-02	5.69E-04	2.28E-05	1.35E-04	3.43E-06	2.90E-02
P99.9	7.54	-191.41	2861.21	6.26E-02	1.66E-02	9.95E-05	1.51E-02	1.48E-04	2.57E-05	4.11E-03	3.90E-03	4.37E-02	7.03E-04	3.01E-05	1.35E-04	3.60E-06	4.72E-02
Maximum	7.54	-190.49	3044.51	6.69E-02	1.75E-02	1.01E-04	1.63E-02	1.48E-04	2.67E-05	4.11E-03	3.90E-03	4.69E-02	7.26E-04	3.12E-05	1.35E-04	3.61E-06	5.04E-02
Permafrost I: FeS(am) coupled																	
	pH	Eh(mV)	TDS(mg/l)	IonicStr	mNa	mK	mCa	mMg	mFe+2	mC	AlkTot	mCl	mS(VI)	mS(-II)	mSi	mP	Na+K+2Mg+2Ca
N total	28044	28044	28044	28044	28044	28044	28044	28044	28044	28044	28044	28044	28044	28044	28044	28044	28044
Mean	8.03	-265.02	644.17	1.31E-02	4.14E-03	4.15E-05	2.86E-03	6.29E-05	6.29E-06	1.66E-03	1.57E-03	8.18E-03	2.24E-04	7.57E-06	1.39E-04	1.02E-06	1.00E-02
Standard Deviation	0.63	40.21	938.24	2.11E-02	5.28E-03	2.72E-05	5.25E-03	4.53E-05	7.62E-06	1.12E-03	9.10E-04	1.51E-02	2.10E-04	8.89E-06	4.81E-06	9.04E-07	1.58E-02
Minimum	6.69	-336.70	81.53	1.32E-03	4.31E-04	1.31E-05	2.49E-04	9.13E-06	7.74E-07	2.32E-04	3.12E-04	4.65E-04	3.30E-05	1.02E-06	1.29E-04	6.27E-08	9.99E-04
P0.1	6.71	-334.88	83.63	1.35E-03	4.64E-04	1.45E-05	2.53E-04	1.18E-05	7.93E-07	2.98E-04	3.65E-04	4.84E-04	4.04E-05	1.17E-06	1.30E-04	8.59E-08	1.03E-03
P5	6.87	-319.43	110.90	1.86E-03	6.95E-04	1.73E-05	3.30E-04	1.86E-05	1.10E-06	5.10E-04	5.84E-04	7.38E-04	5.55E-05	1.51E-06	1.32E-04	2.08E-07	1.43E-03
Median	8.16	-272.80	267.10	4.80E-03	1.93E-03	2.98E-05	8.58E-04	4.41E-05	2.96E-06	1.23E-03	1.26E-03	2.30E-03	1.33E-04	3.58E-06	1.38E-04	6.25E-07	3.78E-03
P95	8.88	-191.58	2837.45	6.20E-02	1.65E-02	9.93E-05	1.50E-02	1.48E-04	2.56E-05	3.83E-03	3.40E-03	4.33E-02	7.00E-04	2.99E-05	1.48E-04	2.96E-06	4.68E-02
P99.9	9.12	-181.66	5948.60	1.36E-01	3.15E-02	1.29E-04	3.46E-02	1.48E-04	3.86E-05	4.01E-03	3.71E-03	9.78E-02	1.09E-03	4.42E-05	1.57E-04	3.32E-06	1.01E-01
Maximum	9.15	-180.98	6338.08	1.45E-01	3.34E-02	1.33E-04	3.70E-02	1.48E-04	3.98E-05	4.04E-03	3.77E-03	1.05E-01	1.13E-03	4.55E-05	1.58E-04	3.39E-06	1.08E-01
Permafrost II: FeS(am) coupled																	
	pH	Eh(mV)	TDS(mg/l)	IonicStr	mNa	mK	mCa	mMg	mFe+2	mC	AlkTot	mCl	mS(VI)	mS(-II)	mSi	mP	Na+K+2Mg+2Ca
N total	28044	28044	28044	28044	28044	28044	28044	28044	28044	28044	28044	28044	28044	28044	28044	28044	28044
Mean	8.21	-276.81	517.12	1.05E-02	3.26E-03	3.46E-05	2.32E-03	4.98E-05	4.99E-06	1.33E-03	1.30E-03	6.52E-03	1.78E-04	5.94E-06	1.41E-04	7.48E-07	8.03E-03
Standard Deviation	0.66	42.15	765.88	1.72E-02	4.30E-03	2.22E-05	4.29E-03	3.68E-05	6.20E-06	9.31E-04	7.85E-04	1.23E-02	1.71E-04	7.07E-06	7.23E-06	6.73E-07	1.29E-02
Minimum	6.78	-358.13	55.23	8.21E-04	1.88E-04	1.22E-05	1.88E-04	7.88E-06	4.96E-07	2.08E-04	3.01E-04	1.93E-04	2.40E-05	8.05E-07	1.30E-04	5.49E-08	5.92E-04
P0.1	6.81	-355.74	57.70	8.67E-04	2.13E-04	1.24E-05	1.93E-04	8.59E-06	5.20E-07	2.59E-04	3.36E-04	2.26E-04	2.54E-05	8.31E-07	1.31E-04	7.31E-08	6.31E-04
P5	6.97	-333.68	85.59	1.38E-03	4.88E-04	1.52E-05	2.58E-04	1.43E-05	8.08E-07	3.96E-04	4.82E-04	4.99E-04	4.30E-05	1.20E-06	1.33E-04	1.50E-07	1.05E-03
Median	8.38	-286.94	203.56	3.64E-03	1.42E-03	2.45E-05	6.58E-04	3.34E-05	2.21E-06	9.29E-04	9.76E-04	1.71E-03	1.00E-04	2.70E-06	1.40E-04	4.36E-07	2.84E-03
P95	9.10	-198.59	2320.43	5.09E-02	1.35E-02	8.32E-05	1.23E-02	1.23E-04	2.09E-05	3.09E-03	2.76E-03	3.53E-02	5.73E-04	2.40E-05	1.56E-04	2.08E-06	3.83E-02
P99.9	9.43	-188.39	4841.73	1.11E-01	2.56E-02	1.07E-04	2.82E-02	1.42E-04	3.14E-05	3.81E-03	3.51E-03	7.94E-02	8.84E-04	3.54E-05	1.78E-04	3.02E-06	8.22E-02
Maximum	9.47	-186.68	5298.19	1.21E-01	2.79E-02	1.13E-04	3.09E-02	1.48E-04	3.33E-05	4.00E-03	3.70E-03	8.73E-02	9.49E-04	3.76E-05	1.82E-04	3.30E-06	9.01E-02
Permafrost III: FeS(am) coupled																	
	pH	Eh(mV)	TDS(mg/l)	IonicStr	mNa	mK	mCa	mMg	mFe+2	mC	AlkTot	mCl	mS(VI)	mS(-II)	mSi	mP	Na+K+2Mg+2Ca
N total	28044	28044	28044	28044	28044	28044	28044	28044	28044	28044	28044	28044	28044	28044	28044	28044	28044
Mean	8.60	-302.06	358.45	7.31E-03	2.14E-03	2.54E-05	1.66E-03	3.18E-05	3.35E-06	8.55E-04	8.86E-04	4.53E-03	1.17E-04	3.96E-06	1.50E-04	4.20E-07	5.54E-03
Standard Deviation	0.73	46.68	587.54	1.32E-02	3.32E-03	1.71E-05	3.26E-03	2.80E-05	4.81E-06	7.13E-04	6.06E-04	9.31E-03	1.33E-04	5.34E-06	1.47E-05	4.39E-07	9.87E-03
Minimum	6.88	-367.19	47.50	6.80E-04	9.22E-05	1.10E-05	1.74E-04	5.73E-06	4.26E-07	1.97E-04	2.94E-04	1.04E-04	1.72E-05	6.81E-07	1.31E-04	5.16E-08	4.71E-04
P0.1	6.95	-366.28	48.08	6.89E-04	1.01E-04	1.12E-05	1.76E-04	6.18E-06	4.30E-07	2.12E-04	3.21E-04	1.11E-04	1.82E-05	7.01E-07	1.32E-04	6.06E-08	4.79E-04
P5	7.12	-356.54	57.25	8.66E-04	2.04E-04	1.23E-05	1.95E-04	8.33E-06	5.17E-07	2.53E-04	3.73E-04	2.28E-04	2.46E-05	8.15E-07	1.34E-04	7.99E-08	6.27E-04
Median	8.82	-315.55	119.17	2.03E-03	7.58E-04	1.80E-05	3.78E-04	2.00E-05	1.21E-06	5.51E-04	6.21E-04	8.81E-04	5.95E-05	1.61E-06	1.46E-04	2.31E-07	1.57E-03
P95	9.45	-207.82	1833.18	4.02E-02	1.05E-02	6.71E-05	9.71E-03	9.33E-05	1.62E-05	2.39E-03	2.18E-03	2.77E-02	4.49E-04	1.82E-05	1.79E-04	1.39E-06	3.02E-02
P99.9	9.58	-197.62	3511.09	8.02E-02	1.85E-02	8.37E-05	2.04E-02	1.21E-04	2.31E-05	3.13E-03	2.87E-03	5.72E-02	6.47E-04	2.58E-05	1.95E-04	2.18E-06	5.96E-02
Maximum	9.60	-192.72	3990.90	9.15E-02	2.09E-02	9.40E-05	2.33E-02	1.48E-04	2.64E-05	3.77E-03	3.27E-03	6.55E-02	7.35E-04	2.96E-05	1.97E-04	2.84E-06	6.78E-02
Permafrost IV: FeS(am) coupled																	
	pH	Eh(mV)	TDS(mg/l)	IonicStr	mNa	mK	mCa	mMg	mFe+2	mC	AlkTot	mCl	mS(VI)	mS(-II)	mSi	mP	Na+K+2Mg+2Ca
N total	28044	28044	28044	28044	28044	28044	28044	28044	28044	28044	28044	28044	28044	28044	28044	28044	28044
Mean	9.01	-328.42	120.59	2.26E-03	6.23E-04	1.49E-05	5.12E-04	1.30E-05	1.16E-06	3.51E-04	4.35E-04	1.22E-03	4.36E-05	1.34E-06	1.57E-04	1.19E-07	1.69E-03
Standard Deviation	0.35	22.28	67.67	1.52E-03	4.13E-04	2.71E-06	3.65E-04	5.07E-06	6.56E-07	1.32E-04	1.17E-04	1.07E-03	1.88E-05	5.96E-07	1.33E-05	5.94E-08	1.14E-03
Minimum	7.84	-372.27	44.34	6.27E-04	4.35E-05	1.05E-05	1.77E-04	4.66E-06	3.99E-07	1.43E-04	2.29E-04	8.18E-05	1.41E-05	6.30E-07	1.37E-04	2.99E-08	4.22E-04
P0.1	8.03	-369.19	47.33	6.91E-04	7.51E-05	1.07E-05	1.79E-04	4.83E-06	4.26E-07	1.50E-04	2.35E-04	1.32E-04	1.53E-05	6.41E-07	1.37E-04	3.20E-08	4.74E-04
P5	8.35	-356.99	58.10	8.87E-04	2.01E-04	1.18E-05	1.99E-04	6.73E-06	5.25E-07	1.87E-04	2.88E-04	2.43E-04	2.27E-05	7.70E-07	1.40E-04	4.68E-08	6.43E-04
Median	9.08	-332.71	95.85	1.68E-03	4.94E-04	1.41E-05	3.66E-04	1.14E-05	9.20E-07	3.10E-04	4.06E-04	8.14E-04	3.77E-05	1.12E-06	1.55E-04	1.02E-07	1.26E-03
P95	9.45	-286.43	264.16	5.47E-03	1.48E-03	2.01E-05	1.27E-03	2.21E-05	2.57E-06	5.88E-04	6.41E-04	3.43E-03	8.10E-05	2.61E-06	1.80E-04	2.23E-07	4.10E-03
P99.9	9.62	-265.28	487.72	1.08E-02	2.61E-03	2.79E-05	2.67E-03	3.80E-05	4.00E-06	1.04E-03	1.07E-03	7.34E-03	1.30E-04	4.11E-06	2.00E-04	4.43E-07	7.98E-03
Maximum	9.66	-253.31	579.67	1.30E-02	3.03E-03	3.31E-05	3.24E-03	4.80E-05	4.86E-06	1.32E-03	1.32E-03	8.90E-03	1.64E-04	5.37E-06	2.06E-04	6.07E-07	9.57E-03

Table A4-12. Statistical results for the main geochemical parameters obtained with the geochemical variant case 3 (Hem uncoup) over the glacial period with frozen ground (permafrost) in the repository volume. Chemical components in mol/kg, TDS in mg/L, pH in standard units and Eh in mV.

Permafrost 0: Hematite Uncoupled																	
	pH	Eh(mV)	TDS(mg/l)	IonicStr	mNa	mK	mCa	mMg	mFe+2	mC	AlkTot	mCl	mS(VI)	mS(-II)	mSi	mP	Na+K+2Mg+2Ca
N total	28044	28044	28044	28044	28044	28044	28044	28044	28044	28044	28044	28044	28044	28044	28044	28044	28044
Mean	7.28	-201.98	988.07	1.85E-02	7.48E-03	8.14E-05	3.44E-03	1.48E-04	1.25E-06	3.93E-03	3.53E-03	1.05E-02	4.40E-04	1.00E-15	1.34E-04	3.16E-06	1.47E-02
Standard Deviation	0.13	22.61	355.45	8.33E-03	1.75E-03	3.48E-06	2.21E-03	2.76E-07	9.45E-08	1.17E-04	2.15E-04	6.37E-03	4.34E-05	2.03E-19	3.87E-07	2.26E-07	6.18E-03
Minimum	6.84	-245.50	644.51	1.06E-02	5.75E-03	7.79E-05	1.33E-03	1.46E-04	1.07E-06	3.49E-03	2.75E-03	4.17E-03	3.97E-04	1.00E-15	1.32E-04	2.39E-06	8.79E-03
P0.1	6.86	-244.87	646.87	1.06E-02	5.77E-03	7.80E-05	1.34E-03	1.46E-04	1.08E-06	3.51E-03	2.78E-03	4.22E-03	3.97E-04	1.00E-15	1.32E-04	2.42E-06	8.83E-03
P5	6.99	-229.54	717.31	1.22E-02	6.13E-03	7.87E-05	1.77E-03	1.47E-04	1.14E-06	3.66E-03	3.04E-03	5.54E-03	4.06E-04	1.00E-15	1.33E-04	2.67E-06	1.01E-02
Median	7.31	-207.65	863.66	1.56E-02	6.87E-03	8.02E-05	2.66E-03	1.48E-04	1.22E-06	3.97E-03	3.59E-03	8.24E-03	4.25E-04	1.00E-15	1.34E-04	3.21E-06	1.26E-02
P95	7.44	-152.25	1808.14	3.77E-02	1.15E-02	8.94E-05	8.54E-03	1.48E-04	1.46E-06	4.06E-03	3.77E-03	2.52E-02	5.40E-04	1.00E-15	1.35E-04	3.44E-06	2.90E-02
P99.9	7.54	-128.99	2858.78	6.26E-02	1.66E-02	9.95E-05	1.51E-02	1.48E-04	1.59E-06	4.12E-03	3.88E-03	4.37E-02	6.66E-04	1.00E-15	1.35E-04	3.62E-06	4.73E-02
Maximum	7.54	-126.20	3041.98	6.69E-02	1.75E-02	1.01E-04	1.63E-02	1.48E-04	1.61E-06	4.12E-03	3.89E-03	4.69E-02	6.88E-04	1.00E-15	1.35E-04	3.62E-06	5.05E-02
Permafrost I: Hematite Uncoupled																	
	pH	Eh(mV)	TDS(mg/l)	IonicStr	mNa	mK	mCa	mMg	mFe+2	mC	AlkTot	mCl	mS(VI)	mS_{-II}	mSi	mP	Na+K+2Mg+2Ca
N total	28044	28044	28044	28044	28044	28044	28044	28044	28044	28044	2.80E+04	28044	28044	28044	28044	28044	28044
Mean	8.03	-296.06	642.80	1.31E-02	4.14E-03	4.15E-05	2.87E-03	6.29E-05	5.13E-07	1.67E-03	1.56E-03	8.18E-03	2.10E-04	5.90E-08	1.39E-04	1.03E-06	1.01E-02
Standard Deviation	0.63	83.14	937.82	2.11E-02	5.28E-03	2.72E-05	5.26E-03	4.53E-05	5.10E-07	1.12E-03	9.11E-04	1.51E-02	2.01E-04	3.18E-08	4.75E-06	9.14E-07	1.58E-02
Minimum	6.69	-401.00	80.47	1.32E-03	4.31E-04	1.31E-05	2.50E-04	9.13E-06	5.81E-09	2.34E-04	2.99E-04	4.65E-04	2.56E-05	1.00E-15	1.29E-04	6.38E-08	1.00E-03
P0.1	6.70	-400.20	82.57	1.35E-03	4.64E-04	1.45E-05	2.55E-04	1.18E-05	8.09E-09	3.00E-04	3.52E-04	4.84E-04	3.28E-05	1.00E-15	1.30E-04	8.72E-08	1.03E-03
P5	6.86	-389.03	109.84	1.86E-03	6.95E-04	1.73E-05	3.32E-04	1.86E-05	2.75E-08	5.13E-04	5.70E-04	7.38E-04	4.75E-05	1.00E-15	1.32E-04	2.10E-07	1.44E-03
Median	8.15	-322.79	265.92	4.80E-03	1.93E-03	2.98E-05	8.62E-04	4.41E-05	3.11E-07	1.24E-03	1.25E-03	2.30E-03	1.23E-04	7.22E-08	1.38E-04	6.29E-07	3.78E-03
P95	8.88	-129.39	2835.03	6.20E-02	1.65E-02	9.93E-05	1.50E-02	1.48E-04	1.59E-06	3.85E-03	3.39E-03	4.33E-02	6.63E-04	8.99E-08	1.48E-04	2.98E-06	4.69E-02
P99.9	9.12	-100.09	5945.55	1.36E-01	3.15E-02	1.29E-04	3.46E-02	1.48E-04	1.84E-06	4.02E-03	3.70E-03	9.78E-02	1.03E-03	9.46E-08	1.56E-04	3.33E-06	1.01E-01
Maximum	9.14	-97.98	6334.97	1.45E-01	3.34E-02	1.33E-04	3.71E-02	1.48E-04	1.87E-06	4.05E-03	3.75E-03	1.05E-01	1.08E-03	9.65E-08	1.57E-04	3.41E-06	1.08E-01
Permafrost II: Hematite Uncoupled																	
	pH	Eh(mV)	TDS(mg/l)	IonicStr	mNa	mK	mCa	mMg	mFe+2	mC	AlkTot	mCl	mS(VI)	mS_{-II}	mSi	mP	Na+K+2Mg+2Ca
N total	28044	28044	28044	28044	28044	28044	28044	28044	28044	28044	28044	28044	28044	28044	28044	28044	28044
Mean	8.21	-314.89	515.85	1.05E-02	3.26E-03	3.46E-05	2.32E-03	4.98E-05	3.85E-07	1.33E-03	1.28E-03	6.52E-03	1.65E-04	6.81E-08	1.41E-04	7.55E-07	8.05E-03
Standard Deviation	0.66	81.98	765.55	1.72E-02	4.30E-03	2.22E-05	4.29E-03	3.68E-05	4.28E-07	9.37E-04	7.85E-04	1.23E-02	1.64E-04	2.58E-08	7.14E-06	6.79E-07	1.29E-02
Minimum	6.78	-410.17	54.12	8.21E-04	1.88E-04	1.22E-05	1.88E-04	7.88E-06	1.06E-09	2.09E-04	2.87E-04	1.93E-04	1.68E-05	1.00E-15	1.30E-04	5.58E-08	5.93E-04
P0.1	6.80	-409.66	56.60	8.68E-04	2.13E-04	1.24E-05	1.94E-04	8.59E-06	1.32E-09	2.61E-04	3.22E-04	2.26E-04	1.82E-05	4.44E-09	1.31E-04	7.41E-08	6.32E-04
P5	6.97	-399.68	84.53	1.38E-03	4.88E-04	1.52E-05	2.60E-04	1.43E-05	9.03E-09	3.98E-04	4.68E-04	4.99E-04	3.54E-05	1.67E-08	1.33E-04	1.51E-07	1.05E-03
Median	8.37	-349.01	202.44	3.64E-03	1.42E-03	2.45E-05	6.61E-04	3.34E-05	1.90E-07	9.32E-04	9.63E-04	1.71E-03	9.12E-05	7.96E-08	1.40E-04	4.39E-07	2.85E-03
P95	9.10	-144.27	2317.96	5.09E-02	1.35E-02	8.32E-05	1.23E-02	1.23E-04	1.31E-06	3.11E-03	2.74E-03	3.53E-02	5.43E-04	9.29E-08	1.56E-04	2.10E-06	3.83E -02
P99.9	9.43	-114.17	4839.12	1.11E-01	2.56E-02	1.07E-04	2.82E-02	1.42E-04	1.52E-06	3.82E-03	3.50E-03	7.94E-02	8.42E-04	9.69E-08	1.77E-04	3.04E-06	8.23E -02
Maximum	9.46	-110.30	5296.02	1.21E-01	2.79E-02	1.13E-04	3.10E-02	1.48E-04	1.58E-06	4.01E-03	3.68E-03	8.73E-02	9.05E-04	9.74E-08	1.81E-04	3.32E-06	9.02E -02
Permafrost III: Hematite Uncoupled																	
	pH	Eh(mV)	TDS(mg/l)	IonicStr	mNa	mK	mCa	mMg	mFe+2	mC	AlkTot	mCl	mS(VI)	mS_{-II}	mSi	mP	Na+K+2Mg+2Ca
N total	28044	28044	28044	28044	28044	28044	28044	28044	28044	28044	28044	28044	28044	28044	28044	28044	28044
Mean	8.60	-347.14	357.26	7.32E-03	2.14E-03	2.54E-05	1.66E-03	3.18E-05	2.18E-07	8.60E-04	8.72E-04	4.53E-03	1.06E-04	8.06E-08	1.50E-04	4.24E-07	5.55E-03
Standard Deviation	0.73	78.89	587.30	1.32E-02	3.32E-03	1.71E-05	3.27E-03	2.80E-05	3.35E-07	7.18E-04	6.07E-04	9.31E-03	1.27E-04	1.96E-08	1.45E-05	4.44E-07	9.88E-03
Minimum	6.87	-411.60	46.37	6.79E-04	9.22E-05	1.10E-05	1.74E-04	5.73E-06	3.73E-10	1.99E-04	2.80E-04	1.04E-04	1.01E-05	1.00E-15	1.31E-04	5.25E-08	4.72E-04
P0.1	6.95	-411.08	46.95	6.88E-04	1.01E-04	1.12E-05	1.77E-04	6.18E-06	4.44E-10	2.13E-04	3.07E-04	1.11E-04	1.11E-05	1.84E-08	1.32E-04	6.14E-08	4.79E-04
P5	7.11	-409.03	56.15	8.66E-04	2.04E-04	1.23E-05	1.96E-04	8.33E-06	1.21E-09	2.54E-04	3.59E-04	2.28E-04	1.74E-05	3.73E-08	1.33E-04	8.09E-08	6.28E-04
Median	8.82	-385.26	118.12	2.03E-03	7.58E-04	1.80E-05	3.80E-04	2.00E-05	3.61E-08	5.53E-04	6.08E-04	8.81E-04	5.15E-05	8.89E-08	1.46E-04	2.33E-07	1.57E-03
P95	9.44	-163.99	1831.32	4.02E-02	1.05E-02	6.71E-05	9.73E-03	9.33E-05	1.02E-06	2.41E-03	2.17E-03	2.77E-02	4.25E-04	9.71E-08	1.79E-04	1.41E-06	3.02E-02
P99.9	9.58	-136.12	3509.04	8.03E-02	1.85E-02	8.37E-05	2.04E-02	1.21E-04	1.28E-06	3.14E-03	2.86E-03	5.72E-02	6.15E-04	9.86E-08	1.94E-04	2.20E-06	5.97E-02
Maximum	9.59	-126.65	3988.50	9.15E-02	2.09E-02	9.40E-05	2.34E-02	1.48E-04	1.47E-06	3.79E-03	3.26E-03	6.55E-02	6.99E-04	9.89E-08	1.96E-04	2.86E-06	6.79E-02
Permafrost IV: Hematite Uncoupled																	
	pH	Eh(mV)	TDS(mg/l)	IonicStr	mNa	mK	mCa	mMg	mFe+2	mC	AlkTot	mCl	mS(VI)	mS_{-II}	mSi	mP	Na+K+2Mg+2Ca
N total	28044	28044	28044	28044	28044	28044	28044	28044	28044	28044	28044	28044	28044	28044	28044	28044	28044
Mean	9.01	-386.11	119.54	2.26E-03	6.23E-04	1.49E-05	5.14E-04	1.30E-05	3.20E-08	3.53E-04	4.21E-04	1.22E-03	3.58E-05	9.38E-08	1.57E-04	1.20E-07	1.69E-03
Standard Deviation	0.35	22.33	67.68	1.52E-03	4.13E-04	2.71E-06	3.65E-04	5.07E-06	4.91E-08	1.33E-04	1.17E-04	1.07E-03	1.82E-05	3.54E-09	1.31E-05	5.98E-08	1.14E-03
Minimum	7.84	-411.43	43.20	6.27E-04	4.35E-05	1.05E-05	1.77E-04	4.66E-06	1.59E-10	1.44E-04	2.16E-04	8.18E-05	7.05E-06	6.94E-08	1.37E-04	3.06E-08	4.22E-04
P0.1	8.02	-411.08	46.19	6.91E-04	7.51E-05	1.07E-05	1.80E-04	4.83E-06	2.37E-10	1.51E-04	2.22E-04	1.32E-04	8.29E-06	7.64E-08	1.37E-04	3.27E-08	4.75E-04
P5	8.35	-408.75	57.00	8.87E-04	2.01E-04	1.18E-05	1.99E-04	6.73E-06	1.07E-09	1.88E-04	2.74E-04	2.43E-04	1.56E-05	8.75E-08	1.39E-04	4.76E-08	6.44E-04
Median	9.08	-394.04	94.81	1.68E-03	4.94E-04	1.41E-05	3.68E-04	1.14E-05	8.44E-09	3.12E-04	3.92E-04	8.14E-04	3.02E-05	9.49E-08	1.55E-04	1.04E-07	1.27E-03
P95	9.45	-337.38	263.10	5.47E-03	1.48E-03	2.01E-05	1.28E-03	2.21E-05	1.47E-07	5.91E-04	6.28E-04	3.43E-03	7.20E-05	9.82E-08	1.79E-04	2.25E-07	4.10E-03
P99.9	9.61	-293.89	486.60	1.08E-02	2.61E-03	2.79E-05	2.68E-03	3.80E-05	3.17E-07	1.05E-03	1.05E-03	7.34E-03	1.19E-04	9.95E-08	1.99E-04	4.46E-07	7.99E-03
Maximum	9.66	-274.06	578.58	1.30E-02	3.03E-03	3.31E-05	3.24E-03	4.80E-05	4.25E-07	1.32E-03	1.31E-03	8.90E-03	1.52E-04	9.96E-08	2.06E-04	6.11E-07	9.58E-03

Table A4-13. Statistical results for the main geochemical parameters obtained with the geochemical Base case over the submerged period (under fresh and marine waters) in the repository volume. Chemical components in mol/kg, TDS in mg/L, pH in standard units and Eh in mV. Columns in red indicate the values taken from the geochemical variant Cases 1 and 2 together (Bace Case for the redox parameters).

Submerged under Marine Water: Base Case (red cells, Hem coup + FeS coup)																	
	pH	Eh(mV) (HemC+ FeSc)	TDS(mg/l)	IonicStr	mNa	mK	mCa	mMg	mFe(II) (HemC+ FeSc)	mC	AlkTot	mCl	mS(VI)	mS(-II) (HemC+ FeSc)	mSi	mP	Na+K+2Mg+2Ca
N total	35762	71524	35762	35762	35762	35762	35762	35762	71524	35762	35762	35762	35762	71524	35762	35762	35762
Mean	7.64	-227.35	11638.49	2.70E-01	6.48E-02	3.02E-04	6.72E-02	9.55E-04	6.48E-06	6.27E-04	5.72E-04	1.99E-01	2.27E-03	1.34E-05	1.28E-04	2.82E-07	2.01E-01
Standard Deviation	0.44	35.84	4430.84	1.05E-01	2.66E-02	4.41E-04	2.84E-02	2.44E-03	7.34E-06	8.53E-04	7.20E-04	7.78E-02	1.21E-03	7.54E-06	2.50E-06	5.45E-07	7.74E-02
Minimum	6.83	-278.73	622.07	1.02E-02	5.61E-03	5.26E-05	1.26E-03	1.93E-05	3.83E-08	5.38E-05	8.11E-05	4.06E-03	3.91E-04	4.63E-06	1.23E-04	4.04E-09	8.49E-03
P0.1	6.85	-274.80	710.48	1.22E-02	6.10E-03	5.68E-05	1.78E-03	2.21E-05	5.71E-08	5.62E-05	8.27E-05	5.71E-03	4.03E-04	5.32E-06	1.24E-04	4.34E-09	1.00E-02
P5	6.93	-269.67	2299.00	5.04E-02	1.38E-02	7.42E-05	1.19E-02	2.80E-05	8.41E-08	5.99E-05	8.53E-05	3.54E-02	5.95E-04	5.92E-06	1.25E-04	4.75E-09	3.81E-02
Median	7.69	-235.24	13087.30	3.03E-01	7.17E-02	1.63E-04	7.60E-02	7.24E-05	5.26E-06	1.88E-04	2.05E-04	2.24E-01	2.27E-03	1.08E-05	1.27E-04	2.63E-08	2.27E-01
P95	8.17	-149.74	16609.20	3.92E-01	1.03E-01	1.37E-03	1.02E-01	6.86E-03	2.27E-05	2.68E-03	2.25E-03	2.87E-01	4.77E-03	2.90E-05	1.33E-04	1.60E-06	2.88E-01
P99.9	8.24	-121.52	18046.30	4.27E-01	1.45E-01	2.96E-03	1.11E-01	1.58E-02	3.08E-05	3.83E-03	3.58E-03	3.13E-01	8.22E-03	3.46E-05	1.35E-04	3.15E-06	3.14E-01
Maximum	8.29	-117.82	18528.30	4.38E-01	1.51E-01	3.17E-03	1.15E-01	1.70E-02	3.26E-05	3.96E-03	3.75E-03	3.21E-01	8.66E-03	3.63E-05	1.35E-04	3.43E-06	3.22E-01
Submerged under Fresh Water: Base Case																	
	pH	Eh(mV) (HemC+ FeSc)	TDS(mg/l)	IonicStr	mNa	mK	mCa	mMg	mFe(II) (HemC+ FeSc)	mC	AlkTot	mCl	mS(VI)	mS(-II) (HemC+ FeSc)	mSi	mP	Na+K+2Mg+2Ca
N total	28044	56088	28044	28044	28044	28044	28044	28044	56088	28044	28044	28044	28044	56088	28044	28044	28044
Mean	8.71	-304.08	913.19	2.14E-02	4.35E-03	2.01E-05	5.63E-03	6.53E-06	1.16E-06	1.03E-04	1.43E-04	1.54E-02	1.18E-04	9.79E-07	1.46E-04	1.73E-08	1.56E-02
Standard Deviation	0.26	17.42	188.27	4.47E-03	9.31E-04	2.98E-06	1.17E-03	4.60E-06	1.34E-06	1.28E-04	1.18E-04	3.25E-03	2.68E-05	1.15E-06	3.80E-06	4.79E-08	3.27E-03
Minimum	7.25	-344.62	167.93	3.65E-03	6.95E-04	1.17E-05	9.67E-04	4.31E-06	2.65E-10	5.92E-05	1.00E-04	2.48E-03	2.29E-05	6.89E-09	1.34E-04	5.66E-09	2.65E-03
P0.1	7.42	-339.38	207.46	4.60E-03	8.89E-04	1.21E-05	1.21E-03	4.35E-06	3.74E-10	6.49E-05	1.01E-04	3.18E-03	2.78E-05	7.13E-08	1.35E-04	5.72E-09	3.34E-03
P5	8.05	-320.11	589.21	1.38E-02	2.75E-03	1.62E-05	3.62E-03	4.77E-06	1.55E-09	2.36E-03	1.03E-04	9.86E-03	7.57E-05	1.06E-07	1.37E-04	5.94E-09	1.00E-02
Median	8.79	-307.86	922.44	2.16E-02	4.37E-03	1.98E-05	5.64E-03	5.24E-06	9.79E-07	5.96E-05	1.09E-04	1.55E-02	1.18E-04	4.37E-07	1.47E-04	6.78E-09	1.58E-02
P95	8.93	-261.40	1193.58	2.80E-02	5.74E-03	2.54E-05	7.36E-03	1.43E-05	3.29E-06	6.06E-05	3.41E-04	2.02E-02	1.61E-04	2.85E-06	1.50E-04	6.73E-08	2.04E-02
P99.9	9.20	-219.45	1480.89	3.50E-02	7.13E-03	4.65E-05	9.21E-03	6.83E-05	8.41E-06	3.17E-04	1.64E-03	2.54E-02	2.58E-04	8.81E-06	1.62E-04	8.65E-07	2.55E-02
Maximum	9.26	-192.66	1541.98	3.65E-02	7.53E-03	5.75E-05	9.59E-03	8.94E-05	1.23E-05	1.78E-03	2.16E-03	2.64E-02	3.35E-04	1.39E-05	1.65E-04	1.37E-06	2.66E-02

Under Marine waters (equivalent to year 3000 BC).

Under Fresh waters (equivalent to the final stage of the glacial period Ice 0r).

Table A4-14. Statistical results for the main geochemical parameters obtained with the geochemical variant case 1 (Hem coup) over the submerged period (under fresh and marine waters) in the repository volume. Chemical components in mol/kg, TDS in mg/L, pH in standard units and Eh in mV.

Submerged under Marine Water: Eq. Hematite Coupled																	
	pH	Eh(mV)	TDS(mg/l)	IonicStr	mNa	mK	mCa	mMg	mFe+2	mC	AlkTot	mCl	mS(VI)	mS(-II)	mSi	mP	Na+K+2Mg+2Ca
N total	35762	35762	35762	35762	35762	35762	35762	35762	35762	35762	35762	35762	35762	35762	35762	35762	35762
Mean	7.64	-216.59	11638.49	2.70E-01	6.48E-02	3.02E-04	6.72E-02	9.55E-04	8.95E-07	6.27E-04	5.72E-04	1.99E-01	2.27E-03	1.34E-05	1.28E-04	2.82E-07	2.01E-01
Standard Deviation	0.44	40.30	4430.84	1.05E-01	2.66E-02	4.41E-04	2.84E-02	2.44E-03	9.32E-07	8.53E-04	7.20E-04	7.78E-02	1.21E-03	7.54E-06	2.50E-06	5.45E-07	7.74E-02
Minimum	6.83	-265.73	622.07	1.02E-02	5.61E-03	5.26E-05	1.26E-03	1.93E-05	3.83E-08	5.38E-05	8.11E-05	4.06E-03	3.91E-04	4.63E-06	1.23E-04	4.04E-09	8.49E-03
P0.1	6.85	-262.09	710.48	1.22E-02	6.10E-03	5.68E-05	1.78E-03	2.21E-05	5.57E-08	5.62E-05	8.27E-05	5.71E-03	4.03E-04	5.32E-06	1.24E-04	4.34E-09	1.00E-02
P5	6.93	-257.81	2299.00	5.04E-02	1.38E-02	7.42E-05	1.19E-02	2.80E-05	7.59E-08	5.99E-05	8.53E-05	3.54E-02	5.95E-04	5.92E-06	1.25E-04	4.75E-09	3.81E-02
Median	7.69	-229.48	13087.30	3.03E-01	7.17E-02	1.63E-04	7.60E-02	7.24E-05	5.50E-07	1.88E-04	2.05E-04	2.24E-01	2.27E-03	1.08E-05	1.27E-04	2.63E-08	2.27E-01
P95	8.17	-135.72	16609.20	3.92E-01	1.03E-01	1.37E-03	1.02E-01	6.86E-03	2.83E-06	2.68E-03	2.25E-03	2.87E-01	4.77E-03	2.90E-05	1.33E-04	1.60E-06	2.88E-01
P99.9	8.24	-120.67	18046.30	4.27E-01	1.45E-01	2.96E-03	1.11E-01	1.58E-02	5.67E-06	3.83E-03	3.58E-03	3.13E-01	8.22E-03	3.46E-05	1.35E-04	3.15E-06	3.14E-01
Maximum	8.29	-117.82	18528.30	4.38E-01	1.51E-01	3.17E-03	1.15E-01	1.70E-02	7.10E-06	3.96E-03	3.75E-03	3.21E-01	8.66E-03	3.63E-05	1.35E-04	3.43E-06	3.22E-01
Submerged under Marine Water: Eq. Hematite coupled																	
	pH	Eh(mV)	TDS(mg/l)	IonicStr	mNa	mK	mCa	mMg	mFe+2	mC	AlkTot	mCl	mS(VI)	mS(-II)	mSi	mP	Na+K+2Mg+2Ca
N total	28044	28044	28044	28044	28044	28044	28044	28044	28044	28044	28044	28044	28044	28044	28044	28044	28044
Mean	8.71	-299.30	913.19	2.14E-02	4.35E-03	2.01E-05	5.63E-03	6.53E-06	1.20E-08	1.03E-04	1.43E-04	1.54E-02	1.18E-04	1.08E-07	1.46E-04	1.73E-08	1.56E-02
Standard Deviation	0.26	17.25	188.27	4.47E-03	9.31E-04	2.98E-06	1.17E-03	4.60E-06	4.67E-08	1.28E-04	1.18E-04	3.25E-03	2.68E-05	3.90E-09	3.80E-06	4.79E-08	3.27E-03
Minimum	7.25	-337.90	167.93	3.65E-03	6.95E-04	1.17E-05	9.67E-04	4.31E-06	2.65E-10	5.92E-05	1.00E-04	2.48E-03	2.29E-05	6.89E-09	1.34E-04	5.66E-09	2.65E-03
P0.1	7.42	-333.79	207.46	4.60E-03	8.89E-04	1.21E-05	1.21E-03	4.35E-06	3.42E-10	6.49E-05	1.01E-04	3.18E-03	2.78E-05	4.97E-08	1.35E-04	5.72E-09	3.34E-03
P5	8.05	-313.67	589.21	1.38E-02	2.75E-03	1.62E-05	3.62E-03	4.77E-06	1.23E-09	2.36E-03	1.03E-04	9.86E-03	7.57E-05	1.04E-07	1.37E-04	5.94E-09	1.00E-02
Median	8.79	-304.21	922.44	2.16E-02	4.37E-03	1.98E-05	5.64E-03	5.24E-06	2.33E-09	5.96E-05	1.09E-04	1.55E-02	1.18E-04	1.09E-07	1.47E-04	6.78E-09	1.58E-02
P95	8.93	-255.65	1193.58	2.80E-02	5.74E-03	2.54E-05	7.36E-03	1.43E-05	5.67E-08	6.06E-05	3.41E-04	2.02E-02	1.61E-04	1.11E-07	1.50E-04	6.73E-08	2.04E-02
P99.9	9.20	-210.33	1480.89	3.50E-02	7.13E-03	4.65E-05	9.21E-03	6.83E-05	6.95E-07	3.17E-04	1.64E-03	2.54E-02	2.58E-04	1.14E-07	1.62E-04	8.65E-07	2.55E-02
Maximum	9.26	-192.66	1541.98	3.65E-02	7.53E-03	5.75E-05	9.59E-03	8.94E-05	1.11E-06	1.78E-03	2.16E-03	2.64E-02	3.35E-04	1.15E-07	1.65E-04	1.37E-06	2.66E-02

Table A4-15. Statistical results for the main geochemical parameters obtained with the geochemical variant case 2 (FeS coup) over the submerged period (under fresh and marine waters) in the repository volume. Chemical components in mol/kg, TDS in mg/L, pH in standard units and Eh in mV.

Submerged under Marine Water: Eq. FeS(am) Coupled																		
	pH	Eh(mV)	TDS(mg/l)	IonicStr	mNa	mK	mCa	mMg	mFe+2	mC	AlkTot	mCl	mS(VI)	mS(-II)	mSi	mP	Na+K+2Mg+2Ca
N total	35762	35762	35762	35762	35762	35762	35762	35762	35762	35762	35762	35762	35762	35762	35762	35762	35762
Mean	7.64	-238.10	11639.99	2.70E-01	6.48E-02	3.02E-04	6.72E-02	9.55E-04	1.21E-05	6.13E-04	5.82E-04	1.99E-01	2.29E-03	1.34E-05	1.28E-04	2.76E-07	0.20
Standard Deviation	0.44	26.72	4430.57	1.05E-01	2.66E-02	4.41E-04	2.84E-02	2.44E-03	6.66E-06	8.47E-04	7.19E-04	7.78E-02	1.21E-03	7.54E-06	2.44E-06	5.38E-07	0.08
Minimum	6.83	-278.73	623.58	1.02E-02	5.61E-03	5.26E-05	1.25E-03	1.93E-05	4.74E-06	4.82E-05	9.31E-05	4.06E-03	4.07E-04	4.63E-06	1.23E-04	3.41E-09	0.01
P0.1	6.85	-275.31	712.08	1.22E-02	6.10E-03	5.68E-05	1.77E-03	2.21E-05	5.22E-06	5.06E-05	9.46E-05	5.71E-03	4.22E-04	5.32E-06	1.24E-04	3.66E-09	0.01
P5	6.93	-271.15	2301.03	5.04E-02	1.38E-02	7.42E-05	1.18E-02	2.80E-05	5.65E-06	5.38E-05	9.72E-05	3.54E-02	6.22E-04	5.92E-06	1.25E-04	4.04E-09	0.04
Median	7.69	-241.17	13088.65	3.03E-01	7.17E-02	1.63E-04	7.60E-02	7.24E-05	9.78E-06	1.77E-04	2.15E-04	2.24E-01	2.28E-03	1.08E-05	1.27E-04	2.41E-08	0.23
P95	8.17	-195.57	16610.80	3.92E-01	1.03E-01	1.37E-03	1.02E-01	6.86E-03	2.62E-05	2.65E-03	2.26E-03	2.87E-01	4.79E-03	2.90E-05	1.33E-04	1.57E-06	0.29
P99.9	8.24	-190.27	18047.80	4.27E-01	1.45E-01	2.96E-03	1.11E-01	1.58E-02	3.12E-05	3.83E-03	3.59E-03	3.13E-01	8.24E-03	3.46E-05	1.35E-04	3.13E-06	0.31
Maximum	8.29	-189.30	18529.80	4.38E-01	1.51E-01	3.17E-03	1.15E-01	1.70E-02	3.26E-05	3.95E-03	3.77E-03	3.21E-01	8.67E-03	3.63E-05	1.35E-04	3.42E-06	0.32
Submerged under Fresh Water: Eq. FeS(am) Coupled																		
	pH	Eh(mV)	TDS(mg/l)	IonicStr	mNa	mK	mCa	mMg	mFe+2	mC	AlkTot	mCl	mS(VI)	mS(-II)	mSi	mP	Na+K+2Mg+2Ca
N total	28044	28044	28044	28044	28044	28044	28044	28044	28044	28044	28044	28044	28044	28044	28044	28044	28044
Mean	8.73	-308.85	914.25	1.56E-04	4.35E-03	2.01E-05	5.62E-03	6.53E-06	2.31E-06	1.00E-04	2.14E-02	1.54E-02	1.26E-04	1.85E-06	1.46E-04	1.68E-08	1.56E-02
Standard Deviation	0.26	16.23	188.28	1.18E-04	9.31E-04	2.98E-06	1.17E-03	4.60E-06	9.76E-07	1.27E-04	4.47E-03	3.25E-03	2.75E-05	1.06E-06	3.93E-06	4.72E-08	3.27E-03
Minimum	7.26	-344.62	169.01	1.13E-04	6.95E-04	1.17E-05	9.66E-04	4.31E-06	9.78E-07	5.69E-05	3.65E-03	2.48E-03	3.00E-05	7.60E-07	1.34E-04	5.30E-09	2.65E-03
P0.1	7.42	-340.75	208.53	1.13E-04	8.89E-04	1.21E-05	1.21E-03	4.35E-06	1.08E-06	5.72E-05	4.60E-03	3.18E-03	3.49E-05	8.11E-07	1.35E-04	5.37E-09	3.34E-03
P5	8.05	-322.16	590.26	1.15E-04	2.75E-03	1.62E-05	3.61E-03	4.77E-06	1.68E-06	5.84E-05	1.38E-02	9.86E-03	8.34E-05	1.22E-06	1.37E-04	5.60E-09	1.00E-02
Median	8.81	-313.56	923.50	1.22E-04	4.37E-03	1.98E-05	5.64E-03	5.24E-06	2.04E-06	6.29E-05	2.16E-02	1.55E-02	1.25E-04	1.54E-06	1.47E-04	6.44E-09	1.58E-02
P95	8.94	-267.50	1194.62	3.53E-04	5.74E-03	2.54E-05	7.36E-03	1.43E-05	4.55E-06	3.12E-04	2.80E-02	2.02E-02	1.72E-04	4.22E-06	1.51E-04	6.55E-08	2.04E-02
P99.9	9.21	-227.03	1481.96	1.65E-03	7.13E-03	4.65E-05	9.20E-03	6.83E-05	9.54E-06	1.77E-03	3.50E-02	2.54E-02	2.75E-04	1.04E-05	1.63E-04	8.55E-07	2.55E-02
Maximum	9.27	-216.49	1543.04	2.17E-03	7.53E-03	5.75E-05	9.59E-03	8.94E-05	1.23E-05	2.35E-03	3.65E-02	2.64E-02	3.55E-04	1.39E-05	1.66E-04	1.35E-06	2.66E-02

Table A4-16. Statistical results for the main geochemical parameters obtained with the geochemical variant case 3 (Hem uncoup) over the submerged period (under fresh and marine waters) in the repository volume. Chemical components in mol/kg, TDS in mg/L, pH in standard units and Eh in mV.

Submerged under Marine Water Hematite Uncoupled																	
	pH	Eh(mV)	TDS(mg/l)	IonicStr	mNa	mK	mCa	mMg	mFe+2	mCtot	AlkTot	mCl	mS(VI)	mS(-II)	mSi	mP	Na+K+2Mg+2Ca
N total	35762	35762	35762	35762	35762	35762	35762	35762	35762	35762	35762	35762	35762	35762	35762	35762	35762
Mean	7.61	-241.55	11638.29	2.70E-01	6.47E-02	3.02E-04	6.72E-02	9.55E-04	1.35E-06	6.28E-04	5.72E-04	1.99E-01	2.27E-03	4.58E-07	1.28E-04	2.83E-07	0.20
Standard Deviation	0.42	67.62	4430.72	1.05E-01	2.66E-02	4.41E-04	2.84E-02	2.44E-03	7.89E-07	8.53E-04	7.20E-04	7.78E-02	1.21E-03	1.08E-06	2.51E-06	5.45E-07	0.08
Minimum	6.82	-337.10	621.92	1.02E-02	5.61E-03	5.26E-05	1.26E-03	1.93E-05	5.40E-07	5.44E-05	8.10E-05	4.06E-03	3.91E-04	4.00E-09	1.23E-04	4.11E-09	0.01
P0.1	6.84	-332.99	710.35	1.22E-02	6.10E-03	5.68E-05	1.78E-03	2.21E-05	5.92E-07	5.68E-05	8.27E-05	5.71E-03	4.03E-04	5.00E-09	1.24E-04	4.41E-09	0.01
P5	6.92	-324.96	2299.03	5.04E-02	1.38E-02	7.42E-05	1.19E-02	2.80E-05	7.78E-07	6.05E-05	8.53E-05	3.54E-02	5.95E-04	2.61E-08	1.25E-04	4.82E-09	0.04
Median	7.66	-250.09	13086.95	3.03E-01	7.17E-02	1.63E-04	7.60E-02	7.24E-05	1.15E-06	1.89E-04	2.05E-04	2.24E-01	2.27E-03	6.98E-08	1.27E-04	2.66E-08	0.23
P95	8.12	-128.93	16608.90	3.92E-01	1.03E-01	1.37E-03	1.02E-01	6.86E-03	3.27E-06	2.68E-03	2.25E-03	2.87E-01	4.76E-03	3.07E-06	1.33E-04	1.60E-06	0.29
P99.9	8.18	-115.54	18045.90	4.27E-01	1.45E-01	2.96E-03	1.11E-01	1.58E-02	5.80E-06	3.83E-03	3.58E-03	3.13E-01	8.22E-03	7.01E-06	1.35E-04	3.15E-06	0.31
Maximum	8.24	-112.92	18528.00	4.38E-01	1.51E-01	3.17E-03	1.15E-01	1.70E-02	6.01E-06	3.96E-03	3.75E-03	3.21E-01	8.65E-03	7.53E-06	1.35E-04	3.43E-06	0.32
Submerged under Fresh Water Hematite Uncoupled																	
	pH	Eh(mV)	TDS(mg/l)	IonicStr	mNa	mK	mCa	mMg	mFe+2	mCtot	AlkTot	mCl	mS(VI)	mS(-II)	mSi	mP	Na+K+2Mg+2Ca
N total	28044	28044	28044	28044	28044	28044	28044	28044	28044	28044	28044	28044	28044	28044	28044	28044	28044
Mean	8.71	-360.99	913.19	2.14E-02	4.35E-03	2.01E-05	5.63E-03	6.53E-06	5.48E-08	1.03E-04	1.43E-04	1.54E-02	1.18E-04	9.79E-08	1.46E-04	1.75E-08	1.56E- 02
Standard Deviation	0.26	28.75	188.27	4.47E-03	9.31E-04	2.98E-06	1.17E-03	4.60E-06	6.24E-08	1.28E-04	1.18E-04	3.25E-03	2.68E-05	3.21E-09	3.75E-06	4.79E-08	3.27E-03
Minimum	7.25	-381.67	167.93	3.65E-03	6.94E-04	1.17E-05	9.67E-04	4.31E-06	1.53E-09	5.99E-05	1.00E-04	2.48E-03	2.28E-05	4.04E-08	1.34E-04	5.76E-09	2.65E- 03
P0.1	7.42	-380.25	207.45	4.60E-03	8.89E-04	1.21E-05	1.22E-03	4.35E-06	2.27E-09	6.03E-05	1.01E-04	3.18E-03	2.77E-05	5.51E-08	1.35E-04	5.83E-09	3.34E- 03
P5	8.05	-375.57	589.20	1.38E-02	2.75E-03	1.62E-05	3.62E-03	4.77E-06	1.55E-08	6.13E-05	1.03E-04	9.86E-03	7.56E-05	9.24E-08	1.37E-04	6.05E-09	1.00E- 02
Median	8.79	-371.81	922.43	2.16E-02	4.36E-03	1.98E-05	5.65E-03	5.24E-06	3.69E-08	6.56E-05	1.09E-04	1.55E-02	1.17E-04	9.87E-08	1.46E-04	6.89E-09	1.58E- 02
P95	8.92	-284.89	1193.58	2.80E-02	5.73E-03	2.54E-05	7.36E-03	1.43E-05	1.87E-07	3.18E-04	3.41E-04	2.02E-02	1.61E-04	9.92E-08	1.50E-04	6.75E-08	2.04E -02
P99.9	9.20	-208.91	1480.88	3.50E-02	7.13E-03	4.65E-05	9.21E-03	6.83E-05	6.86E-07	1.78E-03	1.64E-03	2.54E-02	2.58E-04	9.97E-08	1.62E-04	8.66E-07	2.55E -02
Maximum	9.26	-186.96	1541.96	3.65E-02	7.53E-03	5.75E-05	9.59E-03	8.94E-05	8.84E-07	2.36E-03	2.16E-03	2.64E-02	3.35E-04	9.98E-08	1.65E-04	1.37E-06	2.66E -02

Table A4-17. Statistical results for the main geochemical parameters obtained with the Base Case geochemical simluation over the temperate period in the vertical section parallel to the coast and cross-cutting the repository. Chemical components in mol/kg, TDS in mg/L, pH in standard units and Eh in mV. Columns in red indicate the values taken from the geochemical variant Cases 1 and 2 together (Bace Case for the redox parameters).

2000 AD: Base Case, Hem coupled (black cells), Hem coup + FeS coup (red cells)																	
	pH	Eh(HemC+FeSc)	TDS(mg/l)	IonicStrength	mNa	mK	mCa	mMg	Fe(II)(HemC+FeSc)	mC	AlkalinityTot	mCl	mS(VI)	S(-II)(HemC+FeSc)	mSi	mP	Na+K+2Ca+2Mg
N total samples	33114	66228	33114	33114	33114	33114	33114	33114	66228	33114	33114	33114	33114	66228	33114	33114	33114
Mean	7.58	-224.90	14604.81	3.41E-01	7.67E-02	2.52E-04	8.72E-02	4.31E-04	6.48E-06	2.18E-03	2.06E-03	2.49E-01	2.49E-03	7.42E-06	1.25E-04	2.04E-06	2.52E-01
Standard Deviation	0.46	39.48	16984.85	4.04E-01	8.29E-02	2.34E-04	1.07E-01	1.10E-03	8.76E-06	1.79E-03	1.75E-03	2.97E-01	2.26E-03	1.02E-05	1.19E-05	2.13E-06	2.96E-01
Minimum	6.73	-278.16	464.37	6.53E-03	4.77E-03	6.84E-05	2.76E-04	2.36E-05	2.66E-08	3.68E-05	5.28E-05	6.49E-04	3.66E-04	2.55E-16	8.81E-05	9.85E-10	5.71E-03
P0.1	6.75	-270.12	464.61	6.53E-03	4.78E-03	7.23E-05	2.76E-04	4.58E-05	2.67E-08	3.68E-05	5.28E-05	6.49E-04	3.70E-04	3.84E-16	8.81E-05	9.85E-10	5.71E-03
P5	6.85	-270.01	464.92	6.54E-03	4.79E-03	7.60E-05	2.76E-04	5.47E-05	2.69E-08	6.78E-05	8.32E-05	6.50E-04	3.73E-04	2.17E-13	1.06E-04	4.30E-09	5.71E-03
Median	7.77	-238.37	5901.44	1.30E-01	3.72E-02	1.76E-04	2.85E-02	1.46E-04	2.33E-06	2.26E-03	1.85E-03	9.65E-02	1.61E-03	4.83E-06	1.30E-04	1.19E-06	1.01E-01
P95	8.15	-136.69	42305.80	9.99E-01	2.11E-01	6.54E-04	2.62E-01	2.09E-03	2.80E-05	4.35E-03	4.33E-03	7.33E-01	6.08E-03	3.16E-05	1.37E-04	5.24E-06	7.35E-01
P99.9	8.15	-106.25	78621.88	1.87E+00	3.80E-01	2.00E-03	4.94E-01	1.06E-02	3.87E-05	4.35E-03	4.33E-03	1.37E+00	9.68E-03	4.46E-05	1.37E-04	5.24E-06	1.37E+00
Maximum	8.25	-103.97	78621.88	1.87E+00	3.80E-01	2.51E-03	4.94E-01	1.34E-02	4.09E-05	4.35E-03	4.33E-03	1.37E+00	9.68E-03	4.71E-05	1.37E-04	5.24E-06	1.37E+00
5000 Base Case																	
	pH	Eh(HemC+FeSc)	TDS(mg/l)	IonicStrength	mNa	mK	mCa	mMg	Fe(II)(HemC+FeSc)	mC	AlkalinityTot	mCl	mS(VI)	S(-II)(HemC+FeSc)	mSi	mP	Na+K+2Ca+2Mg
N total samples	33114	66228	33114	33114	33114	33114	33114	33114	66228	33114	3.31E+04	33114	33114	66228	33114	33114	33114
Mean	7.54	-219.55	13196.97	3.08E-01	6.85E-02	1.97E-04	7.93E-02	1.90E-04	7.12E-06	2.45E-03	2.30E-03	2.24E-01	2.20E-03	8.21E-06	1.26E-04	2.29E-06	2.28E-01
Standard Deviation	0.51	45.24	16695.65	3.97E-01	8.18E-02	1.64E-04	1.05E-01	4.20E-04	1.03E-05	1.75E-03	1.72E-03	2.92E-01	2.23E-03	1.19E-05	1.18E-05	2.14E-06	2.91E-01
Minimum	6.66	-270.18	464.76	6.54E-03	4.78E-03	7.07E-05	2.76E-04	3.65E-05	2.67E-08	3.68E-05	5.28E-05	6.49E-04	3.68E-04	1.68E-16	8.81E-05	9.85E-10	5.71E-03
P0.1	6.66	-270.12	464.83	6.54E-03	4.79E-03	7.35E-05	2.76E-04	4.77E-05	2.67E-08	3.68E-05	5.28E-05	6.49E-04	3.71E-04	2.60E-16	8.81E-05	9.85E-10	5.71E-03
P5	6.80	-270.07	464.90	6.54E-03	4.79E-03	7.60E-05	2.76E-04	5.78E-05	2.68E-08	6.90E-05	8.40E-05	6.49E-04	3.73E-04	1.67E-14	1.06E-04	4.41E-09	5.71E-03
Median	7.70	-234.78	3339.53	7.29E-02	2.08E-02	1.15E-04	1.67E-02	1.47E-04	2.33E-06	2.86E-03	2.34E-03	5.24E-02	9.49E-04	4.83E-06	1.32E-04	1.76E-06	5.57E-02
P95	8.15	-123.52	41509.33	9.80E-01	2.07E-01	4.46E-04	2.57E-01	4.39E-04	3.14E-05	4.35E-03	4.33E-03	7.19E-01	6.03E-03	3.54E-05	1.37E-04	5.24E-06	7.21E-01
P99.9	8.15	-98.44	78621.88	1.87E+00	3.80E-01	1.55E-03	4.94E-01	8.16E-03	4.62E-05	4.35E-03	4.33E-03	1.37E+00	9.68E-03	5.35E-05	1.37E-04	5.24E-06	1.37E+00
Maximum	8.15	-97.13	78621.88	1.87E+00	3.80E-01	2.00E-03	4.94E-01	1.06E-02	4.67E-05	4.35E-03	4.33E-03	1.37E+00	9.68E-03	5.41E-05	1.37E-04	5.24E-06	1.37E+00
10000 Base Case																	
	pH	Eh(HemC+FeSc)	TDS(mg/l)	IonicStrength	mNa	mK	mCa	mMg	Fe(II)(HemC+FeSc)	mC	AlkalinityTot	mCl	mS(VI)	S(-II)(HemC+FeSc)	mSi	mP	Na+K+2Ca+2Mg
N total samples	33114	66228	33114	33114	33114	33114	33114	33114	66228	33114	33114	33114	33114	66228	33114	33114	33114
Mean	7.51	-216.59	11574.26	2.70E-01	6.02E-02	1.74E-04	6.93E-02	1.40E-04	7.45E-06	2.69E-03	2.52E-03	1.96E-01	1.96E-03	8.65E-06	1.27E-04	2.52E-06	1.99E-01
Standard Deviation	0.53	48.55	16037.41	3.81E-01	7.87E-02	1.44E-04	1.00E-01	8.73E-05	1.11E-05	1.67E-03	1.66E-03	2.81E-01	2.14E-03	1.29E-05	1.15E-05	2.11E-06	2.80E-01
		--															
Minimum	6.65	-270.12	464.70	6.53E-03	4.79E-03	7.27E-05	2.76E-04	4.56E-05	2.67E-08	3.68E-05	5.28E-05	6.49E-04	3.70E-04	5.17E-17	8.81E-05	9.85E-10	5.71E-03
P0.1	6.65	-270.12	464.90	6.54E-03	4.79E-03	7.47E-05	2.76E-04	5.08E-05	2.67E-08	3.68E-05	5.28E-05	6.49E-04	3.72E-04	5.90E-17	8.81E-05	9.85E-10	5.71E-03
P5	6.75	-270.12	464.90	6.54E-03	4.79E-03	7.60E-05	2.76E-04	6.16E-05	2.67E-08	7.30E-05	8.68E-05	6.49E-04	3.73E-04	2.56E-15	1.07E-04	4.78E-09	5.71E-03
Median	7.60	-230.00	2033.74	4.25E-02	1.37E-02	9.26E-05	9.33E-03	1.48E-04	2.32E-06	3.27E-03	2.73E-03	2.94E-02	7.02E-04	4.19E-06	1.33E-04	2.23E-06	3.29E-02
P95	8.15	-114.86	40419.73	9.55E-01	2.02E-01	4.30E-04	2.50E-01	2.45E-04	3.41E-05	4.35E-03	4.33E-03	7.01E-01	5.91E-03	3.86E-05	1.37E-04	5.24E-06	7.02E-01
P99.9	8.15	-92.28	78621.88	1.87E+00	3.80E-01	8.22E-04	4.94E-01	9.76E-04	4.70E-05	4.35E-03	4.33E-03	1.37E+00	9.68E-03	5.43E-05	1.37E-04	5.24E-06	1.37E+00
Maximum	8.15	-91.71	78621.88	1.87E+00	3.80E-01	1.02E-03	4.94E-01	5.27E-03	4.72E-05	4.35E-03	4.33E-03	1.37E+00	9.68E-03	5.46E-05	1.37E-04	5.24E-06	1.37E+00
15000 Base Case																	
	pH	Eh(HemC+FeSc)	TDS(mg/l)	IonicStrength	mNa	mK	mCa	mMg	Fe(II)(HemC+FeSc)	mC	AlkalinityTot	mCl	mS(VI)	S(-II)(HemC+FeSc)	mSi	mP	Na+K+2Ca+2Mg
N total samples	33114	66228	33114	33114	33114	33114	33114	33114	66228	33114	33114	33114	33114	66228	33114	33114	33114
Mean	7.51	-215.74	10450.06	2.43E-01	5.46E-02	1.63E-04	6.23E-02	1.33E-04	7.53E-06	2.84E-03	2.66E-03	1.76E-01	1.80E-03	8.78E-06	1.28E-04	2.68E-06	1.80E-01
Standard Deviation	0.54	49.88	15464.84	3.67E-01	7.59E-02	1.39E-04	9.68E-02	4.12E-05	1.14E-05	1.61E-03	1.61E-03	2.71E-01	2.07E-03	1.32E-05	1.12E-05	2.08E-06	2.70E-01
Minimum	6.65	-270.12	464.80	6.54E-03	4.79E-03	7.39E-05	2.76E-04	4.66E-05	2.67E-08	3.68E-05	5.28E-05	6.49E-04	3.71E-04	3.40E-17	8.81E-05	9.85E-10	5.71E-03
P0.1	6.65	-270.12	464.90	6.54E-03	4.79E-03	7.53E-05	2.76E-04	5.41E-05	2.67E-08	3.68E-05	5.28E-05	6.49E-04	3.72E-04	3.72E-17	8.81E-05	9.85E-10	5.71E-03
P5	6.73	-270.12	464.90	6.54E-03	4.79E-03	7.60E-05	2.76E-04	6.49E-05	2.67E-08	8.20E-05	9.46E-05	6.49E-04	3.73E-04	1.07E-15	1.07E-04	5.67E-09	5.71E-03
Median	7.56	-228.00	1487.77	2.99E-02	1.07E-02	8.51E-05	6.12E-03	1.48E-04	2.32E-06	3.50E-03	3.02E-03	1.96E-02	5.95E-04	2.86E-06	1.34E-04	2.54E-06	2.34E-02
P95	8.15	-110.81	39398.50	9.30E-01	1.98E-01	4.19E-04	2.43E-01	1.93E-04	3.52E-05	4.35E-03	4.33E-03	6.82E-01	5.81E-03	3.98E-05	1.37E-04	5.24E-06	6.84E-01
P99.9	8.15	-90.86	78621.88	1.87E+00	3.80E-01	8.22E-04	4.94E-01	3.43E-04	4.69E-05	4.35E-03	4.33E-03	1.37E+00	9.68E-03	5.42E-05	1.37E-04	5.24E-06	1.37E+00
Maximum	8.15	-90.40	78621.88	1.87E+00	3.80E-01	8.22E-04	4.94E-01	9.04E-04	4.72E-05	4.35E-03	4.33E-03	1.37E+00	9.68E-03	5.45E-05	1.37E-04	5.24E-06	1.37E+00

Table A4-18. Statistical results for the main geochemical parameters obtained with the geochemical variant case 1 (Hem coup) over the temperate period in the vertical section parallel to the coast and cross-cutting the repository. Chemical components in mol/kg, TDS in mg/L, pH in standard units and Eh in mV.

2000 AD: Eq. Hematite Coupled																	
	pH	Eh(mV)	TDS(mg/l)	IonicStrength	mNa	mK	mCa	mMg	mFe(II)	mC	AlkalinityTot	mCl	mS(VI)	mS(-II)	mSi	mP	Na+K+2Ca+2Mg
N total samples	33114	33114	33114	33114	33114	33114	33114	33114	33114	33114	33114	33114	33114	33114	33114	33114	33114
Mean	7.58	-213.77	14604.81	3.41E-01	7.67E-02	2.52E-04	8.72E-02	4.31E-04	1.14E-06	2.18E-03	2.06E-03	2.49E-01	2.49E-03	3.25E-07	1.25E-04	2.04E-06	2.52 E-01
Standard Deviation	0.46	45.23	16984.85	4.04E-01	8.29E-02	2.34E-04	1.07E-01	1.10E-03	1.74E-06	1.79E-03	1.75E-03	2.97E-01	2.26E-03	6.49E-07	1.19E-05	2.13E-06	2.96E-01
Minimum	6.73	-265.11	464.37	6.53E-03	4.77E-03	6.84E-05	2.76E-04	2.36E-05	2.66E-08	3.68E-05	5.28E-05	6.49E-04	3.66E-04	2.55E-16	8.81E-05	9.85E-10	5.71E-03
P0.1	6.75	-260.03	464.61	6.53E-03	4.78E-03	7.23E-05	2.76E-04	4.58E-05	2.67E-08	3.68E-05	5.28E-05	6.49E-04	3.70E-04	3.25E-16	8.81E-05	9.85E-10	5.71E-03
P5	6.85	-260.03	464.92	6.54E-03	4.79E-03	7.60E-05	2.76E-04	5.47E-05	2.67E-08	6.78E-05	8.32E-05	6.50E-04	3.73E-04	1.75E-14	1.06E-04	4.30E-09	5.71E-03
Median	7.77	-235.30	5901.44	1.30E-01	3.72E-02	1.76E-04	2.85E-02	1.46E-04	3.71E-07	2.26E-03	1.85E-03	9.65E-02	1.61E-03	2.11E-07	1.30E-04	1.19E-06	1.01E -01
P95	8.15	-125.51	42305.80	9.99E-01	2.11E-01	6.54E-04	2.62E-01	2.09E-03	5.30E-06	4.35E-03	4.33E-03	7.33E-01	6.08E-03	9.70E-07	1.37E-04	5.24E-06	7.35 E-01
P99.9	8.15	-105.28	78621.88	1.87E+00	3.80E-01	2.00E-03	4.94E-01	1.06E-02	1.17E-05	4.35E-03	4.33E-03	1.37E+00	9.68E-03	7.05E-06	1.37E-04	5.24E-06	1.37 E+00
Maximum	8.25	-103.97	78621.88	1.87E+00	3.80E-01	2.51E-03	4.94E-01	1.34E-02	1.23E-05	4.35E-03	4.33E-03	1.37E+00	9.68E-03	8.72E-06	1.37E-04	5.24E-06	1.37 E+00
5000 AD: Eq. Hematite Coupled																	
	pH	Eh(mV)	TDS(mg/l)	IonicStrength	mNa	mK	mCa	mMg	mFe(II)	mC	AlkalinityTot	mCl	mS(VI)	mS(-II)	mSi	mP	Na+K+2Ca+2Mg
N total samples	33114	33114	33114	33114	33114	33114	33114	33114	33114	33114	3.31E+04	33114	33114	33114	33114	33114	33114
Mean	7.54	-205.96	13196.97	3.08E-01	6.85E-02	1.97E-04	7.93E-02	1.90E-04	1.00E-06	2.45E-03	2.30E-03	2.24E-01	2.20E-03	1.80E-07	1.26E-04	2.29E-06	2.28 E-01
Standard Deviation	0.51	52.38	16695.65	3.97E-01	8.18E-02	1.64E-04	1.05E-01	4.20E-04	1.14E-06	1.75E-03	1.72E-03	2.92E-01	2.23E-03	2.96E-07	1.18E-05	2.14E-06	2.91E-01
Minimum	6.66	-260.09	464.76	6.54E-03	4.78E-03	7.07E-05	2.76E-04	3.65E-05	2.67E-08	3.68E-05	5.28E-05	6.49E-04	3.68E-04	1.68E-16	8.81E-05	9.85E-10	5.71E-03
P0.1	6.66	-260.03	464.83	6.54E-03	4.79E-03	7.35E-05	2.76E-04	4.77E-05	2.67E-08	3.68E-05	5.28E-05	6.49E-04	3.71E-04	2.16E-16	8.81E-05	9.85E-10	5.71E-03
P5	6.80	-260.03	464.90	6.54E-03	4.79E-03	7.60E-05	2.76E-04	5.78E-05	2.67E-08	6.90E-05	8.40E-05	6.49E-04	3.73E-04	3.19E-15	1.06E-04	4.41E-09	5.71E-03
Median	7.70	-230.17	3339.53	7.29E-02	2.08E-02	1.15E-04	1.67E-02	1.47E-04	4.22E-07	2.86E-03	2.34E-03	5.24E-02	9.49E-04	2.05E-07	1.32E-04	1.76E-06	5.57E -02
P95	8.15	-115.65	41509.33	9.80E-01	2.07E-01	4.46E-04	2.57E-01	4.39E-04	3.23E-06	4.35E-03	4.33E-03	7.19E-01	6.03E-03	4.32E-07	1.37E-04	5.24E-06	7.21 E-01
P99.9	8.15	-97.87	78621.88	1.87E+00	3.80E-01	1.55E-03	4.94E-01	8.16E-03	6.72E-06	4.35E-03	4.33E-03	1.37E+00	9.68E-03	5.06E-06	1.37E-04	5.24E-06	1.37E +00
Maximum	8.15	-97.13	78621.88	1.87E+00	3.80E-01	2.00E-03	4.94E-01	1.06E-02	9.02E-06	4.35E-03	4.33E-03	1.37E+00	9.68E-03	7.05E-06	1.37E-04	5.24E-06	1.37E +00
10000 AD: Eq. Hematite Coupled																	
	pH	Eh(mV)	TDS(mg/l)	IonicStrength	mNa	mK	mCa	mMg	mFe(II)	mC	AlkalinityTot	mCl	mS(VI)	mS(-II)	mSi	mP	Na+K+2Ca+2Mg
N total samples	33114	33114	33114	33114	33114	33114	33114	33114	33114	33114	33114	33114	33114	33114	33114	33114	33114
Mean	7.51	-201.62	11574.26	2.70E-01	6.02E-02	1.74E-04	6.93E-02	1.40E-04	9.20E-07	2.69E-03	2.52E-03	1.96E-01	1.96E-03	1.48E-07	1.27E-04	2.52E-06	1.99 E-01
Standard Deviation	0.53	56.54	16037.41	3.81E-01	7.87E-02	1.44E-04	1.00E-01	8.73E-05	9.09E-07	1.67E-03	1.66E-03	2.81E-01	2.14E-03	1.60E-07	1.15E-05	2.11E-06	2.80E-01
Minimum	6.65	-260.03	464.70	6.53E-03	4.79E-03	7.27E-05	2.76E-04	4.56E-05	2.67E-08	3.68E-05	5.28E-05	6.49E-04	3.70E-04	5.17E-17	8.81E-05	9.85E-10	5.71E-03
P0.1	6.65	-260.03	464.90	6.54E-03	4.79E-03	7.47E-05	2.76E-04	5.08E-05	2.67E-08	3.68E-05	5.28E-05	6.49E-04	3.72E-04	5.64E-17	8.81E-05	9.85E-10	5.71E-03
P5	6.75	-260.03	464.90	6.54E-03	4.79E-03	7.60E-05	2.76E-04	6.16E-05	2.67E-08	7.30E-05	8.68E-05	6.49E-04	3.73E-04	7.76E-16	1.07E-04	4.78E-09	5.71E-03
Median	7.60	-223.16	2033.74	4.25E-02	1.37E-02	9.26E-05	9.33E-03	1.48E-04	5.33E-07	3.27E-03	2.73E-03	2.94E-02	7.02E-04	1.85E-07	1.33E-04	2.23E-06	3.29E -02
P95	8.15	-108.02	40419.73	9.55E-01	2.02E-01	4.30E-04	2.50E-01	2.45E-04	2.56E-06	4.35E-03	4.33E-03	7.01E-01	5.91E-03	4.08E-07	1.37E-04	5.24E-06	7.02 E-01
P99.9	8.15	-92.11	78621.88	1.87E+00	3.80E-01	8.22E-04	4.94E-01	9.76E-04	3.43E-06	4.35E-03	4.33E-03	1.37E+00	9.68E-03	8.81E-07	1.37E-04	5.24E-06	1.37E +00
Maximum	8.15	-91.71	78621.88	1.87E+00	3.80E-01	1.02E-03	4.94E-01	5.27E-03	8.36E-06	4.35E-03	4.33E-03	1.37E+00	9.68E-03	3.55E-06	1.37E-04	5.24E-06	1.37E +00
15000 AD: Eq. Hematite Coupled																	
	pH	Eh(mV)	TDS(mg/l)	IonicStrength	mNa	mK	mCa	mMg	mFe(II)	mC	AlkalinityTot	mCl	mS(VI)	mS(-II)	mSi	mP	Na+K+2Ca+2Mg
N total samples	33114	33114	33114	33114	33114	33114	33114	33114	33114	33114	33114	33114	33114	33114	33114	33114	33114
Mean	7.51	-200.30	10450.06	2.43E-01	5.46E-02	1.63E-04	6.23E-02	1.33E-04	8.95E-07	2.84E-03	2.66E-03	1.76E-01	1.80E-03	1.38E-07	1.28E-04	2.68E-06	1.80E-01
Standard Deviation	0.54	58.20	15464.84	3.67E-01	7.59E-02	1.39E-04	9.68E-02	4.12E-05	8.67E-07	1.61E-03	1.61E-03	2.71E-01	2.07E-03	1.50E-07	1.12E-05	2.08E-06	2.70E-01
Minimum	6.65	-260.03	464.80	6.54E-03	4.79E-03	7.39E-05	2.76E-04	4.66E-05	2.67E-08	3.68E-05	5.28E-05	6.49E-04	3.71E-04	3.40E-17	8.81E-05	9.85E-10	5.71E-03
P0.1	6.65	-260.03	464.90	6.54E-03	4.79E-03	7.53E-05	2.76E-04	5.41E-05	2.67E-08	3.68E-05	5.28E-05	6.49E-04	3.72E-04	3.62E-17	8.81E-05	9.85E-10	5.71E-03
P5	6.73	-260.03	464.90	6.54E-03	4.79E-03	7.60E-05	2.76E-04	6.49E-05	2.67E-08	8.20E-05	9.46E-05	6.49E-04	3.73E-04	3.67E-16	1.07E-04	5.67E-09	5.71E-03
Median	7.56	-220.53	1487.77	2.99E-02	1.07E-02	8.51E-05	6.12E-03	1.48E-04	5.48E-07	3.50E-03	3.02E-03	1.96E-02	5.95E-04	1.69E-07	1.34E-04	2.54E-06	2.34E-02
P95	8.15	-104.03	39398.50	9.30E-01	1.98E-01	4.19E-04	2.43E-01	1.93E-04	2.36E-06	4.35E-03	4.33E-03	6.82E-01	5.81E-03	3.84E-07	1.37E-04	5.24E-06	6.84E-01
P99.9	8.15	-90.74	78621.88	1.87E+00	3.80E-01	8.22E-04	4.94E-01	3.43E-04	3.09E-06	4.35E-03	4.33E-03	1.37E+00	9.68E-03	8.81E-07	1.37E-04	5.24E-06	1.37E+00
Maximum	8.15	-90.40	78621.88	1.87E+00	3.80E-01	8.22E-04	4.94E-01	9.04E-04	4.04E-06	4.35E-03	4.33E-03	1.37E+00	9.68E-03	8.81E-07	1.37E-04	5.24E-06	1.37E+00

Table A4-19. Statistical results for the main geochemical parameters obtained with the geochemical variant case 2 (FeS coup) over the temperate period in the vertical section parallel to the coast and cross-cutting the repository. Chemical components in mol/kg, TDS in mg/L, pH in standard units and Eh in mV.

2000 AD: Eq. FeS(am) Coupled																	
	pH	Eh(mV)	TDS(mg/l)	IonicStrength	mNa	mK	mCa	mMg	mFe(II)	mC	AlkalinityTot	mCl	mS(VI)	mS(-II)	mSi	mP	Na+K+2Ca+2Mg
N total samples	33114	33114	33114	33114	33114	33114	33114	33114	33114	33114	33114	33114	33114	33114	33114	33114	33114
Mean	7.61	-236.02	14606.50	3.41E-01	7.67E-02	2.52E-04	8.72E-02	4.31E-04	1.18E-05	2.17E-03	2.07E-03	2.49E-01	2.51E-03	1.45E-05	1.25E-04	2.03E-06	2.52 E-01
Standard Deviation	0.47	28.72	16984.74	4.04E-01	8.29E-02	2.34E-04	1.07E-01	1.10E-03	9.66E-06	1.80E-03	1.75E-03	2.97E-01	2.26E-03	1.03E-05	1.17E-05	2.13E-06	2.96E-01
Minimum	6.74	-278.16	465.84	6.53E-03	4.77E-03	6.84E-05	2.72E-04	2.36E-05	2.32E-06	3.20E-05	6.45E-05	6.49E-04	3.78E-04	4.47E-06	8.93E-05	7.96E-10	5.70E-03
P0.1	6.76	-270.12	466.05	6.53E-03	4.78E-03	7.23E-05	2.72E-04	4.58E-05	2.32E-06	3.20E-05	6.45E-05	6.49E-04	3.82E-04	4.83E-06	8.93E-05	7.96E-10	5.70E-03
P5	6.86	-270.12	466.40	6.54E-03	4.79E-03	7.60E-05	2.72E-04	5.47E-05	2.32E-06	5.97E-05	9.40E-05	6.50E-04	3.84E-04	4.84E-06	1.06E-04	3.54E-09	5.70E-03
Median	7.82	-248.86	5903.68	1.30E-01	3.72E-02	1.76E-04	2.85E-02	1.46E-04	7.77E-06	2.22E-03	1.86E-03	9.65E-02	1.64E-03	9.84E-06	1.30E-04	1.17E-06	1.01E -01
P95	8.15	-190.38	42307.46	9.99E-01	2.11E-01	6.54E-04	2.62E-01	2.09E-03	3.09E-05	4.34E-03	4.35E-03	7.33E-01	6.10E-03	3.47E-05	1.37E-04	5.25E-06	7.35 E-01
P99.9	8.16	-183.83	78623.35	1.87E+00	3.80E-01	2.00E-03	4.94E-01	1.06E-02	3.95E-05	4.34E-03	4.35E-03	1.37E+00	9.69E-03	4.54E-05	1.37E-04	5.25E-06	1.37 E+00
Maximum	8.29	-182.74	78623.36	1.87E+00	3.80E-01	2.51E-03	4.94E-01	1.34E-02	4.09E-05	4.34E-03	4.35E-03	1.37E+00	9.69E-03	4.71E-05	1.37E-04	5.25E-06	1.37E+00
5000 AD: Eq. FeS(am) Coupled																	
	pH	Eh(mV)	TDS(mg/l)	IonicStrength	mNa	mK	mCa	mMg	mFe(II)	mC	AlkalinityTot	mCl	mS(VI)	mS(-II)	mSi	mP	Na+K+2Ca+2Mg
N total samples	33114	33114	33114	33114	33114	33114	33114	33114	33114	33114	3.31E+04	33114	33114	33114	33114	33114	33114
Mean	7.56	-233.14	13198.72	3.08E-01	6.85E-02	1.97E-04	7.93E-02	1.90E-04	1.32E-05	2.43E-03	2.31E-03	2.24E-01	2.22E-03	1.62E-05	1.26E-04	2.28E-06	2.28E-01
Standard Deviation	0.51	31.32	16695.58	3.97E-01	8.18E-02	1.64E-04	1.05E-01	4.20E-04	1.16E-05	1.75E-03	1.72E-03	2.92E-01	2.23E-03	1.25E-05	1.17E-05	2.14E-06	2.91E-01
Minimum	6.67	-270.18	466.21	6.53E-03	4.78E-03	7.07E-05	2.72E-04	3.65E-05	2.32E-06	3.20E-05	6.45E-05	6.49E-04	3.80E-04	4.83E-06	8.93E-05	7.96E-10	5.70E-03
P0.1	6.67	-270.12	466.31	6.53E-03	4.79E-03	7.35E-05	2.72E-04	4.77E-05	2.32E-06	3.20E-05	6.45E-05	6.49E-04	3.83E-04	4.83E-06	8.93E-05	7.96E-10	5.70E-03
P5	6.81	-270.12	466.38	6.54E-03	4.79E-03	7.60E-05	2.72E-04	5.78E-05	2.32E-06	6.06E-05	9.48E-05	6.49E-04	3.84E-04	4.83E-06	1.07E-04	3.64E-09	5.70E-03
Median	7.72	-243.22	3341.38	7.29E-02	2.08E-02	1.15E-04	1.67E-02	1.47E-04	8.13E-06	2.83E-03	2.34E-03	5.24E-02	9.82E-04	1.03E-05	1.32E-04	1.74E-06	5.57E -02
P95	8.15	-187.19	41510.99	9.80E-01	2.07E-01	4.46E-04	2.57E-01	4.39E-04	3.48E-05	4.34E-03	4.35E-03	7.19E-01	6.04E-03	3.98E-05	1.37E-04	5.25E-06	7.21E-01
P99.9	8.15	-178.70	78623.35	1.87E+00	3.80E-01	1.55E-03	4.94E-01	8.16E-03	4.64E-05	4.34E-03	4.35E-03	1.37E+00	9.69E-03	5.38E-05	1.37E-04	5.25E-06	1.37E+00
Maximum	8.16	-178.47	78623.36	1.87E+00	3.80E-01	2.00E-03	4.94E-01	1.06E-02	4.67E-05	4.34E-03	4.35E-03	1.37E+00	9.69E-03	5.41E-05	1.37E-04	5.25E-06	1.37E+00
10000 AD: Eq. FeS(am) Coupled																	
	pH	Eh(mV)	TDS(mg/l)	IonicStrength	mNa	mK	mCa	mMg	mFe(II)	mC	AlkalinityTot	mCl	mS(VI)	mS(-II)	mSi	mP	Na+K+2Ca+2Mg
N total samples	33114	33114	33114	33114	33114	33114	33114	33114	33114	33114	33114	33114	33114	33114	33114	33114	33114
Mean	7.53	-231.56	11576.05	2.70E-01	6.02E-02	1.74E-04	6.93E-02	1.40E-04	1.40E-05	2.67E-03	2.53E-03	1.96E-01	1.98E-03	1.72E-05	1.27E-04	2.51E-06	1.99E-01
Standard Deviation	0.53	32.69	16037.39	3.81E-01	7.87E-02	1.44E-04	1.00E-01	8.73E-05	1.27E-05	1.68E-03	1.66E-03	2.81E-01	2.15E-03	1.37E-05	1.14E-05	2.12E-06	2.80E-01
Minimum	6.66	-270.12	466.18	6.53E-03	4.79E-03	7.27E-05	2.72E-04	4.56E-05	2.32E-06	3.20E-05	6.45E-05	6.49E-04	3.82E-04	4.83E-06	8.93E-05	7.96E-10	5.70E-03
P0.1	6.66	-270.12	466.32	6.54E-03	4.79E-03	7.47E-05	2.72E-04	5.08E-05	2.32E-06	3.20E-05	6.45E-05	6.49E-04	3.83E-04	4.83E-06	8.93E-05	7.96E-10	5.70E-03
P5	6.76	-270.12	466.38	6.54E-03	4.79E-03	7.60E-05	2.72E-04	6.16E-05	2.32E-06	6.43E-05	9.76E-05	6.49E-04	3.84E-04	4.83E-06	1.07E-04	3.96E-09	5.70E-03
Median	7.62	-237.01	2035.78	4.25E-02	1.37E-02	9.26E-05	9.31E-03	1.48E-04	8.47E-06	3.25E-03	2.75E-03	2.94E-02	7.29E-04	1.08E-05	1.33E-04	2.20E-06	3.28E -02
P95	8.15	-184.28	40421.46	9.55E-01	2.02E-01	4.30E-04	2.50E-01	2.45E-04	3.83E-05	4.34E-03	4.35E-03	7.01E-01	5.93E-03	4.39E-05	1.37E-04	5.25E-06	7.02E-01
P99.9	8.15	-178.18	78623.35	1.87E+00	3.80E-01	8.22E-04	4.94E-01	9.76E-04	4.71E-05	4.34E-03	4.35E-03	1.37E+00	9.69E-03	5.44E-05	1.37E-04	5.25E-06	1.37E+00
Maximum	8.16	-178.13	78623.35	1.87E+00	3.80E-01	1.02E-03	4.94E-01	5.27E-03	4.72E-05	4.34E-03	4.35E-03	1.37E+00	9.69E-03	5.46E-05	1.37E-04	5.25E-06	1.37E+00
15000 AD: Eq. FeS(am) Coupled																	
	pH	Eh(mV)	TDS(mg/l)	IonicStrength	mNa	mK	mCa	mMg	mFe(II)	mC	AlkalinityTot	mCl	mS(VI)	mS(-II)	mSi	mP	Na+K+2Ca+2Mg
N total samples	33114	33114	33114	33114	33114	33114	33114	33114	33114	33114	33114	33114	33114	33114	33114	33114	33114
Mean	7.52	-231.17	10451.87	2.43E-01	5.46E-02	1.63E-04	6.23E-02	1.33E-04	1.42E-05	2.82E-03	2.67E-03	1.76E-01	1.83E-03	1.74E-05	1.28E-04	2.67E-06	1.80 E-01
Standard Deviation	0.54	33.34	15464.85	3.67E-01	7.59E-02	1.39E-04	9.68E-02	4.12E-05	1.31E-05	1.62E-03	1.62E-03	2.71E-01	2.07E-03	1.42E-05	1.11E-05	2.09E-06	2.70E-01
Minimum	6.66	-270.12	466.28	6.53E-03	4.79E-03	7.39E-05	2.72E-04	4.66E-05	2.32E-06	3.20E-05	6.45E-05	6.49E-04	3.83E-04	4.83E-06	8.93E-05	7.96E-10	5.70E-03
P0.1	6.66	-270.12	466.32	6.54E-03	4.79E-03	7.53E-05	2.72E-04	5.41E-05	2.32E-06	3.20E-05	6.45E-05	6.49E-04	3.84E-04	4.83E-06	8.93E-05	7.96E-10	5.70E-03
P5	6.75	-270.12	466.38	6.54E-03	4.79E-03	7.60E-05	2.72E-04	6.49E-05	2.32E-06	7.26E-05	1.05E-04	6.49E-04	3.84E-04	4.83E-06	1.08E-04	4.74E-09	5.70E-03
Median	7.57	-234.21	1489.73	2.99E-02	1.07E-02	8.51E-05	6.10E-03	1.48E-04	8.42E-06	3.48E-03	3.03E-03	1.96E-02	6.20E-04	1.08E-05	1.34E-04	2.51E-06	2.34E -02
P95	8.15	-183.31	39400.78	9.30E-01	1.98E-01	4.19E-04	2.43E-01	1.93E-04	3.95E-05	4.34E-03	4.35E-03	6.82E-01	5.82E-03	4.54E-05	1.37E-04	5.25E-06	6.84 E-01
P99.9	8.15	-178.24	78623.35	1.87E+00	3.80E-01	8.22E-04	4.94E-01	3.43E-04	4.70E-05	4.34E-03	4.35E-03	1.37E+00	9.69E-03	5.43E-05	1.37E-04	5.25E-06	1.37 E+00
Maximum	8.15	-178.13	78623.35	1.87E+00	3.80E-01	8.22E-04	4.94E-01	9.04E-04	4.72E-05	4.34E-03	4.35E-03	1.37E+00	9.69E-03	5.45E-05	1.37E-04	5.25E-06	1.37 E+00

Table A4-20. Statistical results for the main geochemical parameters obtained with the geochemical variant case 3 (Hem uncoup) over the temperate period in the vertical section parallel to the coast and cross-cutting the repository. Chemical components in mol/kg, TDS in mg/L, pH in standard units and Eh in mV.

2000 AD: Hematite Uncoupled																	
	pH	Eh(mV)	TDS(mg/l)	IonicStrength	mNa	mK	mCa	mMg	mFe(II)	mC	AlkalinityTot	mCl	mS(VI)	mS(-II)	mSi	mP	Na+K+2Ca+2Mg
N total samples	33114	33114	33114	33114	33114	33114	33114	33114	33114	33114	33114	33114	33114	33114	33114	33114	33114
Mean	7.58	-246.61	14604.56	3.41E-01	7.67E-02	2.52E-04	8.72E-02	4.31E-04	1.59E-06	2.18E-03	2.06E-03	2.49E-01	2.49E-03	1.62E-07	1.25E-04	2.04E-06	2.52 E-01
Standard Deviation	0.46	78.80	16984.50	4.04E-01	8.29E-02	2.34E-04	1.07E-01	1.10E-03	8.66E-07	1.79E-03	1.75E-03	2.97E-01	2.26E-03	4.91E-07	1.19E-05	2.13E-06	2.96E-01
Minimum	6.73	-338.01	464.34	6.53E-03	4.77E-03	6.84E-05	2.74E-04	2.36E-05	4.95E-07	3.68E-05	5.20E-05	6.49E-04	3.66E-04	1.00E-15	8.81E-05	9.86E-10	5.70E-03
P0.1	6.75	-337.95	464.55	6.53E-03	4.78E-03	7.23E-05	2.74E-04	4.58E-05	6.09E-07	3.68E-05	5.20E-05	6.49E-04	3.70E-04	1.00E-15	8.81E-05	9.86E-10	5.71E-03
P5	6.85	-337.90	464.89	6.54E-03	4.79E-03	7.60E-05	2.74E-04	5.47E-05	6.09E-07	6.84E-05	8.31E-05	6.50E-04	3.73E-04	1.00E-15	1.06E-04	4.35E-09	5.71E-03
Median	7.77	-279.59	5901.25	1.30E-01	3.72E-02	1.76E-04	2.85E-02	1.46E-04	1.39E-06	2.26E-03	1.85E-03	9.65E-02	1.61E-03	2.63E-08	1.30E-04	1.20E-06	1.01E -01
P95	8.15	-118.10	42306.02	9.99E-01	2.11E-01	6.54E-04	2.62E-01	2.09E-03	3.00E-06	4.34E-03	4.33E-03	7.33E-01	6.08E-03	9.07E-07	1.37E-04	5.25E-06	7.35 E-01
P99.9	8.15	-102.43	78619.95	1.87E+00	3.80E-01	2.00E-03	4.94E-01	1.06E-02	4.63E-06	4.35E-03	4.33E-03	1.37E+00	9.68E-03	4.67E-06	1.37E-04	5.25E-06	1.37E+00
Maximum	8.25	-101.23	78619.96	1.87E+00	3.80E-01	2.51E-03	4.94E-01	1.34E-02	4.91E-06	4.35E-03	4.33E-03	1.37E+00	9.68E-03	5.93E-06	1.37E-04	5.25E-06	1.37E+00
5000 AD: Hematite Uncoupled																	
	pH	Eh(mV)	TDS(mg/l)	IonicStrength	mNa	mK	mCa	mMg	mFe(II)	mC	AlkalinityTot	mCl	mS(VI)	mS(-II)	mSi	mP	Na+K+2Ca+2Mg
N total samples	33114	33114	33114	33114	33114	33114	33114	33114	33114	33114	3.31E+04	33114	33114	33114	33114	33114	33114
Mean	7.54	-238.29	13196.73	3.08E-01	6.85E-02	1.97E-04	7.93E-02	1.90E-04	1.49E-06	2.45E-03	2.30E-03	2.24E-01	2.20E-03	4.84E-08	1.26E-04	2.29E-06	2.28 E-01
Standard Deviation	0.51	86.21	16695.32	3.96E-01	8.18E-02	1.64E-04	1.05E-01	4.20E-04	8.38E-07	1.74E-03	1.72E-03	2.92E-01	2.23E-03	1.87E-07	1.19E-05	2.14E-06	2.91E-01
Minimum	6.66	-337.95	464.71	6.53E-03	4.78E-03	7.07E-05	2.74E-04	3.65E-05	6.09E-07	3.68E-05	5.20E-05	6.49E-04	3.68E-04	1.00E-15	8.81E-05	9.86E-10	5.71E-03
P0.1	6.66	-337.95	464.80	6.53E-03	4.79E-03	7.35E-05	2.74E-04	4.77E-05	6.09E-07	3.68E-05	5.20E-05	6.49E-04	3.71E-04	1.00E-15	8.81E-05	9.86E-10	5.71E-03
P5	6.80	-337.95	464.88	6.53E-03	4.79E-03	7.60E-05	2.74E-04	5.78E-05	6.09E-07	6.96E-05	8.40E-05	6.49E-04	3.73E-04	1.00E-15	1.06E-04	4.46E-09	5.71E-03
Median	7.69	-266.82	3339.53	7.30E-02	2.08E-02	1.15E-04	1.67E-02	1.47E-04	1.33E-06	2.86E-03	2.34E-03	5.24E-02	9.49E-04	2.06E-08	1.32E-04	1.77E-06	5.57E -02
P95	8.15	-109.84	41507.24	9.80E-01	2.07E-01	4.46E-04	2.57E-01	4.39E-04	2.88E-06	4.35E-03	4.33E-03	7.19E-01	6.03E-03	1.61E-07	1.37E-04	5.25E-06	7.21 E-01
P99.9	8.15	-89.38	78619.95	1.87E+00	3.80E-01	1.55E-03	4.94E-01	8.16E-03	4.63E-06	4.35E-03	4.33E-03	1.37E+00	9.68E-03	3.58E-06	1.37E-04	5.25E-06	1.37E +00
Maximum	8.15	-88.81	78619.96	1.87E+00	3.80E-01	2.00E-03	4.94E-01	1.06E-02	4.63E-06	4.35E-03	4.33E-03	1.37E+00	9.68E-03	4.67E-06	1.37E-04	5.25E-06	1.37E +00
10000 AD: Hematite Uncoupled																	
	pH	Eh(mV)	TDS(mg/l)	IonicStrength	mNa	mK	mCa	mMg	mFe(II)	mC	AlkalinityTot	mCl	mS(VI)	mS(-II)	mSi	mP	Na+K+2Ca+2Mg
N total samples	33114	33114	33114	33114	33114	33114	33114	33114	33114	33114	33114	33114	33114	33114	33114	33114	33114
Mean	7.51	-234.27	11574.04	2.70E-01	6.02E-02	1.74E-04	6.93E-02	1.40E-04	1.42E-06	2.69E-03	2.52E-03	1.96E-01	1.96E-03	2.10E-08	1.27E-04	2.52E-06	1.99 E-01
Standard Deviation	0.53	89.91	16037.09	3.81E-01	7.87E-02	1.44E-04	1.00E-01	8.73E-05	8.13E-07	1.67E-03	1.66E-03	2.81E-01	2.14E-03	3.79E-08	1.15E-05	2.11E-06	2.80E-01
Minimum	6.65	-337.95	464.68	6.53E-03	4.79E-03	7.27E-05	2.74E-04	4.56E-05	6.09E-07	3.68E-05	5.20E-05	6.49E-04	3.70E-04	1.00E-15	8.81E-05	9.86E-10	5.71E-03
P0.1	6.65	-337.95	464.82	6.53E-03	4.79E-03	7.47E-05	2.74E-04	5.08E-05	6.09E-07	3.68E-05	5.20E-05	6.49E-04	3.72E-04	1.00E-15	8.81E-05	9.86E-10	5.71E-03
P5	6.75	-337.95	464.88	6.53E-03	4.79E-03	7.60E-05	2.74E-04	6.16E-05	6.09E-07	7.36E-05	8.69E-05	6.49E-04	3.73E-04	1.00E-15	1.07E-04	4.84E-09	5.71E-03
Median	7.59	-251.11	2033.77	4.25E-02	1.37E-02	9.26E-05	9.33E-03	1.48E-04	1.29E-06	3.27E-03	2.73E-03	2.94E-02	7.02E-04	1.27E-08	1.33E-04	2.23E-06	3.29E -02
P95	8.15	-103.06	40419.59	9.55E-01	2.02E-01	4.30E-04	2.50E-01	2.45E-04	2.80E-06	4.35E-03	4.33E-03	7.01E-01	5.91E-03	6.79E-08	1.37E-04	5.25E-06	7.02 E-01
P99.9	8.15	-87.78	78619.95	1.87E+00	3.80E-01	8.22E-04	4.94E-01	9.76E-04	4.63E-06	4.35E-03	4.33E-03	1.37E+00	9.68E-03	3.88E-07	1.37E-04	5.25E-06	1.37E +00
Maximum	8.15	-87.50	78619.95	1.87E+00	3.80E-01	1.02E-03	4.94E-01	5.27E-03	4.63E-06	4.35E-03	4.33E-03	1.37E+00	9.68E-03	2.28E-06	1.37E-04	5.25E-06	1.37E +00
15000 AD: Hematite Uncoupled																	
	pH	Eh(mV)	TDS(mg/l)	IonicStrength	mNa	mK	mCa	mMg	mFe(II)	mC	AlkalinityTot	mCl	mS(VI)	mS(-II)	mSi	mP	Na+K+2Ca+2Mg
N total samples	33114	33114	33114	33114	33114	33114	33114	33114	33114	33114	33114	33114	33114	33114	33114	33114	33114
Mean	7.51	-233.48	10449.86	2.43E-01	5.46E-02	1.63E-04	6.23E-02	1.33E-04	1.37E-06	2.84E-03	2.66E-03	1.76E-01	1.80E-03	1.45E-08	1.28E-04	2.68E-06	1.80 E-01
Standard Deviation	0.54	91.60	15464.54	3.67E-01	7.59E-02	1.39E-04	9.69E-02	4.12E-05	7.93E-07	1.61E-03	1.61E-03	2.71E-01	2.07E-03	1.67E-08	1.12E-05	2.08E-06	2.70E-01
Minimum	6.65	-337.95	464.78	6.53E-03	4.79E-03	7.39E-05	2.74E-04	4.66E-05	6.09E-07	3.68E-05	5.20E-05	6.49E-04	3.71E-04	1.00E-15	8.81E-05	9.86E-10	5.71E-03
P0.1	6.65	-337.95	464.83	6.53E-03	4.79E-03	7.53E-05	2.74E-04	5.41E-05	6.09E-07	3.68E-05	5.20E-05	6.49E-04	3.72E-04	1.00E-15	8.81E-05	9.86E-10	5.71E-03
P5	6.73	-337.95	464.88	6.53E-03	4.79E-03	7.60E-05	2.74E-04	6.49E-05	6.09E-07	8.27E-05	9.49E-05	6.49E-04	3.73E-04	1.00E-15	1.07E-04	5.75E-09	5.71E-03
Median	7.55	-246.10	1487.80	2.99E-02	1.07E-02	8.51E-05	6.12E-03	1.48E-04	1.25E-06	3.50E-03	3.02E-03	1.96E-02	5.95E-04	8.05E-09	1.34E-04	2.54E-06	2.34E -02
P95	8.15	-100.66	39396.89	9.30E-01	1.98E-01	4.19E-04	2.43E-01	1.93E-04	2.74E-06	4.35E-03	4.33E-03	6.82E-01	5.81E-03	4.44E-08	1.37E-04	5.25E-06	6.84 E-01
P99.9	8.15	-87.61	78619.95	1.87E+00	3.80E-01	8.22E-04	4.94E-01	3.43E-04	4.63E-06	4.35E-03	4.33E-03	1.37E+00	9.68E-03	1.11E-07	1.37E-04	5.25E-06	1.37E +00
Maximum	8.15	-87.38	78619.95	1.87E+00	3.80E-01	8.22E-04	4.94E-01	9.04E-04	4.63E-06	4.35E-03	4.33E-03	1.37E+00	9.68E-03	3.37E-07	1.37E-04	5.25E-06	1.37E +00

Appendix 5

Distribution of mass fractions of the reference waters over the time

This Appendix shows the distribution of the mixing proportions of all the end members over the whole glacial Cycle. This distribution has been plotted in two different planes: a horizontal plane located at the repository depth (500 m in Laxemar) and a vertical plane cross-cuting the repository with a NW-SE direction. Moreover, there are two sets of plots for each end member and plane, the first showing the complete cycle considering an unfrozen ground during the glacial period, and the other comparing the results obtained when considering the ground unfrozen or frozen.

I all the cases, mixing proportions for the temperate and the submerged under marine conditions periods have been calculated and provided by the hydrogeologists. For the glacial, Periglacial and submerged under fresh water periods, the mixing proportions have been calculated by this group from the salinities provided by the hydrogeologists through an interface developed for SR-Site (see Chapter 3 for more detailed information on the procedure). Due to the limited information and the simplication of this metodology, mixing proportions for Littorina and Old Meteoric end members cannot be calculated fo these glacial, periglacial and submerged under fresh water periods. Figures A5-13 and A5-14 show the mixing proportions for these two end members only for the temperate and submerged under marine water periods.

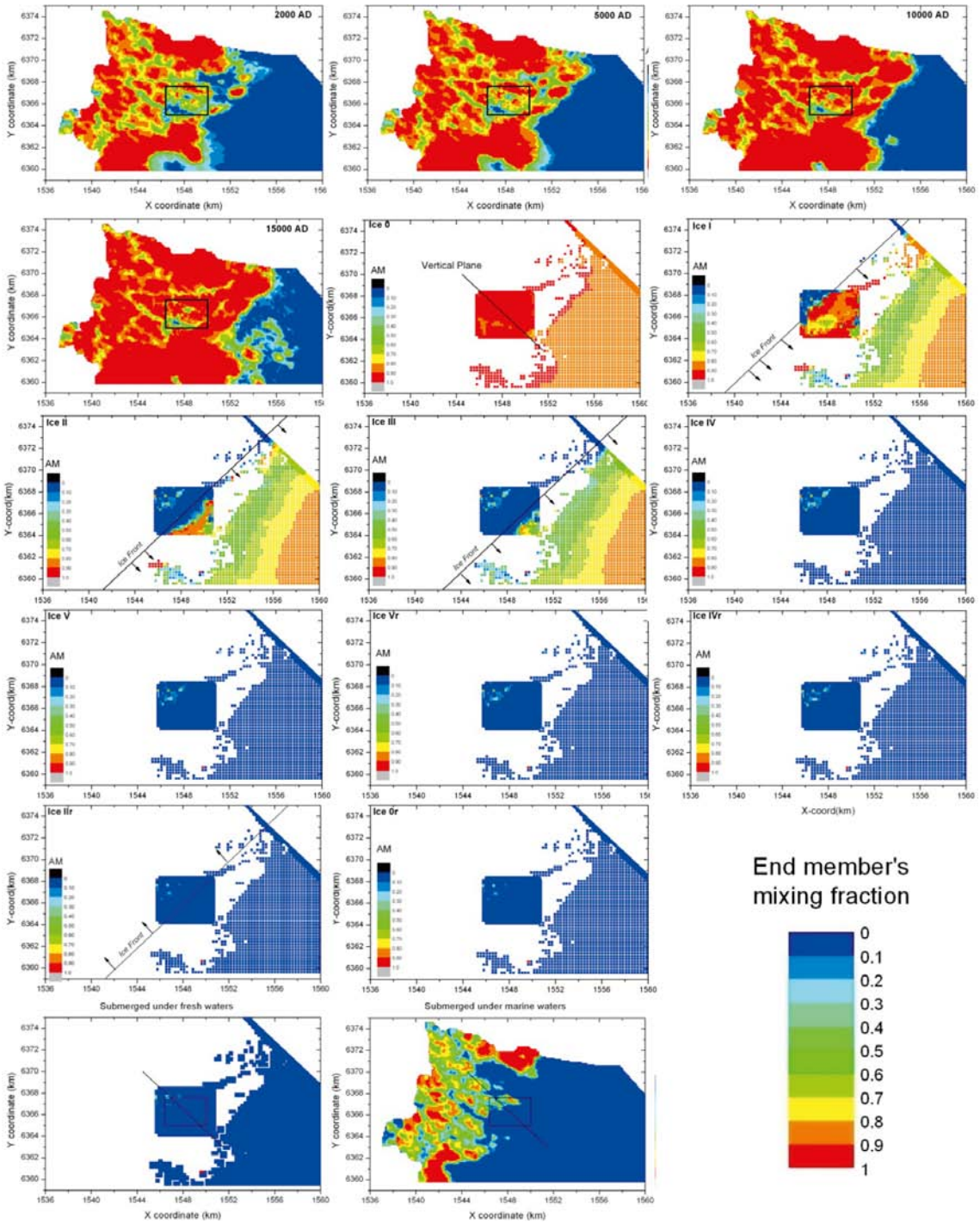

Figure A5-1. *Sequence of Altered Meteoric mixing proportion (AM) time frames as estimated by the hydrological calculations in a 500 m depth plane over the whole glacial cycle. For this and the rest of the plots in this Appendix, mixing proportions for the temperate and submerged under marine water periods have been provided by the hydrogeologists, while mixing proportions for the rest of the remaining glacial cycle including the submerged under fresh water period, have been calculated by this group from the salinities provided by the hydrogeologists through an interface developed for SR-Site.*

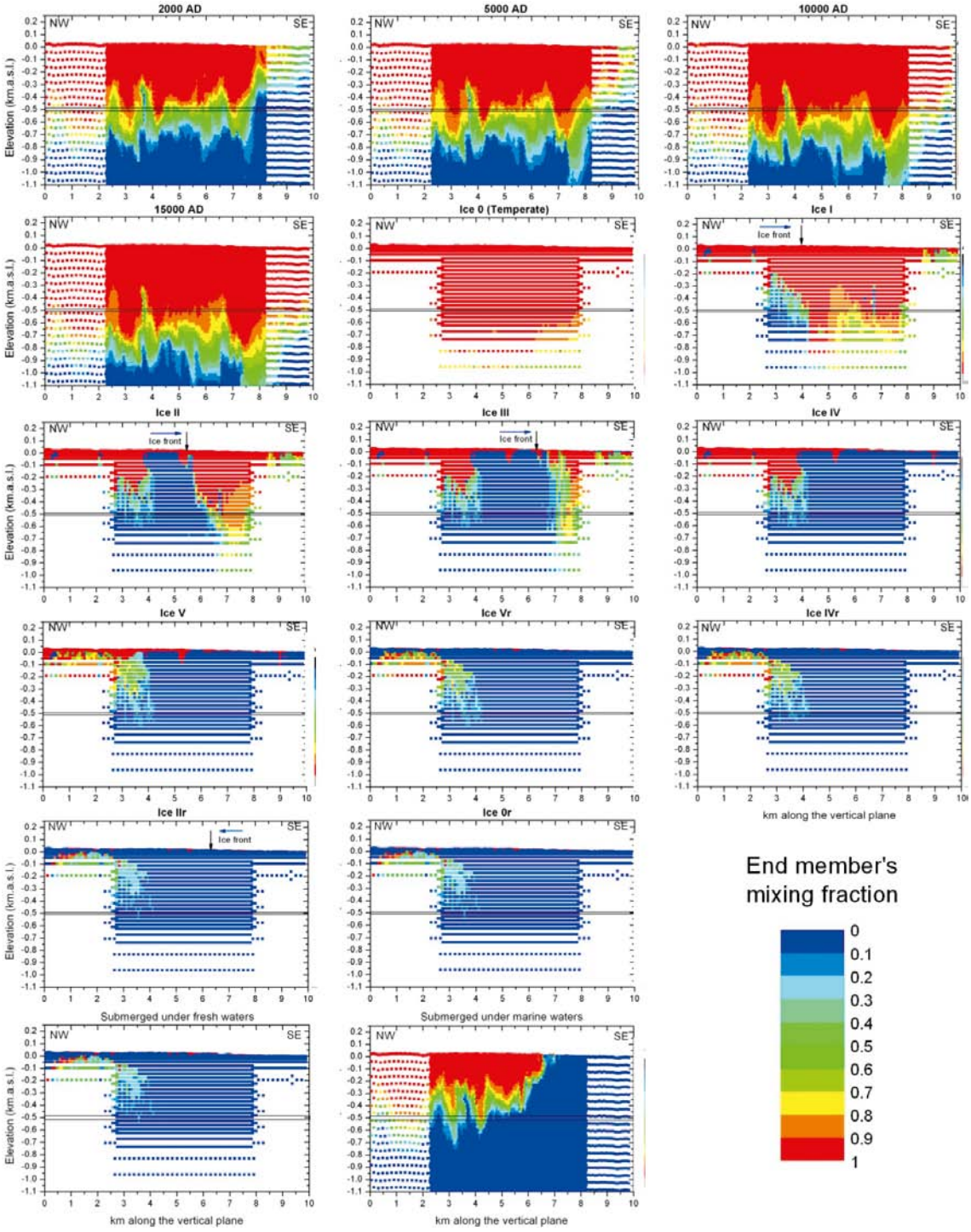

Figure A5-2. *Sequence of Altered Meteoric mixing proportion (AM) time frames as estimated by the hydrological calculations in a vertical section parallel to the coast cross-cutting the repository volume, over the whole glacial cycle. The vertical scale is enlarged 20 times with respect to the horizontal scale. See the caption of Figure A5-1 for more details.*

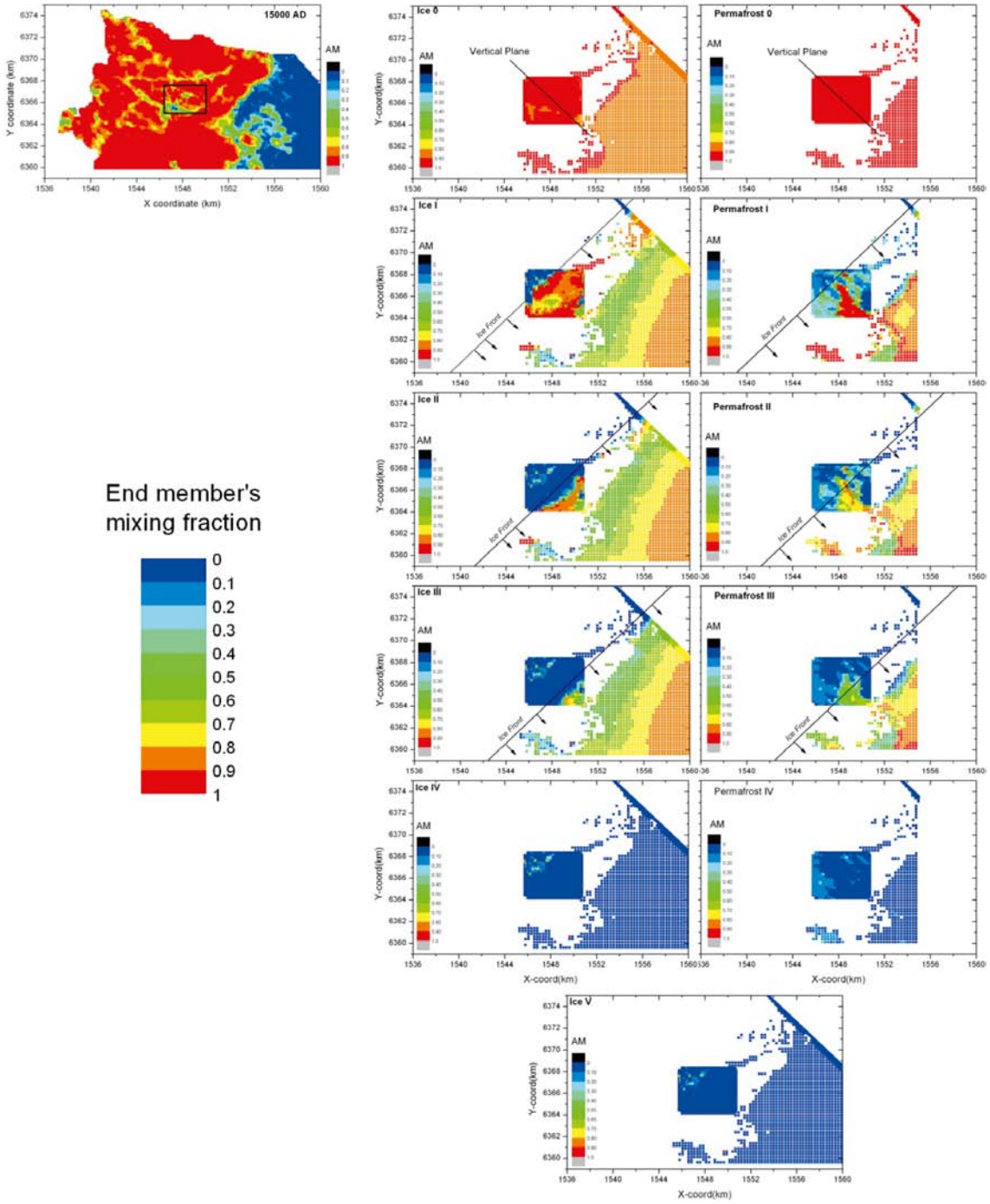

Figure A5-3. *Sequence of Altered Meteoric mixing proportion (AM) time frames as estimated by the hydrological calculations in a 500 m depth plane, for the transition from the end of the temperate period to the first stages of the glacial period (advance) without (left plots) and with permafrost (right plots) development. See the caption of Figure A5-1 for more details.*

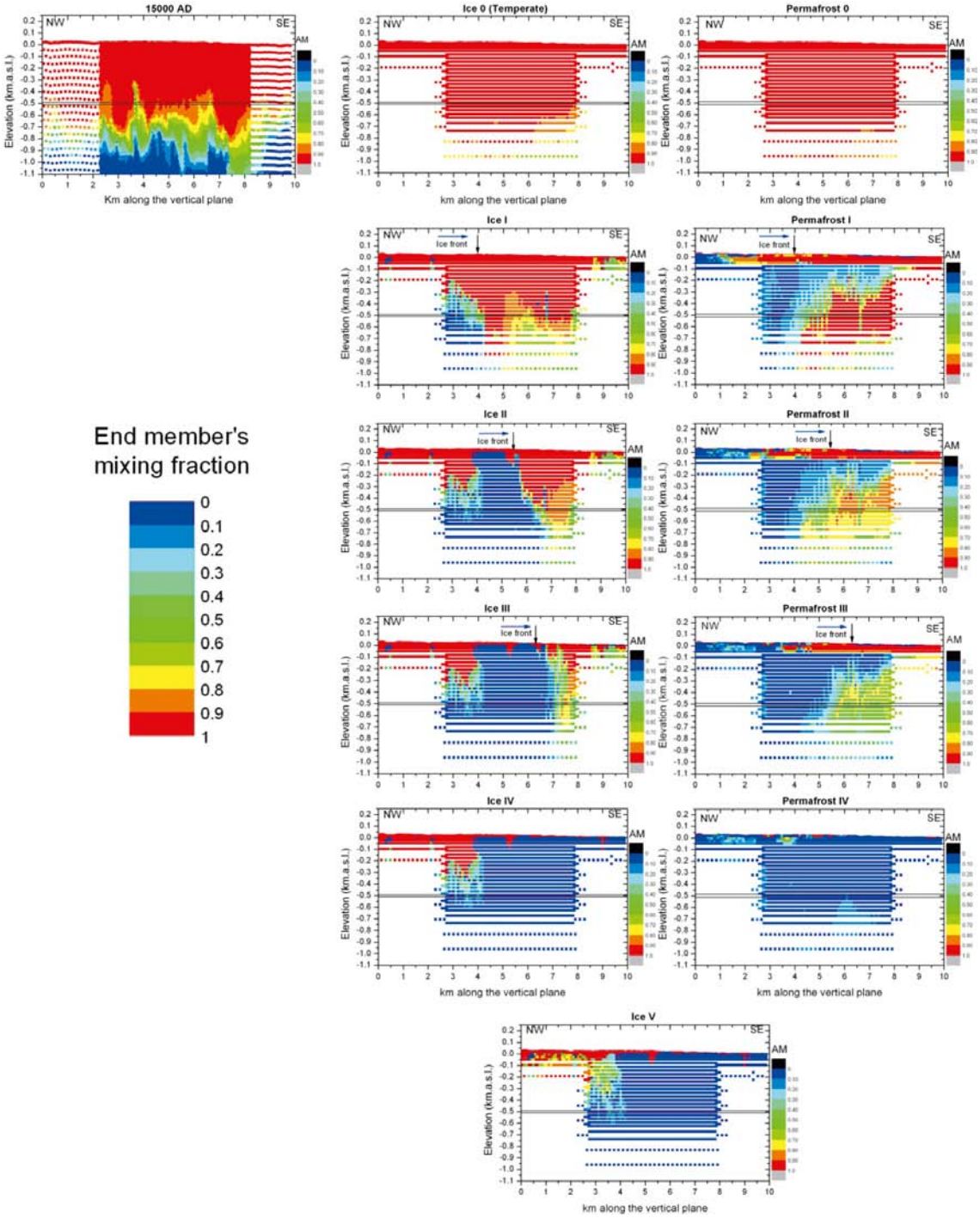

Figure A5-4. *Sequence of Altered Meteoric mixing proportion (AM) time frames as estimated by the hydrological calculations in a vertical section parallel to the coast cross-cutting the repository volume, for the transition from the end of the temperate period to the first stages of the glacial period (advance) without (left plots) and with permafrost (right plots) development. The vertical scale is enlarged 20 times with respect to the horizontal scale. See the caption of Figure A5-1 for more details.*

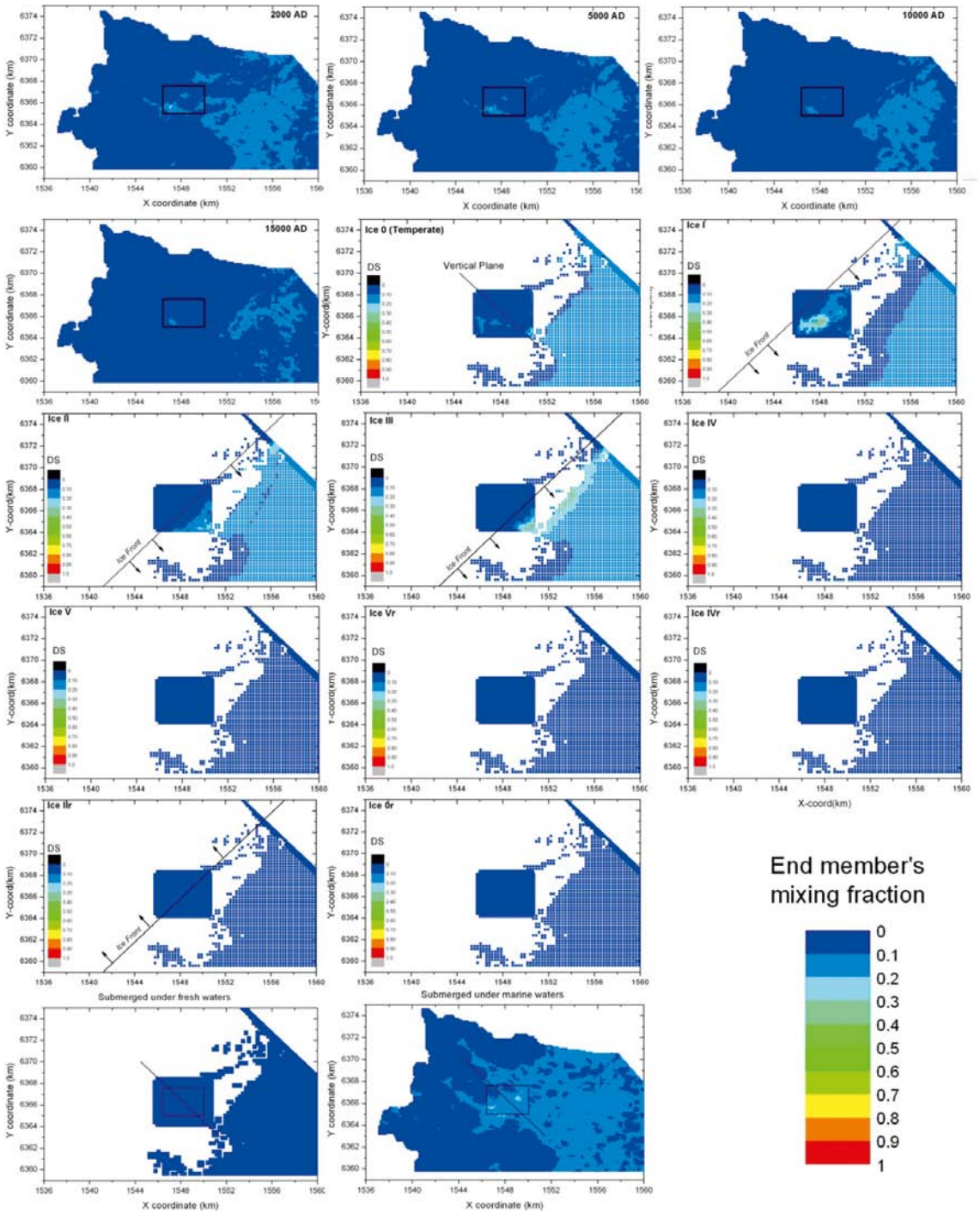

Figure A5-5. *Sequence of Deep Saline mixing proportion (DS) time frames as estimated by the hydrological calculations in a 500 m depth plane over the whole glacial cycle. See the caption of Figure A5-1 for more details.*

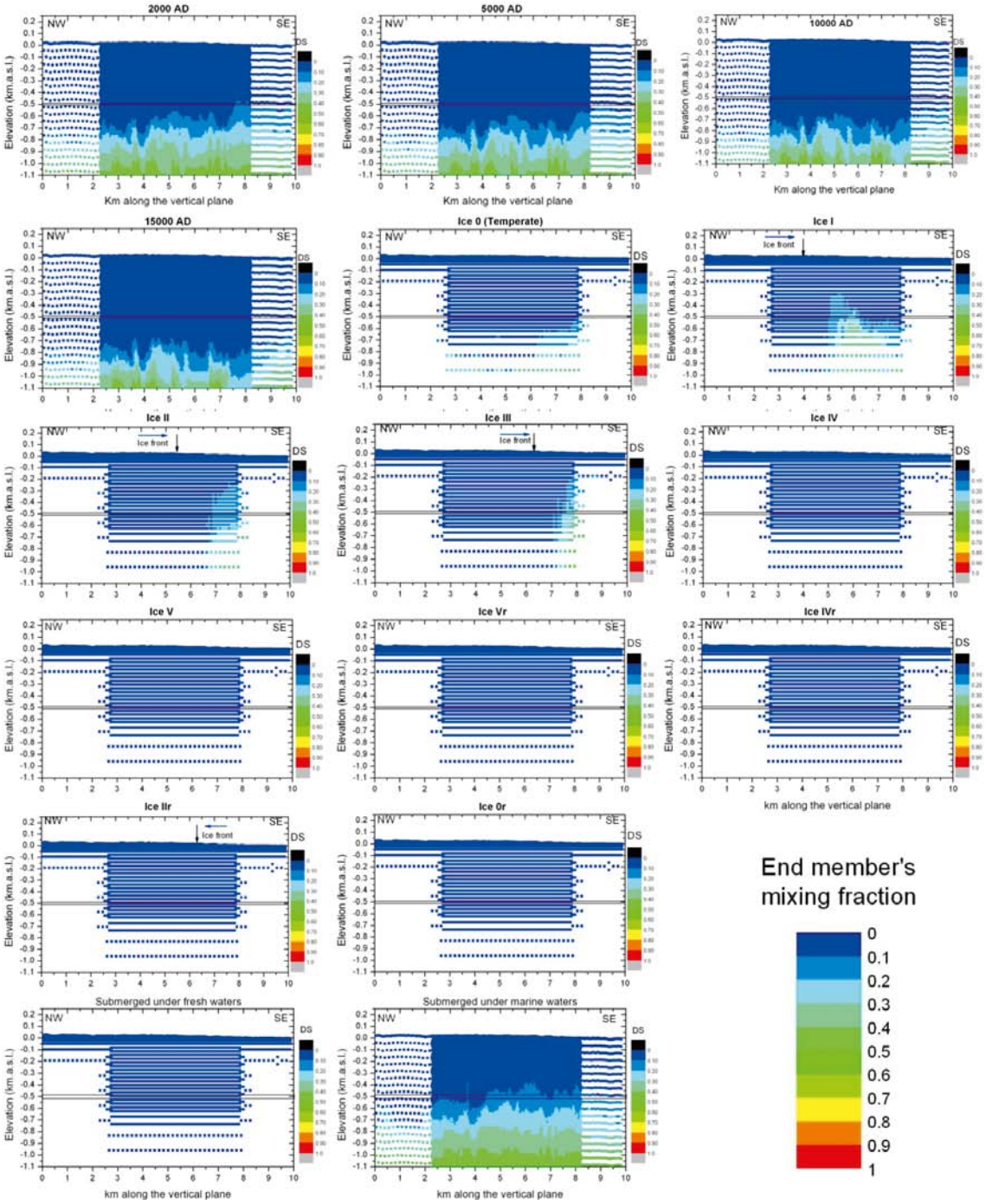

Figure A5-6. *Sequence of Deep Saline mixing proportion (DS) time frames as estimated by the hydrological calculations in a vertical section parallel to the coast cross-cutting the repository volume, over the whole glacial cycle. The vertical scale is enlarged 20 times with respect to the horizontal scale. See the caption of Figure A5-1 for more details.*

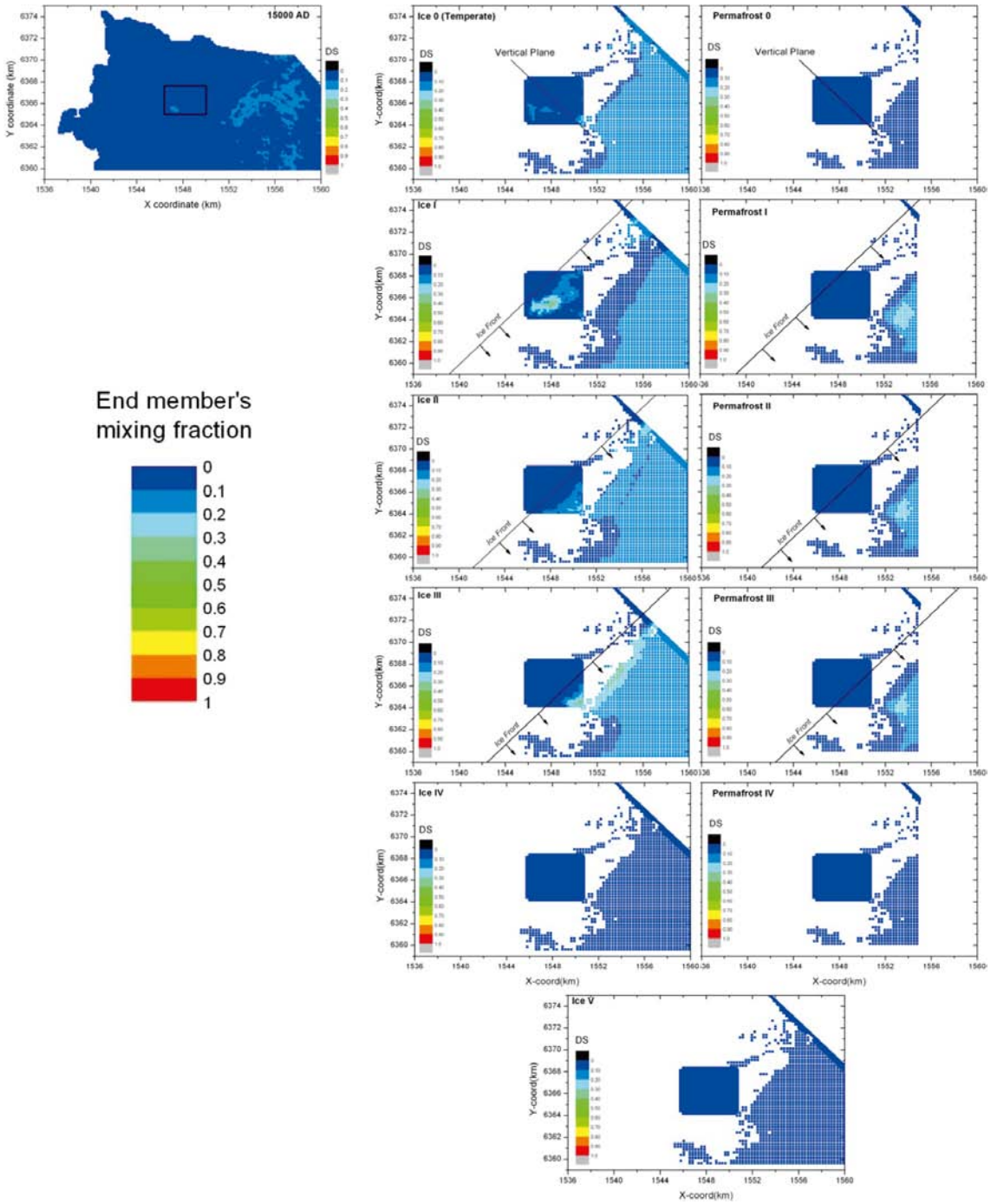

Figure A5-7. *Sequence of Deep Saline mixing proportion (DS) time frames as estimated by the hydrological calculations in a 500 m depth plane, for the transition from the end of the temperate period to the first stages of the glacial period (advance) without (left plots) and with permafrost (right plots) development. See the caption of Figure A5-1 for more details.*

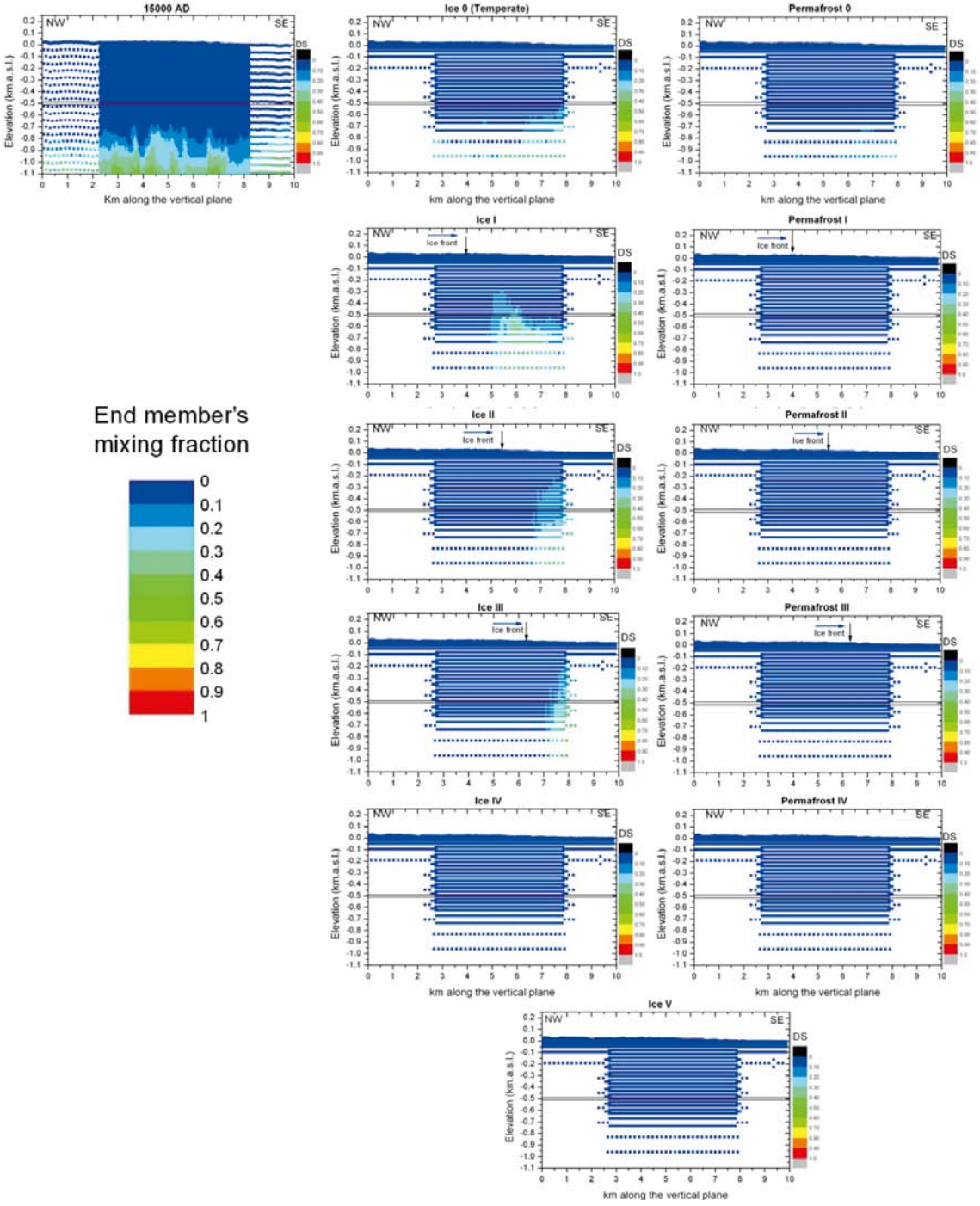

Figure A5-8. *Sequence of Deep Saline mixing proportion (DS) time frames as estimated by the hydrological calculations in a vertical section parallel to the coast cross-cutting the repository volume, for the transition from the end of the temperate period to the first stages of the glacial period (advance) without (left plots) and with permafrost (right plots) development. The vertical scale is enlarged 20 times with respect to the horizontal scale. See the caption of Figure A5-1 for more details.*

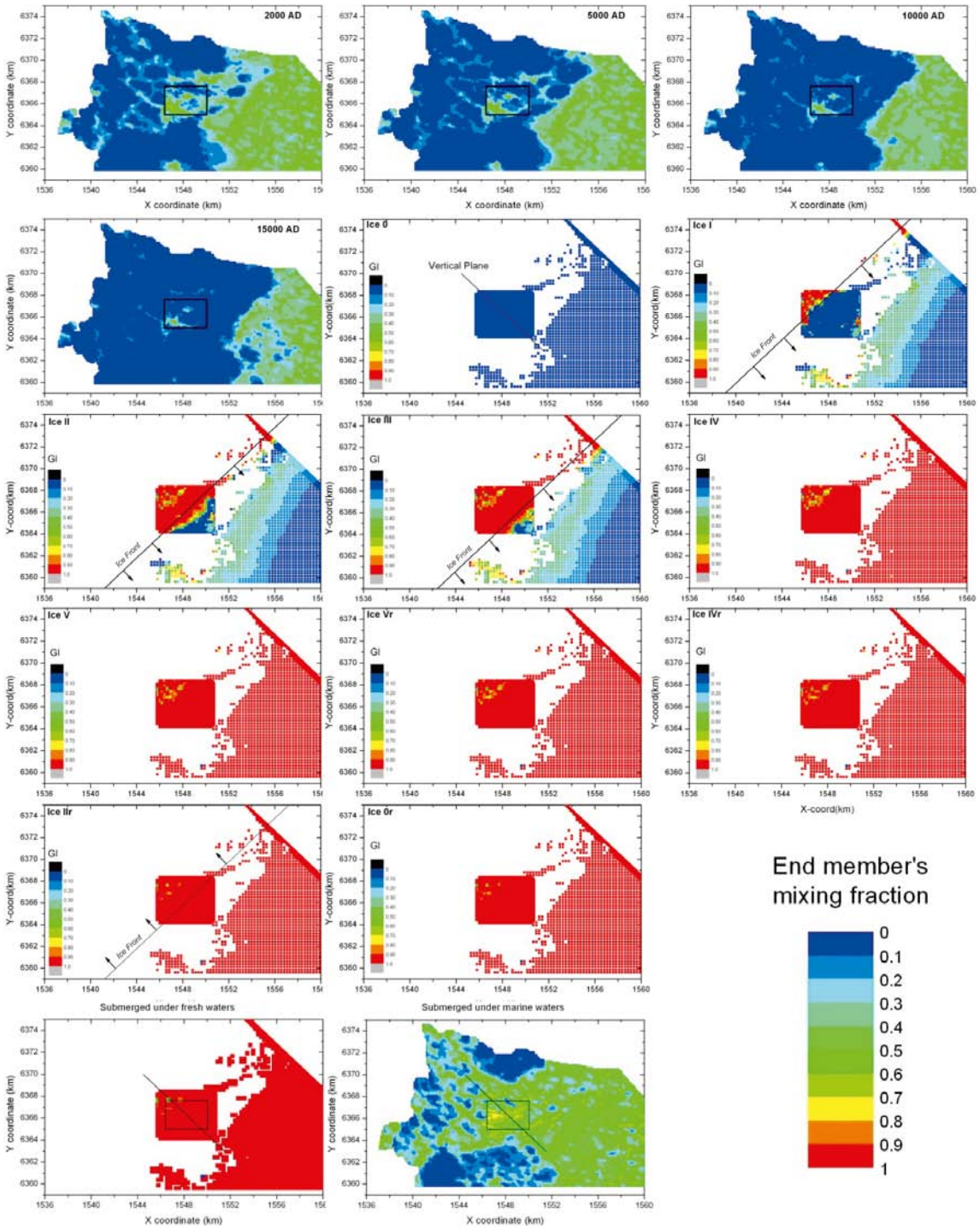

Figure A5-9. *Sequence of glacial mixing proportion (Gl) time frames as estimated by the hydrological calculations in a 500 m depth plane over the whole glacial cycle. See the caption of Figure A5-1 for more details.*

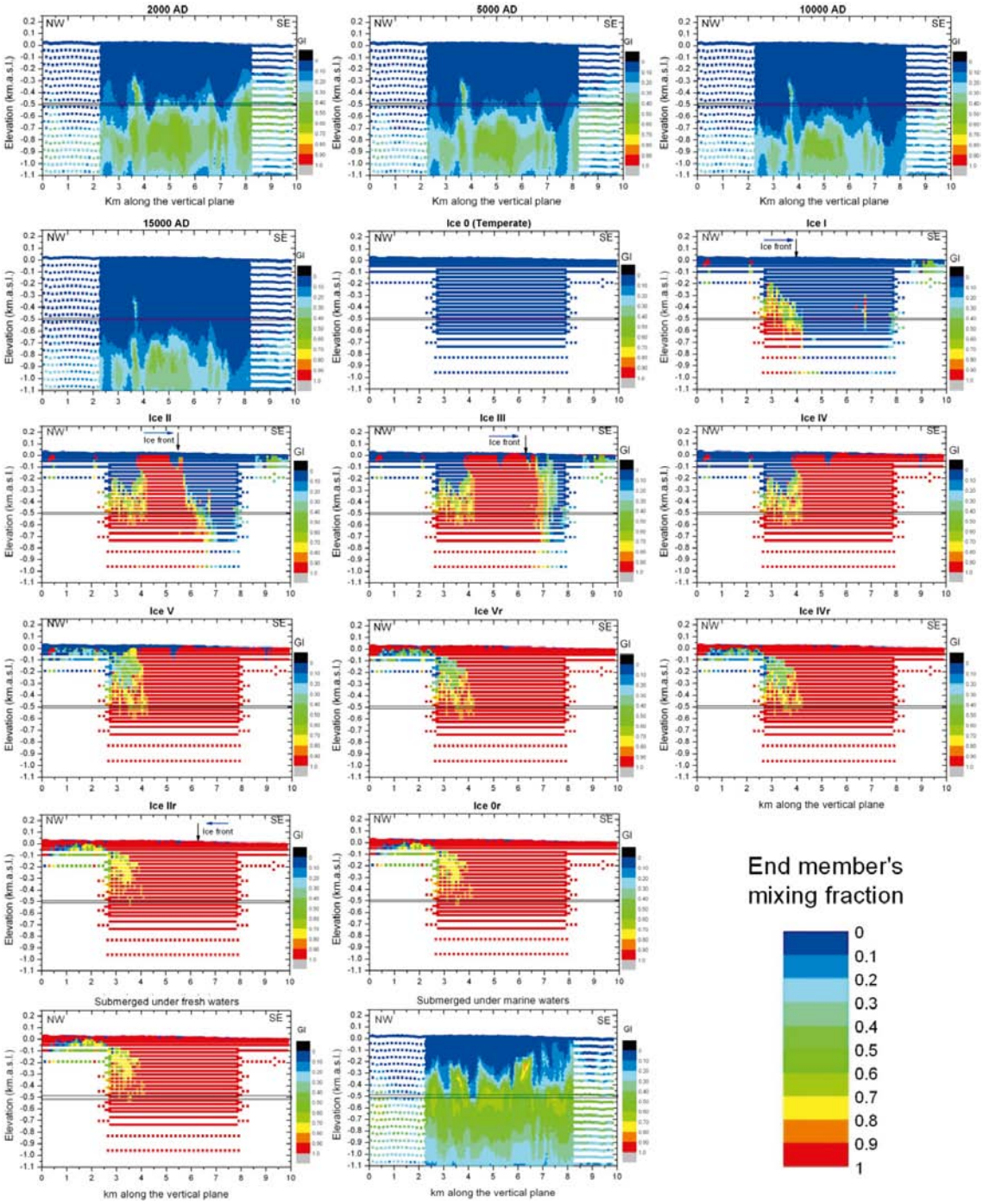

Figure A5-10. *Sequence of glacial mixing proportion (Gl) time frames as estimated by the hydrological calculations in a vertical section parallel to the coast cross-cutting the repository volume, over the whole glacial cycle. The vertical scale is enlarged 20 times with respect to the horizontal scale. See the caption of Figure A5-1 for more details.*

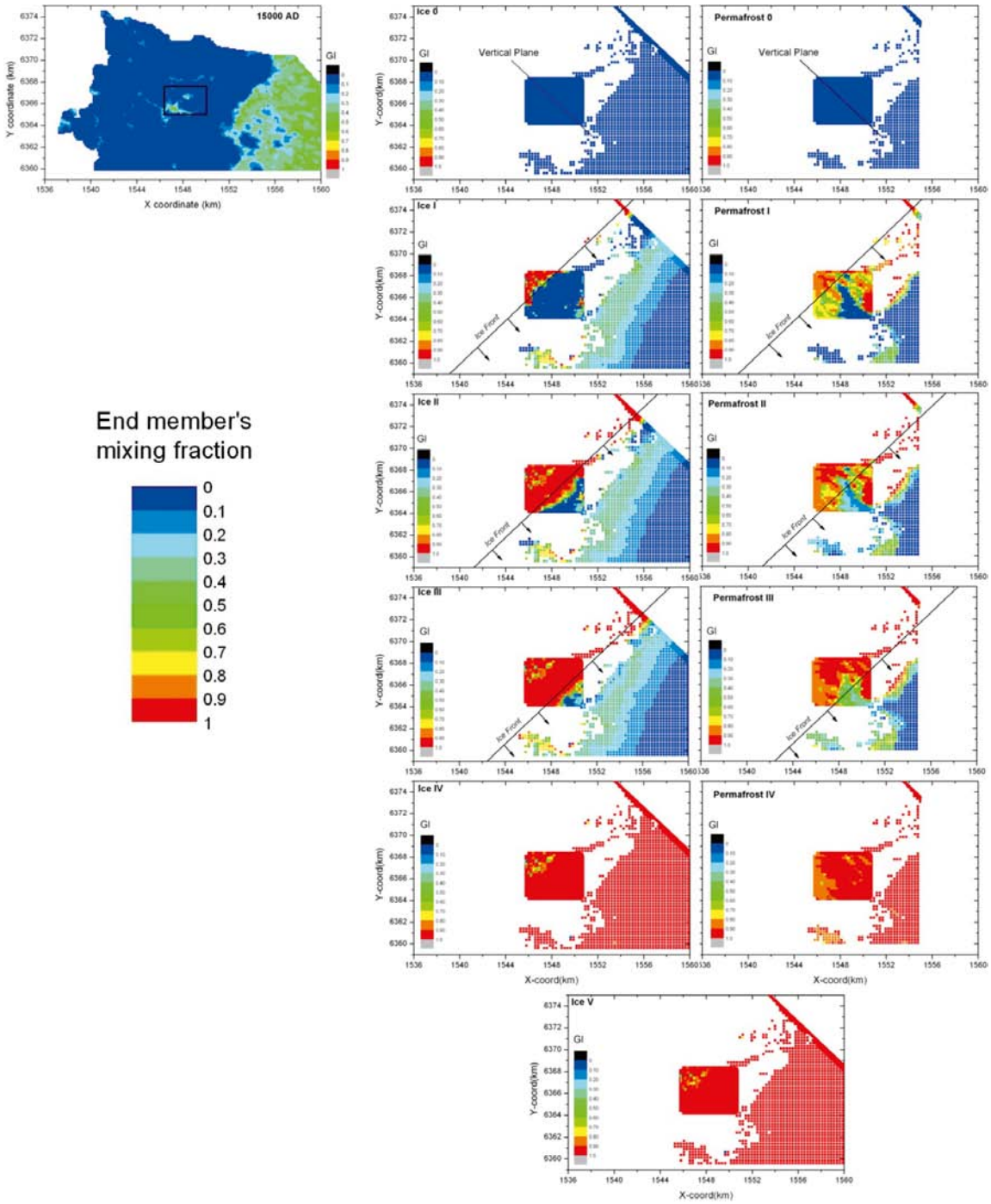

Figure A5-11. *Sequence of glacial mixing proportion (Gl) time frames as estimated by the hydrological calculations in a 500 m depth plane, for the transition from the end of the temperate period to the first stages of the glacial period (advance) without (left plots) and with permafrost (right plots) development. See the caption of Figure A5-1 for more details.*

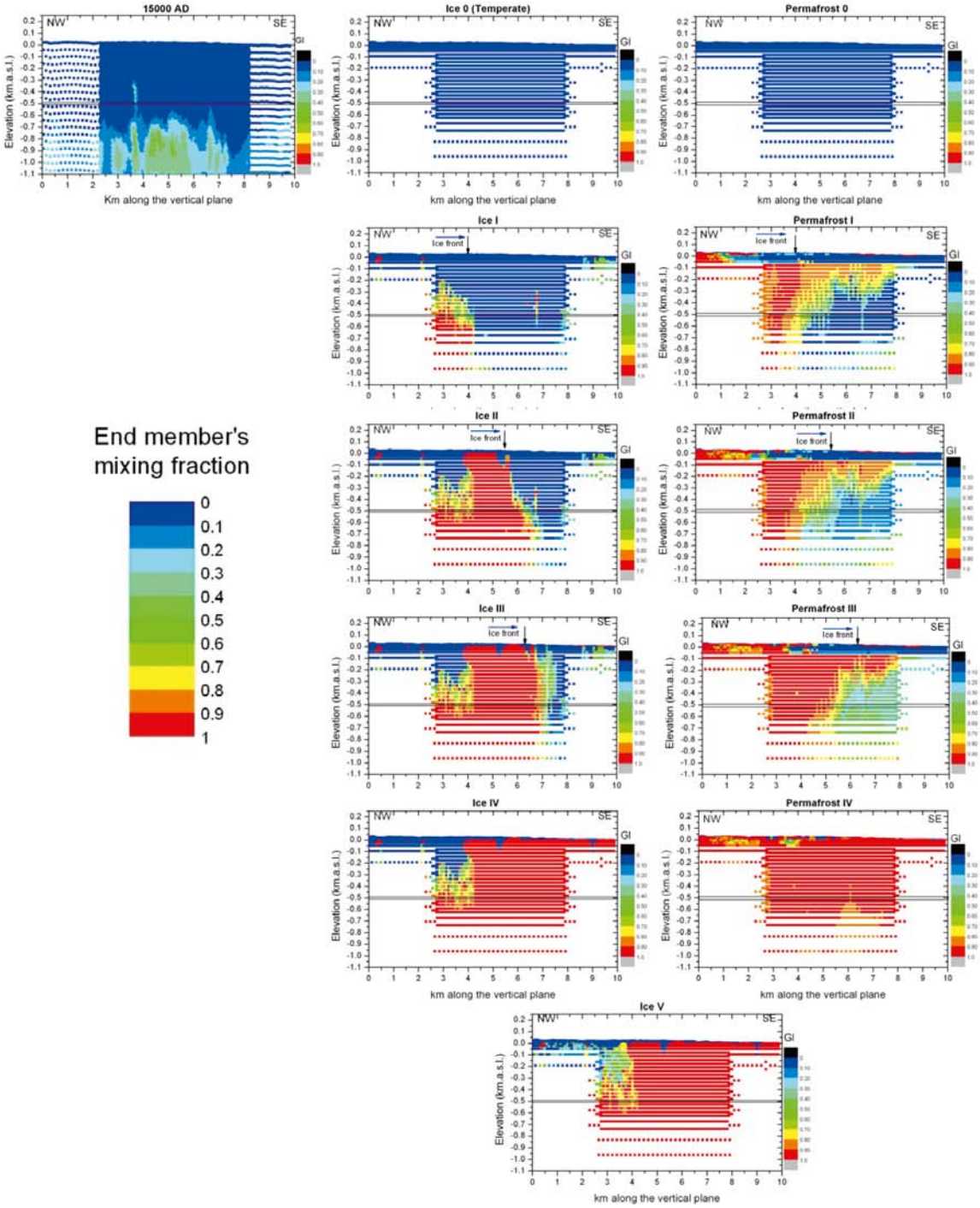

Figure A5-12. *Sequence of glacial mixing proportion (Gl) time frames as estimated by the hydrological calculations in a vertical section parallel to the coast cross-cutting the repository volume, for the transition from the end of the temperate period to the first stages of the glacial period (advance) without (left plots) and with permafrost (right plots) development. The vertical scale is enlarged 20 times with respect to the horizontal scale. See the caption of Figure A5-1 for more details.*

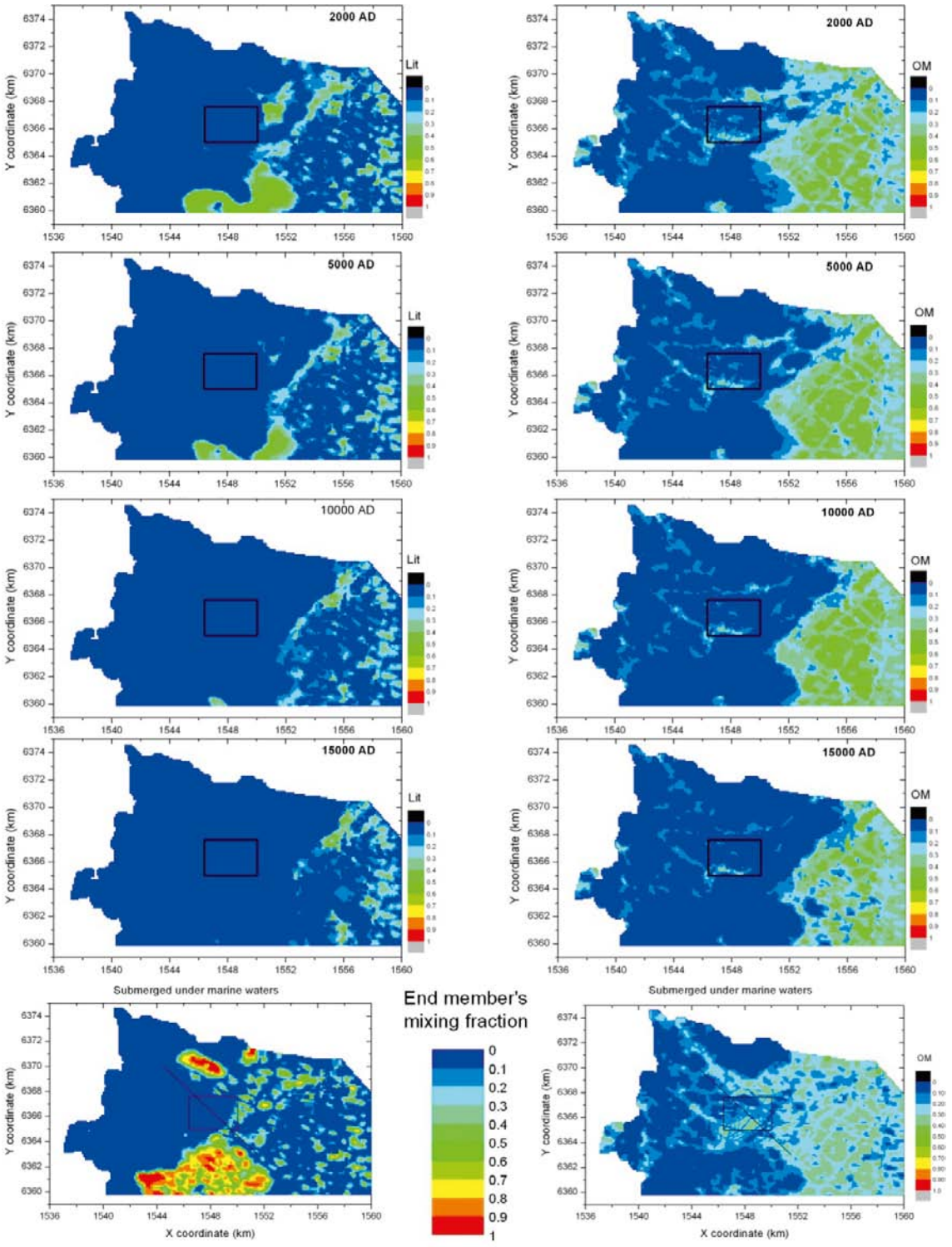

Figure A5-13. *Sequence of Littorina (left) and Old Meteoric (right) mixing proportion time frames as estimated by the hydrological calculations in a 500 m depth plane over the temperate and the submerged under marine water periods (provided by the hydrogeologists, SERCO).*

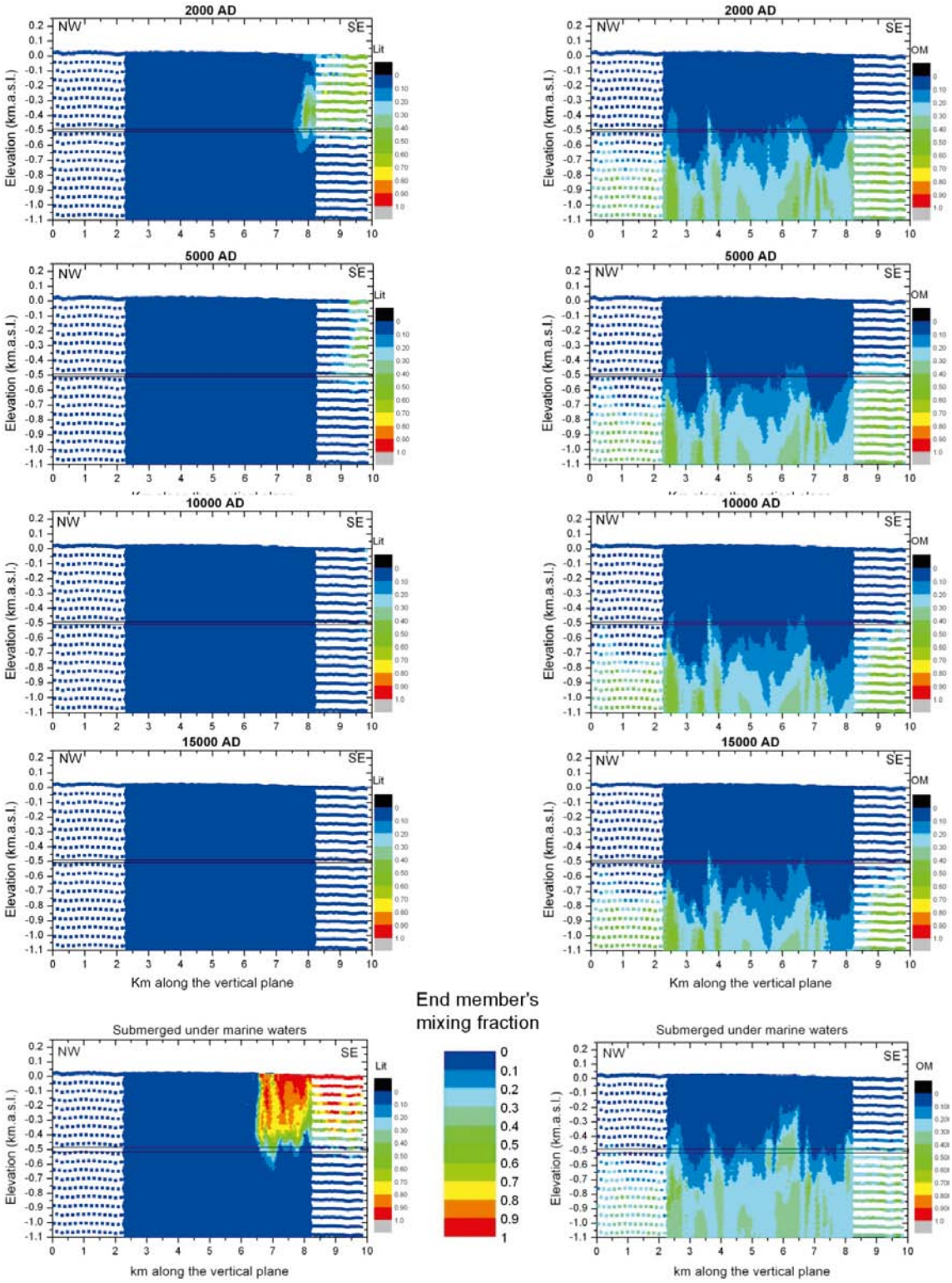

Figure A5-14. *Sequence of Littorina (left; Litt) and Old Meteoric (right; OM) mixing proportion time frames as estimated by the hydrological calculations in a vertical section parallel to the coast cross-cutting the repository volume, over the temperate and the submerged under marine water periods (provided by the hydrogeologists, SERCO). The vertical scale is enlarged 20 times with respect to the horizontal scale.*

Appendix 6

Additional plots with statistical results

This chapter includes a series of plots with the statistical results for the major components (and some interesting minor components) mentioned in Chapter 4. Their evolution over the whole glacial cycle is shown in Figure A6-1 to A6-4. The results correspond to the simulation of the Base Case over the grid points included in the repository volume.

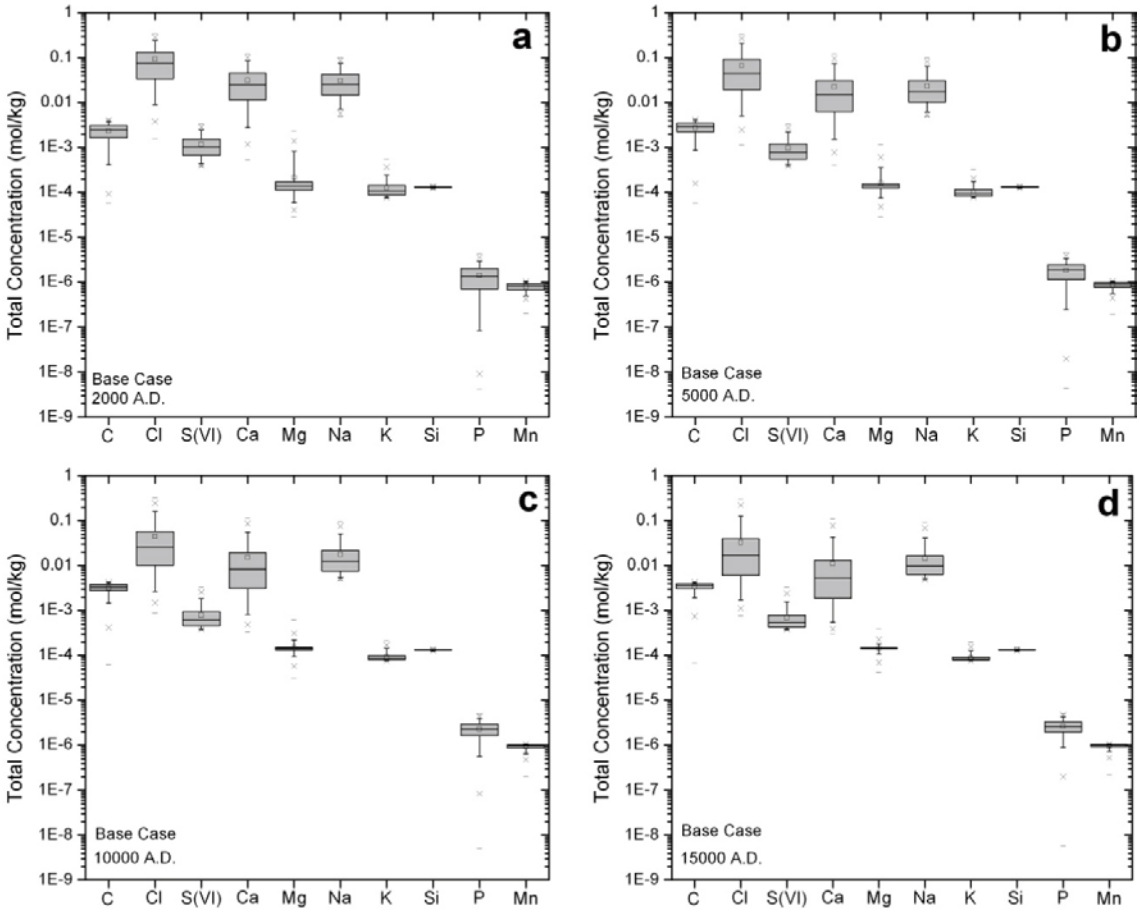

Figure A6-1. *Box-and-whisker plots showing the statistical distribution of the total concentration for the different major water components (in m/kg) calculated with the Base Case over the temperate period for the groundwaters located within the candidate repository volume at Laxemar. The statistical measures plotted here and in all the following box and whisker plots, are the median (horizontal line inside the grey box), the 25th and 75th percentiles (bottom and top of the box), the mean (square), the 5th and 95th percentiles ("whiskers"), the 1st and 99th percentile (crosses) and the maximum and the minimum values (horizontal bars).*

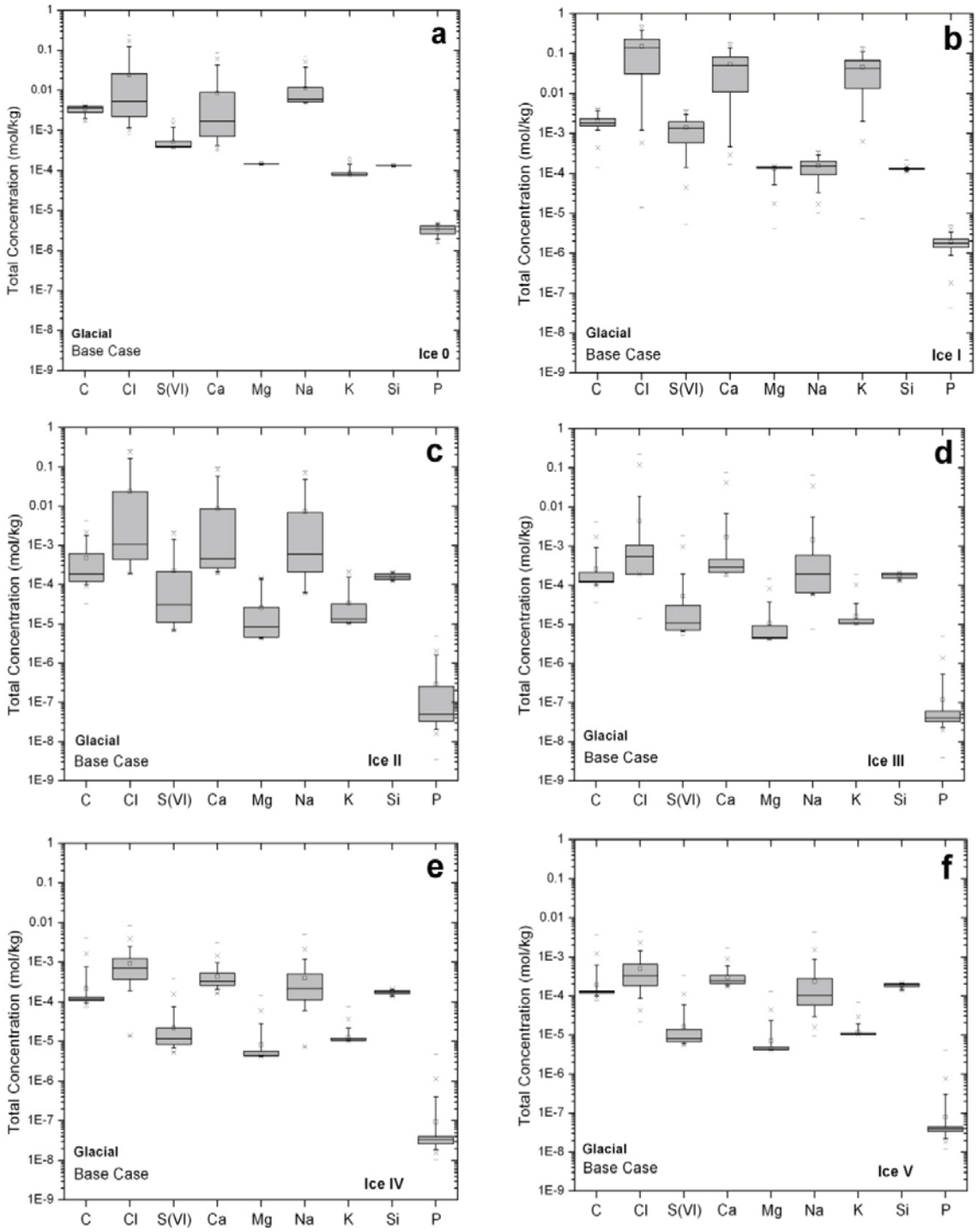

Figure A6-2. *Box-and-whisker plots showing the statistical distribution of the total concentration for the different major water components (in m/kg) calculated with the Base Case over the advance stages of the Glacial period (panels a to f) for the groundwaters located within the candidate repository volume at Laxemar. The statistical values are the same as indicated in Figure A6-1 caption.*

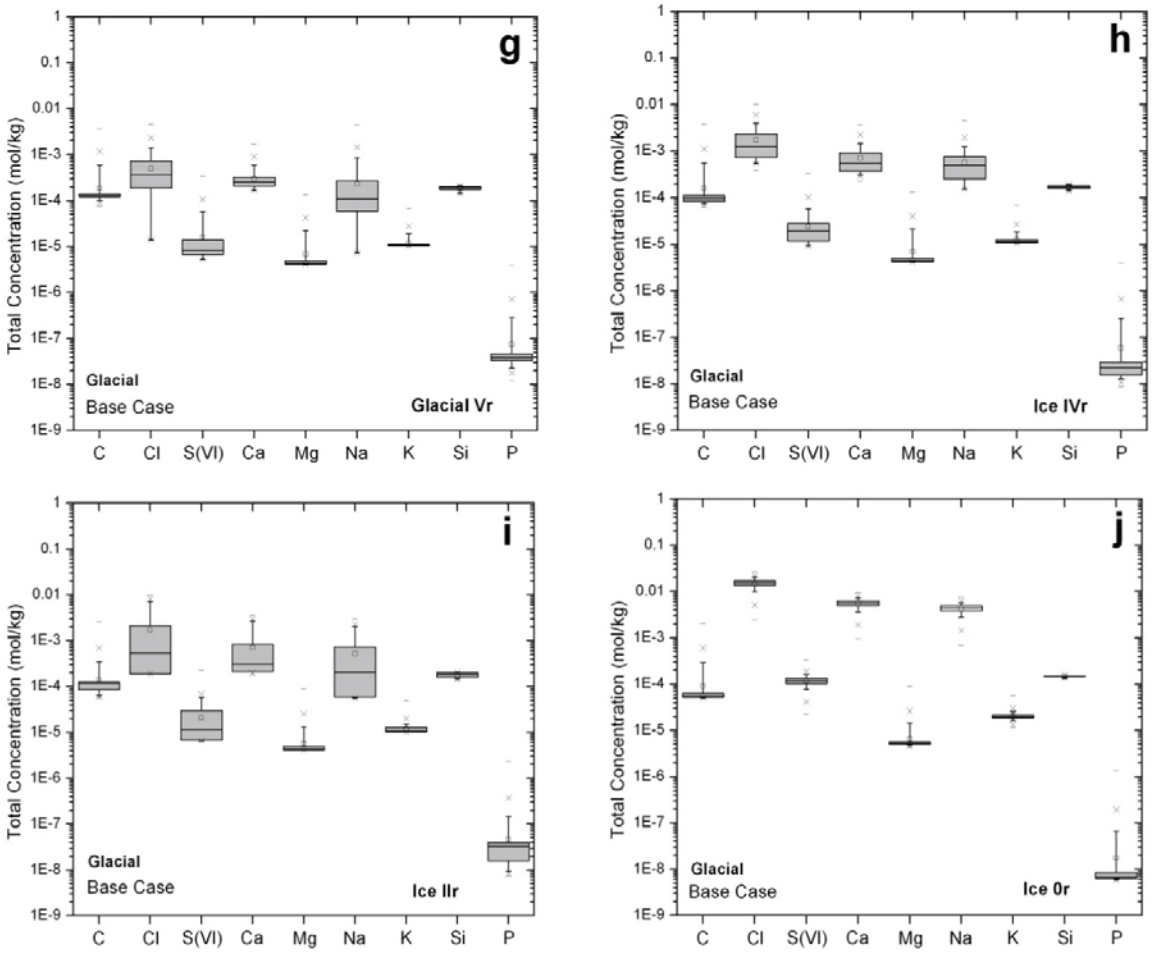

Figure A6-2. *Continuation.*

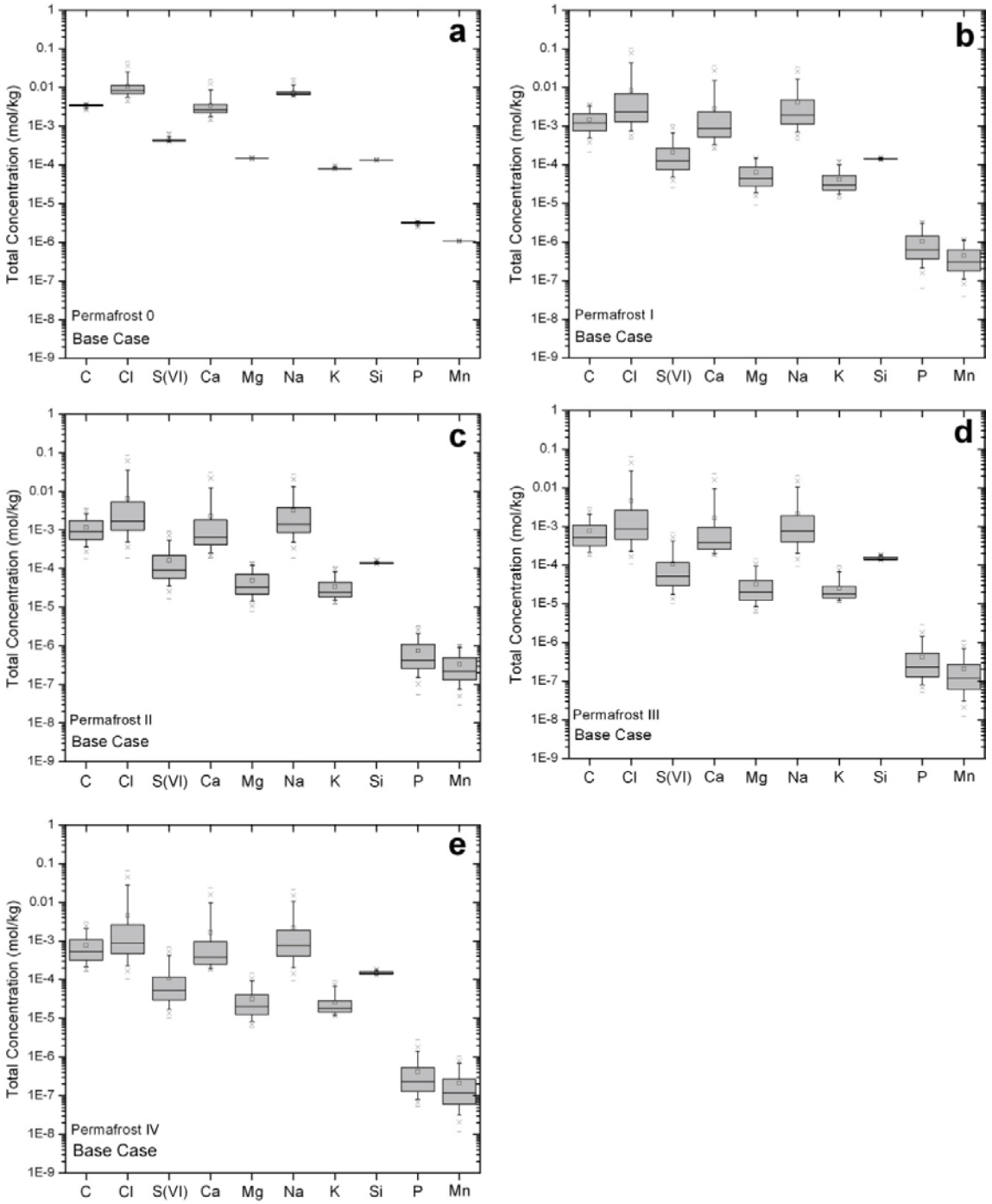

Figure A6-3. *Box-and-whisker plots showing the statistical distribution of the total concentration for the different major water components (in m/kg) calculated with the Base Case over the first stages of the Glacial period when considering the frozen ground (permafrost) for the groundwaters located within the candidate repository volume at Laxemar. The statistical values are the same as indicated in Figure A6-1 caption.*

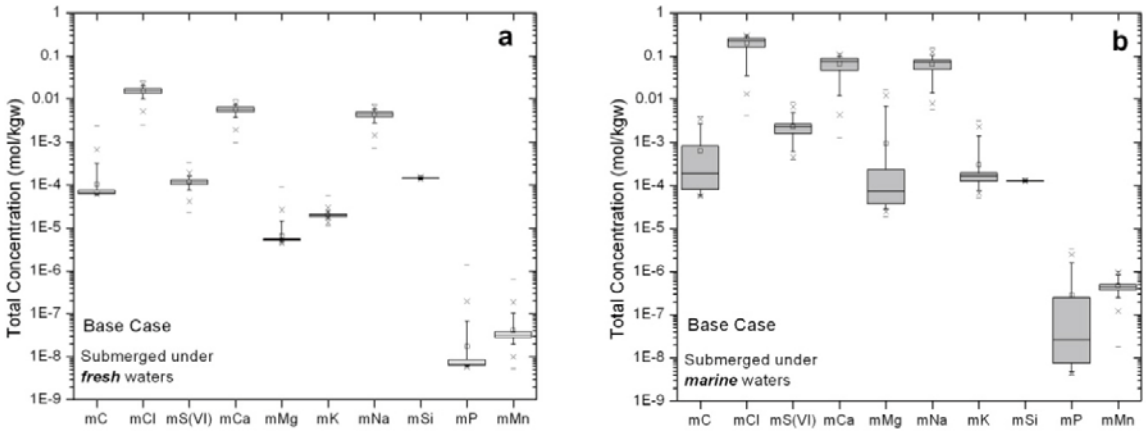

Figure A6-4. *Box-and-whisker plots showing the statistical distribution of the total concentration for the different major water components (in m/kg) calculated with the Base Case over the submerged period (under fresh, a, and marine, b, waters) for the groundwaters located within the candidate repository volume at Laxemar. The statistical values are the same as indicated in Figure A6-1 caption.*